Second Edition

Eastern Economy Edition

Chemical Process Modelling and Computer Simulation

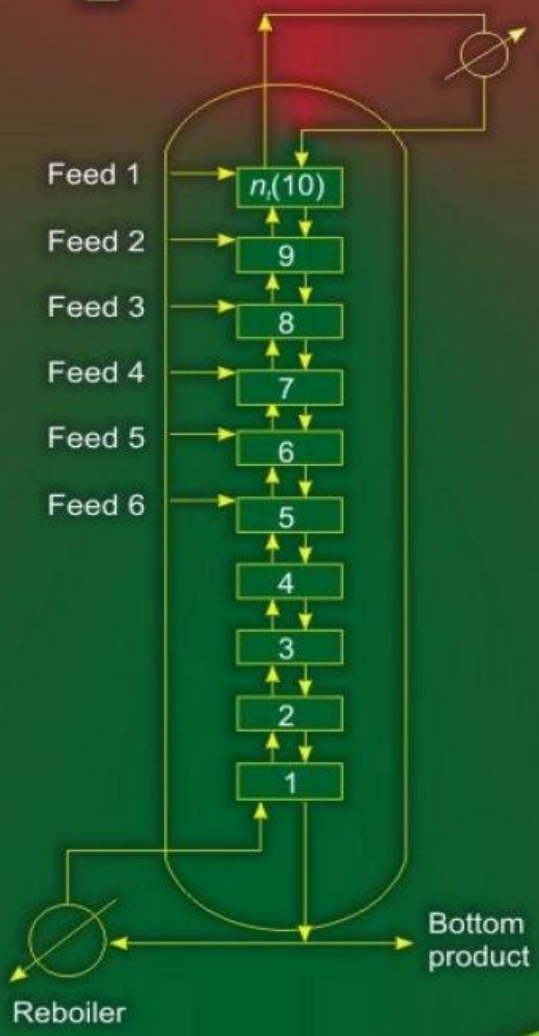

PHI

Amiya K. Jana

Chemical Process Modelling and Computer Simulation

SECOND EDITION

Amiya K. Jana
Department of Chemical Engineering
Indian Institute of Technology Kharagpur

PHI Learning Private Limited
Delhi-110092
2011

CHEMICAL PROCESS MODELLING AND COMPUTER SIMULATION, Second Edition
Amiya K. Jana

ISBN-978-81-203-4477-8

Third Printing (Second Edition) … … … November, 2011

Published by Asoke K. Ghosh, PHI Learning Private Limited, 111, Patparganj Industrial Estate, Delhi-110092 and Printed by Raj Press, New Delhi-110012.

To

My mother Minati
and wife Mahua

The ideals which have lighted my way,
and time after time have given me new courage to face life cheerfully,
have been Kindness, Beauty, and Truth.
The trite subjects of human efforts, possessions, outward success, luxury
have always seemed to me contemptible.

Albert Einstein

Contents

Preface

The first edition of this book appeared three years ago. This edition is a major revision and expansion to the first edition. Two new chapters have been added and several chapters have been expanded. The objective of the book, however, remains the same as in the first edition, "to model and simulate the practical processes for investigating the dynamic behaviour".

To improve the design, operability, safety and productivity of a process with minimum capital and operating costs, it is necessary to understand the detailed process dynamics and plant behaviour. The process characteristics can be predicted by solving the mathematical model in a dynamic simulator. We can say that the process simulator is actually used as a diagnostic tool to identify the operating problems.

Moreover, for the control engineers, knowledge on the mathematical process model is very important mainly for two reasons. Firstly, they must need an overall idea on the process characteristics at different conditions and situations, and secondly, they use the process model for designing the advanced control schemes. In addition, the model is required to develop appropriate controller settings.

In addition to the two new chapters, 15 (Reactive Distillation Column) and 16 (Vaporizing Exchangers), the following chapters have been expanded with several interesting topics:

Chapter 2 with a few more numerical integration techniques for solving differential equations
Chapter 3 with modelling of the semi-batch reactor
Chapter 4 with multiple steady state analysis and control of the CSTR, and a pH neutralization reactor modelling
Chapter 5 with batch and fed-batch modelling and dynamics
Chapter 9 with soft-sensor for the distillation column
Chapter 14 with a refinery distillation model validation and control

It is a great pleasure to acknowledge the valuable contributions provided by many of my well-wishers. I wish to express my heartfelt gratitude and indebtedness to Prof. A.N. Samanta, Prof. S. Ray and Prof. D. Mukherjee, department of chemical engineering, IIT Kharagpur. IIT Kharagpur undergraduate and postgraduate students have contributed to the book by their questions, youthful enthusiasm and genuine interest in the subject.

I am greatly indebted to the editorial staff of the publisher, PHI Learning, for their constant encouragement and their unstinted efforts in bringing out the book in its present form.

The book could not have been completed without the patience, support and forbearance of my mother Minati and wife Mahua.

In the spirit of continuous improvement, we are interested in receiving "feedback" from students, practitioners and faculty who use this book.

Amiya K. Jana

Preface to the First Edition

The chemical process industries are faced with an increasingly competitive environment, ever-changing market conditions, and government regulations. Notwithstanding these constraints, the industries have to continuously keep on increasing their productivity and profitability for survival in the market. In order to achieve this goal, it is most important that the chemical plants are operated with optimum efficiency in spite of the different constraints confronting them.

To improve the design, operability, safety, and productivity of a process with minimum capital and operating costs, it is necessary to understand the detailed process dynamics and plant behaviour. The process characteristics can be predicted by solving the mathematical model in a dynamic simulator. Such a process simulator can also be used as a diagnostic tool to identify the operational problems.

In addition, for the control engineers, a sound knowledge of the mathematical process model is essential on account of two reasons. First, they must have an overall idea of the process characteristics at different conditions and situations, and second, they should be able to use the process model for designing the advanced control schemes. Moreover, the model is required to develop appropriate controller settings, and so on.

Presently, most of the books available on this topic give simplified process models and their simulations. The simplified or approximate models cannot always represent real processes, and they are therefore useful only for academic purposes. This book presents the development of mathematical models for many realistic chemical processes. The examples or case studies include: tanks, heat exchanger, chemical reactors (both continuous and batch), biochemical reactor, distillation columns (both continuous and batch), equilibrium flash vaporizer, and the refinery debutanizer column. Besides, the dynamic simulations of these process models are also included. In this book, many process simulators or different parts of the simulators are programmed using Fortran (90) language. Such detailed programs using an easy language like Fortran (90) should help students to understand this subject matter clearly. Also, it is not difficult to transform the reported Fortran programs to some other convenient language.

For the development of mathematical models of several chemical processes, the readers need to be familiar with the fundamentals of activity coefficient models, equation of state models, vapour–liquid equilibrium, kinetic models, and so on. Again to simulate the mathematical model structures, the readers should also be knowledgeable about different numerical techniques for solving the ordinary differential equations and nonlinear algebraic equations. In the initial chapters, the details of all these fundamentals are addressed. The readership for this book, therefore, comprises senior undergraduate students, first-year postgraduate students, research scientists and practising engineers.

It is a great pleasure to acknowledge the valuable contributions provided by many of my well-wishers. I wish to express my heartfelt gratitude and indebtedness to Prof. A.N. Samanta and Prof. S. Ganguly, both of the department of chemical engineering, IIT Kharagpur, for their invaluable suggestions and constructive criticism throughout the development of many of the process simulators. I am grateful to Prof. S. Ray, Prof. D. Mukherjee and Prof. A.K. Biswas, all of the department of chemical engineering, IIT Kharagpur, for their constant encouragement to complete this book. I am thankful for the support received throughout the development of the manuscript from the department of chemical engineering, BITS, Pilani.

Special thanks go to my former colleagues, Prof. R.P. Vaid, Prof. B.V. Babu, Dr. H.K. Mohanta and Dr. Arvind Kumar Sharma for the support I received from all of them while at BITS, Pilani. Special mention must be made of Prof. Massimiliano Barolo, Università di Padova, Italy, for offering many helpful suggestions. I wish to acknowledge the important suggestions of Prof. James
B. Riggs, Texas Tech University, Lubbock.

I am greatly indebted to the staff members of the publisher, PHI Learning, for their constant cooperation and unstinted efforts in publishing the book in its present form.

The book could not have been completed without the patience, support, and forbearance of my mother and my wife. Finally, to my relatives goes my eternal gratitude for their love, support and dedication.

All comments and suggestions for improvement of the book would be gratefully acknowledged.

Amiya K. Jana

Part I

Introduction

1

Introduction to Modelling and Simulation

1.1 DEFINITIONS

The course that we are going to study is named *Chemical Process Modelling and Computer Simulation*. The technical words (terms), which are assembled to form the title of the course, are required to be explained first. It is true that the subject matter of this book is a small part of the discipline *Modelling and Simulation*.

Definition of modelling and simulation: Modelling and simulation is a discipline for developing a level of understanding of the behaviour of the parts of a system, and of the system as a whole.

Modelling and simulation is very much an art. One can understand about riding a bicycle from reading a book. To really learn to ride a bicycle, one must actively practice with a bicycle. Modelling and simulation follows much the same principle. You can learn much about modelling and simulation from reading books and talking with modellers. Skill and talent in developing models and performing simulations are only developed through building models and simulating them.

Let us discuss first the modelling and then we will study the simulation in subsection 1.6.

Models are used particularly in the *basic sciences* and *engineering* disciplines (such as chemistry, physics, biology, chemical engineering, mechanical engineering, electrical engineering, etc.) and also in the *social sciences* (such as sociology, economics, political science, etc.). Therefore, first we wish to know the general definition of the *model* and then we will know the definition of the *process model*.

Definition of model: A model is a simplified representation of a system at some particular point in time and/or space intended to promote understanding of the real system.

The word *model* actually comes from the Latin word *modus*, which means *a measure*. Used as a noun, it means *a small representation of a planned or existing object* (Webster's New World Dictionary). Remember that in many textbooks and articles, the model is also referred to as a mathematical model.

The above two definitions (modelling and simulation, and model) include a new term *system*. The word *system* probably has more varied meanings than any other word in use today. We may consider the following general definition for the system.

Definition of system: A system typically consists of components (or elements) which are connected together in order to facilitate the flow of information, matter or energy….

Therefore, in brief, a system is an assemblage of several elements comprising a unified whole. From Latin and Greek, the term *system* means to combine, to set up, to place together. In chemical engineering discipline, a system is composed of chemical unit operations, such as distillation columns, chemical reactors, evaporators, heat exchangers, etc. A system may produce the desired product using a single distillation column, then that system is said to be the distillation system.

Like the process control, the process model is typically used in chemical engineering discipline. It may be defined as given below.

Definition of process model: A process model comprises of a set of equations that permits us to predict

the dynamics of a chemical process.

Notice that the process model includes the necessary input data for solving the modelling equations. Although the process model may be a specific type of the model, in the present study we will use the terms, model, mathematical model and process model to mean the same thing. Moreover, in the present study, we prefer to consider a process as a unit operation. Accordingly, in several chapters of this book, the distillation column, for example, will be called as the distillation process. Therefore, we can say that the process may be a *part* of a system or a *complete* system.

However, there are no such clear-cut definitions for these terms so that they can always be defined uniformly. For example, in process control (Stephanopoulos, 1998), a system (closed-loop) may be comprised of the process (e.g., distillation column), controller (e.g., proportional integral (PI) controller), final control element (e.g., valve), and measuring device (e.g., thermocouple). In contrary, the process is also commonly called in that subject as a system (e.g., first-order system, second-order system, etc.).

1.2 CONSERVATION PRINCIPLE

The basis for virtually all theoretical process models is the general conservation principle. It is written as an equation form in the following manner

$$[\text{Accumulation}] = [\text{Input}] - [\text{Output}] + [\text{Internal Production}] \qquad (1.1)$$

It should be more appropriate if the conservation principle is presented in terms of *rates* (per unit time), in which case, Equation (1.1) becomes

$$\begin{bmatrix}\text{Rate of}\\ \text{accumulation of } S\end{bmatrix} = \begin{bmatrix}\text{Rate of}\\ \text{input of } S\end{bmatrix} - \begin{bmatrix}\text{Rate of}\\ \text{output of } S\end{bmatrix} + \begin{bmatrix}\text{Rate of}\\ \text{production of } S\end{bmatrix} \qquad (1.2)$$

where, S is a conserved quantity within the boundaries of a system. Now applying this general conservation principle, the basic model structure of a chemical process can be developed making balance in terms of three fundamental quantities—mass, energy and momentum. It is conventional to refer to the mathematical modelling equations obtained from Equation (1.2) as mass, energy or momentum balances, depending on which of these quantities represents.

The mass balance equation may be developed with respect to the total mass or the mass of individual components in a mixture. The balance equation that is derived with respect to total mass is known as *total mass balance* or *overall mass balance* equation. Similarly, the modelling equation that is built in terms of the mass of an individual component is referred to as *component mass balance* or *partial mass balance* equation. Remember that in many textbooks (e.g. Luyben, 1990), total mass balance and component mass balance equations are called as *total continuity* and *component continuity* equations, respectively. The general form of the mass balance equation is

$$\begin{bmatrix}\text{Rate of}\\ \text{accumulation of mass}\end{bmatrix} = \begin{bmatrix}\text{Rate of}\\ \text{input of mass}\end{bmatrix} + \begin{bmatrix}\text{Rate of}\\ \text{generation of mass}\end{bmatrix} - \begin{bmatrix}\text{Rate of}\\ \text{output of mass}\end{bmatrix} - \begin{bmatrix}\text{Rate of}\\ \text{depletion of mass}\end{bmatrix} \qquad (1.3)$$

Now we wish to develop the mass balance equations for a mixture that has total n number of components. Employing Equation (1.3), we can obtain one total mass balance equation along with n component mass balance equations (one for each component), total $(n + 1)$ equations.

It should be noted that the total mass balance equation does not have any generation or depletion term (both are always zero) because mass can never be totally created or totally destroyed in a system that

operates under nonrelativistic conditions. But the mass of an individual component within a system may change, for example, because of chemical reaction. One component (say, reactant) that disappears may appear as another component (product).

The general form of energy balance equation can be obtained by modifying Equation (1.2) as:

$$\begin{bmatrix}\text{Rate of}\\ \text{accumulation of energy}\end{bmatrix}=\begin{bmatrix}\text{Rate of}\\ \text{input of energy}\end{bmatrix}+\begin{bmatrix}\text{Rate of}\\ \text{generation of energy}\end{bmatrix}-\begin{bmatrix}\text{Rate of}\\ \text{output of energy}\end{bmatrix}-\begin{bmatrix}\text{Rate of}\\ \text{expenditure of energy}\end{bmatrix} \tag{1.4}$$

It is important to note that the first law of thermodynamics is a statement of the conservation of energy for thermodynamic systems. In chemical process modelling, the energy balance equations are also sometimes named as heat balance or enthalpy balance equations.

Similarly, the general form of a momentum balance equation is given in the following manner:

$$\begin{bmatrix}\text{Rate of accumulation}\\ \text{of momentum}\end{bmatrix}=\begin{bmatrix}\text{Rate of input}\\ \text{of momentum}\end{bmatrix}+\begin{bmatrix}\text{Rate of forces}\\ \text{acting on volume element}\end{bmatrix}-\begin{bmatrix}\text{Rate of}\\ \text{output of momentum}\end{bmatrix} \tag{1.5}$$

It is a fact that any generation of momentum must be the result of the forces acting on the volume element. Again it should be noted that the above momentum balance equation is a generalization of Newton's law of motion which states that force is the product of mass and acceleration.

1.3 MODEL REPRESENTATION

Mathematical modelling is an art. It takes talent, practice, and experience to be a successful mathematical modeller. The mathematical model usually describes a system by a set of variables and a set of equations that establish relationships between the variables. In general, there are six basic groups of variables: decision variables, input variables, state variables, exogenous variables, random variables, and output variables. The following groups of variables are commonly used to describe a chemical process: input variables, state variables, and output variables. If there are many variables of each type, the variables may be represented by vectors.

Note that in addition to the above three groups of variables, parameters or constant parameters (also sometimes known as exogenous variables) are also present in the mathematical model of the chemical processes. A parameter is typically a physical or chemical property value. The values of parameters, such as density, heat capacity, viscosity, activation energy, thermal conductivity, heat transfer coefficient, mass transfer coefficient, etc., must be known or specified for solving a problem.

All the process variables we mentioned above, such as input, state, or output variables, depend on time and/or spatial position. Therefore, they all are considered as *dependent* variables. Whereas, time and the spatial coordinate variables are the *independent* variables.

Perhaps the best way to illustrate the foregoing discussion is by presenting an example. Let us consider the liquid tank as shown in Figure 1.1. Here, F_i is the volumetric flow rate of an inlet stream, F_o the volumetric flow rate of an outlet stream, h the height of the liquid in the tank, V the volume of the liquid in the tank and A the cross sectional area of the tank. Now the variables can be defined as follows: F_i is the input variable, F_o the output variable and V (or h) the state variable. Obviously, the cross sectional area

A is regarded as a constant.

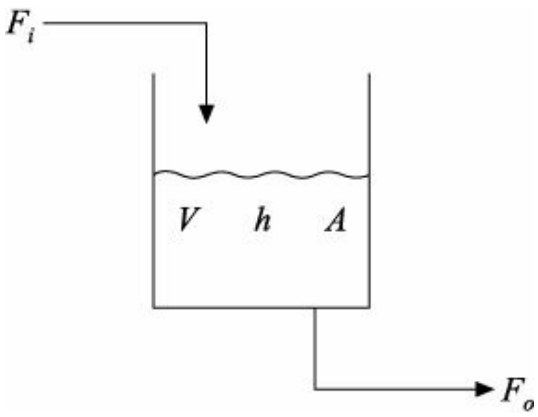

FIGURE 1.1 The liquid tank.

The input variables of a process are normally specified by an engineer who has expertise of the process being considered. The input variables typically include flow rates, compositions, temperatures, and pressures of fluids entering a process. In the process control, the input variables are again classified into two categories: load variables (or disturbances) and manipulated (or adjustable) variables. Interestingly, sometimes the output flow rate is considered as an input variable (i.e., manipulated variable). For example, in Figure 1.1, the liquid volume (or height) in the tank can be maintainted (or controlled) by adjusting (or manipulating) the flow rate of the outlet stream F_O. It implies that F_O is the manipulated variable, i.e., input variable.

Furthermore, the output variables are dependent on the state variables. Figure 1.2 shows the dependency of the output variable y on the state variable x. In the pictorial illustrations, g has been considered as a nonlinear function of x.

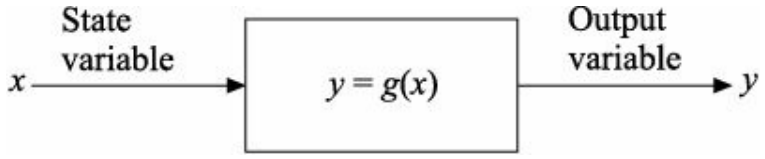

FIGURE 1.2 State variable–output variable map.

For a linear case, $g(x)$ may be represented as:

$$g(x) = Cx \qquad (1.6)$$

that implies,

$$y = Cx \qquad (1.7)$$

Now it is clear that when C is unity, the output variable and state variable are the same.

Now we will concentrate our discussion on the state variables and state equations. In chemical engineering, mass, energy and momentum are three fundamental quantities whose values describe the natural *state* of a processing system. These three fundamental quantities can be charaterized by variables, such as composition (or mole fraction), temperature, etc., and these variables are called *state variables*. A state variable arises naturally in the accumulation term of a dynamic balance equation. For example, in case of a distillation column, tray temperature is a state variable that arises when dynamic enthalpy balance is performed around a tray; composition is also a state variable in the dynamic component mass balance equation; and sometimes liquid holdup on a tray is also considered as a state variable that arises from a dynamic overall mass balance around a tray.

The conservation of mass is a fundamental concept of physics along with the conservation of energy and the conservation of momentum. As stated previously, the *conservation principle* provides the basic

blueprint for building the mathematical models of interest. The equations, which are derived by the application of the conservation principle on the fundamental quantities to relate the state variables with the other variables (including other state variables), are called *state equations*.

Let us consider the example of the liquid tank (Figure 1.1). The principle of conservation of mass implies

[Rate of mass accumulation] = [Rate of mass input] – [Rate of mass output] (1.8)

If the liquid density (^) is assumed constant, then

Rate of mass input = F_i^

Rate of mass output = F_o^

$$\text{Rate of mass accumulation} = \frac{dm}{dt} = \frac{d(V\rho)}{dt} = \rho\frac{dV}{dt}$$

where m represents the mass (= volume ≒ density).

Equation (1.8) finally gives

$$\frac{dV}{dt} = F_i - F_o \qquad (1.9)$$

Obviously, Equation (1.9) is the state equation and V is the state variable. In the above state equation, V is dependent on the input variable F_i since F_o is a function of V (we will see in Equation (1.10)). Time (t) is commonly regarded as an independent variable.

If we assume that the outflow from the tank F_o is proportional to the square root of the volume of liquid in the tank V as:

$$F_o \propto \sqrt{V} \qquad (1.10)$$

then we have

$$\begin{cases} y = F_o \\ x = V \\ g(x) = C'\sqrt{V} \end{cases} \qquad (1.11)$$

where, $F_o = C'\sqrt{V}$, and C⊣ represents the constant of proportionality. We can observe from Equation (1.11) that the state-output map $g(x)$ is represented by a nonlinear expression. Substituting $F_o = C'\sqrt{V}$ in Equation (1.9), one can easily see that the state variable V is dependent on the input variable F_i only.

1.4 TYPES OF MODELLING EQUATIONS

A mathematical process model usually consists of the following types of equations:

- Algebraic equations (AEs)
- Ordinary differential equations (ODEs)
- Partial differential equations (PDEs)

In different chapters of this textbook, the development of several complex chemical process models

will be discussed. At that time, we will observe that all the mathematical model structures include the ordinary differential equations along with the algebraic equations. Actually, we need to solve a set of algebraic equations for finding the numerical solution of a set of ordinary differential equations. Although none of our process models will include the partial differential equations, one of the leading methods for solving PDEs is based on converting a partial differential equation to a set of ordinary differential equations. Then we can use a suitable technique to solve the transformed ordinary differential equations. Several numerical methods for solving ODEs are explained in Chapter 2 of this book. However, in the subsequent discussion, we will not talk anymore about PDEs.

Now we will discuss the mathematical model of the liquid tank. Follow the schematic diagram of the tank as shown in Figure 1.1. The mass balance equation is already developed and is given in Equation (1.9). The model structure of the liquid tank consists of a balanced ordinary differential equation (Equation (1.9)) along with an algebraic equation as given below:

$$\begin{cases} \text{ODE:} & \dfrac{dV}{dt} = F_i - F_o \\ \text{AE:} & V = Ah \end{cases} \qquad (1.12)$$

Substitution of AE in the ODE yields the final form of the model structure as:

$$A\frac{dh}{dt} = F_i - F_o \qquad (1.13)$$

1.5 TYPES OF MATHEMATICAL MODELS

Mathematical models can be classified in several ways, some of which are described here.

Linear model vs. nonlinear model

At this moment, it is noteworthy to mention that most of the chemical processes are inherently nonlinear. It is also true that the nonlinear equations can be transformed to the approximately linear form of equations. This approximate linearization was commonly done in the past. At present, many advanced tools are available to deal with the nonlinear equations. However, the linearization of nonlinear equations is beyond the scope of this book. For your own interest, you can follow any process control textbook (e.g. Stephanopoulos, 1998).

Now, we will consider a process as shown in Figure 1.3 that has the linear model. The pressure at the bottom of the sample liquid tank can be represented by the following *linear* algebraic equation:

$$P = P_0 + h\hat{} \qquad (1.14)$$

where, P = pressure at depth h (kg/m^2) (depth is in m)

P_0 = pressure above surface (kg/m^2)

$\hat{}$ = liquid density (kg/m^3)

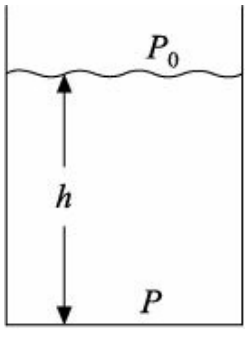

FIGURE 1.3 Example of a linear process.

Using Equation (1.14), one can easily calculate the pressure P at any liquid depth h in the vessel.

Now we wish to discuss a process that has the nonlinear modelling equation. Same liquid tank process as exampled above can provide nonlinear equation for the liquid streams that flow through the valves. In the discussion, we consider Figure 1.4.

The flow of liquid through the valve is given by the following *nonlinear* relationship:

$$F = C_V \sqrt{\frac{\Delta P}{G_F}} \qquad (1.15)$$

where, F = flow through valve (m^3/s)

C_V = valve coefficient $(m^3/(s)(kg/m^2)^{1/2})$

P = pressure drop across valve (kg/m^2)

G_F = specific gravity of liquid (dimensionless)

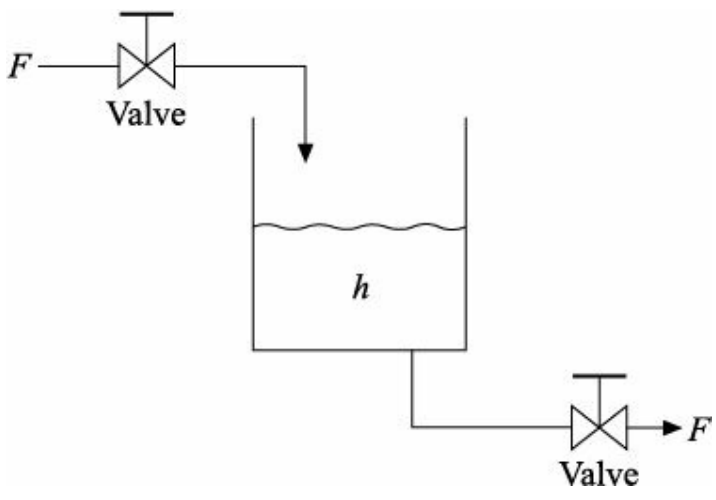

FIGURE 1.4 Flow of liquid streams through the valves.

Notice that in the above discussion of linear model vs. nonlinear model, we have considered two examples—one is modelled developing a linear equation and the other one is modelled by a nonlinear equation. But both the modelling equations have algebraic forms. We have to remember that a process model is said to be linear if the model comprises of either linear AE(s) or linear ODE(s) or both. Linear models never include any nonlinear equation. On the other hand, the nonlinear model structure consists the nonlinear AE(s) and/or nonlinear ODE(s). Also, the nonlinear models may include linear form of equations.

Static model vs. dynamic model

The steady state material and energy balance concepts are generally presented in any introductory textbook on chemical engineering principles. We have already covered this part at the early stage of your

bachelor degree course and the present study will extend the steady state concept to the dynamic state concept.

A *static model* is one, which is developed based on the steady state information, in which nothing changes with time. On the otherhand, in the *dynamic model*, the variables change with time. Static models are typically represented with algebraic equations, whereas dynamic models are described by differential equations. To explain the static model vs. dynamic model, we will consider again the liquid tank (Figure 1.1) that is mathematically represented by the following form:

$$A\frac{dh}{dt} = F_i - F_o \qquad \text{[from Equation (1.13)]}$$

Obviously, Equation (1.13) represents a dynamic model since practically all the variables, h (state variable), F_i (input variable) and F_O (output variable), vary with time.

At steady state, Equation (1.13) becomes:

$$A\frac{dh_s}{dt} = F_{is} - F_{os} \qquad (1.16)$$

where, h_S, F_{iS} and F_{OS} are the steady state values of h, F_i and F_O respectively. We can say that Equation (1.16) is the static model or steady state model of the example liquid tank. Further simplification of Equation (1.16) is also commonly done. Since, h_S is a constant quantity, it remains unchanged with time, i.e.,

$$\frac{dh_s}{dt} = 0 \qquad (1.17)$$

It implies,

$$F_{is} = F_{os} \qquad (1.18)$$

which is an algebraic equation. So, the static model, which comprises of a set of algebraic equations, is obtained from the dynamic modelling equations considering no change of any variable with time including the rate of accumulation terms, equal to zero. Notice that the static model is suitable to use only for steady state analysis. In the past, chemical processes were designed based solely on steady state analysis. However, in general, the static models do not provide satisfactory results in dynamic situations. Therefore, the dynamic model can be employed to predict the process behaviours adequately at static as well as dynamic conditions. Again, many processes, such as batch reactors, batch distillation columns, etc., are inherently dynamic. For these processes, it is essential to use the dynamic model only.

Lumped parameter model vs. distributed parameter model

There are processes in which the dependent variables may be considered as being uniform throughout the entire system, varying only with one independent variable (time, for example, but not space). These processes are called as *lumped parameter systems* because the dependency of all the observed variations have been lumped into one single independent variable.

A typical example of a lumped parameter system is a perfectly mixed (stirred) heating tank as shown in Figure 1.5, where the temperature is uniform throughout the tank. Now we will

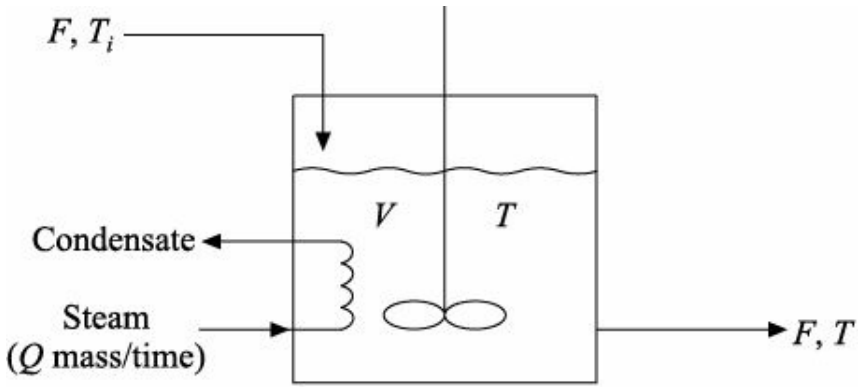

FIGURE 1.5 Stirred heating tank.

develop a mathematical model for the example of lumped system and that model will be referred to as *lumped parameter model*. This model is generally described by ordinary differential equations.

In order to develop the model, we consider the following assumptions:

- The content of the tank is perfectly mixed so that the liquid temperature in the tank and the temperature of the outflow liquid are the same (T).
- The liquid density ($\hat{}$), heat capacity (C_p) and latent heat of vaporization of steam ($\neg$) vary negligibly with temperature.
- No heat accumulation in the coils from the steam; the heat given up by the steam through condensation is completely received by the tank liquid.
- Heat losses from the process to the atmosphere are negligible.

The overall mass balance for the concerned stirred heating tank finally yields:

$$\frac{dV}{dt} = F - F = 0 \qquad (1.19)$$

As Equation (1.9) has been developed for the liquid tank (Figure 1.1), Equation (1.19) can also be derived using Equation (1.8) for the heating tank. Since the volumetric flow rates of inlet and outlet streams are equal (F), Equation (1.19) implies that the volume of liquid mixture in the tank (V) remained constant.

Now we will proceed to develop the energy balance equation. For the process example, the principle of conservation of energy (Equation (1.4)) provides:

$$\begin{bmatrix}\text{Rate of energy}\\ \text{accumulation}\end{bmatrix} = \begin{bmatrix}\text{Rate of energy}\\ \text{input}\end{bmatrix} - \begin{bmatrix}\text{Rate of energy}\\ \text{output}\end{bmatrix} \qquad (1.20)$$

Here

$$\text{Rate of energy accumulation} = \rho C_p \frac{d}{dt}[V(T - T_{\text{ref}})]$$

$$\text{Rate of energy input} = \begin{bmatrix}\text{Rate of energy input}\\ \text{through inlet stream}\end{bmatrix} + \begin{bmatrix}\text{Rate of energy input}\\ \text{through steam}\end{bmatrix}$$

$$= \hat{} FC_p(T_i - T_{\text{ref}}) + \neg Q$$

$$\text{Rate of energy output} = \hat{} FC_p(T - T_{\text{ref}})$$

In the present discussion, T_{ref} is the reference temperature, Q the steam flow rate and T_i the inlet liquid temperature. Substitution of all the above terms into Equation (1.20) yields:

$$\rho C_p \frac{d}{dt}[V(T - T_{\text{ref}})] = \rho F C_p (T_i - T_{\text{ref}}) + \lambda Q - \rho F C_p (T - T_{\text{ref}}) \qquad (1.21)$$

After simplification,

$$\frac{dT}{dt} = \frac{F}{V}(T_i - T) + \frac{\lambda}{\rho V C_p} Q \qquad (1.22)$$

where, V/F is the *residence time*. The above ordinary differential Equation (1.22) is a lumped parameter model that represents the variation of temperature T with a single independent variable, time t. Apart from the state variables, the other dependent variables may also vary with time.

When the variables of a process vary with both spatial position and time, such a process is referred to a s *distributed parameter system*. There are more than one independent variable, and the observed process variations are distributed among them. The mathematical model that represents a distributed system is called *distributed parameter model*. This model typically takes the form of partial differential equations so that the additional variation with spatial position be accounted for properly.

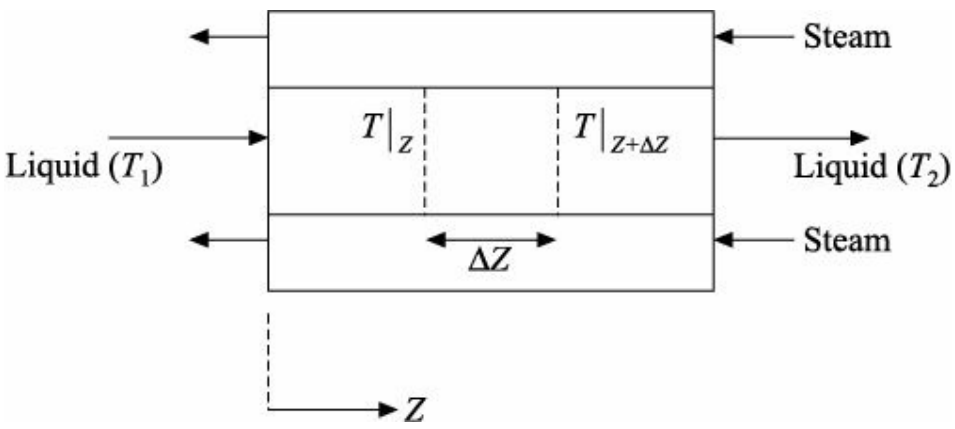

FIGURE 1.6 Shell-and-tube heat exchanger.

Consider a counterflow shell-and-tube heat exchanger as shown in Figure 1.6. Now we will develop the mathematical model of the tubular heat exchanger and observe that the model is a distributed parameter model because the temperature of the liquid stream can change along the length of the heat exchanger and also with time.

A liquid stream with temperature T_1, density ^ and heat capacity C_p is continuously fed to the tube side. The liquid flows through the tube of the heat exchanger with velocity v. The process stream is being heated by the steam that flows counter-currently around the tube. The outlet temperature of the liquid is T_2. In the present situation, the state variable of interest for the tubular heat exchanger is the temperature T of the heated liquid. Therefore, we need to develop the model, making balance in terms of energy. To perform the energy balance, consider the infinitesimally sized element, as shown in Figure 1.6, with length ≡ Z within which the changes are taking place during the infinitesimally small time period ≡ t. The following assumptions are used to build the heat exchanger model:

- The liquid within the element is assumed at a uniform temperature T, but the temperature at the boundaries of the element are $T|_Z$ and $T|_{Z+\Delta Z}$.

- The temperature does not change along the radius of the tube.
- Physical properties are assumed constant.
- The average velocity of the liquid (v) is assumed constant.
- The shell-side steam is assumed to be at a constant temperature T_{st}.
- The dynamics of the tube and shell walls are negligibly small. Any accumulation of energy within the element is due entirely to the liquid occupying the element, not in the heat exchanger wall.

Based on these assumptions, let us develop the energy balance equation for the heat exchanger. For the present case, Equation (1.20) becomes:

[Accumulation of energy] = [Input of energy] – [Output of energy] (1.23)

Here

Amount of energy accumulated during the time period Δt

$$= \rho C_p A \, \Delta Z \left[(T)\big|_{t+\Delta t} - (T)\big|_t \right]$$

Amount of energy input during the time period Δt

$$= \begin{bmatrix} \text{Amount of energy in at } Z \\ \text{with flowing liquid during } \Delta t \end{bmatrix} + \begin{bmatrix} \text{Amount of energy in from the steam to} \\ \text{the liquid through the wall during } \Delta t \end{bmatrix}$$

$$= \rho C_p v A (T)\big|_Z \, \Delta t + Q \, \Delta t (\pi D \, \Delta Z)$$

Amount of energy out at $Z + \Delta Z$ with flowing liquid during the time period Δt

$$\Delta t = \rho \, C_p \, v \, A (T)\big|_{Z+\Delta Z} \, \Delta t$$

In the above discussion, Q is the rate of heat transferred from the shell-side steam to the tube-side liquid per unit heat transfer area, D the external diameter of the tube, and A the cross-sectional area of the tube.

Inserting the above terms into Equation (1.23), we obtain

$$\rho \, C_p A \Delta Z \left[(T)\big|_{t+\Delta t} - (T)\big|_t \right]$$
$$= \rho C_p \, v \, A (T)\big|_Z \, \Delta t + Q \Delta t (\pi D \Delta Z) - \rho C_p v A (T)\big|_{Z+\Delta Z} \, \Delta t \qquad (1.24)$$

Rearranging, we have

$$\rho C_p \, A \, \Delta Z \left[(T)\big|_{t+\Delta t} - (T)\big|_t \right]$$
$$= \rho C_p v \, A (T)\big|_Z \, \Delta t - \rho C_p v \, A (T)\big|_{Z+\Delta Z} \, \Delta t + Q \Delta t (\pi D \, \Delta Z) \qquad (1.25)$$

Dividing both sides of the above equation by $\Delta t \, \Delta Z$ and then assuming $\Delta t \to 0$ and $\Delta Z \to 0$, we finally get

$$\frac{\partial T}{\partial t} + v \frac{\partial T}{\partial Z} = \frac{\pi \, DU}{\rho C_p A} (T_{st} - T) \qquad (1.26)$$

where

$$Q = U(T_{st} - T) \qquad (1.27)$$

Here, U is the overall heat transfer coefficient between the steam and the liquid. The partial differential Equation (1.26) represents a distributed parameter model because the liquid temperature T varies with two independent variables, time t and length Z.

Fundamental model vs. empirical model

The *fundamental* models, also called *first-principles* models, are based on physical–chemical relationships. Actually, these models are derived by applying the conservation principle and may also include transport phenomena, reaction kinetics, and thermodynamic (e.g. phase equilibrium) relationships. For example, Equation (1.22) represents a fundamental model for a stirred heating tank since this model is constructed based on the principle of conservation of energy.

The fundamental models offer several potential benefits. Since these models include detailed physical–chemical relationships, they can better represent the nonlinear behaviour and process dynamics; this allows the model to be used beyond the operating range in which the model was constructed. Another advantage of utilizing the first-principles approach is that the states are generally physical variables such as temperature or concentration that can be directly measured. However, the fundamental models are time consuming to develop and they often have a large number of equations with many parameters that need to be estimated. But in this book, we would prefer to develop the fundamental process models.

The *empirical* model is generally developed to use when the actual process is too complex and the underlying phenomena are not well understood or when the numerical solution of the fundamental model is quite difficult or when the empirical model provides satisfactory predictions of the process characteristics. Experimental plant data are used to develop a relationship between the process input and process output as an empirical model using a mathematical framework such as artificial neural network (ANN) (Rojas, 1996), least square method (LSM) (Jain, Iyengar, and Jain, 1995), etc. Although the time requirement to obtain this type of models is often significantly reduced, the empirical models generally can be used with confidence only for the operating range in which they are constructed. Since these models do not account for the underlying physics, practical insight into the problem may be lost as physical variables of the process, such as temperature, concentration, etc., are generally not the states of the empirical model (Parker, 1999).

Another type of model is the *mixed* or *hybrid* model. The mixed models are developed, as the name suggests, by combining the fundamental and empirical models, thus utilizing the benefits of both. As an example, the mixed modelling techniques have been used to model the polymerization reactors. The mass balance equations for the reactants are developed within the fundamental modelling approach, whereas the unknown rates of the reactions taking place are modelled within the empirical approach (Azevedo, Dahm, and Oliveira, 1997). For more information about the hybrid model, the reader may consult the work presented by Psichogios and Ungar (1992).

1.6 COMPUTER SIMULATION

The mathematical model structures that are developed in several chapters of this book for many nonlinear chemical processes comprise ordinary differential equations in addition to algebraic equations. In order to investigate the dynamic behaviour of a chemical process, we have to simulate the resulting modelling equations. By *simulate*, we mean that the transient response of the state variables can be found by numerically solving the differential–algebraic equations (DAEs). Notice that the nonlinear differential and/or algebraic equations cannot, in general, be solved analytically. Several numerical techniques for

solving the algebraic equations, as well as the ordinary differential equations are explained in Chapter 2. As noted previously, to solve a partial differential equation, first the PDE is converted to a set of ordinary differential equations. Then we can select an appropriate solution technique for solving those ordinary differential equations.

In order to perform the simulation of a process model, the following information is required to specify: initial values of the dependent variables including the values of the inputs as functions of time, and constant parameters. Today, computer simulation is used extensively to analyze the dynamics of chemical processes or aid in the design of controllers and study their effectiveness in controlling a process. The needs of computer simulation are discussed in detail in the following text.

1.7 USE OF SIMULATED PROCESS MODEL

A model is nothing more than a mathematical abstraction of an actual process. The equation or set of equations that consist the mathematical model do not represent exactly the real process. In other words, the process model cannot incorporate all of the features of the true process. Again, sometimes the simplified reduced-order models are preferred to develop for avoiding the complexity and computational load. However, if few details are included in the model, one runs the risk of missing relevant process information and the resultant plant model does not promote understanding. If too many details are included in the model, the model may become overly complicated and difficult to understand.

The process model can be used for the following purposes:

- *To improve understanding of the process:* The process behaviour (how the process reacts to various inputs) can be investigated by the computer simulation of a dynamic process model. This technique is useful before the plant is actually constructed or when it is not feasible to carry out the dynamic experiments in the plant since the experimentation is usually very costly.
- *To train plant operating personnel:* Assuming the process simulator as a real plant, many realistic situations are irritated. Plant operators are trained to familiarize with these problems and how to tackle the emergency situations. Again by interfacing the process simulator to standard control devices, a realistic environment can be created for operator training without the costs or exposure to dangerous conditions that might exist in an actual plant situation.
- *To design the process controller:* The dynamic process model may be employed to develop appropriate controller settings. This can be done either by direct analysis or by computer simulation of the dynamic model. For some processes, this approach is very useful since it is not always feasible to perform experiments that would lead to better controller settings. Moreover, a process model permits to design different possible control configurations and to select the best pairing of the controlled variable vs. the manipulated variable.
- *To design the advanced controller:* Modern control strategies, such as model predictive controller (e.g. dynamic matrix controller, model algorithmic controller, etc.) and model-based controller (e.g. globally linearizing controller, generic model controller, etc.), are designed using the mathematical process model. For these controllers, the design complexity and computational burden are greatly influenced by the order of accuracy of the process model.
- *To optimize process operating conditions:* Many times, we are unable to find the best operating policy for a plant which will minimize the operating cost or maximize the profit. This deficiency is due to the enormous complexity of the chemical plant. In such cases, the process model and appropriate economic information can be used to analyze the prevailing situation and to determine

the most profitable process conditions, as in supervisory control.

1.8 SUMMARY AND CONCLUSIONS

In this chapter, we have first studied about several important terms, such as model, process model, system, etc., and their details. These terms are frequently used in the course of *Process Modelling and Computer Simulation*. Then the general form of the conservation principle is outlined in terms of three fundamental quantities—mass, energy and momentum. Subsequently, different groups of variables including the state variable, and the state equation are presented in detail with a liquid tank example. Also, three different types of modelling equations are discussed in brief. Next, different types of mathematical models are explained by taking appropriate chemical process examples. We have also studied briefly about the computer simulation of the process model. Finally, the important uses of the simulated process model have been reported.

EXERCISES

1.1 Keenan and Keyes (1959) proposed the following boiling relation for water [pressure (P) in atm and temperature (T) in K]:

$$\log_{10}\left(\frac{218}{P}\right)=\frac{x}{499}\left(\frac{3.346+4.14\times10^{-2}x}{1+1.38\times10^{-2}x}\right) \qquad (1.28)$$

where $x = 647.27 - T$.

Is it a linear/nonlinear relation? Why? Verify the relation with the help of steam table data.

1.2 What is the key difference between the independent variable and the dependent variable?

1.3 Write the general forms of mass, energy and momentum balance equations based on the conservation law.

1.4 When is a system at steady state?

1.5 What is the difference between the state variable and the output variable of a process?

1.6 What do you mean by a differential–algebraic equation (DAE) system?

1.7 What is the main difference between the lumped parameter model and the distributed parameter model?

1.8 Is it possible to obtain the steady state model from the given dynamic model of a process? If yes, how?

1.9 It is well-known that the distillation column is a unit operation. Sometimes, the distillation column is also called as distillation system. How can you explain it?

1.10 Consider a perfectly insulated, well-stirred tank, as shown in Figure 1.7, where a hot liquid stream at 75°C is mixed with a cold liquid stream at 15°C. Is it a lumped parameter system or a distributed parameter system? Explain why.

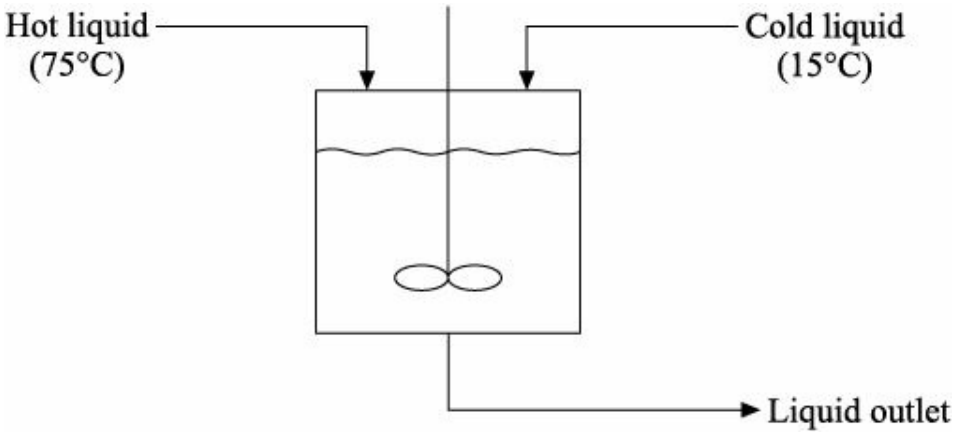

FIGURE 1.7 The mixing tank.

1.11 Consider a conical receiver shown in Figure 1.8. The inlet and outlet liquid volumetric flow rates are F_1 and F_2, respectively.

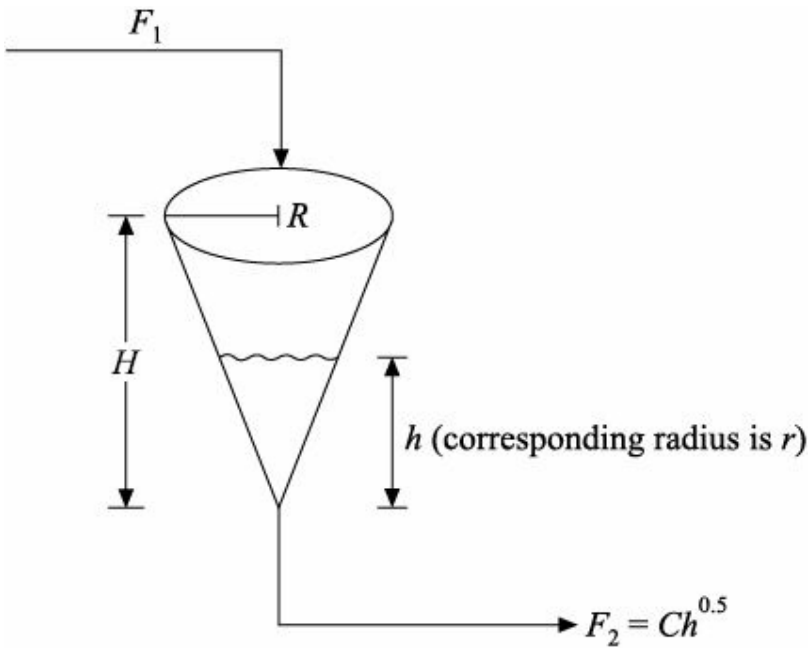

FIGURE 1.8 A conical tank.

(i) Develop the model equation with necessary assumption(s) with respect to the liquid height h.

(ii) What type of mathematical model is this?

Hint: Model: $\frac{dV}{dt} = F_1 - F_2$, where the volume $V = \frac{1}{3}\pi r^2 h = \frac{1}{3}\pi \frac{R^2}{H^2} h^3$, since $\frac{r}{h} = \frac{R}{H}$. Substitute V and F_2 expressions and get the final form.

1.12 Derive the dynamic mass balance equations for the following two simple cases (Figure 1.9 represents Case 1 and Figure 1.10 represents Case 2). Assume (i) a linear relationship between liquid level and flow rate through the outlet valve, and (ii) constant liquid density.

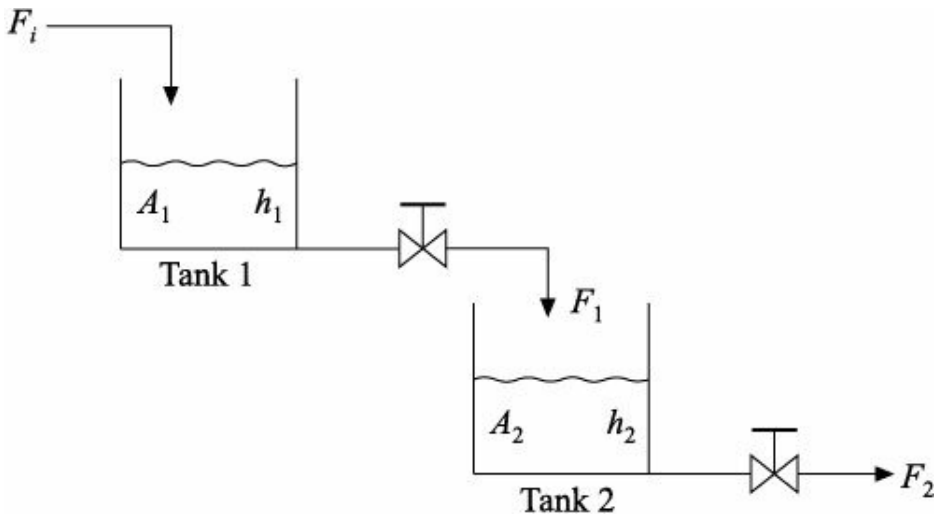

FIGURE 1.9 Two noninteracting tanks in series (Case 1).

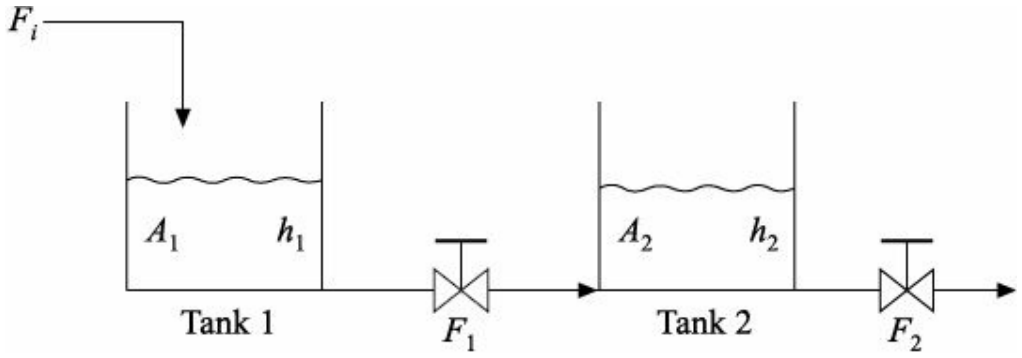

FIGURE 1.10 Two interacting tanks in series (Case 2).

1.13 Consider a liquid level system as shown in Figure 1.11. Derive the mathematical model. What type of model is it? Why?

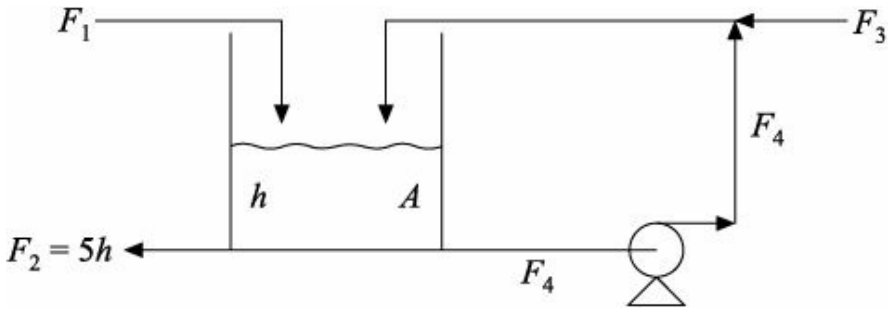

FIGURE 1.11 Liquid level system.

REFERENCES

Azevedo, de S.F., Dahm, B., and Oliveira, F.R. (1997). Hybrid modelling of biochemical processes: a comparison with the conventional approach, *Comput. Chem. Eng.*, S751–S756.

Jain, M.K., Iyengar, S.R.K., and Jain, R.K. (1995). *Numerical Methods for Scientific and Engineering Computation,* 3rd ed., New Age International, New Delhi.

Keenan, J.H., and Keyes, F.G. (1959). *Thermodynamic Properties of Steam*, 1st ed., John Wiley, New York.

Luyben, W.L. (1990). *Process Modeling, Simulation, and Control for Chemical Engineers*, 2nd ed., McGraw-Hill Book Company, Singapore.

Parker, R.S. (1999). *Model-based analysis and control for biosystems*, Ph.D thesis, Department of Chemical Engineering, University of Delaware.

Psichogios, D., and Ungar, L.H. (1992). A hybrid neural network—first principles approach to process modeling, *AIChE J*., 38, 1499–1511.

Rojas, R. (1996). *Neural Networks: A Systematic Introduction*, 1st ed., Springer-Verlag, Berlin.

Stephanopoulos, G. (1998). *Chemical Process Control: An Introduction to Theory and Practice*, 6th ed., Prentice-Hall of India, New Delhi.

2

Numerical Methods

2.1 INTRODUCTION

Mathematical modelling of most of the chemical processes leads to a system of complex model equations. In order to investigate the process characteristics, it is necessary to solve the modelling equations. The solution of a system of nonlinear equations is one of the challenging tasks and it is well-known that no completely satisfactory method exists for it. However, there are at present two ways of finding solutions, namely, analytical method and numerical method. An analytical method produces, when possible, exact solutions usually in the form of general mathematical expressions (like $e^{3\pi}/\sqrt{29}$). For example, analytical solutions of differential equations give expressions for functions, which are distinct from discrete numerical values. Numerical methods, on the other hand, produce approximate solutions in the form of discrete values or numbers.

Realistic mathematical process models in chemical engineering field usually consist of ordinary differential equations (ODEs) coupled with nonlinear algebraic equations. The ODEs are generally derived making mass and energy balance, and the supporting algebraic equations usually correlate the parameters with the process variables. Let us take an example of a distillation column. An ODE is formed if a mass balance is made around a tray, whereas an algebraic equation correlates the vapour–liquid equilibrium coefficient with the phase composition, temperature and pressure.

The simplest of the equations mentioned above is a linear algebraic equation. The exact solution of this linear equation is immediate and consists of a single value or point. Algebraic quadratic equations can also be solved exactly, if solutions exist, leading to two solutions. In general, finding exact solutions to higher-order algebraic equations is not a feasible task and numerical methods must be employed to find approximate solutions. For a system having two or more coupled nonlinear algebraic equations, numerical methods are routinely employed to find approximate solutions.

Ordinary differential equations are in general much more difficult to solve exactly. Exact analytical solutions are available only for linear differential equations. For the case of nonlinear ODEs, explicit exact solutions are quite impossible and numerical methods are employed. Recall that for solving a partial differential equation (PDE), it is common to convert the PDE to a set of ordinary differential equations and the standard techniques are followed for solving those transformed ODEs.

In this book, the mathematical model of several chemical processes has been developed. The dynamic simulations of those models are also incorporated for detailed analysis of the process. Whenever we proceed to develop the dynamic process simulator after the mathematical model development, we must have good knowledge of the numerical methods. Now we will discuss some common numerical techniques that will be employed to solve the nonlinear differential and algebraic equations.

2.2 ITERATIVE CONVERGENCE METHODS

2.2.1 Bisection Method (Interval Halving)

Suppose that we would like to solve a nonlinear algebraic equation of the form:

$$y = f(x) = 0 \qquad (2.1)$$

We can use the following steps according to the Bisection method (Finlayson, 1980; Riggs, 1988).

Step 1: Find two guess values of x (say x_1 and x_2 at the first iteration), so that one where $f(x)$ is negative (< 0) and another where $f(x)$ is positive (> 0).

Step 2: Find the midpoint and then evaluate $f(x)$ at that point. (For example, at the first iteration, the midpoint is x_3 [$= (x_1 + x_2)/2$] and naturally, the function to be evaluated is $f(x_3)$).

Step 3: Among the two guess values of x, one should be replaced by the value of x at midpoint. Replace the bracket limit that has the same sign as the function value at the midpoint, with the midpoint value. [If the value of $f(x_1)$ has the same sign with the value of $f(x_3)$, then x_1 will be replaced by x_3, otherwise x_2 will be replaced.]

Step 4: Check for convergence. If not converged, go back to Step 2.

This *iterative* process continues until the size of the interval shrinks below a convergence tolerance level. If the interval shrinks below a tolerance level, we have found an approximate value of the root. The Bisection method is also known as *interval halving* method since it can halve the size of the interval in each iteration. Figure 2.1 describes this numerical technique.

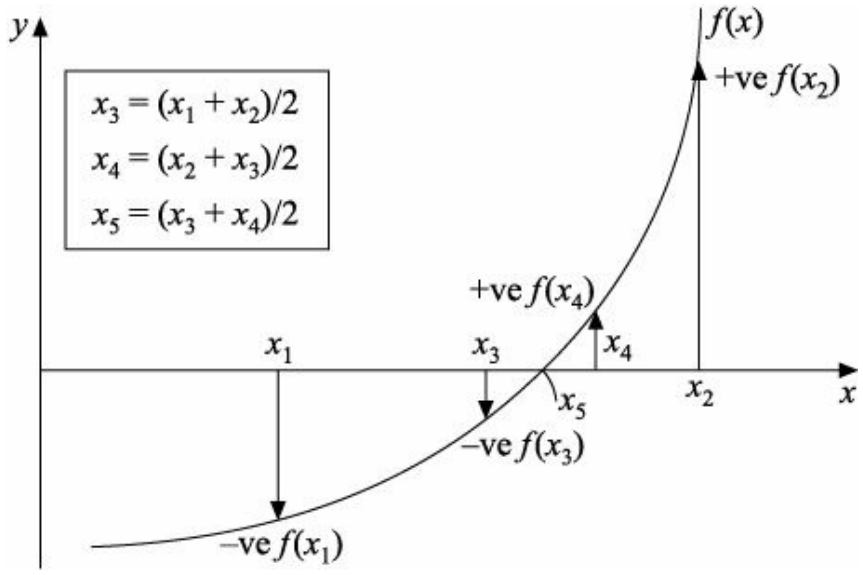

FIGURE 2.1 Illustration of the Bisection method.

The Bisection method actually locates a root by repeatedly narrowing the distance between the two guesses. When an interval contains a root, this simple numerical method never fails. However, the main drawback of the Bisection technique is the slow convergence rate. Also, it is not easily extended to multivariable systems.

2.2.2 Secant Method

Because of the slow convergence provided by the Bisection approach, the Secant method (Finlayson, 1980; Riggs, 1988; Burden and Faires, 1985) receives the attention as an alternative iterative technique. Although this approach is similar to the Bisection method, instead of using the average of the interval endpoints to select the next root estimate, it is required to construct a secant line and find its x-intercept as the next root estimate.

Suppose we are looking for a root of Equation (2.1). Let x_{k-1} and x_k are two approximations to the root. Now construct a straight line through the points (x_{k-1}, f_{k-1}) and (x_k, f_k), where $f_{k-1} = f(x_{k-1})$ and $f_k = f(x_k)$. Note that this line is a *secant* (or *chord*) of the function f.

The slope of the straight line is:

$$m = \frac{f_k - f_{k-1}}{x_k - x_{k-1}} \qquad (2.2)$$

Now take the point of intersection of the straight line with the x-axis as the next approximation to the root. To compute the next approximation x_{k+1}, we need to form an equation of straight line as:

$$f_{k+1} - f_k = m(x_{k+1} - x_k) = \frac{f_k - f_{k-1}}{x_k - x_{k-1}}(x_{k+1} - x_k) \qquad (2.3)$$

For finding its x-intercept, let $y = f_{k+1} = 0$. Simplifying, one obtains

$$x_{k+1} = x_k - \frac{x_k - x_{k-1}}{f_k - f_{k-1}} f_k \qquad (2.4)$$

Further simplifying, we get

$$x_{k+1} = \frac{x_{k-1} f_k - x_k f_{k-1}}{f_k - f_{k-1}} \qquad (2.5)$$

This is called the *Secant* or the *Chord* method and this approach involves iterating on this process until the guess is sufficiently close to the root. This numerical algorithm is illustrated graphically in Figure 2.2.

If the approximations are such that $f_k f_{k-1} < 0$, then the approach, as represented by Equation (2.4) or Equation (2.5), is known as the *False Position* or *Regula Falsi* method. Similar to the Secant method, the False Position algorithm also uses a straight line to approximate the function in the local region of interest. This technique is illustrated in

Figure 2.3. Note that the main difference between these two convergence techniques is that the Secant method retains the most recent two estimates, while the False Position method keeps the most recent estimate and the next recent one which has an opposite sign in the function value. However, this approach may provide a lower and uncertain convergence rate compared to the

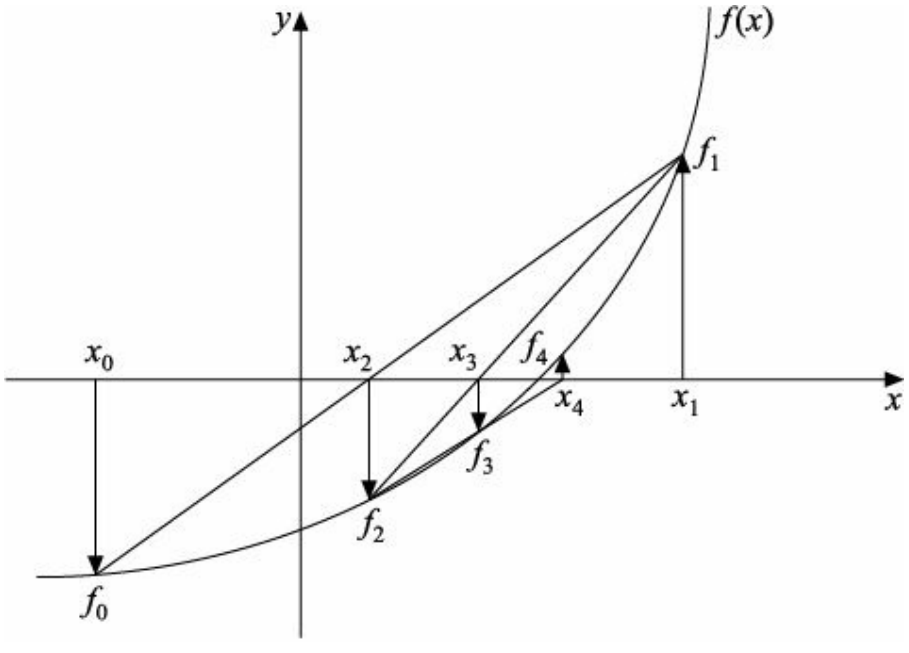

FIGURE 2.2 Illustration of the Secant method.

Secant method because the False Position approach sometimes retains an older reference point to

maintain an opposite sign bracket around the root.

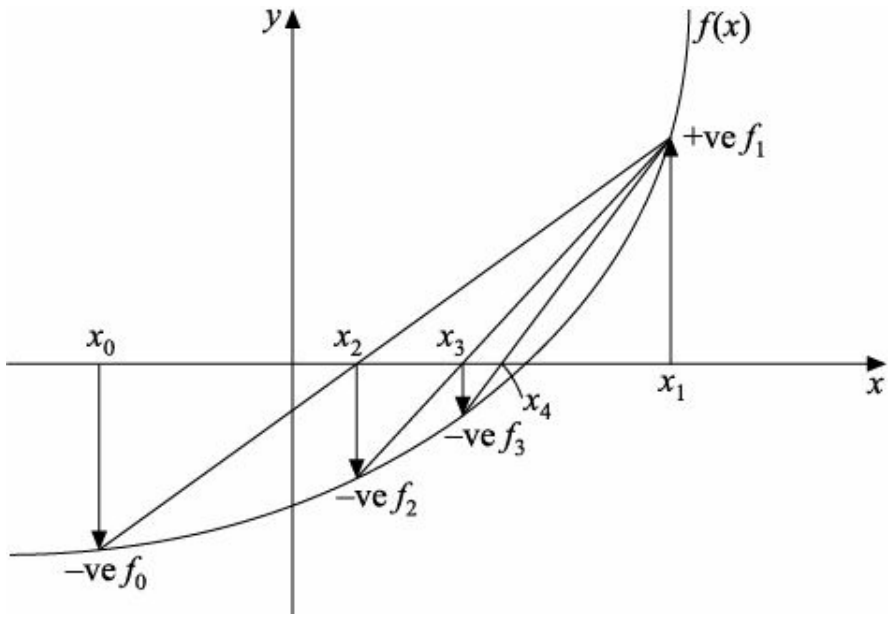

FIGURE 2.3 Illustration of the False Position method.

2.2.3 Newton–Raphson Method

The Newton–Raphson method (Finlayson, 1980; Goldstine, 1977) is the most common and popular method for solving nonlinear algebraic equations. This iterative convergence algorithm, also known as Newton's method, can be derived from Taylor series expansion of $f(x)$:

$$f(x+\Delta x)=f(x)+\frac{\partial f(x)}{\partial x}\frac{\Delta x}{1!}+\frac{\partial^2 f(x)}{\partial x^2}\frac{(\Delta x)^2}{2!}+\frac{\partial^3 f(x)}{\partial x^3}\frac{(\Delta x)^3}{3!}+\cdots=0 \qquad (2.6)$$

If we neglect all terms of order two and higher, Equation (2.6) yields:

$$f(x)+\frac{\partial f(x)}{\partial x}\Delta x=0 \qquad (2.7)$$

That means,

$$\Delta x=\frac{-f(x)}{f'(x)} \qquad (2.8)$$

where $f'(x)=\dfrac{\partial f(x)}{\partial x}$

We need to calculate the guess for x at iteration $k+1$ as a function of the value at iteration k by defining:

$$\Delta x_{k+1}=x_{k+1}-x_k \qquad (2.9)$$

As assumed $f_k=f(x_k)$, Equation (2.8) gives:

$$\Delta x_{k+1}=\frac{-f_k}{f'_k} \qquad (2.10)$$

From Equations (2.9) and (2.10), we obtain

$$x_{k+1} = x_k - \frac{f_k}{f_k'} \qquad (2.11)$$

The above equation represents the *Newton–Raphson* convergence method for a single-variable problem. Equation (2.11) may also be derived from the formula of the Secant method [Equation (2.4)] using the following finite difference approximation

$$f_k' \approx \frac{f_k - f_{k-1}}{x_k - x_{k-1}} \qquad (2.12)$$

The graphical representation of the Newton's method is shown in Figure 2.4.

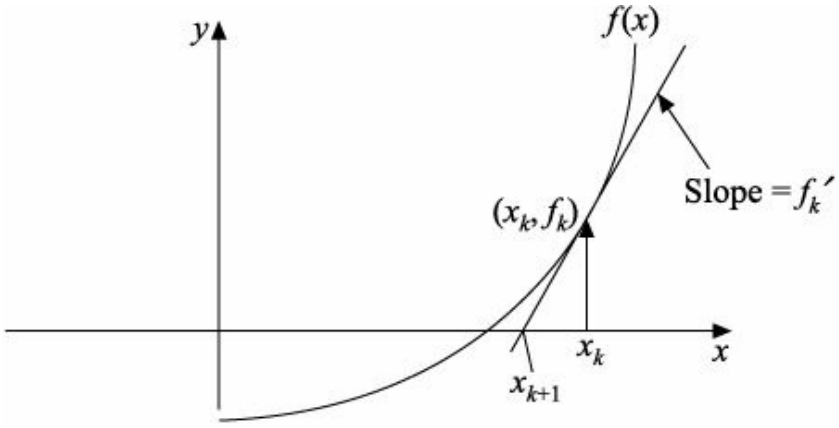

FIGURE 2.4 Illustration of the Newton–Raphson method.

The extension of the Newton–Raphson algorithm to multivariable systems is fairly simple and straightforward. Let us consider a multivariable system represented by:

$$\mathbf{f(x)} = 0 \qquad (2.13)$$

This equation consists of a set of n equations with n variables ($x_1, x_2, ..., x_n$) as:

$$\begin{bmatrix} f_1(x_1, x_2, ..., x_n) \\ f_2(x_1, x_2, ..., x_n) \\ \vdots \\ f_n(x_1, x_2, ..., x_n) \end{bmatrix} = \begin{bmatrix} 0 \\ 0 \\ \vdots \\ 0 \end{bmatrix} \qquad (2.14)$$

The Taylor series gives for each f_i after neglecting the second and higher-order derivative terms as:

$$f_i(\mathbf{x} + \Delta\mathbf{x}) = f_i(\mathbf{x}) + \sum_{j=1}^{n} \frac{\partial f_i(\mathbf{x})}{\partial x_j} \Delta x_j = 0 \qquad (2.15)$$

The above equation yields the following matrix form:

$$\mathbf{f(x)} + \mathbf{J}^{\boxminus}\ \mathbf{x} = 0 \qquad (2.16)$$

where the *Jacobian* matrix

$$\mathbf{J} = \begin{bmatrix} \frac{\partial f_1}{\partial x_1} & \frac{\partial f_1}{\partial x_2} & \cdots & \frac{\partial f_1}{\partial x_n} \\ \vdots & \vdots & \cdots & \vdots \\ \frac{\partial f_n}{\partial x_1} & \frac{\partial f_n}{\partial x_2} & \cdots & \frac{\partial f_n}{\partial x_n} \end{bmatrix}$$

From Equation (2.16),

$$\equiv \mathbf{x} = -\mathbf{J}^{-1}\mathbf{f}(\mathbf{x}) \qquad (2.17)$$

To obtain the guess for x at iteration $k + 1$, Equation (2.17) gives:

$$\mathbf{x}_{k+1} - \mathbf{x}_k = -\mathbf{J}_k^{-1}\,\mathbf{f}(\mathbf{x}_k) \qquad (2.18)$$

That is,

$$\mathbf{x}_{k+1} = \mathbf{x}_k - \mathbf{J}_k^{-1}\,\mathbf{f}_k \qquad (2.19)$$

Remember that $\mathbf{x}_k$ is a vector of values at iteration k. For a single variable system, obviously Equation (2.19) yields:

$$x_{k+1} = x_k - \frac{f_k}{f_k'} \qquad \text{[from Equation (2.11)]}$$

The Newton–Raphson method is very efficient iterative convergence technique compared to many other simple methods. However, at each step, this method requires the calculation of the derivative of a function at the reference point, which is not always easy. It also may sometimes lead to stability problems particularly if the function is strongly nonlinear and if the initial guess is very poor.

2.2.4 Muller Method

This is an iterative convergence method (Jain, Iyengar and Jain, 1995) based on second-degree (quadratic) equation. Let us consider a polynomial of degree 2:

$$p(x) = a_0x^2 + a_1x + a_2 = 0 \qquad (2.20)$$

where $a_0(\neq 0)$, a_1 and a_2 are three arbitrary parameters. In this convergence approach, three values of the unknown x variable are guessed. Let, x_{k-2}, x_{k-1} and x_k are three approximations to the actual root r of $f(x) = 0$. To obtain a_0, a_1 and a_2, we may use the following conditions:

$$p_{k-2} = f_{k-2} = a_0x_{k-2}^2 + a_1x_{k-2} + a_2 \qquad (2.21a)$$

$$p_{k-1} = f_{k-1} = a_0x_{k-1}^2 + a_1x_{k-1} + a_2 \qquad (2.21b)$$

$$p_k = f_k = a_0x_k^2 + a_1x_k + a_2 \qquad (2.21c)$$

and then substituting a_0, a_1 and a_2 in Equation (2.20), finally we obtain

$$p(x)=\frac{(x-x_{k-1})(x-x_k)}{(x_{k-2}-x_{k-1})(x_{k-2}-x_k)}f_{k-2}+\frac{(x-x_{k-2})(x-x_k)}{(x_{k-1}-x_{k-2})(x_{k-1}-x_k)}f_{k-1}$$
$$+\frac{(x-x_{k-2})(x-x_{k-1})}{(x_k-x_{k-2})(x_k-x_{k-1})}f_k=0 \qquad (2.22)$$

In Equations (2.21a, 2.21b and 2.21c), $p_{k-2}=p(x_{k-2})$, $p_{k-1}=p(x_{k-1})$ and $p_k=p(x_k)$. Equation (2.22) can be converted to:

$$\frac{g(g+g_k)}{g_{k-1}(g_{k-1}+g_k)}f_{k-2}-\frac{g(g+g_k+g_{k-1})}{g_kg_{k-1}}f_{k-1}+\frac{(g+g_k)(g+g_k+g_{k-1})}{g_k(g_k+g_{k-1})}f_k=0 \qquad (2.23)$$

where $g=x-x_k$, $g_k=x_k-x_{k-1}$ and $g_{k-1}=x_{k-1}-x_{k-2}$. Further assuming $\neg=g/g_k$, $\neg_k=g_k/g_{k-1}$ and $\in_k=1+\neg_k$, Equation (2.23) gets the form:

$$\lambda^2c_k+\lambda h_k+\delta_kf_k=0 \qquad (2.24)$$

where
$$h_k=\lambda_k^2f_{k-2}-\delta_k^2f_{k-1}+(\lambda_k+\delta_k)f_k$$
$$c_k=\lambda_k(\lambda_kf_{k-2}-\delta_kf_{k-1}+f_k)$$

Dividing Equation (2.24) by $\neg^2$, we obtain

$$\frac{\delta_kf_k}{\lambda^2}+\frac{h_k}{\lambda}+c_k=0 \qquad (2.25)$$

Solving this quadratic equation for $1/\neg$, we get

$$\lambda=\frac{2\delta_kf_k}{-h_k\pm\sqrt{(h_k^2-4\delta_kf_kc_k)}}=\lambda_{k+1} \qquad (2.26)$$

The selection of the sign in the denominator in Equation (2.26) should be such that $\neg_{k+1}$ has the smallest absolute value.

Recall the assumption, $\neg=g/g_k$. It implies,

$$\lambda_{k+1}=\frac{x-x_k}{x_k-x_{k-1}} \qquad (2.27)$$

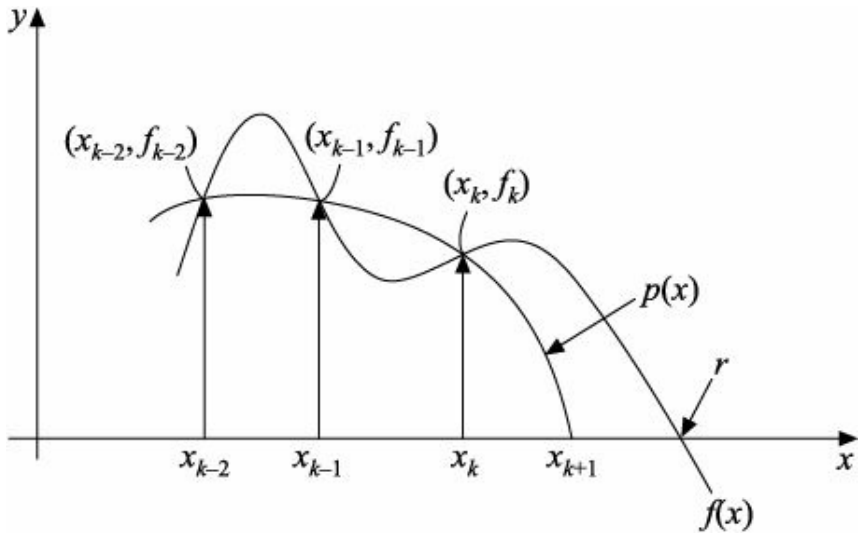

FIGURE 2.5 Illustration of the Muller method.

Rearranging,

$$x = x_k + \lambda_{k+1}(x_k - x_{k-1}) \qquad (2.28)$$

Replacing x by x_{k+1},

$$x_{k+1} = x_k + \lambda_{k+1}(x_k - x_{k-1}) \qquad (2.29)$$

This equation represents the *Muller* method. It is illustrated in Figure 2.5. In this convergence approach, the next approximation x_{k+1} is obtained as the zero of the second-degree curve passing through the points (x_{k-2}, f_{k-2}), (x_{k-1}, f_{k-1}) and (x_k, f_k).

To obtain an approximate root of a nonlinear equation, the Muller method uses a polynomial of degree two (quadratic equation), whereas the Newton–Raphson method uses a straight line (linear equation). Faster rate of convergence is achieved by the Muller method compared to the Newton–Raphson method when the functions are highly curvilinear.

2.3 NUMERICAL INTEGRATION OF ORDINARY DIFFERENTIAL EQUATIONS

Now we will study several numerical methods that are commonly used for solving first-order ODEs. Any higher-order ordinary differential equation can easily be transformed to a set of first-order ODEs. To make it clear, let us consider a system represented by a second-order ODE:

$$p(x)\frac{d^2y}{dx^2} + q(x)\frac{dy}{dx} = r(x) \qquad (2.30)$$

If we assume $y(x) = y_1(x)$ and $\frac{dy_1}{dx} = y_2(x)$, then the above system becomes:

$$\begin{cases} \dfrac{dy_1}{dx} = y_2(x) \\ \dfrac{dy_2}{dx} = \dfrac{r(x) - q(x)y_2(x)}{p(x)} \end{cases} \qquad (2.31)$$

Similarly, an nth-order ODE can be reduced to:

$$\frac{dy_k(x)}{dx} = f_k(x, y_1, y_2, ..., y_n), \quad \text{where } k = 1, 2, ..., n. \qquad (2.32)$$

In the subsequent sections, different types of commonly used numerical integration algorithms will be discussed in detail.

2.3.1 Euler Methods

Consider an ODE with the form

$$\frac{dx}{dt} = f(x, t) \qquad (2.33)$$

where $f(x, t)$ is, in general, a nonlinear function and the initial condition for x is as: $x(0) = x_0$ at time $t = 0$.

Equation (2.33) can be solved employing the Euler method by two different ways, namely explicit approach and implicit approach.

Explicit Euler approach

A forward difference approximation of Equation (2.33) yields:

$$\frac{dx}{dt} \approx \frac{x_{k+1} - x_k}{t_{k+1} - t_k} \qquad (2.34)$$

It implies,

$$\frac{x_{k+1} - x_k}{\Delta t} = f(x_k, t_k) \qquad (2.35)$$

where $\Delta t = t_{k+1} - t_k$. The time increment Δt is known as the *step size* or *integration interval*. We can rearrange Equation (2.35) as:

$$x_{k+1} = x_k + \Delta t\, f(x_k, t_k) \qquad (2.36)$$

That is,

$$x_{k+1} = x_k + \Delta t \left(\frac{dx}{dt}\right)_{(x_k, t_k)} \qquad (2.37)$$

Equation (2.36) or (2.37) represents the *Explicit Euler* method. This integration approach is graphically illustrated in Figure 2.6. From the figure, it is clear that if sufficiently small integration step size Δt is taken, the estimate of x_{k+1} will be very close to the correct value.

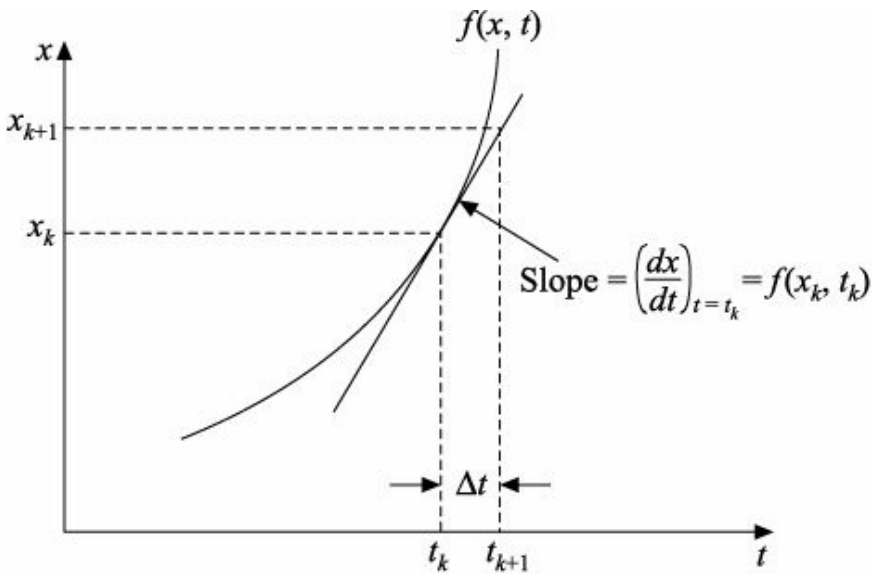

FIGURE 2.6 Illustration of the Explicit Euler method.

Now we wish to solve a system having two simultaneously coupled ODEs:

$$\frac{dx_1}{dt} = f_1(x_1, x_2, t) \qquad (2.38)$$

$$\frac{dx_2}{dt} = f_2(x_1, x_2, t) \qquad (2.39)$$

Using the Explicit Euler algorithm,

$$x_{1,k+1} = x_{1k} + \Delta t \left(\frac{dx_1}{dt} \right)_{(x_{1k}, x_{2k}, t_k)} \qquad (2.40)$$

$$x_{2,k+1} = x_{2k} + \Delta t \left(\frac{dx_2}{dt} \right)_{(x_{1k}, x_{2k}, t_k)} \qquad (2.41)$$

The Euler integration approach is extremely simple to implement for solving even highly nonlinear multivariable complex systems having a large number of ODEs.

Implicit Euler approach

This approach uses a backward difference approximation and accordingly, Equation (2.33) gives:

$$\frac{x_{k+1} - x_k}{\Delta t} = f(x_{k+1}, t_{k+1}) \qquad (2.42)$$

Rearranging, we obtain

$$x_{k+1} = x_k + \Delta t\, f(x_{k+1}, t_{k+1}) \qquad (2.43)$$

That is,

$$x_{k+1} = x_k + \Delta t \left(\frac{dx}{dt} \right)_{(x_{k+1}, t_{k+1})} \qquad (2.44)$$

Equation (2.43) or (2.44) represents the *Implicit Euler* method. This method in Equation (2.44) indicates that we need to evaluate the derivative at the next step in time t_{k+1}. How is it possible without knowing x_{k+1}? But, it is very simple for a linear system. Let us take an example considering a simple linear ODE:

$$\frac{dx}{dt} = x + 1 \qquad (2.45)$$

From Equation (2.44), we may write

$$x_{k+1} = x_k + \Delta t\,(x_{k+1} + 1) \qquad (2.46)$$

Simplifying, we get

$$x_{k+1} = \frac{x_k + \Delta t}{1 - \Delta t} \qquad (2.47)$$

However, for a nonlinear system, the Implicit Euler method is not performed so straightforwardly. To explain it, consider a nonlinear ODE:

$$\frac{dx}{dt} = x^{17} + e^{3x} \qquad (2.48)$$

Equation (2.44) gives:

$$x_{k+1} = x_k + \Delta t[x_{k+1}^{17} + e^{3x_{k+1}}] \qquad (2.49)$$

In order to solve this equation for x_{k+1}, a nonlinear algebraic solution technique, such as the Newton–Raphson convergence method, can be used. In case of nonlinear ODE, obviously the Implicit Euler technique allows a much larger time for performing the iterations in every time step. However, it offers

some advantages. The implicit approach is stable for almost any value of Δt and will not oscillate. The Explicit Euler method, on the other hand, may have instability problem with oscillating outputs for a large step size. One well-known and efficient implicit approach is the Gear's method (Gear, 1971).

2.3.2 Heun Method

We will now discuss a better numerical integration method than Euler's for solving the same kind of initial value problem. In developing the Heun technique, the Euler method is used and for this reason, the Heun algorithm is sometimes called the *Improved Euler method*.

Equation (2.33) can be rewritten as:

$$\frac{dx(t)}{dt} = x'(t) = f[x(t), t] \qquad (2.50)$$

Integrating, we get

$$\int_{t_k}^{t_{k+1}} f[x(t), t]\, dt = \int_{t_k}^{t_{k+1}} x'(t)\, dt = x(t_{k+1}) - x(t_k) = x_{k+1} - x_k \qquad (2.51)$$

Rearranging, we have

$$x_{k+1} = x_k + \int_{t_k}^{t_{k+1}} f[x(t), t]\, dt \qquad (2.52)$$

To approximate the definite integral term in the above equation, the trapezoidal rule is used with step size $\Delta t = t_{k+1} - t_k$. Accordingly, we have

$$x_{k+1} \approx x_k + \frac{\Delta t}{2}[f(x_k, t_k) + f(x_{k+1}, t_{k+1})] \qquad (2.53)$$

Applying the explicit Euler equation (2.36), we get

$$x_{k+1} = x_k + \frac{\Delta t}{2}\{f(x_k, t_k) + f[x_k + \Delta t\, f(x_k, t_k), t_{k+1}]\} \qquad (2.54)$$

This equation can be presented by the following form:

$$\begin{cases} P_{k+1} = x_k + \Delta t\, f(x_k, t_k), & t_{k+1} = t_k + \Delta t \\ x_{k+1} = x_k + \dfrac{\Delta t}{2}[f(x_k, t_k) + f(P_{k+1}, t_{k+1})] \end{cases} \qquad (2.55)$$

This is the Heun algorithm, in which, the first equation represents the explicit Euler approach. The Euler method is described as a predictor algorithm, whereas the Heun method is described as a predictor-corrector algorithm.

2.3.3 Taylor Method

The Taylor method is one of the oldest numerical methods for solving ordinary differential equations. It was already used by Euler and Newton. The formulation is quite simple. Let us start with Equation (2.50):

$$\frac{dx(t)}{dt} = x'(t) = f[x(t), t]$$

Now, the value of the solution at t_{k+1} (that is, x_{k+1}) is approximated from the nth degree Taylor series of $x(t)$ at $t = t_{k+1}$. Denoting $\Delta t = t_{k+1} - t_k$, we have

$$x(t_{k+1}) = x_{k+1} = x_k + \frac{d_1 \Delta t}{1!} + \frac{d_2 \Delta t^2}{2!} + \frac{d_3 \Delta t^3}{3!} + \cdots + \frac{d_n \Delta t^n}{n!} \qquad (2.56)$$

where $d_j = x^{(j)}(t_k) = x_k^{(j)}$ for $j = 1, 2, 3, \ldots, n$. It implies $d_1 = x'_k$, $d_2 = x''_k$, etc.

The Taylor algorithm can be devised to have any specified degree of accuracy. The degree of accuracy can be improved by increasing the order (n) of the Taylor series. The Taylor method is the standard to which we test the accuracy of any other numerical integration algorithm.

2.3.4 Runge–Kutta (RK) Methods

The Runge–Kutta method (Lapidus and Seinfeld, 1971; Davis, 1984) is commonly chosen as a better explicit integration algorithm than the standard Explicit Euler method mainly for two reasons. Firstly, the truncation error per step associated with the Euler method is larger than that associated with the Runge–Kutta approach. Secondly, the Explicit Euler technique is prone to numerical instabilities. Now we will discuss different Runge–Kutta approaches as the tools for solving ODEs. Note that the Euler integration technique is sometimes called the *first-order* Runge–Kutta method.

Second-order Runge–Kutta (RK2) approach

The second-order Runge–Kutta method is also known as the *Midpoint Euler* method. This integration approach is an extension of the first-order Euler scheme. In this approach, first the Euler technique is employed to predict x at the midpoint of the integration interval (step size = $\Delta t/2$). If k_1 be the slope (dx/dt) at the initial point ($\Delta t = 0$), then from Equation (2.33):

$$k_1 = f(x_k, t_k) \qquad (2.57)$$

Consequently, x at the midpoint will be $x_k + (\Delta t/2)k_1$. The next step involved in this approach is the evaluation of the derivative (slope k_2) at the midpoint, which implies,

$$k_2 = f\left(x_k + \frac{\Delta t}{2} k_1, t_k + \frac{\Delta t}{2}\right) \qquad (2.58)$$

Finally, the value of x at the end of the step (step size = Δt) is estimated as:

$$x_{k+1} = x_k + \Delta t k_2 \qquad (2.59)$$

The second-order Runge–Kutta algorithm consists of Equations (2.57), (2.58) and (2.59). This integration technique provides better accuracy than the Explicit Euler method but the Euler approach runs almost two times faster.

Fourth-order Runge–Kutta (RK4) approach

The concepts involved in the fourth-order Runge–Kutta approach (Lapidus and Seinfeld, 1971) for estimating x_{k+1} are outlined below. First, the initial slope k_1 is used to generate a first estimate for x at

the midpoint [i.e., $x_k + (\Delta t/2)k_1$]. Secondly, the first estimate of x is used to find the slope k_2 at the midpoint. Subsequently, a corrected midpoint slope k_3 is evaluated by using k_2. Slope k_4 is then found at the end of integration interval. Finally, a weighted average of these slopes is used to obtain the final estimate of x, which is x_{k+1}. The complete fourth-order Runge–Kutta algorithm consists of the following equations:

$$k_1 = f(x_k, t_k) \qquad \text{[from Equation (2.57)]}$$

$$k_2 = f\left(x_k + \frac{\Delta t}{2}k_1, t_k + \frac{\Delta t}{2}\right) \qquad \text{[from Equation (2.58)]}$$

$$k_3 = f\left(x_k + \frac{\Delta t}{2}k_2, t_k + \frac{\Delta t}{2}\right) \qquad (2.60)$$

$$k_4 = f(x_k + \Delta t k_3, t_k + \Delta t) \qquad (2.61)$$

$$x_{k+1} = x_k + \Delta t\left[\frac{k_1}{6} + \frac{k_2}{3} + \frac{k_3}{3} + \frac{k_4}{6}\right] \qquad (2.62)$$

Comparing the second-order and fourth-order Runge–Kutta integration approaches, it is easy to observe that the complexity as well as computational time increases with the increase of the order. To obtain greater accuracy in estimation, the fourth-order Runge–Kutta method is preferred over the Euler and the second-order Runge–Kutta approaches. The fourth-order Runge–Kutta method requires four derivative evaluations compared to only one for the Euler per ODE at every time step. Therefore, the Euler algorithm is almost four times faster than this fourth-order scheme. Notice that it is straightforward to extend the Runge–Kutta methods for multivariable systems.

Runge–Kutta–Fehlberg (RKF45) approach

Another efficient and popular technique for solving ODEs is the Runge–Kutta–Fehlberg 4th-5th order (RKF45) method (Fehlberg, 1964; 1969; Gupta, 1995). This ODE integrator can exert some adaptive control over its own performance, making frequent changes in its step size (Δt). At each step, the RKF45 technique produces two estimates of a state variable (one denoted by x_{k+1} and another by $\bar{x}_{k+1}$). These two estimates are involved in the determination of the proper step size. Here, a numerical estimate of the error, $(\bar{x}_{k+1} - x_{k+1})/\Delta t_k$, is required to be computed at each time step. If the estimated error is less than the tolerance level (ε_0), the step size, Δt_{k+1}, to be used in the next step to generate x_{k+2} is increased to speed up the computations. Again, if the error exceeds the desired value, a lower value of Δt (= $\Delta t_{k,\text{new}}$) is used and the calculation is repeated. If the value of error is nearly equal to ε_0, the two estimates are in close agreement and the value of step size is accepted without any correction.

In order to solve Equation (2.33), each Runge–Kutta–Fehlberg step requires the use of the following six values:

$$k_1 = f(x_k, t_k) \qquad \text{[from Equation (2.57)]}$$

$$k_2 = f\left(x_k + \frac{k_1}{4}, t_k + \frac{\Delta t}{4}\right) \qquad (2.63)$$

$$k_3 = f\left(x_k + \frac{3}{32}k_1 + \frac{9}{32}k_2, t_k + \frac{3\Delta t}{8}\right) \tag{2.64}$$

$$k_4 = f\left(x_k + \frac{1932}{2197}k_1 - \frac{7200}{2197}k_2 + \frac{7296}{2197}k_3, t_k + \frac{12\Delta t}{13}\right) \tag{2.65}$$

$$k_5 = f\left(x_k + \frac{439}{216}k_1 - 8k_2 + \frac{3680}{513}k_3 - \frac{845}{4104}k_4, t_k + \Delta t\right) \tag{2.66}$$

$$k_6 = f\left(x_k - \frac{8}{27}k_1 + 2k_2 - \frac{3544}{2565}k_3 + \frac{1859}{4104}k_4 - \frac{11}{40}k_5, t_k + \frac{\Delta t}{2}\right) \tag{2.67}$$

Then the two estimates can be obtained using the following two equations:

$$x_{k+1} = x_k + \Delta t\left[\frac{25}{216}k_1 + \frac{1408}{2565}k_3 + \frac{2197}{4104}k_4 - \frac{1}{5}k_5\right] \tag{2.68}$$

$$\bar{x}_{k+1} = x_k + \Delta t\left[\frac{16}{135}k_1 + \frac{6656}{12825}k_3 + \frac{28561}{56430}k_4 - \frac{9}{50}k_5 + \frac{2}{55}k_6\right] \tag{2.69}$$

We must note that x_{k+1} in Equation (2.68) and $\bar{x}_{k+1}$ in Equation (2.69) are obtained using the Runge–Kutta method of order four and order five respectively.

The optimal step size $\equiv t_{k,\text{new}}$ can be determined using:

$$\Delta t_{k,\text{new}} = \Delta t_k\left(\frac{\varepsilon\,\Delta t_k}{2\left|\bar{x}_{k+1} - x_{k+1}\right|}\right)^{0.25} \tag{2.70}$$

The above equation can be rewritten as:

$$\Delta t_{k,\text{new}} = 0.840896\,\Delta t_k\left(\frac{\varepsilon\,\Delta t_k}{\left|\bar{x}_{k+1} - x_{k+1}\right|}\right)^{0.25} \tag{2.71}$$

It is obvious that the calculations involved in this approach are tedious and time consuming. But this method gives more accurate results. The generalization of this method to deal with systems of coupled first-order ODEs is fairly obvious.

2.3.5 Predictor-Corrector Method

For solving the ordinary differential equations, so far we discussed the single-step numerical methods (Euler, Heun, Taylor and Runge–Kutta). They are called so because they need only the information from one previous point for computing the successive point. For example, to generate (t_{k+1}, x_{k+1}), the initial point (t_0, x_0) should be known.

Now we will discuss a multi-step predictor-corrector method of Adams–Bashforth–Moulton. The idea is to predict x_{k+1} using the Adams–Bashforth method and then to correct its value using the corresponding Adams–Moulton approach. At the starting, this four-step approach requires total four initial points, namely (t_0, x_0), (t_1, x_1), (t_2, x_2) and (t_3, x_3), in advance in order to compute the next points $[(t_{k+1}, x_{k+1})$ for $k \geq 3]$.

This multi-step algorithm is developed based on the fundamental theorem of calculus:

$$x_{k+1} = x_k + \int_{t_k}^{t_{k+1}} f[t, x(t)]\, dt \qquad \text{[from Equation (2.52)]}$$

One needs to integrate over a finite step using a simple interpolating polynomial approximation for $f(t, x)$ over the interval.

Adams–Bashforth method (predictor step)

Under this step, we need to fit a cubic polynomial to the function $f(t, x)$ through the points (t_{k-3}, f_{k-3}), (t_{k-2}, f_{k-2}), (t_{k-1}, f_{k-1}) and (t_k, f_k). The function is then integrated over the interval t_k to t_{k+1} and the Adams–Bashforth predictor is obtained as:

$$P_{k+1} = x_k + \frac{\Delta t}{24}(55 f_k - 59 f_{k-1} + 37 f_{k-2} - 9 f_{k-3}) \qquad (2.72)$$

Adams–Moulton method (corrector step)

By the similar way, the corrector is devised. A second cubic polynomial for $f(t, x)$ is constructed based on the points (t_{k-2}, f_{k-2}), (t_{k-1}, f_{k-1}), (t_k, f_k) and the new point (t_{k+1}, f_{k+1}), where $f_{k+1} = f(t_{k+1}, P_{k+1})$. Integrating over t_k to t_{k+1}, the Adams–Moulton corrector is obtained as:

$$x_{k+1} = x_k + \frac{\Delta t}{24}(9 f_{k+1} + 19 f_k - 5 f_{k-1} + f_{k-2}) \qquad (2.73)$$

As mentioned, the Adams–Bashforth–Moulton algorithm requires four initial points in advance. Typically, for an initial value problem, x_0 is only given and t_0 is obviously zero. In this multi-step method, three additional starting values, x_1, x_2 and x_3, are usually computed using the Runge–Kutta approach.

The Adams–Bashforth–Moulton algorithm is of forth order. This method is faster than the forth-order Runge–Kutta approach since only two new functional evaluations are involved in each step. However, this algorithm is not self-starting and, therefore, the RK method is needed to initiate this multi-step approach. The four-step algorithm is given below.

Computational steps

Step 1: Use the RK method to determine x_1, x_2 and x_3 (x_0 is known).

Step 2: Calculate P_{k+1} using Equation (2.72).

Step 3: Evaluate $f_{k+1} = f(t_{k+1}, P_{k+1})$ and compute x_{k+1} using Equation (2.73).

Step 4: Increment the t interval and go to Step 2.

2.4 NUMERICAL SOLUTION OF PARTIAL DIFFERENTIAL EQUATIONS

It is well known that a differential equation involving more than one independent variable is known as a partial differential equation (PDE). As mentioned earlier, in many practical situations, it is exceedingly difficult and sometimes impossible to obtain the analytical solution. Now, we will briefly know the finite-difference models that can be used for approximating the first and second derivatives of a function.

In the following, the various forms of approximation (Chu, 1969) based on the use of central, forward and backward differences are listed.

2.4.1 First-order Approximations

Central difference

$$\left(\frac{\partial x}{\partial z}\right)_n = \frac{x_{n+1} - x_{n-1}}{2\Delta z} \tag{2.74}$$

$$\left(\frac{\partial^2 x}{\partial z^2}\right)_n = \frac{x_{n+1} - 2x_n + x_{n-1}}{\Delta z^2} \tag{2.75}$$

Forward difference

$$\left(\frac{\partial x}{\partial z}\right)_n = \frac{x_{n+1} - x_n}{\Delta z} \tag{2.76}$$

$$\left(\frac{\partial^2 x}{\partial z^2}\right)_n = \frac{x_{n+2} - 2x_{n+1} + x_n}{\Delta z^2} \tag{2.77}$$

Backward difference

$$\left(\frac{\partial x}{\partial z}\right)_n = \frac{x_n - x_{n-1}}{\Delta z} \tag{2.78}$$

$$\left(\frac{\partial^2 x}{\partial z^2}\right)_n = \frac{x_n - 2x_{n-1} + x_{n-2}}{\Delta z^2} \tag{2.79}$$

2.4.2 Second-order Central Difference Approximations

$$\left(\frac{\partial x}{\partial z}\right)_n = \frac{-x_{n+2} + 8x_{n+1} - 8x_{n-1} + x_{n-2}}{12\Delta z} \tag{2.80}$$

$$\left(\frac{\partial^2 x}{\partial z^2}\right)_n = \frac{-x_{n+2} + 16x_{n+1} - 30x_n + 16x_{n-1} - x_{n-2}}{12\Delta z^2} \tag{2.81}$$

2.5 SUMMARY AND CONCLUSIONS

This chapter presents a detailed description of several numerical methods, which are commonly used in the simulation of several chemical engineering process models. At the beginning, different solution techniques for nonlinear algebraic equations and then the numerical solution of differential equations have been discussed. The practical chemical engineering problems are represented by a set of coupled differential–algebraic equations. We will discuss the simultaneous solutions of such systems using these numerical methods in the subsequent chapters.

EXERCISES

2.1 Are the Heun method and RK2 the same? Explain them.

2.2 The following expressions are given (Fonyo et al., 1995) for pure water:

Steam pressure:

$$P_{\text{steam}} = \exp\left(11.6859 - \frac{3822.3186}{227.47 + T}\right) \qquad (2.82)$$

Latent heat:

$$\neg_{\text{steam}} = 2500.43 - 2.3387T + 1.675 \times 10^{-5}T^2 - 1.1145 \times 10^{-5}T^3 \qquad (2.83)$$

Enthalpy of liquid water:

$$H^{L}_{\text{water}} = 0.0188 + 4.1968T - 4.754 \times 10^{-4}T^2 + 3.881 \times 10^{-6}T^3 \qquad (2.84)$$

where T is the temperature (°C). The units of P_{steam}, $\neg_{\text{steam}}$ and H^{L}_{water} are bara, kJ/kg and kJ/kg, respectively. Develop a computer code for computing the enthalpy of water vapour with the given P_{steam}.

2.3 Use the Bisection method to find a root of

$$f(x) = 1 - 2e^{x}$$

to two significant digits.

2.4 Find the three smallest positive roots of

$$f(x) = x - \cot(x)$$

to an accuracy of 10^{-4}.

2.5 Consider the following nonlinear algebraic equation to find the root

$$f(x) = x^3 - 5x^2 + 6x - 1$$

employing the

(i) Bisection method (ii) Secant method

2.6 Find the root of the following equations:

(a) $f(x) = x^3 - 5x + 1$

(b) $f(x) = x^2e^x - 1$

using the

(i) Bisection method (ii) Secant method

(iii) False Position method (iv) Newton–Raphson method

2.7 Find the root of the following equation using the Muller method:

$$f(x) = \cos(x) - xe^{x}$$

The initial approximations are: $x_0 = -1.0$, $x_1 = 0.0$, and $x_2 = 1.0$.

2.8 Perform three iterations using the Muller method for the following equations:

(a) $x^3 - 0.5 = 0$, $x_0 = 0.0$, $x_1 = 1.0$, $x_2 = 0.5$

(b) $\log x - x + 3 = 0$, $x_0 = 0.25$, $x_1 = 0.5$, $x_2 = 1.0$

2.9 An equimolal mixture of ethanol and water is fed to a distillation tray at 1 atm. Develop the computer code for determining the bubble point temperature and vapour composition using the

(a) Newton–Raphson method

(b) Muller method

2.10 Use the Explicit Euler method to solve numerically the initial value problem

$$\frac{dP}{dt} = 2P^2 - 5P + 1$$

with $P_0 = 1.0$ and $\Delta t = 0.5$.

2.11 Consider a first-order process representing

$$\frac{dx}{dt} = -\frac{2x}{\tau}$$

Solve this equation using the Explicit Euler method and the fourth-order Runge–Kutta method, and then compare the results.

Given: $x_0 = 3.0$, $\tau = 3.0$, and $\Delta t = 1.0$.

2.12 Consider the following ODE

$$\frac{dy}{dt} = 4y - e^{-t}$$

Solve this ODE employing the RKF45 algorithm with $y_0 = 1.0$.

2.13 Consider the scaled predator–prey equations

$$\begin{cases} \dfrac{dx_1}{dt} = \alpha_1(1 - x_2)x_1 \\ \dfrac{dx_2}{dt} = -\alpha_2(1 - x_1)x_2 \end{cases}$$

(a) Simulate these coupled equations using the

(i) Explicit Euler method

(ii) Heun method

(iii) Second-order Runge–Kutta method

(iv) Fourth-order Runge–Kutta method

(b) Investigate the effect of initial conditions on the response of x_1 and x_2.

Given: $\alpha_1 = \alpha_2 = 0.5$, $x_{1,0} = 1.0$, $x_{2,0} = 0.75$ and $\Delta t = 0.5$.

2.14 Perform three iterations using the Taylor method for the following equation:

$$x' = \frac{t - x}{3} \text{ with } x_0 = 2 \text{ and } \Delta t = 0.25 .$$

2.15 In a thermostatic bath shown in Figure 2.7, the temperature of a water stream circulating at a low velocity is maintained by means of a coil in which water vapour circulates. The sample process is represented by the following energy balance equation:

$$MC_p \frac{dT}{dt} = FC_p(T_{in} - T) + UA(T_v - T) \qquad (2.85)$$

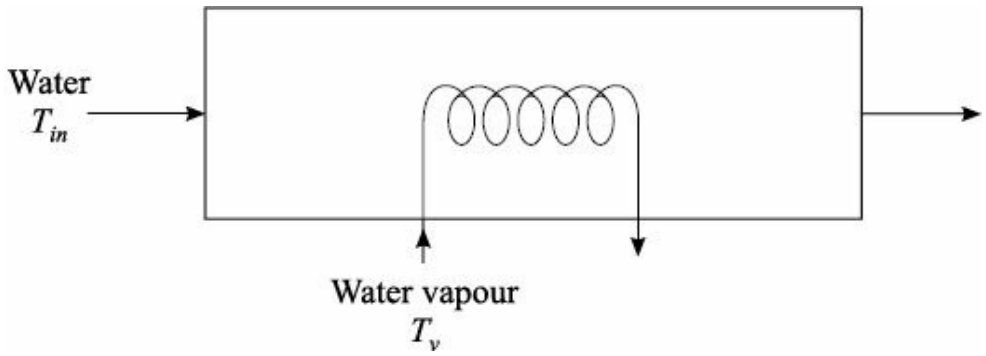

FIGURE 2.7 Thermostatic bath.

System specifications are given in Table 2.1.

Table 2.1 System specifications

Water flow rate (F) = 25 kg/min
Inlet water temperature (T_{in}) = 294 K
Bath temperature (T) = 303 K
Vapour temperature (T_v) = 407.5 K
Water mass to heat (M) = 70 kg
Overall heat transfer coefficient (UA) = 9000 J/min.K
Heat capacity of liquid water (C_p) = 4180 J/kg.K

(i) Simulate the energy balance equation using the RKF45 method.

(ii) Observe the process dynamics with introducing a 10% step increase in water flow rate F.

(iii) Design and employ a classical PI controller for maintaining the bath temperature T by the adjustment of vapour temperature T_v.

(iv) Investigate the control performance with giving a pulse change in water flow rate F (disturbance variable).

2.16 The Van de Vusse reaction operated in a continuous stirred tank reactor (CSTR) is given as follows (Stack and Doyle III, 1997):

$$A \circ B \circ C$$

$$2A \circ D$$

The component material balance equations are described as:

$$\begin{cases} \dfrac{dC_A}{dt} = -k_1 C_A - k_3 C_A^2 + \dfrac{F}{V}(C_{Af} - C_A) \\ \dfrac{dC_B}{dt} = k_1 C_A - k_2 C_B - \dfrac{F}{V} C_B \end{cases} \tag{2.86}$$

(i) Compute the steady state values of C_A and C_B using the data reported in Table 2.2.

(ii) Simulate the modelling equations employing the fourth-order Runge–Kutta method for dynamics study.

Table 2.2 The Van de Vusse CSTR model parameter values

Reactor volume (V) = 1 l
Feed flow rate (F) = 25 l/h
Feed concentration of reactant A(C_{Af}) = 10 mol/l
Kinetic constant (k_1) = 50 h^{-1}

Kinetic constant (k_2) = 100 h^{-1}
Kinetic constant (k_3) = 10 l/mol.h

REFERENCES

Burden, R.L., and Faires, J.D. (1985). *Numerical Analysis*, 3rd ed., Prindle, Weber and Schmidt, Boston, MA.

Chu, Y. (1969). *Digital Simulation of Continuous Systems*, 1st ed., McGraw Hill, New York.

Davis, M.E. (1984). *Numerical Methods and Modeling for Chemical Engineers*, 2nd ed., John Wiley & Sons, New York.

Fehlberg, E. (1964). *Z. Angewandte Mathem. Mech.*, 44, 17.

Fehlberg, E. (1969). Low-order Classical Runge–Kutta Formulas with Stepsize Control and their application to some heat transfer problems, *NASA Technical Report*, NASA TR R-315.

Finlayson, B.A. (1980). *Nonlinear Analysis in Chemical Engineering*, 1st ed., McGraw Hill, New York.

Fonyo, Z., Kurrat, R., Rippin, D.W.T., and Meszaros, I. (1995). Comparative analysis of various heat pump schemes applied to C_4 splitters, *Comput. Chem. Eng.*, 19, S1–S6.

Gear, C.W. (1971). *Numerical Initial Value Problems in Ordinary Differential Equations* , Prentice-Hall, Englewood Cliffs, NJ.

Goldstine, H.H. (1977). *A History of Numerical Analysis from the 16th, thru the 19th Century*, Springer Verlag, New York.

Gupta, S.K. (1995). *Numerical Methods for Engineers*, 1st ed., New Age International, New Delhi.

Jain, M.K., Iyengar, S.R.K., and Jain, R.K. (1995). *Numerical Methods for Scientific and Engineering Computation*, 3rd ed., New Age International, New Delhi.

Lapidus, L., and Seinfeld, J.H. (1971). *Numerical Solution of Ordinary Differential Equations*, Academic, New York.

Riggs, J.B. (1988). *An Introduction to Numerical Methods for Chemical Engineers*, 1st ed., Texas Tech. University Press, Lubbock, TX.

Stack, A.J., and Doyle III, F.J. (1997). Application of a control-law nonlinearity measure to chemical reactor analysis, *AIChE J.*, 43, 425–447.

Part II
Reactor

Chemical reactors are very important unit operations in industrial practice. The reaction occurred in a reactor can either give off heat (*exothermic*) or absorb heat (*endothermic*). The reactor is generally assembled with a jacket or coil in order to maintain the reaction temperature properly. If heat is evolved due to exothermic reaction, a coolant stream is required to pass through the jacket (or coil) to remove the extra heat. On the other hand, if endothermic reaction occurs in the system, the flow of a heating medium is considered through the surrounded jacket (or immersed coil) to maintain the reactor temperature at its expected value.

The range of forms of chemical reactors is so wide that it is really difficult to establish a complete, systematic classification. However, the primary classification can be based on the number of phases to be involved. When only one phase is required, the system is said to be *homogeneous*. If more than one phase are present, the system is a *heterogeneous* one.

The chemical reactors also can be classified based on the feeding mechanism as: batch, semi-batch and continuous flow reactors. In the *batch reactor*, a certain amount of material is introduced first, but there is no further inflow or outflow of materials as the reaction proceeds. For the case of *semi-batch reactor*, some components are either fed in or withdrawn as the reaction occurs. The name *continuous flow reactor* indicates that this reactor runs with continuous flow of reactants and products.

Chemical reactors are usually vessel type. There are two main basic vessel type reactors, which are designed as *tank reactor* (a tank) and *tubular reactor* (a pipe or tube). Batch, semi-batch and many continuous flow reactors are generally tank reactors. *Plug flow reactor* (PFR) is an example of tubular reactor. The tubular reactors are operated only with a continuous mode. Indeed, there are two distinct types of reactors in continuous processes: *continuous stirred tank reactor* (CSTR) and PFR.

Also, we may consider the following types of reactors. When a reactor operates at a constant temperature, then that is called as the *isothermal reactor*. If any exothermic or endothermic reactions are involved in the reactor, the temperature of the reaction mixture varies with time and we need to develop the energy balance equation for this *non-isothermal reactor*. It is well-known that the term *adiabatic* means “no interchange of heat between the system and the surroundings”. So, usually no heating and cooling arrangements are provided with the *adiabatic reactor*. In addition, no heat transfer is involved in between the well-insulated reactor and the external environment. For the case of *non-adiabatic reactor*, there is heat flow into or out of the reactor.

One interesting feature of a non-isothermal CSTR, in which exothermic reaction takes place, is the *multiple steady states* (for a particular value of the input variable, several values of the output variable may be obtained). Multiple steady states may be the result of energy feedback and the highly nonlinear behaviour of the reaction rate constant (according to Arrhenius law). This steady state multiplicity can result in an unstable operating condition leading to a quench (the reaction stops) or a runaway (the reactor overheats).

An important area of attention is the development of reactor models with practical relevance. In this book, we will study the detailed mathematical modelling and dynamic simulation of chemical and biochemical reactors.

3

Batch Reactor

3.1 INTRODUCTION

In a batch reactor, a given amount of material is introduced first, and no material is fed or collected as the reaction proceeds. After a certain period of time, the operation is stopped and the product is withdrawn. Then the batch product is sometimes further treated in order to achieve the required product purity to satisfy the commercial requirements and relevant regulatory authorities.

For large-scale production, continuous processing is almost always economically beneficial to batch processing. However, there are many industries in which batch processing is consistently used in the manufacture of relatively small volumes of high-value added products. The inherent flexibility offered by the batch mode of operation allows us to produce different materials, or grades of material, using the same equipment, thereby reducing the initial investment. The batch processing is also preferred when the product is highly sensitive and regulated, as in the food and pharmaceutical industries. If something is made in a batch reactor, it can be tested and certified batch by batch, and from a regulatory point of view, it is easier to deal with.

The following cases are efficiently handled by the batch mode of operation. (i) Slow reactions are frequently best handled in batch processing. To accelerate some slow reactions, the temperature and pressure, which are much easier to control in batch units, are adjusted. (ii) Solids are easy to mix and handle in a batch process. (iii) Oxygen from the air may interfere with the reaction. Some reactions with air may be explosive. Air is difficult to exclude completely from continuous flow systems and batch processes are usually used to operate under such situations.

Although the batch reactor is very flexible, its operation and product quality control are usually difficult. Batch processes are inherently transient in nature (no steady state) and this behaviour leads to operation under a wide range of conditions. However, a realistic dynamic process model can be used as a diagnostic tool to identify the operating problems. Also remember that an efficient controller can maximize the yield of desired product.

In the present study, we will develop a mathematical model for a batch reactor. The dynamic simulation of the process model will also be included in our study. It is recognized that the control of a batch reactor system provides an interesting challenge in that the system has no steady state. Although our objective is not to design an advanced controller, we are interested to observe the *closed-loop process response*[1] by implementing a conventional proportional integral (PI) controller. Finally, the mathematical modelling of a semi-batch reactor will also be covered.

[1] If a process is under control by the use of a controller, the dynamic behaviour provided by that process is called the *closed-loop process response*. For *open-loop response,* no controller is included with the process.

3.2 THE PROCESS AND THE MODEL

3.2.1 Process Description

Consider a batch reactor shown in Figure 3.1. The reactor is filled with reactant and then sealed. The contents of the reactor are heated up to the reaction temperature with saturated steam supplied to the

jacket at temperature T_S. Condensed steam is collected in a steam trap. The reaction mixture is continuously stirred at a fixed rpm. The reactor is fitted with a cooling coil through which chilled water is passed and the exothermic heat is removed to move the system temperature along a predetermined desired temperature–time trajectory. To follow the prescribed trajectory, both heating and cooling of the process unit is necessary.

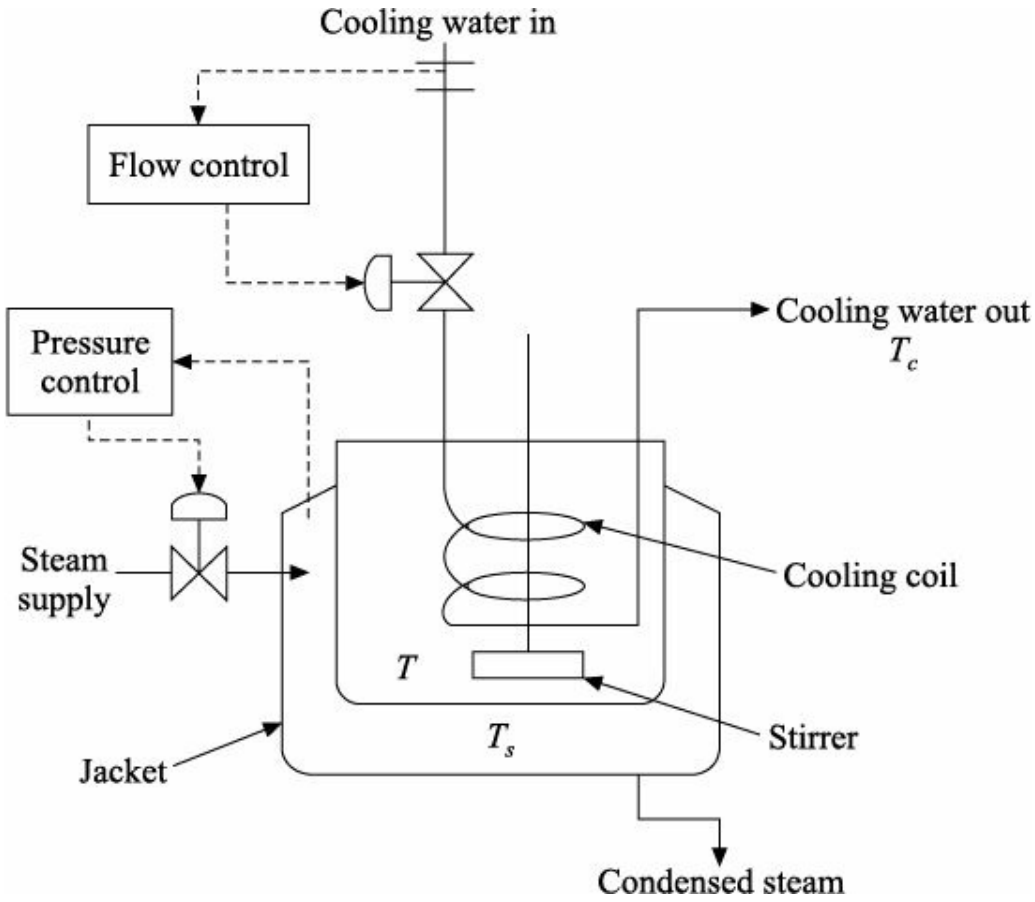

FIGURE 3.1 Schematic representation of the batch reactor example.

Consider the following consecutive reactions that take place in the reactor:

$$A \xrightarrow{k_1} B \xrightarrow{k_2} C$$

It is assumed that $A \rightarrow B$ has second-order kinetics, whereas $B \rightarrow C$ has first-order kinetics. In this batch operation, B is the desired product. If the reaction goes on for a long time, the yield of undesired waste C will be high. Again if we stop the reaction too early, the conversion of A may be very low. In both situations, the yields of desired product B are low. Therefore, there is an optimum time when we can stop the operation and get the maximum amount of desired product. This time is known as *batch time*.

3.2.2 Mathematical Model

Assumptions

We make the following assumptions to develop the process model.

- Both the chemical reactions occurred in the example, batch reactor, are exothermic.
- The reactor is well-insulated such that there is negligible heat exchange in between the reactor and the external environment. Some parts of the cooling water and steam supply lines, which are exposed to the environment, are also insulated.
- The inlet and outlet coolant temperatures do not vary much due to a sufficiently rapid flow rate of the

coolant stream. Therefore, an average water coolant temperature T_c is used in the mathematical model.

- The condensed steam is discharged at its saturation temperature (no subcooling).
- We assume constant volume (V) reactor with constant mixture heat capacity (C_p). Note that here the volume refers to the volume of reaction mixture, not the volume of reactor.
- The reactor contents are perfectly mixed and do not exhibit significant gradients of species concentrations or temperature in any part of the reactor.
- The overall heat transfer coefficient for heating jacket U_j is assumed constant but the overall heat transfer coefficient for the cooling coil U_c is assumed to be a function of the coolant flow rate F_c as:

$$\frac{1}{U_c} = \frac{1}{4550 F_c^{0.8}} + \frac{1}{10.8} \qquad (3.1)$$

Model development

The basis of most of reactor modelling is a set of fundamental balance equations. These equations are mathematical statements of physical laws that require conservation of mass, energy, momentum, and quantities of particular chemical species. Details of the conservation principle are provided in Chapter 1. The basic balance equation is:

$$\begin{bmatrix}\text{Rate of accumulation}\\ \text{within the system}\end{bmatrix} = \begin{bmatrix}\text{Rate of flow}\\ \text{into the system}\end{bmatrix} - \begin{bmatrix}\text{Rate of flow out}\\ \text{of the system}\end{bmatrix} + \begin{bmatrix}\text{Rate of generation}\\ \text{by chemical reaction}\\ \text{within the system}\end{bmatrix} \qquad (3.2)$$

More simply,

$$\begin{bmatrix}\text{Rate of accumulation}\\ \text{within the system}\end{bmatrix} = \begin{bmatrix}\text{Net rate of flow}\\ \text{into the system}\end{bmatrix} + \begin{bmatrix}\text{Rate of generation}\\ \text{by chemical reaction}\\ \text{within the system}\end{bmatrix} \qquad (3.3)$$

In the SI system, all the terms in the above Equations (3.2) and (3.3) have the unit of kilo-mole per second (kmol/s) or kilogram per second (kg/s) for mass balance and kilo-joule per second (kJ/s) for energy balance.

Total Continuity Equation

In the batch operation,

Net flow rate of mass into the reactor = 0,

Rate of generation of mass within the reactor = 0, and

Rate of accumulation of mass within the reactor = $\frac{d(\rho V)}{dt}$.

Since ρ is the mixture density and V is the mixture volume, and ρV becomes the total mass inside the reactor. Substituting all these terms in Equation (3.3), we get the total continuity equation as:

$$\frac{d(\rho V)}{dt} = 0 \qquad (3.4)$$

We have assumed that V is constant and therefore according to the total continuity equation, ρ remains unchanged (constant).

Component Continuity Equations

For component A (*reactant*)

In the component balance equation for species A,

Net flow rate of component A into the reactor = 0,

Rate of generation of component A by chemical reaction = $-(-r_A)V$

$= (r_A)V$, and

Rate of accumulation of component A within the reactor = $\frac{dN_A}{dt}$.

By convention, $(-r_A)$ is the rate of disappearance of species A; consequently, (r_A) is the rate of formation of A. Here, N_A represents the number of moles of species A in the system at time t. Now Equation (3.3) gives the following form for species A as:

$$\frac{dN_A}{dt} = -(-r_A)V \quad (3.5)$$

that is,

$$\frac{1}{V}\frac{dN_A}{dt} = \frac{d(N_A/V)}{dt} = \frac{dC_A}{dt} = -(-r_A) \qquad (3.6)$$

where C_A is the concentration of species A. Since the reaction $A \xrightarrow{k_1} B$ has second-order kinetics, so

$$(-r_A) = k_1 C_A^2 \qquad (3.7)$$

where k_1 represents the reaction rate constant. Substitution of Equation (3.7) into Equation (3.6) gives:

$$\frac{dC_A}{dt} = -k_1 C_A^2 \qquad (3.8)$$

This is the component continuity or component mass balance equation for species A.

For component B (*desired product*)

In the component balance equation for species B,

Net flow rate of component B into the reactor = 0,

Rate of generation of component B by chemical reaction = $-(-r_B)V$, and

Rate of accumulation of component B within the reactor = $\frac{dN_B}{dt}$.

Here, $(-r_B)$ is the rate of disappearance of species B and N_B denotes the number of moles of species B in the system at time t. After rearranging Equation (3.3) for the case of component B, we obtain

$$\frac{dN_B}{dt} = -(-r_B)V \qquad (3.9)$$

Based on the specified reactions as stated earlier, we can write

$$(-r_B) = k_2 C_B - k_1 C_A^2 \quad (3.10)$$

where C_B is the concentration of species B and k_2 denotes the reaction rate constant. Substituting Equation (3.10) into Equation (3.9), finally we get

$$\frac{dC_B}{dt} = k_1 C_A^2 - k_2 C_B \qquad (3.11)$$

This is the component continuity equation for species B.

Reaction Rate Constant

Common sense and chemical intuition suggest that the higher the temperature (T), the faster a given chemical reaction will proceed. Quantitatively this relationship between the rate of reaction and its temperature is determined by the *Arrhenius equation*. According to the Arrhenius rate law, the *reaction rate constant*[2], k (also known as *specific reaction rate constant*) is expressed by

[2] In many textbooks, k is referred to as *reaction rate* or *specific reaction rate* (do not confuse with *rate of reaction, r*) because k is not truly a constant, but it is only independent of the concentrations of the species involved in the reactions.

$$k = \alpha \exp\left(\frac{-E}{RT}\right) \qquad (3.12)$$

where α = frequency factor or pre-exponential factor

E = activation energy

R = universal gas constant

The exponential temperature-dependent function in the kinetic Equation (3.12) represents one of the severe nonlinearities in chemical engineering systems. For the sample batch reactor, the Arrhenius equation [Equation (3.12)] gives the following forms:

$$k_1 = \alpha_{10} \exp\left(\frac{-E_1}{RT}\right) \qquad (3.13)$$

$$k_2 = \alpha_{20} \exp\left(\frac{-E_2}{RT}\right) \qquad (3.14)$$

The above two equations have been used in the component continuity and energy balance equations.

Energy Balance Equation

For the concerned batch reactor, Equation (3.3) can be expressed in terms of energy as:

$$\begin{bmatrix}\text{Rate of energy}\\ \text{accumulation}\end{bmatrix} = \begin{bmatrix}\text{Net rate of}\\ \text{energy input}\end{bmatrix} + \begin{bmatrix}\text{Rate of energy added}\\ \text{by exothermic}\\ \text{chemical reactions}\end{bmatrix} \qquad (3.15)$$

Now,

Net rate of energy input = $\begin{bmatrix}\text{Rate of heat input}\\ \text{from the heating}\\ \text{jacket to the reactor}\end{bmatrix} - \begin{bmatrix}\text{Rate of heat output}\\ \text{from the reactor to}\\ \text{the cooling coil}\end{bmatrix}$

$$= U_j A_j (T_S - T) - U_c A_c (T - T_c)$$

Here, A_j and A_c are the heat transfer areas of the heating jacket and the cooling coil respectively. Since we have assumed that the reactor is well-insulated and, therefore, no heat exchange in between the reactor and the environment is accounted.

Again, rate of energy added by the exothermic reactions

$$= \sum_{i=1}^{n} (-\Delta H_i)(-r_i)V$$

$$= (-\Delta H_1) k_1 C_A^2 V + (-\Delta H_2) k_2 C_B V$$

Clearly, $n = 2$. The subscripts 1 and 2 are used for the reactions $A \xrightarrow{k_1} B$ and $B \xrightarrow{k_2} C$ respectively. Here, $(-\Delta H_1)$ and $(-\Delta H_2)$ are the exothermic heats of reaction for the two reactions. It is well-known that the heat of reaction is negative for the exothermic reaction and positive for the endothermic reaction.

Now, rate of accumulation of energy = $\dfrac{d(\rho V h)}{dt} = \rho V C_p \dfrac{dT}{dt}$

Here, ρ, V and C_p all are constants, and h is the enthalpy ($= C_p T$). Substituting all these energy terms in Equation (3.15), we obtain the following form:

$$\rho C_p V \frac{dT}{dt} = (-\Delta H_1) k_1 C_A^2 V + (-\Delta H_2) k_2 C_B V + U_j A_j (T_s - T) - U_c A_c (T - T_c) \qquad (3.16)$$

Rearranging,

$$\frac{dT}{dt} = \frac{(-\Delta H_1)}{\rho C_p} k_1 C_A^2 + \frac{(-\Delta H_2)}{\rho C_p} k_2 C_B + \frac{U_j A_j}{\rho C_p V} (T_s - T) - \frac{U_c A_c}{\rho C_p V} (T - T_c) \qquad (3.17)$$

This is the energy balance equation for the sample batch reactor.

3.2.3 Application of Control Algorithm

Now we will discuss the control of the example batch reactor under the assumption that some of the basic control theories are familiar to the reader. The control of a batch reactor system is a great challenge because the system has no steady state. From Figure 3.1, it is clear that the cooling rate is controlled by manipulating the water flow rate (F_C) through the cooling coil. Again, the control of the heating rate is accomplished by regulating the steam pressure, and hence, the steam temperature (T_S). Actually the controller manipulates both these variables (F_C and T_S) simultaneously to regulate the reactor temperature (T).

In order to achieve a maximum yield of the desired product, it is always necessary to create a reaction-friendly environment in the reactor. For the present case, the set point temperature in the reactor should be

changed precisely and the dynamic set point is given as a desired temperature–time trajectory (Kravaris and Chung, 1987):

$$T_d(t) = 54 + 71 \exp(-2.5 \times 10^{-3} t) \qquad (3.18)$$

In general practice, one output variable (here T) is controlled using only a single manipulated variable (say, T_S). If we use another manipulated variable F_C [or U_C since they are easily correlated according to Equation (3.1)] simultaneously to drive T, the control system will be over-determined. A way of solving this difficulty is to introduce a single parametric variable u, defined in the following manner (Jutan and Uppal, 1984):

$$T_S = (T_{S,\max} - T_{S,\min})u + T_{S,\min} \qquad (3.19)$$

$$U_C = (U_{C,\min} - U_{C,\max})u + U_{C,\max} \qquad (3.20)$$

where the maximum and minimum values of T_S and U_C are chosen from process or safety limits. Clearly, $u = 0$ represents the maximum cooling of the system and $u = 1$, maximum heating. This parametric variable is used as a single manipulated variable in the prescribed batch control problem. After substituting Equations (3.19) and (3.20) into Equation (3.17) and rearranging, we obtain

$$\frac{dT}{dt} = \gamma_1 k_1 C_A^2 + \gamma_2 k_2 C_B + (a_1 + a_2 T) + (b_1 + b_2 T)u \qquad (3.21)$$

where

$$\gamma_1 = (-\Delta H_1)/\rho C_p \qquad (3.22)$$

$$\gamma_2 = (-\Delta H_2)/\rho C_p \qquad (3.23)$$

$$a_1 = (U_j A_j T_{s,\min} + U_{c,\max} A_c T_c)/\rho C_p V \qquad (3.24)$$

$$a_2 = -(U_j A_j + U_{c,\max} A_c)/\rho C_p V \qquad (3.25)$$

$$b_1 = [U_j A_j (T_{s,\max} - T_{s,\min}) - (U_{c,\max} - U_{c,\min}) A_c T_c]/\rho C_p V \qquad (3.26)$$

$$b_2 = (U_{c,\max} - U_{c,\min}) A_c/\rho C_p V \qquad (3.27)$$

Now u can be obtained by employing a control algorithm. Here, a classical PI controller (Stephanopoulos, 1998) will be implemented to regulate the temperature in the batch reactor. The PI controller equation is

$$u_t = u_s + K_c \left(e_t + \frac{1}{\tau_i} \int e_t \, dt \right) \qquad (3.28)[3]$$

3 Obviously, $\frac{d}{dt}[\int e_t \, dt] = \frac{d}{dt}(error\ \text{int}) = e_t$. So we can write, $error\ \text{int}(k+1) = error\ \text{int}(k) + \Delta t\, e(k)$.

where u_S is the controller's bias signal, K_C the proportional gain (tuning parameter), τ_i the integral time constant (tuning parameter) and the error to the controller $e_t = T_{dt} - T_t$. The values of the tuning parameters are arbitrarily chosen as: $K_C = 0.1(°C^{-1})$ and $\tau_i = 360$ (s).

3.2.4 Dynamic Simulation

We will now proceed to develop the dynamic simulator based on the derived process model. The batch reactor model comprises of the ordinary differential equations (ODEs) (two component continuity

equations and one energy balance equation) supported by the algebraic form of equations (two reaction rate equations). The ordinary differential equations have been solved using the classical fourth-order Runge–Kutta method (details in Chapter 2). An option is also provided in the simulator for solving the ODEs using the Euler integration approach (see Chapter 2 for details). In order to observe the closed-loop process response under PI control, the control scheme is also implemented in the simulator. The start-up conditions and systems characteristics are reported in Table 3.1. Complete batch simulator is programmed using
Fortran (90) computer language and is given in Program 3.1.

Figure 3.2 depicts the tracking performance provided by the designed PI controller [Equation (3.28)]. A satisfactory temperature tracking is obtained by adjustment of heating and cooling rate through manipulation of the parametric variable u. The values of the two manipulated variables, steam temperature and coolant flow rate, are also shown in the figure.

Table 3.1 Start-up conditions and systems characteristics

C_{A0}	concentration of species A at start-up, kmol/m^3	1.0
C_{B0}	concentration of species B at start-up, kmol/m^3	0.0
γ_1	frequency factor of reaction $A \rightarrow B$, m^3/(kmol)(s)	1.1
γ_2	frequency factor of reaction $B \rightarrow C$, s^{-1}	172.2
E_1	activation energy for reaction $A \rightarrow B$, kJ/kmol	2.09×10^4
E_2	activation energy for reaction $B \rightarrow C$, kJ/kmol	4.18×10^4
$(-\Delta H_1)$	heat of reaction for reaction $A \rightarrow B$, kJ/kmol	4.18×10^4
$(-\Delta H_2)$	heat of reaction for reaction $B \rightarrow C$, kJ/kmol	8.36×10^4
C_p	heat capacity, kJ/(kg)(°C)	1.0
ρ	density, kg/m^3	1000.0
T_c	coolant temperature, °C	25.0
U_j	overall heat transfer coefficient of jacket, kJ/(m^2)(°C)(s)	1.16
$U_{c,\max}$	maximum value of U_c, kJ/(m^2)(°C)(s)	4.42
$U_{c,\min}$	minimum value of U_c, kJ/(m^2)(°C)(s)	1.39
$T_{\max}$	maximum value of T, °C	125.0
$T_{\min}$	maximum value of T_s, °C	25.0
$T_{s,\max}$	minimum value of T_s, °C	150.0
$T_{s,\min}$	universal gas constant, kJ/(kmol)(K)	70.0
R	$A_c/V = 17.0$ m^2/m^3	8.314
	$A_j/V = 30.0$ m^2/m^3	
	Batch time = 1 h	
	Integration time interval = 0.1 s	

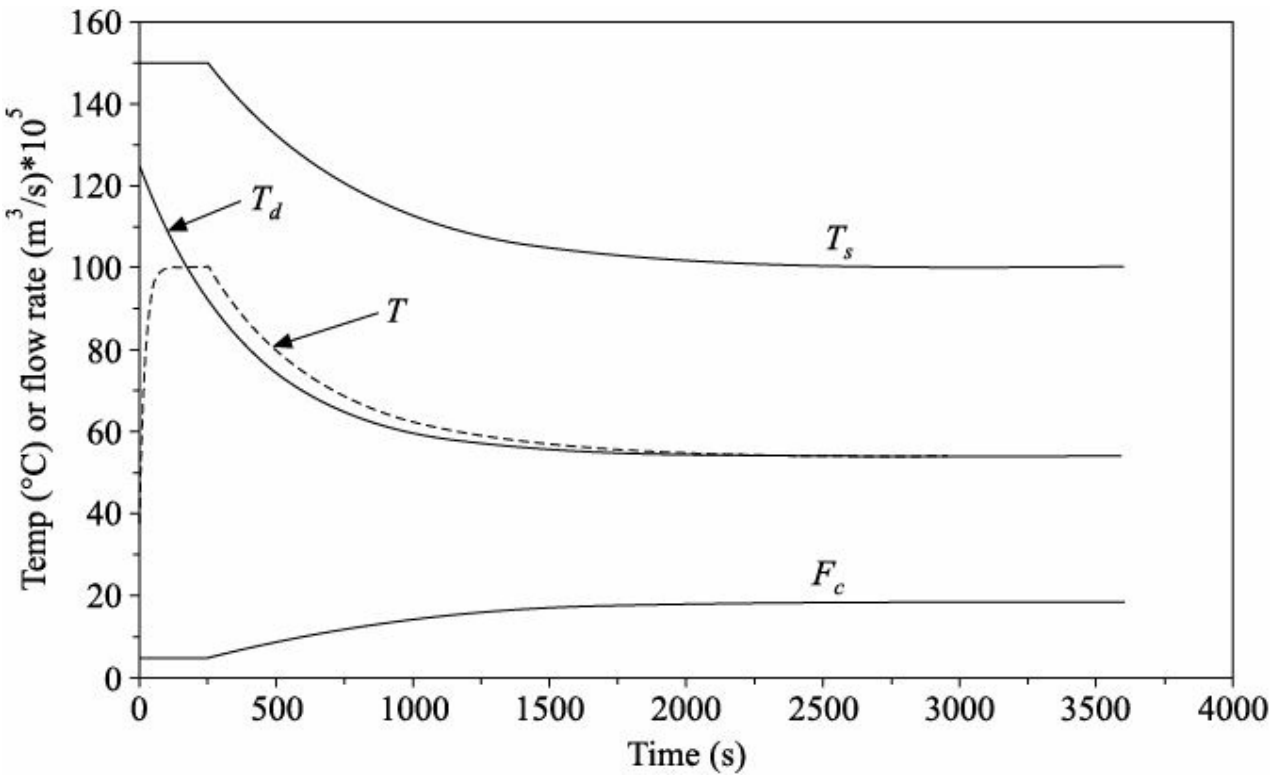

FIGURE 3.2 Temperature tracking provided by the PI controller.

PROGRAM 3.1 *Closed-loop Batch Reactor*

```
! Notations

! A10, A20 = Frequency factors
! Ca = Concentration of species A
! Cb = Concentration of species B
! Fc = Coolant flow rate
! Kc = PI controller gain
! T = Reactor temperature
! TAUI = Integral time constant
! Td = Desired (set-point) temperature
! Ts = Steam temperature
! U = Parametric variable (manipulated variable)
! Uc = Overall heat transfer coefficient of cooling coil
PROGRAM BATCH_REACTOR
IMPLICIT NONE

! Declaration
!————————

INTEGER::K
INTEGER,PARAMETER::N=40000
REAL::T0,T1,T2,T3,Ca0,Ca1,Ca2,Ca3,Cb0,Cb1,Cb2,Cb3
REAL::k1,k11,k12,k2,k21,k22,k3,k31,k32,k4,k41,k42
REAL,DIMENSION(N)::ER,ERINT,U,Fc
REAL,DIMENSION(N)::Td,T,Ca,Cb,Ts,Uc,Time
REAL,PARAMETER::Y1=41.8,Y2=83.6,dt=0.1
REAL,PARAMETER::A1=4.3145,A2=-0.10994,A10=1.1,A20=172.2
REAL,PARAMETER::B1=1.49625,B2=0.05151
REAL,PARAMETER::X=2513.8321,Z=5027.6642
REAL,PARAMETER::Kc=0.1,TAUI=360.0

OPEN(unit=1,file="PI_BATCH.dat")

! Initialization
!—————————
```

```
T(1)=25.00
Ca(1)=1.00
Cb(1)=0.00
Time(1)=0.00

ER(1)=100.00
ERINT(1)=0.0
U(1)=1.00

!————————————Starting of main loop————————————————!
!———————————————————————————————————————————————!

DO K=1,N
Time(K+1)=Time(K)+dt
Td(K+1)=54+71*EXP(-0.0025*Time(K+1))

!———————————Starting of Euler method———————————————!

! T(k+1)=T(k)+dt*((Y1*A10*EXP(-X/(273.00+T(K)))*
! & Ca(K)*Ca(K)+(Y2*A20*EXP(-Z/(273.00+T(K)))*Cb(K))+
! & (A1+A2*T(K))+((B1+B2*T(K))*U(K)))

! Ca(k+1)=Ca(k)-dt*(A10*EXP(-X/(273.00+T(K)))*Ca(k)*Ca(k))

! Cb(k+1)=Cb(k)+dt*((A10*EXP(-X/(273.00+T(K)))*Ca(K)*Ca(K))-
! & (A20*EXP(-Z/(273.00+T(K)))*Cb(k)))

!————————————————End of Euler method————————————————!

!———————Starting of fourth-order Runge—Kutta method——————————!

T0=T(K)
Ca0=Ca(K)
Cb0=Cb(K)

k1=(Y1*A10*EXP(-X/(273.00+T0))*Ca0*Ca0)+
& (Y2*A20*EXP(-Z/(273.00+T0))*Cb0)+
& (A1+A2*T0)+((B1+B2*T0)*U(K))

k11=(-1)*(A10*EXP(-X/(273.00+T0))*Ca0*Ca0)

k12=(A10*EXP(-X/(273.00+T0))*Ca0*Ca0)-
& (A20*EXP(-Z/(273.00+T0))*Cb0)

!———————

T1=T(K)+(k1*dt/2)
Ca1=Ca(K)+(k11*dt/2)
Cb1=Cb(K)+(k12*dt/2)

k2=(Y1*A10*EXP(-X/(273.00+T1))*Ca1*Ca1)+
& (Y2*A20*EXP(-Z/(273.00+T1))*Cb1)+
& (A1+A2*T1)+((B1+B2*T1)*U(K))

k21=(-1)*(A10*EXP(-X/(273.00+T1))*Ca1*Ca1)

k22=(A10*EXP(-X/(273.00+T1))*Ca1*Ca1)-
& (A20*EXP(-Z/(273.00+T1))*Cb1)

!———————

T2=T(K)+(k2*dt/2)
Ca2=Ca(K)+(k21*dt/2)
Cb2=Cb(K)+(k22*dt/2)
k3=(Y1*A10*EXP(-X/(273.00+T2))*Ca2*Ca2)+
& (Y2*A20*EXP(-Z/(273.00+T2))*Cb2)+
& (A1+A2*T2)+((B1+B2*T2)*U(K))
```

```
k31=(-1)*(A10*EXP(-X/(273.00+T2))*Ca2*Ca2)

k32=(A10*EXP(-X/(273.00+T2))*Ca2*Ca2)-
& (A20*EXP(-Z/(273.00+T2))*Cb2)

!———————

T3=T(K)+(k3*dt)
Ca3=Ca(K)+(k31*dt)
Cb3=Cb(K)+(k32*dt)

k4=(Y1*A10*EXP(-X/(273.00+T3))*Ca3*Ca3)+
& (Y2*A20*EXP(-Z/(273.00+T3))*Cb3)+
& (A1+A2*T3)+((B1+B2*T3)*U(K))

k41=(-1)*(A10*EXP(-X/(273.00+T3))*Ca3*Ca3)

k42=(A10*EXP(-X/(273.00+T3))*Ca3*Ca3)-
& (A20*EXP(-Z/(273.00+T3))*Cb3)

!———————

T(K+1)=T(K)+dt*(k1/6.0+k2/3.0+k3/3.0+k4/6.0)

Ca(K+1)=Ca(K)+dt*(k11/6.0+k21/3.0+k31/3.0+k41/6.0)

Cb(K+1)=Cb(K)+dt*(k12/6.0+k22/3.0+k32/3.0+k42/6.0)

!———————————End of fourth-order Runge—Kutta method———————————!

!——————————PI controller——————————!

ERINT(K+1)=ERINT(K)+dt*ER(K)
ER(K+1)=Td(K+1)-T(K+1)
U(K+1)=U(1)+Kc*(ER(K+1)+ERINT(K+1)/TAUI)

IF(U(K+1)>=1.00)U(K+1)=1.00
IF(U(K+1)<=0)U(K+1)=0.00

!———————————————————————————————!

Ts(K+1)=80*U(K+1)+70
Uc(K+1)=4.42-3.03*U(K+1)
Fc(K+1)=((10.8*Uc(K+1))/(4550.00*(10.8-Uc(K+1))))**1.25

PRINT*,Time(K+1),Td(K+1),T(K+1),Ts(K+1),Fc(K+1)*10**5
WRITE(1,10)Time(K+1),Td(K+1),T(K+1),Ts(K+1),Fc(K+1)*10**5

10 FORMAT (1X,5(2X,F10.5))

END DO

!———————————————End of main loop———————————————!

END PROGRAM BATCH_REACTOR
```

3.3 MATHEMATICAL MODEL OF A SEMI-BATCH REACTOR

Here we discuss a dynamical model for a semi-batch reactor shown in Figure 3.3. The following highly exothermic thiosulphate reaction is considered in the present study:

$$\underset{B}{Na_2S_2O_3} + \underset{A}{2H_2O_2} \rightarrow \underset{C}{\frac{1}{2}Na_2S_3O_6} + \underset{D}{\frac{1}{2}Na_2SO_4} + \underset{E}{2H_2O}$$

The reaction rate is assumed to be proportional to the first order of the concentration of reactants A and B, and the solution density (^) to be constant:

$$-r = kC_AC_B \qquad (3.29)$$

where k is a function of the temperature according to the Arrhenius expression [Equation (3.12)].

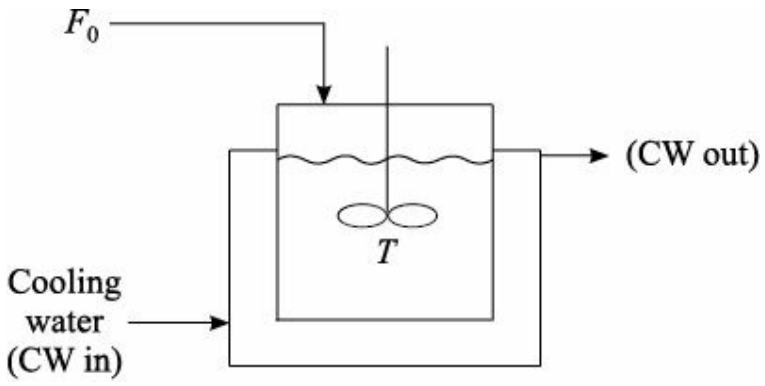

FIGURE 3.3 Schematic representation of the semibatch reactor.

The dynamic behaviour of the sample semi-batch reactor could be described by a set of differential equations resulting from mass and energy balances of the reaction mixture, the energy balance of the jacket wall and the circulating fluid (cooling water) inside the jacket.

Total Mass Balance Equation

$$\frac{d(\rho V)}{dt} = F_0\rho \qquad (3.30)$$

That is,

$$\frac{dV}{dt} = F_0 \qquad (3.31)$$

Here, V represents the volume of reaction mass and F_0 is the addition flow rate of reagent A(H_2O_2).

Component Mass Balance Equations

$$\frac{d(VC_A)}{dt} = F_0C_{A0} - VakC_AC_B \qquad (3.32)$$

$$\frac{d(VC_B)}{dt} = -VbkC_AC_B \qquad (3.33)$$

Here, C_A is the concentration of reactant A, C_{A0} the initial concentration of reactant A, C_B the concentration of reactant B, and a (= 2) and b (= 1) are the stoichiometric factors of reactant A and B, respectively.

Energy Balance Equations

For semi-batch reactor

$$\frac{dT}{dt} = \frac{F_0(T_{ad} - T)}{V} + \frac{(-\Delta H)kC_AC_B}{\rho C_p} - \frac{Q_M}{V\rho C_p} \qquad (3.34)$$

Here, T is the reactor temperature, T_{ad} the temperature of H_2O_2 added, (–≡ H) the heat of reaction, C_p

the heat capacity and the inside heat transfer rate:

$$Q_M = h_i A_i (T - T_M) \qquad (3.35)$$

where h_i represents the inside heat transfer coefficient, A_i the inside heat transfer area and T_M the wall temperature.

For jacket wall

$$\frac{dT_M}{dt} = \frac{Q_M - Q_J}{V_M \rho_M C_M} \qquad (3.36)$$

Here, V_M is the wall volume, $\hat{} _M$ the density of wall, C_M the heat capacity of wall and the outside heat transfer rate:

$$Q_J = h_0 A_0 (T_M - T_J) \qquad (3.37)$$

where h_0 denotes the outside heat transfer coefficient, A_0 the outside heat transfer area and T_J the jacket temperature.

For jacket fluid

$$\frac{dT_J}{dt} = \frac{F_W (T_{J0} - T_J)}{V_J} + \frac{Q_J}{V_J \rho_J C_J} \qquad (3.38)$$

where F_W is the flow rate of jacket fluid stream, T_{J0} the inside jacket fluid temperature, V_J the jacket volume, $\hat{} _J$ the density of jacket fluid and C_J the heat capacity of jacket fluid. It should be noted that the behaviour of the jacket fluid has been considered as a perfect mixing.

3.4 SUMMARY AND CONCLUSIONS

In this chapter, we have first developed a mathematical model for a batch reactor. The reactor is inherently transient in nature and the modelling equations are strongly nonlinear. The model structure consists of mass balance, energy balance and reaction rate equations. In order to carry out the closed-loop simulation experiments, the process simulator is developed with solving the coupled model equations. Then, a conventional PI controller is employed to move the simulated process temperature along a predetermined desired temperature–time trajectory. Finally, the model of a semi-batch reactor is developed for a highly exothermic thiosulphate reaction. The simulation part is left for the students.

EXERCISES

3.1 What are the advantages and disadvantages of the batch processing over the continuous operation?

3.2 What cases are efficiently handled by the batch mode of operation?

3.3 Solve the developed model structure of the batch reactor using both the Euler and fourth-order Runge–Kutta methods, and then compare the results.

3.4 Develop a mathematical model (mass and energy balance equations) for a non-adiabatic batch reactor considering convective heat loss to the atmosphere. You may assume that T_e is the temperature of the environment, h_e is the convective heat transfer coefficient in the environment and no insulation is provided for the cooling coil outside the reactor. Other conditions of this reactor are same with that of

the reactor presented in this chapter.

3.5 Derive the modelling equations for a batch reactor considering the following consecutive exothermic reactions:

$$A \xrightarrow{k_1} B \xrightarrow{k_2} C$$

where both $A \circ B$ and $B \circ C$ have first-order kinetics. Other conditions and notations are same as considered in the present chapter.

3.6 Develop the mathematical model for a batch reactor where the following reactions take place:

$$A \xrightarrow{k_1} B \xrightarrow{k_2} C$$

$$A \xrightarrow{k_3} D$$

All are endothermic, first-order reactions. The reacting mixture is heated by a saturated steam, which flows through a jacket around the reactor with a rate of Q (mass/time).

REFERENCES

Jutan, A., and Uppal, A. (1984). Combined feedforward-feedback servo control scheme for an exothermic batch reactor, *Ind. Eng. Chem. Process Des. Dev.*, 23, 597–602.

Kravaris, C., and Chung, C.-B. (1987). Nonlinear state feedback synthesis by global input/output linearization, *AIChE J.*, 33, 592–603.

Stephanopoulos, G. (1998). *Chemical Process Control: An Introduction to Theory and Practice*, 6th ed., Prentice-Hall of India, New Delhi.

4

Continuous Stirred Tank Reactor

4.1 INTRODUCTION

The *continuous stirred tank reactor* (CSTR) or *backmix reactor* is a very common processing unit in chemical and polymer industry. The name suggests that it is a tank type reactor in which the contents are well stirred and it runs with continuous flow of reactants as well as products. In order to meet the market specifications, sometimes the product stream is further purified in the downstream section of the reactor employing suitable separation techniques.

The CSTR is normally run at steady state. The main feature of this type of reactor is the complete uniformity of concentration and temperature throughout the reactor due to the perfect mixing. Also, the concentration and temperature of the material leaving the tank must be exactly the same as those of the material in the tank. The CSTR is widely used for large-scale produc-tion, whereas the batch processing is preferred in case of small-scale operation. Moreover, compared to the batch processing, the continuous operation results in more consistent product properties, an improved energy consumption (for example, the exothermic heat can be utilized to heat feed streams) and a higher productivity through the reduction of inactive periods (filling, heating, cooling and emptying).

To ensure the successful operation of a continuous stirred tank reactor, it is very much necessary to understand the dynamic characteristics. Realistic process model can predict the dynamic behaviours of a plant. If there is any fault in the plant, the process engineer may realize it through the discrepancy between the model predictions and plant outputs. Then the necessary corrective measures can be taken accordingly.

The present chapter covers:

- The detailed derivation of a fundamental model for a *non-isothermal* continuous stirred tank reactor.
- The development of the dynamic process simulator for solving the balance equations.
- The concept of multiple steady states (MSS) for the simplified form of the example CSTR.
- The design of a classical proportional integral (PI) control scheme to run the chemical reactor at unstable steady state operating point.
- The modelling of a pH neutralization reactor.

4.2 THE PROCESS AND THE MODEL

4.2.1 Process Description

Schematic of the example CSTR process is depicted in Figure 4.1. The following first-order, exothermic, irreversible chemical reaction takes place in the reactor:

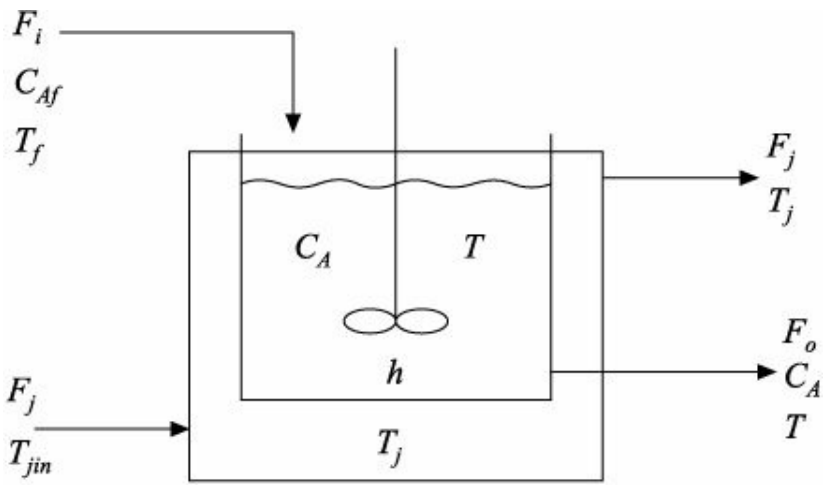

FIGURE 4.1 Schematic representation of the example CSTR.

$$A \xrightarrow{k} B$$

Reactant A is continuously supplied to the reactor with a volumetric flow rate F_i, a molar concentration (or composition) C_{Af} and a temperature T_f. The contents of the reactor are mixed with a motorized agitator. An exit stream, which contains a mixture of both the reactant A and product B, is withdrawn from the reactor continuously with a volumetric flow rate F_O, a composition C_A and a temperature T. To remove the exothermic heat that is generated due to the prescribed chemical reaction, a cooling jacket surrounds the reactor. A coolant stream with a volumetric flow rate F_j and an inlet temperature T_{jin} ($< T$) continuously takes out the heat to maintain the desired reaction temperature.

4.2.2 Mathematical Model

Assumptions

The assumptions made in the development of the reactor model are summarized below.

- The heat losses from the process (well-insulated) to the atmosphere are negligible.
- The mixture density (ρ) and heat capacity (C_p) are assumed constant.
- The coolant is perfectly mixed and therefore the temperature everywhere in the jacket is the same (T_j).
- The mass of the metal walls is negligible so the *thermal inertia* of the metal need not be considered. It is reasonably a good assumption (Luyben, 1990) because the heat capacity of steel is only about 0.1 Btu/(lb_m)(°F), which is an order of magnitude less than that of water.
- There are no spatial variations in concentration, temperature, or reaction rate throughout the reactor.
- The exit stream has the same concentration and temperature as the entire reactor liquid.
- The overall heat transfer coefficient (U_i) is assumed constant.
- No energy balance around the jacket is considered. Indeed, the cooling jacket temperature (T_j) can directly be manipulated in order to control the desired reactor temperature (T).
- The reactor is a flat-bottomed vertical cylinder and the jacket is around the outside and the bottom.

Model development

Total Continuity Equation

For the sample CSTR,

Mass flow rate into the reactor = F_i^ ,

Mass flow rate out of the reactor = F_O^ ,

Rate of production of mass within the reactor = 0, and

Rate of accumulation of mass within the reactor $= \frac{d(\rho V)}{dt} = \frac{d(\rho A_c h)}{dt}$

Here, A_C is the cross-sectional area of the reactor, h the height of reactor liquid and $V(= A_C h)$ the volume of reactor liquid. Substituting all these terms (mass/time) in Equation (3.2), we get

$$\frac{d(\rho V)}{dt} = F_i \rho - F_o \rho \qquad (4.1)$$

We have assumed that the density of liquid inside the reactor is equal to the feed density and is constant in time. Therefore, the above equation becomes:

$$\frac{dV}{dt} = F_i - F_o \qquad \text{[from Equation (1.9)]}$$

Now we need a hydraulic relationship between the reactor holdup (in terms of V or h) and the exit flow rate F_O. We can assume (Stephanopoulos, 1998):

$$F_o \propto \sqrt{V} \qquad \text{[from Equation (1.10)]}$$

For the example CSTR, the above equation can be expressed as:

$$F_o = \sqrt{10 A_c h} \qquad (4.2)$$

Now inserting Equation (4.2) into Equation (1.9) and rearranging, we finally obtain the following total mass balance equation:

$$\frac{dh}{dt} = \frac{F_i}{A_c} - \sqrt{\frac{10h}{A_c}} \qquad (4.3)$$

Component Continuity Equation

We know,

Flow rate of component A into the reactor = $F_i C_{Af}$,

Flow rate of component A out of the reactor = $F_O C_A$,

Rate of generation of component A by chemical reaction = $-(-r_A)V$, and

Rate of accumulation of component A within the reactor = $\frac{d(VC_A)}{dt}$

Here, $(-r_A)$ is the rate of disappearance of species A. Substituting all these terms (mol/time) in the basic balance Equation (3.2), we obtain

$$\frac{d(VC_A)}{dt} = F_i C_{Af} - F_o C_A - (-r_A)V \qquad (4.4)$$

that is,

$$C_A \frac{dV}{dt} + V \frac{dC_A}{dt} = F_i C_{Af} - F_o C_A - (-r_A)V \qquad (4.5)$$

Substituting Equation (1.9) in Equation (4.5) and simplifying, we get

$$\frac{dC_A}{dt} = \frac{F_i}{A_c h}(C_{Af} - C_A) - (-r_A) \qquad (4.6)$$

For the given first-order reaction, $A \rightarrow B$ the rate of disappearance is

$$(-r_A) = kC_A \qquad (4.7)$$

Using the Arrhenius rate Equation (3.12), we obtain

$$(-r_A) = \alpha \exp\left(\frac{-E}{RT}\right) C_A \qquad (4.8)$$

Substituting Equation (4.8) into Equation (4.6), we finally obtain the following component mass balance equation:

$$\frac{dC_A}{dt} = \frac{F_i}{A_c h}(C_{Af} - C_A) - \alpha \exp\left(\frac{-E}{RT}\right) C_A \qquad (4.9)$$

Energy Balance Equation

In the energy balance equation,

Rate of energy input into the reactor = $F_i \rho C_p T_f$,

Rate of energy out of the reactor = $F_o \rho C_p T + U_i A_h (T - T_j)$,

Rate of energy added by the exothermic reaction = $(-\Delta H) V k C_A$

$$= (-\Delta H) V \alpha \exp\left(\frac{-E}{RT}\right) C_A, \text{ and}$$

Rate of accumulation of energy = $\frac{d(V \rho C_p T)}{dt}$.

Here, A_h is the heat transfer area and $(-\Delta H)$ represents the heat of reaction. Using Equation (3.15), we get the following form:

$$\frac{d(V \rho C_p T)}{dt} = F_i \rho C_p T_f - F_o \rho C_p T - U_i A_h (T - T_j) + (-\Delta H) V \alpha \exp\left(\frac{-E}{RT}\right) C_A \qquad (4.10)$$

Using Equation (1.9) and simplifying, we get

$$\frac{dT}{dt} = \frac{F_i}{A_c h}(T_f - T) + \left(\frac{-\Delta H}{\rho C_p}\right) \alpha \exp\left(\frac{-E}{RT}\right) C_A - \frac{U_i A_h}{\rho C_p A_c h}(T - T_j) \qquad (4.11)$$

This is the final form of the energy balance equation.

We have assumed that the example CSTR is a flat-bottomed vertical cylinder and the jacket is around the outside and the bottom. Therefore, the heat transfer area is

$$A_h = (\pi/4)d^2 + \pi dh \qquad (4.12)$$

or

$$A_h = A_c + \pi dh \qquad (4.13)$$

where d is the diameter of the cylindrical reactor. Many reactors are such that the jacket is only around the outside, not around the bottom of the reactor, and then

$$A_h = \pi dh \qquad (4.14)$$

4.2.3 Dynamic Simulation

The mathematical model of the non-isothermal continuous stirred tank reactor is composed of the mass and energy balance equations, plus accessory equations for the calculation of rate of reaction and heat transfer area. Among the three balance ordinary differential equations (ODEs), Equation (4.3) represents the total or overall mass balance, Equation (4.9) represents the component or partial mass balance, and Equation (4.11) represents the energy or heat balance. The supporting Equation (4.8) for rate of reaction and Equation (4.13) for heat transfer area can directly be substituted into the modelling equations.

The steady state and operating conditions are reported in Table 4.1. To solve the ODEs, the second-order Runge–Kutta technique (details in Chapter 2) has been used. The process simulator is developed using Fortran (90) language and is given in Program 4.1. In the program, another option to solve the ODEs using the Euler method is also provided. In the simulator, the jacket temperature (T_j) and feed flow rate or flow rate of reactant (F_i) are considered as input variable and their values are provided at each time step. Actually, the jacket temperature and flow rate of reactant are usually considered as manipulated variable for controlling the reactor temperature and liquid height in the reactor respectively. Note that in order to observe the dynamic process response, the value of feed temperature (T_f) (disturbance or load variable) has been changed in the simulator from 25 (steady state value) to 20°C.

Table 4.1 Steady state and operating conditions

A_c	cross-sectional area of the reactor, m^2	
C_A	concentration of reactant A in the exit stream, $kmol/m^3$	4.2822
C_{Af}	concentration of A in the feed stream, $kmol/m^3$	8.56303
d	diameter of the cylindrical reactor, m	10.0
E	activation energy, kcal/kmol	2.335
F_i	volumetric feed flow rate, m^3/h	11843.0
h	height of the reactor liquid, m	10.0
$(-\Delta H)$	heat of reaction, kcal/kmol	2.335201
R	universal gas constant, kcal/(kmol)(K)	5960.0
ρC_p	frequency factor, h^{-1}	1.987
T	multiplication of mixture density and heat capacity, $kcal/(m^3)(°C)$	34930800.0
T_f	reactor temperature, °C	500.0
T_j	feed temperature, °C	38.17771
U_i	jacket temperature, °C	25.0
	overall heat transfer coefficient, $kcal/(m^2)(°C)(h)$	25.0
	Integration time interval = 0.005 h	70.0

PROGRAM 4.1 *Dynamic CSTR*

```
! Notations

! AC = Cross sectional area
```

```
! AH = Heat transfer area
! Ca = Concentration of reactant A in the exit stream
! Caf = Concentration of reactant A in the feed stream
! d = Diameter of the reactor
! Fi = Feed flow rate
! h = Height of reactor liquid
! Me = Ui/(Row*Cp)
! T = Reactor temperature
! Tf = Feed temperature
! Tj = Jacket temperature
! X = (-H*Z)/(Row*Cp)
! Y = E/R
! Z = Frequency factor

PROGRAM CSTR
IMPLICIT NONE

! Declaration
!————————

INTEGER::m
INTEGER,PARAMETER::n=10000
REAL::Tf,AH
REAL,PARAMETER::d=2.335,AC=4.2822,Caf=10.0,Me=0.14
REAL,DIMENSION(n)::T,Ca,h,Tj,Fi,Time
REAL::T0,T1,Ca0,Ca1,h0,h1
REAL::k1,k11,k12,k2,k21,k22
REAL,PARAMETER::Y=5960.24157,dt=0.005
INTEGER,PARAMETER::Z=34930800,X=416375136

OPEN(UNIT=1,FILE="CSTR.DAT")
! Initialization
!————————

T(1)= 38.17771
Ca(1)= 8.56303
h(1)= 2.335201

Time(1)=0.00

!——————————Starting of main loop————————————————!
!———————————————————————————————————————————————!

DO m=1,n
Tj(m)=25.0
Fi(m)=10.0
Tf=20.0

!————————————Starting of Euler method——————————!

! AH=Ac+3.14159*d*h(m)

! T(m+1)=T(m)+dt*((X*Ca(m)*exp(-Y/(273.0+T(m))))-(((Me*AH)/
! &  (AC*h(m)))*(T(m)-Tj(m)))+((Tf-T(m))*(Fi(m)/(AC*h(m)))))

! Ca(m+1)=Ca(m)+dt*(((Fi(m)/(AC*h(m)))*(Caf-Ca(m)))-(Z*Ca(m)*
! & exp(-Y/(273.0+T(m)))))

! h(m+1)=h(m)+dt*((Fi(m)/AC)-((10.0*h(m)/AC)**0.5))

!————————————End of Euler method——————————————!

!————————Starting of second-order Runge-Kutta method———————!
```

```
T0=T(m)
Ca0=Ca(m)
h0=h(m)

k1=(X*Ca0*exp(-Y/(273.0+T0)))-(((Me*(Ac+3.14159*d*h0))/
&  (AC*h0))*(T0-Tj(m)))+((Tf-T0)*(Fi(m)/(AC*h0)))

k11=((Fi(m)/(AC*h0))*(Caf-Ca0))-(Z*Ca0*exp(-Y/(273.0+T0)))

k12=(Fi(m)/AC)-((10.0*h0/AC)**0.5)

!------

T1=T(m)+(k1*dt/2)
Ca1=Ca(m)+(k11*dt/2)
h1=h(m)+(k12*dt/2)

k2=(X*Ca1*exp(-Y/(273.0+T1)))-(((Me*(Ac+3.14159*d*h1))/
&  (AC*h1))*(T1-Tj(m)))+((Tf-T1)*(Fi(m)/(AC*h1)))

k21=((Fi(m)/(AC*h1))*(Caf-Ca1))-(Z*Ca1*exp(-Y/(273.0+T1)))

k22=(Fi(m)/AC)-((10.0*h1/AC)**0.5)

!------
T(m+1)=T(m)+(dt*k2)

Ca(m+1)=Ca(m)+(dt*k21)

h(m+1)=h(m)+(dt*k22)
!----------End of second-order Runge-Kutta method----------!

Time(m+1)=Time(m)+dt

PRINT*,Time(m),T(m),Ca(m),h(m)

WRITE(1,FMT=100)Time(m),T(m),Ca(m),h(m)

100 FORMAT(1X,4(2X,F10.5))

END DO

!----------End of main loop----------!

END PROGRAM CSTR
```

4.3 MULTIPLE STEADY STATES (MSS)

4.3.1 Representative Process

To analyze the steady state multiplicities, the CSTR problem discussed above is further simplified. Additionally, a constant reactor volume (V) of 10 m^3 is assumed. It implies that $F_i = F_o (= F)$. Accordingly, the model consisting of the component continuity and energy balance equation finally gets the following form (Jana et al., 2005):

$$\frac{dC_A}{dt} = \frac{F}{V}(C_{Af} - C_A) - \alpha \exp\left(\frac{-E}{RT}\right) C_A \qquad (4.15)$$

$$\frac{dT}{dt} = \frac{F}{V}(T_f - T) + \left(\frac{-\Delta H}{\rho C_p}\right) \alpha \exp\left(\frac{-E}{RT}\right) C_A - \frac{U_i A_h}{V \rho C_p}(T - T_j) \qquad (4.16)$$

where $\frac{U_i A_h}{V}$ = 150 kcal/m^3.°C.h. Note that Program 4.1 can easily be modified and used to simulate the model structure of this constant volume CSTR process.

4.3.2 Steady State Solution

At steady state, these two modelling equations become:

$$\frac{dC_{AS}}{dt} = 0 = \frac{F}{V}(C_{AfS} - C_{AS}) - \alpha \exp\left(\frac{-E}{RT_S}\right) C_{AS} \qquad (4.17)$$

$$\frac{dT_S}{dt} = 0 = \frac{F}{V}(T_{fS} - T_S) + \left(\frac{-\Delta H}{\rho C_p}\right) \alpha \exp\left(\frac{-E}{RT_S}\right) C_{AS} - \frac{U_i A_h}{V \rho C_p}(T_S - T_{jS}) \qquad (4.18)$$

Subscript '*S*' is used to represent the steady state. To solve the steady state model consisting of Equations (4.17) and (4.18), all parameters and variables except for T and C_A should be specified. An iterative convergence method (see Chapter 2) can be used for finding T_S and C_{AS}.

When selecting the initial guess values for the numerical technique, we must have some idea about the probable range of solutions. In the present case, T and C_A have to be initialized. We know that the feed concentration of component A is 10 kmol/m^3 and this value can be used as the upper limit for C_A. The lower limit is obviously zero. So the probable range is $0 < C_A < 10$. Again, if there is no reaction occurred in the tank, the lower bound for reactor temperature will be 25°C since both the feed and jacket temperatures are 25°C.

Depending on the initial guess values for temperature and concentration, the steady state model provides three sets of solutions. The results are summarized in Table 4.2. It should be noted that other initial guesses do not lead to any other solutions.

Table 4.2 Steady state operating points

C_A (guess) (kmol/m^3)	T (guess) (°C)	C_{AS} (kmol/m^3)	T_S (°C)	Steady state point
9	26	8.5615	38.2	*SS*1
5	77	5.518	66.1	*SS*2
1	150	2.359	95.1	*SS*3

4.3.3 MSS Behaviour

In the above, it is found that the sample process has three steady states. In the present discussion, we wish to observe how multiple steady states might arise.

Rearranging Equation (4.17), we get

$$C_{AS} = \frac{\frac{F}{V} C_{AfS}}{\frac{F}{V} + \alpha \exp\left(\frac{-E}{RT_S}\right)} \qquad (4.19)$$

Similarly, Equation (4.18) yields:

$$T_{jS} = T_S + \frac{F\rho C_p(T_S - T_{fS}) - (-\Delta H)V\alpha C_{AS}\exp\left(\frac{-E}{RT_S}\right)}{U_i A_h} \qquad (4.20)$$

Again, Equation (4.18) can be rewritten as:

$$\frac{F}{V}(T_S - T_{fS}) + \frac{U_i A_h}{V\rho C_p}(T_S - T_{jS}) = \left(\frac{-\Delta H}{\rho C_p}\right)\alpha\exp\left(\frac{-E}{RT_S}\right)C_{AS} \qquad (4.21)$$

Multiplying both sides by $V\rho C_p$, we obtain

$$\underbrace{F\rho C_p(T_S - T_{fS}) + U_i A_h(T_S - T_{jS})}_{\text{Heat removed } (Q_r)} = \underbrace{(-\Delta H)V\alpha C_{AS}\exp\left(\frac{-E}{RT_S}\right)}_{\text{Heat generated } (Q_g)} \qquad (4.22)$$

where

$$Q_g = (-\Delta H)V\alpha C_{AS}\exp\left(\frac{-E}{RT_S}\right) \qquad (4.23)$$

$$\begin{aligned} Q_r &= F\rho C_p(T_S - T_{fS}) + U_i A_h(T_S - T_{jS}) \\ &= (F\rho C_p + U_i A_h)T_S + (-F\rho C_p T_{fS} - U_i A_h T_{jS}) \end{aligned} \qquad (4.24)$$

From the above analysis, we notice that the heat generated by the exothermic reaction is a non-linear function of reactor temperature [Equation (4.23)]. On the other hand, the heat removed by flow and heat exchange is a linear function of reactor temperature [Equation (4.24)]. The slope of the straight line is ($F\rho C_p + U_i A_h$) and the intercept is ($-F\rho C_p T_{fS} - U_i A_h T_{jS}$). It is true that any change in feed or jacket temperature affects the intercept, but not the slope. However, changes in $U_i A_h$ or feed rate shift both the slope and intercept.

Heat generation and heat removal curves

To investigate the interesting behaviour of the constant volume CSTR, we first attempt to produce the heat generation and heat removal curves. For this purpose, the reactor temperature is considered as an independent variable and it is varied typically from 27 to 107°C with an increment of 2°C. As mentioned previously, if there is no reaction at all, the lower bound for reactor temperature will be 25°C. However, in the simulation, the starting temperature of 27°C is considered. At every temperature step, the concentration is determined from Equation (4.19) keeping the values of all other parameters and variables fixed. Then the corresponding Q_g and Q_r are calculated from Equations (4.23) and (4.24), respectively.

A computer code (Program 4.2) is written with the Fortran 90 language and the simulation results obtained are plotted in Figure 4.2. It is a fact that at steady state, the heat released by the reaction must be equal to the heat removed. Three steady states, *SS*1, *SS*2 and *SS*3, as reported in Table 4.2 are marked in Figure 4.2.

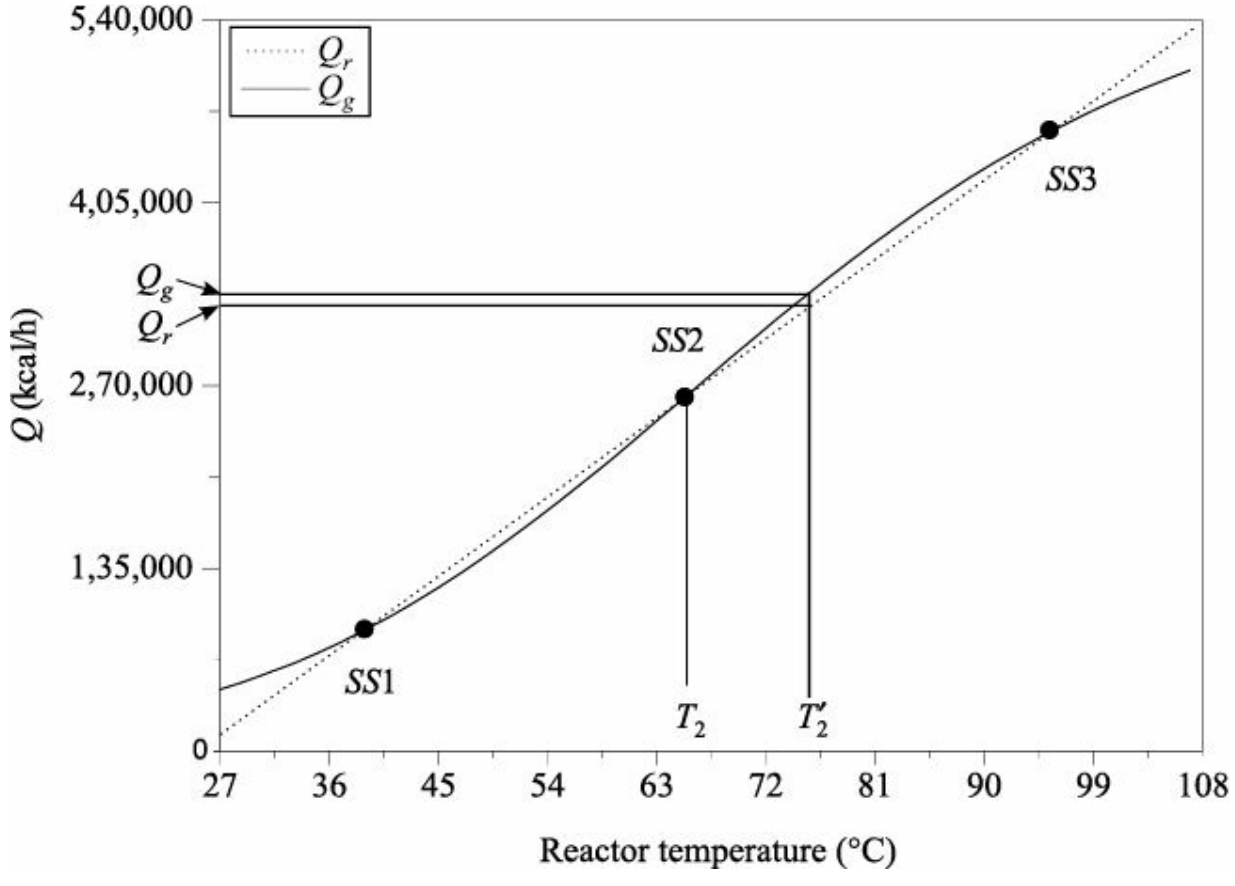

FIGURE 4.2 Multiple steady states.

Among the three steady states, the intermediate one (*SS*2) is unstable and the other two (*SS*1 and *SS*3) are stable steady states. To understand this point, let us consider the CSTR operated at the temperature T_2 and the concentration C_{A2} that corresponds to this temperature. At a particular instant, it is supposed that the feed temperature (T_f) increases causing an increase in the reactor temperature, say $T¢_2$. Figure 4.2 shows that at $T¢_2$ the heat generated by the exothermic reaction (Q_g) is higher than the heat removed (Q_r). It leads to increase the reactor temperature and consequently to increase the rates of reaction. Increased rates of reaction produce larger amounts of heat released by the reaction, which in turn lead to higher temperatures. By this way, the reactor temperature eventually reaches the value of stable steady state point *SS*3. Similarly, if T_f decreases, the reactor temperature will finally reach the value of stable steady state *SS*1. By contrast, if the reactor operates at *SS*1 or *SS*3 and we perturb the operation of the reactor, it will return naturally back to *SS*1 or *SS*3 from which it started.

PROGRAM 4.2 *Heat Generation and Heat Removal*

```
! Notations
! f = (-H*V*Z)/(Ui*Ah)
! Y = E/R
! Z = Frequency factor
! Qr = heat removed
! Qg = heat generated

Program HEAT_SS
IMPLICIT NONE

! Declaration
!————————

INTEGER::m
```

```
INTEGER,PARAMETER::n=41,dt=2,f=1387917120,Z=34930800
REAL*8,DIMENSION(n)::Ca,T,Qr,Qg
REAL,PARAMETER::Y=5960.24157

OPEN(Unit=1,File="Heat.dat")

T(1)=27.00

!————————————————

DO m=1,n
Ca(m)=((10)/(1+Z*EXP(-Y/(273+T(m)))))
Qr(m)=(1500+5000)*T(m)-(1500*25)-(5000*25)
Qg(m)=1500*Ca(m)*f*(EXP(-Y/(273+T(m))))
T(m+1)=T(m)+dt

PRINT*,T(m),Ca(m),Qr(m),Qg(m)
WRITE(1,FMT=100)T(m),Ca(m),Qr(m),Qg(m)
100 FORMAT (1X,4(2X,F15.7))

END DO
END FILE 1
REWIND 1
CLOSE(2)
END PROGRAM HEAT_SS
```

Multiplicity curve for reactor temperature and concentration

To produce the multiplicity curve for reactor temperature and concentration, the reactor temperature is varied from 27 to 107°C, and the corresponding concentration and jacket temperature have been calculated from Equations (4.19) and (4.20), respectively. To carry out this job, a computer code (Program 4.3) has been developed using the Fortran 90 language. The simulation results are plotted accordingly. Figure 4.3 describes the steady state reactor temperature as a function of jacket temperature, whereas Figure 4.4 demonstrates the steady state reactor concentration as a function of T_j.

PROGRAM 4.3 *Multiplicities in Reactor Temperature and Concentration*

```
! Notations
! f = (-H*V*Z)/(Ui*Ah)
! Y = E/R
! Z = Frequency factor

Program Multiple_SS
IMPLICIT NONE

! Declaration
!————————

INTEGER::m
INTEGER,PARAMETER::n=41,dt=2,f=1387917120,Z=34930800
REAL::Ca(n),T(n),Tj(n)
REAL,PARAMETER::Y=5960.24157

OPEN(Unit=1,File="multi_ss.dat")

T(1)=27.00

!————————————————————

DO m=1,n
Ca(m)=((10)/(1+Z*EXP(-Y/(273+T(m)))))
Tj(m)=T(m)+(10.0/3.0)*(T(m)-25)-f*EXP(-Y/(273+T(m)))*Ca(m)
T(m+1)=T(m)+dt
```

```
PRINT*,T(m),Tj(m),Ca(m)
WRITE(1,FMT=100)T(m),Tj(m),Ca(m)
100 FORMAT (1X,3(2X,F11.5))
END DO
END FILE 1
REWIND 1
CLOSE(2)
END PROGRAM MULTIPLE_SS
```

To explain the hysteresis behaviour (Bequette, 1998) observed in Figure 4.3, let us start the process with a low T_j that corresponds to a low operating temperature (point 1). The reactor temperature increases smoothly with the increase of jacket temperature until point 4 (low temperature limit point) is reached. If the jacket temperature is slightly increased further, the reactor temperature jumps (also called *ignition*) to a high temperature (point 8). Beyond point 8, the reactor temperature increases smoothly.

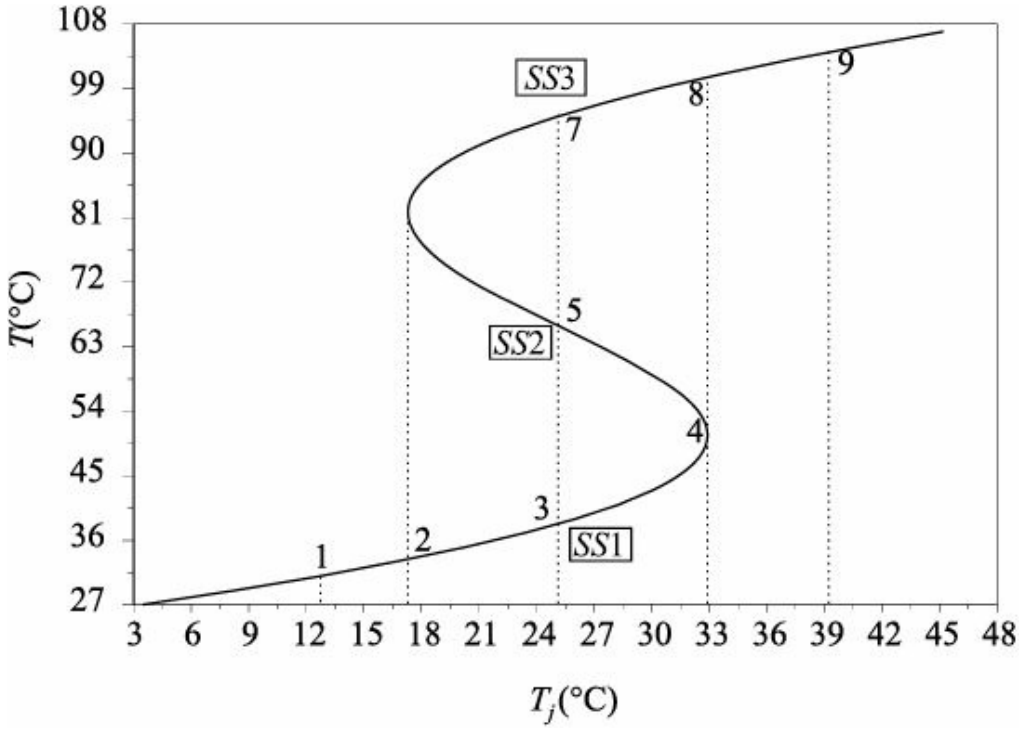

FIGURE 4.3 Steady state reactor temperature vs. jacket temperature.

Contrast the typical behaviour explained above (starting at a low jacket temperature) with that of the case of starting at a high T_j. Now start the process with a high temperature operating point (point 9). The reactor temperature decreases smoothly up to point 6 through point 8 and then point 7 as T_j is decreased. As the jacket temperature is decreased slightly lower than point 6 (high temperature limit point), the reactor temperature drops (also called *extinction*) to a low temperature (point 2). Further decreases in T_j lead to small decreases in reactor temperature.

This hysteresis behaviour is also referred to as *ignition-extinction* behaviour. We can also discuss this interesting behaviour with Figure 4.4. It is worthy to mention that the region between two limit points (points 4 and 6) appears to be unstable because the reactor does not appear to operate in this region. Remember that the unstable steady state point *SS*2 appears in this region.

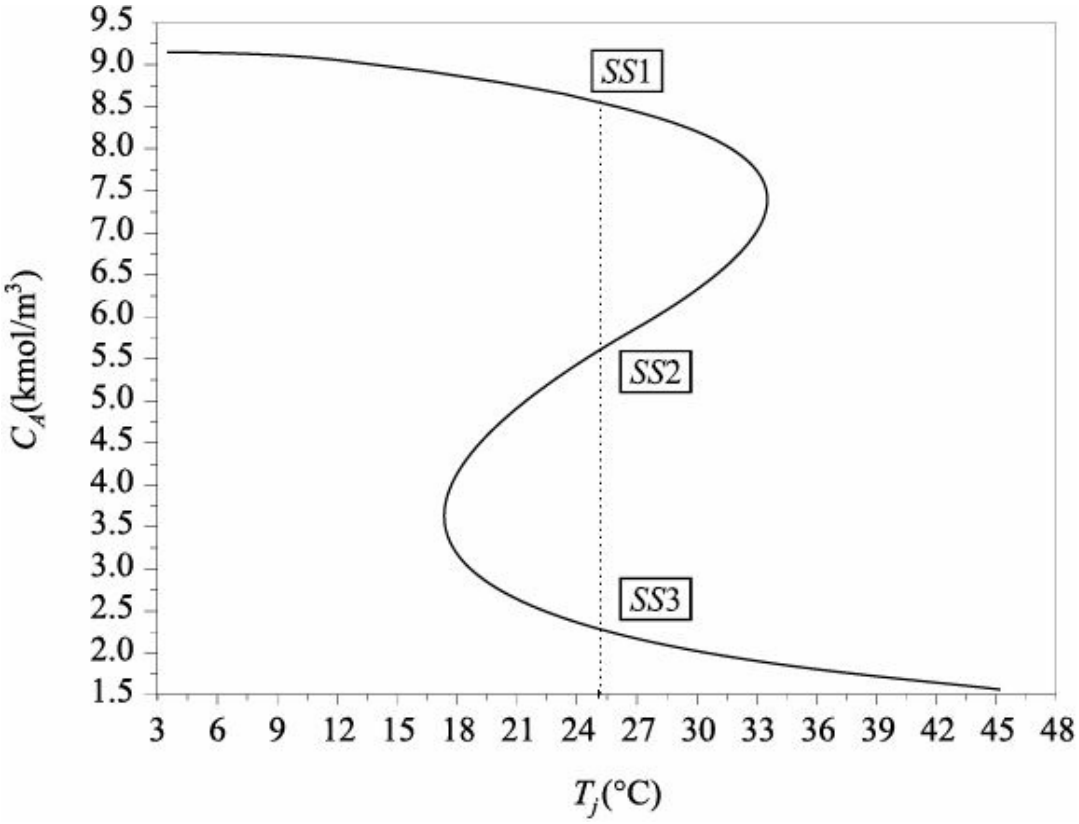

FIGURE 4.4 Steady state concentration vs. jacket temperature.

4.3.4 Process Control

The presence of steady state multiplicities is an interesting feature of the sample reactor. The reactor at minimum steady state temperature (38.2°C) is stable but is of course of no economic interest due to the low conversion. It should be better to operate the reactor at the high temperature steady state operating point (*SS*3) for high conversion. However, sometimes the high temperature steady state may be very high, causing unsafe conditions, destroying the catalyst for a catalytic reactor, degrading the product, and so on. In such a situation, the reactor is operated preferably at the unstable steady state operating point (*SS*2) with medium conversion.

Open-loop response

Previously we determined three steady state solution points while solving the process model. Recall that point *SS*2 corresponds to an unstable steady state operating point. Now we wish to study the dynamic characteristics of the reacting system. For this purpose, three initial conditions for two state variables (C_A and T) have been chosen arbitrarily. The summary of the dynamic simulation results is reported in Table 4.3. As mentioned previously, it is straight-forward to develop the dynamic simulation code for this constant volume CSTR with a little modification of Program 4.1.

Table 4.3 Summary of the open-loop response

C_A (guess) (kmol/m^3)	T (guess) (°C)	*Observation*
9	26	State variables converge to *SS*1 (see Figure 4.5)
5	50	State variables converge to *SS*1 (see Figure 4.6)
1	120	State variables converge to *SS*3 (see Figure 4.7)

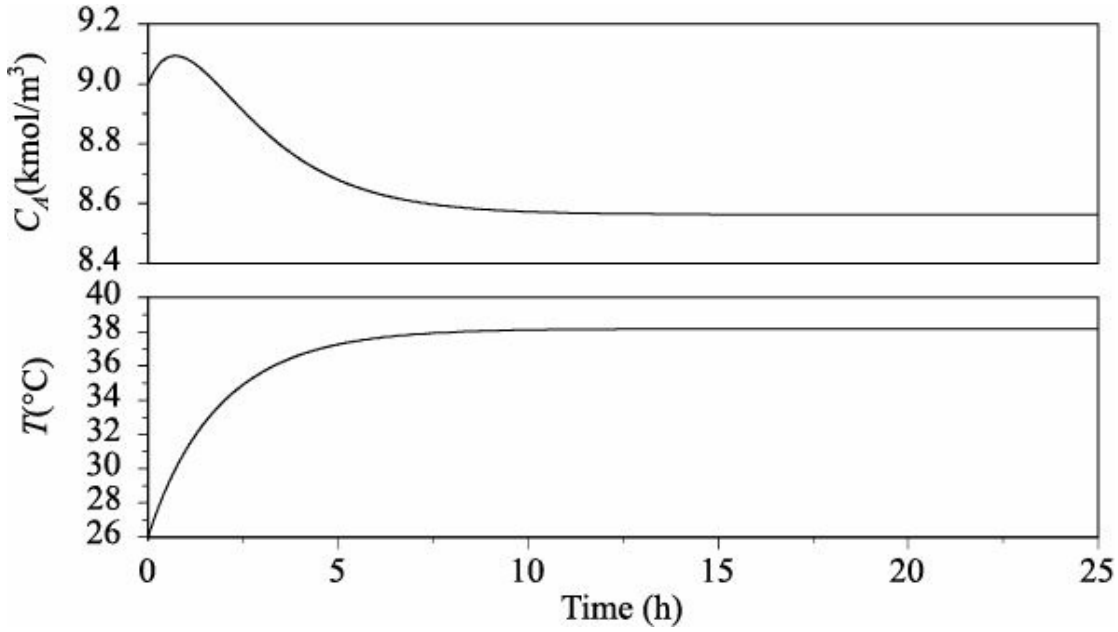

FIGURE 4.5 Dynamic response with C_A (guess) = 9 and T (guess) = 26.

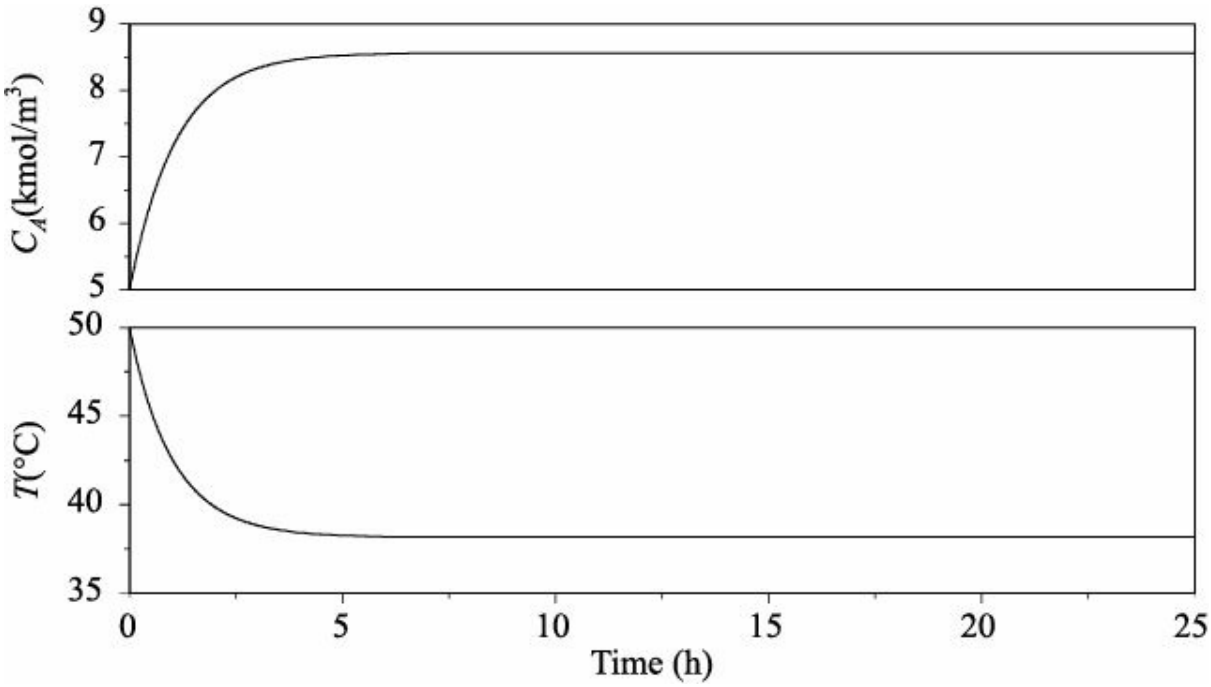

FIGURE 4.6 Dynamic response with C_A (guess) = 5 and T (guess) = 50.

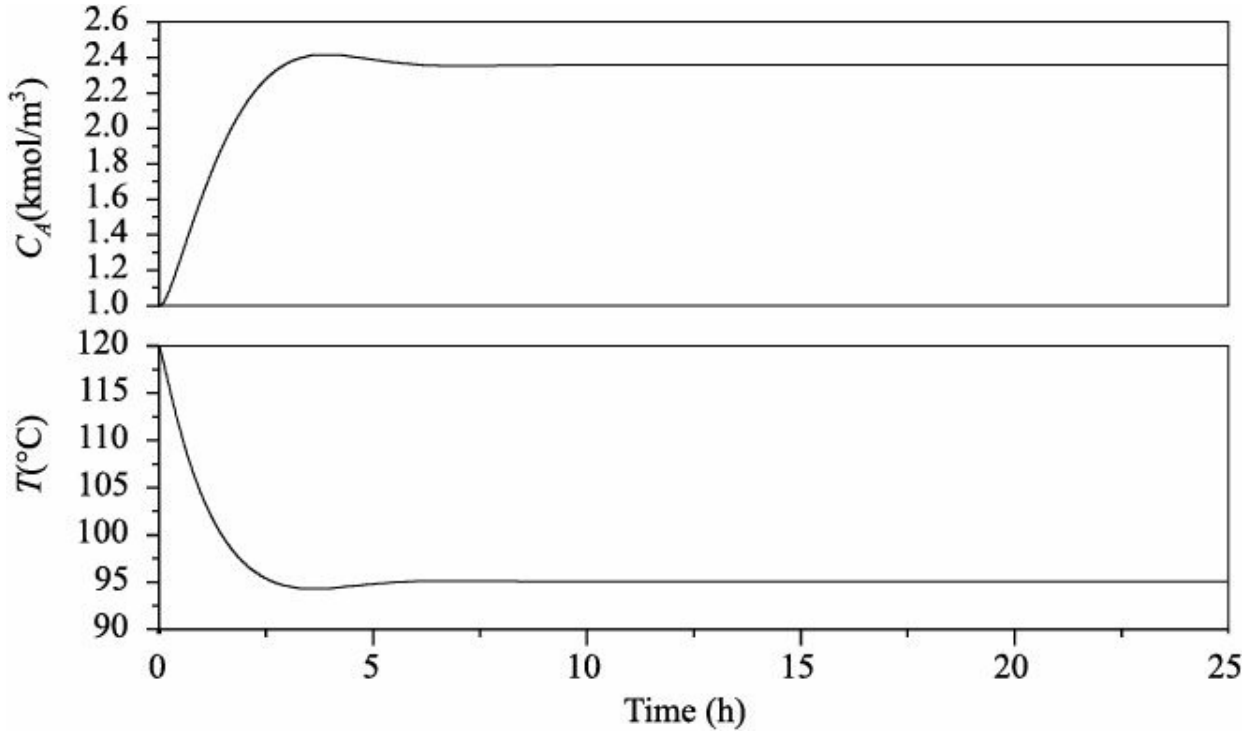

FIGURE 4.7 Dynamic response with C_A (guess) = 1 and T (guess) = 120.

It is evident from the open-loop process response that even if the initial condition is close to the intermediate temperature steady state, the temperature always converges to either the low temperature or high temperature steady state, but not the intermediate temperature steady state. We discussed earlier the rationale behind the operation of the reactor at the unstable steady state operating point (*SS*2). It is now clear to us that the operation at unstable point can only be performed by the employment of a control algorithm and the following discussion covers the closed-loop reactor control.

Closed-loop response

A single-loop PI control scheme is designed to maintain the reactor temperature (T) at its desired set point (T_{sp}) by the manipulation of coolant jacket temperature (T_j). The standard form of the classical PI controller is given as:

$$T_j = T_{jS} + K_c\left(e_t + \frac{1}{\tau_i}\int e_t\, dt\right), \quad \text{where } e_t = T_{sp} - T \tag{4.25}$$

Values of the controller parameters used are as follows: K_c = 100, τ_i = 20 h. The jacket temperature is bounded as $15 \leq T_j \leq 65$°C.

Figure 4.8 displays the servo performance for three consecutive set point step changes in reactor temperature (38.2 → 66.1, 66.1 → 95.1 and 95.1 → 66.1). What is most important is that the PI controller is able to stabilize the process at the unstable operating point. But the control actions provide large overshoot and a slow approach to reach the target temperature. To tackle this situation efficiently, a high quality control system is required to implement. Interested readers can consult the paper by Jana et al. (2005) for the advanced model-based control of the example system.

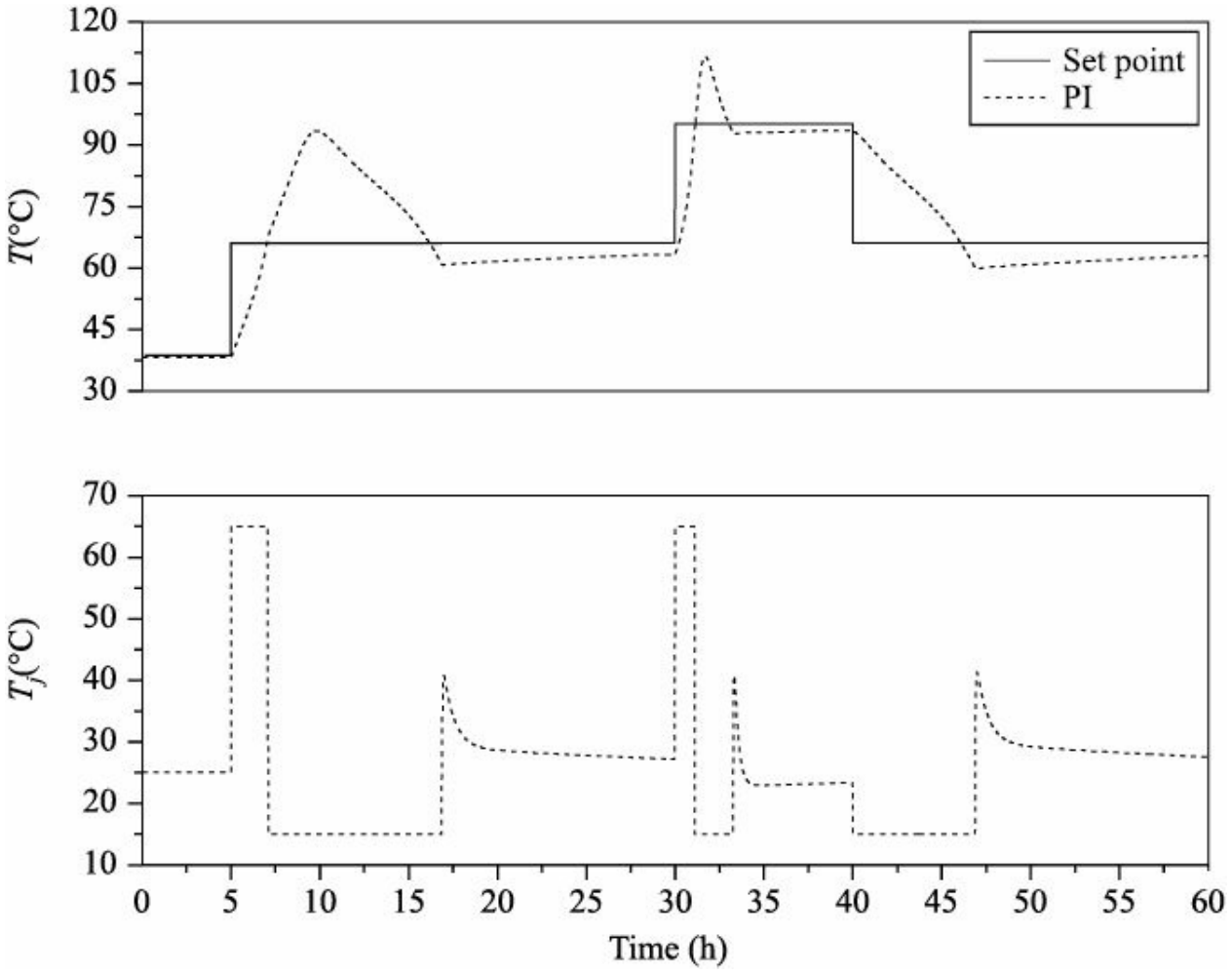

FIGURE 4.8 Servo performance of the PI control algorithm.

4.4 PH NEUTRALIZATION REACTOR: A CSTR EXAMPLE

4.4.1 Process Description

The control of pH is quite common in the chemical process and biotechnological industries. For instance, the pH of effluent streams from wastewater treatment plants should be maintained within stringent environmental limits. When a stream is acidic, some source of OH^- ions (e.g., NaOH) is used to bring the pH up to the specification of seven. Here, an example is taken to know more about a pH process.

Figure 4.9 depicts a CSTR, where an acidic solution having a volumetric flow rate, F_A, with a composition, $x_{1,i}$, is neutralized with an alkaline solution having a volumetric flow, F_B, with a composition of base, $x_{2,i}$, and buffer agent, $x_{3,i}$.

We must know that the resistance of a solution to changes in H^+ ion concentration upon the addition of small amounts of acid or alkali is referred to as *buffer action* (Rakshit, 1993). Solutions that possess such properties are called *buffer solutions* or simply, *buffers*. Usually, the buffer solutions consist of mixtures of solutions of a weak acid or base and its salt.

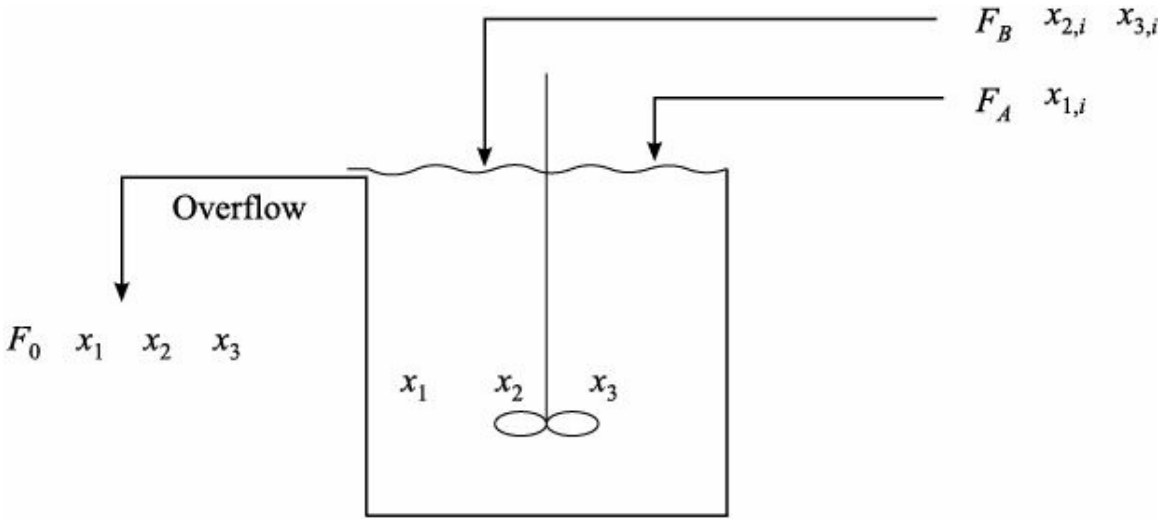

FIGURE 4.9 The pH neutralization reactor.

4.4.2 Mathematical Model

Assumptions

The model (Galan et al., 2000) of a pH neutralization reactor is developed based on the following assumptions:

- The tank is assumed to be perfectly mixed and isothermal.
- The reactor volume is maintained constant using an overflow weir.
- The chemical and electrical equilibrium conditions are prevailed due to the fact that the reaction rates in acid-base systems between dissolved compounds are extremely high.
- The acid used is strong acid, and the base and buffer agents are both highly soluble salts.
- The solution in the reactor is electrically neutral.

Reactions

The neutralization reaction takes place between a strong acid (say, HA) and a strong base (say, BOH) in the presence of a buffer agent (say, BX). The system experiences the following chemical reactions:

$$HA \xleftrightarrow{K_A} H^+ + A^- \qquad (4.26a)$$

$$BOH \xleftrightarrow{K_B} B^+ + OH^- \qquad (4.26b)$$

$$BX \xleftrightarrow{K_C} B^+ + X^- \qquad (4.26c)$$

$$H_2O + X^- \xleftrightarrow{K_D} HX + OH^- \qquad (4.26d)$$

$$H_2O \xleftrightarrow{K_E} H^+ + OH^- \qquad (4.26e)$$

First three equations (i.e., 4.26a–c) represent the acid, base and buffer dissociation, respectfully. Next reaction (4.26d) defines the buffer action that works as a weak base and final reaction (4.26e) represents the water dissociation. The following chemical equilibrium conditions are obtained by supposing the high reaction rates of the acid-base reactions (instantaneous):

$$K_A = \frac{[H^+][A^-]}{[HA]} \qquad (4.27a)$$

$$K_B = \frac{[B^+][OH^-]}{[BOH]} \qquad (4.27b)$$

$$K_C = \frac{[B^+][X^-]}{[BX]} \qquad (4.27c)$$

$$K_D = \frac{[HX][OH^-]}{[X^-]} \qquad (4.27d)$$

$$K_E = [OH^-][H^+] \qquad (4.27e)$$

In the above expressions of equilibrium constants, the concentration of any species, say s, is represented by [s].

For water dissociation, the equilibrium constant is given in terms of activity (denoted by a) as:

$$K_E = \frac{a_{H^+} \times a_{OH^-}}{a_{H_2O}} \qquad (4.28)$$

The activity of water, a_{H_2O} in the pure state or in dilute solution is constant and is taken as unity. Therefore, for the dilute acid-base solution in the example reactor, we have:

$$K_E = a_{H^+} \times a_{OH^-} \qquad (4.29)$$

Expressing activity as the product of concentration and activity coefficient (γ), we obtain:

$$K_E = [H^+]\gamma_{H^+}\,[OH^-]\gamma_{OH^-} \qquad (4.30)$$

In dilute solutions or pure water, the activity coefficients γ_{H^+} and γ_{OH^-} are almost unity. As a result, Equation (4.30) yields Equation (4.27e).

At this point, it is important to mention that usually the acid-base systems are modelled by the use of *invariant* chemical species. The term *invariant* is used for process state variables, which are not affected by the chemical reactions occurring in the system (Fjeld et al., 1974). For the example system, the invariant chemical species are selected as material balances on the irreducible ions associated with the acid (A^-), base (B^+) and buffer agent (X^-).

Charge balance: The pH equation

Supposing the electroneutrality condition, the charge balance establishes that the net charge in an ionic solution is zero. The charge balance yields:

$$[H^+] + [B^+]_{total} - [A^-] - [OH^-] - [X^-] = 0 \qquad (4.31)$$

The sources of B^+ are the base as well as the buffer agent. Accordingly,

$$[B^+]_{total} = [B^+]_{base} + [B^+]_{buffer} \qquad (4.32)$$

The invariant species for the example system are given below:

$$x_1 = [HA] + [A^-] \qquad (4.33a)$$

$$x_2 = [BOH] + [BX] + [B^+] \qquad (4.33b)$$

$$x_3 = [BX] + [HX] + [X^-] \qquad (4.33c)$$

Notice that the invariant species [(4.33a), (4.33b) and (4.33c)] are associated with the species A (acid), B (base) and X (buffer), respectively. Since HA is considered as a strong acid, it is completely dissociated. It implies,

$$[HA] = 0$$

$$= K_A \quad 0 \quad \dashv|$$

Similarly, the base and buffer agents are both highly soluble. Therefore,

$$[BOH] = 0$$

$$= K_B \quad 0 \quad \dashv|$$

and

$$[BX] = 0$$

$$= K_C \quad 0 \quad \dashv|$$

Now Equations (4.33a–c) give:

$$x_1 = [A^-] \qquad (4.34a)$$

$$x_2 = [B^+] \qquad (4.34b)$$

$$x_3 = [HX] + [X^-] \qquad (4.34c)$$

We can rewrite Equation (4.32) as:

$$[B^+]_{total} = [B^+]_{from\ BOH} + [B^+]_{from\ BX} \qquad (4.35)$$
$$= x_2 + x_3$$

The second right-hand term in the above equation indicates the same number of moles of BX added, i.e., [HX] + [X$^-$]. Substituting [HX] from Equation (4.27d) into Equation (4.34c) and rearranging, we obtain:

$$[X^-] = \frac{x_3}{1 + \frac{K_D}{[OH^-]}} \qquad (4.36)$$

Substituting $[B^+]_{total}$ from Equation (4.35), [A$^-$] from Equation (4.34a), [OH$^-$] from Equation (4.27e) and [X$^-$] from Equation (4.36) into Equation (4.31), we obtain:

$$[H^+] + x_2 + x_3 - x_1 - \frac{K_E}{[H^+]} - \frac{x_3}{1 + \frac{K_D[H^+]}{K_E}} = 0 \qquad (4.37)$$

This correlation is referred to as the *pH equation*. Once [H$^+$] is known, the pH can be determined from the following expression:

$$\mathrm{pH} = -\log_{10}[\mathrm{H}^+] \qquad (4.38)$$

Material balance equations

Total material balance

Since the reactor volume is assumed constant, the overall balance yields for the case of constant density:

$$F_A + F_B = F_o \qquad (4.39)$$

Component material balance

It is easy to write for acid:

$$V\frac{dx_1}{dt} = F_A x_{1,i} - F_o x_1 \qquad (4.40)$$

Substituting Equation (4.39) and rearranging, we get:

$$\frac{dx_1}{dt} = \frac{F_A}{V}(x_{1,i} - x_1) - \frac{F_B}{V}x_1 \qquad (4.41)$$

In the same fashion, we obtain two component material balance equations, respectively, for base and buffer:

$$\frac{dx_2}{dt} = \frac{F_B}{V}(x_{2,i} - x_2) - \frac{F_A}{V}x_2 \qquad (4.42)$$

$$\frac{dx_3}{dt} = \frac{F_B}{V}(x_{3,i} - x_3) - \frac{F_A}{V}x_3 \qquad (4.43)$$

The dynamic model structure of the representative pH neutralization reactor system derived using conservation equations and equilibrium relations is summarized below:

Model of the pH neutralization reactor

$$F_A + F_B = F_o \qquad (4.39)$$

$$\frac{dx_1}{dt} = \frac{F_A}{V}(x_{1,i} - x_1) - \frac{F_B}{V}x_1 \qquad (4.41)$$

$$\frac{dx_2}{dt} = \frac{F_B}{V}(x_{2,i} - x_2) - \frac{F_A}{V}x_2 \qquad (4.42)$$

$$\frac{dx_3}{dt} = \frac{F_B}{V}(x_{3,i} - x_3) - \frac{F_A}{V}x_3 \qquad (4.43)$$

$$[\mathrm{H}^+] + x_2 + x_3 - x_1 - \frac{K_E}{[\mathrm{H}^+]} - \frac{x_3}{1 + \frac{K_D[\mathrm{H}^+]}{K_E}} = 0 \qquad (4.37)$$

with

$$\mathrm{pH} = -\log_{10}[\mathrm{H}^+] \qquad (4.38)$$

In the present study, the computer simulation of the reactor model is not covered. A set of model parameters is given in Table 4.4 (Galan et al., 2000) for interested readers for simulation. The pH system for which the data are given receives an acid stream (HCL solution) and an alkaline stream (NaOH and $NaHCO_3$ solution).

Table 4.4 Model parameters for the pH system

Parameter	*Value*
$x_{1,i}$	0.0012 mol/l HCL
$x_{2,i}$	0.002 mol/l NaOH
$x_{3,i}$	0.0025 mol/l $NaHCO_3$
K_D	10^{-7} mol/l
K_E	10^{-14} mol^2/l^2
F_A	1 l/min (16.67 ml/s)
F_B	0.14 l/min
V	2.5 l

4.5 SUMMARY AND CONCLUSIONS

The detailed development of a mathematical model for a non-isothermal continuous stirred tank reactor is presented in this chapter. The process model consists of balance ordinary differential equations supported by algebraic form of equations for the calculation of rate of reaction and heat transfer area. In order to predict the reactor dynamics, the process simulator is also developed by solving the model equations. Next, the CSTR model has been simplified and used to analyze the steady state multiplicities. The control of the simplified CSTR process is also covered. Finally, the model structure for a pH neutralization reactor is formulated.

EXERCISES

4.1 Why is CSTR called so?

4.2 Develop a dynamic simulator for the example non-isothermal reactor if the jacket is only around the outside, not around the bottom.

4.3 Investigate the closed-loop performance of the example simulated reactor by employing a multi-loop proportional integral (PI) controller as given below:

$$T_j = T_{js} + K_{CT}\left(e_t + \frac{1}{\tau_T}\int e_t\,dt\right) \tag{4.44}$$

$$F_i = F_{is} + K_{CF}\left(e_F + \frac{1}{\tau_F}\int e_F\,dt\right) \tag{4.45}$$

where

$T_{js} = 25.0°C$

$F_{is} = 10.0\ m^3/h$

$e_t = (T_{sp} - T)°C$

$e_F = (h_{sp} - h)\ m$

$K_{CT} = 100.0$ (unitless)

$\tau_T = 25.0\ h$

$K_{CF} = 50.0\ m^2/h$

$\tau_F = 10.0\ h$

4.4 Consider a stirred heating tank as shown in Figure 4.10. Liquid at temperature T_i flowing into the tank at a volumetric flow rate F, is heated by steam flowing through the steam coil arrangement at a rate Q

(mass/time). The heated fluid, now at temperature T, is withdrawn at the same volumetric rate F. The tank volume is V and the latent heat of vaporization of steam is ¬ . You may consider constant density (^) and heat capacity (C_p) of the reacting material.

(i) Derive the overall mass and energy balance equations making appropriate assumptions.

(ii) Solve the modelling equations employing the fourth-order Runge–Kutta approach.

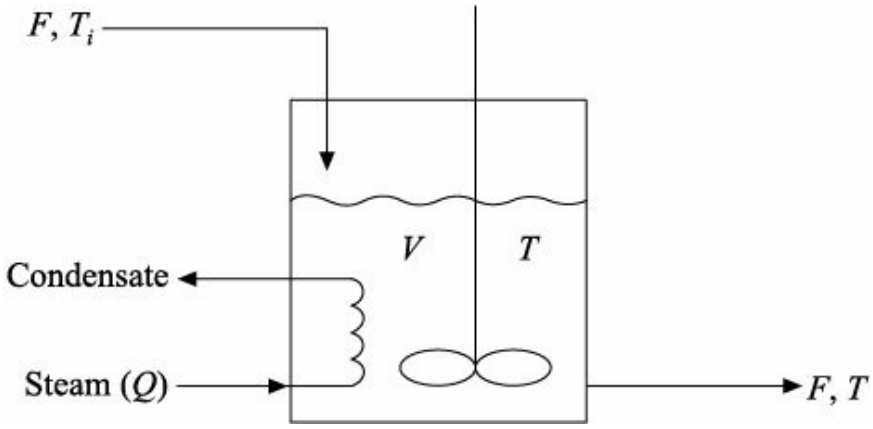

FIGURE 4.10 The stirred heating tank.

4.5 Consider a non-isothermal CSTR as shown in Figure 4.11, in which a second-order, irreversible, exothermic chemical reaction $A \xrightarrow{k} B$ is taking place. Feed material containing C_{Af} mol/volume of A enters the reactor at temperature T_f, and constant

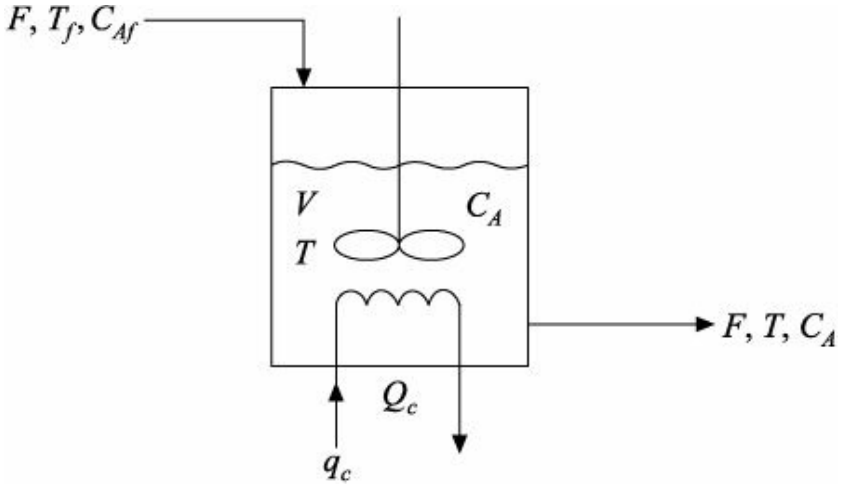

FIGURE 4.11 The non-isothermal CSTR.

volumetric flow rate F. Product is withdrawn from the reactor at the same volumetric flow rate F having composition C_A and temperature T. The rate of heat transfer to the cooling coil is Q_c (energy/time) and the reactor volume is V. You may assume constant density (^) and heat capacity (C_p) of the reactor liquid.

(i) Develop the mathematical model consisting of mass and energy balance equations.

(ii) Simulate the model structure using the RKF45 method (details in Chapter 2).

4.6 In a CSTR shown in Figure 4.12, the following parallel reactions take place:

$$A \xrightarrow{k_1} U_1$$

$$A \xrightarrow{k_2} U_2$$

$$A \xrightarrow{k_d} D$$

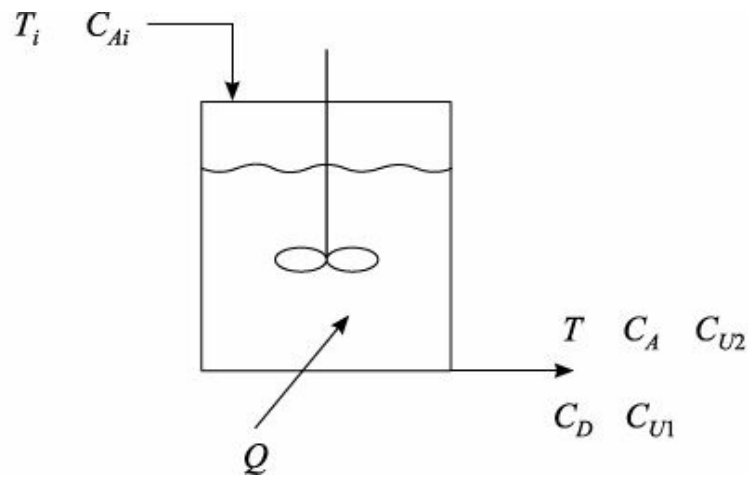

FIGURE 4.12 The CSTR.

Here, U_1 and U_2 are the undesired side products, and D is the desired product. It is assumed that the feed to the reactor does not contain U_1, U_2 or D. The dependence of the reaction rate constants k_1, k_2 and k_d on temperature is given by:

$$k_i = Z_i \exp\left(\frac{-E_{a_i}}{RT}\right), i = 1, 2 \tag{4.46}$$

$$k_d = Z_d \exp\left(\frac{-E_{a_d}}{RT}\right) \tag{4.47}$$

(i) Derive the following model structure mentioning the required assumptions.

$$\begin{cases} \dfrac{dC_A}{dt} = R_A(C_A, T) + \dfrac{C_{Ai} - C_A}{\tau} \\ \dfrac{dT}{dt} = \dfrac{R_H(C_A, T)}{\rho c} + \dfrac{T_i - T}{\tau} + \dfrac{Q}{\rho c V} \\ \dfrac{dC_D}{dt} = R_D(C_A, T) - \dfrac{C_D}{\tau} \end{cases} \tag{4.48}$$

where the rate expressions R_A, R_H and R_D are given by:

$$R_A = -k_1 C_A^{n1} - k_2 C_A^{n2} - k_d C_A^{nd} \tag{4.49}$$

$$R_H = (-\Delta H_1) k_1 C_A^{n1} + (-\Delta H_2) k_2 C_A^{n2} + (-\Delta H_d) k_d C_A^{nd} \tag{4.50}$$

$$R_D = k_d C_A^{nd} \tag{4.51}$$

(ii) Simulate the above model structure using the parameter values and operating conditions given in Table 4.5.

Table 4.5 Parameter values and operating conditions for the CSTR

Universal gas constant, $kJ.kmol^{-1}.K^{-1}$	8.345

R	Frequency factor for reaction 1, $m^6.kmol^{-2}.s^{-1}$	2.0×10^3
Z_1	Frequency factor for reaction 2, $kmol^{0.5}.m^{-1.5}.s^{-1}$	3.4×10^6
Z_2	Frequency factor for desirable reaction, s^{-1}	2.63×10^5
Z_d	Activation energy for reaction 1, $kJ.kmol^{-1}$	4.9×10^4
$(-\Delta H_1)$	Activation energy for reaction 2, $kJ.kmol^{-1}$	6.5×10^4
$(-\Delta H_2)$	Activation energy for desirable reaction, $kJ.kmol^{-1}$	5.7×10^4
$(-\Delta H_d)$	Heat of reaction 1, $kJ.kmol^{-1}$	4.5×10^4
n_1	Heat of reaction 2, $kJ.kmol^{-1}$	5.0×10^4
n_2	Heat of desirable reaction, $kJ.kmol^{-1}$	6.0×10^4
n_d	Order of reaction 1	3.0
α	Order of reaction 2	5.0×10^{-1}
c	Order of desirable reaction	1.0
C_{Ai}	Density of reacting mixture, $kg.m^{-3}$	1.0×10^3
V	Heat capacity of reacting mixture, $kJ.kg^{-1}.K^{-1}$	4.2
T_i	Inlet concentration of reactant A, $kmol.m^{-3}$	1.0×10^1
	Volume of the reacting mixture, m^3	1.0×10^{-2}
	CSTR residence time, s	3.0×10^2
	Temperature of inlet stream, K	2.952×10^2

Initial (*subscript* 0) *and steady state* (*subscript S*) *values*

$C_{A0} = 1.0 \times 10^{-1}$ kmol.m^{-3}	$C_{D0} = 0.0$ kmol.m^{-3}
$T_0 = 2.952 \times 10^2$ K	$T_S = 4.0 \times 10^2$ K
$C_{AS} = 1.3204$ kmol.m^{-3}	$C_{DS} = 4.0$ kmol.m^{-3}

Q_S	Steady state rate of heat input to reactor, $kJ.s^{-1}$	−1.0303

(iii) Investigate the existence of multiple steady states (*SS*1, *SS*2 and *SS*3) having the values listed in Table 4.6.

Table 4.6 Steady state operating points corresponding to $Q_S = -1.0303$ kJ.s^{-1}

Steady state operating point	C_{AS} (kmol/m^3)	C_{DS} (kmol/m^3)	T_S (K)
*SS*1	7.925	0.178	310.8
*SS*2	3.321	2.520	370.0
*SS*3	1.320	4.000	400.0

4.7 Consider a jacketed CSTR in nonisothermal operation, where the following exothermic irreversible reaction between sodium thiosulphate and hydrogen peroxide is taking place (Vejtasa and Schmitz, 1970; Kazantzis et al., 2000):

$$2Na_2S_2O_3 + 4H_2O_2 \rightarrow Na_2S_3O_6 + Na_2SO_4 + 4H_2O$$

By using the letters A, B, C, D and E, we represent the chemical compounds $Na_2S_2O_3$, H_2O_2, $Na_2S_3O_6$, Na_2SO_4 and H_2O, respectively. The reaction kinetic law is reported (Vejtasa and Schmitz, 1970) as:

$$-r_A = k(T)C_AC_B = k_0 \exp\left(-\frac{E}{RT}\right)C_AC_B \qquad (4.52)$$

where $k(T)$ is the reaction rate constant, k_0 the reaction frequency factor, E the reaction activation energy, R the gas constant, T the temperature, and C_A and C_B the concentrations of species A and B, respectively. Assume stoichiometric proportion of species A and B in the feed stream for all times, i.e.,

$C_B(t) = 2C_A(t)$.

(i) Mentioning the standard assumptions, derive the following nonlinear dynamic process model:

$$\begin{cases} \dfrac{dC_A}{dt} = \dfrac{F}{V}(C_{A,in} - C_A) - 2k(T)C_A^2 \\ \dfrac{dT}{dt} = \dfrac{F}{V}(T_{in} - T) + 2\dfrac{(-\Delta H)}{\rho C_p}k(T)C_A^2 - \dfrac{UA}{V\rho C_p}(T - T_j) \end{cases} \tag{4.53}$$

where F is the feed flow rate, V the reactor volume, $C_{A,in}$ the inlet concentration, T_{in} the inlet temperature, T_j the jacket temperature, ^ the density of the reacting mixture, C_p the heat capacity of the reacting mixture, $(-\Delta H)$ the heat of reaction, U the overall heat transfer coefficient, and A the heat exchange area.

(ii) Simulate the above CSTR model using the process parameter values given in Table 4.7.

Table 4.7 Process parameter values

F	20 l/s
V	100 l
T_{in}	275 K
UA	20,000 J/s.K
^	1000 g/l
C_p	4.2 J/g.K
$(-\Delta H)$	5,96,619 J/mol
k_0	6.85E + 11 l/s.mol
E	76,534.704 J/mol
R	8.314 J/mol.K
T_j	250 K
$C_{A,in}$	1 mol/l

(iii) Perform the multiple steady state analysis, and show that the upper and lower steady states are stable ones, whereas the middle one is unstable. At the unstable steady state, $C_A = 0.666$ mol/l, $T = 308.489$ K and $F = 20$ l/s.

4.8 Consider a jacketed CSTR, where an exothermic irreversible first-order reaction takes place. The material and energy balances based on the assumptions of constant volume inside the reactor, perfect mixing and constant physical parameters allow to obtain the dynamical model. The constructive features of the reactor are demonstrated in Figure 4.13.

(i) Derive the following differential equations written in a dimensionless form (Russo and Bequette, 1995):

$$\begin{cases} \dfrac{dx_1}{d\tau} = q(x_{1f} - x_1) - \phi x_1 \kappa(x_2) \\ \dfrac{dx_2}{d\tau} = q(x_{2f} - x_2) - \delta(x_2 - x_3) - \beta\phi x_1 \kappa(x_2) \\ \dfrac{dx_3}{d\tau} = \delta_1[q_c(x_{3f} - x_3) + \delta\,\delta_2(x_2 - x_3)] \end{cases} \tag{4.54}$$

where the dimensionless Arrhenius reaction rate constant ( ) has the following form:

$$\kappa(x_2) = \exp\left(\frac{x_2}{1 + x_2/\gamma}\right) \qquad (4.55)$$

The state variables x_1, x_2 and x_3 stand for the dimensionless reactant concentration, the reactor temperature and the cooling jacket temperature, respectively. τ represents the dimensionless time, q the reactor feed flow rate, x_{1f} the dimensionless reactor feed concentration, x_{2f} the dimensionless reactor feed temperature, x_{3f} the dimensionless cooling-jacket feed temperature, β the nominal Damkohler number based on the reaction feed, γ the dimensionless heat-transfer coefficient, κ the dimensionless heat of reaction, γ_1 the reactor to cooling-jacket volume ratio, γ_2 the reactor to cooling-jacket density heat capacity ratio and q_c the cooling jacket flow rate.

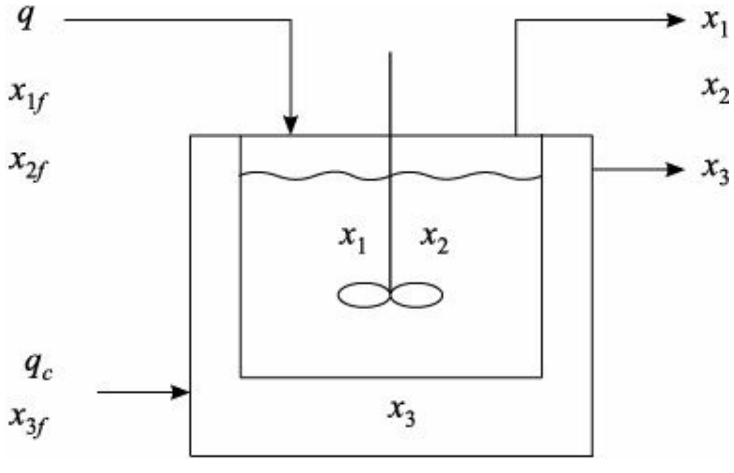

FIGURE 4.13 Schematic representation of the jacketed CSTR.

(ii) Simulate the model structure using the data given in Table 4.8.

Table 4.8 CSTR model parameter values

β	0.072
κ	8.0
γ	0.3
χ	20
q	1.0
γ_1	10
γ_2	1.0
x_{1f}	1.0
x_{2f}	0.0
x_{3f}	−1.0
q_c	0.5

(iii) The representative CSTR shows multiplicity behaviour with respect to the jacket temperature and jacket flow rate. Investigate the existence of open-loop instability when the temperature inside the reactor is between 1.5 and 3.0.

REFERENCES

Bequette, B.W. (1998). *Process Dynamics, Modeling, Analysis, and Simulation*, 1st ed., Prentice-Hall, Upper Saddle River, New Jersey.

Fjeld, M., Asbjornsen, O.A., Astrom, K.J. (1974). Reaction invariants and their importance in the analysis of eigenvectors, state observability and controllability of the continuous stirred tank reactor, *Chem. Eng. Sci.*, 29, 1917–1926.

Galan, O., Romagnoli, J.A., and Palazoglu, A. (2000). Robust $H_{\perp|}$ control of nonlinear plants based on multi-linear models: An application to a bench-scale pH neutralization reactor, *Chem. Eng. Sci*., 55, 4435–4450.

Jana, A.K., Samanta, A.N., and Ganguly, S. (2005). Globally linearized control on diabatic continuous stirred tank reactor: a case study, *ISA Transactions*, 44, 423–444.

Kazantzis, N., Kravaris, C., and Wright, R.A. (2000). Nonlinear observer design for process monitoring, *Ind. Eng. Chem. Res*., 39, 408–419.

Luyben, W.L. (1990). *Process Modeling, Simulation, and Control for Chemical Engineers*, 2nd ed., McGraw-Hill Book Company, Singapore.

Rakshit, P.C. (1993). *Physical Chemistry*, Sarat Book House, Calcutta, India.

Russo, L.P., and Bequette, B.W. (1995). Impact of process design on the multiplicity behaviour of a jacketed exothermic CSTR, *AIChE J*., 41, 135–147.

Stephanopoulos, G. (1998). *Chemical Process Control: An Introduction to Theory and Practice*, 6th ed., Prentice-Hall of India, New Delhi.

Vejtasa, S.A., and Schmitz, R.A. (1970). An experimental study of steady-state multiplicity and stability in an adiabatic stirred reactor, *AIChE J*., 3, 410–419.

5

Bioreactor

5.1 CHEMICAL ENGINEERING IN BIOPROCESS INDUSTRY

Humans are a home to a myriad of living creatures. From head to toes, our *cells*, exposed to the outside world, are hosts to a number of tiny living organisms, called *microorganisms*, including bacteria, protozoa, algae, fungi and viruses, which can be seen with the aid of a microscope. The microorganisms are also known as *microbes*. As a rough rule of thumb, most microorganisms have a diameter of 0.1 mm or less.

It is fairly accurate to say that we are a veritable garden of microorganisms. Most of these microorganisms are not only innocuous but play a useful, yet unseen, role in our lives. They protect against the few harmful disease-causing microorganisms (called *pathogens*) that we encounter each day; they provide vitamins and nutrients and help digest food. Apart from the direct involvement in the human body, the microorganisms contribute a lot to us and to our surroundings. Even the microorganisms play a primary role in the capture of energy from the sun.

Until the time of Louis Pasteur in 1857, *alcoholic fermentation* was deemed to be a chemical process in which the sugars were getting converted to alcohol. Subsequently, it was realized that the conversion of sugar to alcohol was affected by living microorganisms which were the silent workers. This has opened up a wide range of interrelationships between various disciplines in science. The commercial success of the production of *penicillin* during the Second World War period proved the advantages of engineering miracles. The biochemical engineers, who were responsible for providing a favourable and contamination-free environment, have proved that they are needed to ensure the operation successful.

Subsequently, *biotechnology* has evolved into a multidisciplinary stream, drawing upon science (including biological science) and technology. The word biotechnology, short form for biological technology, came in general use in mid-1970s. Biotechnology, relying on renewable resources, is a sustainable technology which may eventually replace many of the current non-renewable resource-dependent production methods. Depletion of finite resources, resulting changes in production economics, environmental factors and improvements in biotechnology-based production, will drive the industrial restructuring.

At the present stage of our ongoing discussion, it is good to know the difference between several interrelated disciplines or branches. They are briefly described in Figure 5.1. Now, naturally one question arises: what role the chemical engineers play in biotechnology? Just as the chemical industry before it, industrial biotechnology needs people capable of developing production processes with the bioscientists (biochemists, microbiologists, geneticists, etc.), and transforming these processes into economically viable large-scale plants for products and services. These processes and process plants have to be designed, built, operated and controlled. Thus arose the profession of chemical engineers. They are well-known as biochemical or bioprocess engineers.

The emergence of *biochemical engineering* is of more recent origin. Processing of biological materials and processing using biological agents such as cells, enzymes, or antibodies are the central domains of biochemical engineering. The biochemical engineering (Moo-Young and Chisti, 1994) combines the bioprocess-relevant chemical engineering knowhow (process modelling and control,

bioreaction and reactor engineering, transport phenomena, fluid mechanics, thermodynamics, unit operations, bioseparations, process design and economics, etc.) with regard to biological systems (microbiology, biochemistry, biocatalysis, etc.) and pharmaceutical systems. Applications of biochemical engineering are wide ranging, covering such major facets of civilization as healthcare, agriculture and food, resource recovery, bulk and fine chemicals, energy and environmental pollution abatement.

Discipline/Branch	*Definition*
Chemical engineering	Chemical engineering is an engineering discipline that is concerned with the translation of discoveries in chemistry into commercial processes for the manufacture of new chemical entities.
Biochemistry	Biochemistry is a branch of chemistry and it deals with the chemical characteristics of a particular living system or biological substance.
Biomedical engineering	Biomedical engineering is a discipline concerned with the development and manufacture of prostheses[1], diagnostic devices, drugs, and other therapies. It is more concerned with biological, safety and regulatory issues than other forms of engineering.
Biotechnology	Biotechnology is not a single subject, but a collective term for all the scientific and engineering disciplines that are involved in the translation of new discoveries in the life sciences to practical outcomes.
Biochemical engineering	Biochemical engineering concerns the design and construction of unit processes, and the translation of discoveries in biochemistry and medicine into commercial processes for new biological entities such as medicines and therapeutics. Its applications are mainly employed in the pharmaceutical, biotechnology, and water treatment industries.

FIGURE 5.1 Definitions of some allied disciplines or branches.

[1] Prosthesis is an artificial device used to replace a missing body part, such as a limb, tooth, eye, heart valve, etc.

5.2 OPERATIONAL STAGES IN A BIOPROCESS

In a bioprocess, microbes or living organisms play an important role in getting transformation of the feed into useful products. The total mass (or weight) of all living organisms in a biological system is commonly termed as *biomass*. The main constituent of the feed stream is the *substrate* (portion of a *medium*[1] metabolized by the organisms) along with the other components of the medium. In addition to the substrate, the medium is prepared with minerals, carbon, nitrogen, water, vitamins and so on. Here, we prefer to use the term *nutrient* to mean a medium constituent. Notice that a catalyst may be present along with the nutrients in the medium. *Enzyme* (a protein) is used as a biological catalyst to increase the rate of biochemical reactions taking place within living systems.

[1] It is a mixture of nutrient substances required by cells for growth and metabolism in an artificial environment.

In a simple way, we can say that the biomass consists of cells that consume the substrate and other essential nutrients. For example, the biomass is generally used to *eat* waste chemicals (substrate) in the wastewater treatment process. In this process, the key component of wastewater (raw material) is the substrate. Other essential nutrients may be supplied for proper treatment of wastewater.

A bioprocess is typically made up of *three* steps (Moo-Young and Blanch, 1981) as shown in Figure

5.2. The raw material, which may be of biological or non-biological origin, is first converted to a form suitable for processing. This is done in a *pretreatment* or *upstream processing* step which involves chemical or enzymatic hydrolysis, preparation of liquid medium, separation of particulate and inhibitory chemicals, sterilization (an operation in which all microorganisms and their propagules are killed by exposure to heat, radiation or chemicals, or removed by filtration), air purification and other preparatory operations.

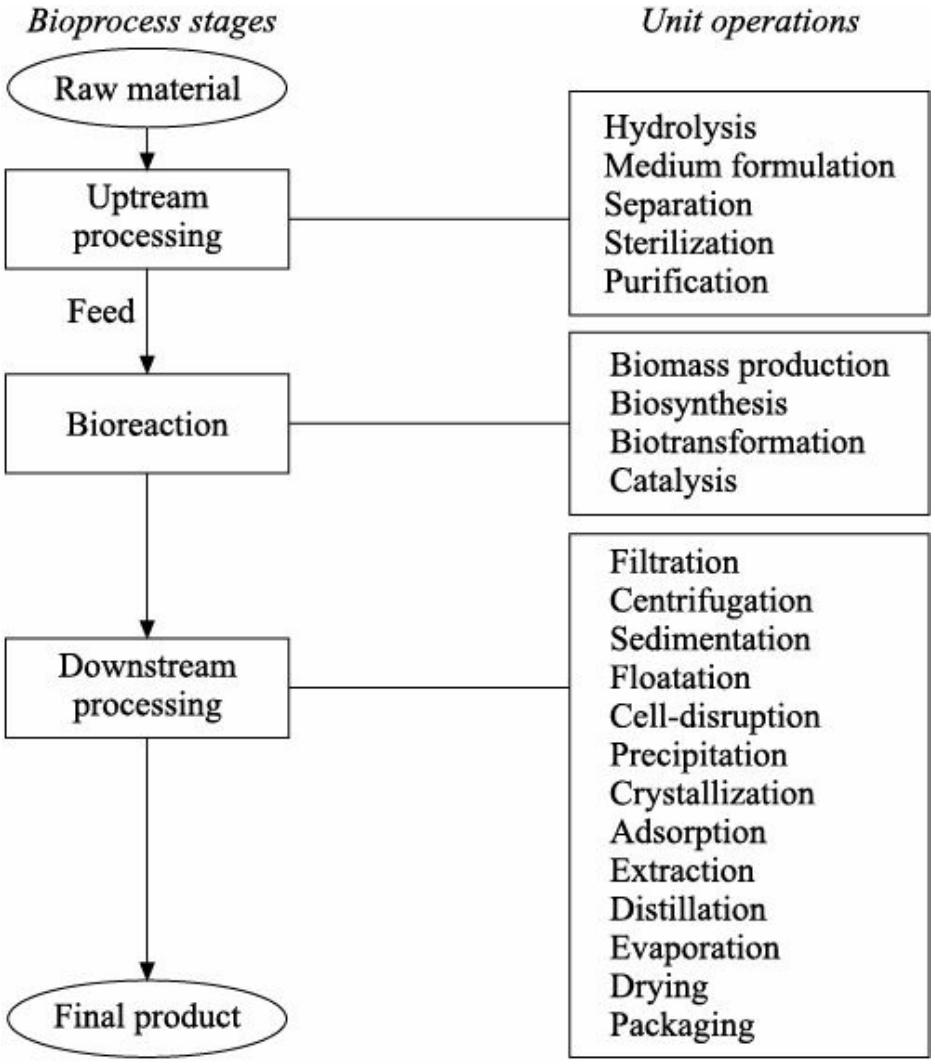

FIGURE 5.2 Bioprocess stages and involved operations.

The pretreatment step is followed by one or more *bioreaction* stages. The *biochemical reactors* or *bioreactors* form the core of the bioreaction step. In this step, the following operations are performed: production of biomass (through the conversion of a substrate to biomass, or biomass and some biochemical including enzymes), metabolize biosynthesis (it takes place within living organisms generally in presence of enzyme catalyst to produce several chemical compounds, including proteins, vitamins and antibiotics[2]) and biotransformation (alteration of the structure of a compound by a living organism or enzyme). The biochemical reactors use the enzyme systems of microbial and other cells to carry out the required biosynthesis, biodegradation or biotransformation. Actually, biodegradation refers to the breakdown of organic materials into simpler components by microorganisms.

2 Antibiotic is a specific type of chemical substance that is administered to fight infections caused usually by bacteria, in humans or animals. Many antibiotics are produced by microorganisms; some are chemically synthesized (Ghose, 1990).

Finally, the material produced in bioreactors must be processed further in the downstream section of the process to convert it to a useful form. *Downstream processing* consists of predominantly physical separation operations which are aimed at purification and concentration of the product. Some commonly

used operations are solid–liquid separation (filtration, centrifugation, sedimentation, floatation, etc.), cell-disruption [a technique to isolate the metabolic product from the solids (usually cells)], precipitation, crystallization, adsorption, liquid-liquid extraction, distillation, evaporation, drying, etc. The purified product may have to be in different physical forms (liquid, slurry, powder, crystalline, emulsions, etc.) and additional steps for product stabilization and formulation may be needed.

Based on the above discussion it is true to say that the chemical engineers play a vital role in all three steps of bioprocessing. Depending on the type of product, the concentration levels it is produced and the purity desired, the second step (bioreaction) might constitute anywhere between 5–50% of the total fixed and operating costs of the process. Therefore, optimal design and operation of bioreactor frequently dominates the overall technological and economic performance of the process.

5.3 BIOCHEMICAL REACTOR

The biochemical reactor is an essential unit operation in a wide variety of biotechnological processes. In biochemical engineering, generally, we use terms like biochemical reactor, biological reactor, bioreactor, fermenter, microbial reactor, which are all synonymous. Actually, *fermentation* is a process of growing microorganisms to produce various chemical or pharmaceutical compounds. Microbes are usually incubated under specific conditions in a large tank called *fermenter*. It is the heart of bioprocessing.

The discoveries of Louis Pasteur soon led to the development of bioreactors for the large-scale *culture* (a growth of living cells or microorganisms in a prepared medium) of bacteria and *yeasts* (microscopic fungi whose metabolic processes are responsible for fermentation, and they are used for leavening bread and in the making of cheese, beer and wine). Small cultures originally were performed in dishes that could not create appreciable quantities of fermentation products (such as acetone, ethyl alcohol, etc.). These products had value if they could be produced in large volumes. To achieve this goal, the development of bioreactors was required (beginning in the early 1900s) that could culture at least a few litres of cells and media. Eventually, the bioreactors would be able to ferment thousands of litres at a time.

The biochemical reactors are employed to produce a large number of intermediate and final products, including medicinal products (e.g., antibiotics, vaccines[3], etc.), food and beverages, and industrial solvents. Like chemical reactors, the biochemical reactors also can be classified based on the feeding approach into three different categories: continuous, batch and semi-batch or semi-continuous or fed-batch. In the following text, they are discussed briefly.

[3] Vaccine is a suspension of attenuated or killed bacteria or virus or portions thereof, injected to produce active immunity (Ghose, 1990).

In the continuous mode of operation, the feed is continuously added into the system and the effluent stream is removed simultaneously from the system. The continuous processes offer advantages, such as higher productivity, and ease of operation and control. But they have certain disadvantages, such as equipment failures, infection by other microorganisms, and low conversion per unit reactor volume. Moreover, the continuous flow fermenter has the drawback that the cells are washed away in the outlet continuously.

In a batch mode, all the materials are added at the beginning of the batch and the contents are sealed. The batch products are withdrawn after the reaction time is over. The batch (and semi-batch) bioreactors have the advantage of avoiding excessive substrate feed which can inhibit microorganism growth. Since the product is also recovered at the end of the batch operation, sterilized conditions can be maintained during process operation. However, the operating costs of batch operations are high, and hence large-scale production is not economical.

As already mentioned in the general description of the reactor (just before Chapter 3), the semi-batch or semi-continuous operation is intermediate to batch operation and continuous operation, and hence the name. The semi-batch reactors are widely used in biochemical operations, and they are popularly known as fed-batch reactors. It offers a good control over the reaction speed (progress) and microorganism growth, as the supply of one of the reactants is under supervision. However, it is usually difficult to analyze the data of the semi-batch reactor operations compared to the batch and continuous systems. Furthermore, there are difficulties in operation and control since the semi-batch processes, like batch processes, are inherently dynamic.

This chapter covers:

- The formulation of a mathematical model for a continuous stirred tank biochemical reactor (also referred to as a continuous fermenter)
- The dynamics of the example continuous-flow bioreactor
- The modelling of a (fed-)batch bioreactor and simulation results.

5.4 CONTINUOUS STIRRED TANK BIOREACTOR (CSTB)

5.4.1 Process Description

In a simple way, the biochemical reactor can be defined as a tank in which several biological reactions occur simultaneously in a liquid medium. In the bioreactor, the fermentation process is commonly performed with the substrate, in presence of other nutrients in the media, by the action of microorganisms, under optimum biological conditions. The fermentations give rise to a variety of products (Rao, 2005), such as: primary metabolites (e.g., alcohol, citric acid, etc.), biomass [e.g., baker's yeast, single cell protein (SCP), etc.], transformed substrates (e.g., steroids), and purified solvents as in the case of water treatment.

In a simple biochemical reactor case study, we have considered two components, biomass and substrate. The substrate is the feed source for the cells. Consider the schematic of a biochemical reactor in Figure 5.3, where x is the biomass concentration (= mass of cells/volume) and S the substrate concentration (= mass of substrate/volume). F represents the volumetric flow rate of the feed stream, V the volume of the bioreactor, and x_f and S_f the biomass and substrate concentrations respectively in the feed stream.

In the sample bioreactor, the feed is supplied continuously. To keep the cells in suspension, gentle stirring is allowed in the reactor. The agitator speed is chosen to provide sufficient mixing while avoiding excessive shear forces that may damage the cells (Lee, 1992). A stream is removed continuously from the bioreactor. The effluent stream contains unreacted substrate and biomass. The growth of microbial cells in a suitable medium results in the consumption of substrate and the formation of products. Here, the desired products are the cells themselves.

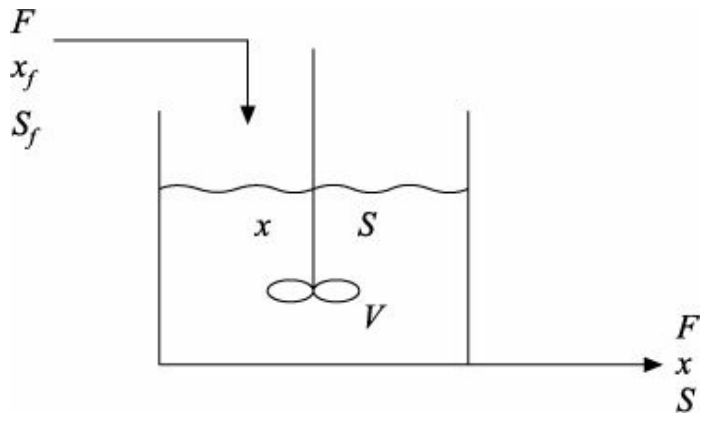

FIGURE 5.3 Schematic representation of the example CSTB.

This system is chosen because, despite this process being the simplest one, its dynamic behaviour is complex (Agrawal, Lee, Lim, and Ramkrishna, 1982). Moreover, several important industrial processes belong to this class (e.g., wastewater treatment process).

The bioreactor model will be constructed in the following way based on the conservation principle and biochemical reaction kinetics.

5.4.2 Mathematical Model

Assumptions

The following assumptions have been made to develop the mathematical model for the bioreactor.

- The reactor contents are perfectly mixed.
- The reactor is operating at a constant temperature (i.e., it is isothermal).
- The feed is sterile (i.e., no biomass in the feed stream).
- The feed stream and reactor contents have equal and constant density ($\hat{}$).
- The feed and product streams have the same flow rate (F).
- The microbial culture involves a single biomass growing on a single substrate.

Model development

Total Continuity Equation

Making overall mass balance, it is easy to get the following equation:

$$\frac{d(\rho V)}{dt} = F\rho - F\rho = 0 \qquad (5.1)$$

Now it is obvious that the reactor volume (V) is constant since $\frac{dV}{dt} = 0$.

Biomass Continuity Equation

We know,

Flow rate of biomass into the bioreactor = Fx_f,

Flow rate of biomass out of the bioreactor = Fx,

Rate of generation of biomass by reaction = Vr_1, and

Rate of accumulation of biomass within the bioreactor $= \frac{d(Vx)}{dt}$.

Substituting all these terms (mass/time) in Equation (3.2), we have

$$\frac{d(Vx)}{dt} = Fx_f - Fx + Vr_1 \qquad (5.2)$$

where r_1 is the rate of cell generation [= (mass of cells generated)/(volume) (time)]. Dividing both sides of the above equation by V, one obtains

$$\frac{dx}{dt} = \frac{F}{V}x_f - \frac{F}{V}x + r_1 \qquad (5.3)$$

In the chemical reaction engineering, F/V is called *space velocity* (time^{-1}) and V/F the *residence time* (time). But in biochemical engineering, F/V is referred to as the *dilution rate*[4], probably due to the dilution of the biomass in the reactor with the addition of fresh feed. Accordingly, Equation (5.3) yields

[4] It is defined as the number of tank liquid volumes (reactor volumes) that pass through the tank per unit time.

$$\frac{dx}{dt} = Dx_f - Dx + r_1 \qquad (5.4)$$

or

$$\frac{dx}{dt} = D(x_f - x) + r_1 \qquad (5.5)$$

where D denotes the dilution rate.

Substrate Continuity Equation

For the substrate balance,

Flow rate of substrate into the bioreactor = FS_f,

Flow rate of substrate out of the bioreactor = FS,

Rate of generation of substrate by reaction = $-Vr_2$, and

Rate of accumulation of substrate within the bioreactor $= \frac{d(VS)}{dt}$.

Equation (3.2) gives

$$\frac{d(VS)}{dt} = FS_f - FS - Vr_2 \qquad (5.6)$$

Rearranging the above equation, we get

$$\frac{dS}{dt} = D(S_f - S) - r_2 \qquad (5.7)$$

where r_2 is the rate of substrate consumption [= (mass of substrate consumed)/(volume) (time)].

Biochemical Reaction Kinetics

It is well-known that for the *chemical* reaction,

$$A \xrightarrow{k} P$$

we can write

$$(-r_A) = k(C_A)^n \qquad (5.8)$$

or

$$(r_A) = -k(C_A)^n \qquad (5.9)$$

where $(-r_A)$ = rate of disappearance of reactant A

(r_A) = rate of formation of A

k = reaction rate constant

C_A = concentration of reactant A

n = order of the reaction with respect to component A

For a first-order reaction, $n = 1$ and accordingly,

$$(-r_A) = kC_A \qquad \text{[from Equation (4.7)]}$$

The reaction kinetics involved in biochemical operations is comparatively complicated than the chemical reaction kinetics. The interested reader may consult the book by Bailey and Ollis (1986) for details about the biochemical reaction kinetics. In general, a biochemical reaction proceeds with the intervention of living organisms (or cells) in the presence of nutrients of the medium under optimum conditions of temperature, pH etc. The cells grow by consuming the substrate and essential nutrients from the medium of fermentation. Remember that the growth pattern is not same for all types of the cells. The growth processes of interest to us have two different manifestations. The *unicellular* organisms (organisms that composed of one cell only), which eventually divide as they grow, increase in the number of cells (population growth) or increase the biomass, whereas the *moulds* [fungi that grow as a mesh of fine branched filaments (mycelium)] increase in size and hence density of the cells but not necessarily in numbers. Notice that two interacting systems are involved in the biochemical operation—the biological phase consisting of a cell population and the environmental phase or growth medium. Indeed, various parameters of the *broth* (a fluid culture medium) have been changed with the cell growth.

In the sample bioreactor, (i) the cell population is treated as one component solute with cell-to-cell homogeneity, (ii) there are no intracellular reactions occurring within the cell, and (iii) the growth phenomena are described based on a single limiting substrate. The mathematical model of such a biochemical reactor is commonly referred to as *unstructured* model. This model describes a condition called *balanced growth*. This is a quasi-steady state assumption, which requires that the environment of the biomass changes sufficiently slowly so that the biomass can adjust its internal composition to adapt to the changes. For the example CSTB, this is often a fairly good assumption because the cell population can adjust to a steady environment and achieve or closely approximate a state of balanced growth.

In the following, the cell population kinetics has been discussed for the unstructured models where balanced growth condition is assumed. In the component mass balance Equations (5.5) and (5.7), r_1 and r_2 represent the rate of cell growth and rate of substrate consumption respectively. The following form of equation normally represents the net rate of cell mass growth:

$$r_1 = \mu x \qquad (5.10)$$

where μ is known as the *specific growth rate* or *specific growth rate coefficient* (time^{-1}). We may think that μ is similar to the first-order reaction rate constant k [Equation (4.7)]. However, μ is originally not a constant. It is true that the microorganisms cannot grow without the supply of food. In the subsequent discussion, we will see that the specific growth rate is a function of the concentration of some

nutrient(s).

Now we wish to define the term *yield*. It is generally defined as the ratio of mass or moles of product formed to the mass or moles of reactants consumed. It is also called *yield factor* or *yield coefficient* or *yield production coefficient*. The yield Y of product P with respect to the reactant A is expressed by:

$$Y = \frac{\text{mass of } P \text{ formed}}{\text{mass of } A \text{ consumed}} \qquad (5.11)$$

For the case of bioreactor,

$$Y = \frac{\text{mass of cells formed}}{\text{mass of substrate consumed}} \qquad (5.12)$$

It gives

$$Y = \frac{r_1}{r_2} \qquad (5.13)$$

or

$$r_2 = \frac{r_1}{Y} \qquad (5.14)$$

Inserting Equation (5.10) into Equation (5.14), one obtains:

$$r_2 = \frac{\mu x}{Y} \qquad (5.15)$$

Actually, the yield coefficient varies linearly with the substrate concentration (Ramaswamy, Cutright and Qammar, 2005) as:

$$Y(S) = a + bS \qquad (5.16)$$

where a and b are positive constants. In the present case study, we have assumed that Y is a constant parameter.

Final Form of Modelling Equations

Substituting Equation (5.10) into Equation (5.5) and Equation (5.15) into Equation (5.7), the following equations are obtained respectively as:

$$\frac{dx}{dt} = D(x_f - x) + \mu x \qquad (5.17)$$

$$\frac{dS}{dt} = D(S_f - S) - \frac{\mu x}{Y} \qquad (5.18)$$

We have assumed that the feed stream does not contain any biomass, i.e., $x_f = 0$. Therefore, the bioreactor modelling equations finally get the following forms:

$$\frac{dx}{dt} = (\mu - D)x \qquad (5.19)$$

$$\frac{dS}{dt} = D(S_f - S) - \frac{\mu x}{Y} \qquad \text{[from Equation (5.18)]}$$

Specific Growth Rate

As previously mentioned, the specific growth rate is not a constant parameter; it is generally a function of the concentration of some nutrient(s). In the following, we will know a little more about it.

The general goal of a medium in the biochemical operations is to support handsome growth and/or high rates of product synthesis. It does not necessarily mean that all medium constituents or nutrients should be supplied to the reactor in great excess. Notice that excessive concentration of a nutrient may inhibit or even poison cell growth. Moreover, if the cells grow too extensively, their accumulated metabolic end products will often disrupt the normal biochemical processes of the cells. Therefore, it is common practice to control total cell growth by limiting the amount of one nutrient in the medium. Often, a single substrate exerts a dominant influence on rate of growth and this component is known as the *growth limiting substrate*, or more simply, the *limiting substrate*.

Now we will discuss the *Monod* model. This model is used to express growth based on a single limiting substrate S. The Monod model is commonly employed in the biochemical reactor modelling and is the basis of almost all growth models.

Monod model

If the concentration of the limiting substrate is varied, experimental study shows that the specific growth rate typically changes in a hyperbolic fashion, as Figure 5.4 shows. Obviously, the growth rate passes through various phases, such as high growth phase, low growth phase and finally cessation. The variation of specific growth rate with the concentration of the growth limiting substrate is well explained by an empirical equation proposed by Monod in 1942. This equation has the following form:

$$\mu = \frac{\mu_m S}{K_m + S} \qquad (5.20)$$

where μ_m is the maximum achievable specific growth rate and K_m represents the limiting substrate concentration when the specific growth rate is equal to half of the maximum specific growth rate, as illustrated in Figure 5.4. These parameters are obtained experimentally and generally they do not have a direct physical interpretation (Bailey and Ollis, 1986).

Substitution of $\mu = (\mu_m/2)$ in Equation (5.20) and after simplification, we get $K_m = S$. Marison (1988) has reported some typical values of K_m. Note that the Monod equation is valid only for balanced growth and should not be applied when growth conditions are changing rapidly.

Monod Equation (5.20) has the same form as the Langmuir adsorption isotherm and the standard rate equation for enzyme-catalyzed reactions with a single substrate (Michaelis–Menten kinetics). If S is very large, Equation (5.20) yields:

$$\mu \approx \frac{\mu_m S}{S} \approx \mu_m \qquad (5.21)$$

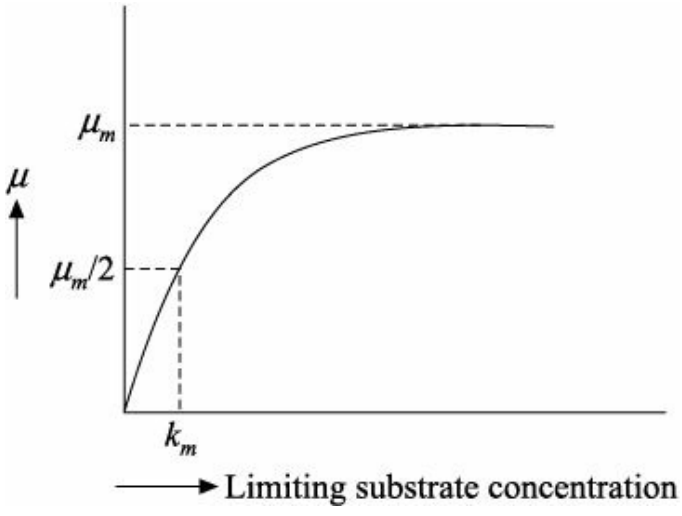

FIGURE 5.4 Dependence of ⌙ on the concentration of the limiting substrate.

Inserting ⌙ ₂₀ ⌙ m in Equation (5.10), we have

$$r_1 \text{ ₂₀ } \llcorner \; m^x \qquad (5.22)$$

It reveals that the Monod description is similar to a first-order reaction when S is very high.

Similarly, if S is very small, the Monod equation gives:

$$\mu \approx \frac{\mu_m S}{K_m} \qquad (5.23)$$

and the rate of cell growth is represented by the following form:

$$r_1 \approx \frac{\mu_m}{K_m} Sx \qquad (5.24)$$

Therefore, when S is very low, the Monod growth kinetics is similar to a second-order (bimolecular) reaction kinetics.

From some studies of the cell's biochemistry, it is apparent that the Monod equation is a great over-simplification. However, there are variants to the Monod model that have also been used, such as the models by Tessier, Moser, Contois, etc., reported in Table 5.1. These models differ in their substrate dependence and some include terms to account for saturation due to high substrate concentration and inhibition due to product or a competing inhibitor. But these models do not differ significantly from the Monod model in the fact that they are empirical and represent all of the cellular processes with just a single equation for the specific growth rate.

Table 5.1 Kinetic structures of fermentation models

Monod (1942)	$\mu(S)=\frac{\mu_m S}{K_m+S}$
Tessier (1942)	$\mu(S)=\mu_m\left(1-\exp\left(-\frac{S}{K_m}\right)\right)$
Moser (1958)	$\mu(S)=\frac{\mu_m S^\lambda}{K_m+S^\lambda},\ \lambda>0$
Contois (1959)	$\mu(S,x)=\frac{\mu_m S}{K_c x+S}$
Aiba et al. (1965)	$\mu(S,P)=\mu_m\left[\frac{S}{K_m+S}\right]\left[\frac{1}{1+(P/K_p)}\right]$
Powell (1967)	$\mu(S)=\frac{\mu_m}{2K_m}(K_m+S-\sqrt{K_m+S^2-4K_m S})$
Edwards (1970)	

Peringer et al. (1972)	$\mu(S)=\dfrac{\mu_m S}{\quad}$ $\mu(S,A)=\mu_m^a\dfrac{S}{K_m+S}\left(\dfrac{A}{K_a+A}+\dfrac{1}{1+K_bA}\right)+\mu_m^b,\ \mu_m=2\mu_m^a+\mu_m^b$
Jackson and Edwards (1975)	$\mu(S,H^+)=\dfrac{\mu_m S}{\left(1+\dfrac{K_2}{H^+}+\dfrac{H^+}{K_1}\right)(K_m+S+S^2/K_i(1+K_3/H^+))}$
Olsson (1976)	$\mu(S,A)=\mu_m\dfrac{SA}{(K_m+S)(K_a+A)}$
Dourado and Calvet (1983)	$\mu(S,P)=\mu_m\dfrac{S}{(K_m+S+(S^2/K_i))}\dfrac{K_p}{(K_p+P)}\left(1-\dfrac{P}{P_f}\right)$
Williams et al. (1984)	$\mu(S,A,P)=\left(\dfrac{K_1S}{K_m+S}+\dfrac{K_2P}{K_p+P}\right)\left(\dfrac{A}{K_a+A}+K_3A-K_4\right)$

S = substrate concentration, x = cell mass concentration, P = product concentration, P_f = inhibition constant, A = dissolved oxygen concentration, H^+ = hydrogen ion concentration, $K_{(\text{any subscript})}$ = constant, μ = specific growth rate, μ_m = maximum specific growth rate.

5.4.3 Dynamic Simulation

In order to know the dynamic behaviour of the sample biochemical reactor, we have to simulate the developed model. The model structure of the CSTB is comprised of the following set of equations:

$$\begin{cases} \dfrac{dx}{dt}=(\mu-D)x \\ \dfrac{dS}{dt}=D(S_f-S)-\dfrac{\mu x}{Y} \\ \mu=\dfrac{\mu_m S}{K_m+S} \end{cases} \qquad (5.25)$$

For solving the above differential–algebraic system, the required data are given in Table 5.2. In the preceding chapters, we have used the fourth-order Runge–Kutta method (Chapter 3) and the second-order Runge–Kutta method (Chapter 4) to solve the ordinary differential equations. Here, the Euler method (detailed in Chapter 2) has been used to simulate the model. The bioreactor simulator is developed using Fortran (90) programming language and is given in Program 5.1. Considering different initial guesses of x and S, we obtain two steady state solutions as:

Equilibrium 1: $x_S = 0.0$ $S_S = 4.0$ (guess values: $x = 0.0$; $S = 1.0$)

Equilibrium 2: $x_S = 1.53735$ $S_S = 0.15653$ (guess values: $x = 1.0$; $S = 1.0$)

Here the subscript s indicates steady state. The unit of both x and S is g/litre.

Table 5.2 Steady state data for the bioreactor

μ_m	$0.53\ \text{h}^{-1}$
K_m	0.12 g/litre
D	$0.3\ \text{h}^{-1}$
S_f	4.0 g/litre
Y	0.4

Integration time interval = 0.005 h

PROGRAM 5.1 *Dynamic CSTB*

```
PROGRAM CSTB
IMPLICIT NONE
```

```
! Declaration
!———————

INTEGER::k
INTEGER,PARAMETER::n=10000
REAL,DIMENSION(n)::X,S,mu,Time
REAL,PARAMETER::D=0.3,mumax=0.53,Km=0.12,Y=0.4,Sf=4.0,dt=0.005
OPEN(UNIT=1,FILE="CSTB.DAT")

! Initialization
!———————

X(1)= 1.0
S(1)= 1.0
Time(1)=0.00

!——————————Starting of main loop——————————!
!———————————————————————————————!

DO k=1,n

mu(k)=(mumax*S(k))/(Km+S(k))

!———————Starting of Euler integration————————!

X(k+1)=X(k)+dt*X(k)*(mu(k)-D)
S(k+1)=S(k)+dt*D*(Sf-S(k))-dt*(mu(k)*X(k)/Y)

!————————End of Euler integration——————————!
Time(k+1)=Time(k)+dt

PRINT*,Time(k),X(k),S(k)
WRITE(1,FMT=500)Time(k),X(k),S(k)
500 FORMAT(1X,3(2X,F10.5))

END DO

!——————————End of main loop———————————————!

END PROGRAM CSTB
```

5.4.4 Multiple Steady States (MSS)

At steady state, the balanced differential Equations (5.18) and (5.19) give

$$\begin{cases} \dfrac{dx_s}{dt} = 0 = (\mu_s - D_s)x_s \\ \dfrac{dS_s}{dt} = 0 = D_s(S_{fs} - S_s) - \dfrac{\mu_s x_s}{Y} \end{cases} \qquad (5.26)$$

Recall that the above set of equations can be obtained for the case of sterile feed ($x_f = 0$). There are two different steady state solutions to Equation (5.26). If more than one steady state (multiple steady states) are there, then it is convenient to classify them into two classes: a *trivial* steady state and *nontrivial* steady state(s). For the present case, we will consider in the following that $x_S = 0$ for trivial or *washout* solution, and x_S ≠ 0 for a single nontrivial solution.

Trivial solution

It is apparent from Equation (5.26) that there may be two cases:

(i) $x_S = 0$ when ($\mu_S - D_S$) ≠ 0 *trivial* case

(ii) $x_S \neq 0$ when $(\mu_S - D_S) = 0$ *nontrivial* case

If $x_S = 0$, then accordingly we obtain

$$D_s(S_{fs} - S_s) = \frac{\mu_s x_s}{Y} = 0 \qquad (5.27)$$

or

$$S_S = S_{fS} \qquad (5.28)$$

since $D_S \neq 0$ for the continuous flow reactor. Hence, the trivial solution includes: $x_S = 0$ and $S_S = S_{fS}$. It clearly shows that no reaction takes place in the reactor, and that is why the concentrations of biomass and substrate in the CSTB are same with that in the feed stream. Since the feed does not contain any biomass, there is also no biomass in the bioreactor. It indicates that all of the cells have been *washed out* of the reactor and therefore this condition is also called as the *washout* condition.

Nontrivial solution

In this case, we assume $x_S \neq 0$. Accordingly, we get the following relationship based on Equation (5.26):

$$\mu_S = D_S \qquad (5.29)$$

It reveals that at steady state, the specific growth rate is equal to the dilution rate. We know,

$$D_s(S_{fs} - S_s) = \frac{\mu_s x_s}{Y} \qquad (5.30)$$

Inserting Equation (5.29) in Equation (5.30) and rearranging, we obtain

$$x_S = Y(S_{fS} - S_S) \qquad (5.31)$$

Next we have to find out S_S. For this, we can start from Monod growth kinetics [Equation (5.20)]. It provides the following expression for the specific growth rate at steady state condition:

$$\mu_s = \frac{\mu_m S_s}{K_m + S_s} \qquad (5.32)$$

Solving the above equation for S_S, we get

$$S_s = \frac{\mu_s K_m}{\mu_m - \mu_s} \qquad (5.33)$$

Since $\mu_S = D_S$,

$$S_s = \frac{D_s K_m}{\mu_m - D_s} \qquad (5.34)$$

Hence in the case of nontrivial steady state, x_S and S_S are found out from Equations (5.31) and (5.34) respectively. At this point, it is good to crosscheck the steady state values obtained for equilibrium 1 (trivial) and 2 (nontrivial) (Subsection 5.4.3).

It is important to mention here that in Equation (5.34), μ_m should be greater than D_S (i.e., $D_S < \mu_m$). Again in Equation (5.31), the highest value of S_S can be S_{fS}. Otherwise, x_S becomes negative. Supposing $S_S = S_{fS}$, the maximum D_S in reality is:

$$D_s < \frac{\mu_m S_{fs}}{K_m + S_{fs}} \qquad (5.35)$$

Notice that the interested reader may further proceed to know (Agrawal, Lee, Lim, and Ramkrishna, 1982) about the stability of steady states, existence and stability character of limit cycles and so on.

5.5 (FED-)BATCH BIOREACTOR

The increasing emphasis on energy efficient and green manufacturing has paved the way for the biological route towards manufacturing. In addition, many important chemical and pharmaceutical compounds are now made in biological reactors. The (fed-)batch mode of bioreactor operation is most commonly used in the fermentation industry aiming to maintain sterility, avoid product and/or substrate inhibition and to ensure operational flexibility in order to keep pace with the changing market requirements. This section discusses the production of ethanol in a baker's yeast fermenter operated in both batch and fed-batch modes.

5.5.1 Model Development

Here, the model of a fed-batch bioreactor is developed. This model can also be modified to represent the batch operation by simply considering zero feed rates.

The process considered for modelling is a fed-batch biochemical reactor growing *Saccharomyces cerevisiae*, known as baker's yeast, on glucose (substrate) in a biological environment. The substrate is added continuously to the ethanol fermentation process during the period of operation. The feed is sterile, i.e., it contains neither the biomass nor the product.

Total Continuity Equation

$$\frac{d(\rho V)}{dt} = \rho F \qquad (5.36)$$

Assuming constant density (^), we obtain

$$\frac{dV}{dt} = F \qquad (5.37)$$

Component Continuity Equation

As obtained for the CSTB, the biomass mass balance equation has the following form:

$$\frac{d(Vx)}{dt} = r_1 V$$

$$= \llcorner xV \qquad (5.38)$$

Rearranging, we obtain

$$\frac{dx}{dt} = \mu x - \frac{F}{V}x \quad (5.39)$$

By the similar way, the substrate and product mass balance equations can be derived, respectively, as:

$$\frac{dS}{dt} = -\sigma x + \frac{F}{V}(S_f - S) \qquad (5.40)$$

$$\frac{dP}{dt} = \pi x - \frac{F}{V}P \qquad (5.41)$$

The above equations have two new terms, namely ° (the substrate consumption rate) and □ (the product formation rate). The complete fed-batch bioreactor model structure includes the following rate expressions along with Equations (5.37), (5.39), (5.40) and (5.41):

$$\mu = \frac{0.408S}{0.22+S} e^{-0.028P} \qquad (5.42)$$

$$\sigma = \frac{\mu}{0.1} \qquad (5.43)$$

$$\pi = \frac{S}{0.44+S} e^{-0.015P} \qquad (5.44)$$

The conservation of volume, as represented by Equation (5.37), is very appropriate in biochemical reactions as it permits to neglect the volume of the gases released on account of reaction (i.e., CO_2). Although the volume of CO_2 in the gaseous phase may be very significant, the equivalent volume in the condensed phase is assumed to be negligible (Mangesh and Jana, 2008).

5.5.2 Dynamic Simulation Results

In order to understand the example system behaviour, simulation runs are carried out. For the computer simulation of the above four state macroscopic bioreactor model structure, the required data are given in Table 5.3. The development of computer code is left as an exercise for the reader.

Table 5.3 Required data and system specifications

Initial biomass concentration (x_0), g/l	0.2
Initial glucose concentration (S_0), g/l	100.0
Initial ethanol concentration (P_0), g/l	0.0
Initial reactor volume (V_0), l	1.0
Total batch time, h	20.0
Feed rate (throughout the fed-batch operation) (F), l/h	1.0
Integration time interval = 0.004 h	

It is true that the sample bioreactor in batch as well as in fed-batch mode is inherently an unsteady state process. To obtain the concentration and rate profiles, each run continues for the duration of 20 h (batch time) with the initial conditions as tabulated.

Figure 5.5 describes the growth behaviour under batch mode of biological process operation with no feed input. It is observed that the concentrations of biomass and product ethanol increase exponentially up to almost 12th hour. However, once the amount of glucose is completely consumed, the ethanol concentration remains constant and the simulated model does not capture the biomass growth on the product. As a consequence, the biomass concentration also remains unchanged beyond 12th hour.

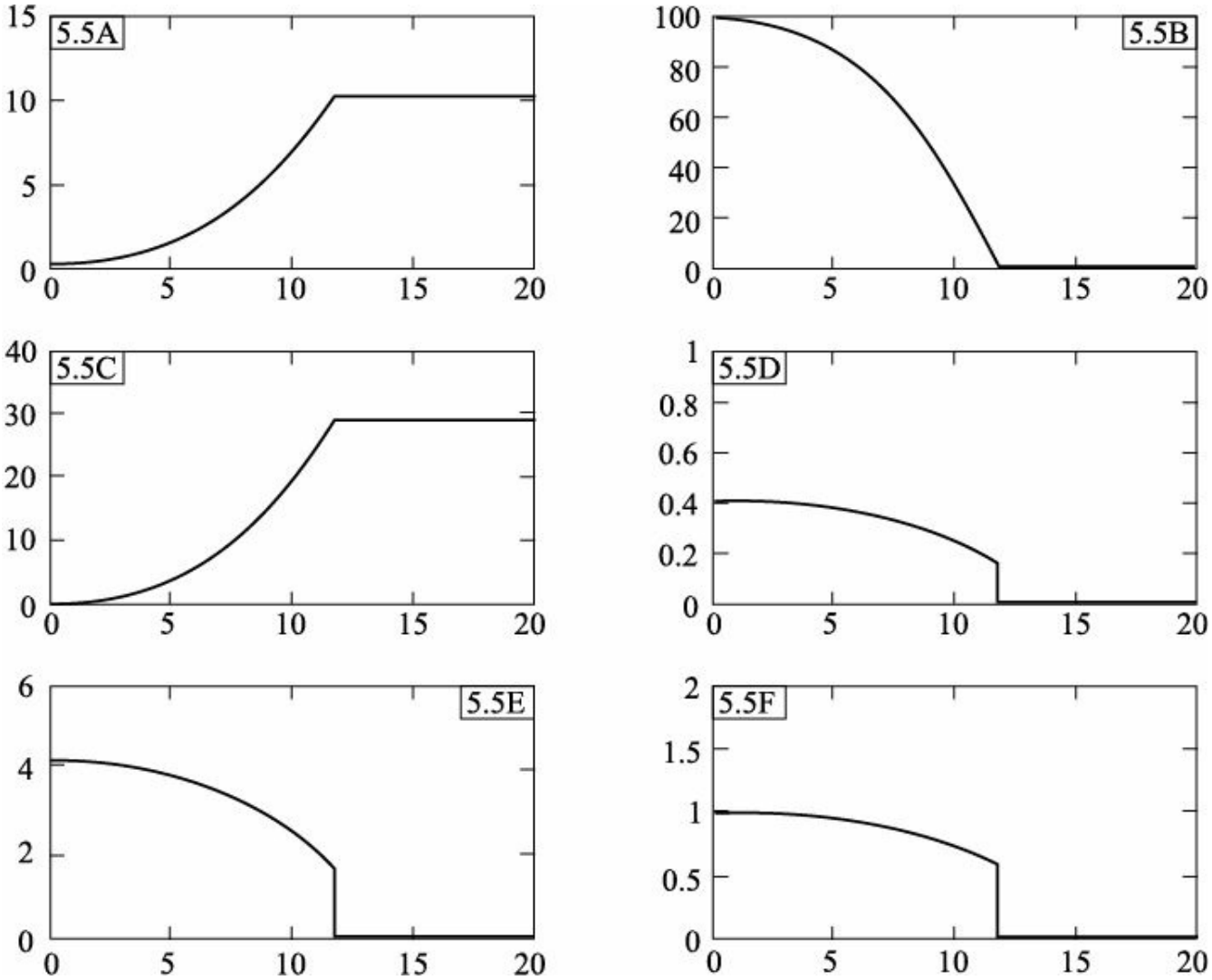

FIGURE 5.5 Concentration and rate profiles of the simulated process in batch mode [5.5A: *x* (ordinate) vs. time *t* (abscissa), 5.5B: *S* vs. *t*, 5.5C: *P* vs. *t*, 5.5D: ⌙ vs. *t*, 5.5E: ⌔ vs. *t*, 5.5F: ⌑ vs. *t*].

Figure 5.6 demonstrates the dynamic behaviour of the simulated reaction system under fed-batch condition. The concentration and rate profiles are shown in the figure for the constant feed rate of 1 l/h throughout the operation. It is supposed that the feed is completely sterile and it has substrate concentration of 100 g/l. It is obvious based on the simulation experiment that the biomass growth and product formation continue as long as the substrate is present there. The results also show that the specific growth rate and product formation rate decrease slowly with the gradual consumption of glucose.

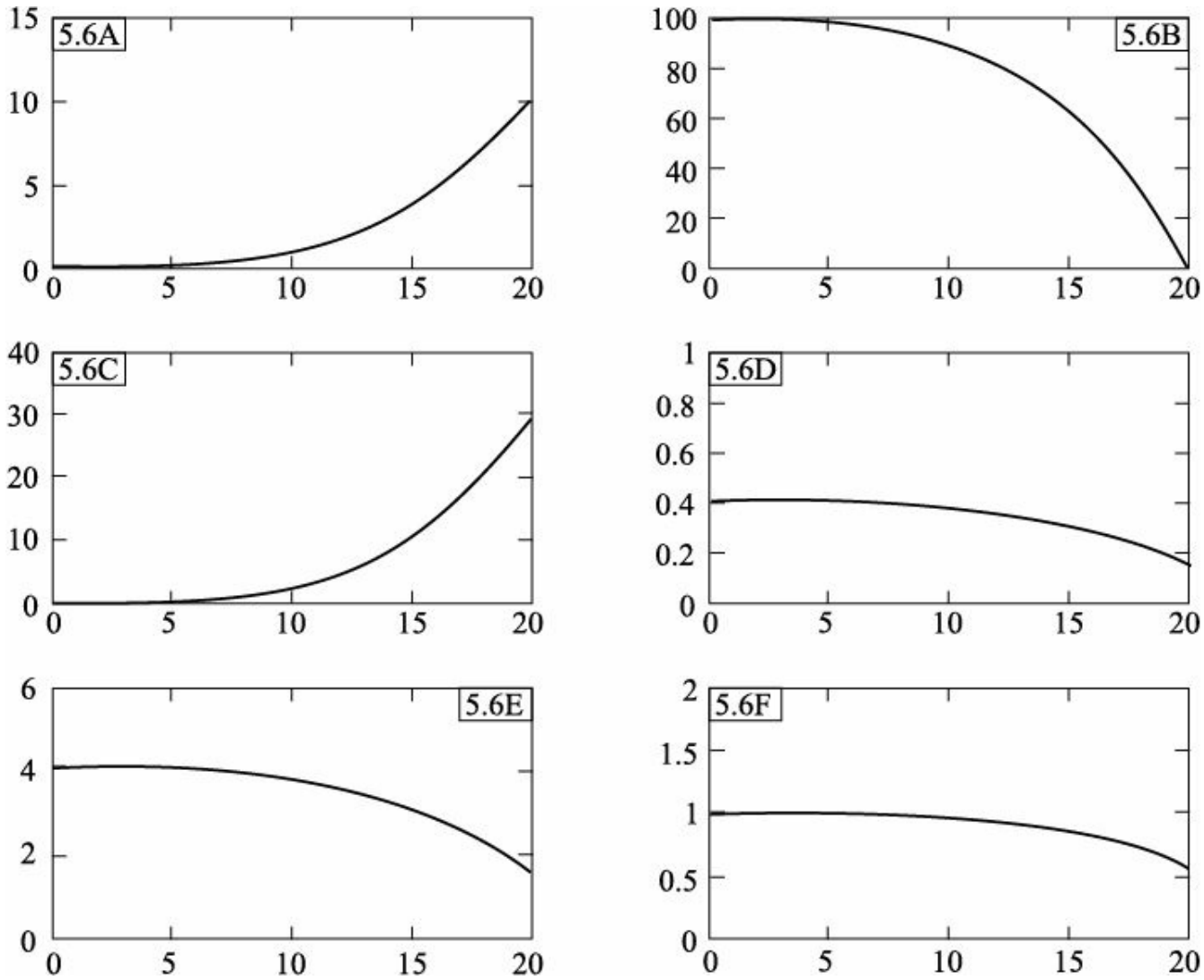

FIGURE 5.6 Concentration and rate profiles of the simulated process in fed-batch mode [5.6A: x vs. time t, 5.6B: S vs. t, 5.6C: P vs. t, 5.6D: $\llcorner$ vs. t, 5.6E: $\subset$ vs. t, 5.6F: $\sqsupset$ vs. t].

5.6 SUMMARY AND CONCLUSIONS

At the beginning of this chapter, we have studied the role of chemical engineers in the bioprocessing. The importance of biochemical reactors in the three step biotechnological operations is also explained. The study includes the development of mathematical modelling equations of a continuous stirred tank bioreactor. The model incorporates the biochemical reaction kinetics. The derived model structure is then solved in the process simulator. The interesting feature of the prescribed biochemical reactor, multiple steady states, is also analyzed.

In the next phase, a bioreactor is modelled in order to operate in both batch and fed-batch modes. The process considered is a reactor growing *S. cerevisiae* on glucose in a biological environment. The four state macroscopic reactor model with lumped biological representation has been simulated for dynamics study. Interested reader may consult the journal paper (Pham, Larsson and Enfors, 2000) for a detailed model that describes precisely the metabolism in aerobic fed-batch cultures of *S.cerevisiae*.

EXERCISES

5.1 Explain the following terms:

(i) Microorganisms

(ii) Fermentation

(iii) Medium
(iv) Biosynthesis
(v) Biocatalysis
(vi) Biodegradation
(vii) Antibiotics
(viii) Culture
(ix) Vaccines

5.2 What role do the chemical engineers play in bioprocessing?

5.3 Describe the multidisciplinary nature of biotechnology.

5.4 Describe how the various physico-chemical and thermal parameters of the broth are affected with the change of cell population.

5.5 Explain how the different parameters involved in the Monod growth kinetics [Equation (5.20)] are determined.

5.6 How are the biochemical reactions different from the chemical reactions?

5.7 Describe the kinetic equation for cell growth.

5.8 Define the yield coefficient and its variation with substrate concentration.

5.9 What is 'growth limiting substrate'?

5.10 Describe the limitations of the Monod model.

5.11 Explain how you determine μ_m and K_m in the Monod model by linearizing it.

5.12 Define the term 'dilution rate' in the biochemical reactor modelling equation.

5.13 Describe the concept of unstructured models. If there is a structured model, how can you define it?

5.14 Sometimes the specific growth rate increases at low substrate concentration and decreases at high substrate concentration, as shown in Figure 5.7. Probably the main reason behind this fact is that the substrate has a toxic effect on the biomass cells at a higher concentration. This effect is commonly known as the *substrate inhibition* and is represented by the following form of expression:

$$\mu = \frac{\mu_m S}{K_m + S + K_1 S^2} \qquad (5.45)$$

where K_1 is the inhibition constant. Obviously, when $K_1 = 0$, the above equation becomes Monod equation. Now

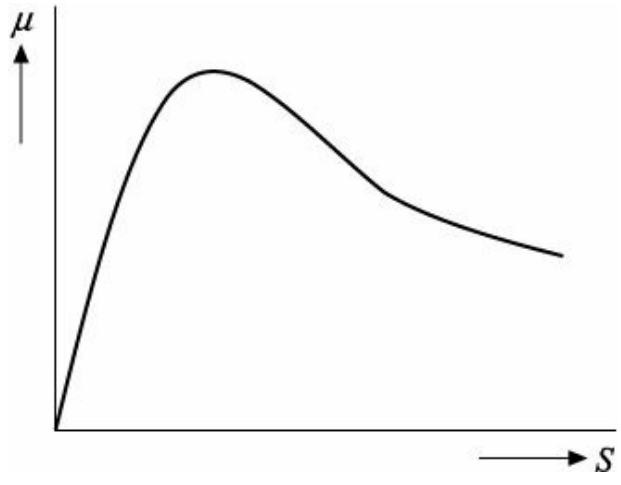

FIGURE 5.7 Influence of S on μ.

(i) Simulate the developed continuous stirred tank bioreactor model [Equation (5.25)] only replacing the Monod model by the above substrate inhibition model [Equation (5.45)]. Take the steady state data from Table 5.2 including $K_1 = 0.4545$ l/g.

(ii) Compare the process outputs obtained by simulating the CSTB with Monod model and that with substrate inhibition model.

(iii) Analyze the multiple steady states for the case of substrate inhibition.

5.15 Consider a biochemical reactor where the consumption of substrate (S) promotes the growth of biomass (x) and formation of product (P). The mathematical dynamical model (Farza, Busawon and Hammouri, 1998) of the process is constituted by the following three balance equations associated with x, S and P, respectively:

$$\begin{cases} \dfrac{dx}{dt} = r_1 - Dx \\ \dfrac{dS}{dt} = -y_1 r_1 - y_2 r_2 + D(S_f - S) \\ \dfrac{dP}{dt} = r_2 - DP \end{cases} \qquad (5.46)$$

where r_1 and r_2, respectively, denote the growth and the biosynthesis reaction rate; y_1 and y_2 are yield coefficients. D and S_f represent the dilution rate and the substrate concentration in the feed stream, respectively. Consider the following kinetic expressions:

$$\begin{cases} r_1 = \mu x \\ r_2 = \nu x \end{cases} \qquad (5.47)$$

with

$$\begin{cases} \mu = \mu_m \dfrac{S}{(K_{m1} + S + (S^2/K_1))} \dfrac{K_P}{(K_P + P)} \left(1 - \dfrac{P}{P_f}\right) \\ \nu = \nu_m \dfrac{S}{(K_{m2} + S)} \end{cases} \qquad (5.48)$$

where μ_m and ν_m are the biomass' maximum specific growth rate and the product's maximum specific synthesis rate respectively; K_{m1} and K_{m2} are the saturation constants; K_1, P_f and K_P are the inhibition constants. Simulate the prescribed bioreactor model to find out the steady state values of x, S and P (all are in g/l) under the following conditions:

$D = 0.15\ \text{h}^{-1}$, $y_1 = 5.1$, $y_2 = 1.5$, $\mu_m = 0.3\ \text{h}^{-1}$, $K_{m1} = 0.26$ g/l,

$K_1 = 297\ (\text{g/l})^2$, $P_f = 85$ g/l, $K_P = 8$ g/l, $\nu_m = 0.11\ \text{h}^{-1}$,

$K_{m2} = 9.5$ g/l, $S_f = 95$ g/l.

5.16 Consider a biological reactor in which a simple microbial culture involves a single biomass (x) growing on a single substrate (S) and yielding a single product (P). The reactor model (Bequette, 1998) comprises the following set of equations:

$$\begin{cases} \dfrac{dx}{dt} = (\mu - D)x \\ \dfrac{dS}{dt} = D(S_f - S) - \dfrac{\mu x}{Y} \\ \dfrac{dP}{dt} = -DP + (\alpha_1 \mu + \alpha_2)x \\ \mu = \mu_m \dfrac{S}{K_m + S + K_1 S^2}\left(1 - \dfrac{P}{P_f}\right) \end{cases} \tag{5.49}$$

where ⌙ is the specific growth rate, D the dilution rate, S_f the inlet substrate concentration, Y the yield coefficient, ⌙ $_m$ the maximum specific growth rate, K_m the saturation constant, and K_1 and P_f the inhibition constants. The necessary data are presented below:

$x = 6$ g/l, $S = 5$ g/l, $P = 19.14$ g/l, $Y = 0.4$ g/g,

¬↗1 = 2.2 g/g, ¬↗2 = 0.2 h^{-1}, $P_f = 50$ g/l, $K_1 = 0.04545$ l/g, $D = 0.202$ h^{-1},

⌙ $_m = 0.48$ h^{-1}, $K_m = 1.2$ g/l, $S_f = 20$ g/l.

(i) Develop the process simulator with computer code based on the above modelling equations of the biological reactor.

(ii) Verify that the steady state values for x, S and P given above are correct.

(iii) Analyze the multiply steady states (if exist).

5.17 The dynamic model of the baker's yeast production process in a fed-batch reactor is given as follows:

$$\begin{cases} \dfrac{dx}{dt} = \mu(S)x - \dfrac{F}{V}x \\ \dfrac{dS}{dt} = -\dfrac{\mu(S)x}{Y_x} - \dfrac{vx}{Y_P} + \dfrac{F}{V}(S_f - S) \\ \dfrac{dP}{dt} = vx - \dfrac{F}{V}P \\ \dfrac{dV}{dt} = F \end{cases} \tag{5.50}$$

with

$$\mu(S) = \frac{\mu_m S}{K_m + S + (S^2/K_1)} \tag{5.51}$$

Here, ⌙ $_m$, K_m, K_1 and ⌐ are the kinetic parameters, and Y_x and Y_P are the yield coefficients.

(i) Develop the model structure [Equation (5.50)].

(ii) Simulate the model using the data tabulated in Table 5.4 and considering total run time (t_f) of 150 h.

Table 5.4 Model parameters and initial conditions

⌙ $_m$

K_m	0.02 l/h
K_1	0.05 g/l
Y_x	5.0 g/l
Y_P	0.5 g [*x*]/g [*S*]
=	1.2 g [*P*]/g [*S*]
S_f	0.004 l/h
F	200 g/l
x_0	0.5 l/h
S_0	1.0 g/l
P_0	0.5 g/l
V_0	0.0 g/l
	150 l

REFERENCES

Agrawal, P., Lee, C., Lim, H.C., and Ramkrishna, D. (1982). Theoretical investigations of dynamic behavior of isothermal continuous stirred tank biological reactors, *Chem. Eng. Sci.*, 37, 453–462.

Aiba, S., Humphrey, A.E., and Millis, N.F. (1965). *Biochemical Engineering*, Academic Press, New York.

Bailey, J.E., and Ollis, D.F. (1986). *Biochemical Engineering Fundamentals*, 2nd ed., McGraw-Hill, Singapore.

Bequette, B.W. (1998). *Process dynamics: Modeling, Analysis, and Simulation*, 1st ed., Prentice-Hall, New Jersey.

Contois, D. (1959). Kinetics of bacterial growth relationship between population density and specific growth rate of continuous cultures, *J. Gen. Microbiol.*, 21, 40–50.

Dourado, A., and Calvet, J.L. (1983). Static optimization of ethanol production in a cascade reactor, In A. Halme, *Modelling and Control of Biotechnical Processes*, Oxford.

Edwards, V.H. (1970). The influence of high substrate concentration on microbial kinetics, *Biotechnol. Bioeng.*, 12, 679–712.

Farza, M., Busawon, K., and Hammouri, H. (1998). Simple nonlinear observers for on-line estimation of kinetic rates in bioreactors, *Automatica*, 34, 301–318.

Ghose, T.K. (1990). *Bioprocess Computations in Biotechnology*, 1st ed., Vol. 1, Ellis Horwood, London.

Jackson, J.V., and Edwards, V. H. (1975). Kinetics of substrate inhibition if exponential yeast growth, *Biotechnol. Bioeng.*, 17, 943–964.

Lee, J.M. (1992). *Biochemical Engineering,* 1st ed., Prentice-Hall, Englewood Cliffs, New Jersey.

Mangesh, G.M., and Jana, A.K. (2008). A comparison of three sets of DSP algorithms for monitoring the production of ethanol in a fed-batch baker's yeast fermenter, *Measurement*, 41, 970–985.

Marison, I.W. (1988). *Biotechnology for Engineers*, Ellis Horwood, Chichester.

Monod, J. (1942). *Recherches sur la croissance des cultures bacteriennes*, Paris, Hermann.

Moo-Young, M., and Blanch, H.W. (1981). Design of biochemical reactors: Mass transfer criteria for simple and complex systems, *Advances in Biochemical Engineering*, Fiechter, A. (Ed.), Vol. 19, Springer-Verlag, Berlin, pp. 1–69.

Moo-Young, M., and Chisti, Y. (1994). Biochemical engineering in biotechnology, *Pure & Appl. Chem.*, 66, 117–136.

Moser, H. (1958). *The Dynamics of Bacterial Populations in the Chemostat*, Carnegie Inst. Publication,

n 614, Washington.

Olsson, G. (1976). State of art in sewage treatment plant control, *AIChE Symposium Series*, 72, 52–76.

Peringer, P., Blachere, H., Corrieu, G., and Lane, A.G. (1972). Mathematical model of the kinetics of growth of Saccharomyces cerevisiae, *4th International Fermentation Symposium*, Kyoto, Japan.

Pham, H.T.B., Larsson, G., and Enfors, S.O. (2000). Growth and energy metabolism in aerobic fed-batch cultures of *Saccharomyces cerevisiae*: Simulation and model verification, *Biotechnol. Bioeng.*, 60, 474–482.

Powell, E. (1967). Growth rate of microorganisms as a function of substrate consumption. Microbial physiology and continuous culture, London: *3rd Symposium HMSO*.

Ramaswamy, S., Cutright, T.J., and Qammar, H.K. (2005). Control of a continuous bioreactor using model predictive control, *Process Biochem.*, 40, 2763–2770.

Rao, D.G. (2005). *Introduction to Biochemical Engineering*, 1st ed., Tata McGraw-Hill, New Delhi.

Tessier, G. (1942). Croissance des populations bacteriennes et quantites d'aliments disponsibles, *Review Science Paris*, 80–209.

Williams, D., Yousefpour, P., and Swanick, B.H. (1984). On-line adaptive control of a fermentation process, *IEE Proc.*, 131, 117–124.

Part III

Distillation

Distillation is a very old separation technology for separating liquid mixtures that can be traced back to the chemists in Alexandria in the first century AD. At the early stage, the distillation was mainly employed to manufacture the perfumes, brandy and other spirits from wine. With time, the distillation process has gained tremendous importance as a separation unit and today it is recognized as the heart of many industries. Distillation has an important role in our everyday life. It plays a role in the fuel we put in our cars, the perfumes we wear, the two-for-one cocktails we have at happy hour, and even the water we drink.

Distillation (the Latin root of the word refers to dropping or trickling) is a mass transfer operation, in which, the physical separation of a liquid or vapour or liquid–vapour mixture (*feed* stream) of two or more substances into its component fractions that have different boiling points is performed. The separation of a liquid mixture in a distillation column is carried out based on the differences in *volatility* (the ability to vaporize), and it occurs by the application and removal of heat. Distillation is an energy-intensive method of performing separations in the petroleum refinery, petrochemicals, natural gas processing, chemical processing, food, pulp and paper, and pharmaceutical industries. In the chemical and petroleum industries alone, this mass transfer unit is used to make almost 95% of all separations. Surprisingly, distillation processes account for approximately 8% of the total energy use of the U.S. industrial sector[1]. Mix et al.[2] found that 60% of energy used by chemical industry is for distillation.

1 Information collected from the report prepared for the U.S. Department of Energy (June 1993).

2 Mix, T.J., Dueck, J.S., and Weinberg, M. (1978). Energy conservation in distillation, *Chemical Engineering Progress,* 74, 49–55.

Types of Distillation Operation

There are three basic types of distillation: flash distillation, differential batch distillation, and fractional distillation. In a *flash distillation*, also known as *equilibrium distillation* or *equilibrium flash vaporization,* a liquid feed stream is brought into a flash drum or tank where the feed is partially vaporized when the pressure suddenly drops. As a result, liquid and vapour phases are produced, and these phases are in equilibrium with each other because they are in contact for a sufficiently long time. Flash distillation may be batchwise or continuous. However, this is the simplest and cheapest form of distillation, and is frequently used as a *pre-separator* before some equipment. The details of this type of separation are given in Chapter 12.

The second type of distillation is *differential batch distillation*, or more simply *differential distillation*. In this separation technique, the liquid that to be separated is placed in a still or a pot, and this still is then heated. The lowest boiling component vaporizes first as the still is heated. The produced vapours are then condensed and collected in the distillate pot. As the component with the lower boiling point is removed, the boiling point of the remaining liquid in the still gradually increases. This operation continues until the desired quantity of distillate having specified quality is collected in the distillate pot. The details of batch distillation dynamics are reported in Chapters 9 and 11 for binary and multicomponent mixture separations, respectively.

Another type of distillation is *fractional distillation* o r *continuous fractional distillation*, in which, a distillation column, a condenser, and a reboiler are often utilized. Continuous distillation, as the name says, continuously takes a feed and separates it into two or more products. Note that the present discussion focuses on the plate type distillation column, not the packed type column. Feed to the distillation column enters on a tray (called as *feed tray*) somewhere in between the top tray and the bottom tray. The portion of the column above the feed plate is the *rectifying section* or *enriching section* or *absorption section* and that below is the *stripping section* or *exhausting section* or *desorption section*. All vaporous feed travels up the column into rectifying section, while all liquid feed travels down into the stripping section of the column. The column comprises of several trays, which permit the simultaneous travel of liquid down the tray and vapour up the tray, allowing mixing of the two phases and therefore equilibrium. The overhead vapour that leaves the top plate of the column enters the *condenser* where it is either partially or completely condensed. The condensed liquid is then collected in an *accumulator* (also known as *reflux drum*). A fraction of this accumulated liquid is recycled back to the top tray of the column as *reflux* to promote separation and another fraction of the rest liquid is withdrawn as *distillate* (also called *top product* or *overhead product*). When the overhead vapour is totally condensed to the liquid phase and the top product is withdrawn as a liquid, the condenser is called a *total condenser*. The *partial condenser* provides the liquid reflux in addition to vapour distillate or in addition to both liquid and vapour distillates. The liquid leaving the bottom plate of the column is fed into the *reboiler* where heat input causes a portion of liquid to vaporize. The vapour produced (called as *boilup vapour*) is allowed to flow back up through the column, and the liquid product is withdrawn from the reboiler which is called the *bottoms* or *bottom product*. The bottom product contains mostly low volatile components, whereas the overhead product is richer in the more volatile components. Remember that the bottom product is almost exclusively liquid, while the distillate may be a liquid or a vapour or both. Several continuous distillation columns are dealt in details in different chapters (6, 7, 10, 14 and 15) of this book.

Based on the number of components present in the feed mixture, the distillation column is also categorized. When a mixture having two components is fractionated in a distillation column, that process is called *binary distillation* column. For three-

component feed mixture, the process is *ternary distillation* column. The *multicomponent distillation* column can separate a mixture of more than two components and so the ternary distillation is a multicomponent distillation column. A good example of a binary distillation is separating ethyl alcohol (ethanol) from water. The crude distillation column, which is frequently used to separate a complex mixture of hydrocarbons, is an example of the multicomponent distillation. Nearly all commercial distillation columns are the multicomponent distillations.

6

Compartmental Distillation Model

6.1 INTRODUCTION

Continuous distillation is an important commercial process that is widely used in the petroleum, chemical and food industries as a separation or purification unit. This process is most often used with big volume products. Distillation columns are generally employed to separate two or more products that have sufficiently different boiling points, to remove a volatile solvent from a nonvolatile product and to separate a volatile product from nonvolatile impurities. In order to predict the dynamics of a distillation column, it is essential to develop the mathematical model of the column.

The *low-order* (sometimes called *reduced-order* or *approximate*) process models are usually preferred for use in the closed-loop systems for the reduction of design complexity as well as computational load involved in the implementation of advanced nonlinear control schemes (Jana and Samanta, 2006). A low-order modelling technique for separation processes is developed by considering a staged column as a compartment system in which a number of stages are lumped to form an equivalent stage. This method helps to produce the reduced-order models of separation processes directly and without linearization. For distillation column, this approximate model is commonly known as *compartmental distillation model*.

In this chapter, the compartmental modelling of a binary distillation column is carried out. The dynamic mathematical model is comprised of total and component continuity equations along with vapour–liquid equilibrium (VLE) relationship. In addition, the dynamic simulation of the example column has been presented in this chapter through computer programming.

6.2 AN OVERVIEW

Distillation is an *equilibrium stage operation*. In each stage of a distillation column, the boiling of a liquid stream evolves a vapour stream. The vapour composition is generally different from the liquid composition. When the vapour composition is the same as the liquid, the system is termed a *constant boiling* or *azeotropic* mixture. Usually, in every stage, a vapour phase is contacted with a liquid phase and accordingly the mass transfer takes place. The *less volatile* (also called *heavy* or *high boiling)* components concentrate in the liquid-phase and the *more volatile* (*light* or *low boiling*) components concentrate in the vapour-phase. The vapour and liquid streams leaving a stage are said to be in physical equilibrium if the following conditions are satisfied (Denbigh, 1955).

1. The temperature of the vapour phase is equal to the temperature of the liquid phase—*thermal equilibrium.*
2. The total pressure throughout the vapour phase is equal to the total pressure throughout the liquid phase—*mechanical equilibrium.*
3. The tendency of each component to escape from the liquid phase to the vapour phase is exactly equal to its tendency to escape from the vapour phase to the liquid phase—*phase equilibrium.*

Actually in phase equilibrium, the chemical potential (function of temperature, pressure and phase

composition) of each component in the liquid phase is the same with that in the vapour phase. Suppose the two phases are in thermal and mechanical equilibrium. Now to attain the phase equilibrium, additionally there should be no composition change in both the phases due to the equal rate of vaporization and condensation of each species.

Now consider an ideal case where the above mentioned third condition may be represented as:

$$P_i^S x_i = P_t y_i \qquad (6.1)$$

where P_i^S is the vapour pressure of pure component i, P_t the total pressure, x_i the mole fraction of component i in the liquid-phase and y_i the mole fraction of component i in the vapour-phase. However, Equation (6.1) can be rewritten as:

$$\frac{y_i}{x_i} = \frac{P_i^S}{P_t} \qquad (6.2)$$

For vapour–liquid equilibrium, *k*-value (or *vapour–liquid equilibrium coefficient*) is defined by:

$$k = \frac{y}{x} \qquad (6.3)$$

For any component i,

$$k_i = \frac{y_i}{x_i} = \frac{P_i^S}{P_t} \qquad (6.4)$$

From Equation (6.4), it is obvious that the equilibrium coefficient depends on temperature (since according to Antoine equation, vapour pressure is a function of solely the temperature) and pressure. In the following passages, two nonideal cases have been considered.

If the liquid-phase nonideality is taken into account, Equation (6.4) is modified to:

$$k_i = \frac{\gamma_i P_i^S}{P_t} \qquad (6.5)$$

where γ_i is the liquid-phase activity coefficient of component i. The details of liquid-phase nonideality are dealt in Chapter 8.

Again for both liquid and vapour-phase nonidealities, the vapour–liquid equilibrium coefficient is expressed as:

$$k_i = \frac{\hat{f}_i^L / x_i P_t}{\hat{f}_i^V / y_i P_t} \qquad (6.6)$$

where $\hat{f}_i^V$ and $\hat{f}_i^L$ are the fugacities of component i in the vapour and liquid mixtures, respectively. Chapter 13 presents the details of nonidealities that exist in vapour as well as in liquid phases. We must note that the equilibrium coefficient for the above two nonideal cases is a function of phase composition(s), temperature and pressure.

For vapour–liquid separation processes, an index of the relative separability of two chemical components i and j is represented by the *relative volatility* α_{ij} defined as the ratio of their *k*-values:

$$\alpha_{ij} = \frac{k_i}{k_j} \qquad (6.7)$$

Inserting Equation (6.4) in the above equation, we obtain

$$\alpha_{ij} = \frac{y_i / x_i}{y_j / x_j} \qquad (6.8)$$

For a binary system, it is well-known that

$$x_i + x_j = 1 \qquad (6.9)$$

$$y_i + y_j = 1 \qquad (6.10)$$

Therefore, Equation (6.8) yields

$$\alpha_{ij} = \frac{y_i / x_i}{(1 - y_i)/(1 - x_i)} \qquad (6.11)$$

After rearranging, the simple VLE relationship for a binary mixture can be obtained as:

$$y_i = \frac{\alpha_{ij} x_i}{1 + (\alpha_{ij} - 1) x_i} \qquad (6.12)$$

In a similar way, it is easily possible to derive the VLE relationship for the multicomponent mixtures as:

$$y_i = \frac{\alpha_{ij} x_i}{1 + \sum_{i=1}^{N_c} (\alpha_{ij} - 1) x_i} \qquad (6.13)$$

where N_c is the number of components present in the mixture and j is the reference component.

6.3 THE PROCESS AND THE MODEL

6.3.1 Process Description

The main objective of the present study is to develop the compartmental binary distillation model. The distillation column, which is sketched in Figure 6.1, contains one feed stream and two product streams (distillate and bottoms). A saturated liquid mixture containing two components (1-propanol and ethanol) is fed in the column, onto the feed tray f, with a flow rate F and a mole fraction (or composition) of more volatile component (ethanol) Z. The overhead vapour stream with a flow rate V_R and a mole fraction y_R is totally condensed (not subcooled) in a total condenser and then the condensed liquid is temporarily held in the reflux drum. A fraction of this accumulated liquid is pumped back in the column as reflux stream with a flow rate R. Also, a part of the liquid is withdrawn from the reflux drum as distillate product with a flow rate D. Let m_D be the liquid holdup in the reflux drum having composition x_D. Then it is obvious that x_D is the composition of both the reflux and distillate streams. Note that y_R is not equal, dynamically, to x_D. Only at steady state, y_R and x_D are equal. The liquid with a flow rate L_S leaving the stripping section is accumulated at the base of the distillation column and then that liquid stream flows into the reboiler, which is a partial one. A fraction of this liquid, which is vaporized in the reboiler,

returns to the stripping section with a flow rate V. Some of the liquid is withdrawn from the reboiler as bottom product with a flow rate B and a composition x_B. Let m_B be the liquid holdup at the bottom section of the column having composition x_B.

6.3.2 Mathematical Model

Assumptions

The following assumptions have been made to construct the mathematical model.

- The vapour holdup in each compartment is negligible compared to the liquid holdup. Although the vapour volume is relatively large, the number of moles is generally small because the vapour density is considerably much smaller than the liquid density. Of course, this assumption is not valid in high-pressure columns.
- Constant liquid holdup in each compartment (including reflux drum and column base) is considered.
- Constant molal overflow is assumed. Actually, the molar flow rates of vapour and liquid are nearly constant in each compartment (or envelope or section) of the column. It also ensures that the operating lines on the familiar McCabe–Thiele diagram are straight lines. This results from nearly equal molar heats of vaporization, so that each mole of condensing vapour releases sufficient heat to vaporize about one mole of liquid.
- The liquids in each section (including reflux drum and column base) are perfectly mixed.
- The heat losses to and from the column are small and neglected.
- The relative volatility remains constant with time and throughout the column.
- Each tray is 100% efficient (*ideal* or *theoretical tray*), which reveals that the outgoing liquid and vapour streams are in equilibrium with each other.
- The dynamics of the condenser and reboiler are neglected. This assumption is usually not a good one for most of the commercial-scale distillation columns. In those columns, the dynamic response of these peripheral heat exchangers is much faster than the response of the column itself.
- The liquids in the reboiler and in the column base are perfectly mixed together and have the total holdup m_B having composition x_B.

Model development

The total (or overall) and component (or partial) material balance equations will be derived based on the following dynamics:

$$\left[\frac{\text{Input of material}}{\text{time}}\right]-\left[\frac{\text{Output of material}}{\text{time}}\right]=\left[\frac{\text{Accumulation of material}}{\text{time}}\right] \qquad (6.14)$$

In this balance equation, all the three terms are in gm-moles per minute (gmol/min). For the sample distillation column (see Figure 6.1), the flow rate of a liquid leaving the rectifying section (L_R) is equal to the reflux flow rate (R), which means,

$$L_R = R \qquad (6.15)$$

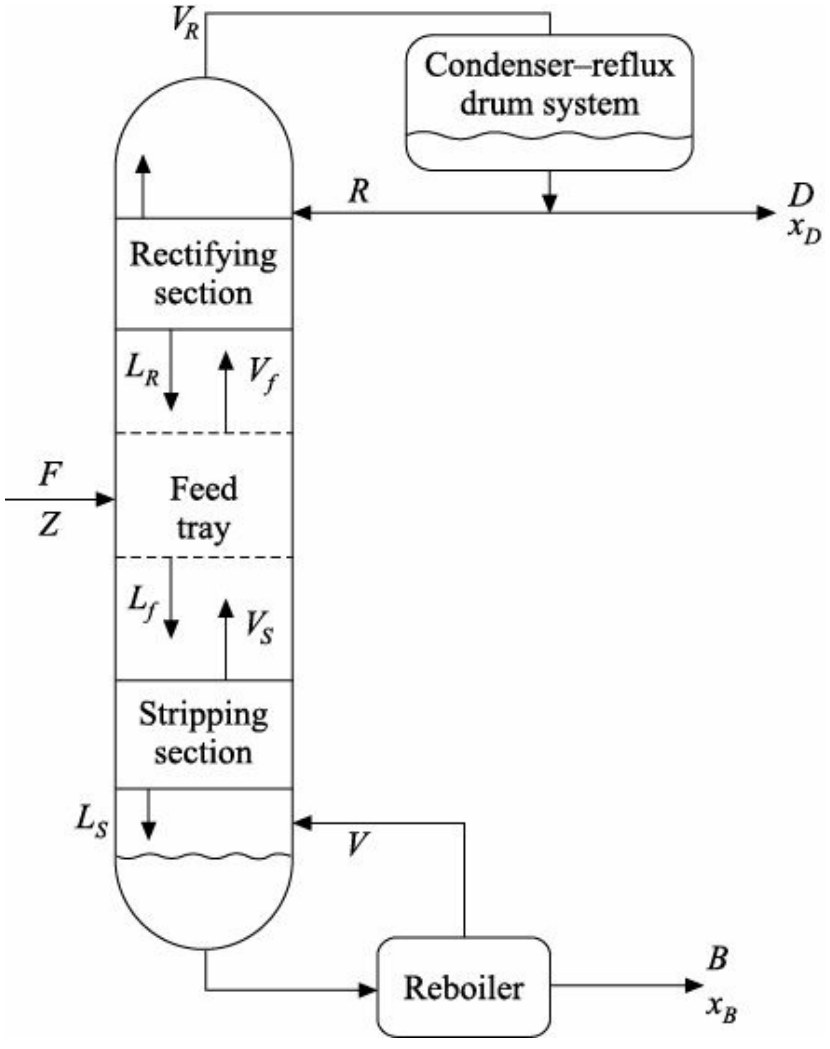

FIGURE 6.1 Schematic representation of the example distillation column.

Similarly, the flow rate of a liquid leaving the feed tray (L_f) is equal to that of a liquid leaving the stripping section (L_S) and so

$$L_f = L_S = R + F \qquad (6.16)$$

The vapour flow rate through all trays of the column is the same. Hence,

$$V_R = V_f = V_S = V \qquad (6.17)$$

where the suffix 'R' represents the rectifying section, 'f' the feed tray and 'S' the stripping section. All these flow rate relationships [Equations (6.15) to (6.17)] are applicable at dynamic as well as steady state. Remember that these liquid and vapour flow rates are not necessarily constant with time. In general practice, R and V are manipulated by the employed control scheme to control x_D and x_B respectively.

In the following, all compartments of the distillation column have been modelled based on the assumptions adopted.

Condenser–Reflux Drum System (subscript 'D')

The input and output flows and their respective compositions are shown for the condenser–reflux drum system in Figure 6.2. The balance equations in terms of total mass and a lighter component (ethanol) mass have been formulated [based on Equation (6.14)] as below.

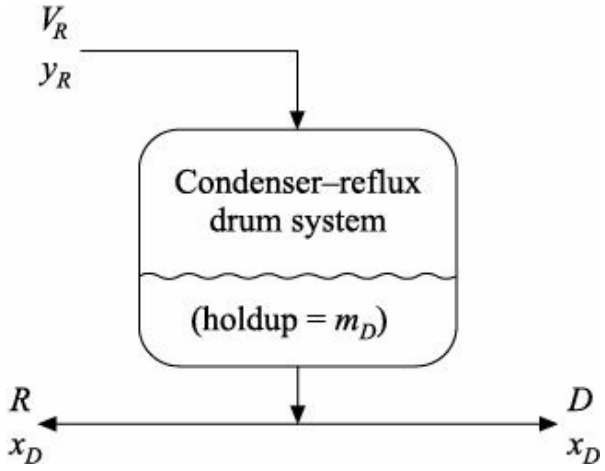

FIGURE 6.2 Condenser–reflux drum system.

Total continuity equation

$$\dot{m}_D = \frac{dm_D}{dt} = V_R - R - D \qquad (6.18)$$

The dot symbol (.) (over-dot) is used throughout this chapter to represent the time (t) derivative. Since constant liquid holdup is assumed, the above equation becomes:

$$V = R + D \qquad (6.19)$$

Component continuity equation

$$\dot{m}_D \dot{x}_D = \frac{d(m_D x_D)}{dt} = V_R y_R - (R + D)x_D \qquad (6.20)$$

Inserting Equation (6.19) into Equation (6.20) and rearranging, we obtain

$$\dot{x}_D = \frac{V}{m_D}(y_R - x_D) \qquad (6.21)$$

Rectifying Section (subscript '*R*')

Total and component mass balance equations can be derived for the rectifying section considering the incoming and outgoing flows as shown in Figure 6.3.

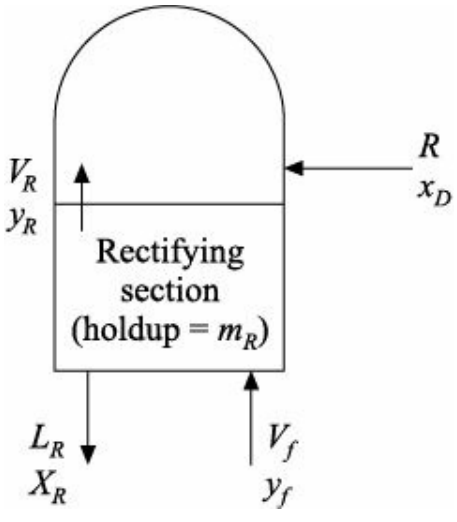

FIGURE 6.3 Rectifying section.

Total continuity equation

$$\dot{m}_R = R + V_f - L_R - V_R \qquad (6.22)$$

Since $V_R = V_f = V$ and m_R is constant, the above equation becomes Equation (6.15).

Component continuity equation

$$\dot{m}_R \dot{x}_R = Rx_D + V_f y_f - L_R x_R - V_R y_R \quad (6.23)$$

Substituting $L_R = R$, and $V_R = V_f = V$ and rearranging, we get

$$\dot{x}_R = \frac{1}{m_R}[R(x_D - x_R) + V(y_f - y_R)] \qquad (6.24)$$

Feed Tray (subscript '*f*')

The schematic representation of the feed tray is shown in Figure 6.4. Let q_F represent the *quality* of the feed stream, where $q_F = L_F/F$ and therefore, $1 - q_F = V_F/F$. Here, L_F and V_F are the flow rates of liquid and vapour feeds respectively, and obviously $F = L_F + V_F$. The flow rate of a vapour stream leaving the feed stage (V_f) can be expressed as:

$$V_f = V_S + V_F = V_S + F(1 - q_F) \qquad (6.25)$$

Similarly, the flow rate of a liquid stream leaving the feed tray can be expressed as:

$$L_f = L_R + L_F = L_R + Fq_F \qquad (6.26)$$

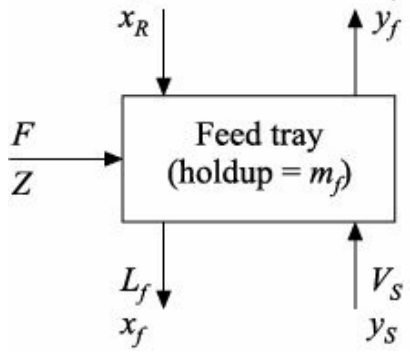

FIGURE 6.4 Feed tray.

Hence, for the case of a partially vaporized feed, Equation (6.16) must be modified to the following form of equation:

$$L_f = L_S = L_R + Fq_F = R + Fq_F \qquad (6.27)$$

and Equation (6.17) should be modified to the following two equations:

$$V_S = V \qquad (6.28)$$

$$V_f = V_R = V_S + F(1 - q_F) \qquad (6.29)$$

Now it is not difficult to develop the material balance equations for the feed tray.

The quality of the feed stream can be expressed by $q_F = (L_f - L_R)/F$. Notice that q_F has the following numerical limits for the various conditions:

Superheated vapour feed, $q_F < 0$

Saturated vapour feed, $q_F = 0$

Partially vaporized feed, $0 < q_F < 1$

Saturated liquid feed, $q_F = 1$

Subcooled liquid feed, $q_F > 1$.

For the example distillation column, a saturated liquid feed ($q_F = 1$) has been considered. And so the balance equations can be derived as reported in the following text.

Total continuity equation

$$\dot{m}_f = L_R + F + V_S - L_f - V_f \qquad (6.30)$$

For the prescribed column, $V_S = V_f = V$ and m_f is assumed constant. Therefore, the above equation gives $L_f = L_R + F$.

Component continuity equation

$$\dot{m}_f \dot{x}_f = L_R x_R + FZ + V_S y_S - L_f x_f - V_f y_f \qquad (6.31)$$

After substituting, $L_f = L_R + F$ and $V_S = V_f = V$, and rearranging, we finally get

$$\dot{x}_f = \frac{1}{m_f}[L_R(x_R - x_f) + F(Z - x_f) + V(y_S - y_f)] \qquad (6.32)$$

Stripping Section (subscript '*S*')

The compartment representing the stripping section is shown in Figure 6.5. Making balance around the stripping section, the following continuity equations can be obtained.

Total continuity equation

$$\dot{m}_S = L_f + V - L_S - V_S \qquad (6.33)$$

which implies that $L_S = L_f$.

Component continuity equation

$$\dot{m}_S \dot{x}_S = L_f x_f + V y_B - L_S x_S - V_S y_S \qquad (6.34)$$

Considering $L_f = L_S$, $V_S = V$ and constant liquid holdup, we finally obtain

$$\dot{x}_S = \frac{1}{m_S}[L_S(x_f - x_S) + V(y_B - y_S)] \qquad (6.35)$$

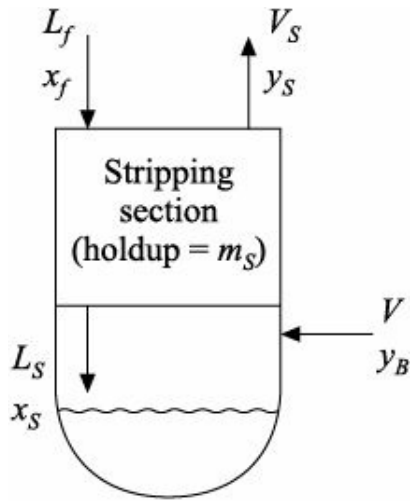

FIGURE 6.5 Stripping section.

Reboiler–Column Base System (subscript '*B*')

Figure 6.6 depicts a typical equilibrium stage (vapour stream *V* is in equilibrium with liquid stream *B*) comprising of a partial reboiler and the base of the distillation column. This combined system can mathematically be represented by the following material balance equations.

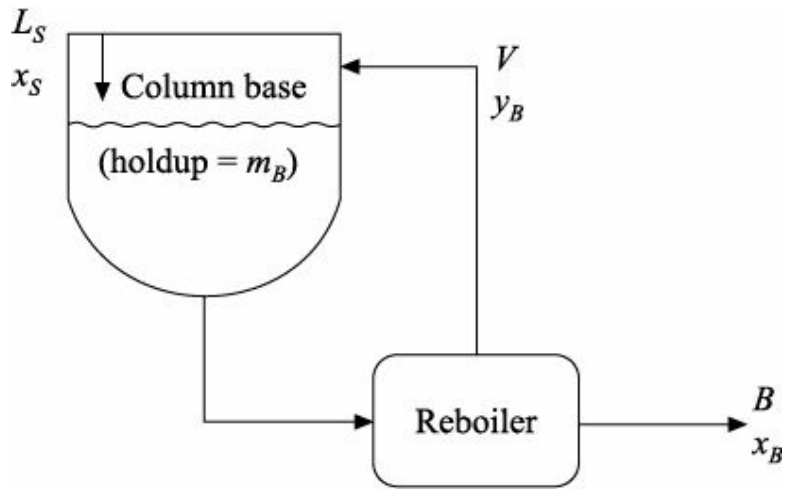

FIGURE 6.6 Reboiler–Column base system.

Total continuity equation

$$\dot{m}_B = L_S - B - V \qquad (6.36)$$

Since m_B is constant, so $B = L_S - V$.

Component continuity equation

$$\dot{m}_B \dot{x}_B = L_S x_S - B x_B - V y_B \qquad (6.37)$$

Simplifying,

$$\dot{x}_B = \frac{1}{m_B}[L_S x_S - B x_B - V y_B] \qquad (6.38)$$

The concept of distillation model reveals that in addition to the derived material balance and fluid flow equations for all envelopes, the bulk of the model involves VLE calculations. For the present case, a simple relative volatility-based VLE relationship [Equation (6.12)] has been employed to calculate the vapour-phase composition. As stated earlier, all trays are assumed to be ideal since efficiency is 100%.

6.4 DYNAMIC SIMULATION

The developed compartmental distillation model includes a set of ordinary differential equations (ODEs) and algebraic equations (AEs). In this differential–algebraic system, the ODEs represent the material balances, whereas the AEs represent the flow rates in addition to the vapour-liquid equilibrium. In the process simulator, the total continuity equations are used to calculate the flow rates, component continuity equations are employed to compute the liquid-phase compositions, and the vapour-phase compositions are calculated using the VLE relationship. For the concerned distillation column, the operating and steady state conditions are reported in Table 6.1 as well as in Program 6.1. The developed dynamic process model will be simulated according to the following sequential steps:

Step 1: Input data for variables: Liquid-phase compositions, x for all compartments (including reflux drum and column base).

Step 2: Input data for constant inputs/parameters: Feed rate F, with composition Z, relative volatility α, and liquid holdups m, for all compartments (including reflux drum and column base). Note the fact that the values of input disturbance as well as uncertain modelling parameter may change sometimes during the operation.

Step 3: Input the value for manipulated variables at each time step: In real-time operations, the reflux flow rate R, and vapour boil-up rate V, are considered as manipulated variable for controlling the distillate composition x_D, and bottom product composition x_B, respectively. In the present case, no controllers are implemented and we input the value for these flow rates at every time step.

Step 4: Calculate the vapour-phase composition y, for all sections (excluding reflux drum since there is no vapour).

Step 5: Compute the internal liquid flow rates along with the bottom product flow rate.

Step 6: Update the liquid-phase compositions on all trays (including reflux drum and column base) for the next time step. The numerical integration is done by using the classical Euler method (details in Chapter 2).

Step 7: To predict the distillation column dynamics for the next step in time, go back to Step 3.

Table 6.1 Operating and steady state conditions

Binary system: 1-propanol/ethanol	
Distillate composition (mol fraction), x_D	0.7504868
Composition of liquid in rectifying section (mol fraction), x_R	0.6006191
Composition of liquid on feed plate (mol fraction), x_f	0.4735253
Composition of liquid in stripping section (mol fraction), x_S	0.3665335
Bottoms composition (mol fraction), x_B	0.2495303
Feed flow rate (gmol/min), F	100.00
Feed composition (mol fraction), Z	0.5
Distillate flow rate (gmol/min), D	50.00
Reflux flow rate (gmol/min), R	128.01
Bottoms flow rate (gmol/min), B	50.00
Vapour boil-up rate (gmol/min), V	178.01
Tray holdups (gmol), $m_R = m_f = m_S$	10.00
Reflux drum holdup (gmol), m_D	100.00
Bottom (column base + reboiler) holdup (gmol), m_B	100.00
Integration time interval (min), dt	0.005
Relative volatility, α	2.0

A computer program (Fortran 90) is assembled in Program 6.1 to demonstrate the dynamic simulation of the prescribed distillation column. Note that the reported distillation simulator (Program 6.1) provides steady state process response because the given initial values for all variables are steady state values. To

investigate the dynamic process response, it is sufficient to change the value of any input variable, e.g., reflux flow rate, vapour boil-up rate (both are considered as input variables since they are manipulated by a control algorithm), feed rate, feed composition, etc., and consequently, the process simulator will reach at a new steady state.

PROGRAM 6.1 *Dynamic Distillation Simulator*

```
! ALPHA = Relative volatility
! B = Bottoms flow rate
! dt = Integration time interval
! F = Feed flow rate
! L = Internal liquid flow rate
! M = Liquid holdup in the compartment
! R = Reflux flow rate
! V = Vapour flow rate
! X = Liquid composition
! Y = Vapour composition
! Z = Feed composition
PROGRAM COMPARTMENTAL_DISTILLATION_MODEL
IMPLICIT NONE

! Declaration

INTEGER::n
INTEGER,PARAMETER::j=5000
REAL,PARAMETER::ALPHA=2.0,dt=0.005
REAL,DIMENSION(j)::XB,XS,XF,XR,XD,YB,YS,YF,YR
REAL,DIMENSION(j)::LR,R,LS,B,V
REAL,DIMENSION(j)::Time
REAL::MB,MD,MS,MF,MR,Z,F
OPEN(UNIT=2,File="dynamic_state.dat")

! Initialization

XB(1)=0.2495303
XS(1)=0.3665335
XF(1)=0.4735253
XR(1)=0.6006191
XD(1)=0.7504868

MB=100.00
MD=100.00
MS=10.00
MF=10.00
MR=10.00

Z=0.5
F=100.0

Time(1)=0.00

DO n=1,j !——Starting of main loop——!

R(n)=128.01
V(n)=178.01

YB(n)=(Alpha*XB(n))/(1+(Alpha-1)*XB(n))
YS(n)=(Alpha*XS(n))/(1+(Alpha-1)*XS(n))
YF(n)=(Alpha*XF(n))/(1+(Alpha-1)*XF(n))
YR(n)=(Alpha*XR(n))/(1+(Alpha-1)*XR(n))

LR(n)=R(n)
```

```
LS(n)=R(n)+F
B(n)=LS(n)-V(n)

! Reboiler-column base system

XB(n+1)=XB(n)+(1/MB)*dt*((LS(n)*XS(n))-
& (B(n)*XB(n))-(V(n)*YB(n)))

! Stripping section

XS(n+1)=XS(n)+(1/MS)*dt*((LS(n)*(XF(n)-
& XS(n)))+(V(n)*(YB(n)-YS(n))))
! Feed plate

XF(n+1)=XF(n)+(1/MF)*dt*((LR(n)*XR(n))-
& (LS(n)*XF(n))+(F*Z)+(V(n)*(YS(n)-YF(n))))

! Rectifying section

XR(n+1)=XR(n)+(1/MR)*dt*((LR(n)*(XD(n)-
& XR(n)))+(V(n)*(YF(n)-YR(n))))

! Condenser-reflux drum system

XD(n+1)=XD(n)+(1/MD)*dt*(V(n)*(YR(n)-XD(n)))

Time(n+1)=Time(n)+dt

PRINT*,Time(n+1),XD(n+1),XR(n+1),XF(n+1),XS(n+1),XB(n+1)
WRITE(2,FMT=100)Time(n+1),XD(n+1),XR(n+1),XF(n+1),XS(n+1),XB(n+1)
100 FORMAT (1X,6(2X,F10.5))

END DO !——End of main loop——!

END FILE 2
REWIND 2
CLOSE(2)

END PROGRAM COMPARTMENTAL_DISTILLATION_MODEL
```

6.5 SUMMARY AND CONCLUSIONS

In this chapter, the detailed development of a low-order compartmental distillation model is presented. The process model includes the material balance equations supported by the relative volatility-based VLE relationship. This chapter also describes the dynamic simulation of the developed distillation model through computer programming.

EXERCISES

6.1 What are the different types of distillation columns? How they differ from each other?

6.2 Why is distillation an important separation technique in many industries? Mention the significant advantages and disadvantages of this process.

6.3 Why are the partial condenser and reboiler considered as equilibrium stage?

6.4 Why is sometimes the equilibrium flash vaporizer employed in the up-stream section to produce the feed mixture (vapour + liquid) for the continuous distillation column?

6.5 What is thermodynamic equilibrium? How is the phase equilibrium attained?

6.6 Suppose that the vapour and liquid phases in a distillation tray are in thermal and mechanical equilibrium. Can we say that they are also in phase equilibrium? Give reasons.

6.7 Why is the process model, which is constructed in this chapter, called 'compartmental distillation model'?

6.8 Is it practical to assume 'constant relative volatility throughout the distillation column'? Please explain in support of your answer.

6.9 What are the basic differences between the conventional distillation and crude distillation column?

6.10 Develop the mathematical model for a compartmental distillation column considering variation in liquid holdups in each compartment (including reflux drum and column base). Discuss the calculation of all process variables.

6.11 It is well known that the equilibrium vapour composition is calculated from the following form of equation:

$$y_i = \frac{\alpha_{ij} x_i}{\sum_{i=1}^{N_c} \alpha_{ij} x_i} \qquad (6.39)$$

Now derive Equation (6.13) from the above correlation.

REFERENCES

Denbigh, K. (1955). *The Principles of Chemical Equilibrium*, Cambridge University Press, New York.

Jana, A.K., and Samanta, A.N. (2006). A hybrid feedback linearizing—Kalman filtering control algorithm for a distillation column, *ISA Transactions*, 45, 87–98.

7

Ideal Binary Distillation Column

7.1 INTRODUCTION

Distillation columns fractionate a feed mixture to produce product streams of desired purity, either for direct sale or for use in other processes. As mentioned in Chapter 6, when a distillation column separates a feed mixture of two components, that process is called as *binary distillation* column. If an ideal mixture having two components is dealt in a fractionating column, the column is usually referred to as *ideal binary distillation* column. In another sense, if all the trays of a binary distillation are ideal (100% efficient), then the column may be called ideal binary distillation column.

The previous chapter develops a mathematical model for a simple staged distillation distillation column. The column has been considered as a compartment system, in which, a number of stages are lumped. In this chapter, we will develop a dynamic model for a little more complex distillation process. Few assumptions, which are used to simplify a distillation model to a compartmental distillation model, will be avoided in the derivation of the ideal binary distillation column model. The present study also includes the dynamic simulation of the process model.

7.2 THE PROCESS AND THE MODEL

7.2.1 Process Description

The schematic diagram of a distillation column, which is dealt here, is shown in Figure 7.1. It consists of 15 trays, a reboiler and a partial condenser. The trays are numbered from the bottom to the top; the bottom tray has number 1 and the top tray has number 15. The feed is a mixture of components 1-propanol and ethanol. On the fifth tray of the column, a partially vaporized feed (liquid + vapour) is introduced. The overhead vapour is partly condensed in the partial condenser and the noncondensed vapour (not superheated) is withdrawn from the reflux drum as vapour distillate. A fraction of the condensed liquid (not subcooled) is recycled back in the column as reflux stream and some of the liquid is removed as liquid distillate product. At the base of the column, the bottom product is collected as a liquid stream. The boil-up vapour is generated using steam as a heating medium in the reboiler and the produced vapour returns to the bottom plate. The vapour and liquid distillates in the reflux drum, and the boil-up vapour and bottom product streams in the reboiler are in equilibrium.

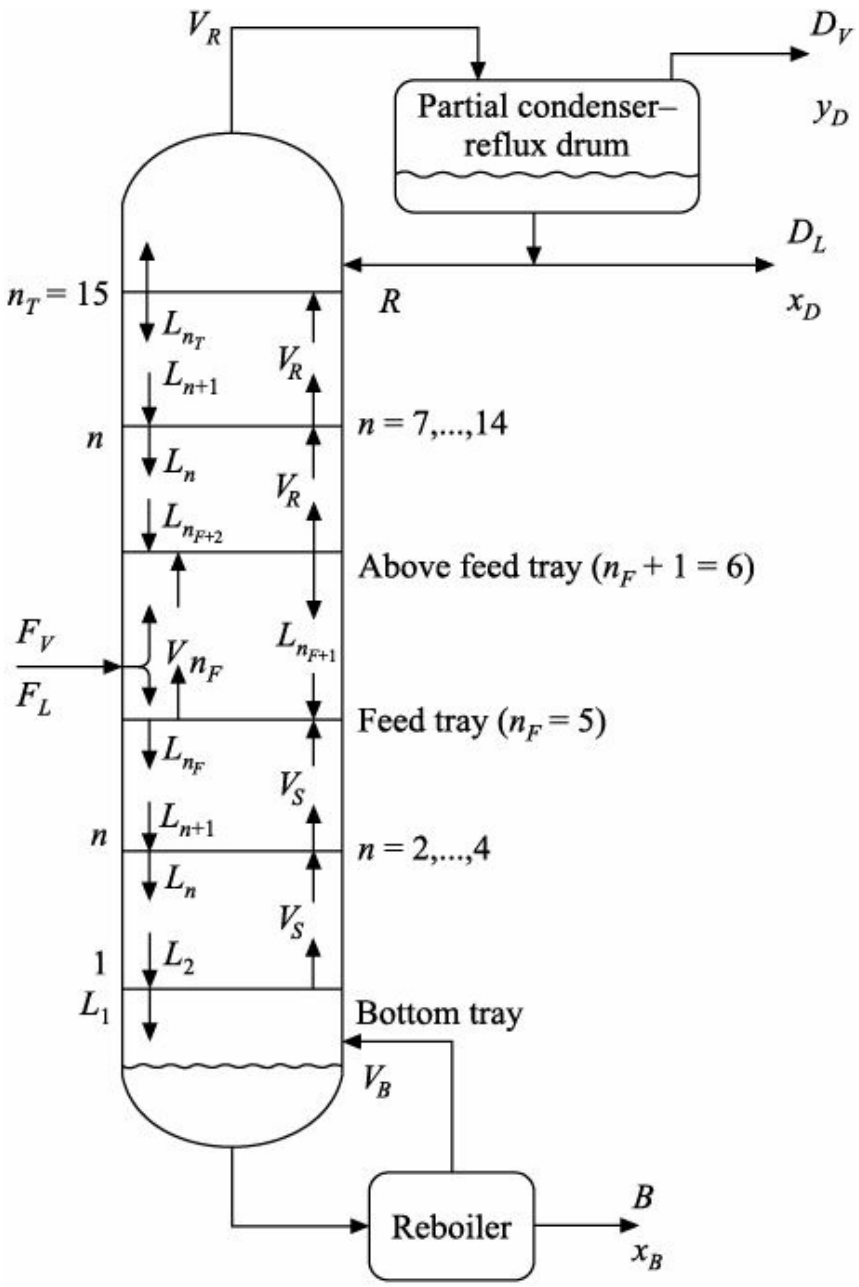

FIGURE 7.1 Schematic representation of the example of distillation column.

7.2.2 Mathematical Model

Assumptions

The following assumptions have been adopted to develop the mathematical process model.

- Negligible vapour holdup is assumed.
- The molar heats of vaporization of both components are about the same.
- The liquid holdup varies on each tray (excluding reflux drum and column base), and the liquid hydraulics are calculated from the Francis weir formula. In practice, the liquid holdups in reflux drum and column base are generally tightly controlled implementing level controllers with the manipulation of distillate and bottom product flow rates respectively.
- The liquid is perfectly mixed on each stage. For the nth stage, it reveals that

$$\text{liquid composition anywhere on the stage} = x_n \qquad (7.1)$$

- The total amount of liquid accumulated in the reboiler as well as in the base of the column is

considered as the column base holdup.

- The heat losses from the column to the surroundings are assumed to be negligible.
- The relative volatility is invariant with time and with column length.
- Each tray is assumed to be ideal (i.e., 100% efficient).
- Coolant and steam dynamics are negligible in the condenser and reboiler respectively. The book by Franks (1972) can be consulted for details about the condenser and reboiler dynamics.

Model development

As was mentioned above, in the present study, the distillation process considers varying liquid holdups on each tray excluding reflux drum and column base. The internal liquid flow rate leaving a stage $n(L_n)$ is determined by means of the linearized version of the Francis weir formula:

$$L_n = L_{n0} + \frac{m_n - m_{n0}}{\beta} \qquad (7.2)$$

where L_{n0} is the reference value of the internal liquid flow rate, and m_n and m_{n0} are the actual and reference molar holdups respectively on tray n. The hydraulic time constant τ is typically 3 to 6 seconds per tray (Luyben, 1990).

If V_B be the vapour boil-up rate, V_S the vapour flow rate throughout the stripping section (tray 1 to tray 4) and V_{n_F} the vapour flow rate leaving the feed plate (n_F), the stated assumptions imply that:

$$V_{n_F} = V_S = V_B \qquad (7.3)$$

and

$$V_R = V_{n_F} + F_V = V_B + F_V \qquad (7.4)$$

In the above equation, F_V is the flow rate of vapour feed and V_R the vapour flow rate along the rectifying section (tray 6 to tray 15). Note that these V terms are not necessarily constant with time. In the industrial column, usually the bottom product composition (x_B) is controlled by manipulating the flow rate of boil-up vapour (or steam input to the reboiler). Therefore, the other vapour flow rates are also changed accordingly.

Here, the vapour–liquid equilibrium (VLE) describes the relation between the vapour-phase composition of more volatile component (here ethanol) y and the liquid-phase composition of ethanol x for any stage n of the column. The relationship is given below as a nonlinear expression (details in Chapter 6):

$$y_n = \frac{\alpha x_n}{1 + (\alpha - 1)x_n} \qquad (7.5)$$

where α (or α_{12}) is the relative volatility of component 1 (here ethanol) with respect to component 2 (here 1-propanol).

In the following, the tray-wise modelling equations for the complete distillation column will be derived based on the assumptions made.

Condenser–Reflux Drum System (subscript '*D*')

The partial condenser and the reflux drum are shown as a combined system in Figure 7.2. The total and

component continuity equations, which represent the mathematical model of the combined system, can be obtained by making balance based on the following form:

Rate of input – Rate of output = Rate of accumulation (7.6)

Here, this relationship will be used with the unit of pound-moles per hour (lbmol/h) and to derive the continuity model of all the distillation trays.

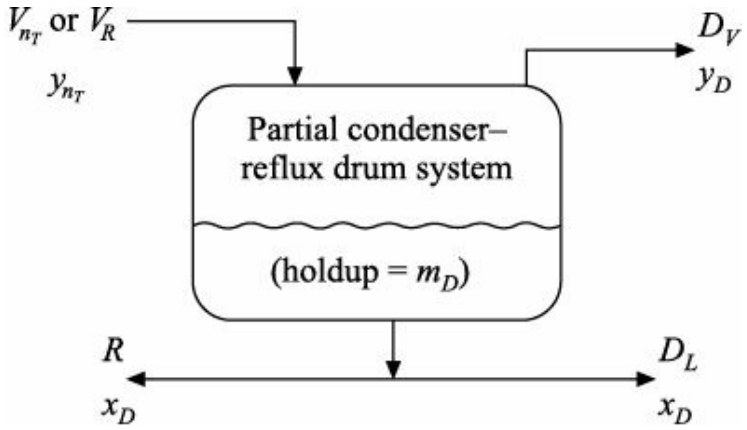

FIGURE 7.2 Condenser–Reflux drum system.

Total continuity equation

$$\dot{m}_D = \frac{dm_D}{dt} = V_{n_T} - R - D_L - D_V \qquad (7.7)$$

In this equation, V_{n_T} is the flow rate of a vapour stream with composition y_{n_T} leaving top tray (nT), R the reflux flow rate having composition x_D, D_L the flow rate of the liquid distillate having composition x_D and D_V the flow rate of the vapour distillate with composition y_D. Since the liquid holdup in the reflux drum (m_D) is assumed constant and $V_{n_T} = V_R$, therefore

$$D_L = V_R - R - D_V \qquad (7.8)$$

Component continuity equation

$$\dot{m}_D \dot{x}_D = \frac{d(m_D x_D)}{dt} = V_{n_T} y_{n_T} - D_V y_D - (D_L + R) x_D \qquad (7.9)$$

Rearranging

$$\dot{x}_D = \frac{1}{m_D}[V_R y_{n_T} - D_V y_D - (D_L + R) x_D] \qquad (7.10)$$

Top Tray (subscript 'nT')

The top tray along with the associated flow schemes is shown in Figure 7.3. To represent this tray mathematically, the balance equations have been derived as follows:

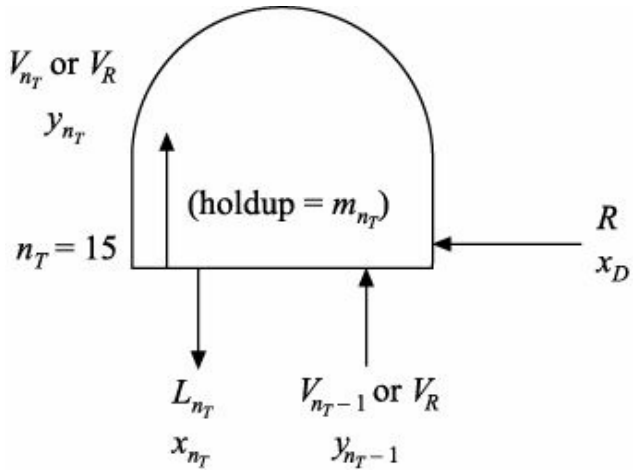

FIGURE 7.3 Top tray.

Total continuity equation

$$\dot{m}_{n_T} = R + V_{n_T-1} - L_{n_T} - V_{n_T} \tag{7.11}$$

Since $V_{n_T} = V_{n_T-1} = V_R$, so

$$\dot{m}_{n_T} = R - L_{n_T} \tag{7.12}$$

Component continuity equation

$$\dot{m}_{n_T}\dot{x}_{n_T} = R_{x_D} + V_{n_T-1}y_{n_T-1} - L_{n_T}x_{n_T} - V_{n_T}y_{n_T} \tag{7.13}$$

This equation gives

$$m_{n_T}\dot{x}_{n_T} + x_{n_T}\dot{m}_{n_T} = R_{x_D} + V_{n_T-1}y_{n_T-1} - L_{n_T}x_{n_T} - V_{n_T}y_{n_T} \tag{7.14}$$

or

$$m_{n_T}\dot{x}_{n_T} + x_{n_T}(R - L_{n_T}) = R_{x_D} + V_{n_T-1}y_{n_T-1} - L_{n_T}x_{n_T} - V_{n_T}y_{n_T} \tag{7.15}$$

Simplifying,

$$\dot{x}_{n_T} = \frac{1}{m_{n_T}}[R(x_D - x_{n_T}) + V_R(y_{n_T-1} - y_{n_T})] \tag{7.16}$$

***n*th Tray** (subscript '*n*', where $n = 7, ..., 14$)

The sketch of the incoming and outgoing flow streams in addition to the liquid holdup is shown for *n*th tray in Figure 7.4. The following continuity equations can represent the *n*th tray model.

Total continuity equation

$$\dot{m}_n = L_{n+1} + V_{n-1} - L_n - V_n \tag{7.17}$$

Simplifying

$$\dot{m}_n = L_{n+1} - L_n \tag{7.18}$$

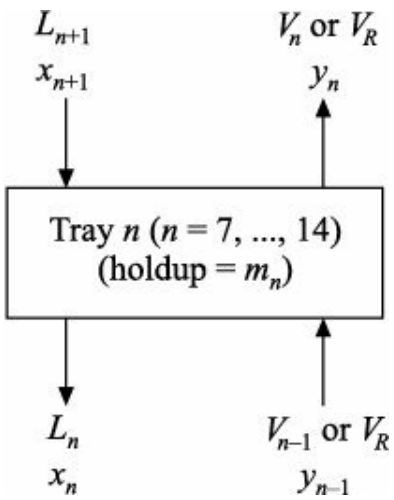

FIGURE 7.4 *n*th tray.

Component continuity equation

$$\dot{m}_n \dot{x}_n = L_{n+1} x_{n+1} + V_{n-1} y_{n-1} - L_n x_n - V_n y_n \tag{7.19}$$

Considering dynamic tray holdup and rearranging, we obtain:

$$\dot{x}_n = \frac{1}{m_n}[L_{n+1}(x_{n+1} - x_n) + V_R(y_{n-1} - y_n)] \tag{7.20}$$

Above Feed Tray (subscript 'n_F+1')

The feed stream of the sample distillation column is a mixture of both liquid and vapour streams. The feeding of this mixture to the column leads to the down flow of the liquid feed (F_L) through tray n_F and up flow of the vapour feed (F_V) through tray n_F + 1. The material balance equations for tray n_F + 1 have been derived as per the description given in Figure 7.5.

Total continuity equation

$$\dot{m}_{n_F+1} = L_{n_F+2} + F_V + V_{n_F} - L_{n_F+1} - V_{n_F+1} \tag{7.21}$$

Here, $V_{n_F+1} = V_R$ and $V_{n_F} = V_S$, and

$$V_{n_F+1} = F_V + V_{n_F} \tag{7.22}$$

Then, Equation (7.21) yields

$$\dot{m}_{n_F+1} = L_{n_F+2} - L_{n_F+1} \tag{7.23}$$

Component continuity equation

$$\dot{m}_{n_F+1}\dot{x}_{n_F+1} = x_{n_F+2} + F_V Z_V + V_{n_F} y_{n_F} - L_{n_F+1} x_{n_F+1} - V_{n_F+1} y_{n_F+1} \tag{7.24}$$

where Z_V is the composition of vapour feed. Substituting Equation (7.23), the above equation simplifies to

$$\dot{x}_{n_F+1} = \frac{1}{m_{n_F+1}}[L_{n_F+2}(x_{n_F+2} - x_{n_F+1}) + F_V Z_V + V_S y_{n_F} - V_R y_{n_F+1}] \tag{7.25}$$

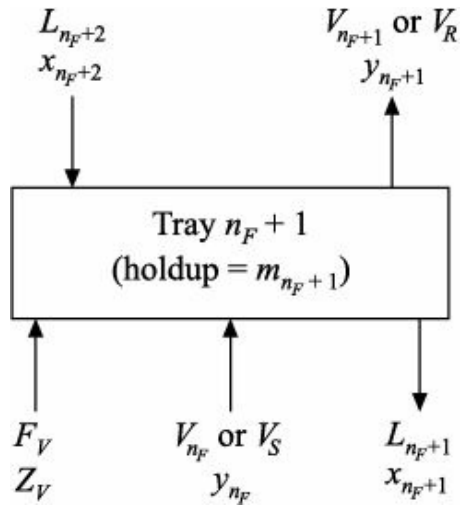

FIGURE 7.5 Above feed tray.

Feed Tray (subscript 'nF')

Figure 7.6 illustrates the feed tray. Here, the liquid feed is considered as an incoming stream to the feed tray. Notice that the input and output vapour flow rates are equal. The mathematical representation of this feed tray is provided by the following balance equations.

Total continuity equation

$$\dot{m}_{n_F} = L_{n_F+1} + F_L + V_{n_F-1} - L_{n_F} - V_{n_F} \tag{7.26}$$

Substituting $V_{n_F} = V_{n_F-1} = V_S$, we get

$$\dot{m}_{n_F} = L_{n_F+1} + F_L - L_{n_F} \tag{7.27}$$

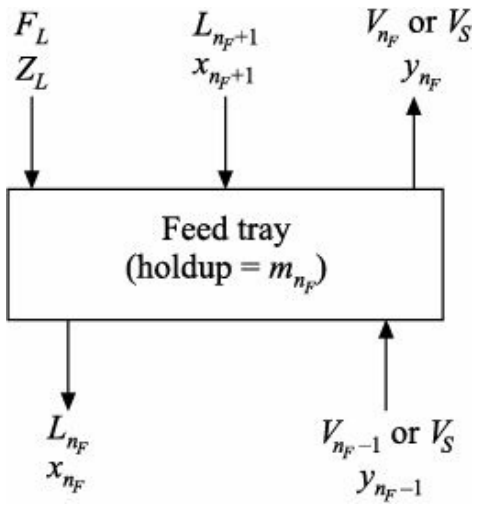

FIGURE 7.6 Feed tray.

Component continuity equation

$$\dot{m}_{n_F}\dot{x}_{n_F} = L_{n_F+1}x_{n_F+1} + F_L Z_L + V_{n_F-1}y_{n_F-1} - L_{n_F}x_{n_F} - V_{n_F}y_{n_F} \tag{7.28}$$

where Z_L is the composition of liquid feed. Simplifying the above equation, we have

$$\dot{x}_{n_F} = \frac{1}{m_{n_F}}[L_{n_F+1}(x_{n_F+1} - x_{n_F}) + F_L(Z_L - x_{n_F}) + V_S(y_{n_F-1} - y_{n_F})] \tag{7.29}$$

***n*th Tray** (subscript 'n', where $n = 2, ..., 4$)

This *n*th tray (n = 2, ..., 4) is not same with the previous *n*th tray (n = 7, ..., 14). The input and output flows of this tray are demonstrated in Figure 7.7. Now the modelling equations may be derived by the following way.

Total continuity equation

$$\dot{m}_n = L_{n+1} + V_{n-1} - L_n - V_n \qquad \text{[from Equation (7.17)]}$$

We know $V_n = V_{n-1} = V_S$ and therefore, the above equation yields

$$\dot{m}_n = L_{n+1} - L_n \qquad \text{[from Equation (7.18)]}$$

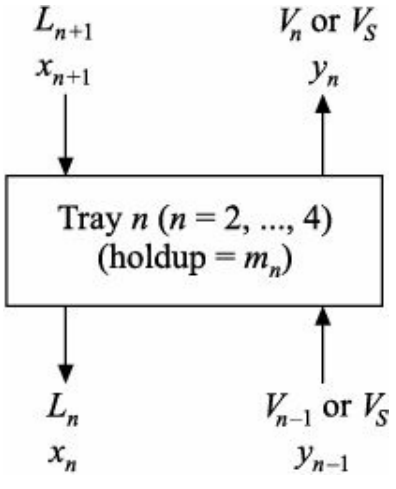

FIGURE 7.7 *n*th tray.

Component continuity equation

$$\dot{m}_n \dot{x}_n = L_{n+1}x_{n+1} + V_{n-1}y_{n-1} - L_n x_n - V_n y_n \qquad \text{[from Equation (7.19)]}$$

Considering dynamic holdup and rearranging, we obtain

$$\dot{x}_n = \frac{1}{m_n}[L_{n+1}(x_{n+1} - x_n) + V_S(y_{n-1} - y_n)] \qquad (7.30)$$

Bottom Tray (subscript '1')

Figure 7.8 represents the bottom (1st) tray of the distillation column. The following total and component mass balance equations describe this tray.

Total continuity equation

$$\dot{m}_1 = L_2 + V_B - L_1 - V_1 \qquad (7.31)$$

It is assumed that $V_1 = V_S = V_B$ and hence, the above equation reduces to

$$\dot{m}_1 = L_2 - L_1 \qquad (7.32)$$

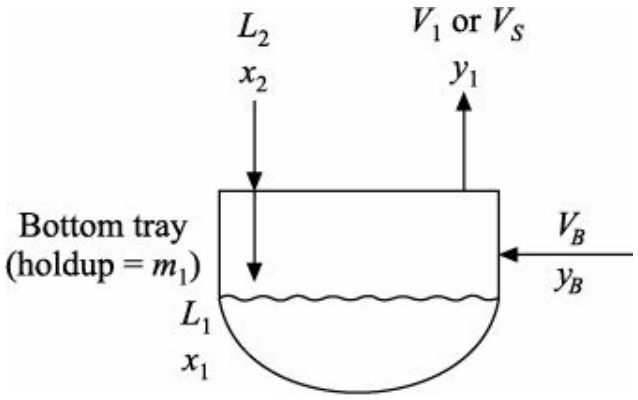

FIGURE 7.8 Bottom tray.

Component continuity equation

$$\dot{m}_1\dot{x}_1 = L_2x_2 + V_By_B - L_1x_1 - V_1y_1 \qquad (7.33)$$

Inserting Equation (7.32) into Equation (7.33), one finally obtains

$$\dot{x}_1 = \frac{1}{m_1}[L_2(x_2 - x_1) + V_By_B - V_Sy_1] \qquad (7.34)$$

Reboiler–Column Base System (subscript '*B*')

Figure 7.9 describes an equilibrium stage that comprises of a reboiler and the base of the distillation column. The total liquid holdup in this combined system is m_B and the flow rates are shown in the figure. The model can be developed as follows.

Total continuity equation

$$\dot{m}_B = L_1 - B - V_B \qquad (7.35)$$

Since the liquid holdup is constant,

$$B = L_1 - V_B \quad (7.36)$$

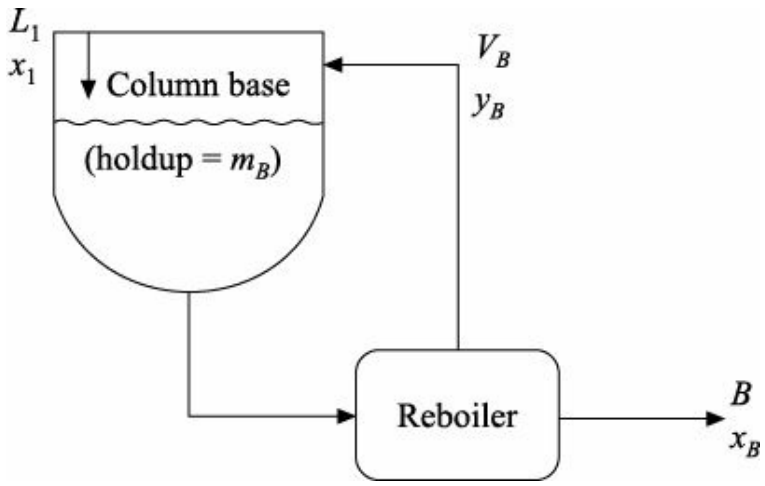

FIGURE 7.9 Reboiler–Column base system.

Component continuity equation

$$\dot{m}_B\dot{x}_B = L_1x_1 - Bx_B - V_By_B \qquad (7.37)$$

Equation (7.37) yields at constant liquid holdup,

$$\dot{x}_B = \frac{1}{m_B}[L_1 x_1 - B x_B - V_B y_B] \qquad (7.38)$$

7.3 DYNAMIC SIMULATION

In order to predict the ideal binary distillation column dynamics, we need to simulate the developed mathematical model. The process model comprises of a set of ordinary differential equations (ODEs) in addition to the algebraic equations (AEs). Among the ODEs, the total continuity equations are used to compute the holdups of tray liquids and the component continuity equations are employed to determine the liquid-phase compositions on all trays. Among the algebraic form of equations, the VLE relationship [Equation (7.5)] provides the vapour-phase compositions and the Francis weir formula [Equation (7.2)] calculates the internal liquid flow rates. In addition, the vapour flow rates are calculated using Equations (7.3) and (7.4). Therefore, apart from the vapour rate calculations, there are two ODEs (a total continuity equation and a light component continuity equation) and two AEs (a VLE relationship and a liquid-hydraulic relationship) per tray. The operating and steady state conditions of the example distillation column are reported in Table 7.1.

Table 7.1 Operating and steady state conditions

Binary system: 1-propanol/ethanol	
Flow rate of liquid distillate (lbmol/h), D_L	27.8
Composition of liquid distillate (mol fraction), x_D	0.899
Flow rate of vapour distillate (lbmol/h), D_V	200.0
Composition of vapour distillate (mol fraction), y_D	0.947
Liquid holdup in reflux drum (lbmol), m_D	8.056
Reflux flow rate (lbmol/h), R	400.864
Flow rate of liquid feed (lbmol/h), F_L	800.0
Composition of liquid feed (mol fraction), Z_L	0.60
Flow rate of vapour feed (lbmol/h), F_V	200.0
Composition of vapour feed (mol fraction), Z_V	0.53
Composition of bottom product (mol fraction), x_B	0.481
Liquid holdup in column base (lbmol), m_B	4.897
Vapour boil-up rate (lbmol/h), V_B	428.66
Hydraulic time constant (s), ⌙	3.6
Relative volatility, ¬	2.0
Integration time interval (h), dt	0.0001

The dynamic process simulator that solves the differential-algebraic system can be developed according to the following logic.

Step 1: Input data for variables: liquid-phase compositions x for all trays (including reflux drum and column base) and liquid holdups m for all trays (excluding reflux drum and column base).

Step 2: Input data for constant inputs/outputs/parameters: liquid feed rate F_L with composition Z_L, vapour feed rate F_V with composition Z_V, vapour distillate rate D_V, hydraulic time constant ⌙, relative volatility ¬, and liquid holdups in reflux drum m_D and in column base m_B. Note that the values of input disturbances, outputs and uncertain parameters may change during the plant operation.

Step 3: Either input the values of reflux flow rate R and vapour boil-up rate V_B or manipulate these flow rates employing the controllers. In our case, no controllers have been implemented and the values of these manipulated inputs are supplied at each time step.

Step 4: Calculate the internal liquid flow rate L using the Francis weir formula [Equation (7.2)] for all trays. Also compute the vapour flow rate V employing Equations (7.3) and (7.4) for all trays.

Step 5: Calculate the vapour-phase composition y for all trays (including reflux drum and column base) from Equation (7.5).

Step 6: Compute the liquid distillate flow rate D_L using Equation (7.8) and bottoms flow rate B from Equation (7.36).

Step 7: Update the liquid-phase compositions on all trays (including reflux drum and column base) and liquid holdups on all trays (excluding reflux drum and column base) for the next time step. The Euler method (details in Chapter 2) is used to integrate the ODEs.

Step 8: To predict the column dynamics for the future time step, go back to Step 3.

The complete computer program (Fortran 90 code) for the prescribed ideal binary distillation column is given in Program 7.1. Note that if you run Program 7.1, you shall get the dynamic process response for a step change in liquid feed composition from 0.60 (steady state value) to 0.55 at time equal to zero.

PROGRAM 7.1 *Dynamic Distillation Simulator*

```
! B = Bottoms flow rate
! DL = Liquid distillate flow rate
! DV = Vapour distillate flow rate
! FL = Liquid feed flow rate
! FV = Vapour feed flow rate
! L = Internal liquid flow rate
! M = Liquid holdup on the tray
! MB = Liquid holdup in the column base
! MD = Liquid holdup in the reflux drum
! NF = Feed tray
! NT = Total number of trays
! R = Reflux flow rate
! VB = Vapour boil-up rate
! VR = Vapour flow rate throughout the rectifying section
! VS = Vapour flow rate throughout the stripping section
! X = Liquid-phase composition
! XB = Composition of bottom product
! XD = Composition of liquid distillate
! XF = Composition of liquid feed
! Y = Vapour-phase composition
! YB = Composition of boil-up vapour
! YD = Composition of vapour distillate
! YF = Composition of vapour feed

PROGRAM DYNAMIC_IBDC
IMPLICIT NONE

! Declaration

INTEGER::K,n
INTEGER,PARAMETER::NT=15,i=5000,NF=5
REAL*8::FL,FV,XF,YF,DV
REAL*8,DIMENSION(NT,i)::X,Y,M,L,L0
REAL*8,DIMENSION(i)::XD,XB,Time,R,VB,B,DL,YB,YD
REAL*8::VS(NF,i),VR(NF+1:NT,i)
REAL*8::MD,MB
REAL*8,PARAMETER:: BETA=0.001 D0,ALPHA=2.0 D0,dt=0.0001 D0
REAL*8,PARAMETER::R0=400.8636170476530082 D0

OPEN(UNIT=2,File="IBDC_DS.dat")

! Initial data

XD(1)=0.8993283514871822 D0
```

```
XB(1)=0.4812223878557398 D0

MD=8.0557290338576260 D0
MB=4.8969852099258300 D0

FL=800.0 D0
FV=200.0 D0
DV=200.0 D0
XF=0.55 D0
YF=0.53 D0

Time(1)=0.00 D0

! Tray-wise holdups and compositions

M(1,1)=2.3838602106839941 D0
X(1,1)=0.5413852549176267 D0

M(2,1)=2.5699186724215152 D0
X(2,1)=0.5601978537566697 D0

M(3,1)=2.7363668003742906 D0
X(3,1)=0.5657826798790962 D0

M(4,1)=2.8625585439519976 D0
X(4,1)=0.5674147929146519 D0

M(5,1)=2.9135632410532013 D0
X(5,1)=0.5678895664968068 D0

M(6,1)=3.0847017035199670 D0
X(6,1)=0.5042202331519813 D0

M(7,1)=3.3039534593441741 D0
X(7,1)=0.5165359860620628 D0

M(8,1)=3.4025198348688281 D0
X(8,1)=0.5334695233306152 D0

M(9,1)=3.4534614354834354 D0
X(9,1)=0.5563081868270025 D0

M(10,1)=3.4804263798593035 D0
X(10,1)=0.5863240475565120 D0

M(11,1)=3.4947818851582641 D0
X(11,1)=0.6244582053050142 D0

M(12,1)=3.5025169721393036 D0
X(12,1)=0.6708738701789345 D0

M(13,1)=3.5067720060071967 D0
X(13,1)=0.7245107163243557 D0

M(14,1)=3.5091445478460969 D0
X(14,1)=0.7828961533779115 D0

M(15,1)=3.5083822933519770 D0
X(15,1)=0.8424573558588187 D0

DO K=1,i !——Starting of main loop——!

R(K) =400.8636170476530082 D0
VB(K)=428.6624377313841023 D0

! Liquid flow rates

DO n=1,NF
```

```
L0(n,k)=R0+FL
END DO

DO n=NF+1,NT
L0(n,k)=R0
END DO

DO n=1,NT
L(n,k)=L0(n,k)+((M(n,k)-M(n,1))/Beta)
END DO

! Vapour flow rates

DO n=1,NF
VS(n,k)=VB(K)
END DO

DO n=NF+1,NT
VR(n,k)=VB(k)+FV
END DO

! Vapour-phase compositions
YB(K)=(Alpha*XB(K))/(1+(Alpha-1)*XB(K))

DO n=1,NT
Y(n,K)=(Alpha*X(n,K))/(1+(Alpha-1)*X(n,K))
END DO

YD(K)=(Alpha*XD(K))/(1+(Alpha-1)*XD(K))

! Product flow rates

DL(K)=VR(15,K)-DV-R(K)
B(k)=L(1,k)-VB(k)

! Liquid-phase compositions and liquid holdups

XB(k+1)=XB(k)+(dt/MB)*((L(1,k)*X(1,k))-
& (VB(k)*YB(k))-(B(k)*XB(k)))
IF(XB(k+1)>1.0 D0)XB(k+1)=1.0 D0
IF(XB(k+1)<0.0 D0)XB(k+1)=0.0 D0

M(1,k+1)=M(1,k)+dt*(L(2,k)-L(1,k))
X(1,k+1)=X(1,k)+(dt/M(1,k))*((L(2,k)*(X(2,k)-
& X(1,k)))+(VB(k)*YB(k))-(VS(1,K)*Y(1,k)))
IF(X(1,k+1)>1.0 D0)X(1,k+1)=1.0 D0
IF(X(1,k+1)<0.0 D0)X(1,k+1)=0.0 D0

DO n=2,4
M(n,k+1)=M(n,k)+dt*(L(n+1,k)-L(n,k))

X(n,k+1)=X(n,k)+(dt/M(n,k))*((L(n+1,k)*
& (X(n+1,k)-X(n,k)))+(VS(n-1,k)*Y(n-1,k))-(VS(n,k)*Y(n,k)))
IF(X(n,k+1)>1.0 D0)X(n,k+1)=1.0 D0
IF(X(n,k+1)<0.0 D0)X(n,k+1)=0.0 D0
END DO

M(5,k+1)=M(5,k)+dt*(L(6,k)-L(5,k)+FL)
X(5,k+1)=X(5,k)+(dt/M(5,k))*((L(6,k)*(X(6,k)-
& X(5,k)))+(VS(4,K)*Y(4,k))-(VS(5,k)*Y(5,k))+(FL*(XF-X(5,k))))
IF(X(5,k+1)>1.0 D0)X(5,k+1)=1.0 D0
IF(X(5,k+1)<0.0 D0)X(5,k+1)=0.0 D0

M(6,k+1)=M(6,k)+dt*(L(7,k)-L(6,k))
X(6,k+1)=X(6,k)+(dt/M(6,k))*((L(7,k)*(X(7,k)-
```

```
& X(6,k)))+(VS(5,k)*Y(5,k))-(VR(6,k)*Y(6,k))+(FV*YF))
IF(X(6,k+1)>1.0 D0)X(6,k+1)=1.0 D0
IF(X(6,k+1)<0.0 D0)X(6,k+1)=0.0 D0

DO n=7,14
M(n,k+1)=M(n,k)+dt*(L(n+1,k)-L(n,k))

X(n,k+1)=X(n,k)+(dt/M(n,k))*((L(n+1,k)*
& (X(n+1,k)-X(n,k)))+(VR(n-1,k)*Y(n-1,k))-(VR(n,k)*Y(n,k)))
IF(X(n,k+1)>1.0 D0)X(n,k+1)=1.0 D0
IF(X(n,k+1)<0.0 D0)X(n,k+1)=0.0 D0
END DO
M(15,k+1)=M(15,k)+dt*(R(k)-L(15,k))
X(15,k+1)=X(15,k)+(dt/M(15,k))*((R(k)*(XD(k)-
& X(15,k)))+(VR(14,k)*Y(14,k))-(VR(15,K)*Y(15,k)))
IF(X(15,k+1)>1.0 D0)X(15,k+1)=1.0 D0
IF(X(15,k+1)<0.0 D0)X(15,k+1)=0.0 D0

XD(k+1)=XD(k)+(dt/MD)*((VR(15,k)*Y(15,k))-
& (R(k)*XD(k))-(DL(k)*XD(k))-(DV*YD(K)))
IF(XD(k+1)>1.0 D0)XD(k+1)=1.0 D0
IF(XD(k+1)<0.0 D0)XD(k+1)=0.0 D0

Time(k+1)=Time(k)+dt

PRINT*,Time(k),XB(k),X(1:15,K),M(1:15,K),XD(k)
WRITE(2,FMT=100)Time(k),XB(k),X(1:15,K),M(1:15,K),XD(k)
100 FORMAT (1X,33(2X,F21.16))

END DO !——End of main loop——!
END FILE 2
REWIND 2
CLOSE(2)

END PROGRAM DYNAMIC_IBDC
```

7.4 SUMMARY AND CONCLUSIONS

This chapter presents the detailed modelling and simulation of an ideal distillation column. A binary 1-propanol/ethanol mixture has been fractionated in the prescribed operation. In the process simulator, a relative-volatility-based VLE relationship has been used to predict the equilibrium properties. In addition, the internal liquid flow rates have been calculated using a simple Francis weir formula. Energy balance equations, phase nonidealities, rigorous tray hydraulics and some other vital considerations have been omitted from the process model for simplicity. In the subsequent chapters, of course, several realistic distillation simulators will be developed considering all these issues.

EXERCISES

7.1 Why is the distillation column that is considered in this chapter called ‘ideal distillation column’? Explain it.

7.2 What is the physical significance of the term ‘hydraulic time constant’ in the Francis weir formula?

7.3 Why are the energy balance equations not included in the developed model of the ideal binary distillation column?

7.4 Why is the pressure in the base usually higher than that at the top of the distillation column?

7.5 Simulate the model structure, which is developed in this chapter for an ideal binary distillation column, using the fourth-order Runge–Kutta algorithm.

7.6 Develop a mathematical model for an ideal binary distillation column considering two partially vaporized feed streams. One is fed on 5th tray and other one is introduced on 10th tray. The same assumptions and equipment configurations as we considered in this chapter can be used.

REFERENCES

Franks, R.G.E. (1972). *Modeling and Simulation in Chemical Engineering*, 1st ed., John Wiley & Sons, New York.

Luyben, W.L. (1990). *Process Modeling, Simulation, and Control for Chemical Engineers*, 2nd ed., McGraw-Hill Book Company, Singapore.

8

Activity Coefficient Models

8.1 INTRODUCTION

A significant fraction of chemical process design is concerned with separation of fluid mixtures by several operations. All design methods for the separations require quantitative estimates of fluid-phase equilibria. This chapter explains how to make such estimates for liquid-phase mixtures where nonideality is sufficiently strong.

Before describing the activity coefficient models, let us briefly discuss the preliminaries. In distillation column design, the required phase equilibrium information is commonly expressed by *k*-factors as:

$$k_i = \frac{y_i}{x_i} \qquad (8.1)$$

where y_i is the equilibrium composition (mole fraction) of component i in the vapour phase and x_i the corresponding composition (mole fraction) of component i in the liquid phase. Using standard thermodynamics

$$k_i = \frac{\gamma_i^L f_i^0}{\hat{\phi}_i^V P} \qquad (8.2)$$

where γ_i^L (or $\text{≥}i$) is the liquid-phase *activity coefficient*, f_i^0 the standard-state *fugacity*, $\hat{\phi}_i^V$ the *mixture fugacity coefficient* in the vapour phase, and P the total pressure.

For condensable components, f_i^0 is the fugacity of pure component i in the liquid phase (denoted by f_i^L) at system temperature T and pressure P, and it can be expressed as:

$$f_i^0 = f_i^L = P_i^S \phi_i^S \exp\left[\int_{P_i^S}^{P} \frac{V_i}{RT} dP\right] \qquad (8.3)$$

where R is the universal gas constant. For pure liquid i, P_i^S is the saturation (vapour) pressure, ϕ_i^S the fugacity coefficient at saturation, and V_i the liquid molar volume, all at temperature T. The exponential term within the integration is called the *Poynting factor*. If the effect of pressure on the molar volume of the liquid is neglected, Equation (8.3) becomes

$$f_i^L = P_i^S \phi_i^S \exp\left[\frac{V_i(P - P_i^S)}{RT}\right] \qquad (8.4)$$

Normally, at low pressures, the fugacity coefficients $\hat{\phi}_i^V$ (in the mixture) and ϕ_i^S (pure i at saturation) do not deviate much from unity, and f_i^L is nearly equal to P_i^S. Accordingly, Equation (8.2) yields

$$k_i = \frac{\gamma_i^L P_i^S}{P} \qquad (8.5)$$

The combination of Equations (8.1) and (8.5) gives

$$y_i = \frac{\gamma_i^L x_i P_i^S}{P} \qquad (8.6)$$

This equation is generally used for the distillation column operated at low pressure to calculate the mole fraction of component *i* in the vapour phase. Not only that, but this equation is also used to compute the tray temperature (boiling point) of the distillation processes. For ideal mixtures, phase nonideality is not accounted and $\gamma_i^L = 1.0$.

8.2 ACTIVITY COEFFICIENT MODELS FOR LIQUID MIXTURES

Liquid-phase activity coefficient γ_i is determined from an expression for the excess Gibbs energy. For a mixture of *N* species, the *excess Gibbs free energy* G^E is defined as:

$$G^E = RT \sum_{i=1}^{N} n_i \ln \gamma_i \qquad (8.7)$$

where n_i denotes the number of moles of species *i*. The *molar excess Gibbs free energy*[1] g^E is related to G^E by the following equation:

[1] The molar excess free energy is the difference in free energy of one mole of the actual mixture minus the free energy which the mixture would have if it were an ideal solution.

$$g^E = \frac{G^E}{n_T} \qquad (8.8)$$

where n_T is the total number of moles and is given by

$$n_T = \sum_{i=1}^{N} n_i \qquad (8.9)$$

and so the liquid-phase composition is

$$x_i = \frac{n_i}{n_T} \qquad (8.10)$$

The solution models, which relate activity coefficients to liquid composition, satisfy the well-known Gibbs–Duhem equation at constant temperature and pressure

$$\sum_{i=1}^{N} x_i \, (d \ln \gamma_i)_{T,P} = 0 \qquad (8.11)$$

A common procedure in activity coefficient model development is the first to relate the molar excess free energy to the liquid composition. Then the activity coefficient γ_i is found employing

$$RT \ln \gamma_i = \left(\frac{\partial G^E}{\partial n_i} \right)_{T,P,n_{j \neq i}} = \left(\frac{\partial n_T g^E}{\partial n_i} \right)_{T,P,n_j} \tag{8.12}$$

where n_j indicates that all mole numbers except n_i are held constant in the differentiation.

Wohl (1946) has shown that the Margules, Van Laar, and Scatchard–Hamer equations can all be developed as variations of one mathematical scheme. In the derivation, the molar excess free energy of the mixture is equated to a sum of empirical interaction terms

$$\frac{g^E}{2.303\, RT \sum_{i=1}^{N} s_i x_i} = \sum_{i=1}^{N}\sum_{j=1}^{N} z_i z_j a_{ij} + \sum_{i=1}^{N}\sum_{j=1}^{N}\sum_{k=1}^{N} z_i z_j z_k a_{ijk} + \cdots \tag{8.13}$$

where s_i is called the *effective molar volume* of the *i*th component. The *effective volumetric fraction* z_i is defined as:

$$z_i = \frac{s_i x_i}{\sum_{j=1}^{N} s_j x_j} = \frac{s_i n_i}{\sum_{j=1}^{N} s_j n_j} \tag{8.14}$$

where a_{ij} and a_{ijk} the interaction parameters, and $a_{ii} = a_{iii} = 0$. The first term in the right hand side of Equation (8.13) is included for the interactions of two unlike molecules, and the second term is included for the interactions of three unlike molecules, and so on. The groups of three unlike molecules include the groups of two like and one unlike molecules. If Equation (8.13) only retains the first term, it is known as the two-suffix equation; if that retains the first two terms, it is known as the three-suffix equation.

To apply Equation (8.6), it is necessary to know the activity coefficient. The following methods, which estimate the activity coefficients, provide a reliable model to the process engineer for predicting equilibrium conditions.

8.2.1 The Margules Model (developed by Margules in 1895)

The Margules activity coefficient model is mathematically very simple. This solution model can be derived from the two-suffix form of Equation (8.13). For ternary and binary mixtures, the model is given in the following subsections.

For Ternary System

$$\begin{aligned}\log_{10} \gamma_1 = {} & x_2^2[A_{12} + 2x_1(A_{21} - A_{12})] + x_3^2[A_{13} + 2x_1(A_{31} - A_{13})] \\ & + x_2 x_3[(A_{21} + A_{12} + A_{31} + A_{13} - A_{23} - A_{32})/2 \\ & + x_1(A_{21} - A_{12} + A_{31} - A_{13}) + (x_2 - x_3)(A_{23} - A_{32}) - (1 - 2x_1)C^*]\end{aligned} \tag{8.15}$$

$$\begin{aligned}\log_{10} \gamma_2 = {} & x_3^2[A_{23} + 2x_2(A_{32} - A_{23})] + x_1^2[A_{21} + 2x_2(A_{12} - A_{21})] \\ & + x_3 x_1[(A_{32} + A_{23} + A_{12} + A_{21} - A_{31} - A_{13})/2 \\ & + x_2(A_{32} - A_{23} + A_{12} - A_{21}) + (x_3 - x_1)(A_{31} - A_{13}) - (1 - 2x_2)C^*]\end{aligned} \tag{8.16}$$

$$\log_{10}\gamma_3 = x_1^2[A_{31} + 2x_3(A_{13} - A_{31})] + x_2^2[A_{32} + 2x_3(A_{23} - A_{32})]$$
$$+ x_1x_2[(A_{13} + A_{31} + A_{23} + A_{32} - A_{12} - A_{21})/2$$
$$+ x_3(A_{13} - A_{31} + A_{23} - A_{32}) + (x_1 - x_2)(A_{12} - A_{21}) - (1 - 2x_3)C^*] \quad (8.17)$$

For Binary System

$$\log_{10}\gamma_1 = x_2^2[A_{12} + 2x_1(A_{21} - A_{12})] \quad (8.18)$$

$$\log_{10}\gamma_2 = x_1^2[A_{21} + 2x_2(A_{12} - A_{21})] \quad (8.19)$$

The above equations represent the Margules activity coefficient model. Equations (8.15) to (8.17) are employed for the ternary system, and Equations (8.18) and (8.19) for the binary system. In this thermodynamic model, A_{ij} and A_{ji} are the Margules interaction constants. If the activity coefficient expression for any one component is derived, it is easy to develop the expressions for the other two components of a ternary system by the *rotation* principle

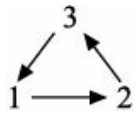

The Margules equations for a two-component solution require only binary-pair constants, whereas the model equations for a ternary system involve the parameters of the three constituent binary systems and a single ternary parameter (C^*). However, the ternary parameter can be set equal to zero for systems in which the ternary interactions are negligible (Wohl, 1953). As a result, only binary-pair constants are needed to represent a ternary system and the required data are listed in Table 8.1.

8.2.2 The Van Laar Model (developed by Van Laar in 1913)

The Van Laar equations, one of the most well-known classical activity coefficient models, may be derived from the two-suffix form of Equation (8.13). The expressions of this model for the multicomponent and binary mixtures are reported in this section.

For Multicomponent System (developed by Null in 1970)

$$\log_{10}\gamma_i = \frac{\sum_{j=1}^{N}(x_j\bar{A}_{ij})}{1 - x_i}\left[1 - \frac{x_i\sum_{j=1}^{N}(x_j\bar{A}_{ij})}{x_i\sum_{j=1}^{N}(x_j\bar{A}_{ij}) + (1 - x_i)\sum_{j=1}^{N}(x_j\bar{A}_{ji})}\right]^2 \quad (8.20)$$

For Binary System (developed by Carlson and Colburn in 1942)

$$\log_{10}\gamma_1 = \frac{\bar{A}_{12}}{\left(1 + \frac{x_1\bar{A}_{12}}{x_2\bar{A}_{21}}\right)^2} \quad (8.21)$$

$$\log_{10}\gamma_2 = \frac{\bar{A}_{21}}{\left(1+\frac{x_2\bar{A}_{21}}{x_1\bar{A}_{12}}\right)^2} \qquad (8.22)$$

Equation (8.20) is restricted to conditions where all Van Laar interaction constants $\bar{A}_{ij}$ and $\bar{A}_{ji}$ pairs are of the same sign. All self-interaction constants in this model, $\bar{A}_{ii}$ should be zero, that means $\bar{A}_{ii} = \bar{A}_{jj} = 0$. But the ratio $\bar{A}_{ii}/\bar{A}_{jj}$ must be unity. This can be achieved in computer calculation by setting all A_{ii} equal to a very small number.

Actually, $\bar{A}_{ij}$ and $\bar{A}_{ji}$ vary with temperature. These coefficients are constant only for a particular binary pair at a certain temperature. However, this thermodynamic model provides good performance even with the assumption of no variation of Van Laar constants with temperature. A multicomponent mixture of N species has $N(N-1)/2$ binary pairs. For example, when $N = 4$, 6 binary pairs can be constituted. Now it is obvious that the Van Laar expression depends only on liquid compositions and the binary constants. The binary interaction constants for different pairs are given in Table 8.1.

Table 8.1 Wilson, Van Laar and Margules parameters

Reference component (1)	*Component* (2)	¬12 − ¬11 (cal/gmol)	¬21 − ¬22 (cal/gmol)	*Pressure* (mm Hg)/ *Temp.* (°C)			A_{12}	A_{21}
Acetone	Benzene	494.92	–167.91	760	0.2039	0.1563	0.2012	0.1533
	Carbon tetrachloride	651.76	–12.67	760	0.3889	0.3301	0.3874	0.3282
	Chloroform	–72.20	–332.23	760	–0.3045	–0.2709	–0.3051	–0.2676
	2,3-Dimethyl butane	948.29	234.96	760	0.6345	0.6358	0.6345	0.6358
	Ethanol	38.17	418.96	760	0.2574	0.2879	0.2569	0.2870
	Methanol	–214.95	664.08	760	0.2635	0.2801	0.2634	0.2798
	n-Pentane	996.75	262.74	760	0.7403	0.6364	0.7386	0.6329
	2-Propanol	127.43	284.99	760	0.2186	0.2690	0.2152	0.2688
	Water	439.64	1405.49	760	0.9972	0.6105	0.9709	0.5576
Acetonitrile	Water	694.08	1610.07	760	1.0680	0.8207	1.0489	0.8231
Benzene	Acetone	–167.91	494.93	760	0.1563	0.2039	0.1533	0.2012
	1-Butanol	160.12	817.67	760	0.3594	0.5865	0.3449	0.5651
	Carbon tetrachloride	–103.41	204.82	760	0.0360	0.0509	0.0359	0.0488
	Chloroform	141.62	–204.22	760	–0.0858	–0.0556	–0.0824	–0.0532
	Cyclohexane	187.23	80.02	760	0.1466	0.1646	0.1462	0.1640
	Cyclopentane	266.56	–24.18	760	0.1655	0.1302	0.1634	0.1290
	Ethanol	131.47	1297.90	760	0.5804	0.7969	0.5718	0.7883
	n-Heptane	99.35	292.94	760	0.0985	0.2135	0.0842	0.1899
	n-Hexane	173.93	169.92	760	0.1457	0.2063	0.1430	0.2010
	Methanol	153.86	1620.36	760	0.7518	0.8975	0.7494	0.8923
	Methyl acetate	229.25	–23.84	760	0.1292	0.0919	0.1219	0.0939
	Methyl cyclohexane	–4.15	360.92	760	0.0910	0.1901	0.0760	0.1760
	Methyl cyclopentane	161.44	97.33	760	0.1360	0.1605	0.1342	0.1606
	1-Propanol	–73.91	1370.32	760	0.3772	0.7703	0.3251	0.7332
	2-Propanol	160.53	1007.94	760	0.4638	0.6723	0.4523	0.6551
1-Butanol	Benzene	817.67	160.12	760	0.5865	0.3594	0.5651	0.3449
	Toluene	887.80	104.68	760	0.5430	0.3841	0.5340	0.3699
Butyl cellosolve	Ethyl cyclohexane	643.51	636.11	400	0.5814	0.5784	0.5814	0.5784
	n-Octane	1070.54	298.62	400	0.6967	0.5318	0.6903	0.5227
Carbon tetrachloride	Acetone	–12.67	651.76	760	0.3301	0.3889	0.3282	0.3874
	Benzene	204.82	–103.41	760	0.0509	0.0360	0.0488	0.0359
	2-Propanol	111.11	1232.94	760	0.4918	0.7868	0.4763	0.7656
Cellosolve	Ethyl benzene	755.77	121.89	760	0.4402	0.3762	0.4379	0.3750
	n-Hexane	834.86	656.23	760	0.6629	0.7206	0.6633	0.7183
	Hexene-1	370.05	705.47	760	0.4367	0.5860	0.4228	0.5818
	n-Octane	989.04	622.77	760	0.6158	0.7507	0.6117	0.7467
Chloroform	Acetone	–332.23	–72.20	760	–0.2709	–0.3045	–0.2676	–0.3051
	Benzene	–204.22	141.62	760	–0.0556	–0.0858	–0.0532	–0.0824
	2,3-Dimethyl butane	213.88	223.69	760	0.1736	0.2790	0.1637	0.2677
	Ethyl acetate	–367.50	–92.50	760	–0.2868	–0.4478	–0.2726	–0.4275
	Methanol	–373.30	1703.68	760	0.4104	0.8263	0.3702	0.7767
	Methyl acetate	–451.09	113.24	760	–0.2249	–0.3343	–0.2112	–0.3270
	Methyl-ethyl-ketone	–231.61	–235.12	760	–0.2990	–0.3486	–0.2938	–0.3507
	Benzene	80.02	187.23	760	0.1646	0.1466	0.1640	0.1462

Cyclohexane	Ethanol	303.42	2151.01	760	0.7811	1.1031	0.7743	1.0699
	Methyl acetate	345.11	691.65	760	0.5799	0.5317	0.5789	0.5313
	2-Propanol	69.02	1734.12	760	0.5322	1.0162	0.5006	0.9539
	Toluene	–414.68	909.36	760	0.0702	0.2578	0.0689	0.1563
Cyclopentane	Benzene	–24.18	266.56	760	0.1302	0.1655	0.1290	0.1634
2,3-Dimethyl-butane	Acetone	234.96	948.29	760	0.6358	0.6345	0.6358	0.6345
	Chloroform	223.69	213.88	760	0.2790	0.1736	0.2677	0.1637
	Methanol	449.08	2771.85	760	1.1276	1.5408	1.1265	1.5255
1,4-Dioxane	*n*-Hexane	806.80	164.58	760	0.5260	0.4850	0.5230	0.4857
	Hexene-1	495.19	176.39	760	0.3578	0.3757	0.3577	0.3755
Ethanol	Acetone	418.96	38.17	760	0.2879	0.2574	0.2870	0.2569
	Benzene	1297.90	131.47	760	0.7969	0.5804	0.7883	0.5718
	Cyclohexane	2151.01	303.42	760	1.1031	0.7811	1.0699	0.7743
	Ethyl acetate	844.69	–178.81	760	0.3972	0.3311	0.3925	0.3313
	n-Heptane	2096.50	617.57	760	1.0832	1.0208	1.0806	1.0226
	n-Hexane	2281.99	283.63	760	1.2005	0.8422	1.1738	0.8337
	Methanol	–511.39	598.44	760	0.0088	0.0254	0.0081	0.0189
	Methyl cyclopentane	2221.47	161.53	760	1.2330	0.7332	1.1965	0.7065
	Toluene	1238.70	251.93	760	0.7067	0.6932	0.7066	0.6933
	Water	382.30	955.45	760	0.7292	0.4104	0.6848	0.3781
Ethyl acetate	Chloroform	–92.50	–367.50	760	–0.4478	–0.2868	–0.4275	–0.2726
	Ethanol	–178.81	844.69	760	0.3311	0.3972	0.3313	0.3925
	Methanol	–200.36	985.69	760	0.4470	0.4227	0.4463	0.4229
	1-Propanol	–198.72	661.24	760	0.2051	0.2893	0.1982	0.2849
	2-Propanol	60.99	289.68	760	0.2113	0.1964	0.2112	0.1961
Ethyl benzene	Cellosolve	121.89	755.77	760	0.3762	0.4402	0.3750	0.4379
	Ethyl cyclohexane	396.01	–240.92	400	0.0821	0.0628	0.0800	0.0626
	Hexylene glycol	52.43	1601.04	400	0.3719	0.8383	0.3105	0.7358
	n-Octane	304.31	–134.87	760	0.0890	0.0902	0.0889	0.0903
Ethyl cyclo-hexane	Butyl cellosolve	636.11	643.51	400	0.5784	0.5814	0.5784	0.5814
	Ethyl benzene	–240.92	396.01	400	0.0628	0.0821	0.0626	0.0800
	Hexylene glycol	76.95	3592.40	400	0.4770	1.1219	0.4293	0.9448
n-Heptane	Benzene	292.94	99.35	760	0.2135	0.0985	0.1899	0.0842
	Ethanol	617.57	2096.50	760	1.0208	1.0832	1.0226	1.0806
	1-Propanol	316.22	1353.98	75°C	0.7719	0.7550	0.7719	0.7548
n-Hexane	Benzene	169.92	173.93	760	0.2063	0.1457	0.2010	0.1430
	Cellosolve	656.23	834.86	760	0.7206	0.6629	0.7183	0.6633
	1,4-Dioxane	164.58	806.80	760	0.4850	0.5260	0.4857	0.5238
	Ethanol	283.63	2281.99	760	0.8422	1.2005	0.8337	1.1738
	Hexene-1	415.18	–279.86	760	0.0393	0.0114	0.0283	0.0078
	Methyl cyclopentane	272.09	–175.70	760	0.0023	0.0226	0.0188	0.0014
	1-Propanol	834.85	812.66	760	0.8734	0.5952	0.8511	0.5763
	1,2,3-Trichloro-propane	116.39	1106.54	760	0.4520	0.7257	0.4298	0.6916
Hexene-1	Cellosolve	705.47	370.05	760	0.5860	0.4367	0.5818	0.4228
	1,4-Dioxane	176.39	495.19	760	0.3757	0.3578	0.3755	0.3577
	n-Hexane	–279.86	415.18	760	0.0114	0.0393	0.0078	0.0283
	1,2,3-Trichloro-propane	156.93	570.31	760	0.3419	0.4372	0.3382	0.4307
Hexylene glycol	Ethylbenzene	1601.04	52.43	400	0.8383	0.3719	0.7358	0.3105
	Ethyl cyclohexane	3592.40	76.95	400	1.1219	0.4770	0.9448	0.4293
Methanol	Acetone	664.08	–214.95	760	0.2801	0.2635	0.2798	0.2634
	Benzene	1620.36	153.86	760	0.8975	0.7518	0.8923	0.7494
	Chloroform	1703.68	–373.30	760	0.8263	0.4104	0.7767	0.3702
	2,3-Dimethyl butane	2771.85	449.08	760	1.5408	1.1276	1.5255	1.1265
	Ethanol	598.44	–511.39	760	0.0254	0.0088	0.0189	0.0081
	Ethyl acetate	985.69	–200.36	760	0.4227	0.4470	0.4229	0.4463
	Methyl acetate	834.06	–78.81	760	0.4394	0.4262	0.4393	0.4261
	2-Propanol	88.02	–30.19	760	–0.0325	–0.0329	–0.0326	–0.0329
	Water	205.30	482.16	760	0.3861	0.2439	0.3794	0.2211
Methyl acetate	Benzene	–23.84	229.25	760	0.0919	0.1292	0.0939	0.1219
	Chloroform	113.24	–451.09	760	–0.3343	–0.2249	–0.3270	–0.2112
	Cyclohexane	691.65	345.11	760	0.5317	0.5799	0.5313	0.5789
	Methanol	–78.81	834.06	760	0.4262	0.4394	0.4261	0.4393
Methyl cyclo-hexane	Benzene	360.92	–4.15	760	0.1901	0.0910	0.1760	0.0760
	2-Propanol	209.75	1831.76	500	0.6886	1.0659	0.6785	1.0343
Methyl cyclo-pentane	Benzene	97.33	161.44	760	0.1605	0.1360	0.1606	0.1342
	Ethanol	161.53	2221.47	760	0.7332	1.2330	0.7065	1.1965
	n-Hexane	–175.70	272.09	760	0.0226	0.0023	0.0014	0.0188
	Toluene	–451.92	957.61	760	0.0717	0.2475	0.0694	0.1627
Methyl-ethyl-ketone	Chloroform	–235.12	–231.61	760	–0.3486	–0.2990	–0.3507	–0.2938
n-Octane	Butyl cellosolve	298.62	1070.54	400	0.5318	0.6967	0.5227	0.6903
	Cellosolve	622.77	989.04	760	0.7507	0.6158	0.7467	0.6117
	Ethyl benzene	–134.87	304.31	760	0.0902	0.0890	0.0903	0.0889
	2-Propanol	422.41	1391.09	400	0.8535	0.8043	0.8524	0.8044
n-Pentane	Acetone	262.74	996.75	760	0.6364	0.7403	0.6329	0.7386
	Benzene	1370.32	–73.91	760	0.7703	0.3772	0.7332	0.3251

1-Propanol	Ethyl acetate	661.24	–198.72	760	0.2893	0.2051	0.2849	0.1982
	n-Heptane	1353.98	316.22	75°C	0.7550	0.7719	0.7548	0.7719
	n-Hexane	812.66	834.85	760	0.5952	0.8734	0.5763	0.8511
	Water	1015.80	1284.61	760	1.1433	0.5037	1.0536	0.4393
2-Propanol	Acetone	284.99	127.43	760				
	Benzene	1007.94	160.53	760				
	Carbon tetrachloride	1232.94	111.11	760				
	Cyclohexane	1734.12	69.02	760				
	Ethyl acetate	289.68	60.99	760				
	Methanol	–30.19	88.02	760				
	Methyl cyclohexane	1831.76	209.75	500				
	n-Octane	1391.09	422.41	400				
	2,2,4-Trimethyl pentane	1231.69	183.12					

760
0.2690
0.6723
0.7868
1.0162
0.1964
–0.0329
1.0659
0.8043
0.6603
0.2186
0.4638
0.4918
0.5322
0.2113
–0.0325
0.6886
0.8535
0.6927
0.2688
0.6551
0.7656
0.9539
0.1961
–0.0329
1.0343
0.8044
0.6601
0.2152
0.4523
0.4763
0.5006
0.2112
–0.0326
0.6785
0.8524
0.6924

Toluene
1-Butanol
Cyclohexane
Ethanol
Methyl cyclopentane

104.68
909.36
251.93
957.61
887.80
–414.68
1238.70
–452.92
760
760
756
760
0.3841
0.2578
0.6932
0.2475
0.5430
0.0702
0.7067
0.0717
0.3699
0.1563
0.6933
0.1627
0.5340
0.0689
0.7066
0.0694

1,2,3-Trichloropropane
n-Hexane
Hexene-1

1106.54
570.31
116.93

156.39
760
760
0.7257
0.4372
0.4520
0.3419
0.6916
0.4307
0.4298
0.3382
2,2,4-Trimeth-
yl pentane
2-Propanol
183.12
1231.69
760
0.6927
0.6603
0.6924
0.6601
Water
Acetone
Acetonitrile
Ethanol
Methanol
1-Propanol
1405.49
1610.07
955.45
482.61
1284.61
439.64
694.08
382.30
205.30
1015.80
760
760
760
760
760
0.6105
0.8207
0.4104
0.2439
0.5037
0.9972
1.0680
0.7292
0.3861
1.1433
0.5576
0.8231
0.3781
0.2211
0.4393
0.9709
1.0489
0.6848
0.3794
1.0536

Reprinted with permission from (Holmes, M.J., and Van Winkle, M. (1970). Prediction of ternary vapor–liquid equilibria from binary data, *Industrial & Engineering Chemistry*, 62, 21–31) American Chemical Society.

For moderately nonideal mixtures, the Margules and Van Laar equations are used extensively. These classical activity coefficient models are mathematically easier to handle. However, for strongly nonideal mixtures, the Margules and Van Laar equations are likely to represent the data with significantly less success.

8.2.3 The Wilson Model (developed by Wilson in 1964)

Wilson proposed an expression for the molar excess free energy that differs from the usual Wohl

expansion. Instead of the polynomial expansion given by Equation (8.13), Wilson proposed the following logarithmic function:

$$\frac{g^E}{RT} = -\sum_{i=1}^{N} x_i \ln\left[\sum_{j=1}^{N} \Lambda_{ij} x_j\right] \tag{8.23}$$

In the following subsection, the Wilson model is represented for the multicomponent and binary systems.

For Multicomponent System

$$\ln \gamma_i = 1 - \ln\left(\sum_{j=1}^{N} x_j \Lambda_{ij}\right) - \sum_{k=1}^{N}\left(\frac{x_k \Lambda_{ki}}{\sum_{j=1}^{N} x_j \Lambda_{kj}}\right) \tag{8.24}$$

where

$$\Lambda_{ij} = \frac{V_j}{V_i}\exp\left[-\frac{(\lambda_{ij} - \lambda_{ii})}{RT}\right]$$
$$\lambda_{ji} = \lambda_{ij}$$
$$\lambda_{ii} \neq \lambda_{jj} \tag{8.25}$$
$$\Lambda_{ji} \neq \Lambda_{ij}$$
$$\Lambda_{ii} = \Lambda_{jj} = \Lambda_{kk} = 1$$

For Binary System

$$\ln \gamma_1 = -\ln(x_1 + \Lambda_{12}x_2) + x_2\left[\frac{\Lambda_{12}}{x_1 + \Lambda_{12}x_2} - \frac{\Lambda_{21}}{x_2 + \Lambda_{21}x_1}\right] \tag{8.26}$$

$$\ln \gamma_2 = -\ln(x_2 + \Lambda_{21}x_1) - x_1\left[\frac{\Lambda_{12}}{x_1 + \Lambda_{12}x_2} - \frac{\Lambda_{21}}{x_2 + \Lambda_{21}x_1}\right] \tag{8.27}$$

For this binary system, ⊣12 and ⊣21 can be estimated from Equation (8.25).

The activity coefficients are predicted accurately using the Wilson thermodynamic model for dilute composition where entropy effects dominate over enthalpy effects. For highly nonideal mixtures, this model becomes markedly superior to the Margules and Van Laar equations. When the Wilson parameter (⊣$_{ij}$) is equal to unity, the solution is at ideal phase. Values of ⊣$_{ij} < 1$ correspond to positive deviations from Raoult's law, while values of ⊣$_{ij} > 1$ correspond to negative deviations. Here, ¬ $_{ij}$ is the energy of interaction between the molecules designated in the subscripts. The Wilson equation involves only two parameters per binary, (¬ $_{ij}$ − ¬ $_{ii}$) and (¬ $_{ji}$ − ¬ $_{jj}$), and these parameters for different binary pairs are listed in Table 8.1. The liquid molar volume V_i for several components is listed in Table 8.2.

Table 8.2 Liquid molar volumes for the Wilson model

Component, *i*	*Temperature* (K)	V_i (cc/gmol)
Acetone	228.15	67.380
	273.15	71.483
	323.15	76.826

Acetonitrile	273.15 303.15 355.15	51.092 53.214 57.4
Benzene	273.15 323.15 373.15	86.783 92.263 98.537
1-Butanol	273.15 343.15 413.15	89.873 97.8 108.7
Butyl cellosolve	293.15 373.15 453.15	130.86 143.1 161.1
Carbon tetrachloride	293.15 353.15 413.15	96.518 104.192 114.379
Cellosolve	293.15 353.15 413.15	96.80 104.1 114.0
Chloroform	273.15 303.15 333.15	78.218 81.185 84.5
Cyclohexane	288.15 306.30 352.35	107.470 109.841 116.630
Cyclopentane	273.15 333.15 373.15	91.9 99.4 105.2
2,3-Dimethyl butane	273.15 303.15 333.15	126.80 132.06 138.03
1,4-Dioxane	293.15 333.15 373.15	85.24 89.3 93.9
Ethanol	273.15 323.15 373.15	57.141 60.356 64.371
Ethyl acetate	273.15 323.15 373.15	95.3 102.1 110.5
Ethyl benzene	273.15 343.15 413.15	120.02 129.09 140.29
Ethyl cyclohexane	293.15 353.15 413.15	142.48 152.1 163.9
n-Heptane	273.15 323.15 373.15	143.045 152.303 163.619
n-Hexane	273.15 323.15 373.15	127.301 136.388 148.211
Hexene-1	273.15 303.15 333.15	121.62 126.80 132.45
Hexylene glycol	273.15 373.15 473.15	122.20 135.0 154.1
Methanol	273.15 373.15	39.556 44.874

	473.15	57.939
Methyl acetate	273.15 373.15 473.15	77.221 90.111 121.443
Methyl cyclohexane	303.15 333.85 372.65	129.116 133.833 140.609
Methyl cyclopentane	273.15 303.15 373.15	109.670 113.810 126.2
Methyl ethyl ketone	273.15 333.15 373.15	87.3 94.5 100.0
n-Octane	273.15 333.15 393.15	158.970 170.630 185.182
n-Pentane	273.15 333.15 373.15	111.8 122.9 131.4
1-Propanol	293.15 343.15 393.15	74.785 78.962 84.515
2-Propanol	298.15 333.15 373.15	77.0 80.5 86.1
Toluene	303.15 353.15 400.00	107.415 113.717 120.879
1,2,3-Trichloropropane	293.15 353.15 433.15	106.22 112.6 124.1
2,2,4-Trimethylpentane	273.15 323.15 373.15	161.26 171.24 183.66
Water	277.13 323.15 373.15	18.060 18.278 18.844

Note: Using the given data in the table, it is easily possible to correlate the liquid molar volume of any component i, V_i, with the temperature by a second-order polynomial as $V_i = a_i + b_i T + c_i T^2$. The molar volume at any temperature could then be calculated.

Reprinted with permission from (Holmes, M.J. and Van Winkle, M. (1970). Prediction of ternary vapor–liq uid equilibria from binary data, *Industrial & Engineering Chemistry*, 62, 21–31) American Chemical Society.

The Wilson equation has two main features, which make it particularly useful for engineering applications. First, one may consider the quantities ($\lambda_{ij} - \lambda_{ii}$) and ($\lambda_{ji} - \lambda_{jj}$) to be independent of temperature, at least over a modest temperature interval. This is an important advantage in the design of isobaric distillation equipment where the temperature varies from plate to plate. If the temperature dependence is completely neglected, then Λ_{ij} and Λ_{ji} may be directly obtained from the experimental data. In this case, the liquid molar volumes are not needed. Second, the Wilson thermodynamic model for a multicomponent solution requires only parameters that can be obtained from binary mixture data. This feature provides an important economic advantage since the amount of experimental work required to characterize a multicomponent solution is thereby very much reduced.

8.2.4 The NRTL Model (nonrandom two-liquid model developed by Renon and Prausnitz in 1968)

The NRTL equation represents an accepted extension of Wilson's concept and was developed on the basis of a *two-liquid* theory. The expression for molar excess Gibbs free energy is as follows:

$$\frac{g^E}{RT} = \sum_{i=1}^{N} x_i \left(\frac{\sum_{j=1}^{N} x_j \tau_{ji} G_{ji}}{\sum_{k=1}^{N} x_k G_{ki}} \right) \qquad (8.28)$$

The NRTL activity coefficient model for the multicomponent and binary mixtures is given below.

For Multicomponent System

$$\ln \gamma_i = \frac{\sum_{j=1}^{N} x_j \tau_{ji} G_{ji}}{\sum_{k=1}^{N} x_k G_{ki}} + \sum_{j=1}^{N} \left[\frac{x_j G_{ij}}{\sum_{k=1}^{N} x_k G_{kj}} \left(\tau_{ij} - \frac{\sum_{k=1}^{N} x_k \tau_{kj} G_{kj}}{\sum_{k=1}^{N} x_k G_{kj}} \right) \right] \qquad (8.29)$$

where $\ln G_{ij} = -\alpha_{ij} \tau_{ij}$ (8.30)

$\ln G_{ji} = -\alpha_{ji} \tau_{ji}$ (8.31)

$\tau_{ij} = \frac{(g_{ij} - g_{jj})}{RT}$ (8.32)

$\tau_{ji} = \frac{(g_{ji} - g_{ii})}{RT}$ (8.33)

$\tau_{ij} \neq \tau_{ji}$

$\tau_{ii} = \tau_{jj} = 0$

$G_{ii} = G_{jj} = 1$

$\alpha_{ij} = \alpha_{ji}$

For Binary System

$$\ln \gamma_1 = x_2^2 \left[\frac{\tau_{21} G_{21}^2}{(x_1 + x_2 G_{21})^2} + \frac{\tau_{12} G_{12}}{(x_2 + x_1 G_{12})^2} \right] \qquad (8.34)$$

$$\ln \gamma_2 = x_1^2 \left[\frac{\tau_{12} G_{12}^2}{(x_2 + x_1 G_{12})^2} + \frac{\tau_{21} G_{21}}{(x_1 + x_2 G_{21})^2} \right] \qquad (8.35)$$

For the binary systems, Equation (8.30) or (8.31) is used to estimate G_{12} and G_{21}, and Equation (8.32) or (8.33) is used to estimate τ_{12} and τ_{21}.

For ideal solutions, $\tau_{ij} = \tau_{ji} = 0$. The NRTL activity coefficient model contains two temperature-dependent parameters, $(g_{ij} - g_{jj})$ and $(g_{ji} - g_{ii})$, in addition to a nonrandomness parameter, α_{ij}, which, to a good approximation, does not depend on temperature and can often be estimated with sufficient

accuracy from the nature of components i and j (Renon and Prausnitz, 1968). For some systems, it appears that $(g_{ij} - g_{jj})$ and $(g_{ji} - g_{ii})$ are linear functions of temperature.

As stated, this model contains three binary interaction parameters for each binary pair, and is applicable to vapour–liquid, liquid–liquid and vapour–liquid–liquid systems, whereas the Wilson equation is, in theory, not applicable to partially miscible solutions.

The parameter $\neg\curlywedge_{ij}$ characterizes the tendency of species i and j to be distributed in a nonrandom fashion. Depending on the chemical nature of the mixture, a value for $\neg\curlywedge_{ij}$ (in between 0.2 and 0.47) must be chosen; the values recommended by Renon and Prausnitz (1968) provide a convenient guide. For most of the binary systems, $\neg\curlywedge_{ij}$ is set according to the following rules.

1. $\neg\curlywedge_{ij}$ = 0.0, which implies that local mole fractions are equal to overall solution mole fractions (not desirable).
2. $\neg\curlywedge_{ij}$ = 0.20 for mixtures of saturated hydrocarbons with polar nonassociated species (e.g., *n*-hexane–acetone or *iso*-octane–nitroethane). Phase splitting occurs at a relatively low degree of nonideality and the nonrandomness, as measured by $\neg\curlywedge_{ij}$, is small.
3. $\neg\curlywedge_{ij}$ = 0.30 for mixtures of nonpolar compounds (e.g., hydrocarbons–carbon tetrachloride, benzene–*n*-heptane), except the mixtures of fluorocarbons and paraffins. The mixtures of nonpolar and polar nonassociated species (e.g., *n*-heptane–methyl ethyl ketone, benzene–acetone, carbon tetrachloride–nitroethane); mixtures of polar species that exhibit negative deviations from Raoult's law (e.g., acetone–chloroform, chloroform–dioxane) and moderate positive deviations (e.g., acetone–methyl acetate, ethanol–water); mixtures of water and polar nonassociated species (e.g., water–acetone) fall in this category.
4. $\neg\curlywedge_{ij}$ = 0.40 for mixtures of saturated hydrocarbons and homolog perfluorocarbons (e.g., *n*-hexane–perfluoro-*n*-hexane).
5. $\neg\curlywedge_{ij}$ = 0.47 for mixtures of an alcohol or other strongly self-associated species with a nonpolar species, like a hydrocarbon or carbon tetrachloride (e.g., ethanol–benzene); mixtures of carbon tetrachloride with polar species (acetonitrile and nitromethane); mixtures of water with a polar self-associated substance (butyl-glycol and pyridine).

The binary parameters ($\neg\curlywedge_{ij}$, $g_{ij} - g_{jj}$ and $g_{ji} - g_{ii}$) for limited nonideal liquid mixtures are listed in Table 8.3.

Table 8.3 Parameters for the NRTL model

System (1)–(2)	$\neg\curlywedge_{12}$	$g_{12} - g_{22}$ (cal/gmol)	$g_{21} - g_{11}$ (cal/gmol)	*Temp.* (°C)
Ethanol-*n*–hexane	0.47	1010.0	1515.0	55.0
Methyl ethyl ketone–*n*-hexane	0.20	253.0	630.0	60.0
1-Propanol–water	0.30	18.0	1735.0	60.0
n-Hexane–nitroethane	0.20	702.0	780.0	25.0
n-Octane–nitroethane	0.20	604.0	1124.0	25.0
iso-Octane–nitroethane	0.20	497.0	1026.0	25.0
Ethyl acetate–water	0.40	1335.0	2510.0	70.0
Water–ethanol	0.30	976.0	88.0	70.0
Ethanol–ethyl acetate	0.30	301.0	322.0	70.0

Reprinted with permission from (Renon, H., and Prausnitz, J.M. (1969). Estimation of parameters for the NRTL equation for excess Gibbs energies of strongly nonideal liquid mixtures, *Ind. Eng. Chem. Process Des. Dev.,* 8, 413–419) American Chemical Society.

8.2.5 The UNIQUAC Model (universal quasi-chemical model developed by Abrams and Prausnitz in 1975)

The molar excess free energy function is taken to be the sum of g^C, the combinatorial part, and g^R, the residual part of the excess free energy as:

$$g^E = g^C + g^R \qquad (8.36)$$

where

$$\frac{g^C}{RT} = \sum_{i=1}^{N} x_i \ln\left(\frac{\Phi_i}{x_i}\right) + \frac{Z}{2}\sum_{i=1}^{N} q_i x_i \ln\left(\frac{\theta_i}{\Phi_i}\right) \qquad (8.37)$$

$$\frac{g^R}{RT} = -\sum_{i=1}^{N} q_i x_i \ln\left(\sum_{j=1}^{N} \theta_j \tau_{ji}\right) \qquad (8.38)$$

For multicomponent and binary solutions, the UNIQUAC activity coefficient model is given in the following subsection.

For Multicomponent System

$$\ln \gamma_i = \underbrace{\ln \gamma_i^C}_{\left[\begin{smallmatrix}\text{combinatorial}\\ \text{part}\end{smallmatrix}\right]} + \underbrace{\ln \gamma_i^R}_{\left[\begin{smallmatrix}\text{residual}\\ \text{part}\end{smallmatrix}\right]} \qquad (8.39)$$

Combinatorial part

$$\ln \gamma_i^C = \ln\left(\frac{\Phi_i}{x_i}\right) + \frac{Z}{2} q_i \ln\left(\frac{\theta_i}{\Phi_i}\right) + l_i - \left(\frac{\Phi_i}{x_i}\right)\sum_{j=1}^{N} x_j l_j \qquad (8.40)$$

where

$$l_i = \frac{Z}{2}(r_i - q_i) - r_i + 1 \qquad (8.41)$$

area fraction $$\theta_i = \frac{x_i q_i}{\sum_{j=1}^{N} x_j q_j} \qquad (8.42)$$

segment fraction $$\Phi_i = \frac{x_i r_i}{\sum_{j=1}^{N} x_j r_j} \qquad (8.43)$$

$Z = 10$

Residual part

$$\ln \gamma_i^R = q_i \left[1 - \ln \left(\sum_{j=1}^{N} \theta_j \tau_{ji} \right) - \sum_{j=1}^{N} \left(\frac{\theta_j \tau_{ij}}{\sum_{k=1}^{N} \theta_k \tau_{kj}} \right) \right] \tag{8.44}$$

where

$$\tau_{ji} = \exp\left[-\frac{(u_{ji} - u_{ii})}{RT} \right] \tag{8.45}$$

$$\tau_{ij} = \exp\left[-\frac{(u_{ij} - u_{jj})}{RT} \right] \tag{8.46}$$

For Binary System

$$\ln \gamma_1 = \ln \left(\frac{\Phi_1}{x_1} \right) + \frac{Z}{2} q_1 \ln \left(\frac{\theta_1}{\Phi_1} \right) + \Phi_2 \left(l_1 - \frac{r_1}{r_2} \times l_2 \right)$$
$$- q_1 \ln (\theta_1 + \theta_2 \tau_{21}) + \theta_2 q_1 \left(\frac{\tau_{21}}{\theta_1 + \theta_2 \tau_{21}} - \frac{\tau_{12}}{\theta_2 + \theta_1 \tau_{12}} \right) \tag{8.47}$$

$$\ln \gamma_2 = \ln \frac{\Phi_2}{x_2} + \frac{Z}{2} q_2 \ln \frac{\theta_2}{\Phi_2} + \Phi_1 \left(l_2 - \frac{r_2}{r_1} \times l_1 \right)$$
$$- q_2 \ln (\theta_2 + \theta_1 \tau_{12}) + \theta_1 q_2 \left(\frac{\tau_{12}}{\theta_2 + \theta_1 \tau_{12}} - \frac{\tau_{21}}{\theta_1 + \theta_2 \tau_{21}} \right) \tag{8.48}$$

Equation (8.41) for l_1 and l_2, Equation (8.42) for ㅂ_1 and ㅂ_2, Equation (8.43) for ㅎ_1 and ㅎ_2, and Equation (8.45) or (8.46) for ㅊ_{12} and ㅊ_{21} are used in the UNIQUAC model for binary systems.

In the above UNIQUAC model, q_i and r_i are the pure-component (i) area and volume parameters respectively, and u_{ji} is a characteristic energy for the $j - i$ interaction. The activity coefficient is relatively insensitive to the choice of the lattice coordination number (Z) provided a reasonable value (6 ㄲ Z ㄲ 12) is chosen. Abrams and Prausnitz (1975) consistently used the value $Z = 10$ in their work.

The first term on the right hand side of Equation (8.36) accounts for combinatorial effects due to differences in size and shape of the molecules, whereas the second term provides a residual contribution owing to differences in intermolecular forces. The main advantage of the UNIQUAC model is that, with only two adjustable parameters per binary ($u_{ij} - u_{jj}$ and $u_{ji} - u_{ii}$), it gives satisfactory representation of both vapour–liquid and liquid–liquid equilibria. Extension to multicomponent systems requires no ternary (or higher) parameters. Abrams and Prausnitz (1975) showed that $u_{ji} = u_{ij}$ and $\text{ㅊ}_{ii} = \text{ㅊ}_{jj} = 1$. Table 8.4 gives the structural parameters (q and r) for some representative nonelectrolyte molecules.

In general, the differences in interaction energies, $(u_{ji} - u_{ii})$ and $(u_{ij} - u_{jj})$, are linear functions of temperature. Neglecting the effect of temperature, these energy parameters can be obtained from experimental results and are reported in Table 8.5 for limited binary systems.

Table 8.4 Pure-component area and volume parameters for the UNIQUAC model

Molecule, i	r_i	q_i
Acetaldehyde	1.90	1.80
Acetone	2.57	2.34
Aniline	3.72	2.83
Benzene	3.19	2.40
Carbon dioxide	1.30	1.12
Chloroform	2.87	2.41
n-Decane	7.20	6.02
Dimethyl amine	2.33	2.09
Ethane	1.80	1.70
Furfural	2.80	2.58
n-Hexadecane	11.24	9.26
Methyl acetate	2.80	2.58
n-Octane	5.84	4.93
Toluene	3.87	2.93
Triethyl amine	5.01	4.26
Water	0.92	1.40

Reprinted with permission from (Abrams, D.S., and Prausnitz, J.M. (1975). Statistical thermodynamics of liquid mixtures: a new expression for the excess Gibbs energy of partly or completely miscible systems, *AIChE J.*, 21, 116–128) American Institute of Chemical Engineers.

Table 8.5 Binary parameters for the UNIQUAC model

System (1)–(2)	$u_{21} - u_{11}$ (cal/gmol)	$u_{12} - u_{22}$ (cal/gmol)	*Pressure* (mm Hg)/ *Temp.* (°C)
Acetone–benzene	331.0	–208.9	45°C
Acetone–chloroform	149.8	–315.5	50°C
Benzene–*iso*-octane	182.1	–76.5	760
Carbon tetrachloride–acetonitrile	–100.1	953.4	45°C
Ethanol–hexane	940.9	–335.0	760
Ethanol–*iso*-octane	968.2	–357.6	50°C
Ethylacetate–ethanol	–292.3	446.5	70°C
Hexane–nitroethane	–36.3	471.6	45°C
iso-octane–nitroethane	5.3	492.3	35°C
Methanol–benzene	1355.8	–417.4	55°C
Methylacetate–ethanol	–40.5	426.5	45°C
Methylacetate–methanol	–233.1	622.1	50°C
Methylcyclopentane–benzene	–36.9	138.1	760
Nitromethane–benzene	309.1	35.45	45°C
Water–ethanol	258.4	378.1	70°C
Water–methyl-ethyl-ketone	622.3	222.2	760

Reprinted with permission from (Abrams, D.S., and Prausnitz, J.M. (1975). Statistical thermodynamics of liquid mixtures: A new expression for the excess Gibbs energy of partly or completely miscible systems, *AIChE J.*, 21, 116–128) American Institute of Chemical Engineers.

Again, for a small temperature range, the effect of temperature on τ_{ij} may be approximated by a linear form:

$$\tau_{ij} = U_{ij} + U'_{ij}T \qquad (8.49)$$

where U_{ij} and U'_{ij} are coefficients related to $u_{ij} - u_{jj}$.

Abrams and Prausnitz (1975) have mentioned that the UNIQUAC model is about as satisfactory as the Wilson equation but no better for miscible systems. They also stated that this model is superior to the NRTL equation for liquid–liquid systems.

8.2.6 The UNIFAC Model (universal quasi-chemical (UNIQUAC) functional group activity coefficients model developed by Fredenslund, Jones, and Prausnitz in 1975)

The UNIFAC group contribution method is based on the solution of groups concept. The groups are structural units which when added form the parent molecules. Instead of considering a liquid mixture as a

solution of molecules, the mixture is considered as a solution of groups. The activity coefficients are then determined by the properties of the groups rather than by those of the molecules.

For more details, let us consider an example of ethanol–*n*-hexane mixture. Ethanol consists of one CH_3, one CH_2 and one OH (hydroxyl)[2] groups (or one CH_3OH and one CH_2 groups), and *n*-hexane contributes two CH_3 and four CH_2 groups. Therefore, the example solution can be treated as a mixture of three CH_3, five CH_2 and one OH functional groups
(or one CH_3OH, two CH_3 and five CH_2 groups). It is also not incorrect to consider
ethanol (C_2H_5OH) as a single group. There are many thousands of multicomponent liquid mixtures that can be constituted from a much smaller (perhaps 50 to 100) number of functional groups.

[2] The UNIFAC group interaction parameters for OH functional group are first reported by Skjold–Jorgensen, Kolbe, Gmehling, and Rasmussen (Skjold–Jorgensen, S., Kolbe, B., Gmehling, J., and Rasmussen, P. (1979). Vapour–liquid equilibria by UNIFAC group contribution. Revision and extension, *Ind. Eng. Chem. Process Des. Dev.,* 18, 714–722).

The UNIFAC method offers several appealing advantages over other activity coefficient models, such as: (i) the parameters are essentially independent of temperature, (ii) predictions can be made with sufficient accuracy over a temperature range of typically 2 to 150°C and up to a pressure of a few atmospheres, (iii) this method can predict the properties of a mixture (by the help of available parameters for a considerably larger number of functional groups) when no mixture data (experimental) at all are available, and (iv) UNIFAC provides a priori estimates of sizes and surface areas.

The UNIFAC model is theoretically based on the UNIQUAC method and therefore,

$$\ln \gamma_i = \ln \gamma_i^C + \ln \gamma_i^R \qquad \text{[from Equation (8.39)]}$$

Combinatorial part

The combinatorial part of UNIFAC model includes Equations (8.40) to (8.43) in addition to $Z = 10$. That means, the combinatorial contribution is the same in both the UNIQUAC and UNIFAC models. In the UNIFAC method, the pure-component area and volume parameters are replaced by:

$$q_i = \sum_k \nu_k^{(i)} Q_k \qquad (8.50)$$

$$r_i = \sum_k \nu_k^{(i)} R_k \qquad (8.51)$$

Residual part

$$\ln \gamma_i^R = \sum_{\substack{k \\ \text{all functional groups in the mixture}}} \nu_k^{(i)} [\ln \Gamma_k - \ln \Gamma_k^{(i)}] \qquad (8.52)$$

where

$$\ln \Gamma_k = Q_k \left[1 - \ln \left(\sum_m \theta_m \psi_{mk} \right) - \sum_m \left(\frac{\theta_m \psi_{km}}{\sum_n \theta_n \psi_{nm}} \right) \right] \qquad (8.53)$$

$$\theta_m = \frac{Q_m X_m}{\sum_n Q_n X_n} \tag{8.54}$$

$$X_m = \frac{\sum_i v_m^{(i)} x_i}{\sum_i \sum_n v_n^{(i)} x_i} \tag{8.55}$$

$$\psi_{mk} = \exp\left[-\frac{a_{mk}}{T}\right] \tag{8.56}$$

$$\psi_{km} = \exp\left[-\frac{a_{km}}{T}\right] \tag{8.57}$$

In the above UNIFAC model, Q_k and R_k are the area and volume parameters, respectively, for the type-k functional group; $v_k^{(i)}$, always an integer, is the number of groups of type k in molecule i; Γ_k is the residual activity coefficient of the functional group k in the actual mixture; $\Gamma_k^{(i)}$ is the residual activity coefficient of group k in a reference mixture containing only molecules of type i; θ_m is the area fraction of group m and X_m is the mole fraction of group m in the mixture. Parameter a_{mk} characterizes the interaction between groups m and k. For each group–group interaction, there are two parameters: a_{mk} and a_{km}. When $m = k$, then $a_{mk} = 0.0$ and $\psi_{mk} = 1.0$.

In Table 8.6, it is obvious that the subgroups ACH (m_1) and AC (m_2) are within the same main group ACH. Now let us consider an example of ACH-R system, where the molecule R is a single functional group (m_3). Notice that all subgroups within the same main group have different values for Q_k and R_k but identical group interaction parameters a_{mk}. It implies that $a_{m1,m3} = a_{m2,m3}$, $a_{m3,m1} = a_{m3,m2}$ and $a_{m1,m2} = a_{m2,m1} = 0.0$.

Table 8.6 Group volume and area parameters for the UNIFAC model

Main group	*Subgroup(s)*	R_k	Q_k	*Sample group assignment*
CH_2	CH_3	0.9011	0.848	Ethane: $2CH_3$
	CH_2	0.6744	0.540	*n*-Butane: $2CH_3$, $2CH_2$
	CH	0.4469	0.228	*iso*-Butane: $3CH_3$, 1CH
	C	0.2195	0.000	2,2-Dimethyl propane: $4CH_3$, 1C
C=C	CH_2=CH	1.3454	1.176	1-Hexene: $1CH_3$, $3CH_2$, $1CH_2$=CH
	CH=CH	1.1167	0.867	2-Hexene: $2CH_3$, $2CH_2$, 1CH=CH
	CH=C	0.8886	0.676	2-Methyl butene-2: $3CH_3$, 1CH=C
	CH_2=C	1.1173	0.988	2-Methyl butene-1: $2CH_3$, $1CH_2$, $1CH_2$=C
ACH	ACH	0.5313	0.400	Benzene: 6ACH
	AC	0.3652	0.120	Styrene: $1CH_2$=CH, 5ACH, 1AC
$ACCH_2$	$ACCH_3$	1.2663	0.968	Toluene: 5ACH, $1ACCH_3$
	$ACCH_2$	1.0396	0.660	Ethyl benzene: $1CH_3$, 5ACH, $1ACCH_2$
	ACCH	0.8121	0.348	Cumene: $2CH_3$, 5ACH, 1ACCH
COH	COH	1.2044	1.124	Ethanol: $1CH_3$, 1COH
	MCOH	1.4311	1.432	Methanol: 1MCOH
	CHOH	0.9769	0.812	*iso*-Propanol: $2CH_3$, 1CHOH

CCOH	CH_2CH_2OH	1.8788	1.664	1-Propanol: $1CH_3$, $1CH_2CH_2OH$
	$CHOHCH_3$	1.8780	1.660	2-Butanol: $1CH_3$, $1CH_2$, $1CHOHCH_3$
	$CHOHCH_2$	1.6513	1.352	3-Octanol: $2CH_3$, $4CH_2$, $1CHOHCH_2$
	CH_3CH_2OH	2.1055	1.972	Ethanol: $1CH_3CH_2OH$
	$CHCH_2OH$	1.6513	1.352	*iso*-Butanol: $2CH_3$, $1CHCH_2OH$
H_2O	H_2O	0.92	1.40	Water: $1H_2O$
ACOH	ACOH	0.8952	0.680	Phenol: 5ACH, 1ACOH
CO	CO	0.7713	0.640	Acetone: $2CH_3$, 1CO
CHO	CHO	0.9980	0.948	Acetaldehyde: $1CH_3$, 1CHO
CH_2CO	CH_3CO	1.6724	1.488	2-Butanone: $1CH_3$, $1CH_2$, $1CH_3CO$
	CH_2CO	1.4457	1.180	3-Pentanone: $2CH_3$, $1CH_2$, $1CH_2CO$
COO	COO	1.002	0.880	Methyl acetate: $2CH_3$, 1COO
COOC	CH_3COO	1.9031	1.728	Butyl acetate: $1CH_3$, $3CH_2$, $1CH_3COO$
	CH_2COO	1.6764	1.420	Butyl propanoate: $2CH_3$, $3CH_2$, $1CH_2COO$
CH_2O	CH_3O	1.1450	1.088	Dimethyl ether: $1CH_3$, $1CH_3O$
	CH_2O	0.9183	0.780	Diethyl ether: $2CH_3$, $1CH_2$, $1CH_2O$
	CH-O	0.6908	0.468	Diisopropyl ether: $4CH_3$, 1CH, 1CH-O
	FCH_2O	0.9183	1.100	Tetrahydrofuran: $3CH_2$, $1FCH_2O$
CNH_2	CH_3NH_2	1.5959	1.544	Methyl amine: $1CH_3NH_2$
	CH_2NH_2	1.3692	1.236	*n*-Propyl amine: $1CH_3$, $1CH_2$, $1CH_2NH_2$
	$CHNH_2$	1.1417	0.924	*iso*-propylamine: $2CH_3$, $1CHNH_2$
CNH	CH_3NH	1.4337	1.244	Dimethyl amine: $1CH_3$, $1CH_3NH$
	CH_2NH	1.2070	0.936	Diethyl amine: $2CH_3$, $1CH_2$, $1CH_2NH$
	CHNH	0.9795	0.624	Diisopropyl amine: $4CH_3$, 1CH, 1CHNH
$ACNH_2$	$ACNH_2$	1.0600	0.816	Aniline: 5ACH, $1ACNH_2$
CCN	CH_3CN	1.8701	1.724	Acetonitrile: $1CH_3CN$
	CH_2CN	1.6434	1.416	Propionitrile: $1CH_3$, $1CH_2CN$
COOH	COOH	1.3013	1.224	Acetic acid: $1CH_3$, 1COOH
	HCOOH	1.5280	1.532	Formic acid: 1HCOOH
CCl	CH_2Cl	1.4654	1.264	Butylchloride: $1CH_3$, $2CH_2$, $1CH_2Cl$
	CHCl	1.2380	0.952	*iso*-propyl chloride: $2CH_3$, 1CHCl
	CCl	0.7910	0.724	*tert*-Butyl chloride: $3CH_3$, 1CCl
CCl_2	CH_2Cl_2	2.2564	1.988	Dichloromethane: $1CH_2Cl_2$
	$CHCl_2$	2.0606	1.684	1,1-Dichloroethane: $1CH_3$, $1CHCl_2$
	CCl_2	1.8016	1.448	2,2-Dichloropropane: $2CH_3$, $1CCl_2$
CCl_3	$CHCl_3$	2.8700	2.410	Chloroform: $1CHCl_3$
	CCl_3*	2.6401	2.184	1,1,1-Trichloroethane: $1CH_3$, $1CCl_3$
CCl_4	CCl_4	3.3900	2.910	Carbon tetrachloride: $1CCl_4$
ACCl	ACCl	1.1562	0.844	Chlorobenzene: 5ACH, 1ACCl
CNO_2	CH_3NO_2	2.0086	1.868	Nitromethane: $1CH_3NO_2$
	CH_2NO_2	1.7818	1.560	1-Nitropropane: $1CH_3$, $1CH_2$, $1CH_2NO_2$
	$CHNO_2$	1.5544	1.248	2-Nitropropane: $2CH_3$, $1CHNO_2$
$ACNO_2$	$ACNO_2$	1.4199	1.104	Nitrobenzene: 5ACH, $1ACNO_2$
CS_2	CS_2	2.0570	1.650	Carbon disulphide: $1CS_2$

* Not to be used with oxygen-containing hydrocarbons or amines.

Reprinted with permission from (Fredenslund, A., Gmehling, J., Michelsen, M.L., Rasmussen, P., and Prausnitz, J.M. (1977). Computerized design of

multicomponent distillation columns using the UNIFAC group contribution method for calculation of activity coefficients, *Ind. Eng. Chem. Process Des. Dev.*, 16, 450–462) American Chemical Society.

Table 8.7 Group interaction parameters a_{mk} (in kelvin) for the UNIFAC model

Group→ ↓	CH_2	C=C	ACH	$ACCH_2$	CCOH	CH_3OH	H_2O	ACOH	CH_2CO	CHO	COOC	CH_2O
CH_2	0.0	–200.0	61.13	76.50	737.5	697.2	1318.0	2789.0	476.4	677.0	232.1	251.5
C=C	2520.0	0.0	340.7	4102.0	535.2	1509.0	599.6	n.a.	524.5	n.a.	n.a.	289.3
ACH	–11.12	–94.78	0.0	167.0	477.0	637.4	903.8	1397.0	25.77	n.a.	5.994	32.14
$ACCH_2$	–69.70	–269.7	–146.8	0.0	469.0	603.3	5695.0	726.3	–52.10	n.a.	5688.0	213.1
CCOH	–87.93	121.5	–64.13	–99.38	0.0	127.4	285.4	257.3	48.16	n.a.	76.20	70.0
CH_3OH	16.51	–52.39	–50.0	–44.50	–80.78	0.0	–181.0	n.a.	23.39	306.4	–10.72	–180.6
H_2O	580.6	511.7	362.3	377.6	–148.5	289.6	0.0	442.0	–280.8	649.1	–455.4	–400.6
ACOH	311.0	n.a.	2043.0	6245.0	–455.4	n.a.	–540.6	0.0	n.a.	n.a.	–713.2	n.a.
CH_2CO	26.76	–82.92	140.1	365.8	129.2	108.7	605.6	n.a.	0.0	–37.36	–213.7	5.202
CHO	505.7	n.a.	n.a.	n.a.	n.a.	–340.2	–155.7	n.a.	128.0	0.0	n.a.	n.a.
COOC	114.8	n.a.	85.84	–170.0	109.9	249.6	1135.0	853.6	372.2	n.a.	0.0	–235.7
CH_2O	83.36	76.44	52.13	65.69	42.00	339.7	634.2	n.a.	52.38	n.a.	461.3	0.0
CNH_2	–30.48	79.40	–44.85	n.a.	–217.2	–481.7	–507.1	n.a.	n.a.	n.a.	n.a.	n.a.
CNH	65.33	–41.32	–22.31	223.0	–243.3	–500.4	–547.7	n.a.	n.a.	n.a.	136.0	–49.30
$ACNH_2$	5339.0	n.a.	650.4	3399.0	–245.0	n.a.	–339.5	n.a.	n.a.	n.a.	n.a.	n.a.
CCN	35.76	26.09	–22.97	–138.4	n.a.	168.8	242.8	n.a.	–275.1	n.a.	–297.3	n.a.
COOH	315.3	349.2	62.32	268.2	–17.59	1020.0	–292.0	n.a.	–297.8	n.a.	–256.3	–338.5
CCl	91.46	–24.36	4.680	122.9	368.6	529.0	698.2	n.a.	286.3	n.a.	n.a.	225.4
CCl_2	34.01	–52.71	n.a.	n.a.	601.6	669.9	708.7	n.a.	423.2	n.a.	–132.9	–197.7
CCl_3	36.70	–185.1	288.5	33.61	491.1	649.1	826.8	n.a.	552.1	n.a.	176.5	–20.93
CCl_4	–78.45	–293.7	–4.70	134.7	570.7	860.1	1201.0	1616.0	372.0	n.a.	129.5	n.a.
ACCl	–141.3	n.a.	–237.7	n.a.	134.1	n.a.	920.4	n.a.	n.a.	n.a.	–299.2	n.a.
CNO_2	–32.69	–49.92	10.38	–97.05	n.a.	252.6	614.2	n.a.	–142.6	n.a.	n.a.	–94.49
$ACNO_2$	5541.0	n.a.	1825.0	n.a.	n.a.	n.a.	360.7	n.a.	n.a.	n.a.	n.a.	n.a.
CS_2	11.46	n.a.	–18.99	n.a.	442.8	914.2	1081.0	n.a.	298.7	n.a.	233.7	79.79

(*Contd.*)

Group→ ↓	CNH_2	CNH	$ACNH_2$	CCN	COOH	CCl	CCl_2	CCl_3	CCl_4	ACCl	CNO_2	$ACNO_2$	CS_2
CH_2	391.5	255.7	1245.0	612.0	663.5	35.93	53.76	24.9	104.3	321.5	661.5	543.0	114.1
C=C	396.0	273.6	n.a.	370.9	730.4	99.61	337.1	4583.0	5831.0	n.a.	542.1	n.a.	n.a.
ACH	161.7	122.8	668.2	212.5	537.4	–18.81	n.a.	–231.9	3.00	538.2	168.1	194.9	97.53
$ACCH_2$	n.a.	–49.29	612.5	6096.0	603.8	–114.1	n.a.	–12.14	–141.3	n.a.	3629.0	n.a.	n.a.
CCOH	110.8	188.3	412.0	n.a.	77.61	–38.23	–185.9	–170.9	–98.66	290.0	n.a.	n.a.	73.52
CH_3OH	359.3	266.0	n.a.	45.54	–289.5	–38.32	–102.5	–139.4	–67.80	n.a.	75.14	n.a.	–31.09
H_2O	357.5	287.0	213.0	112.6	225.4	325.4	370.4	353.7	497.5	678.2	–19.44	399.5	887.1
ACOH	n.a.	n.a.	n.a.	n.a.	n.a.	n.a.	n.a.	n.a.	4894.0	n.a.	n.a.	n.a.	n.a.
CH_2OH	n.a.	n.a.	n.a.	428.5	669.4	–191.7	–284.0	–354.6	–39.20	n.a.	137.5	n.a.	162.3
CHO	n.a.	n.a.	n.a.	n.a.	n.a.	n.a.	n.a.	n.a.	n.a.	n.a.	n.a.	n.a.	n.a.
COOC	n.a.	–73.50	n.a.	533.6	660.2	n.a.	108.9	–209.7	54.47	808.7	n.a.	n.a.	162.7
CH_2O	n.a.	141.7	n.a.	n.a.	664.6	301.1	137.8	–154.3	n.a.	n.a.	95.18	n.a.	151.1
CNH_2	0.0	63.72	n.a.	n.a.	n.a.	n.a.	n.a.	n.a.	n.a.	68.81	n.a.	n.a.	n.a.
CNH	108.8	0.0	n.a.	n.a.	n.a.	n.a.	n.a.	n.a.	71.23	4350.0	n.a.	n.a.	n.a.
$ACNH_2$	n.a.	n.a.	0.0	n.a.	n.a.	n.a.	n.a.	n.a.	8455.0	n.a.	n.a.	–62.73	n.a.
CCN	n.a.	n.a.	n.a.	0.0	n.a.	n.a.	n.a.	–15.62	–54.86	n.a.	n.a.	n.a.	n.a.
COOH	n.a.	n.a.	n.a.	n.a.	0.0	44.42	–183.4	n.a.	212.7	n.a.	n.a.	n.a.	n.a.
CCl	n.a.	n.a.	n.a.	n.a.	326.4	0.0	108.3	249.2	62.42	n.a.	n.a.	n.a.	n.a.
CCl_2	n.a.	n.a.	n.a.	n.a.	1821.0	–84.53	0.0	0.0	56.33	n.a.	n.a.	n.a.	n.a.
CCl_3	n.a.	n.a.	n.a.	74.04	n.a.	–157.1	0.0	0.0	–30.10	n.a.	n.a.	n.a.	256.5
CCl_4	n.a.	91.13	1302.0	492.0	689.0	11.80	17.97	51.90	0.0	475.8	490.9	534.7	132.2
ACCl	203.5	–108.4	n.a.	n.a.	n.a.	n.a.	n.a.	n.a.	–255.4	0.0	–154.5	n.a.	n.a.
CNO_2	n.a.	n.a.	n.a.	n.a.	n.a.	n.a.	n.a.	n.a.	–34.68	794.4	0.0	n.a.	n.a.
$ACNO_2$	n.a.	n.a.	5250.0	n.a.	n.a.	n.a.	n.a.	n.a.	514.6	n.a.	n.a.	0.0	n.a.
CS_2	n.a.	n.a.	n.a.	n.a.	n.a.	n.a.	n.a.	–125.8	–60.71	n.a.	n.a.	n.a.	0.0

n.a. = not available

Reprinted with permission from (Fredenslund, A., Gmehling, J., Michelsen, M.L., Rasmussen, P., and Prausnitz, J.M. (1977). Computerized design of multicomponent distillation columns using the UNIFAC group contribution method for calculation of activity coefficients, *Ind. Eng. Chem. Process Des. Dev.*, 16, 450–462) American Chemical Society.

Group parameters R_k and Q_k are obtained from van der Waals group volumes V_{wk} and surface areas A_{wk}, given by Bondi (1968) as:

$$R_k = \frac{V_{wk}}{15.17} \qquad (8.58)$$

$$Q_k = \frac{A_{wk}}{2.5 \times 10^9} \qquad (8.59)$$

The numbers 15.17 and 2.5 $\times$ 10^9 are normalization factors. Values of R_k and Q_k are reported in Table 8.6, and that of a_{mk} are presented in Table 8.7.

The UNIQUAC method, which uses only molecular compositions, is faster than the UNIFAC method, which uses both molecular and group compositions. Tests for systems where experimental data are available show that activity coefficients calculated from the UNIQUAC model and estimated limiting activity coefficients are, on the average, as accurate as those calculated directly using the UNIFAC method.

8.2.7 The Hildebrand Model (Regular Solution) (developed by Hildebrand and Scott in 1950)

Liquid solutions of hydrocarbons are considered to be regular solutions in this correlation. The *regular solutions* are characterized by their excess entropy being equal to zero. Any nonideal behaviour is due entirely to the heat of solution. The expression for the Hildebrand model is:

$$\ln \gamma_i = \frac{V_i(\delta_i - \bar{\delta})^2}{RT} \qquad (8.60)$$

where

$$\bar{\delta} = \frac{\sum_{i=1}^{N} x_i V_i \delta_i}{\sum_{i=1}^{N} x_i V_i} \qquad (8.61)$$

The above model requires two parameters for each component. These are the solubility parameter δ_i and liquid molar volume V_i. The quantity $\bar{\delta}$ designates an average value of the solubility parameter for the solution.

An important feature of this model is that it requires only pure component property data. The δ_i and V_i of the usually encountered components are given in Table 8.8. A number of these values were determined to fit experimental vapour–liquid equilibrium data. To obtain more accurate predictions, the liquid molar volume of a particular component can be considered as a function of temperature as defined in the equation given in the note below Table 8.2.

The Hildebrand Model performs well only within a restricted range of conditions. Chao and Seader (1961) have strictly recommended the following conditions within which a reasonable accuracy can be achieved by the employment of this regular solution model.

For Hydrocarbons (except methane)

Reduced temperature ($=T/T_{ci}$)*:* 0.5 to 1.3 based on the pure component critical temperature (T_{ci}).

Pressure: up to about 2000 lb/in^2 abs. but not to exceed about 0.8 of the critical pressure of the system (P_c).

For Light Gases (hydrogen and methane)

Temperature: from –100°F to about 0.93 in pseudoreduced temperature of the equilibrium liquid mixture but not to exceed 500°F. The pseudoreduced temperature is based on the molal average of the critical temperatures of the components.

Pressure: up to about 8000 lb/in^2 abs.

Concentration: up to about 20 mole% of other dissolved gases in the liquid.

Table 8.8 Solubility parameters and liquid molar volumes (see Table 8.2) for the Hildebrand model

For Paraffins		
Component, i	δ_i (cal/cc)$^{0.5}$	V_i (cc/gmol)
Methane	5.680	52.0
Ethane	6.050	68.0
Propane	6.400	84.0
iso-Butane	6.730	105.5
n-Butane	6.730	101.4
iso-Pentane	7.020	117.4
n-Pentane	7.020	116.1
neo-Pentane	7.020	123.3
n-Hexane	7.270	131.6
n-Heptane	7.430	147.5
n-Octane	7.551	163.5
n-Nonane	7.650	179.6
n-Decane	7.720	196.0
n-Undecane	7.790	212.2
n-Dodecane	7.840	228.6
n-Tridecane	7.890	244.9
n-Tetradecane	7.920	261.3
n-Pentadecane	7.960	277.8
n-Hexadecane	7.990	294.1
n-Heptadecane	8.030	310.4
For Olefins		
Component, i	δ_i (cal/cc)$^{0.5}$	V_i (cc/gmol)
Ethylene	6.080	61.0
Propylene	6.430	79.0
1-Butene	6.760	95.3
cis-2-Butene	6.760	91.2
trans-2-Butene	6.760	93.8
iso-Butene	6.760	95.4
1,3-Butadiene	6.940	88.0
1-Pentene	7.050	110.4
cis-2-Pentene	7.050	107.8
trans-2-Pentene	7.050	109.0
2-Methyl-1-Butene	7.050	108.7
3-Methyl-1-Butene	7.050	112.8
2-Methyl-2-Butene	7.050	106.7
1-Hexene	7.400	125.8
For Naphthenes		
Component, i	δ_i (cal/cc)$^{0.5}$	V_i (cc/gmol)
Cyclopentane	8.110	94.70
Methyl cyclopentane	7.850	113.10
Cyclohexane	8.200	108.70
Methyl cyclohexane	7.830	128.30

For Aromatics		
Component, i	δ_i (cal/cc)$^{0.5}$	V_i (cc/gmol)
Benzene	9.160	89.40
Toluene	8.920	106.80
o-Xylene	8.990	121.20
m-Xylene	8.820	123.50
p-Xylene	8.770	124.00
Ethyl benzene	8.790	123.10
For hydrogen $\delta = 3.25$ (cal/cc)$^{0.5}$; $V = 31.0$ cc/gmol		

Reprinted with permission from (Chao, K.C., and Seader, J.D. (1961). A general correlation of vapor–liquid equilibria in hydrocarbon mixtures, *AIChE J.*, 7, 598–605) American Institute of Chemical Engineers.

8.3 SUMMARY AND CONCLUSIONS

This chapter describes several activity coefficient models, such as the Margules, Van Laar, Wilson, NRTL, UNIQUAC, UNIFAC and Hildebrand equations, as a powerful tool for the chemical design engineers. For the accurate predictions of the properties of highly nonideal mixtures, it is really difficult to bypass the thermodynamic model.

In chemical engineering, distillation is an important unit operation. To develop a relatively rigorous simulator for binary to multicomponent distillation columns, an activity coefficient model is required to employ for liquid-phase nonideality predictions. Based on the real-time plant data, many researchers determined the interaction and structural parameters for the thermodynamic models. These parameters for several pure-components or mixtures are systematically reported in this chapter.

EXERCISES

8.1 How are the vapour-phase compositions calculated for a distillation column that fractionates an ideal mixture?

8.2 Derive the expressions for molar excess Gibbs free energy for binary systems from
(i) Equation (8.23) for the Wilson model
(ii) Equation (8.28) for the NRTL model
(iii) Equations (8.36), (8.37) and (8.38) for the UNIQUAC model.

8.3 What are the differences between the UNIQUAC and UNIFAC methods based on their advantages and disadvantages?

8.4 Consider a binary mixture of ethanol (E) and *n*-hexane (H), which is at 1 atm (101.3 kPa) pressure. The azeotrope occurs at $x_E = 0.332$, $x_H = 0.668$ and $T = 58°C$ (331.15 K). Now, estimate the activity coefficients at the azeotropic composition using the
(i) Wilson method
(ii) NRTL method
(iii) UNIFAC method.

8.5 The Van Laar constants for the system *n*-hexane (1)–benzene (2) at 71°C temperature are determined to be $\bar{A}_{12} = 0.6224$ and $\bar{A}_{21} = 0.2968$. Predict the Van Laar constants at 35°C temperature. The temperature dependence of the Van Laar constant may be expressed by:

$$\bar{A}_{ij} = \frac{A'_{ij}}{RT} \qquad (8.62)$$

where A_{ij} is in Btu/lb mol.

8.6 The Wilson constants for the ethanol (1)–benzene (2) system at 42°C are: $\Lambda_{12} = 0.121$ and $\Lambda_{21} = 0.520$. Using these constants and the Wilson equations, predict the liquid-phase activity coefficients for this binary system over the entire range of composition (x_1 = 0.05, 0.1, 0.25, 0.4, 0.55, 0.7, 0.85, 0.975).

8.7 At 50°C temperature, using the UNIFAC method, estimate the liquid-phase activity coefficients for 45 mole% liquid solutions of the following hydrocarbons in ethanol.

(i) *n*-butane
(ii) *n*-pentane
(iii) *n*-hexane
(iv) *n*-heptane
(v) *n*-octane.

8.8 Estimate the activity coefficients for the following binary systems employing the Hildebrand model when each system is at 35°C temperature and 1 atm pressure with compositions of $x_1 = 0.35$ and $x_2 = 0.65$.

(i) *n*-octane (1)–ethylbenzene (2)
(ii) toluene (1)–cyclohexane (2)
(iii) benzene (1)–cyclopentane (2).

8.9 Substitution of q_i and r_i equal to unity in Equation (8.47) yields a form of equation. At what conditions that form of equation is identical with the Wilson equation [Equation (8.26)]?

REFERENCES

Abrams, D.S., and Prausnitz, J.M. (1975). Statistical thermodynamics of liquid mixtures: a new expression for the excess Gibbs energy of partly or completely miscible systems, *AIChE J.*, 21, 116–128.

Bondi, A. (1968). *Physical Properties of Molecular Crystals, Liquids and Gases*, John Wiley & Sons, New York.

Carlson, H.C., and Colburn, A.P. (1942). Vapour–liquid equilibria of nonideal solutions: utilization of theoretical methods to extend data, *Industrial and Engineering Chemistry*, 34, 581–589.

Chao, K.C., and Seader, J.D. (1961). A general correlation of vapour–liquid equilibria in hydrocarbon mixtures, *AIChE J.*, 7, 598–605.

Fredenslund, A., Jones, R.L., and Prausnitz, J.M. (1975). Group contribution estimation of activity coefficients in nonideal liquid mixtures, *AIChE J.*, 21, 1086–1099.

Hildebrand, J.H., and Scott, R.L. (1950). *The Solubility of Nonelectrolytes*, 3rd ed., Reinhold, New York.

Margules, S. (1895). math.-naturw. K. Kaiserlichen Akad. Wiss. (Vienna), 104, 1243.

Null, H.R. (1970). *Phase Equilibrium in Process Design*, Interscience Publishers, Inc., New York.

Renon, H. and Prausnitz, J.M. (1968). Local compositions in thermodynamic excess functions for liquid mixtures, *AIChE J.*, 14, 135–144.

Van Laar, J.J. (1913). Zur Theorie der Dampfspannugen, von binaren Gemishen, *Z. Phys. Chem.*, 83, 599–608.

Wilson, G.M. (1964). Vapour–liquid equilibrium. XI. a new expression for the excess free energy of mixing, *J. Amer. Chem. Soc.*, 86, 127–130.

Wohl, K. (1946). *Trans. AIChE*, 42, 215–249.

Wohl, K. (1953). Thermodynamic evaluation of binary and ternary liquid systems, *Chem. Eng. Progr.,* 49, 218–219.

9

Binary Batch Distillation Column

9.1 INTRODUCTION

Distillation processes are among the most important technologies for the separation of a mixture. Distillation can be done either in a continuous operation regime (where the mixture is continuously supplied and the products are continuously let off) or in a discontinuous regime–the so-called batch distillation process (where the apparatus is loaded with the mixture at start-up time and the different fractions are taken out one by one).

Batch distillation is widely used in the fine chemistry, pharmaceutical, biochemical and food industries, especially those related to the production of fine materials with high added value. This is due to the low-scale production, rapid change in market needs and the flexibility in purifying different mixtures under a variety of operational conditions. A single batch column can separate a multicomponent mixture into several products within a single operation; conversely, if the separation were carried out continuously, either a train of columns or a multi-pass operation would be required. In comparison to continuous distillation, batch distillation processes are more flexible and economically attractive for equipment reduction.

The batch operation is conveniently described by dividing into two periods: the start-up period and the production period. The production period is that part of the process operation during which the product is withdrawn from the column. Necessary adjustments to bring the column to an operating condition that produces a distillate with a desired purity are made in the start-up period.

Traditionally, a batch distillation column can be operated in three different ways: constant reflux ratio, constant distillate composition and optimal operation. Usually, the batch process is allowed to approach the steady state first and then the withdrawal of distillate product is started. To achieve the steady state, the distillation is run in the start-up phase at *total reflux* condition. In this situation, all the overhead vapours are condensed and accumulated in the condenser–reflux drum system. Then the condensed liquid completely returns to the column as reflux and subsequently the steady state is reached as no distillate product is removed. Batch distillation operated at total reflux may be considered as another mode of operation in addition to the three ways as mentioned above. Therefore, the four different modes are: total reflux, constant reflux ratio, constant distillate composition and optimal operation. Notice that the total reflux mode of operation is carried out in the start-up phase and the other three modes are used in production period.

Batch distillation operated at a *constant reflux* condition is an unsteady state operation. Actually, in this case, the reflux ratio (or the reflux rate) is kept constant throughout the distillation, which results in a continuously changing distillate composition. This is inherently an open-loop strategy and the average product composition is known at the end of the batch. Therefore, if an off-specification product were obtained, the batch would have to be blended or rerun, with a significant financial loss.

Constant-distillate-composition operation is more difficult. In fact, to keep the distillate composition to the desired value throughout the whole batch, we need to continuously adjust the reflux rate. On the other hand, the product composition can be controlled accurately during batch production, i.e., this mode is inherently a feedback operation.

Another operating mode, *optimal operation*, has gained attention in recent years, and it is determined by maximizing off-line a prespecified profit function (Sorensen, Macchietto, Stuart and Skogestad, 1996). This operating procedure often results in a piecewise constant-reflux-ratio operation, and is normally implemented in an open-loop fashion. Therefore, the drawbacks of optimal operation are somewhat similar to those of constant reflux operation. In fact, the closed-loop implementation of open-loop optimal profiles is still an open issue for research, at least from a control standpoint (Edgar, 1996).

In this chapter, initially we will know the start-up operation of a batch distillation column. The detailed development of modelling equations for a binary batch column will be discussed next. We will carry out the computer simulation of the developed process model. The simulator to be developed in this chapter may be employed to prevail the steady state under total reflux mode. For other three modes of batch operation as mentioned above, we can also use this simulator as a reference distillation process. Finally, the concept and development of the software sensor are presented.

9.2 FEATURES OF BATCH DISTILLATION COLUMN

The essential features (Mujtaba and Macchietto, 1997) of a batch distillation unit (Figure 9.1) are described as follows:

(a) A bottom receiver/reboiler/still pot which is charged with the feed to be processed and which provides the heat transfer surface.

(b) A rectifying column (either a tray or packed column) superimposed on the reboiler, coupled with either a total condenser or a partial condenser system.

(c) A series of product accumulator tanks connected to the product streams to collect the main and or the intermediate distillate fractions.

Operation of such a distillation column involves performing the fractionation until a desired amount has been distilled off. The overhead composition varies during the operation and usually a number of cuts are made (for multicomponent systems). Some of the cuts are desired products while others are intermediate fractions that can be recycled to subsequent batches to obtain further separation. A residual bottom fraction may or may not be recovered as product.

9.3 START-UP PROCEDURE OF A BATCH COLUMN

Previously, the start-up operation is explained in a few words. Here, we will know the sequential steps through which the start-up operation (Sorensen, 1994) of a batch column, packed or tray, usually proceeds.

Step 1: The liquid feed is initially charged to the reboiler or still pot. Heat is introduced in the still for bringing the material to its boiling point temperature.

Step 2: Boiling starts and the produced vapour goes up through the column. Some of the vapour condenses inside the column section.

Step 3: The condenser begins its operation as the vapour reaches the top tray and the reflux drum starts to fill up.

Step 4: When the reflux drum is filled up, the reflux valve is opened and normally, the operation at total reflux starts. However, some product may also be taken out at this point with a given reflux flow instead.

Step 5: The liquid holdup in the top tray starts to increase. The column is gradually filled up from the top and down.

Step 6: The column is then operated under total reflux operation until the distillation unit is taken to a steady state or to a state where the distillate purity reaches the desired product composition.

9.3.1 Simulation Procedures for the Initial Filling

In the above, the six sequential steps in the start-up of a batch distillation are explained. These steps in simulations are usually approximated by supposing that the trays and the reflux drum are initially filled up according to some filling procedures (Sorensen, 1994) described in the following:

Procedure 1: Initially, the feed charge is distributed in the reflux drum, on the trays and in the still. The reflux drum and tray liquid holdups are constant, and the initial compositions are equal to the total reflux compositions (Steps 2–6 negligible).

Procedure 2: The feed charge is initially distributed in the reflux accumulator, on the trays and in the still. The accumulator and tray liquid holdups are constant and all compositions are initially equal to the feed composition.

Procedure 3: The column section and reflux drum are initially empty, and all the feed is in the still. The vapour from the still is condensed and stored in the overhead equipment until liquid first fills the reflux drum and then the column trays. This is equivalent to operating the unit without reflux, i.e., with only one theoretical rectification stage. As soon as the drum is filled up, the trays are filled from the top and down. After a tray has been filled, its liquid holdup is assumed constant.

Procedure 4: Same as Procedure 3 but it is supposed that some of the vapour is condensed on the trays before reaching the reflux accumulator. The trays are then filled up from the top and down.

In this book, we will follow the simulation Procedure 2 for initial filling in the batch distillation columns.

9.4 AN EXAMPLE PROCESS AND THE MODEL

In the sample batch distillation shown in Figure 9.1, a liquid mixture is charged into a vessel (still pot) and heat is added to produce vapour that is fed into a rectifying column. Then the vapours rise up the column becoming enriched in the more volatile (or lightest) component. Before starting up the batch operation, as mentioned, the reflux drum, column trays and still-pot are all initially filled with a material of composition x_{B0} (liquid composition of feed at the beginning).

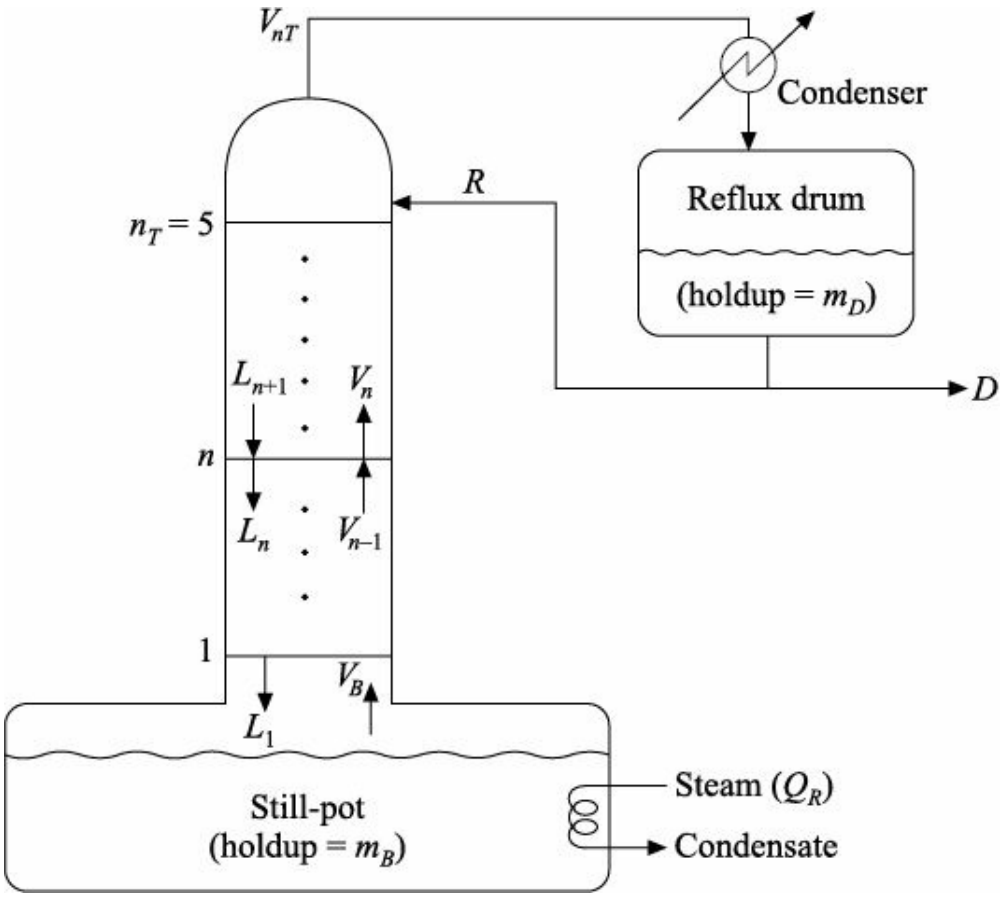

FIGURE 9.1 Schematic representation of the example of batch distillation column.

During the initial start-up period, the sample column operates under total reflux condition in which vapour from the top of the column is condensed and returned to the column. This condition is continued until the process approaches the steady state. After reaching steady state, the production phase may start, i.e., the distillate is withdrawn as a product stream. Now several simulation experiments in open-loop or closed-loop fashion can be performed. Note at this point that it is not compulsory to achieve the steady state condition before withdrawal of the first product. Actually, the distillate product withdrawal is begun when the composition of the lightest component in the distillate reaches its specified purity level.

In order to represent realistic operation of actual batch distillation column, a rigorous nonlinear model is attempted to develop from the first principles involving dynamic material and energy balances, and algebraic enthalpy and tray hydraulic equations supported by vapour–liquid equilibrium (VLE) and physical properties. The batch distillation dynamics simulator has major computation functions like composition, flow rate, tray holdup, enthalpy, average molecular weight and density, and VLE calculations.

To predict the column behaviour, we are intended to develop a rigorous batch distillation simulator. The simulated column separates a highly nonideal ethanol–water mixture. In this alcoholic mixture, ethanol is more volatile component (subscript 1 used for ethanol) and naturally, water is relatively less volatile component (subscript 2 used for water). The start-up conditions and system specifications are reported in Table 9.1.

Table 9.1 Model and system characteristics

Binary system (*ethanol–water*)	
Total feed charge, gmol	10000.0
Feed composition (startup), mole fraction (ethanol–water)	0.3/0.7
Tray holdup (start-up), gmol	30.0
Reflux drum holdup, gmol	1000.0
Heat input to the still, kJ/min	5000.0

Distillate flow rate (production phase), gmol/min	50.0
Distillate composition (steady state), mole fraction	0.8/0.2
Column diameter, cm	125.0
Integration time interval, min	0.005

The main assumptions adopted for the dynamic model development are as follows:

- Staged batch distillation column with trays numbered from the bottom and up (total six trays including still-pot).
- Perfect mixing and equilibrium (thermal) on all trays.
- Atmospheric pressure operation and constant tray efficiency (vapour-phase Murphree efficiency = 80%).
- Negligible vapour holdup.
- Algebraic enthalpy equations.
- Total condensation with no subcooling in the condenser.
- Negligible coolant dynamics in the condenser and steam dynamics in the reboiler.
- Francis weir formula for tray hydraulics calculations.
- Variation of liquid holdup in each tray excluding reflux drum. (Until the steady state condition is prevailed, the reflux drum holdup is assumed constant at total reflux provision. In the production phase, the liquid holdup in reflux drum of most of the industrial-scale columns is perfectly controlled such that the holdup variations are negligibly small.)
- Wilson thermodynamic model (details in Chapter 8) for VLE calculations.

9.4.1 Material and Energy Balance Equations

The balance differential equations are given in the following for different trays including reflux-drum and reboiler.

Reboiler (subscript '*B*')

Total continuity: $$\dot{m}_B = L_1 - V_B = -D \tag{9.1}$$

Component continuity: $$\dot{m}_B \dot{x}_B = L_1 x_1 - V_B y_B \tag{9.2}$$

Energy equation: $$\dot{m}_B \dot{H}_B^L = Q_R + L_1 H_1^L - V_B H_B^V \tag{9.3}$$

Bottom Tray (subscript '1')

Total continuity: $$\dot{m}_1 = L_2 + V_B - L_1 - V_1 \tag{9.4}$$

Component continuity: $$\dot{m}_1 \dot{x}_1 = L_2 x_2 + V_B y_B - L_1 x_1 - V_1 y_1 \tag{9.5}$$

Energy equation: $$\dot{m}_1 \dot{H}_1^L = L_2 H_2^L + V_B H_B^V - L_1 H_1^L - V_1 H_1^V \tag{9.6}$$

Intermediate Trays (subscript '*n*', where *n* = 2 to 4)

Total continuity: $$\dot{m}_n = L_{n+1} + V_{n-1} - L_n - V_n \tag{9.7}$$

Component continuity: $$\dot{m}_n \dot{x}_n = L_{n+1} x_{n+1} + V_{n-1} y_{n-1} - L_n x_n - V_n y_n \tag{9.8}$$

Energy equation: $$\dot{m}_n \dot{H}_n^L = L_{n+1} H_{n+1}^L + V_{n-1} H_{n-1}^V - L_n H_n^L - V_n H_n^V \tag{9.9}$$

Top Tray (subscript 'n_T')

Total continuity: $$\dot{m}_{n_T} = R + V_{n_T-1} - L_{n_T} - V_{n_T} \tag{9.10}$$

Component continuity: $$\dot{m}_{n_T}\dot{x}_{n_T} = Rx_D + V_{n_T-1}y_{n_T-1} - L_{n_T}x_{n_T} - V_{n_T}y_{n_T} \quad (9.11)$$

Energy equation: $$\dot{m}_{n_T}\dot{H}^L_{n_T} = RH^L_D + V_{n_T-1}H^V_{n_T-1} - L_{n_T}H^L_{n_T} - V_{n_T}H^V_{n_T} \quad (9.12)$$

Condenser and Reflux Drum (subscript '*D*')

Total continuity: $$\dot{m}_D = V_{n_T} - R - D \quad (9.13)$$

Component continuity: $$\dot{m}_D\dot{x}_D = V_{n_T}y_{n_T} - (R+D)x_D \quad (9.14)$$

In the above model, x_n is the mole fraction (or composition) of the more volatile component (here ethanol) in a liquid stream leaving *n*th tray, y_n the mole fraction of ethanol in a vapour stream leaving *n*th tray, x_D the mole fraction of ethanol in the liquid distillate, x_B the mole fraction of ethanol in the liquid of the still-pot, L_n the liquid flow rate leaving *n*th tray (gmol/min), V_n the vapour flow rate leaving *n*th tray (gmol/min), R the reflux flow rate (gmol/min), D the distillate flow rate (gmol/min), V_B the vapour boil-up rate (gmol/min), m_n the liquid holdup on *n*th tray (gmol), m_D the liquid holdup in the reflux drum (gmol), m_B the liquid holdup in the still-pot (gmol), H^L_D the enthalpy of distillate (J/gmol), H^L_n the enthalpy of a liquid stream leaving *n*th tray (J/gmol), H^V_n the enthalpy of a vapour stream leaving *n*th tray (J/gmol) and Q_R the heat input to the still-pot (J/min). The dot symbol (.) represents the time derivative. Again, the time derivative of the multiplication of two variables, say *m* and *x*, is denoted here by $\dot{mx}$.

Several numerical techniques (for example, Euler method, fourth order Runge–Kutta method, etc.) are used (details in Chapter 2) to integrate the differential modelling equations. It is important to mention here that the dynamics of internal energies are much faster than that of composition or total holdup on each tray. Therefore, the above energy balance equations are transformed into an algebraic system by substituting zero in the left hand sides of the energy equations. The transformed equations are then employed to calculate the vapour flow rates.

To explain the vapour flow rate calculations in detail, let us consider a case of the reboiler. Assuming right hand side of Equation (9.3) equal to zero and rearranging, we finally get

$$V_B = \frac{Q_R + L_1H^L_1}{H^V_B} \quad (9.15)$$

Similarly, the vapour flow rates for other trays can be calculated based on the concept as described above. Since no vapour flow rate calculation is required for the condenser–reflux drum system, it is unnecessary to formulate the energy balance equation for that system.

At this moment, obviously one question arises: if the balance differential energy equations are used for vapour flow rate calculations, how the liquid and vapour phase enthalpies are estimated? The phase enthalpies are actually estimated from the algebraic form of equations. The enthalpy calculations are discussed in detail in Subsection 9.4.2.

The development of the batch distillation column model is not completed so far. In the subsequent subsections, we will study different algebraic model equations. Actually, these algebraic equations provide some time-dependent data that are required for the numerical solution of the differential modelling equations of the specified batch rectifier [Equations (9.1)–(9.14)].

9.4.2 Enthalpy Calculations

It is very convenient to represent the liquid and ideal gas enthalpy data by analytical equations. In brief, the enthalpy computations are shown in the present subsection. For more details, the reader should refer to Reid, Prausnitz and Sherwood (1977), and Passut and Danner (1972).

For the ethanol–water system, the following algebraic enthalpy equations can be used:

For liquid: $$H^L = a + bT + cT^2 \quad (9.16)$$

For ideal gas: $$H^V = A + BT + CT^2 + DT^3 + ET^4 \quad (9.17)$$

where T is the temperature at which the enthalpies are to be calculated. It should be recognized that Equations (9.16) and (9.17) include the pure component enthalpies as a function of temperature only. The coefficients a, b, c and A, B, C, D, E for different pure components are available in Tables 9.2 (Holland, 1981) and 9.3 (Holland, 1981) respectively. The Fortran (90) codes for the computations of liquid and vapour enthalpies in the batch distillation simulator are given in Programs 9.1 and 9.2 respectively.

Table 9.2 Coefficients for liquid enthalpy (temperature in °R and enthalpy in Btu/lbmol)

Component (formula)	*a*	*b*	*c*
Acetone (C_3H_6O)	–0.115334E + 5	0.1770348E + 2	0.1166435E – 1
Benzene (C_6H_6)	–0.1048661E + 5	0.1197147E + 2	0.1898900E – 1
Chloroform ($CHCl_3$)	–0.1061259E + 5	0.1661526E + 2	0.1018617E – 1
Ethanol (C_2H_6O)	0.4046348E + 3	–0.2410286E + 2	0.4728230E – 1
Methanol (CH_4O)	–0.3119436E + 4	–0.4145198E + 1	0.2131106E – 1
Methyl acetate ($C_3H_6O_2$)	–0.1275019E + 5	0.1831477E + 2	0.1544864E – 1
Methyl cyclohexane (C_7H_{14})	–0.5748773E + 4	0.1415027E + 2	0.3715891E – 1
Phenol (C_6H_6O)	–0.2226400E + 5	0.4839999E + 2	0.0
Toluene (C_7H_8)	–0.5920285E + 4	0.1550792E + 2	0.2143342E – 1
Water (H_2O)	–0.87838059E + 4	0.1758450E + 2	0.3651369E – 3

Table 9.3 Coefficients for ideal gas enthalpy (temperature in °R and enthalpy in Btu/lbmol)

Component (formula)	*A*	*B*	*C*	*D*	*E*
Acetone (C_3H_6O)	0.867332E+4	0.4735799E+1	0.1452860E–1	–0.1121397E–5	–0.2018173E–9
Benzene (C_6H_6)	0.1266990E+5	–0.8743198E+1	0.3191165E–1	–0.7611106E–5	0.7677461E–9
Chloroform ($CHCl_3$)	0.8893305E+4	0.5674799E+1	0.1125665E–1	–0.3292178E–5	0.3790719E–9
Ethanol (C_2H_6O)	0.106486E+5	0.7515997E+1	0.1151360E–1	–0.1682096E–5	0.9036333E–10
Methanol (CH_4O)	0.1174119E+5	0.7121495E+1	0.5579442E–2	–0.4506170E–6	–0.2091904E–10
Methyl acetate ($C_3H_6O_2$)	0.8855164E+4	0.3952399E+1	0.1489360E–1	–0.1066871E–5	–0.2983536E–9
Methylcyclohexane (C_7H_{14})	0.1805154E+5	–1.072998E+0	0.3568761E–1	0.0	0.0
Phenol (C_6H_6O)	–0.400000E+1	0.4839999E+2	0.0	0.0	0.0
Toluene (C_7H_8)	0.1628525E+5	0.6948364E+1	0.1784207E–1	0.0	0.0
Water (H_2O)	0.1545871E+5	0.8022526E+1	–0.4745722E–3	0.6878047E–6	–0.1439752E–9

PROGRAM 9.1 *Computer Program* (*subroutine*) *for Liquid Enthalpy*

```
! Inputs: T (degree C), X (mole fraction)
! Output: HL (J/gmol)
! a, b, c = Coefficients in Equation (9.16)
! HL = Liquid enthalpy
! NC = Number of components
! T = Stage temperature
! TR = Stage temperature in degree R
! X = Liquid-phase mole fraction

SUBROUTINE ENTLIQ(T,X,HL)
IMPLICIT NONE
REAL*8,INTENT(IN)::T,X
REAL*8,INTENT(OUT)::HL
INTEGER,PARAMETER::NC=2
REAL*8,DIMENSION(NC)::a,b,c
REAL*8::TR,ENTL1,ENTL2

!——Initialization——! '1' used for ethanol and '2' for water

a(1)=0.4046348 D+3
a(2)=-0.87838059 D+4

b(1)=-0.2410286 D+2
b(2)=0.175845 D+2

c(1)=0.472823 D-1
c(2)=0.3651369 D-3

TR=(1.8*T)+492.0
ENTL1=a(1)+b(1)*TR+c(1)*TR*TR                                    !Btu/lbmol
ENTL2=a(2)+b(2)*TR+c(2)*TR*TR                                    !Btu/lbmol
HL=(ENTL1*X+ENTL2*(1-X))*2.326            !1 Btu/lbmol = 2.326 J/gmol
RETURN

END SUBROUTINE ENTLIQ
```

PROGRAM 9.2 *Computer Program* (*subroutine*) *for Vapour Enthalpy*

```
! Inputs: T (degree C), Y (mole fraction)
! Output: HV (J/gmol)
! E1, E2, E3, E4, E5 = Coefficients in Equation (9.17) (in place of ! A, B, C, D, E)
! HV = Vapour enthalpy
! T = Stage temperature
! TR = Stage temperature in degree R
! Y = Vapour-phase mole fraction

SUBROUTINE ENTVAP(T,Y,HV)
IMPLICIT NONE
REAL*8,INTENT(IN)::T,Y
REAL*8,INTENT(OUT)::HV
INTEGER,PARAMETER::NC=2
REAL*8,DIMENSION(NC)::E1,E2,E3,E4,E5
REAL*8::TR,ENTV1,ENTV2

!——Initialization——!          '1' used for ethanol and '2' for water

E1(1)=0.106486 D+5
E1(2)=0.1545871 D+5

E2(1)=7.515997 D0
E2(2)=8.022526 D0
```

```
E3(1)=0.115136 D-1
E3(2)=-0.4745722 D-3

E4(1)=-0.1682096 D-5
E4(2)=0.6878047 D-6

E5(1)=0.9036333 D-10
E5(2)=-0.1439752 D-9
TR=(1.8*T)+492.0
ENTV1=E1(1)+E2(1)*TR+E3(1)*TR*TR+E4(1)*(TR**3)+E5(1)*(TR**4)  !Btu/lbmol
ENTV2=E1(2)+E2(2)*TR+E3(2)*TR*TR+E4(2)*(TR**3)+E5(2)*(TR**4)  !Btu/lbmol
HV=(ENTV1*Y+ENTV2*(1-Y))*2.326 !J/gmol
RETURN

END SUBROUTINE ENTVAP
```

9.4.3 Tray Hydraulics

The flow rate of a liquid stream leaving a tray is usually computed using the Francis weir formula that has different forms. The details of tray hydraulics are available elsewhere (Treybal, 1980; Luyben, 1990; Baratti et al., 1995). For the example distillation column, the liquid hydraulics in a particular tray can be calculated solving the following form of Francis weir formula:

$$L = \frac{\text{DENSA} \times W_L \times 999 \left\{ \frac{183.2 \times m \times \text{MWA}}{\text{DENSA} \times \text{DCOL} \times \text{DCOL}} - \frac{W_H}{12} \right\}^{1.5}}{\text{MWA}} \tag{9.18}$$

where

DCOL = column diameter in inches

DENSA = average density of the liquid mixture on the tray in lb/ft^3

L = liquid flow rate in lbmol/h

MWA = average molecular weight of the liquid mixture on the tray in $lb_m/lbmol$

W_H = weir height in inches

W_L = weir length in inches

m = liquid holdup on the tray in lbmol

Note that the distillation column diameter, weir length and weir height can be varied from tray to tray although this fact is not common in practice. However, the values of these design parameters in the stripping section may be different from the values of those in the rectifying section. The Fortran (90) code for the computation of internal liquid flow rates in the batch distillation simulator is given in Program 9.3.

PROGRAM 9.3 *Computer Program* (*subroutine*) *for Tray Hydraulics*

```
! Notice that the unit of L in Equation (9.18) is lbmol/h, whereas ! that of L in the
! subroutine is gmol/min.

! Inputs: M (gmol), X (mole fraction), WH (cm), WL (cm), DCOL (cm)
! Output: L (gmol/min)
! DCOL = Column diameter
! L = Internal liquid flow rate
! M = Tray holdup
! WH = Weir height
! WL = Weir length
! X = Liquid-phase mole fraction
```

```
SUBROUTINE HYDRAU(M,X,L,WH,WL,DCOL)
IMPLICIT NONE
REAL*8,INTENT(IN)::M,X,WH,WL,DCOL
REAL*8,INTENT(OUT)::L
REAL*8::CONST,MWA,DENSA
REAL*8::DCOLs,WHs,WLs,Ms,Ls
CALL MWDENS(X,MWA,DENSA)
DCOLs=DCOL*0.3937                                    !1 cm = 0.3937 in
WHs=WH*0.3937
WLs=WL*0.3937
Ms=M*0.002204586                                !1 gmol = 0.002204586 lbmol
CONST=183.2*Ms*MWA/(DENSA*DCOLs*DCOLs)-WHs/12
IF(CONST .LE. 0.00)GO TO 10
Ls=DENSA*WLs*999*((183.2*Ms*MWA/(DENSA*DCOLs*DCOLs)-WHs/12)**1.5)
& /MWA
L=Ls*7.56                                        !1 lbmol/h = 7.56 gmol/min
RETURN
10 L=0.00 D0
RETURN

END SUBROUTINE HYDRAU
```

9.4.4 Murphree Vapour-phase Tray Efficiency

A Murphree vapour-phase tray efficiency (Treybal, 1980) will be used in the sample batch distillation column to describe the departure from phase equilibrium and can be defined as:

$$\eta_n = \frac{y_n - y_{n-1}}{y_n^* - y_{n-1}} \qquad (9.19)$$

where

y_n^* = composition of vapour in phase equilibrium with liquid on nth tray with composition x_n (or simply, equilibrium vapour composition on nth tray)

y_n = actual composition of vapour leaving nth tray

y_{n-1} = actual composition of vapour entering nth tray

η_n = Murphree vapour-phase efficiency on nth tray

9.4.5 Molecular Weight and Density of the Tray Liquid

The average molecular weight of a liquid mixture on a tray (MWA) is the sum of the fractional molecular weights (MW) of the constituent components (j) of the mixture. It can be computed for a distillation tray using the following equation:

$$\text{MWA} = \sum_{j=1}^{N_c} \text{MW}(j)\, x(j) \qquad (9.20)$$

where N_c is the total number of components present in the tray liquid.

Similarly, the average liquid density (DENSA) can be estimated from the following equation:

$$\text{DENSA} = \sum_{j=1}^{N_c} \text{DENS}(j)\, x(j) \qquad (9.21)$$

In the above equation, DENS denotes the liquid density of the individual component. It should be noted that the average molecular weight and density of a tray liquid are needed for the internal liquid flow rate calculations employing Equation (9.18). Moreover, these terms may also be utilized for tray holdup computations as discussed in Subsection 14.2.2 (Chapter 14). The Fortran (90) code to compute MWA and DENSA in the batch distillation simulator is given in Program 9.4.

PROGRAM 9.4 *Computer Program* (*subroutine*) *for Molecular Weight and Density*

```
! The outputs (average density and molecular weight) of the subroutine ! are in FPS unit
! because they will be used in the tray hydraulic Equation (9.18).
! Input: X1 (mole fraction)
! Outputs: MWA (lb_m/lbmol), DENSA (lb/ft^3)

SUBROUTINE MWDENS(X1,MWA,DENSA)
IMPLICIT NONE
REAL*8,INTENT(IN)::X1
REAL*8,INTENT(OUT)::MWA,DENSA
REAL*8::X2,MW1,MW2,DENS1,DENS2

!——Initialization——!          '1' used for ethanol and '2' for Water

MW1=46.0634 D0
MW2=18.0152 D0

DENS1=0.789*62.42587                          !1 g/cm^3 = 62.42587 lb/ft^3
DENS2=1.00*62.42587

X2=1-X1
MWA=(X1*MW1)+(X2*MW2)
DENSA=(X1*DENS1)+(X2*DENS2)

END SUBROUTINE MWDENS
```

9.4.6 Vapour–Liquid Equilibrium (VLE)

An essential ingredient in the design of distillation column is a knowledge of the vapour–liquid equilibria of the system to be separated. Because the cost and time involved in obtaining experimental equilibrium data increase rapidly with the number of components, the distillation practitioner has turned to thermodynamics in search of effective predictive methods. Many such methods are discussed in Chapter 8.

The *ideal equilibrium stage*, also known as the *theoretical stage* or *theoretical plate* or *ideal stage*, is one which has the exit phases/streams in thermodynamic equilibrium, each phase/stream being removed from the stage without entraining any of the other phase/stream. If the outgoing vapour and liquid streams are in thermal equilibrium (same temperature) but not in phase equilibrium, the tray efficiency is used to correlate the composition in the ideal phase with that in the actual phase as stated for vapour-phase in Subsection 9.4.4. Phase equilibrium exists when the chemical potential (function of temperature, pressure and phase composition) of each component in the liquid phase is the same with that in the vapour phase.

Vapour–liquid equilibrium refers to the relationship between the liquid and vapour compositions in each equilibrium stage. In general, the vapour composition as well as the stage temperature are determined by solving the bubble point correlations with known liquid composition and pressure. The bubble point temperature is the temperature at which a bubble of vapour is formed in a liquid solution. The composition of the bubble is different from the liquid and is richer in the more volatile component. Usually, the bubble point temperature is considered as the stage temperature of a distillation column.

Vapour composition and temperature in an equilibrium stage

Ideal mixtures: If the vapour and liquid both are in ideal state, the calculations of the vapour composition and stage temperature are very simple and straightforward. Now for the ideal case, we will study the useful equations that are involved in VLE predictions for a binary system.

Dalton's law (for ideal vapour-phase):

$$P_i = P_t y_i^* \qquad (9.22)$$

where P_t is the total pressure. For component i, P_i is the partial pressure and y_i^* is the equilibrium vapour composition.

Raoult's law (for ideal liquid-phase):

$$P_i = P_i^S x_i \qquad (9.23)$$

where P_i^S is the vapour pressure of pure component i. Liquids that obey Raoult's law are called *ideal*. Combining Equations (9.22) and (9.23), we have

$$P_i^S x_i = P_t y_i^* \qquad (9.24)$$

Next, we will know several possible ways by which the VLE can be predicted at ideal situation. Mainly based on the available information, we can choose a suitable approach. In the subsequent discussions, subscript '1' will be used for one constituent element and '2' for another constituent element of a binary mixture.

A. Calculation of vapour composition

Initially, we will consider two cases (Case 1 and Case 2) in which no calculation of temperature is involved; only vapour composition is computed. The equilibrium vapour composition of the constituent elements 1 and 2 (y_1^* and y_2^*) can be calculated by the following ways as per the availability of the coefficient.

Case 1

Problem statement:

Given: liquid composition (x_1), equilibrium coefficient (k_1)

Unknowns: vapour compositions (y_1^* and y_2^*)

Solution technique: y_1^* can be computed from the following correlation:

$$y_1^* = k_1 x_1 \qquad (9.25)$$

For a binary mixture,

$$y_2^* = 1 - y_1^* \qquad (9.26)$$

Case 2

Problem statement:

Given: liquid composition (x_1), relative volatility ($\neg\text{ا}12$)

Unknowns: vapour compositions (y_1^* and y_2^*)

Solution technique: y_1^* can directly be obtained using:

$$y_1^* = \frac{\alpha_{12} x_1}{1 + (\alpha_{12} - 1) x_1} \qquad (9.27)$$

Now, y_2^* can be calculated from Equation (9.26). Note that this approach (Case 2) is used in the dynamic simulation of a compartmental distillation model (Chapter 6) and of an ideal binary distillation model (Chapter 7).

B. Calculation of vapour composition and temperature

Problem statement:

Given: liquid composition (x_1), pressure (P_t)

Unknowns: vapour compositions (y_1^* and y_2^*), temperature (T)

Solution technique: In order to compute the unknowns, any iterative convergence technique (details in Chapter 2) is required to use. Here, the Newton–Raphson algorithm is outlined to determine the vapour compositions and temperature for the present problem.

The following computational steps are involved.

Step 1: Guess temperature T (say, at time step t).

Step 2: Calculate vapour pressures P_1^S and P_2^S. The vapour pressure solely depends on the stage temperature according to the following form of Antoine equation:

$$\ln P_i^S = A_i - \frac{B_i}{T + C_i} \qquad (9.28)$$

where A_i, B_i, and C_i are the Antoine constants for pure component i. The constants are reported for various components in Table 9.4.

Table 9.4 Antoine constants (vapour pressure in mm Hg and temperature in K)

Component (formula)	*Temp. range* (K)	*A*	*B*	*C*
Acetic acid ($C_2H_4O_2$)	290–430	16.8080	3405.57	–56.34
Acetone (C_3H_6O)	241–350	16.6513	2940.46	–35.93
Acetylene (C_2H_2)	194–202	16.3481	1637.14	–19.77
Acrylonitrile (C_3H_3N)	255–385	15.9253	2782.21	–51.15
Ammonia (NH_3)	179–261	16.9481	2132.50	–32.98
Benzene (C_6H_6)	280–377	15.9008	2788.51	–52.36
iso-Butane (C_4H_{10})	187–280	15.5381	2032.73	–33.15
n-Butane (C_4H_{10})	195–290	15.6782	2154.90	–34.42
1-Butene (C_4H_8)	190–295	15.7564	2132.42	–33.15
Carbon disulphide (CS_2)	228–342	15.9844	2690.85	–31.62
Carbon tetrachloride (CCl_4)	253–374	15.8742	2808.19	–45.99
Chloroform ($CHCl_3$)	260–370	15.9732	2696.79	–46.16
Cyclopentane (C_5H_{10})	230–345	15.8574	2588.48	–41.79
Cycloheptane (C_7H_{14})	330–435	15.7818	3066.05	–56.80
Cyclohexane (C_6H_{12})	280–380	15.7527	2766.63	–50.50
Ethane (C_2H_6)	130–199	15.6637	1511.42	–17.16
Ethylene (C_2H_4)	120–182	15.5368	1347.01	–18.15
Ethyl acetate ($C_4H_8O_2$)	260–385	16.1516	2790.50	–57.15
Ethyl alcohol (C_2H_6O)	270–369	18.5242	3578.91	–50.50

Ethyl amine (C_2H_7N)	215–316	17.0073	2618.73	–37.30
Ethyl bromide (C_2H_5Br)	226–333	15.9338	2511.68	–41.44
Formaldehyde (CH_2O)	185–271	16.4775	2204.13	–30.15
Glycerol ($C_3H_8O_3$)	440–600	17.2392	4487.04	–140.2
n-Heptane (C_7H_{16})	270–400	15.8737	2911.32	–56.51
n-Hexane (C_6H_{14})	245–370	15.8366	2697.55	–48.78
Methane (CH_4)	93–120	15.2243	597.84	–7.16
Methyl acetate ($C_3H_6O_2$)	245–360	16.1295	2601.92	–56.15
Methyl alcohol (CH_4O)	257–364	18.5875	3626.55	–34.29
Methyl amine (CH_5N)	212–311	17.2622	2484.83	–32.92
Methyl ethyl ketone (C_4H_8O)	257–376	16.5986	3150.42	–36.65
n-Octane (C_8H_{18})	292–425	15.9426	3120.29	–63.63
n-Pentane (C_5H_{12})	220–330	15.8333	2477.07	–39.94
Phenol (C_6H_6O)	345–481	16.4279	3490.89	–98.59
Propane (C_3H_8)	164–249	15.7260	1872.46	–25.16
Propylene (C_3H_6)	160–240	15.7027	1807.53	–26.15
1-Propanol (C_3H_8O)	285–400	17.5439	3166.38	–80.15
Sulphur dioxide (SO_2)	195–280	16.7680	2302.35	–35.97
Sulphur trioxide (SO_3)	290–332	20.8403	3995.70	–36.66
Toluene (C_7H_8)	280–410	16.0137	3096.52	–53.67
Vinyl chloride (C_2H_3Cl)	185–290	14.9601	1803.84	–43.15
Water (H_2O)	284–441	18.3036	3816.44	–46.13

Reprinted with permission from (Reid, R.C., Prausnitz, J.M., and Sherwood, T.K. (1977). *The Properties of Gases and Liquids*, 3rd ed., McGraw-Hill Book Company, New York) McGraw-Hill Companies.

Step 3: Compute equilibrium vapour compositions (y_1^* and y_2^*) using a form of Equation (9.24) as:

$$y_i^* = \frac{P_i^S x_i}{P_t} \qquad (9.29)$$

Step 4: Check whether the absolute value of $\left(\sum_{i=1}^{2} y_i^* - 1\right)$ ≤ tolerance limit (the range of 10^{-5} to 10^{-10} is adequate to achieve reasonable accuracy)? If yes, note down the temperature and vapour compositions and go to Step 7, otherwise go to next step.

Step 5: Let

$$F_t = \sum_{i=1}^{2} y_i^* - 1 = \sum_{i=1}^{2} \left[\frac{P_i^S x_i}{P_t} - 1\right] \qquad (9.30)$$

that means,

$$F_t = \sum_{i=1}^{2} \frac{x_i \exp\left(A_i - \dfrac{B_i}{T + C_i}\right)}{P_t} - 1 \qquad (9.31)$$

and then calculate the derivative of F_t with respect to temperature based on:

$$F_t' = \frac{dF_t}{dT} = \sum_{i=1}^{2} \frac{B_i y_i^*}{(T + C_i)^2} \qquad (9.32)$$

Step 6: Compute T for the next time step $t + 1$ using:

$$T_{t+1} = T_t - \frac{F_t}{F_t'} \qquad (9.33)$$

Next go to Step 2 to continue the iteration.

Step 7: Stop.

Nonideal mixtures: For a nonideal mixture, Equation (9.24) is modified to:

$$\gamma_i P_i^S x_i = P_t y_i^* \qquad (9.34)$$

This is sometimes called modified or extended Raoult's law. Here, γ_i is the liquid-phase activity coefficient of component i. This coefficient is incorporated within the k-value formulation to account for the nonideality, which is generally severe in the liquid phase even at low pressures (close to 1 atm). In general, it is assumed that the vapour phase is remained at ideal state in low pressure operations. Different useful models for activity coefficient predictions are given in details in Chapter 8.

We can notice one point that is obvious in Equation (9.34). Two main factors, which make the vapour and liquid compositions different at equilibrium, are: the pure component vapour pressure and the nonidealities in the liquid phase.

Problem statement:

Given: liquid composition (x_1), pressure (P_t)

Unknowns: vapour compositions (y_1^* and y_2^*), temperature (T)

Solution technique: The solution approach is very similar to the approach as presented previously for ideal mixtures; only the calculation of activity coefficient is included in the present technique. The following computational steps can be followed to solve this problem.

Step 1: Guess temperature T (say, at time step t).

Step 2: Calculate activity coefficients for both the components (1 and 2) using an activity coefficient model. Different coefficient models are: Margules, Van Laar, Wilson, NRTL, UNIQUAC, UNIFAC, Hildebrand equations, etc.

Step 3: Compute vapour pressures P_1^S and P_2^S employing Antoine Equation (9.28).

Step 4: Calculate equilibrium vapour compositions (y_1^* and y_2^*) from:

$$y_i^* = \frac{\gamma_i P_i^S x_i}{P_t} \qquad (9.35)$$

This equation, which is obtained with the rearrangement of Equation (9.34), is the same with Equation (8.6); only difference is in the notations used.

Step 5: Check whether the absolute value of $\left| \sum_{i=1}^{2} y_i^* - 1 \right|$ ≤ tolerance limit? If yes, note down the temperature and vapour compositions and go to Step 8, otherwise go to next step.

Step 6: Suppose

$$F_t = \sum_{i=1}^{2} y_i^* - 1$$

that means,

$$F_t = \sum_{i=1}^{2} \frac{\gamma_i x_i \exp\left(A_i - \dfrac{B_i}{T + C_i}\right)}{P_t} - 1 \qquad (9.36)$$

and then determine the temperature derivative as

$$F_t' = \frac{dF_t}{dT} = \sum_{i=1}^{2} \frac{B_i y_i^*}{(T + C_i)^2} \qquad \text{[from Equation (9.32)]}$$

Step 7: Compute T for the next time step $t + 1$ using Equation (9.33) and then go to Step 2 to repeat computations for the next time step.

Step 8: Stop.

For the prescribed batch distillation column, the above algorithm has been used to compute the equilibrium vapour compositions of the binary components and tray temperature. The liquid-phase activity coefficients have been predicted by the use of the Wilson thermodynamic model. In the example of batch rectifier, the Wilson parameters (Λ_{ij}) are assumed to be temperature independent and constant. The Fortran (90) code for the computations of vapour compositions and tray temperature in the batch distillation simulator is given in Program 9.5.

PROGRAM 9.5 *Computer Program* (*subroutine*) *for Equilibrium Vapour Compositions and Tray Temperature*

```
! Inputs: X1 (mole fraction), P (mm Hg)
! Outputs: T (°C), Y1 (mole fraction)
! A, B, C = Antoine constants
! G = Activity coefficient
! LAMDA = Wilson parameter
! NC = Number of components
! P = Stage pressure
! Ps = Vapour pressure in mm Hg
! T = Stage temperature
! X1, Y1 = Compositions of component 1 in liquid and vapour phase
! respectively
SUBROUTINE BUBBLEPOINT(T,X1,Y1,P)
IMPLICIT NONE
REAL*8,INTENT(IN)::X1,P
REAL*8,INTENT(OUT)::T,Y1
INTEGER,PARAMETER::NC=2
INTEGER::J,LOOP
REAL*8,DIMENSION(NC)::X,Y
REAL*8,DIMENSION(NC)::Ps,A,B,C,G
REAL*8::SUMY,PAR1,PAR2,PAR3,FSLOPE,F
REAL*8,PARAMETER::LAMDA12=0.20916399 D0,LAMDA21=0.82284181 D0
!———Initialization———!        '1' used for ethanol and '2' for water
!—Antoine Constants—!
A(1)=18.5242 D0
```

```
B(1)=3578.91 D0
C(1)=-50.50 D0
A(2)=18.3036 D0
B(2)=3816.44 D0
C(2)=-46.13 D0
X(1)=X1
X(2)=1-X1
LOOP=0
T=95.00
10 LOOP=LOOP+1
IF(LOOP .GT. 1000) GO TO 30   !maximum number of iterations = 1000
SUMY=0.00 D0
PAR1=(LAMDA12/(X(1)+LAMDA12*X(2)))-
& (LAMDA21/(X(2)+LAMDA21*X(1)))
PAR2=DLOG(X(1)+LAMDA12*X(2))
PAR3=DLOG(X(2)+LAMDA21*X(1))
G(1)=EXP(-PAR2+(X(2)*PAR1))
G(2)=EXP(-PAR3-(X(1)*PAR1))
DO 15 J=1,NC
Ps(J)=EXP(A(J)-(B(J)/(T+273+C(J))))
Y(J)=Ps(J)*G(J)*X(J)/P
15 SUMY=SUMY+Y(J)
IF(ABS(SUMY-1) .LT. 0.0000001)RETURN        !tolerance limit =1.0E-7
F=SUMY-1
FSLOPE=0.0 D0
DO 20 J=1,NC
20 FSLOPE=FSLOPE+((Y(J)*B(J))/((T+273+C(J))**2))
T=T-F/FSLOPE
Y1=Y(1)
GO TO 10
30 STOP
END SUBROUTINE BUBBLEPOINT
```

9.5 SOFTWARE SENSOR

9.5.1 What Is Software Sensor?

A software sensor, in brief a soft-sensor, can be defined as the association between an estimator (software) and a sensor (hardware). The estimator is an algorithm based on the dynamic process model and is employed to compute the unmeasured state from the online measurement of secondary variable using the sensor.

9.5.2 Why Is It Required?

In many practical situations, the online measurement of a controlled output (primary measurement) is not advantageous and therefore the issue of controlled variable estimation arises. In such a case, a suitable secondary variable is attempted to measure using the sensor. By using this auxiliary measurement information, the estimation algorithm computes the controlled output. This concept is demonstrated in Figure 9.2. It is worthy to point out at this moment that for computing a single controlled output, the use of more than one secondary measurement is also recommended for improved estimation.

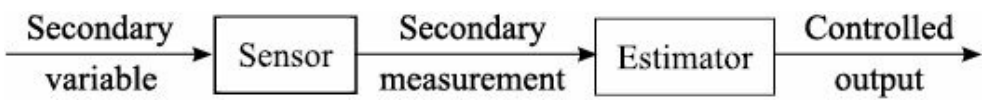

FIGURE 9.2 A soft-sensor.

9.5.3 Development of Soft-Sensor for Distillation Column

The online measurement of product compositions of a distillation column is not advantageous. It is because most product analyzers, like gas chromatographs, provide large delays in the response and high investment and maintenance costs. To tackle this problem, a soft-sensor based on measured temperature can be employed. It is true that the temperature measurement is reliable and inexpensive and has negligible measurement delays. As described in Figure 9.3, the measured tray temperature value, obtained using a thermocouple (say), is used in the temperature–composition (T–x) correlation (estimator) to infer the liquid composition (mole fraction). In the following, we discuss the derivation of T–x correlation with two different examples.

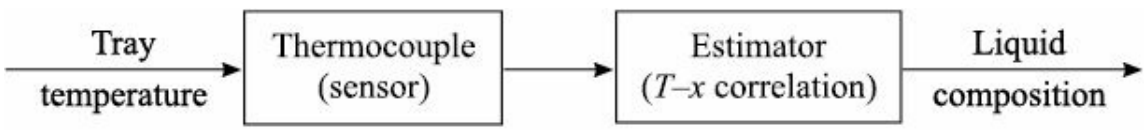

FIGURE 9.3 A soft-sensor for a distillation column.

Example 1: *T–x correlation for the binary systems*

Consider a typical distillation tray containing a liquid of composition x and temperature T. The pressure throughout the binary column is assumed constant and that is denoted by P_t. In this problem, T is a measurable quantity and we wish to estimate x. For this, we need to derive the T–x correlation.

The vapour-phase composition in equilibrium with the liquid-phase is given for the first component (subscript 1) by:

$$y_1^* = k_1(x_1, T, P_t)x_1 \qquad (9.37)$$

Similarly, we can write for the second component (subscript 2) as:

$$1 - y_1^* = k_2(x_2, T, P_t)(1 - x_1) \qquad (9.38)$$

Considering liquid-phase nonideality, the equilibrium coefficients get the following forms from Equation (9.35):

$$k_1 = \left[\frac{\gamma_1 P_1^S(T)}{P_t}\right] \qquad (9.39a)$$

$$k_2 = \left[\frac{\gamma_2 P_2^S(T)}{P_t}\right] \qquad (9.39b)$$

It is obvious from Equations (9.39a) and (9.39b) that the equilibrium coefficient, k, is dependent on x, T and P_t. Therefore, sometimes k is written in the form of $k(x, T, P_t)$. Recall that the Antoine equation [Equation (9.28)] correlates the component (i) vapour-pressure, P_i^S, with temperature.

By summing up Equations (9.37) and (9.38), we obtain

$$1 = k_1x_1 + k_2(1 - x_1) \qquad (9.40)$$

Substituting k_1 and k_2 from Equations (9.39a) and (9.39b) into Equation (9.40) and after rearrangement the following temperature–composition correlation is obtained:

$$x_1 = \frac{P_t - \gamma_2 P_2^S}{\gamma_1 P_1^S - \gamma_2 P_2^S} \qquad (9.41)$$

Now we will consider two cases in the following discussion.

Case 1: Consider the Wilson model, for example, for describing the activity coefficient in Equation (9.41). Accordingly, the calculation of x from Equation (9.41) can be carried out by using an iterative technique because the activity coefficient is a function of liquid composition and temperature.

Case 2: For an ideal case, $\gamma_1 = \gamma_2 = 1$. Accordingly, Equation (9.41) yields

$$x_1 = \frac{P_t - P_2^S}{P_1^S - P_2^S} \qquad (9.42)$$

Since the tray temperature is a measured quantity and the pressure, P_t, is defined, it is straightforward to compute x from Equation (9.42).

Example 2: *T–x correlation for the multicomponent systems*

Let us consider a multicomponent system having N_C number of components. Unlike the previous example, here we wish to derive the T–x correlation aiming to estimate tray temperature T based on measured liquid composition x for an ideal mixture.

The equations used to compute the temperature on any tray are as follows:

$$P_i^S = P_t \frac{y_i^*}{x_i} \qquad \text{[from Equation (9.24)]}$$

$$\frac{y_i^*}{x_i} = \frac{\alpha_{ij}}{\sum_{i=1}^{N_C} \alpha_{ij} x_i} \qquad \text{[from Equation (6.13)]}$$

$$\ln P_i^S = A_i - \frac{B_i}{T + C_i} \qquad \text{[from Equation (9.28)]}$$

Recall that α_{ij} is the relative volatility of any component i with reference to jth component. Combining the above three equations and simplifying, we obtain

$$T = \frac{B_i}{A_i - \ln\left(P_t \alpha_{ij} \Big/ \sum_{i=1}^{N_C} \alpha_{ij} x_i \right)} - C_i \qquad (9.43)$$

This is the final form of the T–x correlation for an ideal multicomponent system.

9.6 SUMMARY AND CONCLUSIONS

This chapter discusses the start-up operation, mathematical modelling and dynamic simulation of a practical binary batch distillation column. The formulation of the soft-sensor is also covered. In the present case study, the number of trays in the column is six including still pot. Indeed, it is very easy to

increase the number of trays in the process model as per the requirements. The higher the number of trays, the better the separation that can be achieved.

All required computations to solve the modelling Equations (9.1)–(9.14) of the sample batch rectifier are shown with detailed computer programming (subroutine). Now, you need to write a *main program* that can use the subroutines for solving the balance differential equations along with the related algebraic equations. For this task, you can follow the computer program (main program) that is given in Chapter 10 for a binary continuous distillation column; only the following concepts have to be implemented for the batch column:

- No stream is withdrawn as bottom product (i.e., $B = 0$, where B is the bottoms flow rate).
- There no feed plate exists (i.e., $F = x_F = T_F = H_F = 0$, where F is the feed flow rate, x_F the feed composition, T_F the feed temperature and H_F the feed enthalpy).
- In the start-up phase, consider that there is no distillate product flow rate (total reflux condition), i.e., $D = 0$. At production phase, distillate is removed with a desired amount from the reflux drum.

EXERCISES

9.1 Which model can provide sufficiently accurate predictions of activity coefficient for the nonideal batch distillation column that is prescribed in this chapter? Give the answer considering the mathematical complexity and computational load.

9.2 Why is the example batch distillation column a nonideal one? What changes are required to make it an ideal column?

9.3 To run the prescribed batch column in closed-loop fashion, we need to select the suitable control configurations. Mention the controlled variables and the corresponding manipulated variables.

9.4 At what situations is the batch distillation operation usually preferred over the continuous distillation operation for the separation of a mixture?

9.5 In this chapter, the liquid hydraulics in a tray are computed using the Francis weir formula [Equation (9.18)]. Convert this hydraulic equation for the tray liquid to CGS as well as SI unit.

9.6 In the computations of vapour–liquid equilibrium, an initial value of the stage temperature is required to guess. Is the convergence affected by the choice of the initial value? If yes, how?

9.7 Consider the separation of a nonideal mixture. Discuss the computational steps that are involved in the calculations of equilibrium vapour compositions and stage temperature using the Muller iterative convergence method.

9.8 Discuss the different modes of batch operation.

9.9 Describe the start-up procedure of batch operation.

9.10 What do you mean by the soft-sensor? Formulate a soft-sensor for a nonideal multi-component mixture.

REFERENCES

Baratti, R., Bertucco, A., Da Rold, A., and Morbidelli, M. (1995). Development of a composition estimator for binary distillation columns. application to a pilot plant, *Chem. Eng. Sci.*, 50, 1541–1550.

Edgar, T.F. (1996). Control of unconventional processes, *J. Process Control*, 6, 99–110.

Holland, C.D. (1981). *Fundamentals of Multicomponent Distillation*, 1st ed., McGraw-Hill Book Company, New York.

Luyben, W.L. (1990). *Process Modeling, Simulation, and Control for Chemical Engineers*, 2nd ed., McGraw-Hill Book Company, Singapore.

Mujtaba, I.M., and Macchietto, S. (1997). Efficient optimization of batch distillation with chemical reaction using polynomial curve fitting techniques, *Ind. Eng. Chem. Res.*, 36, 2287–2295.

Passut, C.A., and Danner, R.P. (1972). Correlation of ideal gas enthalpy, heat capacity, and entropy, *Ind. Eng. Chem. Process Des. Develop.*, 11, 543–546.

Reid, R.C., Prausnitz, J.M., and Sherwood, T.K. (1977). *The Properties of Gases and Liquids*, 3rd ed., McGraw-Hill Book Company, New York.

Sorensen, E. (1994). Studies on optimal operation and control of batch distillation columns, PhD Thesis, University of Trondheim, The Norwegian Institute of Technology.

Sorensen, E., Macchietto, S., Stuart, G., and Skogestad, S. (1996). Optimal control and on-line operation of reactive batch distillation, *Comput. Chem. Eng.*, 20, 1491–1498.

Treybal, R.E. (1980). *Mass-transfer Operations*, 3rd ed., McGraw-Hill Book Company, New York.

10

Binary Continuous Distillation Column

10.1 INTRODUCTION

Distillation is the most common unit operation in the chemical industry and understanding its behaviour has been a defining characteristic of a good chemical engineer. The key objective of developing a mathematical process model is to predict the dynamic characteristics of a plant, whether the model is used for the advanced model-based controller synthesis or for the soft sensor design. When developing a model of a distillation column, several unacceptable assumptions are sometimes adopted aiming to simplify the theory. Unfortunately, the resulting simplified model may fail to capture precisely the nonlinear and interactive distillation dynamics.

Realistic performance of an actual column can seldom be predicted satisfactorily by excluding the simultaneous effects of heat transfer and fluid flow on the trays. The liquid hydraulic in a tray is an important factor in predicting the dynamic performance. The plant dynamics are also greatly influenced by the phase nonidealities. In addition, accurate estimation of the physical properties is also a vital issue.

This chapter presents the development of a dynamic model for a realistic alcohol distillation column taking into consideration all the factors described above, including liquid-phase nonideality, nonequimolal overflow, rigorous tray hydraulics and inefficient trays. The model structure of such a practical column contains a large number of ordinary differential equations (ODEs) along with nonlinear algebraic equations (AEs) that must be solved. Keeping this objective in mind, the dynamic simulation of the example distillation model has also been included with computer program in this chapter.

10.2 THE PROCESS AND THE MODEL

The present study concerns a continuous distillation column with one input feed stream and two liquid products (distillate and bottoms). The example column is actually used to distil ethanol from water. A schematic representation of the distillation column is shown in Figure 10.1.

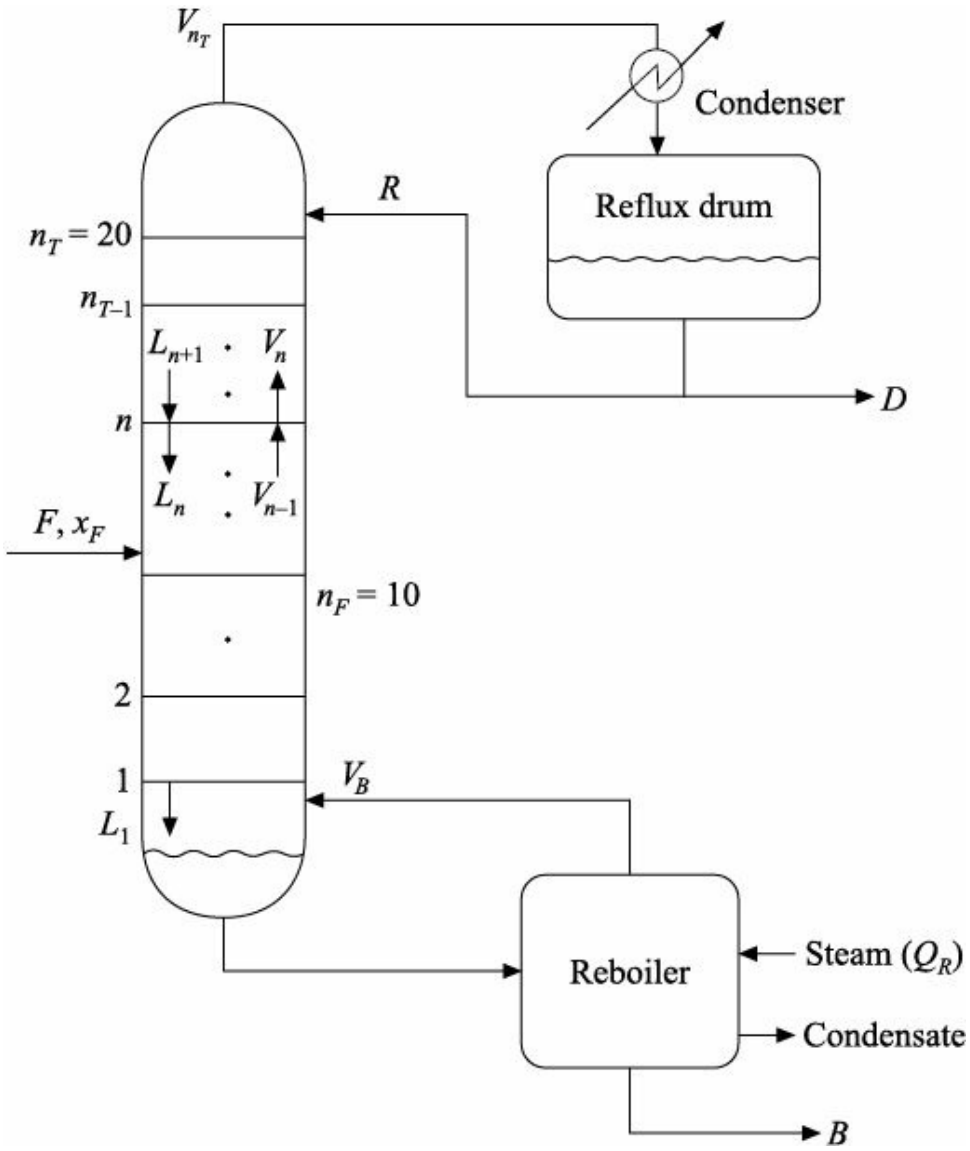

FIGURE 10.1 Schematic representation of the alcohol distillation column example.

The fractionating column is made up of 20 inefficient trays, a reboiler and a total condenser. Numbering of trays is started from the bottom of the column: tray 1 is the bottom tray above the reboiler, tray 2 is the next, etc. The feed (saturated liquid) enters at tray 10. The condensation of overhead vapour is total and the condensed liquid is accumulated in the reflux drum. No vapour distillate is produced here. Some of the condensed liquid (not subcooled) is removed from the reflux drum as the distillate product, and some of it is sent back as a reflux stream to the column to provide liquid flow on the trays. At the base of the column, the bottoms is withdrawn as a liquid product. A reboiler heated by steam, generates the boil-up vapour and the vapour produced flows back to the bottom plate. The reboiler runs like a theoretical tray.

In order to describe detailed distillation operation, we will attempt to develop a rigorous distillation model. The mathematical model, which can represent a binary column, is a large structured system of differential–algebraic equations supported by vapour–liquid equilibrium (VLE) and physical properties. The dynamic distillation simulator involves the computations of composition (or mole fraction), flow rate, tray holdup, enthalpy, average molecular weight and density, and VLE.

The following assumptions have been used to develop the distillation model.

- The liquid is perfectly mixed on each tray. This assumption implies that the liquid on any tray n has the uniform composition x_n.

- The liquid and vapour leaving each tray are in thermal equilibrium.
- The operating pressure is constant (one atmosphere) and pressure drops are negligible.
- The tray efficiency is defined from the Murphree relation and 70% vapour-phase Murphree efficiency has been assumed for every tray.
- The vapour-phase holdup is negligible with regard to the liquid-phase holdup. This assumption is quite reasonable since in most systems, the vapour density is much smaller than the liquid density.
- Algebraic forms of equations are used to calculate the liquid-phase and vapour-phase enthalpies. The energy balance equations (enthalpy derivatives with respect to time) are not used to compute enthalpies; they are generally employed for vapour flow rate calculations.
- The tray hydraulics are modelled with Francis weir relationship (details in Chapter 9).
- Variations of liquid holdups are considered in each tray excluding reflux drum and column base. Indeed, the reflux drum and column base holdups in most of the industrial columns are held almost constant by employing level controllers.
- Coolant and steam dynamics are negligible in the condenser and reboiler, respectively. However, to examine the condenser and reboiler dynamics, an example of a heat exchanger is discussed with the development of dynamic model in Chapter 1.
- Wilson thermodynamic model is used (details in Chapter 8) for VLE predictions.
- The thermal losses are assumed to be negligible.

10.2.1 Material and Energy Balance Equations

A set of ordinary differential equations consisting of total (or overall) continuity, component (or partial) continuity, and energy (or enthalpy) balance equations is given in the following descriptions.

Reboiler–Column Base System (subscript 'B')

Total Continuity: $$\dot{m}_B = L_1 - V_B - B \tag{10.1}$$

Component Continuity: $$\dot{m}_B \dot{x}_B = L_1 x_1 - V_B y_B - B x_B \tag{10.2}$$

Energy equation: $$\dot{m}_B \dot{H}_B^L = Q_R + L_1 H_1^L - V_B H_B^V - B H_B^L \tag{10.3}$$

Bottom Tray (subscript '1')

Total continuity: $$\dot{m}_1 = L_2 + V_B - L_1 - V_1 \tag{10.4}$$

Component continuity: $$\dot{m}_1 \dot{x}_1 = L_2 x_2 + V_B y_B - L_1 x_1 - V_1 y_1 \tag{10.5}$$

Energy equation: $$\dot{m}_1 \dot{H}_1^L = L_2 H_2^L + V_B H_B^V - L_1 H_1^L - V_1 H_1^V \tag{10.6}$$

***n*th Tray** (subscript 'n', where $n = 2$ to $n_F - 1$ and $n_F + 1$ to $n_T - 1$)

Total continuity: $$\dot{m}_n = L_{n+1} + V_{n-1} - L_n - V_n \tag{10.7}$$

Component continuity: $$\dot{m}_n \dot{x}_n = L_{n+1} x_{n+1} + V_{n-1} y_{n-1} - L_n x_n - V_n y_n \tag{10.8}$$

Energy equation: $$\dot{m}_n \dot{H}_n^L = L_{n+1} H_{n+1}^L + V_{n-1} H_{n-1}^V - L_n H_n^L - V_n H_n^V \tag{10.9}$$

Feed Tray (subscript 'n_F')

Total continuity: $$\dot{m}_{n_F} = L_{n_F+1} + F + V_{n_F-1} - L_{n_F} - V_{n_F} \tag{10.10}$$

Component continuity:

$$\dot{m}_{n_F}\dot{x}_{n_F} = L_{n_F+1}x_{n_F+1} + Fx_F + V_{n_F-1}y_{n_F-1} - L_{n_F}x_{n_F} - V_{n_F}y_{n_F} \quad (10.11)$$

Energy equation:

$$\dot{m}_{n_F}\dot{H}^L_{n_F} = L_{n_F+1}H^L_{n_F+1} + FH^L_F + V_{n_F-1}H^V_{n_F-1} - L_{n_F}H^L_{n_F} - V_{n_F}H^V_{n_F} \quad (10.12)$$

Top Tray (subscript 'n_T')

Total continuity: $$\dot{m}_{n_T} = R + V_{n_T-1} - L_{n_T} - V_{n_T} \quad (10.13)$$

Component continuity: $$\dot{m}_{n_T}\dot{x}_{n_T} = Rx_D + V_{n_T-1}y_{n_T-1} - L_{n_T}x_{n_T} - V_{n_T}y_{n_T} \quad (10.14)$$

Energy equation: $$\dot{m}_{n_T}\dot{H}^L_{n_T} = RH^L_D + V_{n_T-1}H^V_{n_T-1} - L_{n_T}H^L_{n_T} - V_{n_T}H^V_{n_T} \quad (10.15)$$

Condenser–Reflux Drum System (subscript 'D')

Total continuity: $$\dot{m}_D = V_{n_T} - R - D \quad (10.16)$$

Component continuity: $$\dot{m}_D\dot{x}_D = V_{n_T}y_{n_T} - (R+D)x_D \quad (10.17)$$

In the above modelling equations, x_n is the mole fraction of a more volatile component (here ethanol) in a liquid stream leaving nth tray, y_n the mole fraction of ethanol in a vapour stream leaving nth tray, x_F the mole fraction of ethanol in the feed stream, x_D the mole fraction of ethanol in the liquid distillate, x_B the mole fraction of ethanol in the bottom product, L_n the liquid flow rate leaving nth tray (gmol/min), V_n the vapour flow rate leaving nth tray (gmol/min), F the feed flow rate (gmol/min), R the reflux flow rate (gmol/min), D the distillate flow rate (gmol/min), B the bottoms flow rate (gmol/min), V_B the vapour boil-up rate (gmol/min), m_n the liquid holdup on nth tray (gmol), m_D the liquid holdup in the reflux drum (gmol), m_B the liquid holdup in the column base (gmol), $H_D{}^L$ the enthalpy of distillate (J/gmol), $H_B{}^L$ the enthalpy of bottom product (J/gmol), $H_F{}^L$ the enthalpy of feed stream (J/gmol), $H_n{}^L$ the enthalpy of a liquid stream leaving nth tray (J/gmol), $H_n{}^V$ the enthalpy of a vapour stream leaving nth tray (J/gmol) and Q_R the heat input to the reboiler (J/min). The dot symbol (.) on a variable is used to denote the time derivative of that variable. Also, $\dot{mx}$ represents the time derivative of mx, i.e., $\dot{mx} = d(mx)/dt$.

It is well-known that the dynamic changes in internal energies on the trays are much faster than the composition or total holdup changes. Therefore, the energy balance Equations (10.3), (10.6), (10.9), (10.12), and (10.15) with putting zero in the left hand sides are commonly (and here also) utilized to compute the vapour flow rates (V_B, V_1, V_n, V_{n_F}, V_{n_T}).

We must remember that it is not necessary to include Equation (10.3) in the reboiler–column base system model if V_B be the manipulated input instead of Q_R for the bottom loop. It is also worthy to mention at this moment that since no vapour flow rate calculation is involved in the condenser–reflux drum system, there is no need to make an energy balance equation for that system. As stated previously, the liquid as well as vapour phase enthalpy is estimated using the algebraic forms of equations.

10.3 DYNAMIC SIMULATION

As mentioned, the dynamic distillation simulator (to be developed), computes the tray holdup, phase composition, flow rate, enthalpy, average molecular weight and density, and vapour–liquid equilibrium.

Tray holdup, liquid-phase composition, and vapour flow rate can be calculated from the derived material and energy balance Equations (10.1) to (10.17). In addition to the balance differential equations, it is necessary to derive some algebraic forms of equations. The algebraic modelling equations can provide the predictions of vapour–liquid equilibrium (already analyzed in Subsection 9.4.6 with computer Program 9.5), the estimations of average molecular weight and density (reported in Subsection 9.4.5 with computer Program 9.4), the calculations of liquid and vapour phase enthalpies (given in Subsection 9.4.2 with computer Programs 9.1 and 9.2), and the computations of internal liquid flow rate (discussed in Subsection 9.4.3 with computer Program 9.3).

All the subsections and the computer programs mentioned above are well-documented in Chapter 9. Actually, the previous chapter describes the separation of a binary ethanol–water mixture using a batch distillation column and here the same mixture is fractionated employing a continuous distillation column. In order to avoid the repetitions, exactly same computational approaches as discussed in Chapter 9 have not been further included in the present study.

The computer program (Fortran 90) providing the simulation of the complete distillation column is given in Program 10.1. All the Fortran subroutines (computer Programs 9.1, 9.2, 9.3, 9.4 and 9.5) are assembled in Program 10.1 along with the *main program*. The steady state and operating conditions of the sample process are reported in Table 10.1 as well as in Program 10.1. Note that a step change in feed temperature (disturbance or load variable) from 50 (steady state value) to 45°C at time equal to zero is introduced in the process simulator (Program 10.1) to observe the dynamic process response. You can change any other variable or parameter in the dynamic simulator according to the requirements.

Table 10.1 Operating and steady state conditions

Binary system: ethanol–water	
Distillate flow rate (gmol/min), D	4075.33
Distillate composition (mol fraction), x_D	0.8066
Feed flow rate (gmol/min), F	7560.0
Feed composition (mol fraction), x_F	0.50
Feed temperature (°C), T_F	50.0
Bottoms flow rate (gmol/min), B	3484.67
Bottoms composition (mol fraction), x_B	0.1414
Reflux flow rate (gmol/min), R	6000.0
Heat input to the reboiler (kJ/min), Q_R	4.0×10^5
Liquid holdup in the reflux drum (gmol), m_D	11564.07
Liquid holdup in the column base (gmol), m_B	24994.76
Integration time interval (min), dt	0.005

The process simulator is developed based on the following computational steps.

Step 1: Input data on the column size (number of total trays and column diameter), weir dimensions (weir height and weir length), feed (components, flow rate, composition and temperature), feed tray position, pressure profile, tray efficiency and initial conditions (liquid compositions and liquid holdups on all trays).

Step 2: In the closed-loop distillation system, the reflux flow rate and heat input to the reboiler (or alternatively vapour boil-up rate) are usually calculated as manipulated variables in the controller model. In the present open-loop case, the values of reflux flow and heat input rates are provided at each time step.

Step 3: Compute the temperature and equilibrium vapour-phase composition on each tray at given pressure and liquid-phase composition (using BUBLEPOINT subroutine). The Newton–Raphson convergence method is used in the subroutine. Subsequently, calculate the actual vapour-phase composition employing Murphree relationship [Equation (9.19)].

Step 4: Calculate the liquid and vapour phase enthalpies for each tray based on the algebraic form of Equations (9.16) and (9.17) respectively (using subroutine ENTLIQ for liquid-phase enthalpy and subroutine ENTVAP for vapour-phase enthalpy).

Step 5: Calculate the internal liquid flow rate for all trays from Francis weir relationship [Equation (9.18)] (using subroutine HYDRAU).

Step 6: Compute all vapour flow rates as described earlier using the energy balance equations. Also calculate the bottoms and distillate flow rates, B and D, from Equations (10.1) and (10.16) respectively (assume constant m_B and m_D).

Step 7: Evaluate the time derivative of all total and component material balance equations except Equations (10.1) and (10.16).

Step 8: Integrate all balance differential equations [except Equations (10.1) and (10.16), and all energy balance equations] using the Euler method. Then calculate the liquid holdups on all trays (excluding reflux drum and column base) and liquid-phase compositions on all trays for the future time step.

Step 9: To run the process simulator for the next time step, go back to Step 2.

PROGRAM 10.1 *Dynamic Distillation Simulator*

```
! B = Bottoms flow rate
! D = Distillate flow rate
! DM = Time derivative of M
! DXB, DXD = Time derivative of XB and XD respectively
! DXM = Time derivative of the multiplication of X and M
! Eff = Tray efficiency
! F = Feed flow rate
! HF = Enthalpy of feed
! HL, HV = Liquid-phase and vapour-phase enthalpy respectively
! HLB, HLD = Liquid enthalpy of bottoms and distillate respectively
! HVB = Enthalpy of boil-up vapour
! L = Internal liquid flow rate
! M = Molar liquid holdup
! MB, MD = Molar liquid holdup in column base and reflux drum
! respectively
! NC = Total number of components
! NF = Feed tray
! NT = Total number of trays
! P = Pressure
! QR = Heat input to the reboiler
! R = Reflux flow rate
! T = Tray temperature
! TF = Feed temperature
! V = Vapour flow rate
! VB = Vapour boil-up rate in the reboiler
! WLS, WHS, DS = Weir length, weir height and column diameter
! respectively in
! stripping section
! WLR, WHR, DR = Weir length, weir height and column diameter
! respectively in
! rectifying section
! X = Liquid-phase composition
! XB = Liquid composition of bottom product
! XD = Liquid composition of distillate product
! XF = Feed composition
! Y = Vapour-phase composition
! YB = Composition of boil-up vapour
! Yeq = Equilibrium vapour composition
```

```
!————————————Starting of Main Program————————————————————!
!———————————————————————————————————————————————————————!

PROGRAM BINARY_DISTILLATION_COLUMN
IMPLICIT NONE

INTERFACE

SUBROUTINE HYDRAU(M,X,L,WH,WL,DCOL)
REAL*8,INTENT(IN)::M,X,WH,WL,DCOL
REAL*8,INTENT(OUT)::L
END SUBROUTINE HYDRAU

SUBROUTINE BUBLEPOINT(T,X1,Y1,P)
REAL*8,INTENT(IN)::X1,P
REAL*8,INTENT(OUT)::T,Y1
END SUBROUTINE BUBLEPOINT

SUBROUTINE MWDENS(X1,MWA,DENSA)
REAL*8,INTENT(IN)::X1
REAL*8,INTENT(OUT)::MWA,DENSA
END SUBROUTINE MWDENS

SUBROUTINE ENTVAP(T,Y,HV)
REAL*8,INTENT(IN)::T,Y
REAL*8,INTENT(OUT)::HV
END SUBROUTINE ENTVAP

SUBROUTINE ENTLIQ(T,X,HL)
REAL*8,INTENT(IN)::T,X
REAL*8,INTENT(OUT)::HL
END SUBROUTINE ENTLIQ
END INTERFACE

!Declaration
!————————!

INTEGER::K,N,j
INTEGER,PARAMETER::NT=20,NC=2,NF=10,i=7000
REAL*8,DIMENSION(i)::XD,XB,YD,YB,DXD,DXB
REAL*8,DIMENSION(i)::Time,HLB,HVB,HLD,VB,QR,R,MB,MD
REAL*8,DIMENSION(i)::D,B,TB,TD
REAL*8,PARAMETER::WLS=121.92 D0,WHS=1.905 D0,DS=182.88 D0
REAL*8,PARAMETER::WLR=121.92 D0,WHR=3.175 D0,DR=182.88 D0
REAL*8,DIMENSION(NT,i)::X,XM,Y,DXM,Yeq
REAL*8,DIMENSION(NT,i)::M,L,HL,HV,V,DM,T
REAL,PARAMETER::dt=0.005,Eff=0.70
REAL*8::HF,P,PB,PD,F,XF,TF

OPEN(UNIT=2,File="BDC_SS.dat")

!Initialization
!————————!

XD(1)= 0.80659971824504 D0
XB(1)= 0.14143012615680 D0

P=760.00 D0
PB=760.00 D0
PD=760.00 D0
F=7560.0 D0
XF=0.50 D0
TF=45.0 D0
```

```
!Liquid compositions
!————————————!

X(1,1)= 0.39621505672092 D0
X(2,1)= 0.46964196245191 D0
X(3,1)= 0.50757565191151 D0
X(4,1)= 0.52743102859236 D0
X(5,1)= 0.53793416441121 D0

X(6,1)= 0.54352752274519 D0
X(7,1)= 0.54651775199382 D0
X(8,1)= 0.54811977334792 D0
X(9,1)= 0.54897906620493 D0
X(10,1)= 0.54944026689427 D0

X(11,1)= 0.59939111353814 D0
X(12,1)= 0.62703561060469 D0
X(13,1)= 0.65128128508155 D0
X(14,1)= 0.67309893894477 D0
X(15,1)= 0.69321494040634 D0

X(16,1)= 0.71220554114628 D0
X(17,1)= 0.73055653434763 D0
X(18,1)= 0.74870931580235 D0
X(19,1)= 0.76710139769909 D0
X(20,1)= 0.78620884696348 D0

! Tray holdups
!————————!

M(1,1)= 3381.89143335566041 D0
M(2,1)= 3218.56027805881558 D0
M(3,1)= 3140.03821131412678 D0
M(4,1)= 3100.79788770943924 D0
M(5,1)= 3080.52860980672222 D0

M(6,1)= 3069.86811270731505 D0
M(7,1)= 3064.20649759588605 D0
M(8,1)= 3061.18394079383188 D0
M(9,1)= 3059.56575271839483 D0
M(10,1)= 3058.69811362274686 D0

M(11,1)= 3040.69798213731428 D0
M(12,1)= 2975.33077698886109 D0
M(13,1)= 2920.02153066220080 D0
M(14,1)= 2871.92959536285662 D0
M(15,1)= 2828.92930230204456 D0

M(16,1)= 2789.46342932412244 D0
M(17,1)= 2752.32604892530162 D0
M(18,1)= 2716.51893206451314 D0
M(19,1)= 2681.14703551736329 D0
M(20,1)= 2645.33059631233482 D0

!————————————————————!

Time(1)=0.00 D0

DO 30 N=1,NT
XM(n,1)=M(n,1)*X(n,1)
30 CONTINUE
DO K=1,i !————————Starting of main loop—————————!

R(K) =6000.00 D0
```

```
QR(K)=400000000.00 D0

MD(K)=11564.06633051157041 D0
MB(K)=24994.76474233236149 D0

!———Bubble point and enthalpy calculations———!
!———————————————————————————!

! Reboiler
!——————!

CALL BUBLEPOINT(TB(K),XB(K),YB(K),PB)
CALL ENTVAP(TB(K),YB(K),HVB(K))
CALL ENTLIQ(TB(K),XB(K),HLB(K))

! 1ST tray
!——————!

CALL BUBLEPOINT(T(1,K),X(1,K),Yeq(1,K),P)
Y(1,K)=YB(K)+Eff*(Yeq(1,K)-YB(K))
CALL ENTVAP(T(1,K),Y(1,K),HV(1,K))
CALL ENTLIQ(T(1,K),X(1,K),HL(1,K))

! 2ND tray to NT tray
!———————————————!

DO 110 n=2,NT
CALL BUBLEPOINT(T(n,K),X(n,k),Yeq(n,k),P)
Y(n,k)=(Yeq(n,k)-Y(n-1,K))*Eff+Y(n-1,k)
CALL ENTVAP(T(n,K),Y(n,K),HV(n,K))
CALL ENTLIQ(T(n,K),X(n,k),HL(n,K))
110 CONTINUE
! Reflux drum
!————————!

CALL BUBLEPOINT(TD(K),XD(k),YD(k),PD)
CALL ENTLIQ(TD(K),XD(K),HLD(K))

!———Internal liquid flow rate calculations———!
!———————————————————————————!

! Stripping section (including feed tray)
!————————————————————————!

DO 270 N=1,NF
CALL HYDRAU(M(N,K),X(n,k),L(N,K),WHS,WLS,DS)
270 CONTINUE
! Rectifying section
!———————————!

DO 273 N=NF+1,NT
CALL HYDRAU(M(N,K),X(n,k),L(N,K),WHR,WLR,DR)
273 CONTINUE

!———Vapour flow rate calculations———!
!————————————————————————————!

VB(K)=(QR(K)-L(1,K)*(HLB(K)-HL(1,K)))/(HVB(K)-HLB(K))
B(K)=L(1,K)-VB(K)
IF(B(K) .LT. 0.0) STOP

V(1,K)=(HL(2,K)*L(2,K)+HVB(K)*VB(K)-HL(1,K)*L(1,K))/HV(1,K)
DO 120 N=2,NF-1
V(N,K)=(HL(N+1,K)*L(N+1,K)+HV(N-1,K)*V(N-1,K)-HL(N,K)*L(N,K))/
& HV(N,K)
```

```
120 CONTINUE

CALL ENTLIQ(TF,XF,HF)
V(NF,K)=(HL(NF+1,K)*L(NF+1,K)+HV(NF-1,K)*V(NF-1,K)-HL(NF,K)*
& L(NF,K)+HF*F)/HV(NF,K)

DO 130 N=NF+1,NT-1
130 V(n,k)=(HL(n+1,k)*L(n+1,k)+HV(n-1,k)*V(n-1,k)-HL(n,k)*L(n,k))/
& HV(n,k)

V(NT,K)=(HLD(K)*R(K)+HV(NT-1,K)*V(NT-1,K)-HL(NT,K)*L(NT,K))/
& HV(NT,K)

D(K)=V(NT,K)-R(K)
IF(D(K) .LT. 0.0) STOP

!————Evaluation of time derivatives————!
!————————————————————————————————————!

DM(1,K)=L(2,K)+VB(K)-V(1,K)-L(1,K)

DO 140 N=2,NF-1
140 DM(N,K)=L(N+1,K)+V(N-1,K)-L(N,K)-V(N,K)

DM(NF,K)=L(NF+1,K)+F+V(NF-1,K)-L(NF,K)-V(NF,K)

DO 150 N=NF+1,NT-1
150 DM(N,K)=L(N+1,K)+V(N-1,K)-L(N,K)-V(N,K)

DM(NT,K)=R(K)+V(NT-1,K)-L(NT,K)-V(NT,K)

DXB(K)=(X(1,K)*L(1,K)-YB(K)*VB(K)-XB(K)*B(K))/MB(K)
DXM(1,K)=X(2,K)*L(2,K)+YB(K)*VB(K)-X(1,K)*L(1,K)-
& Y(1,K)*V(1,K)

DO 165 N=2,NF-1
165 DXM(N,K)=X(N+1,K)*L(N+1,K)+Y(N-1,K)*V(N-1,K)-X(N,K)*L(N,K)
& -Y(N,K)*V(N,K)

DXM(NF,K)=X(NF+1,K)*L(NF+1,K)+Y(NF-1,K)*V(NF-1,K)-X(NF,K)*
& L(NF,K)-Y(NF,K)*V(NF,K)+F*XF

DO 170 N=NF+1,NT-1
170 DXM(N,K)=X(N+1,K)*L(N+1,K)+Y(N-1,K)*V(N-1,K)-X(N,K)*L(N,K)
& -Y(N,K)*V(N,K)

DXM(NT,K)=XD(K)*R(K)+Y(NT-1,K)*V(NT-1,K)-X(NT,K)*L(NT,K)-
& Y(NT,K)*V(NT,K)

DXD(K)=(V(NT,K)*Y(NT,K)-(R(K)+D(K))*XD(K))/MD(k)

!———Integration using Euler method————!
!————————————————————————————————————!

DO 215 N=1,NT
215 M(N,K+1)=M(N,K)+DM(N,K)*dt

XB(K+1)=XB(K)+DXB(K)*dt
IF(XB(K+1)<0.00)XB(K+1)=0.00
IF(XB(K+1)>1.00)XB(K+1)=1.00

DO 225 N=1,NT
XM(N,K+1)=XM(N,K)+DXM(N,K)*dt
X(N,K+1)=XM(N,K+1)/M(N,K+1)
IF(X(N,K+1)<0.00)X(N,K+1)=0.00
IF(X(N,K+1)>1.00)X(N,K+1)=1.00
225 CONTINUE
```

```
XD(K+1)=XD(K)+DXD(K)*dt
IF(XD(K+1)<0.00)XD(K+1)=0.00
IF(XD(K+1)>1.00)XD(K+1)=1.00

Time(K+1)=Time(K)+dt

PRINT*,Time(k),TB(K),XB(k),TD(K),XD(K),
& (X(n,K),n=1,20),
& (M(n,K),n=1,20),
& (T(n,K),n=1,20),
& (L(n,K),n=1,20),
& D(k),B(k),MD(k),MB(K),VB(K)

WRITE(2,FMT=100)Time(k),TB(K),XB(k),TD(K),XD(K),
& (X(n,K),n=1,20),
& (M(n,K),n=1,20),
& (T(n,K),n=1,20),
& (L(n,K),n=1,20),
& D(k),B(k),MD(k),MB(K),VB(K)

100 FORMAT (1X,90(2X,F15.10))

END DO                      !————————End of main loop——————————!
END FILE 2

END PROGRAM BINARY_DISTILLATION_COLUMN

!————————————————————End of Main Program————————————————————!
!——————————————————————————————————————————————————————————!

!———————————————————Starting of Subroutines———————————————————!
!——————————————————————————————————————————————————————————!

!——Subroutine (Program 9.3) for internal liquid flow rate calculations——!
!————————————————————————————————————————————————————————————!

SUBROUTINE HYDRAU(M,X,L,WH,WL,DCOL)
IMPLICIT NONE
REAL*8,INTENT(IN)::M,X,WH,WL,DCOL
REAL*8,INTENT(OUT)::L
REAL*8::CONST,MWA,DENSA
REAL*8::DCOLs,WHs,WLs,Ms,Ls

CALL MWDENS(X,MWA,DENSA)
DCOLs=DCOL*0.3937                                  ! 1 cm = 0.3937 in
WHs=WH*0.3937
WLs=WL*0.3937
Ms=M*0.002204586                              ! 1 gmol = 0.002204586 lbmol

CONST=183.2*Ms*MWA/(DENSA*DCOLs*DCOLs)-WHs/12
IF(CONST .LE. 0.00)GO TO 10
Ls=DENSA*WLs*999*((183.2*Ms*MWA/(DENSA*DCOLs*DCOLs)-WHs/12)**1.5)
& /MWA

L=Ls*7.56                                      ! 1 lbmol/h = 7.56 gmol/min

RETURN
10 L=0.00 D0
RETURN

END SUBROUTINE HYDRAU

!——Subroutine (Program 9.2) for vapour enthalpy calculations———!
!————————————————————————————————————————————————————————————!
SUBROUTINE ENTVAP(T,Y,HV)
```

```
IMPLICIT NONE
REAL*8,INTENT(IN)::T,Y
REAL*8,INTENT(OUT)::HV
INTEGER,PARAMETER::NC=2
REAL*8,DIMENSION(NC)::E1,E2,E3,E4,E5
REAL*8::TR,ENTV1,ENTV2

E1(1)=0.106486 D+5
E1(2)=0.1545871 D+5

E2(1)=7.515997 D0
E2(2)=8.022526 D0

E3(1)=0.115136 D-1
E3(2)=-0.4745722 D-3

E4(1)=-0.1682096 D-5
E4(2)=0.6878047 D-6

E5(1)=0.9036333 D-10
E5(2)=-0.1439752 D-9

TR=(1.8*T)+492.0                                    ! TR in degree R
ENTV1=E1(1)+E2(1)*TR+E3(1)*TR*TR+E4(1)*(TR**3)+E5(1)*(TR**4)
ENTV2=E1(2)+E2(2)*TR+E3(2)*TR*TR+E4(2)*(TR**3)+E5(2)*(TR**4)
                              HV=(ENTV1*Y+ENTV2*(1-Y))*2.326 ! 1 Btu/lbmol = 2.326 J/gmol
RETURN

END SUBROUTINE ENTVAP

!——Subroutine (Program 9.1) for liquid enthalpy calculations———!
!————————————————————————————————————————————————————————————!
SUBROUTINE ENTLIQ(T,X,HL)
IMPLICIT NONE
REAL*8,INTENT(IN)::T,X
REAL*8,INTENT(OUT)::HL
INTEGER,PARAMETER::NC=2
REAL*8,DIMENSION(NC)::C1,C2,C3
REAL*8::TR,ENTL1,ENTL2

C1(1)=0.4046348 D+3
C1(2)=-0.87838059 D+4

C2(1)=-0.2410286 D+2
C2(2)=0.175845 D+2

C3(1)=0.472823 D-1
C3(2)=0.3651369 D-3
TR=(1.8*T)+492.0                                    ! TR in degree R
ENTL1=C1(1)+C2(1)*TR+C3(1)*TR*TR
ENTL2=C1(2)+C2(2)*TR+C3(2)*TR*TR
HL=(ENTL1*X+ENTL2*(1-X))*2.326 ! 1 Btu/lbmol = 2.326 J/gmol
RETURN

END SUBROUTINE ENTLIQ

!—Subroutine (Program 9.4) for molecular weight and density
! calculations—!
!————————————————————————————————————————————————————————————!

SUBROUTINE MWDENS(X1,MWA,DENSA)
IMPLICIT NONE
REAL*8,INTENT(IN)::X1
REAL*8,INTENT(OUT)::MWA,DENSA
```

```
REAL*8::X2,MW1,MW2,DENS1,DENS2

MW1=46.0634 D0
MW2=18.0152 D0

DENS1=0.789*62.42587 ! 1 g/cm^3 = 62.42587 lb/ft^3
DENS2=1.00*62.42587

X2=1-X1
MWA=(X1*MW1)+(X2*MW2)
DENSA=(X1*DENS1)+(X2*DENS2) ! DENSA in lb/ft^3

END SUBROUTINE MWDENS

!——Subroutine (Program 9.5) for bubble point calculations———!
!————————————————————————————————————————————————————————!

SUBROUTINE BUBLEPOINT(T,X1,Y1,P)
IMPLICIT NONE
REAL*8,INTENT(IN)::X1,P
REAL*8,INTENT(OUT)::T,Y1
INTEGER,PARAMETER::NC=2
INTEGER::J,LOOP
REAL*8,DIMENSION(NC)::X,Y
REAL*8,DIMENSION(NC)::Ps,A,B,C,G
REAL*8::SUMY,PAR1,PAR2,PAR3,FSLOPE,F
REAL*8,PARAMETER::LAMDA12=0.20916399 D0,LAMDA21=0.82284181 D0

A(1)=18.5242 D0
B(1)=3578.91 D0
C(1)=-50.50 D0
A(2)=18.3036 D0
B(2)=3816.44 D0
C(2)=-46.13 D0

X(1)=X1
X(2)=1-X1
LOOP=0
T=95.00                    ! guessed value for all tray temperatures

10 LOOP=LOOP+1
IF(LOOP .GT. 1000) GO TO 30
SUMY=0.00 D0

PAR1=(LAMDA12/(X(1)+LAMDA12*X(2)))-
& (LAMDA21/(X(2)+LAMDA21*X(1)))
PAR2=DLOG(X(1)+LAMDA12*X(2))
PAR3=DLOG(X(2)+LAMDA21*X(1))

G(1)=EXP(-PAR2+(X(2)*PAR1))
G(2)=EXP(-PAR3-(X(1)*PAR1))

DO 17 J=1,NC
Ps(J)=EXP(A(J)-(B(J)/(T+273+C(J))))
Y(J)=Ps(J)*G(J)*X(J)/P
17 SUMY=SUMY+Y(J)

IF(ABS(SUMY-1) .LT. 0.0000001)RETURN
F=SUMY-1
FSLOPE=0.0 D0

DO 20 J=1,NC
20 FSLOPE=FSLOPE+((Y(J)*B(J))/((T+273+C(J))**2))
```

```
T=T-F/FSLOPE
Y1=Y(1)

GO TO 10
30 STOP

END SUBROUTINE BUBLEPOINT

!————————————————End of Subroutines————————————————!
!————————————————————————————————————————————————!
```

10.4 SUMMARY AND CONCLUSIONS

This chapter is devoted to develop a mathematical model of a nonideal continuous distillation column. The dynamic simulation of the process model is also presented with detailed computer program. A highly nonideal ethanol–water mixture is used to separate in the example column. A similar distillation simulator is developed by Jana, Samanta, and Ganguly (2005) for controlling the product compositions employing an advanced nonlinear controller. However, after studying this chapter, it is not a difficult task for you to develop a dynamic distillation simulator with different equipment configurations and conditions for the separation of any nonideal feed mixture.

EXERCISES

10.1 From the model structure of a continuous distillation column as reported in this chapter:

(i) Find out the number of state variables and state equations.

(ii) Classify the linear and nonlinear equations.

10.2 How is the steady state model developed from the dynamic model of a process? What are the steady state modelling equations of the distillation column explained in this chapter?

10.3 You have two continuous distillation columns. Except the total number of trays, everything is same in both the columns. What are the possible ways for maintaining the same distillate (liquid) product purity in both the distillation columns?

10.4 Develop a dynamic binary distillation simulator for the separation of an ethanol–water mixture. The same modelling equations as presented in this chapter may be solved in the simulator. Use Francis weir formula [Equation (9.18)] for tray hydraulic calculations. The Wilson parameters that are required for activity coefficient predictions are given in Program 10.1 (subroutine for bubble point calculations) as LAMDA. The operating and steady state conditions are listed in the following text.

Total number of trays (excluding total condenser and reboiler) = 15
Feed tray location = 5
Pressure (constant) throughout the column = 1 atm
Murphree vapour-phase tray efficiency = 60%
Feed (saturated liquid) flow rate = 7560.0 gmol/min
Feed composition = 0.5
Feed temperature = 30°C
Distillate flow rate = 1993.1984 gmol/min
Distillate composition = 0.8022
Distillate temperature = 78.3706°C
Bottoms flow rate = 5566.8016 gmol/min
Bottoms composition = 0.3918
Bottoms temperature = 80.9073°C

Reflux flow rate = 3024.0 gmol/min
Vapour boil-up rate = 6020.56 gmol/min
Holdup in reflux drum = 3628.80 gmol
Holdup in column base = 2222.64 gmol
Sampling time = 0.005 min
Note: If any vital data is missing, please assume that.

REFERENCE

Jana, A.K., Samanta, A.N., and Ganguly, S. (2005). Nonlinear model-based control algorithm for a distillation column using software sensor, *ISA Transactions*, 44, 259–271.

11

Multicomponent Batch Distillation Column

11.1 INTRODUCTION

Up to the end of 1970s, most of the research work on transient distillation calculations has been primarily concerned with continuous distillation rather than with batch distillation, which is inherently an unsteady state process. The reason for this is twofold. First, there is wider industrial interest in continuous distillation, and second, unsteady state continuous distillation models are more easily derived and the related computational problems are less severe than those of batch distillation. For example, transients in continuous distillation are usually in the form of relatively small upsets from steady state operation, whereas in batch distillation, individual components can completely disappear from the column, first from the reboiler (or still-pot) and then from the entire column.

In spite of these difficulties, a remarkable shift toward batch production technologies has been observed from the early of 1980s. One of the reasons is that the market demand is changing much more frequently than in the past, and product specification requirements are becoming stricter and stricter. The flexibility of a batch process is such that these short-term changes and severe purity requirements can be accommodated. Moreover, because the production amounts in a batch process are usually small, the raw material inventories can be kept to a minimum, which often results in an economic incentive.

Batch distillation is a common method for physical separation of binary and multicomponent mixtures. Many different components and multiple product fractions can be separated in the same batch column, and at a much lower capital cost than would be associated with the relevant train of continuous columns. The streams coming from a batch column may be themselves the desired products; in such a case, they can be directly placed in the market. Otherwise, the required product purities can be maintained by implementing an efficient controller.

A detailed dynamic model of a binary batch distillation column is presented in Chapter 9. The functioning of the column is also described there. The present chapter provides the development of mathematical modelling equations of a practical multicomponent batch distillation process and the dynamic simulation of a set of those differential–algebraic equations. The industry needs a process model that can predict the real-time plant dynamics accurately. In order to represent realistic operation of an actual batch distillation column, a rigorous nonlinear model that considers simultaneous effect of heat and mass transfer operations and fluid flow on the plates is needed. Such a batch distillation model is intended to develop in this chapter. The model consists of material and energy balance equations, algebraic enthalpy and tray hydraulics equations, and the equations for vapour–liquid equilibrium (VLE) predictions and physical property estimations.

11.2 THE PROCESS AND THE MODEL

Unlike unsteady state continuous distillation, in which the transient response results from the upsets in the operating conditions of a column at steady state, batch distillation is inherently an unsteady state process. For a batch rectifier, the steady state is achieved at the end of start-up phase under total reflux condition.

After reaching steady state, the production phase may start as distillate is withdrawn. In the present case study, we will develop a mathematical model of a ternary batch distillation column and the simulated model can be employed to predict the process dynamics at start-up phase as well as at production phase.

It should be stated that the reflux drum, column trays and still-pot are all initially filled with fresh feed of same composition. During the column operation under total reflux condition, the concentration of the lightest component buildups on the upper trays in the column, and the concentrations of the intermediate component and heaviest component decrease in the top of the column but increase in the still-pot. When the concentration of the lightest component in the distillate reaches its specified purity level, then the distillate product withdrawal is begun. The total *batch time* corresponds to the time period which starts at the beginning of the distillate withdrawal and finishes when the instantaneous distillate composition meets a preset value. For temperature sensitive compounds, the optimum batch time plays an important role to avoid the thermal degradation.

Batch operation can be performed in closed-loop as well as in open-loop fashion. First we will briefly discuss the batch processing in closed-loop mode (Barolo and Berto, 1998). In this mode of operation, the objective of the ternary separation is to recover the lightest component and then the intermediate component at a constant purity. By this way, multiple products can be made from a single column. In the industrial practice, the column is started up as usual (described in Chapter 9); then, the lightest component is withdrawn at the required constant purity (say, at composition x_{D1}) implementing a controller until the reflux ratio reaches a specified maximum value. At this point, the reflux rate is lowered (for example, following a ramp decrease) in order to allow the intermediate component to reach the top of the column. When this component has reached the desired purity (say, x_{D2}), constant composition control is started again. Therefore, the *slop cut* is started to withdraw as the reflux rate is lowered and until x_{D2} builds up. Note that startups and shutdowns of batch columns are very frequent and therefore, there is a strong economical incentive to reduce the startup time. For this reason, the lightest component (or first product) withdrawal is started as soon as this component met the composition specification, without waiting for the steady state to be attained.

Now we will analyze the batch operation in open-loop mode (Venkateswarlu and Avantika, 2001). When the concentration of the lightest component in the distillate reaches its specification purity, traditionally the distillate product draw-off is begun. Then gradually the composition of lightest component decreases in the still-pot and naturally, the purity of the distillate also drops. A period of time comes when the distillate stream contains too little of the lightest component to be used for that product and also very little of intermediate component to be used for the next heavier product. At this time, the distillate stream is diverted to another tank as the first slop cut. When the composition of the intermediate component in the distillate reaches its specified purity level, the distillate is diverted to another tank in which second product is collected. When the purity of the material in this tank drops to the specified purity level, the distillate stream is diverted into another tank, and the second slop cut is collected until the average composition of the material remaining in the still-pot and on the trays in the column meets the purity specification of the end product. The end product is what is left in the still-pot and on the trays. Batch distillation operated at a constant reflux ratio condition is a well-known operation in open-loop mode. Note that the slop cuts are generally recycled back to the still-pot. Therefore, the liquid mixture that is charged into the reboiler can be a fresh feed and also with any recycled slop cuts.

Figure 11.1 shows a schematic representation of a batch distillation column used. This batch process is employed to separate a hydrocarbon mixture of cyclohexane, *n*-heptane and toluene. Among these, cyclohexane is the lightest component, *n*-heptane is the intermediate component and toluene is the heaviest

component. The start-up conditions and system specifications are given in Table 11.1. Constants for the enthalpy Equation (11.17) are given in Table 11.2.

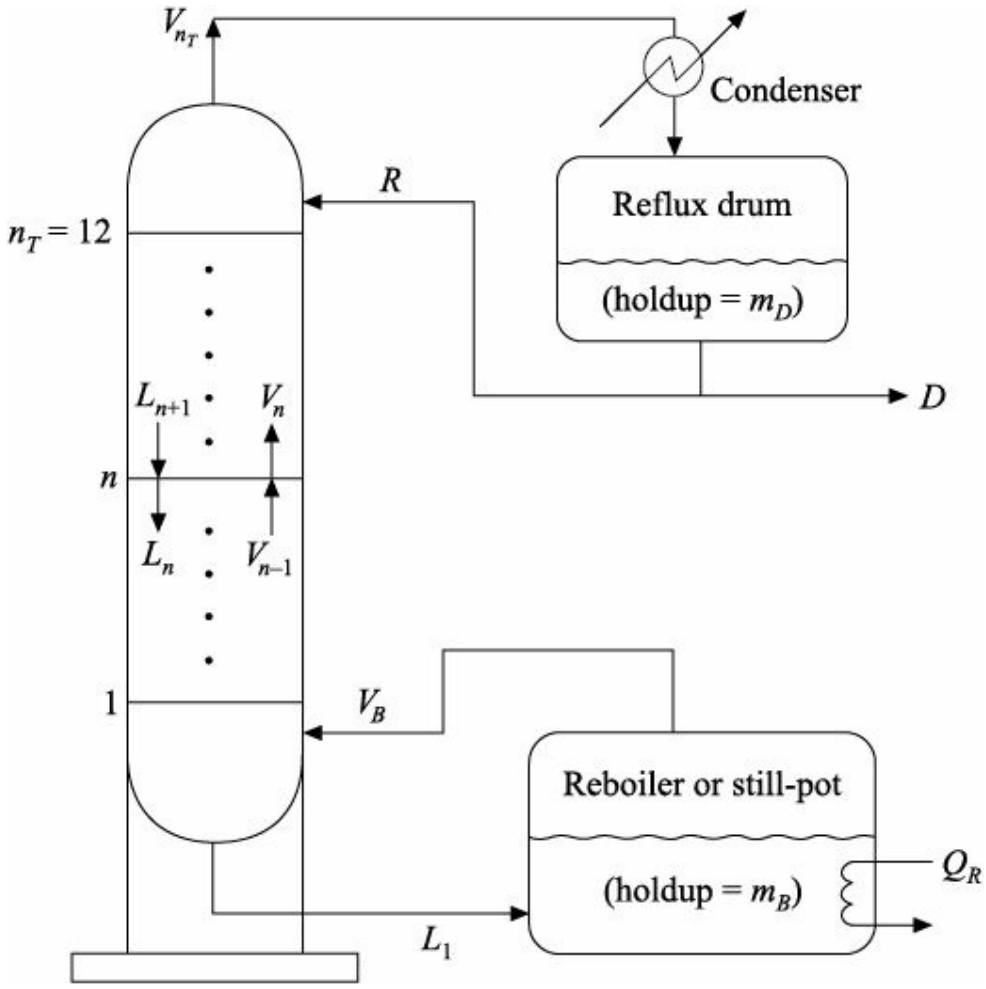

FIGURE 11.1 Schematic representation of the example of multicomponent batch distillation.

Table 11.1 Model and system characteristics

Ternary system: cyclohexane–n-heptane–toluene

Total feed charge, gmol	30000.00
Feed composition (start-up), mol fraction	0.4/0.4/0.2
Tray holdup (start-up), gmol	30.00
Reflux drum holdup, gmol	1000.00
Heat input to the still, kcal/min	200.00
Distillate flow rate (production phase), gmol/min	100.00
Distillate composition (steady state), mol fraction of cyclohexane	0.99
Column diameter, cm	75.00
Integration time interval, min	0.005

Table 11.2 Constants for the enthalpy Equation (11.17)

Component	a_1	a_2	a_3	a_4	*Liquid density* (g/cm^3)
Water	3.224E + 1	1.924E – 3	1.055E – 5	–3.596E – 9	0.998
Carbon monoxide	3.087E + 1	–1.285E – 2	2.789E – 5	–1.272E – 8	0.803
Carbon dioxide	1.980E + 1	7.344E – 2	–5.602E – 5	1.715E – 8	
Carbon disulphide	2.744E + 1	8.127E – 2	–7.666E – 5	2.673E – 8	1.293
Chloroform	2.400E + 1	1.893E – 1	–1.841E – 4	6.657E – 8	1.489
Formaldehyde	2.348E + 1	3.157E – 2	2.985E – 5	–2.300E – 8	0.815
Methane	1.925E + 1	5.213E – 2	1.197E – 5	–1.132E – 8	0.425
Methanol	2.115E + 1	7.092E – 2	2.587E – 5	–2.852E – 8	0.791

Methyl amine	1.148E + 1	1.427E – 1	–5.334E – 5	4.752E – 9	0.703
Acetylene	2.682E + 1	7.578E – 2	–5.007E – 5	1.412E – 8	0.615
Ethylene	3.806E + 0	1.566E – 1	–8.348E – 5	1.755E – 8	0.577
Acetaldehyde	7.716E + 0	1.823E – 1	–1.007E – 4	2.380E – 8	0.778
Ethane	5.409E + 0	1.781E – 1	–6.938E – 5	8.713E – 9	0.548
Ethanol	9.014E + 0	2.141E – 1	–8.390E – 5	1.373E – 9	0.789
Dimethyl amine	–1.717E – 1	2.695E – 1	–1.329E – 4	2.339E – 8	0.656
Propylene	3.710E + 0	2.345E – 1	–1.160E – 4	2.205E – 8	0.612
Acetone	6.301E + 0	2.606E – 1	–1.253E – 4	2.038E – 8	0.790
Propane	–4.224E + 0	3.063E – 1	–1.586E – 4	3.215E – 8	0.582
1-Butene	–2.994E + 0	3.532E – 1	–1.990E – 4	4.463E – 8	0.595
n-Butane	9.487E + 0	3.313E – 1	–1.108E – 4	–2.822E – 9	0.579
iso-Butane	–1.390E + 0	3.847E – 1	–1.846E – 4	2.895E – 8	0.557
Cyclopentane	–5.362E + 1	5.426E – 1	–3.031E – 4	6.485E – 8	0.745
1-Pentene	–1.340E – 1	4.329E – 1	–2.317E – 4	4.681E – 8	0.640
n-Pentane	–3.626E + 0	4.873E – 1	–2.580E – 4	5.305E – 8	0.626
iso-Pentane	–9.525E + 0	5.066E – 1	–2.729E – 4	5.723E – 8	0.620
Chlorobenzene	–3.389E + 1	5.631E – 1	–4.522E – 4	1.426E – 7	1.106
Benzene	–3.392E + 1	4.739E – 1	–3.017E – 4	7.130E – 8	0.885
Phenol	–3.584E + 1	5.983E – 1	–4.827E – 4	1.527E – 7	1.059
Cyclohexane	–5.454E + 1	6.113E – 1	–2.523E – 4	1.321E – 8	0.779
1-Hexene	–1.746E + 0	5.309E – 1	–2.903E – 4	6.054E – 8	0.673
n-Hexane	–4.413E + 0	5.820E – 1	–3.119E – 4	6.494E – 8	0.659
Toluene	–2.435E + 1	5.125E – 1	–2.765E – 4	4.911E – 8	0.867
1-Heptene	–3.303E + 0	6.297E – 1	–3.512E – 4	7.607E – 8	0.697
n-Heptane	–5.146E + 0	6.762E – 1	–3.651E – 4	7.658E – 8	0.684
o-Xylene	–1.585E + 1	5.962E – 1	–3.443E – 4	7.528E – 8	0.880
m-Xylene	–2.917E + 1	6.297E – 1	–3.747E – 4	8.478E – 8	0.864
p-Xylene	–2.509E + 1	6.042E – 1	–3.374E – 4	6.820E – 8	0.861
n-Octane	–6.096E + 0	7.712E – 1	–4.195E – 4	8.855E – 8	0.703
n-Nonane	–8.374E + 0	8.729E – 1	–4.823E – 4	1.031E – 7	0.718

Reprinted with permission from (Reid, R.C., Prausnitz, J.M., and Poling, B.E. (1987). *The Properties of Gases and Liquids*, 4th ed., McGraw-Hill Book Company, New York) the McGraw-Hill Companies.

The mathematical model will be formulated on the following assumptions:

- Staged batch distillation column with trays numbered from the bottom and up (total thirteen trays including still-pot).
- Perfect mixing and thermal equilibrium on all trays.
- Constant stage pressures (one atmosphere).
- Inefficient trays (constant vapour-phase Murphree efficiency = 80%).
- Negligible tray vapour holdups.
- Algebraic vapour and liquid enthalpy equations.
- Total condensation with no subcooling in the condenser.
- Negligible coolant and steam dynamics in the condenser and reboiler respectively.
- Nonlinear Francis weir formula for tray hydraulics calculations.
- Varying liquid holdup in each tray excluding reflux drum. (Supposing the liquid holdup in the reflux drum remains unchanged at total reflux condition. In the production phase, the variations of liquid

holdup in the reflux drum for most of the practical columns are negligibly small due to the nearly perfect level control).

- Hildebrand regular solution model for VLE calculations.

11.2.1 Material and Energy Balance Equations

The total continuity (one per tray), component continuity ($N_C - 1$ per tray, where N_C is the number of components) and energy balance (one per tray) equations for different stages are summarized in the following text.

Reboiler (subscript 'B')

Total continuity: $$\dot{m}_B = L_1 - V_B = -D \tag{11.1}$$

Component continuity: $$\dot{m}_B \dot{x}_{B,j} = L_1 x_{1,j} - V_B y_{B,j} \tag{11.2}$$

Energy equation: $$\dot{m}_B \dot{H}_B^L = Q_R + L_1 H_1^L - V_B H_B^V \tag{11.3}$$

Bottom Tray (subscript '1')

Total continuity: $$\dot{m}_1 = L_2 + V_B - L_1 - V_1 \tag{11.4}$$

Component continuity: $$\dot{m}_1 \dot{x}_{1,j} = L_2 x_{2,j} + V_B y_{B,j} - L_1 x_{1,j} - V_1 y_{1,j} \tag{11.5}$$

Energy equation: $$\dot{m}_1 \dot{H}_1^L = L_2 H_2^L + V_B H_B^V - L_1 H_1^L - V_1 H_1^V \tag{11.6}$$

Intermediate Trays (subscript 'n', where n = 2 to 11)

Total continuity: $$\dot{m}_n = L_{n+1} + V_{n-1} - L_n - V_n \tag{11.7}$$

Component continuity: $$\dot{m}_n \dot{x}_{n,j} = L_{n+1} x_{n+1,j} + V_{n-1} y_{n-1,j} - L_n x_{n,j} - V_n y_{n,j} \tag{11.8}$$

Energy equation: $$\dot{m}_n \dot{H}_n^L = L_{n+1} H_{n+1}^L + V_{n-1} H_{n-1}^V - L_n H_n^L - V_n H_n^V \tag{11.9}$$

Top Tray (subscript 'n_T')

Total continuity: $$\dot{m}_{n_T} = R + V_{n_T-1} - L_{n_T} - V_{n_T} \tag{11.10}$$

Component continuity: $$\dot{m}_{n_T} \dot{x}_{n_T,j} = R x_{D,j} + V_{n_T-1} y_{n_T-1,j} - L_{n_T} x_{n_T,j} - V_{n_T} y_{n_T,j} \tag{11.11}$$

Energy equation: $$\dot{m}_{n_T} \dot{H}_{n_T}^L = R H_D^L + V_{n_T-1} H_{n_T-1}^V - L_{n_T} H_{n_T}^L - V_{n_T} H_{n_T}^V \tag{11.12}$$

Condenser and Reflux Drum (subscript 'D')

Total continuity: $$\dot{m}_D = V_{n_T} - R - D \tag{11.13}$$

Component continuity: $$\dot{m}_D \dot{x}_{D,j} = V_{n_T} y_{n_T,j} - (R + D) x_{D,j} \tag{11.14}$$

In the above mathematical model, $x_{n,j}$ is the mole fraction of component j in a liquid stream leaving nth tray, $y_{n,j}$ the mole fraction of component j in a vapour stream leaving nth tray, $x_{D,j}$ the mole fraction of component j in the liquid distillate, $x_{B,j}$ the mole fraction of component j in the liquid of the still-pot, $y_{B,j}$ the mole fraction of component j in the boil-up vapour, L_n the liquid flow rate leaving nth tray (gmol/min), V_n the vapour flow rate leaving nth tray (gmol/min), R the reflux flow rate (gmol/min), D the distillate flow rate (gmol/min), V_B the vapour boil-up rate (gmol/min), m_n the liquid holdup on nth tray

(gmol), m_D the liquid holdup in the reflux drum (gmol), m_B the liquid holdup in the still-pot (gmol), H_n^L the enthalpy of a liquid stream leaving nth tray (cal/gmol), H_n^V the enthalpy of a vapour stream leaving nth tray (cal/gmol), H_B^V the enthalpy of boil-up vapour (cal/gmol) and Q_R the heat input to the still-pot (cal/min). The over-dot symbol (.) is used to denote the time derivative. The above batch distillation model also includes few terms, for example, $\dot{m}\dot{x}$ that represents the time derivative of the multiplication of variables m and x.

In general, the liquid holdups on all trays are calculated solving the total continuity-equations, and the liquid-phase compositions on all trays including reflux drum and still-pot are calculated from the component continuity equations. Computations of internal liquid flow rates for all trays are performed employing the Francis weir formula. The vapour and liquid enthalpies are preferred to compute using the algebraic form of equations. In other words, the energy balance Equations (11.3), (11.6), (11.9) and (11.12) are not usually employed to calculate the phase enthalpy. Rather, these energy equations, with substituting zero in the left hand sides, have been used for the calculation of vapour flow rates. We must remember that no heat balance equation is included in the model of condenser–reflux drum system because there is no need of vapour flow rate calculations.

Now we wish to study an alternative approach to compute the process variables of a batch distillation column. This approach is proposed by Distefano (1968), and further used by Venkateswarlu and Avantika (2001). Equations (11.2), (11.5), (11.8), (11.11), and (11.14) describe the rate of change of compositions with time; Equations (11.3), (11.6), (11.9), and (11.12) describe vapour flow rates; and Equations (11.4), (11.7), (11.10), and (11.13) describe liquid flow rates. Note that Equation (11.13) is used to calculate R in the open-loop batch operation. In the liquid and vapour rate calculations, the rate of change of holdup and liquid enthalpy is approximated by a numerical differentiation procedure of low order that replaces dm_n/dt (or $\dot{m}_n$) as Δm_n, and dH_n^L/dt (or $\dot{H}_n^L$) as δH_n^L. Since the flow rates are very large compared with the rate of change of holdup and enthalpy over a single integration interval, it is believed that this approximation (which greatly simplifies the computational procedure) is justified. The molar holdup variations on plates (except still-pot) may be considered by assuming volume holdup as constant and variation of liquid density as a function of temperature, pressure and composition.

11.2.2 Enthalpy Calculations

Since the mathematical model involves energy balances, it requires values of the liquid and vapour enthalpies throughout the column and throughout the operation. Therefore, the following *ideal gas enthalpy* (H^V) relationship can be provided at temperature T as:

$$H^V = \int_{T_0}^{T} C_p \, dT = \sum_{k=1}^{4} \frac{a_k (T^k - T_0^k)}{k} \qquad (11.15)$$

where T_0 is the datum temperature. The *heat capacity* of the ideal gas (C_p) is represented by (Reid, Prausnitz and Poling, 1987):

$$C_p = a_1 + a_2 T + a_3 T^2 + a_4 T^3 \qquad (11.16)$$

If the datum temperature is equal to zero (i.e., $T_0 = 0$), then Equation (11.15) yields

$$H^V = a_1 T + \frac{a_2 T^2}{2} + \frac{a_3 T^3}{3} + \frac{a_4 T^4}{4} \qquad (11.17)$$

Values of the four constants a_1 through a_4 with T in K and C_p in J/(gmol)(K) are given for several components in Table 11.2.

Once the ideal gas enthalpy is known, then the enthalpy of a liquid (H^L) can be computed using the following form of relationship:

$$H^L = H^V - \neg \qquad (11.18)$$

Using Clausius–Clapeyron equation,

$$\frac{d \ln P^S}{dP^S} = \frac{\lambda}{RT^2} \qquad (11.19)$$

and the Antoine equation

$$\ln P^S = A - \frac{B}{T + C}, \qquad (11.20)$$

the following expression is obtained for the latent heat of vaporization ($\neg$):

$$\lambda = RT^2 \left[\frac{B}{(C+T)^2} \right] \qquad (11.21)$$

The calculated value of the latent heat of vaporization will be in kJ/gmol if the universal gas constant (R) is equal to 8.314 $\triangleq$ 10^{-3} kJ/(gmol)(K), and the values of vapour pressure (P^S) and temperature (T) are taken in mm Hg and K, respectively. Remember that Equations (11.17) and (11.18) correlate the pure component enthalpies with the temperature. The Fortran (90) code is given in Program 11.1 to provide the step-by-step computations of liquid and vapour enthalpies in the example ternary batch distillation simulator.

PROGRAM 11.1 *Computer Program* (*subroutine*) *for Liquid and Vapour Enthalpies*

```
! Inputs: T (degree C), X (mole fraction), Y (mole fraction)
! Outputs: HL (cal/gmol), HV (cal/gmol)
! A, B, C, D = Constants in ideal gas enthalpy Equation (11.17)
! Ant_B, Ant_C = Antoine constants in Equation (11.21)
! HL, HV = Liquid and vapour phase enthalpies respectively
! Hvap(i) = Enthalpy of a pure component i in the vapour-phase in cal/
! gmol
! Lamda(i) = Latent heat of vaporization of a pure component i in cal/
! gmol
! NC = Number of components
! R = Universal gas constant (= 8.314 ≙ 10^-3 kJ/(gmol)(K))
! T = Tray temperature
! TK = Tray temperature in K
! X(i) = Mole fraction of a component i in the liquid-phase
! Y(i) = Mole fraction of a component i in the vapour-phase

SUBROUTINE ENTH(T,X,Y,HL,HV)
IMPLICIT NONE
INTEGER::i
INTEGER,PARAMETER::NC=3
```

```
REAL*8,INTENT(IN)::T
REAL*8,DIMENSION(NC),INTENT(IN)::X,Y
REAL*8,INTENT(OUT)::HL,HV
REAL*8,PARAMETER::R=8.314 D-3
REAL*8::TK
REAL*8,DIMENSION(NC)::A,B,C,D,Ant_B,Ant_C,Hvap,Lamda

!—Initialization—! '1' denotes for cyclohexane, '2' for n-heptane and
! '3' for toluene

A(1)=-54.54 D0
B(1)= 0.6113 D0
C(1)=-2.523 D-4
D(1)= 1.321 D-8
A(2)=-5.146 D0
B(2)= 0.6762 D0
C(2)=-3.651 D-4
D(2)= 7.658 D-8

A(3)=-24.35 D0
B(3)= 0.5125 D0
C(3)=-2.765 D-4
D(3)= 4.911 D-8

!——Antoine constants——!

Ant_B(1)=2766.63 D0
Ant_B(2)=2911.32 D0
Ant_B(3)=3096.52 D0

Ant_C(1)=-50.50 D0
Ant_C(2)=-56.51 D0
Ant_C(3)=-53.67 D0

TK=T+273.0

!——Calculation of Lamda and HV——!
! 1 kJ/gmol = 238.834 cal/gmol and so, 1 J/gmol = 0.238834 cal/gmol

DO i=1,NC
Hvap(i)=((A(i)*TK)+((B(i)/2.0)*(TK**2))+((C(i)/3.0)*(TK**3))+((D(i)/
& 4.0)*(TK**4)))*0.238834
Lamda(i)=((R*TK*TK*Ant_B(i))/((Ant_C(i)+TK)**2))*238.834
END DO
HV=(Y(1)*Hvap(1))+(Y(2)*Hvap(2))+(Y(3)*Hvap(3))

!——Calculation of HL——!

HL=(X(1)*(Hvap(1)-Lamda(1)))+(X(2)*(Hvap(2)-Lamda(2)))+
& (X(3)*(Hvap(3)-Lamda(3)))

END SUBROUTINE ENTH
```

11.2.3 Tray Hydraulics

In the present study, the nonlinear version of the Francis weir formula is employed to calculate the liquid flow rate leaving a tray. The same formula is also used in the binary distillation columns (Chapters 9 and 10). The equation is restated here as

$$L_n = \frac{\mathrm{DENSA}_n \times W_L \times 999 \left\{ \dfrac{183.2 \times m_n \times \mathrm{MWA}_n}{\mathrm{DENSA}_n \times \mathrm{DCOL} \times \mathrm{DCOL}} - \dfrac{W_H}{12} \right\}^{1.5}}{\mathrm{MWA}_n} \qquad (11.22)$$

where

L_n = liquid flow rate leaving nth tray in lbmol/h

DCOL = column diameter in inch

DENSA_n = average density of the liquid mixture on nth tray in lb/ft^3

m_n = liquid holdup on nth tray in lbmol

MWA_n = average molecular weight of the liquid mixture on nth tray in $\mathrm{lb_m}$/lbmol

W_L = weir length in inch

W_H = weir height in inch

The Fortran (90) code, which provides the computations of the internal liquid flow rates in the ternary batch distillation simulator, is given in Program 11.2.

PROGRAM 11.2 *Computer Program* (*subroutine*) *for Tray Hydraulics*

```
! Note that the output of the subroutine, L is in gmol/min although
! Equation (11.22) is
! derived with different unit.

! Inputs: MG (gmol), X (mole fraction), WH (in), WL (in), DCOL (in)
! Output: L (gmol/min)
! L = Liquid flow rate
! Lfps = Liquid flow rate in lbmol/h
! M = Tray holdup in lbmol
! MG = Tray holdup
! WH, WL, DCOL = Weir height, weir length and column diameter
! respectively
! X = Liquid-phase mole fraction

SUBROUTINE HYDRAU(MG,X,L,WH,WL,DCOL)
IMPLICIT NONE
INTEGER,PARAMETER::NC=3
REAL*8,DIMENSION(NC),INTENT(IN)::X
REAL*8,INTENT(IN)::MG,WH,WL,DCOL
REAL*8,INTENT(OUT)::L
REAL*8::CONST,MWA,DENSA,Lfps,M
CALL MWDENS(X(1:NC),MWA,DENSA)
M=MG*0.0022045855                          ! 1 gmol = 0.0022045855 lbmol
CONST=183.2*M*MWA/(DENSA*DCOL*DCOL)-WH/12
IF(CONST .LE. 0.00)GO TO 10
Lfps=DENSA*WL*999.0*((183.2*M*MWA/(DENSA*DCOL*DCOL)-WH/12)**1.5)/
& MWA
L=Lfps*7.56                                 ! 1 lbmol/h = 7.56 gmol/min
RETURN
10 L=0.00

RETURN

END SUBROUTINE HYDRAU
```

11.2.4 Molecular Weight and Density of the Tray Liquid

The average molecular weight of a liquid mixture (MWA) on the distillation tray can be estimated knowing the molecular weight (MW) and liquid-phase composition (x) of all components. In the sample multicomponent batch simulator, the following equation is used:

$$\text{MWA} = \sum_{j=1}^{N_c} \text{MW}(j)\, x(j) \qquad \text{[from Equation (9.20)]}$$

Similarly, the average mixture density in the liquid-phase (DENSA) may be determined knowing the density (DENS) and liquid-phase composition of all individual components present in the mixture. It is computed employing Equation (9.21):

$$\text{DENSA} = \sum_{j=1}^{N_c} \text{DENS}(j)\, x(j) \qquad \text{[from Equation (9.21)]}$$

The Fortran (90) code, which can compute MWA and DENSA in the distillation simulator, is given in Program 11.3.

PROGRAM 11.3 *Computer Program* (*subroutine*) *for Molecular Weight and Density*

```
! Input: X (mole fraction)
! Outputs: MWA (lbm/lbmol), DENSA (lb/ft3)
! DENS(J) = Density of component J in the liquid-phase in lb/ft3
! DENSA = Average density of a liquid mixture
! MW(J) = Molecular weight of component J in lbm/lbmol
! MWA = Average molecular weight
! X(J) = Mole fraction of component J in the liquid-phase

SUBROUTINE MWDENS(X,MWA,DENSA)
IMPLICIT NONE
INTEGER::J
INTEGER,PARAMETER::NC=3
REAL*8,DIMENSION(NC),INTENT(IN)::X
REAL*8,INTENT(OUT)::MWA,DENSA
REAL*8,DIMENSION(NC)::MW,DENS

!—Initialization—! '1' denotes for cyclohexane, '2' for n-heptane and
! '3' for toluene

MW(1)=84.162 D0
MW(2)=100.205 D0
MW(3)=92.141 D0

DENS(1)=48.63 D0
DENS(2)=42.7 D0
DENS(3)=54.123 D0
DENSA=0.0 D0
MWA=0.00 D0

DO 1 J=1,NC
MWA=X(J)*MW(J)+MWA
1 DENSA=X(J)*DENS(J)+DENSA

RETURN

END SUBROUTINE MWDENS
```

11.2.5 Equilibrium Relationship

The ultimate success of any distillation model depends upon the accuracy of the vapour-liquid equilibrium relationship employed. The most commonly used form of this relationship for multicomponent mixtures is:

$$y^*_{n,j} = k_{n,j}\, x_{n,j} \qquad (11.23)$$

For any tray n, $y^*_{n,j}$ is the equilibrium vapour composition of component j. The vapour–liquid equilibrium coefficient, $k_{n,j}$ is used most frequently as a function of liquid-phase composition (vapour as well as liquid phase composition if the nonideality is considered in both the phases), temperature and pressure. It is assumed that the example batch distillation column is operated at constant atmospheric pressure. Under such assumption, it is reasonable to neglect the vapour-phase nonideality. Therefore, considering only the liquid-phase nonideality, the above Equation (11.23) yields for nth tray:

$$y^*_{n,j} = k_{n,j}\, x_{n,j} = \frac{\gamma_{n,j}\, x_{n,j}\, P^S_{n,j}}{P_t} \qquad (11.24)$$

where γ_j is the activity coefficient of component j in the liquid phase, P^S_j the vapour pressure of component j and P_t the total pressure (one atmosphere). The computational problem here is to find each $k_{n,j}$ such that

$$\sum_{j=1}^{N_c} y^*_{n,j} = 1.0 \qquad (11.25)$$

which is commonly referred to as a *bubble-point* calculation. For the multicomponent batch simulator, the Hildebrand regular solution model is applied to predict the vapour-liquid equilibrium. Details of the Hildebrand model are given in Chapter 8. The Fortran (90) code is developed and given in Program 11.4 to carry out the bubble-point calculations for the batch distillation process.

PROGRAM 11.4 *Computer Program* (*subroutine*) *for Bubble-point Calculations*

```
! Inputs: X (mole fraction), P (mm Hg)
! Outputs: Y (mole fraction), T (degree C)
! A(J), B(J), C(J) = Antoine constants for component J
! del(J) = Solubility parameter of component J in (cal/ml)**0.5
! delavg = Average value of del
! Gama(J) = Activity coefficient of component J
! P = Column pressure
! Ps(J) = Vapour pressure of component J in mm Hg
! R = Universal gas constant in cal/(gmol)(K)
! T = Tray temperature
! TK = Tray temperature in K
! V(J) = Liquid molar volume of component J in ml/gmol
! X(J) = Mole fraction of component J in the liquid-phase
! Y(J) = Mole fraction of component J in the vapour-phase

SUBROUTINE BUBPT(T,X,Y,P)
IMPLICIT NONE
INTEGER,PARAMETER::NC=3
REAL*8,INTENT(IN)::P
REAL*8,DIMENSION(NC),INTENT(IN)::X
```

```
REAL*8,INTENT(OUT)::T
REAL*8,DIMENSION(NC),INTENT(OUT)::Y
INTEGER::J,LOOP
REAL*8,PARAMETER::R=1.987 D0
REAL*8,DIMENSION(NC)::V,del,SON,Gama,Ps,A,B,C,MON,PON
REAL*8::TK,SUMY,delavg,F,FSLOPE

!——Initialization——! ‘1’ denotes for cyclohexane, ‘2’ for n-heptane and
! ‘3’ for toluene

V(1)=108.7 D0
V(2)=147.5 D0
V(3)=106.8 D0

del(1)=8.20 D0
del(2)=7.43 D0
del(3)=8.92 D0

A(1)=15.7527 D0
B(1)=2766.63 D0
C(1)=-50.50 D0
A(2)=15.8737 D0
B(2)=2911.32 D0
C(2)=-56.51 D0

A(3)=16.0137 D0
B(3)=3096.52 D0
C(3)=-53.67 D0

LOOP=0
TK=320.0 D0
11 LOOP=LOOP+1
IF(LOOP .GT. 500) GO TO 31 ! maximum number of iterations = 500

! Calculation of delavg

delavg=((X(1)*V(1)*del(1))+(X(2)*V(2)*del(2))+
& (X(3)*V(3)*del(3)))/((X(1)*V(1))+(X(2)*V(2))+(X(3)*V(3)))

SUMY=0.00 D0
DO 51 J=1,NC

! Calculation of activity coefficients

SON(J)=V(J)*((del(J)-delavg)**2)
Gama(J)=EXP(SON(J)/(R*TK))

! Calculation of vapour pressures

Ps(J)=EXP(A(J)-(B(J)/(TK+C(J))))

! Calculation of component compositions in the vapour-phase

Y(J)=(Gama(J)*Ps(J)*X(J))/P

51 SUMY=SUMY+Y(J)
IF(ABS(SUMY-1) .LT. 0.00001)RETURN ! tolerance limit = 1.0E-5
F=SUMY-1
FSLOPE=0.0 D0
DO 21 J=1,NC
MON(J)=B(J)/((TK+C(J))**2)
PON(J)=SON(J)/(R*(TK**2))
21 FSLOPE=FSLOPE+(Y(J)*(MON(J)-PON(J)))
TK=TK-F/FSLOPE
T=TK-273.0
```

```
GO TO 11

31 STOP

END SUBROUTINE BUBPT
```

11.3 SUMMARY AND CONCLUSIONS

In this chapter, the mathematical model of a practical ternary batch distillation column is presented and a step-by-step calculation procedure is outlined. The dynamic model incorporates total and partial mass balance equations, and energy balance equations together with thermodynamic relations, that include bubble point temperature computation and avoid constant relative volatility concept. The process model also includes the algebraic enthalpy equations along with the nonlinear tray hydraulics equation. The value of Murphree vapour-phase tray efficiency is utilized to compute the actual component composition in the vapour-phase. Details of this are reported in Chapter 9 and hence are not given here again.

The prescribed batch column can work at infinite reflux ratio in order to stabilize it, and then with a finite reflux ratio as the distillate is withdrawn. Notice that the calculation related to the slop cut is not provided in the present chapter. You need to incorporate it for the prescribed batch distillation simulator.

EXERCISES

11.1 What is the maximum number of slop cuts involved in fractionating a mixture having N_C number of components?

11.2 Suppose a multicomponent distillation column is employed to fractionate a mixture of N_C components. Why $N_C - 1$ (instead of N_C) number of component continuity equations are required to derive for each tray?

11.3 The reduced form of the Clapeyron equation is

$$\frac{\lambda}{ZRT_c} = \frac{B}{T_c}\left[\frac{T_r}{T_r + (C/T_c)}\right]^2 \qquad (11.26)$$

where

Z = compressibility factor
R = universal gas constant
T_C = critical temperature
$T_r = T/T_C$ = reduced temperature
B, C = antoine constants
$\neg$ = latent heat of vaporization

Compare the above Clapeyron equation with Equation (11.21) and comment on their applications.

11.4 Develop the dynamic multicomponent batch distillation simulators using the relevant data given in Table 11.1 for the following systems:

(i) cyclohexane–toluene–chlorobenzene
(ii) *n*-butane–*n*-pentane–*n*-hexane
(iii) toluene–*n*-butanol–*n*-octanol (toluene–*n*-butanol form a binary azeotrope and *n*-octanol acts as a solvent to break the azeotrope).

11.5 Modify the ternary batch simulators that are mentioned in the previous Problem 11.4 with increasing

the number of theoretical trays and considering the production of liquid as well as vapour distillate.

11.6 What changes are you expecting due to the increase of number of theoretical trays in a batch rectifier? Please verify your expectations with performing the simulation experiments.

11.7 To investigate the simulated process dynamics for the above three systems (Problem 11.4), plot the compositions of lightest, intermediate and heaviest components in the distillate for the batch time of 40 hours.

REFERENCES

Barolo, M., and Berto, F. (1998). Composition control in batch distillation: binary and multicomponent mixtures, *Ind. Eng. Chem. Res.*, 37, 4689–4698.

Distefano, G.P. (1968). Mathematical modeling and numerical integration of multicomponent batch distillation equations, *AIChE J.*, 14, 190–199.

Reid, R.C., Prausnitz, J.M., and Poling, B.E. (1987). *The Properties of Gases and Liquids*, 4th ed., McGraw-Hill Book Company, New York.

Venkateswarlu, C., and Avantika, S. (2001). Optimal state estimation of multicomponent batch distillation, *Chem. Eng. Sci.*, 56, 5771–5786.

12

Equilibrium Flash Vaporization

12.1 INTRODUCTION

The flash is a single-stage separation technique in which a feed mixture is partially vaporized to produce a vapour that is enriched with more volatile components and a liquid that is richer in the less volatile components. The vapour and liquid streams leaving the drum are in equilibrium, and therefore this operation is called *equilibrium flash vaporization*. The split of a feed mixture in a flash drum can be carried out by two different ways as follows:

(i) by raising the temperature of the liquid feed to a temperature (T), which lies in between the bubble-point temperature and the dew-point temperature of that feed at a specified constant pressure (P), and

(ii) by reducing the pressure on the feed stream.

In practice, this partial vaporization of a multicomponent feed mixture is commonly conducted by reducing the pressure on the feed stream rather than by heating the feed at constant pressure. However, the two types of flash calculations that are commonly made are generally referred to as *isothermal* and *adiabatic* flashes. The present discussion is confined to these two single-stage separation processes.

12.2 ISOTHERMAL FLASH

The name *isothermal flash* reveals that the temperature of the contents of the flash drum as well as the vapour and liquid streams produced by the flash is fixed at T. However, the flash temperature may not be equal to the feed temperature prior to its flashing. The schematic diagram of a flash process is shown in Figure 12.1. Before performing the flash calculations, we need to clear about the known and unknown terms associated in the problem.

An isothermal flash process can mathematically be described by the independent equations, which are given in the following text. The state of equilibrium for a two-phase system may be described as:

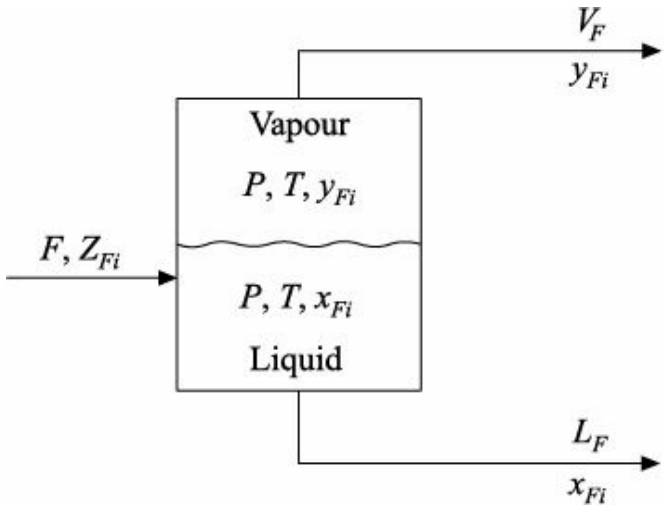

FIGURE 12.1 Flash process.

$$\text{Total } N_c + 2 \text{ equations: } \begin{cases} y_{Fi} = k_{Fi} x_{Fi} \\ \sum_{i=1}^{N_c} y_{Fi} = 1 \\ \sum_{i=1}^{N_c} x_{Fi} = 1 \end{cases} \qquad (i = 1, 2, 3, ..., N_c) \qquad (12.1)$$

where N_c is the total number of components, k_{Fi} represents the equilibrium coefficient of component i evaluated at T and P, and y_{Fi} and x_{Fi} are the compositions of component i in the produced vapour and liquid streams, respectively. In addition, the material balance for any component i around the flash chamber gives:

$$\text{Total } N_c \text{ equations: } \{FZ_{Fi} = V_F y_{Fi} + L_F x_{Fi}\} \qquad (i = 1, 2, 3, ..., N_c) \qquad (12.2)$$

where F is the flow rate of liquid feed, Z_{Fi} is the feed composition for component i, and L_F and V_F are the flow rates of exit liquid and vapour streams, respectively. Equation (12.2) can be extended to:

$$F \sum_{i=1}^{N_c} Z_{Fi} = V_F \sum_{i=1}^{N_c} y_{Fi} + L_F \sum_{i=1}^{N_c} x_{Fi} \qquad (12.3)$$

or

$$F = V_F + L_F \qquad (12.4)$$

By the substitution of the first expression Equation (12.1) (i.e., $y_{Fi} = k_{Fi} x_{Fi}$) into Equation (12.2) and after algebraic simplifications, we obtain

$$x_{Fi} = \frac{Z_{Fi}}{L_F/F + V_F k_{Fi}/F} \qquad (12.5)$$

that is,

$$x_{Fi} = \frac{Z_{Fi}}{(1 - V_F/F) + (V_F k_{Fi}/F)} \qquad (12.6)$$

or

$$x_{Fi} = \frac{Z_{Fi}}{1 - \delta(1 - k_{Fi})} \qquad (12.7)$$

where δ (= V_F/F) is the fraction vaporized in the flash operation.

Now using Equation (12.7), we can write the following expression:

$$F(\delta) = \sum_{i=1}^{N_c} \frac{Z_{Fi}}{[1 - \delta(1 - k_{Fi})]} - 1 \qquad (12.8)$$

Next we need to determine the root δ of the above Equation (12.8) such that $F(\delta) = 0$. In practice, values of δ should be constrained to lie between 0 and 1. Positive value of δ means the flash vaporization occurs, whereas zero value indicates no vaporization.

In the subsequent subsections, the computational approaches have been introduced to deal with the

flash vaporization problems related to ideal and nonideal solutions.

12.2.1 Ideal Mixtures

Problem statement:

Given (N_c + 3): T, P, F, Z_{Fi}

Unknowns ($2N_c$ + 2): V_F, L_F, y_{Fi}, x_{Fi}

where i = 1, 2, 3, ..., N_c.

Solution technique: The following computational steps may help to achieve the desired results for the present type of problems.

Step 1: Calculate vapour–liquid equilibrium coefficient, k_{Fi}, for all components. Using the Antoine Equation (9.28), the vapour pressure of any component $i(P_i^S)$ of a multicomponent mixture with known temperature can be computed easily. Remember that the simple Antoine equation may not be so promising in some cases (e.g., many hydrocarbons). In such situations, an alternative vapour pressure calculating equation[1] can be chosen (details in Chapter 13). However, in case of ideal solutions, the vapour–liquid equilibrium coefficient for any component i may be independent of phase composition. That depends on temperature, if the vapour pressure is a function of temperature only, and total pressure as:

[1] In some correlations as reported in Chapter 13, the vapour pressure is dependent on critical temperature, critical pressure and acentric factor along with system temperature.

$$k_{Fi} = P_i^S/P \qquad (12.9)$$

In the present problem, T and P both are given, so actually k_{Fi}'s are known.

Step 2: Assume δ. The assumed value may be taken as 1.0.

Step 3: Calculate V_F since $\delta = V_F/F$, and then compute L_F from $F = V_F + L_F$.

Step 4: Compute x_{Fi}'s using Equation (12.7).

Step 5: Next it is required to determine y_{Fi}'s using the first expression Equation (12.1).

Step 6: Check the condition $\left|\sum_{i=1}^{N_c} x_{Fi} - 1\right| \leq 1$ tolerance limit. If this condition is satisfied, go to Step 8, otherwise go to the next step.

Step 7: Update δ. The Newton–Raphson convergence technique has been employed here to update δ. The differentiation of Equation (12.8) with respect to δ is represented as follows:

$$F'(\delta) = \sum_{i=1}^{N_c} \frac{Z_{Fi}(1-k_{Fi})}{[1-\delta(1-k_{Fi})]^2} \qquad (12.10)$$

According to the Newton–Raphson method,

$$\delta_{new} = \delta_{old} - \frac{F(\delta)}{F'(\delta)} \qquad (12.11)$$

To continue the iterative procedure, go back to Step 3.

Step 8: Stop.

Application to an ideal system example

In order to apply the simulation technique developed above, we consider a problem (Holland, 1981), in which a feed mixture of three hypothetical components (denoted by 1, 2 and 3) is to be treated. Use the required information provided as follows:

Component (i)	k_{Fi}	Z_{Fi}
1	$k_{F1}=\frac{T}{300\,P}$	0.33333
2	$k_{F2}=\frac{2T}{100\,P}$	0.33333
3	$k_{F3}=\frac{7T}{200\,P}$	0.33333
	T is in °F and P in atm	
F = 100 mol/h T = 100°F P = 1 atm		

By the use of the simulation algorithm, we obtain e_{27} = 0.787 along with the following results.

L_F = 21.314 mol/h $\qquad$ x_F = 0.701/0.187/0.112

V_F = 78.686 mol/h $\qquad$ y_F = 0.234/0.373/0.393

The above results are obtained by developing a Fortran (90) code given in Program 12.1.

PROGRAM 12.1 *Computer Program for Isothermal Flash Calculations* (*ideal mixture*)

```
! DEL = VF/F
! F (and FF) = Feed rate (mol/h)
! K = Vapour-liquid equilibrium coefficient
! LF = Flow rate of exit liquid stream (mol/h)
! NC = Number of components (= 3)
! P (and PF) = Flash pressure (atm)
! T (and TF) = Flash temperature (degree F)
! VF = Flow rate of exit vapour stream (mol/h)
! XF = Mole fraction of exit liquid
! YF = Mole fraction of exit vapour
! Z (and ZF) = Mole fraction of feed

!-------------------------------------------------!

  PROGRAM ISOTHERMAL_FLASH_IDEAL_SYSTEM
  IMPLICIT NONE
  INTERFACE
!---
  SUBROUTINE FEED_FLASH_IDEAL(T,P,Z,F,LF,VF,XF,YF,DEL)
  REAL*8,INTENT(IN)::T,P,F
  REAL*8,DIMENSION(3),INTENT(IN)::Z
  REAL*8,INTENT(OUT)::LF,VF,DEL
  REAL*8,DIMENSION(3),INTENT(OUT)::XF,YF
  END SUBROUTINE FEED_FLASH_IDEAL
!---
  END INTERFACE
!---DECLARATION---!
  REAL*8::LF,VF,DEL
  REAL*8,PARAMETER::TF=100.00 D0, PF=1.00 D0, FF=100.00 D0
  REAL*8,DIMENSION(3)::ZF,XF,YF
!---
```

```
  OPEN(UNIT=2,File="IDEAL_FLASH.dat")
!--INITIALIZATION--!
!-----------------!
  ZF(1)=0.33333 D0
  ZF(2)=0.33333 D0
  ZF(3)=0.33333 D0
!---
  CALL FEED_FLASH_IDEAL(TF,PF,ZF(1:3),FF,LF,VF,XF(1:3),YF(1:3),DEL)
!---
  PRINT*,TF,PF,ZF(1:3),FF,LF,VF,XF(1:3),YF(1:3),DEL
  WRITE(2,FMT=100)TF,PF,ZF(1:3),FF,LF,VF,XF(1:3),YF(1:3),DEL
100 FORMAT (1X,15(2X,F15.10))
  END FILE 2
  END PROGRAM ISOTHERMAL_FLASH_IDEAL_SYSTEM
!-----------SUBROUTINE-----------!
!--------------------------------!
  SUBROUTINE FEED_FLASH_IDEAL(T,P,Z,F,LF,VF,XF,YF,DEL)
  IMPLICIT NONE
  INTEGER,PARAMETER::NC=3
!---
  REAL*8,INTENT(IN)::T,P,F
  REAL*8,DIMENSION(NC),INTENT(IN)::Z
  REAL*8,INTENT(OUT)::LF,VF,DEL
  REAL*8,DIMENSION(NC),INTENT(OUT)::XF,YF
!---
  INTEGER::J,LOOP
  REAL*8,DIMENSION(NC)::K,PAR1,PAR2,PAR3
  REAL*8::SUMXF,FL,FLSLOPE
!---
  K(1)=(T)/(300*P)
  K(2)=(2*T)/(100*P)
  K(3)=(7*T)/(200*P)
!---
  LOOP=0
  DEL=1.0 D0
11 LOOP=LOOP+1
  IF(LOOP .GT. 100) GO TO 31 !i.e. NO.OF ITERATIONS=100
!---
  VF=DEL*F
  LF=F-VF
!---
  SUMXF=0.00 D0
  DO 51 J=1,NC
  PAR1(J)=1-(DEL*(1-K(J)))
  XF(J)=Z(J)/(PAR1(J))
  YF(J)=K(J)*XF(J)
51 SUMXF=SUMXF+XF(J)
  IF(ABS(SUMXF-1) .LT. 0.0001)RETURN
!---
  FL=SUMXF-1
  FLSLOPE=0.0 D0
  DO 21 J=1,NC
  PAR2(J)=Z(J)*(1-K(J))
  PAR3(J)=PAR2(J)/(PAR1(J)**2)
21 FLSLOPE=FLSLOPE+PAR3(J)
  DEL=DEL-FL/FLSLOPE
  GO TO 11
31 STOP
  END SUBROUTINE FEED_FLASH_IDEAL
```

12.2.2 Nonideal Mixtures

Problem statement:

Given ($N_c + 3$): T, P, F, Z_{Fi}

Unknowns ($2N_c + 2$): V_F, L_F, y_{Fi}, x_{Fi}

where $i = 1, 2, 3, ..., N_c$.

Solution technique: For a nonideal mixture, the vapour–liquid equilibrium coefficient depends on temperature, total pressure and phase compositions. To solve the stated problem, the following sequential steps may be followed for a mixture having nonidealities in both vapour as well as liquid phase.

Step 1: Calculate k_{Fi} at ideal state, $(k_{Fi})_{\text{ideal}}$, using Equation (12.9) for all components. Notice that $(k_{Fi})_{\text{ideal}}$ may be a function of T and P in addition with critical temperature, critical pressure and acentric factor. In the present case, both T and P are given, and additionally, the critical properties may have to know.

Step 2: Assume ψ (= 1.0).

Step 3: Compute V_F since $\psi = V_F/F$, and then calculate L_F from Equation (12.4).

Step 4: Calculate x_{Fi}'s using Equation (12.7). Note that only in the first iteration, $k_{Fi} = (k_{Fi})_{\text{ideal}}$, otherwise $k_{Fi} = (k_{Fi})_{\text{nonideal}} = \dfrac{\hat{f}_i^L / P x_{Fi}}{\hat{f}_i^V / P y_{Fi}}$ [see Equation (13.17)].

Step 5: Calculate y_{Fi}'s. Here, first calculate $(y_{Fi})_{\text{alt}}$ (= $k_{Fi}x_{Fi}$) and then check the following conditions:

$$\left| \sum_{i=1}^{N_c} (y_{Fi})_{\text{alt}} - 1 \right| \leq \text{tolerance limit.}$$

$$\left| \sum_{i=1}^{N_c} x_{Fi} - 1 \right| \leq \text{tolerance limit.}$$

If both the conditions are satisfied, then $y_{Fi} = (y_{Fi})_{\text{alt}}$ and go to Step 8, otherwise the vapour compositions are normalized according to the form $y_{Fi} = \dfrac{(y_{Fi})_{\text{alt}}}{\sum_{i=1}^{N_c} (y_{Fi})_{\text{alt}}}$ and go to the next step.

Step 6: Compute $(k_{Fi})_{\text{nonideal}}$ for all components by the use of a thermodynamic property prediction method (any equation of state model; details in Chapter 13). As mentioned, for a solution having nonidealities in both vapour and liquid phases, the equilibrium coefficient is a function of flash temperature and flash pressure (both given), and of liquid and vapour compositions (calculated in Step 4 and Step 5).

Step 7: Update ψ using an iterative convergence approach. To continue the iterative procedure, go back to Step 3.

Step 8: Stop.

Application to a nonideal system example

The isothermal flash calculation method developed for nonideal mixture will be applied on a complex multicomponent debutanizer column (detailed dynamics presented in Chapter 14). The schematic diagram of the debutanizer distillation accompanying with the flash drum is given in Figure 12.2.

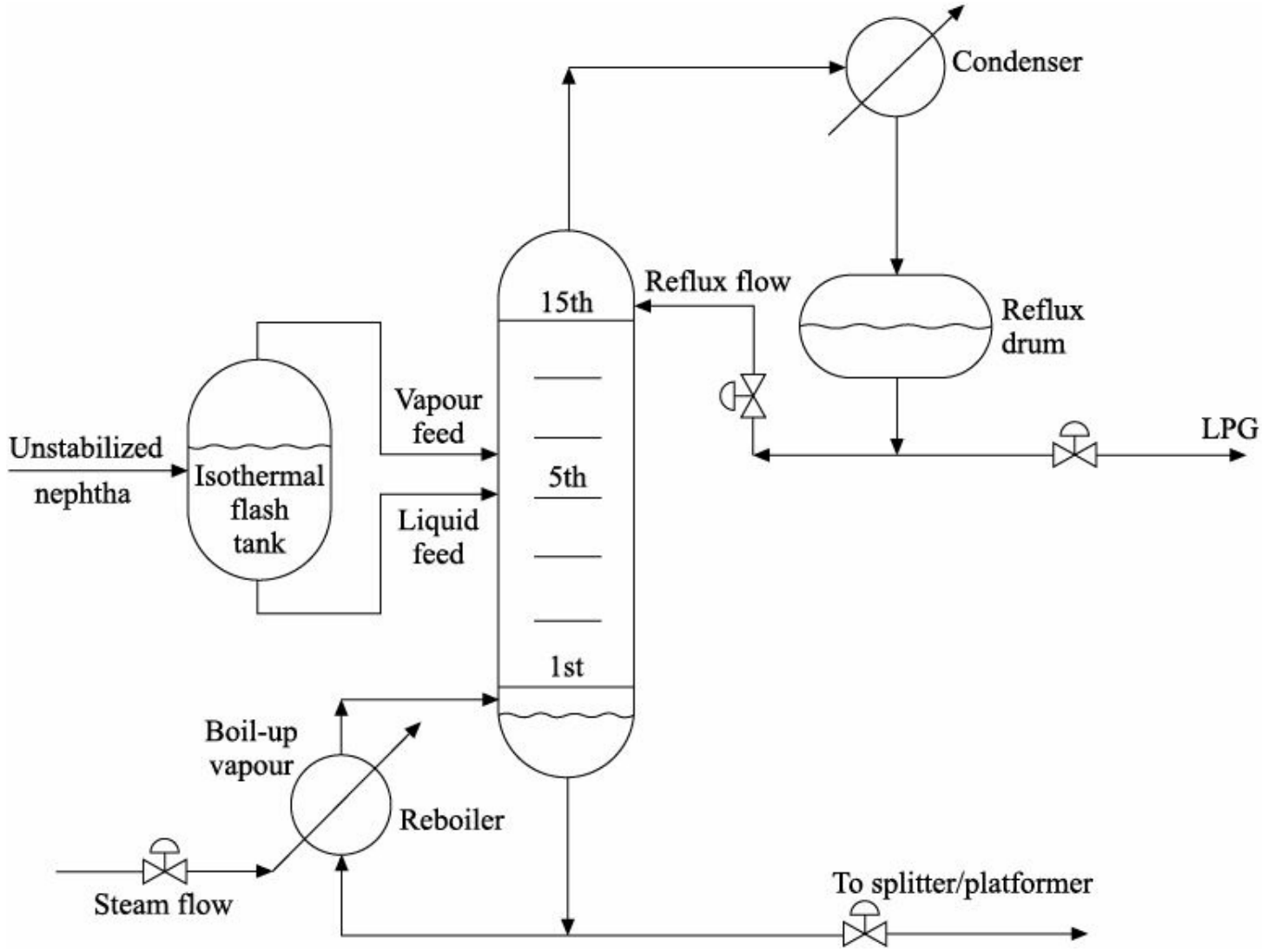

FIGURE 12.2 Schematic diagram of a debutanizer column.

The Fortran (90) code is given in Program 12.2 providing the isothermal flash calculations of a mixture having nonidealities in both vapour and liquid phases. The feed is introduced in a simulated debutanizer column just after splitting the feed into vapour and liquid streams. In the present study, the Soave–Redlich–Kwong (SRK) equation of state has been used to predict the nonidealities. It means the SRK model determines also the vapour–liquid equilibrium coefficient at nonideal condition. Here, the vapour pressure has been calculated using Equation (13.115).

PROGRAM 12.2 *Computer Program* (*subroutine*) *for Isothermal Flash Calculations* (*nonideal mixture*)

```
! Inputs: TF (degree F), P (Psi), X (mole fraction), W, TcF (degree
! F), Pc (Psi), F
! (lbmol/h)
! Outputs: VF (lbmol/h), LF (lbmol/h), YF (mole fraction), XF (mole
! fraction)w

! delta = VF/F
! F = Feed flow rate
! Kay = Vapour-liquid equilibrium coefficient
! LF = Flow rate of exit liquid (from the flash drum)
```

```
! NC = Number of components in the feed
! P = Flash pressure
! Pc = Critical pressure
! Pckp = Critical pressure in kPa
! Press4 = Vapour pressure in kPa
! Pvp = Vapour pressure in Psi
! R = Universal gas constant (= 1.987 Btu/(lbmol)(degree R))
! TcF = Critical temperature
! TcK = Critical temperature in degree K
! TcR = Critical temperature in degree R
! TF = Flash temperature
! Tk = Flash temperature in degree K
! TR = Reduced temperature (degree R/degree R)
! TRK = Reduced temperature (degree K/degree K)
! TTR = Flash temperature in degree R
! VF = Flow rate of exit vapour (from the flash drum)
! W = Acentric factor
! X = Feed composition
! XF = Composition of exit liquid
! YF = Composition of exit vapour

SUBROUTINE NONIDEAL_FEED_FLASH(TF,P,X,F,W,TcF,Pc,VF,LF,XF,YF)
IMPLICIT NONE
INTEGER::i,Loop,j
INTEGER,PARAMETER::NC=8
REAL*8,INTENT(in)::TF,P,F
REAL*8,INTENT(out)::VF,LF
REAL*8,DIMENSION(NC),INTENT(in)::X,W,TcF,Pc
REAL*8,DIMENSION(NC),INTENT(out)::XF,YF
REAL*8::Tk,TTR,VAR,LAR,ZL1,CaL,CbL,ZL2,ZL3,Z_Liq,delta
REAL*8::ZV1,ZV2,ZV3,CaV,CbV,Z_Vap,AAL,AAV,BL,BV,SUMY,SUMX
REAL*8::VAR3,VAR4,LAR3,LAR4,Sumdelta,Func,Derivative
REAL*8,DIMENSION(NC)::Press1,Press2,Press3,Press4,Pvp,Kay,YFalt
REAL*8,DIMENSION(NC)::TR,TRK,TcR,TcK,Pckp,Ym,af,A,B
REAL*8,DIMENSION(NC)::ac,bc,AbarV,AbarL,Derivative1,Derivative2
REAL*8,DIMENSION(NC)::VAR1,VAR2,VVAR,LAR1,LAR2,LLAR
REAL*8,PARAMETER::R=1.987 D0,GA=0.42747 D0,GB=0.08664 D0

!—Unit (temperature) conversion from degree F to degree R and K—!

DO i=1,NC
 TcR(i)=TcF(i)+460.0
 TcK(i)=((5.0/9.0)*(TcF(i)-32.0))+273.0
END DO

!—Unit (pressure) conversion from Psi to kPa—!

DO i=1,NC
 Pckp(i)=Pc(i)*6.89479                ! 1 Psi = 6.89479 kPa
END DO

Tk=((5.0/9.0)*(TF-32.0))+273.0
TTR=TF+460.0

DO i=1,NC
 TRK(i)=TK/TcK(i)
END DO

DO i=1,NC
 Press1(i)=5.92714-(6.09648/TRK(i))-(1.28862*DLOG(TRK(i)))+
 & (0.169347*(TRK(i)**6))
 Press2(i)=15.2518-(15.6875/TRK(i))-(13.4721*DLOG(TRK(i)))+
 & (0.43577*(TRK(i)**6))
```

```
 Press3(i)=Press1(i)+(W(i)*Press2(i))
 Press4(i)=Pckp(i)*EXP(Press3(i))
 Pvp(i)=0.145037*Press4(i)                    ! 1 kPa = 0.145037 Psi
 Kay(i)=Pvp(i)/P
END DO

DO i=1,NC
 Ym(i)=0.480+(1.574*W(i))-(0.176*W(i)*W(i))
END DO

Loop=0
delta=1.0 D0
111 Loop=Loop+1
IF(Loop .GT. 1000) GO TO 133
VF=F*delta
LF=F-VF

DO i=1,NC
 XF(i)=X(i)/(1-(delta*(1-Kay(i))))
 YFalt(i)=Kay(i)*XF(i)
END DO

SumY=0.0 D0
SumX=0.0 D0
DO i=1,NC
 SumY=SumY+YFalt(i)
 SumX=SumX+XF(i)
END DO

IF((ABS(SUMY-1) .LT. 1.0D-4) .AND. (ABS(SUMX-1) .LT. 1.0D-4))THEN
DO i=1,NC
 YF(i)=YFalt(i)
END DO
RETURN

ELSE
DO i=1,NC
 YF(i)=YFalt(i)/SUMY
END DO

DO i=1,NC
 TR(i)=TTR/TcR(i)
 af(i)=1+(Ym(i)*(1-(TR(i)**0.5)))
 ac(i)=GA*R*R*TcR(i)*TcR(i)/Pc(i)
 bc(i)=GB*R*TcR(i)/Pc(i)
 A(i)=((ac(i)**0.5)*af(i))/(R*TTR)
 B(i)=bc(i)/(R*TTR)
END DO

VAR=0.0 D0
LAR=0.0 D0
DO j=1,NC
 VAR=VAR+(YF(j)*A(j))
 LAR=LAR+(XF(j)*A(j))
END DO

DO i=1,NC
 AbarV(i)=A(i)*VAR
 AbarL(i)=A(i)*LAR
END DO

CALL First_Root_Z_Liq(TTR,P,XF(1:NC),W(1:NC),TcF(1:NC),
& Pc(1:NC),ZL1,CaL,CbL)
```

```
CALL Optimum_Z_liq(ZL1,CaL,CbL,ZL2,ZL3,Z_Liq)

CALL First_Root_Z_Vap(TTR,P,YF(1:NC),W(1:NC),TcF(1:NC),
& Pc(1:NC),ZV1,CaV,CbV)
CALL Optimum_Z_Vap(ZV1,CaV,CbV,ZV2,ZV3,Z_vap)

AAL=CaL/P
AAV=CaV/P
BL=CbL/P
BV=CbV/P

!—For vapour—!

DO i=1,NC
 VAR1(i)=(B(i)/Bv)*(Z_vap-1)
 VAR2(i)=(AAv/Bv)*((2*Abarv(i)/AAv)-(B(i)/Bv))
 VAR3=DLOG(1+(Cbv/Z_vap))
 VAR4=DLOG(Z_Vap-Cbv)
 VVAR(i)=EXP(VAR1(i)-(VAR2(i)*VAR3)-VAR4)
END DO

!—For liquid—!

DO i=1,NC
 LAR1(i)=(B(i)/BL)*(Z_liq-1)
 LAR2(i)=(AAL/BL)*((2*AbarL(i)/AAL)-(B(i)/BL))
 LAR3=DLOG(1+(CbL/Z_liq))
 LAR4=DLOG(Z_Liq-CbL)
 LLAR(i)=EXP(LAR1(i)-(LAR2(i)*LAR3)-LAR4)
END DO

!—Equilibrium coefficient (Kay) at nonideal condition—!
DO i=1,NC
 Kay(i)=LLAR(i)/VVAR(i)
END DO

!—Iteration using the Newton-Raphson method—!

Sumdelta=0.0 D0
DO i=1,NC
 Sumdelta=Sumdelta+(X(i)/(1-(delta*(1-Kay(i)))))
END DO
Func=Sumdelta-1.0
Derivative=0.0 D0
DO i=1,NC
 Derivative1(i)=X(i)*(1-Kay(i))
 Derivative2(i)=((1-(delta*(1-Kay(i))))**2)
 Derivative=Derivative+(Derivative1(i)/Derivative2(i))
END DO

delta=delta-Func/Derivative

END IF
GO TO 111

133 STOP

END SUBROUTINE NONIDEAL_FEED_FLASH
```

12.3 ADIABATIC FLASH

The feed mixture to the flash drum may not contain the correct amount of heat needed for vaporization. In such situations, the energy is to be added or withdrawn at the drum as required for the flash operation. In

practice, the heat content of the feed mixture is required to adjust precisely before the feed reaches the flash chamber so that the partial vaporization occurs adiabatically. That means the heat (Q) added at the flash drum is equal to zero. This flash process is usually termed as *adiabatic flash*. It can be described (Holland, 1981) by an enthalpy balance equation in addition to Equations (12.1) and (12.2) that represent the isothermal flash process.

The enthalpy balance gives:

$$FH = V_F H_F + L_F h_F \qquad (12.12)$$

where H is the feed enthalpy, and H_F and h_F are the enthalpies of the exit vapour and liquid streams, respectively. When the produced vapour and liquid streams form ideal solutions, the enthalpies may be computed as follows:

$$\begin{cases} H_F = \sum_{i=1}^{N_c} H_{Fi} y_{Fi} \\ h_F = \sum_{i=1}^{N_c} h_{Fi} x_{Fi} \end{cases} \qquad (12.13)$$

For a nonideal case, we may use Equations (13.32) and (13.34) for the calculations of vapour and liquid enthalpies respectively.

It is worthy to point out that the equations required to represent the adiabatic flash are of precisely the same form as those required to represent the separation process that occurs on the plate of a distillation column in the process of separating a multicomponent mixture.

In the present section, two sets of problems have been taken to illustrate the adiabatic flash process. The first set follows the *problem statement* for ideal mixtures defined in Subsection 12.2.1. In the second set, instead of known flash temperature, the feed enthalpy is assumed as a known quantity. The other given and unknown terms are the same with those terms mentioned in the first set of problem. Let us discuss the problems and their solution techniques in details.

12.3.1 First Set of Problem

Problem statement:

Given ($N_c + 3$): T, P, F, Z_{Fi}

Unknowns ($2N_c + 5$): $V_F, H_F, L_F, h_F, y_{Fi}, H, x_{Fi}$

where $i = 1, 2, 3, ..., N_c$.

Solution technique: This problem is related to the adiabatic flash operation. The solution may be either at ideal state or at nonideal state and so, both the cases will be considered to discuss here.

Case 1 (*ideal mixtures*): From the preceding discussion, we know that total $2N_c + 3$ number of equations [(12.1), (12.2) and (12.12)] is used to describe the adiabatic flash process. In the given problem, total number of unknowns is $2N_c + 5$. Apparently, the problem becomes complicated since the number of unknowns is more than that of independent equations. However, the solution approach is actually straightforward. For an ideal solution, conventionally H_{Fi} and h_{Fi} are the functions of given flash temperature. Therefore, the number of unknowns reduces to $2N_c + 3$. Now, we may note the following computational steps.

Step 1: Calculate V_F, L_F, x_{Fi}'s and y_{Fi}'s employing the solution technique given in Subsection 12.2.1.

Step 2: Compute H_{Fi} and h_{Fi} all constituent components by the use of analytical enthalpy equations as the polynomials of temperature (here, flash temperature). Then calculate H_F and h_F using Equation (12.13).

Step 3: Compute H from Equation (12.12).

Case 2 (*nonideal mixtures*): For an ideal mixture, the enthalpy may be considered as a function of solely the temperature (given). But for a solution having nonidealities in both vapour and liquid phases, the phase enthalpy depends on temperature and pressure (both given) as well as on phase composition (unknown). In the predictions of the thermodynamic properties, equations of state show very good performance. In the present case, the number of unknowns (= $2N_C + 3$) is equal to the number of available equations. Now, we may follow the computational steps as described below.

Step 1: Calculate V_F, L_F, x_{Fi}'s and y_{Fi}'s employing the solution approach described in Subsection 12.2.2.

Step 2: Compute H_F and h_F using a suitable thermodynamic property prediction method. As stated, for a nonideal mixture, an equation of state model is appropriate to employ. In the present status, the information on $\{T, P, y_{Fi}$'s$\}$ and $\{T, P, x_{Fi}$'s$\}$ are available to calculate the vapour and liquid enthalpies, respectively. For this nonideal case, we may employ Equations (13.32) and (13.34).

Step 3: Compute feed enthalpy (H) from Equation (12.12).

Notice that it is a part of your assignment to develop the computer code (Program) for the present problem.

12.3.2 Second Set of Problem

Problem statement:

Given ($N_C + 3$): P, F, H, Z_{Fi}

Unknowns ($2N_C + 5$): $T, V_F, H_F, L_F, h_F, y_{Fi}, x_{Fi}$

where $i = 1, 2, 3, ..., N_C$.

Solution technique: The present problem can be solved for both ideal and nonideal mixtures. In the following, the solution algorithms are outlined in details.

Case 1 (*ideal mixtures*): Actually, the total number of unknowns is $2N_C + 3$ since at ideal condition, the component enthalpy is assumed as a function of temperature only. So, total $2N_C + 3$ unknowns are needed to compute from the equal number of available equations [(12.1), (12.2) and (12.12)]. The computational steps to perform the adiabatic flash calculations are given below.

Step 1: Assume ψ.

Step 2: Assume T.

Step 3: Calculate k_{Fi}'s based on assumed T and given P. For this, we can see Step 1 of Problem set of Subsection 12.2.1.

Step 4: Calculate V_F since $\psi = V_F/F$, and then compute L_F from Equation (12.4).

Step 5: Calculate x_{Fi}'s and y_{Fi}'s according to the descriptions given in Steps 4 and 5 of Problem set of Subsection 12.2.1, respectively. Then use these calculated x_{Fi}'s and y_{Fi}'s to update k_{Fi}'s.

Step 6: Calculate H by using Equation (12.12). The values of H_F and h_F are known since H_{Fi} and h_{Fi} are the functions of assumed T (updated T from the second iteration onwards).

Step 7: Update T and ϕ. Equation (12.8) can be rewritten as:

$$F_1(\delta_n) = \sum_{i=1}^{N_c} \frac{Z_{Fi}}{[1-\delta_n(1-k_{Fin})]} - 1 \qquad (12.14)$$

and let

$$F_2(T_n) = H_n - H \qquad (12.15)$$

where H_n is computed for each T_n, and suffix 'n' denotes the trial number. Employing an iterative convergence algorithm ϕ (as discussed in Problem set of Subsection 12.2.1) and T can be updated. If the convergence conditions, including $|F_1|$ and $|F_2|$ less than the tolerance limit(s), are satisfied, then go to next step, otherwise go to Step 4.

Step 8: Stop.

Case 2 (*nonideal mixtures*): In the present case, also the total number of unknowns is equal to that of independent equations since the phase enthalpy is a function of temperature, pressure and phase composition. The following sequential steps can be developed for computer solution of this problem.

Step 1: Assume ϕ.

Step 2: Assume T.

Step 3: Calculate $(k_{Fi})_{\text{ideal}}$ for all components.

Step 4: Calculate V_F based on assumed/updated ϕ and given F. Then use Equation (12.4) to find L_F.

Step 5: Calculate x_{Fi}'s and y_{Fi}'s according to the descriptions provided in Steps 4 and 5 of problem set of Subsection 12.2.2, respectively. Then calculate $(k_{Fi})_{\text{nonideal}}$'s, using a thermodynamic model, based on T (assumed/updated), P (given) and phase compositions (just calculated).

Step 6: Calculate H_F and h_F by the use of an equation of state model with available $\{T, P, y_{Fi}$'s$\}$ and $\{T, P, x_{Fi}$'s$\}$ respectively. Then, H can be determined from Equation (12.12).

Step 7: Update T and ϕ following the approach as explained in Case 1 (Step 7) of this problem set. If the convergence criterions are not fulfilled, then go to Step 4, otherwise go to next step.

Step 8: Stop.

The development of the computer code for the second set of problem concerning the calculations for the adiabatic flash vaporization has been left for the practice of the students.

12.4 SUMMARY AND CONCLUSIONS

In this chapter, the details of flash calculations are presented. The computer codes are developed to apply the concept of isothermal flash vaporization on two examples, including an industrial debutanizer column. The development of computer codes for the adiabatic flash is left for your practice. Note that going through this chapter, we learn the flash calculations for ideal systems and systems with nonidealities in both liquid and vapour phases. It is now straightforward to perform the flash calculations for a system having nonideality in either of the phases.

Equilibrium flash separations are very common operations in industry, especially in petroleum refining. Even when some other method of separation is to be employed, it is not uncommon to use a *pre-*

flash to reduce the load on the separation itself. The flash calculations are so common in chemical engineering that they are key components of simulation packages like *Hysis*, *Aspen*, etc.

EXERCISES

12.1 What is flash vaporization? Why is it also called equilibrium distillation?

12.2 What are the different types of flash operation? Why are they called so?

12.3 Discuss the computational steps involved in the flash (both isothermal and adiabatic) calculations dealing the ideal as well as nonideal mixture.

12.4 Discuss the operational difficulties involved in the isothermal flash and the adiabatic flash operations.

12.5 It is a common situation in refinery operations that the feed is flashed before introducing it into the fractionating column. What are the main reasons behind this fact?

12.6 What are the different possible ways to produce vapour as well as liquid streams from a liquid feed mixture?

12.7 What are the different possible ways to produce vapour as well as liquid stream from a vapour feed mixture?

12.8 Discuss how the value of $_{27}$ is changed with the vaporization rate in a flash chamber.

12.9 Discuss how the phase nonidealities affect the equilibrium flash calculations. What will be the case if only the liquid phase nonideality is assumed?

12.10 Mention the complete convergence conditions for the second set of problem of the adiabatic flash operation.

12.11 Discuss why the stages in a distillation column are considered as the adiabatic flash chambers.

12.12 Equation (12.8) represents the flash function and an alternative form to this is:

$$F(\delta) = \sum_{i=1}^{N_C} \frac{Z_{Fi}(1 - k_{Fi})}{[1 - \delta(1 - k_{Fi})]} \qquad (12.16)$$

The above equation is obtained by using Equation (12.7) in the following equation:

$$\sum_{i=1}^{N_C} y_{Fi} - \sum_{i=1}^{N_C} x_{Fi} = 0 \qquad (12.17)$$

Using the above flash function [Equation (12.16)], find the bubble point and dew point equations.

[***Hint:*** At the bubble point, $_{27}$ = 0 and $F(_{27}) = 0$; at the dew point, $_{27}$ = 1 and $F(_{27}) = 0$].

REFERENCE

Holland, C.D. (1981). *Fundamentals of Multicomponent Distillation*, 1st ed., McGraw-Hill Book Company, New York.

13

Equation of State Models

13.1 INTRODUCTION

Nonideal solution effects can be incorporated into the formulations of vapour–liquid equilibrium (VLE) coefficient (k). At low pressures, it is generally assumed that the vapour phase is at ideal state but the nonidealities in the liquid phase can be severe. At moderate pressures, a vapour solution may still be ideal although the liquid phase does not follow the ideal law. For high-pressure operations, the nonidealities in both vapour and liquid phases are strictly taken into account. Several activity coefficient models, which predict the liquid-phase nonidealities through the VLE coefficients in distillation columns operated at low pressures, are discussed in Chapter 8. The goal of the present chapter is to provide the different equation of state models to represent the pressure–volume–temperature (P-V-T) relations for nonideal mixtures.

To solve distillation problems, phase enthalpies in addition to phase equilibrium ratios are needed. All these quantities may be obtained in a consistent manner from P-V-T relationships, which are usually referred to as *equations of state*. First, an equation of state model is developed for pure components and subsequently, the model is extended to mixtures through the use of *mixing rules*.

For multicomponent mixtures, graphical representations of properties cannot be used to determine equilibrium-stage requirements. Analytical computational procedures must be applied with thermodynamic properties represented preferably by algebraic equations (e.g., equation of state model). Use of an equation to represent the diverse thermodynamic properties has a number of advantages. It provides thermodynamically consistent values of these properties. Secondly, it facilitates interpolation and extrapolation of experimental data. In addition, calculations involving integration and differentiation can be carried out more readily by an equation than by graphical means. Perhaps most important of all, an equation provides a concise summary of a large mass of data, which, in the case of multicomponent mixtures, may be so extensive as to defy complete numerical tabulation or graphical representation. Motivated by these facts, several equation of state models have been developed by many researchers. These state models are widely used for computing phase equilibrium coefficients and enthalpies of mixtures over wide ranges of conditions.

Although many equations of state are reported so far, this chapter will be concerned with the present-day working state models. It is true that very few state models are suitable for practical design calculations. Before going to describe these models, we need to familiarize ourselves with the following preliminary facts relating to the fundamental thermodynamics.

13.2 MATHEMATICAL REPRESENTATIONS OF USEFUL THERMODYNAMIC QUANTITIES

As a measure of nonideality, the *pure species fugacity* (f_i) is related to pressure (P) through the *pure species fugacity coefficient* (ϕ_i) as:

$$\varphi_i = \frac{f_i}{P} \qquad (13.1)$$

where φ_i is unity for an ideal gas. Lewis and Randall defined first the fugacity concept for mixtures. The fugacity of a component in liquid as well as in vapour phase is a function of temperature, pressure and respective phase composition. For nonideal and ideal solutions, the fugacity is represented in the following way.

For Nonideal Solutions

Vapour phase: $$\hat{f}_i^V = \gamma_i^V y_i f_i^V \qquad (13.2)$$

Liquid phase: $$\hat{f}_i^L = \gamma_i^L x_i f_i^L \qquad (13.3)$$

For Ideal Solutions

Vapour phase: $$\hat{f}_i^V = y_i f_i^V \qquad (13.4)$$

Liquid phase: $$\hat{f}_i^L = x_i f_i^L \qquad (13.5)$$

At equilibrium,

$$\hat{f}_i^V = \hat{f}_i^L \qquad (13.6)$$

where

$\hat{f}_i^V$ = the fugacity of component *i* in the vapour mixture

$\hat{f}_i^L$ = the fugacity of component *i* in the liquid mixture

f_i^V = the fugacity of pure component *i* in the vapour state at *T* and *P* of the vapour mixture

f_i^L = the fugacity of pure component *i* in the liquid state at *T* and *P* of the liquid mixture

γ_i^V = the activity coefficient of pure component *i* in the vapour phase

γ_i^L = the activity coefficient of pure component *i* in the liquid phase

y_i = the composition of component *i* in the vapour phase

x_i = the composition of component *i* in the liquid phase

Equation (13.1) can be extended for *mixture fugacity coefficients* as:

Vapour phase: $$\hat{\varphi}_i^V = \frac{\hat{f}_i^V}{y_i P} \qquad (13.7)$$

Liquid phase: $$\hat{\varphi}_i^L = \frac{\hat{f}_i^L}{x_i P} \qquad (13.8)$$

Here, superscripts '*V*' and '*L*' refer, respectively, to the vapour and liquid phases, and $\hat{\varphi}_i$ is the fugacity coefficient of component *i* in a mixture. The expressions for fugacity of pure component *i* in two phases can be represented by use of the following equations:

Vapour phase: $$\ln \frac{f_i^V}{P} = \int_0^{P_r} (Z-1) \frac{dP_r}{P_r} \qquad (13.9)$$

Liquid phase:
$$f_i^L = P_i^S \varphi_i^S \exp\left[\int_{P_i^S}^{P} \frac{V_i}{RT} dP\right] \qquad (13.10)$$

where P_{ri} is the reduced pressure of component i ($=P/P_{ci}$), P_{ci} the critical pressure of component i, P_i^S the vapour pressure of component i, φ_i^S the fugacity coefficient of pure component i at saturation, V_i the liquid molar volume, R the universal gas constant and Z the compressibility factor. Compressibility expresses how much a gas is behaving like an ideal gas under any conditions. The compressibility equals one, means the gas is behaving exactly like an ideal gas.

Equation (13.9) implies that $f_i^V \to P$ if ideal gas behaviour is assumed and accordingly, Equation (13.1) gives $\varphi_i^V = 1.0.$ Then, according to Equation (13.4), $\hat{f}_i^V \to Py_i$ (i.e., $\hat{f}_i^V \to P_i$) and Equation (13.7) gives $\hat{\varphi}_i^V = 1.0.$ By the same way as described in Chapter 8, if the ideal solution behaviour is approached in the liquid, then Equation (13.10) implies $f_i^L \to P_i^S.$ So Equation (13.1) yields $\varphi_i^L = P_i^S/P.$ Then, according to Equation (13.5), $\hat{f}_i^L \to x_i P_i^S$ and using this in Equation (13.8), one obtains $\hat{\varphi}_i^L = P_i^S/P.$

At a given temperature, the *activity* of a component i(a_{ci}) is defined as the ratio of the fugacity of that component in a mixture to its fugacity in some standard state and can be expressed as:

$$a_{ci} = \frac{\hat{f}_i}{f_i} \qquad (13.11)$$

Comparison of this equation with Equations (13.4) and (13.5) shows that for ideal solutions $a_{ci}^V = y_i$ and $a_{ci}^L = x_i.$

The *activity coefficients* are commonly used to represent the solution nonideality. These coefficients can be obtained for vapour and liquid phases after substituting Equation (13.11) into Equations (13.2) and (13.3), respectively, as:

Vapour phase:
$$\gamma_i^V = \frac{a_{ci}^V}{y_i} \qquad (13.12)$$

Liquid phase:
$$\gamma_i^L = \frac{a_{ci}^L}{x_i} \qquad (13.13)$$

For ideal solutions, $a_{ci}^V = y_i$ and $a_{ci}^L = x_i,$ and consequently, $\gamma_i^V = 1.0$ and $\gamma_i^L = 1.0.$

13.3 VAPOUR–LIQUID EQUILIBRIUM COEFFICIENT

As mentioned earlier, for vapour–liquid equilibrium

$\hat{f}_i^V = \hat{f}_i^L$ [from Equation (13.6)]

For nonideal solutions, substitution of $\hat{f}_i^V$ [from Equation (13.2)] and $\hat{f}_i^L$ [from Equation (13.3)] in Equation (13.6) gives

$$\gamma_i^V y_i f_i^V = \gamma_i^L x_i f_i^L \qquad (13.14)$$

The above equation may be restated as follows:

$$\frac{y_i}{x_i} = \frac{\gamma_i^L f_i^L}{\gamma_i^V f_i^V} \qquad (13.15)$$

Since the vapour–liquid equilibrium coefficient, $k_i = y_i/x_i$, thus

$$k_i = \frac{\gamma_i^L f_i^L}{\gamma_i^V f_i^V} \qquad (13.16)$$

Now Equation (13.16) can be rearranged to

$$k_i = \frac{\hat{f}_i^L / x_i P}{\hat{f}_i^V / y_i P} \qquad (13.17)$$

By the use of Equations (13.7) and (13.8), the following form is obtained:

$$k_i = \frac{\hat{\varphi}_i^L}{\hat{\varphi}_i^V} \qquad (13.18)$$

Again, Equation (13.17) can be written using Equations (13.1), (13.2) and (13.8) as

$$k_i = \frac{\hat{f}_i^L / x_i}{\gamma_i^V f_i^V} = \frac{\hat{\varphi}_i^L P}{\gamma_i^V \varphi_i^V P} \qquad (13.19)$$

that means,

$$k_i = \frac{\hat{\varphi}_i^L}{\gamma_i^V \varphi_i^V} \qquad (13.20)$$

Similarly,

$$k_i = \frac{\gamma_i^L \varphi_i^L}{\hat{\varphi}_i^V} = \frac{\gamma_i^L f_i^L}{\hat{\varphi}_i^V P} \qquad (13.21)$$

Equations (13.16), (13.17) and (13.18) are *symmetrical*, whereas Equations (13.19), (13.20) and (13.21) are *unsymmetrical* formulations. In the Benedict–Webb–Rubin (BWR) and Soave–Redlich–Kwong (SRK) thermodynamic models, Equations (13.17) and (13.18) are used for the prediction of *k*-values. Again, Equation (13.21) has been applied successfully to many important industrial systems by several researchers (Chao and Seader, 1961; Lee, Erbar and Edmister, 1973; Robinson and Chao, 1971).

In the above passages, we have studied the formulations for VLE coefficient for the equation of state models. The application of the VLE formulation is discussed in Chapter 14. The SRK model is employed there to predict the equilibrium coefficients in addition to the phase enthalpies for a refinery debutanizer column.

The *ideal solution k-value* for component *i*, denoted by k_i^{id}, is expressed as

$$k_i^{id} = \frac{f_i^L}{f_i^V} \qquad (13.22)$$

So, Equation (13.16) can be rewritten as

$$k_i = \frac{\gamma_i^L}{\gamma_i^V} k_i^{id} \qquad (13.23)$$

If only the liquid phase forms ideal solution (i.e., $\gamma_i^L = 1.0$), then

$$k_i = \frac{k_i^{id}}{\gamma_i^V} \qquad (13.24)$$

Similarly, if the vapour phase forms ideal solution (i.e., $\gamma_i^V = 1.0$), then

$$k_i = \gamma_i^L k_i^{id} \qquad (13.25)$$

If both the vapour and liquid phases form ideal solutions (i.e., $\gamma_i^V = \gamma_i^L = 1.0$), Equation (13.23) reduces to

$$k_i = k_i^{id} \qquad (13.26)$$

Notice that the vapour–liquid equilibrium coefficient for several components in the mixtures can be predicted using the simple algebraic form of equations. For example,

Hadden (1948) proposed a correlation of k_i with temperature (in °R) at a specified pressure (300 lb/in^2 abs) as

$$\left(\frac{k_i}{T}\right)^{1/3} = \mu_{1i} + \mu_{2i}T + \mu_{3i}T^2 + \mu_{4i}T^3 \qquad (13.27)$$

The constants μ_1, μ_2, μ_3 and μ_4 are specific to component i, and can be determined from the experimental results. At the specified pressure (300 lb/in^2 abs), the values of these constants for different hydrocarbons are given in Table 13.1 (Hadden, 1948). It is worthy to mention that many difficulties are associated with this method. First of all, the phase nonideality, which is a complex and usually a common feature of a mixture, is not properly incorporated within this simple algebraic equation. Secondly, the constants are available only for few hydrocarbons and not even at different pressures.

Table 13.1 Constants for the k_i [Equation (13.27)]

Component	μ_1 ($\equiv 10^2$)	μ_2 ($\equiv 10^5$)	μ_3 ($\equiv 10^8$)	μ_4 ($\equiv 10^{12}$)
Ethane	–9.8400210	67.545943	–37.459290	–9.0732459
Ethylene	–5.1779950	62.124576	–37.562082	8.0145501
iso-Butane	–18.967651	61.239667	–17.891649	–90.855512
iso-Butene	–10.104481	21.400418	38.564266	–353.65419
iso-Pentane	–7.5488400	3.2623631	58.507340	–414.92323
Methane	32.718139	–9.6951405	6.9229334	–47.361298
n-Butane	–14.181715	36.866353	16.521412	–248.23843
n-Heptane	5.5692758	–50.705967	112.17338	–574.89350
n-Hexane	1.1506919	–33.885839	97.795401	–542.35941
n-Octane	7.1714400	–52.608530	103.72034	–496.46551

n-Pentane	–7.5435390	2.0584231	59.138344	–413.12409
Propane	–14.512474	53.638924	–5.3051604	–173.58329
Propylene	–25.098770	102.39287	–75.221710	153.84709

13.4 VAPOUR AND LIQUID ENTHALPY

The *ideal gas heat capacity* can be expressed as a polynomial in temperature (Passut and Danner, 1972):

$$C_p = B + 2CT + 3DT^2 + 4ET^3 + 5FT^4 \qquad (13.28)$$

Now, the *ideal gas enthalpy* (H^0) is related to the heat capacity by the standard thermodynamic formula:

$$\Delta H^0 = \int C_p \, dT \qquad (13.29)$$

Clearly, $C_p = dH^0/dT$ since $\Delta H^0 = H^0 - H^0_{\text{ref}}$ where H^0_{ref} is a reference state for ideal gas enthalpy. After performing integration, the following form of equation (Passut and Danner, 1972) may be obtained to predict the ideal gas enthalpy:

$$H^0 = A + BT + CT^2 + DT^3 + ET^4 + FT^5 \qquad (13.30)$$

where A, B, C, D, E and F are the coefficients. These coefficients for several compounds are reported in Table 13.2. The database used is 0 Btu/lb at 0°R for the enthalpy. It should be noted that this base cannot be used for a system in which a chemical reaction has occurred.

Table 13.2 Coefficients for the ideal gas enthalpy Equation (13.30) (enthalpy in Btu/lb and temperature in °R)

Component	*A*	*B*	*C* ($\times 10^3$)	*D* ($\times 10^6$)	*E* ($\times 10^{10}$)	*F* ($\times 10^{14}$)
Oxygen	–0.98176	0.227486	–0.037305	0.048302	–0.185243	0.247488
Hydrogen	12.32674	3.199617	0.392786	–0.293452	1.090069	–1.387867
Water	–2.46342	0.457392	–0.052512	0.064594	–0.202759	0.236310
Hydrogen sulphide	–0.61782	0.238575	–0.024457	0.041067	–0.130126	0.144852
Nitrogen	–0.68925	0.253664	–0.014549	0.012544	–0.017106	–0.008239
Ammonia	–0.79603	0.476211	–0.070682	0.151983	–0.548226	0.694700
Carbon	4.11552	–0.047746	0.203743	0.019721	–0.332358	0.620433
Carbon monoxide	–0.97557	0.256524	–0.022911	0.022280	–0.056326	0.045588
Carbon dioxide	4.77805	0.114433	0.101132	–0.026494	0.034706	–0.013140
Sulphur dioxide	1.39432	0.110263	0.033029	0.008912	–0.077313	0.129287
Methane	–5.58114	0.564834	–0.282973	0.417399	–1.525576	1.958857
Ethane	–0.76005	0.273088	–0.042956	0.312815	–1.389890	2.007023
Propane	–1.22301	0.179733	0.066458	0.250998	–1.247461	1.893509
n-Butane	29.11502	0.002040	0.434879	–0.081810	0.072349	–0.014560
2-Methyl propane	13.28660	0.036637	0.349631	0.005361	–0.298111	0.538662
n-Pentane	27.17183	–0.002795	0.440073	–0.086288	0.081764	–0.019715
2-Methyl butane	27.62342	–0.031504	0.469884	–0.098283	0.102985	–0.029485
2,2-Dimethyl propane	11.77146	0.004372	0.406465	–0.027646	–0.217453	0.468503
n-Hexane	32.03560	–0.023096	0.461333	–0.097402	0.103368	–0.030643
2-Methyl pentane	47.93127	–0.144726	0.652894	–0.222413	0.436227	–0.245813
3-Methyl pentane	36.03723	–0.040505	0.488067	–0.114855	0.144909	–0.040314
n-Heptane	30.70117	–0.023143	0.460981	–0.098074	0.104752	–0.031340
2-Methyl hexane	20.52402	–0.030355	0.478057	–0.094352	0.040395	0.052751
3-Methyl hexane	13.57672	–0.002985	0.421071	–0.051639	–0.082615	0.141821
n-Octane	29.50114	–0.022402	0.459712	–0.098062	0.104754	–0.031355
2-Methyl heptane	34.08025	–0.095851	0.593907	–0.181654	0.298714	–0.135831
2,2,4-Trimethyl pentane	5.774120	0.021117	0.297026	0.154707	–1.414781	3.128672
n-Nonane	28.56645	–0.021654	0.458518	–0.097973	0.104654	–0.031318
n-Decane	28.48990	–0.023837	0.461164	–0.099786	0.108353	–0.033074
n-Undecane	28.06989	–0.023843	0.460773	–0.099839	0.108415	–0.033122
n-Dodecane	26.21126	–0.018522	0.453893	–0.096464	0.101393	–0.029665
n-Tridecane	26.97706	–0.022933	0.459517	–0.099758	0.108351	–0.033091
n-Tetradecane	26.50692	–0.022048	0.458079	–0.099164	0.107126	–0.032538
n-Pentadecane	26.74860	–0.024114	0.460717	–0.100767	0.110447	–0.034147
n-Hexadecane	26.19390	–0.022825	0.459024	–0.100021	0.108912	–0.033390
n-Heptadecane	26.16214	–0.023563	0.459907	–0.100664	0.110307	–0.034076
n-Octadecane	25.97571	–0.023616	0.459950	–0.100804	0.110587	–0.034205
n-Nonadecane	25.44962	–0.022153	0.457982	–0.099865	0.108644	–0.033275
n-Eicosane	25.43578	–0.022726	0.458663	–0.100313	0.109516	–0.033658
Cyclopentane	57.78000	–0.174553	0.487900	–0.079021	–0.025900	0.187338
Methyl cyclopentane	54.70525	–0.163500	0.531524	–0.123976	0.146551	–0.049768
Ethyl cyclopentane	53.75912	–0.152454	0.527902	–0.123211	0.146775	–0.049978
1,1-Dimethyl cyclopentane	51.71806	–0.167061	0.553236	–0.133894	0.163103	–0.057106
cis-1,2-Dimethyl cyclopentane	53.58792	–0.171032	0.560092	–0.138623	0.174330	–0.063655
trans-1,2-Dimethyl cyclopentane	53.04513	–0.166442	0.554211	–0.135955	0.169209	–0.061040

cis-1,3-Dimethyl cyclopentane	53.04513	–0.166442	0.554211	–0.135955	0.169209	–0.061040
trans-1,3-Dimethyl cyclopentane	53.04513	–0.166442	0.554211	–0.135955	0.169209	–0.061040
Cyclohexane	46.56603	–0.149848	0.457275	–0.038739	–0.179124	0.379353
Methyl cyclohexane	46.25893	–0.168390	0.544484	–0.112689	0.075113	0.060602
Ethyl cyclohexane	26.19627	–0.084958	0.427814	–0.028309	–0.221691	0.455582
1,1-Dimethyl cyclohexane	22.03712	–0.062955	0.364210	0.028180	–0.421880	0.711053
cis-1,2-Dimethyl cyclohexane	32.83805	–0.108227	0.445852	–0.033539	–0.219459	0.466601
trans-1,2-Dimethyl cyclohexane	43.91461	–0.165475	0.561323	–0.130023	0.145736	–0.045846
cis-1,3-Dimethyl cyclohexane	33.67583	–0.115284	0.470036	–0.058996	–0.106752	0.293400
trans-1,3-Dimethyl cyclohexane	31.44064	–0.117151	0.499798	–0.100833	0.090021	–0.018348
cis-1,4-Dimethyl cyclohexane	31.44064	–0.117151	0.499798	–0.100833	0.090021	–0.018348
trans-1,4-Dimethyl cyclohexane	22.48886	–0.064575	0.384794	0.009490	–0.358720	0.632457
Ethene	51.78893	0.020724	0.385431	–0.082721	0.092318	–0.029284
Propene	26.17773	0.044867	0.324263	–0.030604	–0.083732	0.188977
1-Butene	32.74090	–0.018519	0.426345	–0.094058	0.107224	–0.034983
cis-2-Butene	43.74545	–0.042795	0.403432	–0.068428	0.013449	0.087886
trans-2-Butene	20.68885	0.037032	0.355122	–0.056044	0.015847	0.044467
2-Methyl propene	14.96746	0.033009	0.378264	–0.073331	0.069757	–0.017483
1-Pentene	30.15557	–0.006874	0.421053	–0.090830	0.100380	–0.031591
1-Hexene	27.48574	–0.004262	0.419666	–0.088211	0.092532	–0.027052
1-Heptene	27.04731	–0.007807	0.425936	–0.090496	0.095961	–0.028471
1-Octene	27.30859	–0.012888	0.434131	–0.094225	0.103056	–0.031854
Cyclopentene	36.07924	–0.059928	0.295761	0.033290	–0.388533	0.648582
Propadiene	25.33539	0.033745	0.371517	–0.106261	0.186462	–0.143504
1,2-Butadiene	17.65767	0.039560	0.347981	–0.075607	0.084037	–0.026515
1,3-Butadiene	40.76389	–0.100604	0.565187	–0.212346	0.483054	–0.473845
Acetylene	10.52464	0.134680	0.364644	–0.169596	0.465419	–0.522046
Propyne	15.21043	0.080387	0.324007	–0.087975	0.159915	–0.140098
1-Butyne	10.13562	0.053336	0.346106	–0.080330	0.105276	–0.053399
Benzene	36.31430	–0.122662	0.431082	–0.113814	0.149498	–0.056477
Methyl benzene	31.88489	–0.101151	0.422572	–0.106144	0.133765	–0.048407
Ethyl benzene	30.33272	–0.093633	0.439064	–0.112630	0.145822	–0.054320
1,2-Dimethyl benzene	13.97958	–0.014950	0.334243	–0.048408	–0.046017	0.170557
1,3-Dimethyl benzene	25.48862	–0.068902	0.399500	–0.092476	0.105979	–0.034527
1,4-Dimethyl benzene	18.50495	–0.030090	0.330052	–0.039435	–0.082116	0.217324
n-Propyl benzene	32.50404	–0.099907	0.466800	–0.126928	0.176789	–0.069443
Isopropyl benzene	25.26273	–0.084771	0.442557	–0.111294	0.139999	–0.050954
1-Methyl-2-ethyl benzene	20.11249	–0.044156	0.403697	–0.096314	0.116070	–0.040090
1-Methyl-3-ethyl benzene	19.02413	–0.036920	0.363993	–0.056337	–0.044323	0.188858
1-Methyl-4-ethyl benzene	18.47560	–0.030093	0.351431	–0.049197	–0.061535	0.203186
1,2,3-Trimethyl benzene	–1.992290	0.074678	0.185787	0.066551	–0.446036	0.693925
1,2,4-Trimethyl benzene	–3.455730	0.078874	0.184527	0.065059	–0.432780	0.666189
1,3,5-Trimethyl benzene	24.29772	–0.055925	0.391561	–0.086915	0.095603	–0.029628
n-Butyl benzene	29.05375	–0.074034	0.437825	–0.107719	0.133490	–0.047775

Reprinted with permission from (Passut, C.A. and Danner, R.P. (1972). Correlation of ideal gas enthalpy, heat capacity, and entropy, *Ind. Eng. Chem. Process Des. Devel.*, 11, 543–546) American Chemical Society.

The ideal gas law assumption is not valid at high pressure. Therefore, it is required to correct the enthalpy for pressure. For a mixture, the vapour enthalpy at temperature T and pressure P is:

$$H = \left[\sum_{i=1}^{N_c} (y_i H_i^0)\right] + (H - H_v^0) \qquad (13.31)$$

or
$$H = H_v^0 + \Omega_v \qquad (13.32)$$

Similarly, the liquid-phase enthalpy is:

$$h = \left[\sum_{i=1}^{N_c} (x_i H_i^0)\right] + (h - H_L^0) \qquad (13.33)$$

or
$$h = H_L^0 + \Omega_L \qquad (13.34)$$

where N_C is the number of components in a mixture, and $\Omega_v\ (= H - H_v^0)$ and $\Omega_L\ (= h - H_L^0)$ are the *enthalpy departure functions*[1] in vapour and liquid phases, respectively. It is straightforward to convert Equations (13.31) and (13.33) for pure components. Notice that all the enthalpies used in Equations (13.31) to (13.34) are actually molar enthalpies (energy/mole).

[1] The enthalpy of one mole of mixture at the temperature T and pressure P minus the enthalpy of one mole of the same mixture in the perfect gas state at T and at P = 1 atmosphere.

Like the vapour–liquid equilibrium coefficient, the liquid and vapour enthalpies of a pure component i(h_i and H_i) can be predicted employing the algebraic form of equations as developed by Maxwell (1955) at a specified pressure (300 lb/in^2 abs):

$$(h_i)^{1/2} = \theta_{1i} + \theta_{2i}T + \theta_{3i}T^2 \qquad (13.35)$$

$$(H_i)^{1/2} = \sigma_{1i} + \sigma_{2i}T + \sigma_{3i}T^2 \qquad (13.36)$$

where T is in °R and enthalpies are in Btu/lbmol. The constants θ_1, θ_2, θ_3, σ_1, σ_2 and σ_3 are specific to component i, and the values of these constants at pressure 300 lb/in^2 abs are listed in Table 13.3 (Maxwell, 1955). Note that these algebraic Equations (13.27), (13.35), and (13.36) perform well for thermodynamic property predictions over extremely narrow ranges of conditions.

Table 13.3 Constants for the enthalpy Equations (13.35) and (13.36)

Component	θ_1	θ_2 (× 10)	θ_3 (× 10^4)	σ_1	σ_2 (× 10^4)	σ_3 (× 10^6)
Ethane	−8.4857000	1.6286636	−1.9498601	61.334520	588.75430	11.948654
Ethylene	−7.2915000	1.5411962	−1.6088376	56.796380	615.93154	2.4088730
iso-Butane	−16.553405	2.1618650	−3.1476209	147.65414	−1185.2942	152.87778
iso-Butene	−16.553405	2.1618650	−3.1476209	139.17444	−822.39488	120.39298
iso-Pentane	−23.356460	2.5017453	−4.3917897	130.96679	−197.98604	82.549947
Methane	−17.899210	1.7395763	−3.7596114	44.445874	501.04559	7.3207219
n-Butane	−20.298110	2.3005743	−3.8663417	152.66798	−1153.4842	146.64125
n-Heptane	−25.314530	2.8246389	−4.5418718	94.682620	1479.5387	−19.105299
n-Hexane	−23.870410	2.6768089	−4.4197793	85.834950	1522.3917	−34.018595
n-Octane	−22.235050	2.8478429	−3.8850819	106.32806	1328.3949	1.6230737
n-Pentane	−24.371540	2.5636200	−4.6499694	128.90152	2.0509603	64.501496
Propane	−14.500060	1.9802223	−2.9048837	81.795910	389.81919	36.470900
Propylene	−12.427900	1.8834652	−2.4839140	71.828480	658.55130	11.299585

13.5 EQUATION OF STATE MODELS FOR PURE COMPONENTS AND MIXTURES

13.5.1 The Redlich–Kwong (RK) Equation of State Model (developed by Redlich and Kwong in 1949)

Equation of State: $P = \dfrac{RT}{V-b} - \dfrac{aT^{-0.5}}{V(V+b)}$

where $V\left(=\dfrac{ZRT}{P}\right)$ is the molar volume, $a = \left[\sum_{i=1}^{N_c} x_i a_i^{0.5}\right]^2$, and $b = \sum_{i=1}^{N_c} x_i b_i$. By the same way, a and b can be obtained for vapour phase replacing x by y.

For Pure Components

Vapour phase

$$H - H^0 = RT\left[Z_v - 1 - \frac{3A^2}{2B}\ln\left(1 + \frac{BP}{Z_v}\right)\right] \qquad (13.37)$$

$$\ln \frac{f^V}{P} = Z_v - 1 - \ln (Z_v - BP) - \frac{A^2}{B} \ln \left(1 + \frac{BP}{Z_v} \right) \tag{13.38}$$

Liquid phase

$$h - H^0 = RT\left[Z_L - 1 - \frac{3A^2}{2B}\ln\left(1+\frac{BP}{Z_L}\right)\right] \tag{13.39}$$

$$\ln\frac{f^L}{P} = Z_L - 1 - \ln(Z_L - BP) - \frac{A^2}{B}\ln\left(1+\frac{BP}{Z_L}\right) \tag{13.40}$$

For Mixtures

Vapour phase

$$\Omega_v = RT\left[Z_v - 1 - \frac{3A_v^2}{2B_v}\ln\left(1+\frac{B_vP}{Z_v}\right)\right] \tag{13.41}$$

$$\ln\left(\frac{\hat{f}_i^V}{Py_i}\right) = \frac{B_i}{B_v}(Z_v - 1) - \ln(Z_v - B_vP) - \frac{A_v^2}{B_v}\left(\frac{2A_i}{A_v} - \frac{B_i}{B_v}\right)\ln\left(1+\frac{B_vP}{Z_v}\right) \tag{13.42}$$

where

$$A_v = \sum_{i=1}^{N_c} y_i A_i \tag{13.43}$$

$$B_v = \sum_{i=1}^{N_c} y_i B_i \tag{13.44}$$

Liquid phase

$$\Omega_L = RT\left[Z_L - 1 - \frac{3A_L^2}{2B_L}\ln\left(1+\frac{B_LP}{Z_L}\right)\right] \tag{13.45}$$

$$\ln\left(\frac{\hat{f}_i^L}{Px_i}\right) = \frac{B_i}{B_L}(Z_L - 1) - \ln(Z_L - B_LP) - \frac{A_L^2}{B_L}\left(\frac{2A_i}{A_L} - \frac{B_i}{B_L}\right)\ln\left(1+\frac{B_LP}{Z_L}\right) \tag{13.46}$$

where

$$A_L = \sum_{i=1}^{N_c} x_i A_i \tag{13.47}$$

$$B_L = \sum_{i=1}^{N_c} x_i B_i \tag{13.48}$$

Other associated terms in the RK model are defined as

$$a_i = 0.4278\frac{R^2T_{ci}^{2.5}}{P_{ci}} \tag{13.49}$$

$$b_i = 0.0867 \frac{RT_{ci}}{P_{ci}} \qquad (13.50)$$

$$A_i = \frac{a_i^{0.5}}{RT^{1.25}} \qquad (13.51)$$

$$B_i = \frac{b_i}{RT} \qquad (13.52)$$

The following form of cubic equation is used to determine the compressibility factors in the RK equation of state:

$$Z^3 - Z^2 + [A^2P - BP(1 + BP)]Z - A^2PBP = 0 \qquad (13.53)$$

The solution of this equation yields either three real roots or one real root and two conjugate imaginary roots (Sokolnikoff and Sokolnikoff, 1941). For the case where three real roots exist, the largest real root is taken for the vapour phase (*vapour root*) and the smallest real root for the liquid phase (*liquid root*). The intermediate real root has no physical significance. For the case where only one real root exists, that positive real root is obtained at supercritical temperatures (Edmister, 1968) where only a single phase exists. For $T < T_C$, the single real root is a vapour root if the corresponding density is less than the critical density ($\hat{} < \hat{} _C$) and a liquid root if $\hat{} > \hat{} _C$. If $T > T_C$, the single real root corresponds to the vapour phase.

As stated, superscripts or subscripts '*V*' and '*L*' refer, respectively, to the vapour and liquid phases. In the above RK model structure, T_{Ci} is the critical temperature of component *i* and P_{Ci} the critical pressure of component *i*. Values of T_{Ci} and P_{Ci} are given for different components in Table 13.4. Two parameters (*a* and *b*) are mainly involved in this thermodynamic state model and these parameters can be obtained directly by knowing the critical temperature and critical pressure.

Table 13.4 Constants for the vapour pressure Equation (13.113), and molecular weight (Mol. wt.), critical temperature (T_C), critical pressure (P_C) and acentric factor (w) for different components

Component	A_1	A_2	A_3	A_4	*Mol. wt.*	T_c (K)	P_c (bar)	w
Water	–7.76451	1.45838	–2.77580	–1.23303	18.015	647.30	221.20	0.344
Carbon monoxide	–6.20798	1.27885	–1.34533	–2.56842	28.010	132.9	35.0	0.066
Carbon dioxide	–6.95626	1.19695	–3.12614	2.99448	44.010	304.1	73.8	0.239
Carbon disulphide	–6.63896	1.20395	–0.37653	–4.32820	76.131	552.0	79.0	0.109
Chloroform	–6.95546	1.16625	–2.13970	–3.44421	119.378	536.4	53.7	0.218
Formaldehyde	–7.29343	1.08395	–1.63882	–2.30677	30.026	408.0	65.9	0.253
Methane	–6.00435	1.18850	–0.83408	–1.22833	16.043	190.4	46.0	0.011
Methanol	–8.54796	0.76982	–3.10850	1.54481	32.042	512.6	80.9	0.556
Methyl amine	–7.52772	1.81615	–4.20677	–1.22275	31.058	430.0	74.3	0.292
Acetylene	–6.90128	1.26873	–2.09113	–2.75601	26.038	308.3	61.4	0.190
Ethylene	–6.32055	1.16819	–1.55935	–1.83552	28.054	282.4	50.4	0.089
Acetaldehyde	–7.04687	0.12142	–0.02660	–5.90300	44.054	461.0	55.7	0.303
Ethane	–6.34307	1.01630	–1.19116	–2.03539	30.070	305.4	48.8	0.099
Ethanol	–8.51838	0.34163	–5.73683	8.32581	46.069	513.9	61.4	0.644
Dimethyl amine	–7.90295	2.81577	–6.31338	–0.22407	45.085	437.7	53.1	0.302
Propylene	–6.64231	1.21857	–1.81005	–2.48212	42.081	364.9	46.0	0.144
Acetone	–7.45514	1.20200	–2.43926	–3.35590	58.080	508.1	47.0	0.304
Propane	–6.72219	1.33236	–2.13868	–1.38551	44.094	369.8	42.5	0.153
1-Butene	–6.88204	1.27051	–2.26284	–2.61632	56.108	419.6	40.2	0.191
n-Butane	–6.88709	1.15157	–1.99873	–3.13003	58.124	425.2	38.0	0.199
iso-Butane	–6.95579	1.50090	–2.52717	–1.49776	58.124	408.2	36.5	0.183
Cyclopentane	–6.51809	0.38442	–1.11706	–4.50275	70.135	511.7	45.1	0.196
1-Pentene	–7.04875	1.17813	–2.45105	–2.21727	70.135	464.8	35.3	0.233
n-Pentane	–7.28936	1.53679	–3.08367	–1.02456	72.151	469.7	33.7	0.251
iso-Pentane	–7.12727	1.38996	–2.54302	–2.45657	72.151	460.4	33.9	0.227
Chlorobenzene	–7.58700	2.26551	–4.09418	0.17038	112.559	632.4	45.2	0.249
Benzene	–6.98273	1.33213	–2.62863	–3.33399	78.114	562.2	48.9	0.212
Phenol	–8.75550	2.92651	–6.31601	–1.36889	94.113	694.2	61.3	0.438
Cyclohexane	–6.96009	1.31328	–2.75683	–2.45491	84.162	553.5	40.7	0.212
1-Hexene	–7.76467	2.29843	–4.44302	0.89947	84.163	504.0	31.7	0.285
n-Hexane	–7.46765	1.44211	–3.28222	–2.50941	86.178	507.5	30.1	0.299
Toluene	–7.28607	1.38091	–2.83433	–2.79168	92.141	591.8	41.0	0.263

1-Heptene	–8.26875	3.02688	–6.18709	4.33049	98.189	537.3	28.3	0.358
n-Heptane	–7.67468	1.37068	–3.53620	–3.20243	100.205	540.3	27.4	0.349
o-Xylene	–7.53357	1.40968	–3.10985	–2.85992	106.168	630.3	37.3	0.310
m-Xylene	–7.59222	1.39441	–3.22746	–2.40376	106.168	617.1	35.4	0.325
p-Xylene	–7.63495	1.50724	–3.19678	–2.78710	106.168	616.2	35.1	0.320
n-Octane	–7.91211	1.38007	–3.80435	–4.50132	114.232	568.8	24.9	0.398
n-Nonane	–8.24480	1.57885	–4.38155	–4.04412	128.259	594.6	22.9	0.445
n-Decane	–8.56523	1.97756	–5.81971	–0.29982	142.286	617.7	21.2	0.489

The RK equation is commonly considered as one of the best of the two-parameter equations of state. While it can be used to calculate, with a good degree of accuracy, volumetric and thermal properties of pure compounds and of mixtures, its application to multicomponent VLE calculations often gives poor results. However, this Redlich–Kwong equation of state model is recommended for predicting the properties of only the vapour phase although sometimes this model has the ability to approximate the liquid region.

13.5.2 The Soave–Redlich–Kwong (SRK) Equation of State Model (Soave in 1972 modified the RK model to SRK model)

Equation of State: $P = \dfrac{RT}{V-b} - \dfrac{a\alpha}{V(V+b)}$

where $a = \sum_{i=1}^{N_c}\sum_{j=1}^{N_c} x_i x_j (a_i a_j)^{0.5}(1-k_{ij}), b = \sum_{i=1}^{N_c} x_i b_i,$ and ¬ will be defined in the following discussions.

For Pure Components

Vapour phase

$$H - H^0 = RT(Z_v - 1) + \frac{RTA^2}{B}\left(\frac{T}{\alpha}\frac{d\alpha}{dT} - 1\right)\ln\left(1 + \frac{BP}{Z_v}\right) \qquad (13.54)$$

$$\ln\frac{f^V}{P} = Z_v - 1 - \ln(Z_v - BP) - \frac{A^2}{B}\ln\left(1 + \frac{BP}{Z_v}\right) \qquad (13.55)$$

Liquid phase

$$h - H^0 = RT(Z_L - 1) + \frac{RTA^2}{B}\left(\frac{T}{\alpha}\frac{d\alpha}{dT} - 1\right)\ln\left(1 + \frac{BP}{Z_L}\right) \qquad (13.56)$$

$$\ln\left(\frac{f^L}{P}\right) = Z_L - 1 - \ln(Z_L - BP) - \frac{A^2}{B}\ln\left(1 + \frac{BP}{Z_L}\right) \qquad (13.57)$$

For Mixtures

Vapour phase

$$\Omega_v = RT(Z_v - 1) + \frac{RTA_v^2}{B_v}\left[\frac{2T}{A_v^2}\sum_{i=1}^{N_c} y_i \bar{A}_{vi}^2\left(\frac{1}{\alpha_i^{0.5}}\frac{d\alpha_i^{0.5}}{dT}\right) - 1\right]\ln\left(1 + \frac{B_v P}{Z_v}\right) \qquad (13.58)$$

$$\ln\left(\frac{\hat{f}_i^V}{Py_i}\right)=\frac{B_i}{B_v}(Z_v-1)-\frac{A_v^2}{B_v}\left(\frac{2\bar{A}_{vi}^2}{A_v^2}-\frac{B_i}{B_v}\right)\ln\left(1+\frac{B_vP}{Z_v}\right)-\ln(Z_v-B_vP) \tag{13.59}$$

where

$$A_v=\sum_{i=1}^{N_c}y_iA_i \qquad \text{[from Equation (13.43)]}$$

$$B_v=\sum_{i=1}^{N_c}y_iB_i \qquad \text{[from Equation (13.44)]}$$

$$A_v^2=\left(\sum_{i=1}^{N_c}y_iA_i\right)^2=\sum_{i=1}^{N_c}\sum_{j=1}^{N_c}y_iy_jA_iA_j \tag{13.60}$$

$$\bar{A}_{vi}^2=A_i\sum_{j=1}^{N_c}y_jA_j \tag{13.61}$$

Liquid phase

$$\Omega_L=RT(Z_L-1)+\frac{RTA_L^2}{B_L}\left[\frac{2T}{A_L^2}\sum_{i=1}^{N_c}x_i\bar{A}_{Li}^2\left(\frac{1}{\alpha_i^{0.5}}\frac{d\alpha_i^{0.5}}{dT}\right)-1\right]\ln\left(1+\frac{B_LP}{Z_L}\right) \tag{13.62}$$

$$\ln\left(\frac{\hat{f}_i^L}{Px_i}\right)=\frac{B_i}{B_L}(Z_L-1)-\frac{A_L^2}{B_L}\left(\frac{2\bar{A}_{Li}^2}{A_L^2}-\frac{B_i}{B_L}\right)\ln\left(1+\frac{B_LP}{Z_L}\right)-\ln(Z_L-B_LP) \tag{13.63}$$

where

$$A_L=\sum_{i=1}^{N_c}x_iA_i \qquad \text{[from Equation (13.47)]}$$

$$B_L=\sum_{i=1}^{N_c}x_iB_i \qquad \text{[from Equation (13.48)]}$$

$$A_L^2=\left(\sum_{i=1}^{N_c}x_iA_i\right)^2=\sum_{i=1}^{N_c}\sum_{j=1}^{N_c}x_ix_jA_iA_j \tag{13.64}$$

$$\bar{A}_{Li}^2=A_i\sum_{j=1}^{N_c}x_jA_j \tag{13.65}$$

The terms involved in the SRK model can be expressed in the following forms:

$$a_i = 0.42747 \frac{R^2 T_{ci}^2}{P_{ci}} \qquad (13.66)$$

$$b_i = 0.08664 \frac{RT_{ci}}{P_{ci}} \qquad (13.67)$$

$$A_i = \frac{a_i^{0.5} \alpha_i^{0.5}}{RT} \qquad (13.68)$$

$$B_i = \frac{b_i}{RT} \qquad [\text{from Equation (13.52)}]$$

$$\alpha_i^{0.5} = 1 + m_i(1 - T_{ri}^{0.5}) \qquad (13.69)$$

$$m_i = 0.480 + 1.574 w_i - 0.176 w_i^2 \qquad (13.70)$$

The SRK model can be applied to predict the thermodynamic properties of light gases (except hydrogen) such as nitrogen, carbon monoxide, carbon dioxide, and hydrogen sulphide if binary interaction parameters k_{ij} are included as given in the following equations.

Vapour phase

$$A_v^2 = \sum_{i=1}^{N_c} \sum_{j=1}^{N_c} y_i y_j A_i A_j (1 - k_{ij}) \qquad (13.71)$$

$$\bar{A}_{vi}^2 = A_i \sum_{j=1}^{N_c} y_j A_j (1 - k_{ij}) \qquad (13.72)$$

Liquid phase

$$A_L^2 = \sum_{i=1}^{N_c} \sum_{j=1}^{N_c} x_i x_j A_i A_j (1 - k_{ij}) \qquad (13.73)$$

$$\bar{A}_{Li}^2 = A_i \sum_{j=1}^{N_c} x_j A_j (1 - k_{ij}) \qquad (13.74)$$

In the above state model, w_i denotes the Pitzer acentric factor for component i (values given for different components in Table 13.4). Values of the correction factor k_{ij} for many binary pairs have been calculated from experimental data and are reported in Table 13.5 (Erbar, 1973). It was observed (Soave, 1972) that the use of an interaction parameter has greatly improved the predictions. Values of the compressibility factor for vapour and liquid phases are obtained from Equation (13.53).

The major difficulty with the original Redlich–Kwong equation is its failure to predict vapour pressure accurately. To overcome this difficulty, Soave (1972) added a third parameter, the acentric factor (w_i), to the RK equation of state. The SRK model has rapidly gained acceptance by the hydrocarbon processing industry because of the relative simplicity of the equation itself as compared to the more complicated Benedict–Webb–Rubin equation and because of its capability for predicting reasonably accurate

thermodynamic properties in both liquid and vapour phases.

However, the SRK model provides less accurate results for hydrogen-containing mixtures. In addition, this thermodynamic model, like the RK equation, still fails to predict liquid density with good accuracy. The following Peng–Robinson model is more successful in that respect.

Table 13.5 Binary interaction parameter (k_{ij}) for the SRK model

Component	*Carbon dioxide*	*Hydrogen sulphide*	*Nitrogen*	*Carbon monoxide*
Methane	0.12	0.08	0.02	–0.02
Ethylene	0.15	0.07	0.04	
Ethane	0.15	0.07	0.06	
Propylene	0.08	0.07	0.06	
Propane	0.15	0.07	0.08	
iso-Butane	0.15	0.06	0.08	
n-Butane	0.15	0.06	0.08	
iso-Pentane	0.15	0.06	0.08	
n-Pentane	0.15	0.06	0.08	
n-Hexane	0.15	0.05	0.08	
n-Heptane	0.15	0.04	0.08	
n-Octane	0.15	0.04	0.08	
n-Nonane	0.15	0.03	0.08	
n-Decane	0.15	0.03	0.08	
n-Undecane	0.15	0.03	0.08	
Carbon dioxide	...	0.12	...	–0.04
Cyclohexane	0.15	0.03	0.08	
Methyl cyclohexane	0.15	0.03	0.08	
Benzene	0.15	0.03	0.08	
Toluene	0.15	0.03	0.08	
o-Xylene	0.15	0.03	0.08	
m-Xylene	0.15	0.03	0.08	
p-Xylene	0.15	0.03	0.08	
Ethyl benzene	0.15	0.03	0.08	

13.5.3 The Peng–Robinson (PR) Equation of State Model (Peng and Robinson in 1976 modified the RK model to PR model)

Equation of State: $$P = \frac{RT}{V-b} - \frac{a\alpha}{V(V+b)+b(V-b)}$$

where $a = \sum_{i=1}^{N_c}\sum_{j=1}^{N_c} x_i x_j (a_i a_j)^{0.5}(1-k_{ij}), b = \sum_{i=1}^{N_c} x_i b_i,$ and ¬ will be defined in the following discussions.

For Pure Components

Vapour phase

$$H - H^0 = RT(Z_v - 1) + \frac{RTA^2}{2\sqrt{2}B}\left(\frac{T}{\alpha}\frac{d\alpha}{dT} - 1\right)\ln\left[\frac{Z_v + (1+\sqrt{2})BP}{Z_v + (1-\sqrt{2})BP}\right] \qquad (13.75)$$

$$\ln\frac{f^V}{P} = Z_v - 1 - \ln(Z_v - BP) - \frac{A^2}{2\sqrt{2}B}\ln\left[\frac{Z_v + (1+\sqrt{2})BP}{Z_v + (1-\sqrt{2})BP}\right] \qquad (13.76)$$

Liquid phase

$$h - H^0 = RT(Z_L - 1) + \frac{RTA^2}{2\sqrt{2}B}\left(\frac{T}{\alpha}\frac{d\alpha}{dT} - 1\right)\ln\left[\frac{Z_L + (1+\sqrt{2})BP}{Z_L + (1-\sqrt{2})BP}\right] \qquad (13.77)$$

$$\ln\frac{f^L}{P} = Z_L - 1 - \ln(Z_L - BP) - \frac{A^2}{2\sqrt{2}B}\ln\left[\frac{Z_L + (1+\sqrt{2})BP}{Z_L + (1-\sqrt{2})BP}\right] \qquad (13.78)$$

For Mixtures

Vapour phase

$$\Omega_v = RT(Z_v - 1) + \frac{RTA_v^2}{2\sqrt{2}B_v}\left[\frac{2T}{A_v^2}\sum_{i=1}^{N_c} y_i \bar{A}_{vi}^2\left(\frac{1}{\alpha_i^{0.5}}\frac{d\alpha_i^{0.5}}{dT}\right) - 1\right]\ln\left[\frac{Z_v + (1+\sqrt{2})B_vP}{Z_v + (1-\sqrt{2})B_vP}\right] \qquad (13.79)$$

$$\ln\frac{\hat{f}_i^V}{Py_i} = \frac{B_i}{B_v}(Z_v - 1) - \frac{A_v^2}{2\sqrt{2}B_v}\left(\frac{2\bar{A}_{vi}^2}{A_v^2} - \frac{B_i}{B_v}\right)\ln\left[\frac{Z_v + (1+\sqrt{2})B_vP}{Z_v + (1-\sqrt{2})B_vP}\right] - \ln(Z_v - B_vP) \qquad (13.80)$$

where

$$A_v = \sum_{i=1}^{N_c} y_i A_i \qquad \text{[from Equation (13.43)]}$$

$$B_v = \sum_{i=1}^{N_c} y_i B_i \qquad \text{[from Equation (13.44)]}$$

$$A_v^2 = \left(\sum_{i=1}^{N_c} y_i A_i\right)^2 = \sum_{i=1}^{N_c}\sum_{j=1}^{N_c} y_i y_j A_i A_j \qquad \text{[from Equation (13.60)]}$$

$$\bar{A}_{vi}^2 = A_i \sum_{j=1}^{N_c} y_j A_j \qquad \text{[from Equation (13.61)]}$$

Liquid phase

$$\Omega_L = RT(Z_L - 1) + \frac{RTA_L^2}{2\sqrt{2}B_L}\left[\frac{2T}{A_L^2}\sum_{i=1}^{N_c} x_i \bar{A}_{Li}^2 \left(\frac{1}{\alpha_i^{0.5}}\frac{d\alpha_i^{0.5}}{dT}\right) - 1\right]\ln\left[\frac{Z_L + (1+\sqrt{2})B_L P}{Z_L + (1-\sqrt{2})B_L P}\right] \tag{13.81}$$

$$\ln\frac{\hat{f}_i^L}{Px_i} = \frac{B_i}{B_L}(Z_L - 1) - \frac{A_L^2}{2\sqrt{2}B_L}\left(\frac{2\bar{A}_{Li}^2}{A_L^2} - \frac{B_i}{B_L}\right)\ln\left[\frac{Z_L + (1+\sqrt{2})B_L P}{Z_L + (1-\sqrt{2})B_L P}\right] - \ln(Z_L - B_L P) \tag{13.82}$$

where

$A_L = \sum_{i=1}^{N_c} x_i A_i$ [from Equation (13.47)]

$B_L = \sum_{i=1}^{N_c} x_i B_i$ [from Equation (13.48)]

$A_L^2 = \left(\sum_{i=1}^{N_c} x_i A_i\right)^2 = \sum_{i=1}^{N_c}\sum_{j=1}^{N_c} x_i x_j A_i A_j$ [from Equation (13.64)]

$\bar{A}_{Li}^2 = A_i \sum_{j=1}^{N_c} x_j A_j$ [from Equation (13.65)]

Other expressions, which are included in the PR model, are

$$a_i = 0.45724\frac{R^2 T_{ci}^2}{P_{ci}} \tag{13.83}$$

$$b_i = 0.07780\frac{RT_{ci}}{P_{ci}} \tag{13.84}$$

$A_i = \frac{a_i^{0.5}\alpha_i^{0.5}}{RT}$ [from Equation (13.68)]

$B_i = \frac{b_i}{RT}$ [from Equation (13.52)]

$\alpha_i^{0.5} = 1 + m_i(1 - T_{ri}^{0.5})$ [from Equation (13.69)]

$$m_i = 0.37464 + 1.54226w_i - 0.26992w_i^2 \tag{13.85}$$

Values of the compressibility factor for vapour and liquid phases are determined by solving the following form of equation:

$$Z^3 - (1 - BP)Z^2 + [A^2P - BP(2 + 3BP)]Z - BP[A^2P - BP(1 + BP)] = 0 \tag{13.86}$$

The binary interaction parameter k_{ij} can be incorporated in the definitions of A_v^2, $\overline{A}_{vi}^2$, A_L^2 and $\overline{A}_{Li}^2$ as explained in the SRK equation of state model. It is noteworthy that the two binary interaction parameters, k_{ij}'s, in the SRK and PR models are not necessarily the same (Edmister and Lee, 1984). The values of these binary interaction coefficients are usually obtained from experimental VLE data on binary mixtures by using, for example, a least square curve-fitting method. The binary parameters may also be obtained from other sources of experimental data such as second virial coefficients of binary mixtures.

Since two-constant equations have their inherent limitations, and the PR equation is no exception, the justification for this model is the compromise of its simplicity and accuracy. It performs as well as or better than the SRK model and shows its greatest advantages in the prediction of liquid phase densities. Like the SRK model, the PR equation of state model is recommended for computing the thermodynamic properties of both vapour and liquid phases.

13.5.4 The Benedict–Webb–Rubin (BWR) Equation of State Model (developed by Benedict, Webb and Rubin in 1940)

Equation of State: $$P = RT\rho + \left(B_0RT - A_0 - \frac{C_0}{T^2}\right)\rho^2 + (bRT - a)\rho^3 + a\alpha\rho^6 + \frac{c\rho^3}{T^2}(1+\gamma\rho^2)\exp(-\gamma\rho^2)$$

where A_0, B_0, C_0, a, b, c, γ and α are empirical constants, and ρ is the molal density.

For Pure Components

Vapour phase

$$H - H^0 = \left(B_0RT - 2A_0 - \frac{4C_0}{T^2}\right)\rho_v + \left(bRT - \frac{3a}{2}\right)\rho_v^2 + \frac{6a\alpha\rho_v^5}{5} + \frac{c\rho_v^2}{T^2}\left[3\left(\frac{1-\exp(-\gamma\rho_v^2)}{\gamma\rho_v^2}\right) + \left(\gamma\rho_v^2 - \frac{1}{2}\right)\exp\left(-\gamma\rho_v^2\right)\right] \tag{13.87}$$

$$RT\ln\left(\frac{f^V}{P}\right) = RT\ln\left(\frac{\rho_v RT}{P}\right) + 2\left(B_0RT - A_0 - \frac{C_0}{T^2}\right)\rho_v + \frac{3}{2}(bRT - a)\rho_v^2 + \frac{6}{5}a\alpha\rho_v^5 + \frac{c\rho_v^2}{T^2}\left[\frac{1-\exp(-\gamma\rho_v^2)}{\gamma\rho_v^2} + \left(\frac{1}{2} + \gamma\rho_v^2\right)\exp(-\gamma\rho_v^2)\right] \tag{13.88}$$

Liquid phase

$$h - H^0 = \left(B_0RT - 2A_0 - \frac{4C_0}{T^2}\right)\rho_L + \left(bRT - \frac{3a}{2}\right)\rho_L^2 + \frac{6a\alpha\rho_L^5}{5} + \frac{c\rho_L^2}{T^2}\left[3\left(\frac{1-\exp(-\gamma\rho_L^2)}{\gamma\rho_L^2}\right) + \left(\gamma\rho_L^2 - \frac{1}{2}\right)\exp(-\gamma\rho_L^2)\right] \tag{13.89}$$

$$RT\ln\left(\frac{f^L}{P}\right)=RT\ln\left(\frac{\rho_L RT}{P}\right)+2\left(B_0RT-A_0-\frac{C_0}{T^2}\right)\rho_L+\frac{3}{2}(bRT-a)\rho_L^2$$
$$+\frac{6}{5}a\alpha\rho_L^5+\frac{c\rho_L^2}{T^2}\left[\frac{1-\exp(-\gamma\rho_L^2)}{\gamma\rho_L^2}+\left(\frac{1}{2}+\gamma\rho_L^2\right)\exp(-\gamma\rho_L^2)\right] \quad (13.90)$$

For Mixtures

Vapour phase

$$\Omega_v=\left(B_{0v}RT-2A_{0v}-\frac{4C_{0v}}{T^2}\right)\rho_v+\left(b_vRT-\frac{3a_v}{2}\right)\rho_v^2+\frac{6a_v\alpha_v\rho_v^5}{5}$$
$$+\frac{c_v\rho_v^2}{T^2}\left[3\left(\frac{1-\exp(-\gamma_v\rho_v^2)}{\gamma_v\rho_v^2}\right)+\left(\gamma_v\rho_v^2-\frac{1}{2}\right)\exp(-\gamma_v\rho_v^2)\right] \quad (13.91)$$

$$RT\ln\left(\frac{\hat{f}_i^V}{Py_i}\right)=RT\ln\left(\frac{\rho_v RT}{P}\right)+\left[(B_{0v}+B_{0i})RT-2(A_{0v}A_{0i})^{0.5}-2\frac{(C_{0v}C_{0i})^{0.5}}{T^2}\right]\rho_v$$
$$+\frac{3}{2}[RT(b_v^2b_i)^{1/3}-(a_v^2a_i)^{0.5}]\rho_v^2+\frac{3}{5}[a_v(\alpha_v^2\alpha_i)^{1/3}+\alpha_v(a_v^2a_i)^{1/3}]\rho_v^5$$
$$+\frac{3\rho_v^2(c_v^2c_i)^{1/3}}{T^2}\left(\frac{1-\exp(-\gamma_v\rho_v^2)}{\gamma_v\rho_v^2}-\frac{\exp(-\gamma_v\rho_v^2)}{2}\right)$$
$$-\frac{2\rho_v^2c_v}{T^2}\left(\frac{\gamma_i}{\gamma_v}\right)^{0.5}\left(\frac{1-\exp(-\gamma_v\rho_v^2)}{\gamma_v\rho_v^2}-\exp(-\gamma_v\rho_v^2)-\frac{\gamma_v\rho_v^2\exp(-\gamma_v\rho_v^2)}{2}\right) \quad (13.92)$$

where

$$A_{0v}=\left(\sum_{i=1}^{N_c}y_iA_{0i}^{0.5}\right)^2 \quad (13.93)$$

$$B_{0v}=\sum_{i=1}^{N_c}y_iB_{0i} \quad (13.94)$$

$$C_{0v}=\left(\sum_{i=1}^{N_c}y_iC_{0i}^{0.5}\right)^2 \quad (13.95)$$

$$a_v = \left(\sum_{i=1}^{N_c} y_i a_i^{1/3} \right)^3 \quad (13.96)$$

$$b_v = \left(\sum_{i=1}^{N_c} y_i b_i^{1/3} \right)^3 \quad (13.97)$$

$$c_v = \left(\sum_{i=1}^{N_c} y_i c_i^{1/3} \right)^3 \quad (13.98)$$

$$\alpha_v = \left(\sum_{i=1}^{N_c} y_i \alpha_i^{1/3} \right)^3 \quad (13.99)$$

$$\gamma_v = \left(\sum_{i=1}^{N_c} y_i \gamma_i^{0.5} \right)^2 \quad (13.100)$$

$$\rho_v = \sum_{i=1}^{N_c} y_i \rho_{vi} \quad (13.101)$$

Liquid phase

$$\Omega_L = \left(B_{0L} RT - 2A_{0L} - \frac{4C_{0L}}{T^2} \right) \rho_L + \left(b_L RT - \frac{3a_L}{2} \right) \rho_L^2 + \frac{6a_L \alpha_L \rho_L^5}{5} + \frac{c_L \rho_L^2}{T^2} \left[3 \left(\frac{1 - \exp(-\gamma_L \rho_L^2)}{\gamma_L \rho_L^2} \right) + \left(\gamma_L \rho_L^2 - \frac{1}{2} \right) \exp(-\gamma_L \rho_L^2) \right] \quad (13.102)$$

$$RT \ln \left(\frac{\hat{f}_i^L}{P x_i} \right) = RT \ln \left(\frac{\rho_L RT}{P} \right) + \left[(B_{0L} + B_{0i}) RT - 2(A_{0L} A_{0i})^{0.5} - 2 \frac{(C_{0L} C_{0i})^{0.5}}{T^2} \right] \rho_L + \frac{3}{2} [RT (b_L^2 b_i)^{1/3} - (a_L^2 a_i)^{0.5}] \rho_L^2 + \frac{3}{5} [a_L (\alpha_L^2 \alpha_i)^{1/3} + \alpha_L (a_L^2 a_i)^{1/3}] \rho_L^5 + \frac{3\rho_L^2 (c_L^2 c_i)^{1/3}}{T^2} \left(\frac{1 - \exp(-\gamma_L \rho_L^2)}{\gamma_L \rho_L^2} - \frac{\exp(-\gamma_L \rho_L^2)}{2} \right) - \frac{2\rho_L^2 c_L}{T^2} \left(\frac{\gamma_i}{\gamma_L} \right)^{0.5} \left(\frac{1 - \exp(-\gamma_L \rho_L^2)}{\gamma_L \rho_L^2} - \exp(-\gamma_L \rho_L^2) - \frac{\gamma_L \rho_L^2 \exp(-\gamma_L \rho_L^2)}{2} \right) \quad (13.103)$$

where

$$A_{0L} = \left(\sum_{i=1}^{N_c} x_i A_{0i}^{0.5} \right)^2 \qquad (13.104)$$

$$B_{0L} = \sum_{i=1}^{N_c} x_i B_{0i} \qquad (13.105)$$

$$C_{0L} = \left(\sum_{i=1}^{N_c} x_i C_{0i}^{0.5} \right)^2 \qquad (13.106)$$

$$a_L = \left(\sum_{i=1}^{N_c} x_i a_i^{1/3} \right)^3 \qquad (13.107)$$

$$b_L = \left(\sum_{i=1}^{N_c} x_i b_i^{1/3} \right)^3 \qquad (13.108)$$

$$c_L = \left(\sum_{i=1}^{N_c} x_i c_i^{1/3} \right)^3 \qquad (13.109)$$

$$\alpha_L = \left(\sum_{i=1}^{N_c} x_i \alpha_i^{1/3} \right)^3 \qquad (13.110)$$

$$\gamma_L = \left(\sum_{i=1}^{N_c} x_i \gamma_i^{0.5} \right)^2 \qquad (13.111)$$

$$\rho_L = \sum_{i=1}^{N_c} x_i \rho_{Li} \qquad (13.112)$$

In the above equations, $\hat{}_v$ is the molal density in vapour phase and $\hat{}_L$ represents the molal density in liquid phase. As described above, the eight parameters A_0, B_0, C_0, a, b, c, ㄱㅅ and ㄹㅅ are numerical constants for pure species and functions of composition for mixtures. Values of these constants for different pure components are given in Table 13.6. In some correlations, some of these constants are taken to be functions of temperature.

It is noteworthy that the BWR equation of state model for mixtures may be derived from data on pure components alone, without the need for supplementary data on mixtures. Although the BWR equation of state is a complex one involving eight constant parameters for each constituent component, this state model is required to describe accurately the *P-V-T* relations of real fluids over the entire vapour and liquid regions.

Table 13.6 Constants for the BWR model

Component	A_0	B_0	C_0 ($\times 10^{-6}$)	a	b	c ($\times 10^{-6}$)	γ ($\times 10^{3}$)	α ($\times 10^{2}$)
Methane	6995.25	0.682401	275.763	2984.12	0.867325	498.106	511.172	153.961
Ethylene	12593.6	0.89198	1602.28	15645.5	2.20678	4133.14	731.661	236.844
Ethane	15670.7	1.00554	2194.27	20850.2	2.85393	6413.14	1000.44	302.790
Propylene	23049.2	1.36263	5365.97	46758.6	4.79997	20083.0	1873.12	469.325
Propane	25913.4	1.55884	6209.93	57248.0	5.77355	25247.8	2495.77	464.524
iso-Butane	38587.4	2.20329	10384.7	117047.0	10.8890	55977.7	4414.96	872.447
iso-Butylene	33762.9	1.85858	11329.6	102251.0	8.93375	53807.2	3744.17	759.401
n-Butane	38029.6	1.99211	12130.5	113705.0	10.2636	61925.6	4526.93	872.447
iso-Pentane	4825.36	2.56386	21336.7	226902.0	17.1441	136025.0	6987.77	1188.07
n-Pentane	45928.8	2.51096	25917.2	246148.0	17.1441	161306.0	7439.92	1218.86
n-Hexane	5443.4	2.84835	40556.2	429901.0	28.0032	296077.0	11553.9	1711.15
n-Heptane	66070.6	3.18782	57984.0	626106.0	38.9917	483427.0	17905.6	2309.42
n-Octane	55471.799	2.43165	88100.0	1259500.0	73.054599	882303.0	17942.1	2456.80
Benzene	24548.48	0.8057382	41907.7	336468.00	19.663411	230247.3	2877.29	751.841
Hydrogen	585.127	0.3339370	4.1100	98.599000	0.0868200	1.423170	479.116	82.8100
Nitrogen	4496.941	0.7336413	71.9533	900.07000	0.5084650	107.2668	1198.38	192.451
Carbon dioxide	10322.799	0.7994960	1698.00	8264.4600	1.0582000	2919.710	348.000	138.400
Hydrogen sulphide	11701.1	0.5582140	2360.00	8758.2700	1.1354300	3660.180	289.043	116.889

Note: The above BWR constants are derived considering P in lb/in^2 abs., ρ_v and ρ_L in lbmol/ft^3, T in °R, and R = 10.7335 lb ft^3/(in^2. lbmol. °R).

Reprinted with permission from (Benedict, M., Webb, G.B., and Rubin, L.C. (1951). An empirical equation for thermodynamic properties of light hydrocarbons and their mixtures—constants for twelve hydrocarbons, *Chem. Eng. Prog*., 47, 419–422) American Institute of Chemical Engineers.

13.6 VAPOUR PRESSURE: A REVIEW

Here, we will briefly discuss several methods for the estimation of vapour pressure of pure components. It is important to note that if the total pressure is not very high (above about 10 MPa), the influence of total pressure on vapour pressure is not so significant. We can apply a correction, the Poynting correction (see Subsection 8.1), to capture the effect of very high total pressures. Antoine (1888) proposed a simple vapour pressure correlation that has been widely used over limited temperature ranges as:

$$\ln P_i^S = A_i - \frac{B_i}{T + C_i} \qquad \text{[from Equation (9.28)]}$$

Values of the Antoine constants A, B and C for different components (P_i^S in mm Hg and T in K) are reported in Table 9.4. Note that the Antoine correlation does not fit data accurately much above the normal boiling point. In such a situation, the following procedures may be followed.

The vapour pressure can be computed using the following form of correlation (Reid, Prausnitz and Poling, 1987):

$$P_i^S = P_{ci} \exp\left(\frac{A_{1i}\beta_i + A_{2i}\beta_i^{1.5} + A_{3i}\beta_i^3 + A_{4i}\beta_i^6}{1-\beta_i}\right) \qquad (13.113)$$

where

$$\beta_i = 1 - (T/T_{ci}) = 1 - T_{ri} \qquad (13.114)$$

Values of the constants A_1, A_2, A_3 and A_4 for different compounds are reported in Table 13.4. Values are given when P_i^S and P_{ci} are in bar, and T and T_{ci} are in K.

This method can match the critical data exactly, although it cannot be extrapolated above the critical point. In the application of the procedure described above, the main difficulty arises when $T > T_c$. For example, the tray temperature in a typical distillation column may be greater than the critical temperature

of the lightest component. In such a situation, the above method should not be used due to the associated term $[1 - (T/T_c)]^{1.5}$ and the following procedure is recommended (Lee and Kesler, 1975).

The method of Lee and Kesler has gained almost universal acceptance for prediction of the vapour pressure of pure hydrocarbons. According to this method (three-parameter form),

$$P_i^S = P_{ci} \exp (\ln \pi_{1i} + w_i \ln \pi_{2i}) \qquad (13.115)$$

where the correlation terms are

$$\ln \pi_{1i} = 5.92714 - (6.09648/T_{ri}) - 1.28862 \ln T_{ri} + 0.169347 T_{ri}^6 \qquad (13.116)$$

$$\ln \pi_{2i} = 15.2518 - (15.6875/T_{ri}) - 13.4721 \ln T_{ri} + 0.43577 T_{ri}^6 \qquad (13.117)$$

When Equation (13.115) is employed, Lee and Kesler recommended that the following expression be used to compute the acentric factor:

$$w = \frac{-\ln P_c - 5.92714 + (6.09648/T_{br}) + 1.28862 \ln T_{br} - 0.169347 T_{br}^6}{15.2518 - (15.6875/T_{br}) - 13.4721 \ln T_{br} + 0.43577 T_{br}^6} \qquad (13.118)$$

where $T_{br} = T_b/T_c$ and T_b is the normal boiling point temperature. In the above Lee–Kesler method, all pressures are in atm and temperatures are in K. It is obvious that Equation (13.118) is obtained from Equation (13.115) with $T_r = T_{br}$ and $P^S = 1$ atm.

The correlation terms, $\ln \pi_1$ and $\ln \pi_2$, have been tabulated over wide ranges in reduced temperature [Halm and Stiel, 1967; Carruth and Kobayashi, 1972; Technical Data Book—Petroleum Refining (API), 1984]. The Lee–Kesler method is valid only for nonpolar substances and restricted to reduced temperatures above 0.30 or the freezing point, whichever is higher, and below the critical point. The method is most reliable when $0.50 < T_r < 0.95$. Remember that to apply the above vapour pressure estimating methods [Equations (13.113) and (13.115)], one needs the information on the critical properties of the constituent components.

13.7 SUMMARY AND CONCLUSIONS

The present chapter is devoted to a study of different equations of state models and their suitable applications in different systems. The multistage multicomponent separation processes are extensively used in chemical, petroleum and related industries. Simulation of these processes requires accurate and consistent thermodynamic properties such as vapour–liquid equilibrium coefficients and enthalpies over a wide range of conditions. In industrial practice, many distillation systems are operated at sufficiently high pressure. The thermodynamic properties of a mixture in both vapour and liquid phases are severely affected due to the strong nonidealities under high pressure. In such cases, reasonably good predictions of enthalpies and vapour–liquid equilibrium coefficients are provided by the equations of state. Alternatively, the nonidealities in the liquid phase are calculated using activity coefficient models.

The Benedict–Webb–Rubin, Peng–Robinson, Soave–Redlich–Kwong, Redlich–Kwong and UNIFAC are very effective and most useful thermodynamic models in real-time situations. Generally, the activity coefficient-based UNIFAC method should not be used when the operating pressure is above the critical pressure of any of the light components. Additionally, except for low pressure, a fugacity correction for the vapour phase at the operating pressure is very much essential. Therefore, an appropriate alternative is

to employ the equation of state models for more accurate predictions of the thermodynamic properties including vapour–liquid equilibrium coefficients of hydrocarbons and related compounds.

EXERCISES

13.1 What is equation of state and why is it called so?

13.2 At what situations, are the equations of state preferred to employ than the activity coefficient models for the prediction of the thermodynamic properties of a mixture? Give reasons.

13.3 Derive the vapour–liquid equilibrium coefficient for any component i in terms of the symmetrical and unsymmetrical formulations.

13.4 Compare the different equation of state models with respect to their applications and limitations.

13.5 For the RK equation of state model, derive an expression for

$$\left(\frac{\partial Z}{\partial T}\right)_P$$

13.6 The compressibility factors in the RK and SRK models are found out by solving the following form of equation:

$$Z^3 - Z^2 + [A^2P - BP(1 + BP)]Z - A^2PBP = 0 \qquad \text{[from Equation (13.53)]}$$

Why is the same Equation (13.53) used in both the state models? Provide the necessary derivations in support of your answer.

13.7 Derive Equation (13.86) that is used to estimate the compressibility factors in the PR equation of state model.

13.8 For both the vapour and liquid phases, derive the enthalpy and fugacity expressions for pure components [e.g., Equations (13.37) and (13.38)] from the enthalpy and fugacity expressions of mixtures [e.g., Equations (13.41) and (13.42)]. Perform the derivations for the

(i) RK model
(ii) SRK model
(iii) PR model
(iv) BWR model

13.9 Estimate the change in enthalpy for *iso*-butane vapour during isothermal compression from 0.6895 bar to 15.81 bar pressure (abs) at 360 K temperature employing the RK equation of state model.

13.10 The equilibrium phase compositions for a system of methane–*n*-butane–*n*-decane are provided by Reamer, Sage, and Lacey [*Ind. Eng. Chem.,* 43, 1436 (1951)] at 410.8 K temperature and 206.80 bar pressure (abs). The data are given below.

Species	x_i	y_i
Methane	0.5444	0.9140
n-Butane	0.0916	0.0512
n-Decane	0.3640	0.0348

Use the SRK state model to predict for each phase the

(i) mixture fugacity coefficients
(ii) enthalpies
(iii) k-values

13.11 Repeat Problem 13.10 using the PR equation of state.

13.12 Estimate the acentric factor for the following compounds using Equation (13.118)

(i) *n*-Pentane
(ii) *iso*-Pentane
(iii) *n*-Octane

13.13 Discuss the applicability of several vapour pressure estimating methods.

REFERENCES

American Petroleum Institute (1984). *Technical Data Book—Petroleum Refining*, Chapter 5, Washington, D.C.

Antoine, C. (1888). Tension des vapeurs: nouvelle relation entre les tension et les temperatures. *Competes Rendus*, 107, 681–684, 836–837.

Benedict, M., Webb, G.B., and Rubin, L.C. (1940). An empirical equation for the thermo-dynamic properties of light hydrocarbons and their mixtures, *J. Chem. Phys*., 8, 334.

Carruth, G.F., and Kobayashi, R. (1972). Extension to low reduced temperatures of three-parameter corresponding states: vapour pressures, enthalpies and entropies of vaporization, and liquid fugacity coefficients, *Ind. Eng. Chem. Fundam.*, 11, 509–517.

Chao, K.C., and Seader, J.D. (1961). A general correlation of vapour–liquid equilibria in hydrocarbon mixtures, *AIChE J.*, 7, 598–605.

Edmister, W.C. (1968). *Applied Hydrocarbon Thermodynamics*; Part 32—compressibility factors and fugacity coefficients from the Redlich–Kwong equation of state, *Hydrocarbon Processing*, 47, 239–244.

Edmister, W.C., and Lee, B.I. (1984). *Applied Hydrocarbon Thermodynamics*, Vol. 1, 2nd ed., Gulf Publishing Company, Houston.

Erbar, J.H. (1973). Oklahoma State University, Personal Communication.

Hadden, S.T. (1948). Vapour–liquid equilibria in hydrocarbon system, *Chem. Eng. Prog.*, 44, 37.

Halm, R.L., and Stiel, L.I. (1967). A fourth parameter for the vapour pressure and entropy of vaporization of polar fluids, *AIChE J.*, 13, 351–355.

Lee, B.I., Erbar, J.H., and Edmister, W.C. (1973). Properties for low temperature hydrocarbon process calculations, *AIChE J*., 19, 349–356.

Lee, B.I., and Kesler, M.G. (1975). A generalized thermodynamic correlation based on three-parameter corresponding states, *AIChE J*., 21, 510–527.

Maxwell, J.B. (1955). *Data Book on Hydrocarbons*, D. Van Nostrand Company, New York.

Passut, C.A., and Danner, R.P. (1972). Correlation of ideal gas enthalpy, heat capacity, and entropy, *Ind. Eng. Chem. Process Design Devel*., 11, 543–546.

Peng, D.Y., and Robinson, D.B. (1976). A new two-constant equation of state, *Ind. Eng. Chem. Fundam*., 15, 59–64.

Redlich, O., and Kwong, J.N.S. (1949). On the thermodynamics of solutions. V. An equation of state. Fugacities of gaseous solutions, *Chem. Rev*., 44, 233–244.

Reid, R.C., Prausnitz, J.M., and Poling, B.E. (1987). *The Properties of Gases and Liquids*, 4th ed., McGraw-Hill Book Company, New York.

Robinson, R.L., and Chao, K.C. (1971). A correlation of vaporization equilibrium ratios for gas processing systems, *Ind. Eng. Chem. Process Design Devel*., 10, 221–229.

Soave, G. (1972), Equilibrium constants from a modified Redlich–Kwong equation of state, *Chem. Eng. Sci.*, 27, 1197–1203.

Sokolnikoff, I.S., and Sokolnikoff, E.S. (1941), *Higher Mathematics for Engineers and Physicists*, 2nd ed., McGraw-Hill Book Company, New York.

14

Refinery Debutanizer Column

14.1 INTRODUCTION

Distillation is one of the central and critical operating processes in chemical industries. The stagewise multicomponent separation processes are generally represented by an equilibrium stage model and described by the model equations consisting of material balances, equilibrium relationships, heat balances and summation equations. The model equations are numerous and nonlinear in nature.

Even in the mid-1970s, two computational methods, namely traditional methods and methods based on linearization, were conventionally used to predict the nature of a multicomponent distillation process. Traditional methods such as those proposed by Lewis and Matheson (1932), Thiele and Geddes (1933), Sujata (1961), and Wang and Henke (1966) solve the model equations independently to obtain composition, temperature and vapour profiles in a column. Friday and Smith (1964) have reported that the traditional methods are not suitable for a wide range of problems. Subsequently developed methods are based on the concept of linearization and having an advantage of improved convergence characteristics over a relatively wider range of conditions. The examples are the methods proposed by Tomich (1970), Goldstein and Stanfield (1970), Naphtali and Sandholm (1971), Billingsley and Boynton (1971), Ishii and Otto (1973), and Shah and Bishnoi (1978).

Up to the early 1980s, there has been a continuous development of dynamic models of distillation columns with emphasis on process control and fast, approximate models in strategies for maintaining product specifications. Very few of these models, however, consider the solution of the material and energy balances on each plate using models to represent plate hydraulics and approaches to equilibrium. Gani, Ruiz, and Cameron (1986) proposed a generalized model that is flexible enough to handle different column (or columns) configurations and is versatile enough to allow the study of different operations (e.g., start-up).

Dynamic simulation is commonly used to make stability, operability and control analysis. Actually, operating modes near nominal points, determination of new operating points, start-up and shutdown policies, design of optimal control strategies can be studied by means of dynamic simulation procedures. This chapter presents a detailed dynamic modelling, computer simulation and control of a complex debutanizer process. A debutanizer is a multicomponent distillation column frequently encountered in oil refineries. This distillation process is installed in a petroleum refinery industry for different purposes. For example, this unit is used to separate *iso*-butane present in a hydrocarbon mixture for alkylation, to separate lighter hydrocarbons (mainly butane) from the naphtha (that becomes debutanized naphtha) for liquefied petroleum gas (LPG) production, and so on.

In this chapter, first the dynamic model of a debutanizer column is derived. Computer subroutines required for process simulation are also developed. The rigorous distillation model is verified with real plant data. The simulated model is then used for process control. Finally, simulation experiments have been conducted to examine the servo as well as regulatory performance.

14.2 THE PROCESS AND THE MODEL

The debutanizer column, which is dealt in this chapter, receives unstabilized naphtha feed having

components ranging from C_2 (ethane) to C_8 (octane) from the crude distiller. This multicomponent distillation fractionates the naphtha such that the light ends are removed from the top and the debutanized naphtha is removed from the bottom and directed to the splitter/platformer section for further processing. In the overhead section, the condensed liquid is directed to the liquefied petroleum gas section. A portion of the condensed liquid from the overhead is used as a reflux to the column whereas the reboiler provides the heat necessary to partially vaporize the debutanizer bottoms liquid before returning it to the column.

The sample column consists of 15 trays, a reboiler and a total condenser. The trays are numbered from the bottom to the top; the bottom tray has number 1. The liquid feed is flashed isothermally in a flash drum (details in Chapter 12) before introducing it to the fifth tray of the column. The schematic diagram of the example multicomponent distillation system is given in Figure 14.1. The specifications and steady state compositions for the simulated column are reported in Tables 14.1 and 14.2, respectively.

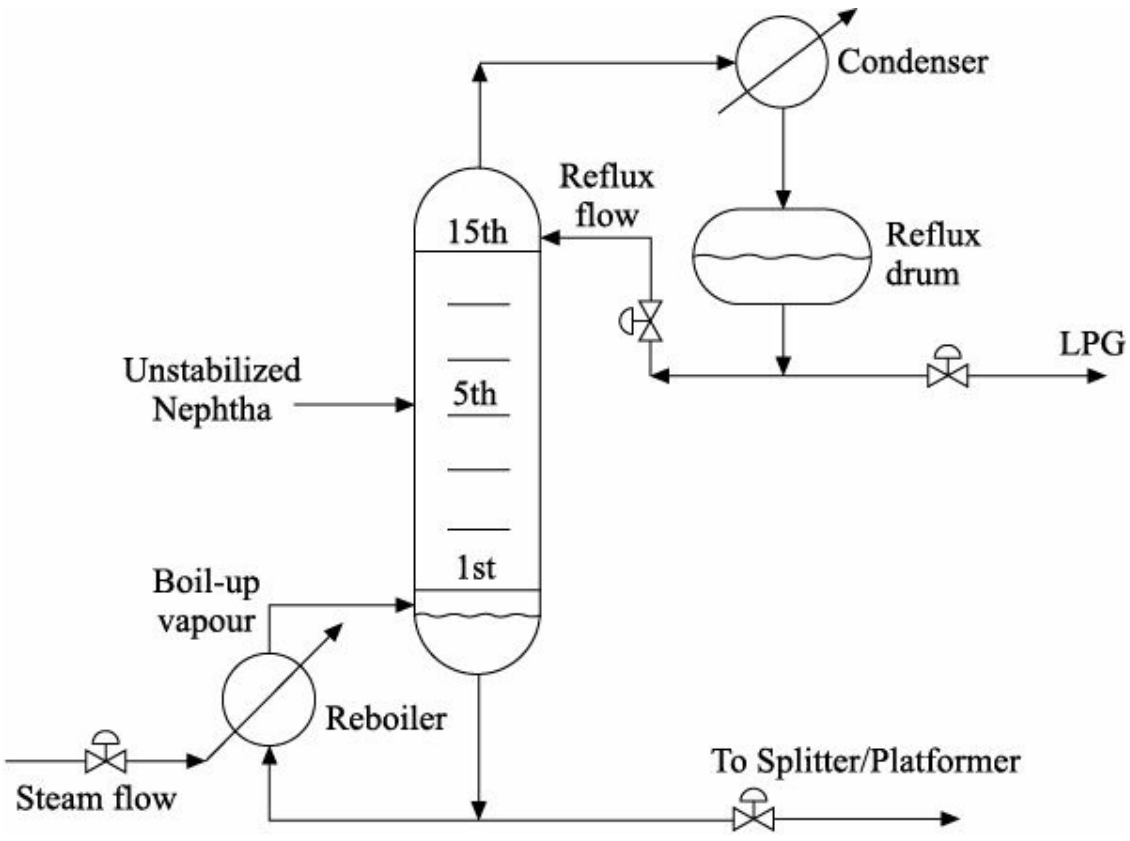

FIGURE 14.1 Schematic representation of the debutanizer column example.

Table 14.1 Simulated debutanizer column specifications

Term	*Value/Condition*	*Unit*
Number of trays	15	—
Number of components	8	—
Plate efficiency	70%	—
Actual feed plate position	5	—
Column diameter	7.958	ft
Type of condenser	Total	—
Feed condition (isothermal flash)	Two phase	—
Flash temperature of feed	180.00	°F
Flash pressure of feed	110.01	Psi
Feed flow rate	880.56	lbmol/h
Distillate temperature	134.88	°F
Distillate flow rate	472.24	lbmol/h
Bottom product temperature	257.65	°F
Bottom product flow rate	408.32	lbmol/h
Vapour boil-up rate	946.10	lbmol/h
Reflux flow rate	750.00	lbmol/h
Reboiler heat input	10000000.0	Btu/h
Integration time interval	0.000025	h

Table 14.2 Steady state compositions for the simulated debutanizer column

Component	*Feed composition*	*Distillate composition*	*Bottoms composition*
Component 1 (C_2)	0.00120174	0.002239600	0.00000006
Component 2 (C_3)	0.00675980	0.012573600	0.00003427
Component 3 (iC_4)	0.24079915	0.427743400	0.02458328
Component 4 (nC_4)	0.31515700	0.514338200	0.08478892
Component 5 (iC_5)	0.12167645	0.034126400	0.22293856
Component 6 (nC_5)	0.10244855	0.008930000	0.21061263
Component 7 (nC_6)	0.13159080	0.000050700	0.28372456
Component 8 (nC_8)	0.08036650	0.000000082	0.17331400

The debutanizer column will be employed for the separation of an eight-component hydrocarbon mixture. The rigorous process model consists of a set of ordinary differential equations (ODEs) coupled with algebraic equations/correlations. The ODEs are obtained from mass and energy balances around each plate of the distillation column. The algebraic equations/correlations are used to predict the thermodynamic and physical properties, plate hydraulics, and actual vapour-phase compositions.

The following assumptions have been made in the development of the process model:

- The molar vapour holdup is negligible compared to the molar liquid holdup.
- The liquid and vapour leaving each plate are in thermal equilibrium.
- The definition of Murphree plate efficiency applies for each plate.
- The liquid is perfectly mixed on each plate.
- No subcooling is considered in the total condenser.
- Coolant and steam dynamics in the condenser and reboiler respectively are neglected.
- Molal liquid holdup varies in each tray (including reflux drum and column base) but the holdups in reflux drum and column base are constant in volume.
- The column operates with the top (P_T) and base (P_B) pressures of 102.98 and 122.70 psia, respectively. The tray-to-tray pressure varies linearly according to the following form of equation:

$$P_n = P_B - \frac{n(P_B - P_T)}{n_T + 1} \qquad (14.1)$$

where P_n is the pressure in nth tray and n_T represents the total number of trays (here 15).

- Liquid hydraulics are calculated from the Francis weir formula (details in Chapter 11).
- Vapour–liquid equilibria (VLE) and enthalpy are calculated based on the Soave–Redlich–Kwong (SRK) equation of state (details in Chapter 13).
- The Muller iteration method based on second-degree equation (details in Chapter 2) is used in the bubble-point calculations.

14.2.1 Material and Energy Balance Equations

For all column trays including a reboiler and a reflux drum, and for a component $i = 1, ..., N_c$, the model ordinary differential equations representing total continuity (one per tray), component continuity ($N_c - 1$

per tray) and energy balance (one per tray) can be obtained as:

Reboiler–Column Base System (subscript 'B')

Total continuity: $$\dot{m}_B = L_1 - V_B - B \tag{14.2}$$

Component continuity: $$\dot{m}_B \dot{x}_{B,i} = L_1 x_{1,i} - V_B y_{B,i} - B x_{B,i} \tag{14.3}$$

Energy equation: $$\dot{m}_B \dot{H}_B^L = Q_R + L_1 H_1^L - V_B H_B^V - B H_B^L \tag{14.4}$$

Bottom Tray (subscript '1')

Total continuity: $$\dot{m}_1 = L_2 + V_B - L_1 - V_1 \tag{14.5}$$

Component continuity: $$\dot{m}_1 \dot{x}_{1,i} = L_2 x_{2,i} + V_B y_{B,i} - L_1 x_{1,i} - V_1 y_{1,i} \tag{14.6}$$

Energy equation: $$\dot{m}_1 \dot{H}_1^L = L_2 H_2^L + V_B H_B^V - L_1 H_1^L - V_1 H_1^V \tag{14.7}$$

***n*th Tray** (subscript 'n', where $n = 2$ to $n_F - 1$ and $n_F + 2$ to $n_T - 1$)

Total continuity: $$\dot{m}_n = L_{n+1} + V_{n-1} - L_n - V_n \tag{14.8}$$

Component continuity: $$\dot{m}_n \dot{x}_{n,i} = L_{n+1} x_{n+1,i} + V_{n-1} y_{n-1,i} - L_n x_{n,i} - V_n y_{n,i} \tag{14.9}$$

Energy equation: $$\dot{m}_n \dot{H}_n^L = L_{n+1} H_{n+1}^L + V_{n-1} H_{n-1}^V - L_n H_n^L - V_n H_n^V \tag{14.10}$$

Feed Tray (subscript 'n_F')

Total continuity: $$\dot{m}_{n_F} = L_{n_F+1} + F^L + V_{n_F-1} - L_{n_F} - V_{n_F} \tag{14.11}$$

Component continuity:

$$\dot{m}_{n_F} \dot{x}_{n_F,i} = L_{n_F+1} x_{n_F+1} + F^L x_{F,i} + V_{n_F-1} y_{n_F-1,i} - L_{n_F} x_{n_F,i} - V_{n_F} y_{n_F,i} \tag{14.12}$$

Energy equation:

$$\dot{m}_{n_F} \dot{H}_{n_F}^L = L_{n_F+1} H_{n_F+1}^L + F^L H_F^L + V_{n_F-1} H_{n_F-1}^V - L_{n_F} H_{n_F}^L - V_{n_F} H_{n_F}^V \tag{14.13}$$

Above Feed Tray (subscript '$n_F + 1$')

Total continuity: $$\dot{m}_{n_F+1} = L_{n_F+2} + F^V + V_{n_F} - L_{n_F+1} - V_{n_F+1} \tag{14.14}$$

Component continuity:

$$\dot{m}_{n_F+1} \dot{x}_{n_F+1,i} = L_{n_F+2} x_{n_F+2,i} + F^V y_{F,i} + V_{n_F} y_{n_F,i} - L_{n_F+1} x_{n_F+1,i} - V_{n_F+1} y_{n_F+1,i} \tag{14.15}$$

Energy equation:

$$\dot{m}_{n_F+1} \dot{H}_{n_F+1}^L = L_{n_F+2} H_{n_F+2}^L + F^V H_F^V + V_{n_F} H_{n_F}^V - L_{n_F+1} H_{n_F+1}^L - V_{n_F+1} H_{n_F+1}^V \tag{14.16}$$

Top Tray (subscript 'n_T')

Total continuity: $$\dot{m}_{n_T} = R + V_{n_T-1} - L_{n_T} - V_{n_T} \tag{14.17}$$

Component continuity: $$\dot{m}_{n_T} \dot{x}_{n_T,i} = R x_{D,i} + V_{n_T-1} y_{n_T-1,i} - L_{n_T} x_{n_T,i} - V_{n_T} y_{n_T,i} \tag{14.18}$$

Energy equation: $$\dot{m}_{n_T} \dot{H}_{n_T}^L = R H_D^L + V_{n_T-1} H_{n_T-1}^V - L_{n_T} H_{n_T}^L - V_{n_T} H_{n_T}^V \tag{14.19}$$

Condenser–Reflux Drum System (subscript '*D*')

Total continuity: $$\dot{m}_D = V_{n_T} - R - D \tag{14.20}$$

Component continuity: $$\dot{m}_D \dot{x}_{D,i} = V_{n_T} y_{n_T,i} - (R + D) x_{D,i} \tag{14.21}$$

In the above distillation modelling equations, $x_{n,i}$ is the mole fraction of component i in a liquid stream leaving nth tray, $y_{n,i}$ the mole fraction of component i in a vapour stream leaving nth tray, $x_{F,i}$ the mole fraction of component i in the liquid feed, $y_{F,i}$ the mole fraction of component i in the vapour feed, $x_{D,i}$ the mole fraction of component i in the distillate, $x_{B,i}$ the mole fraction of component i in the bottom product, L_n the liquid flow rate leaving nth tray (lbmol/h), V_n the vapour flow rate leaving nth tray (lbmol/h), R the reflux flow rate (lbmol/h), D the distillate flow rate (lbmol/h), V_B the vapour boil-up rate (lbmol/h), B the bottom product flow rate (lbmol/h), F^L the flow rate of the liquid feed (lbmol/h), F^V the flow rate of the vapour feed (lbmol/h), m_n the liquid holdup on nth tray (lbmol), m_D the liquid holdup in the reflux drum (lbmol), m_B the liquid holdup in the reboiler–column base system (lbmol), H_n^L the enthalpy of a liquid stream leaving nth tray (Btu/lbmol), H_v^V the enthalpy of a vapour stream leaving nth tray (Btu/lbmol), H_B^L the enthalpy of the bottom product (Btu/lbmol), H_B^V the enthalpy of the boil-up vapour (Btu/lbmol), H_D^L the enthalpy of the distillate (Btu/lbmol), H_F^L the enthalpy of the liquid feed (Btu/lbmol), H_F^V the enthalpy of the vapour feed
(Btu/lbmol), Q_R the heat input to the reboiler (Btu/h), N_c the number of components (here 8) and n_F the feed tray. The time derivative of any variable, say z, and the time derivative of the multiplication of any two variables, say z_1 and z_2, are represented in the above model as $\dot{z}$ and $\dot{z}_1 z_2$, respectively.

The energy balance equations, with substituting zero in the left hand sides, are transformed into a set of algebraic equations since the dynamic changes in internal energies on the trays are much faster than the composition or total holdup changes. These transformed algebraic equations are actually employed to calculate the internal vapour flow rates. Remember that the vapour boil-up rate V_B is not computed from Equation (14.4) when that is the controller output other than Q_R in the closed bottom loop. Interestingly, no heat balance equation is incorporated in the model structure of the condenser–reflux drum system because no vapour flow rate calculation is involved there. As mentioned earlier, the vapour and liquid enthalpies along with the vapour–liquid equilibrium coefficient have been computed using the SRK equation of state model.

14.2.2 Tray Holdup Dynamics

Distefano (1968) has reported a procedure for tray holdup calculations in distillation columns. This approach formulates based on the assumption of constant volume holdup on the plates. Therefore, the molal holdup on nth plate is given by:

$$m_n = \frac{mv_n \rho_{Ln}}{\mathrm{MW}_n} \tag{14.22}$$

where mv_n is the constant volumetric liquid holdup (volume) on any plate n. $\hat{}_{Ln}$ and MW_n represent the average density (mass/volume) and average molecular weight, respectively, of the liquid stream on nth

plate.

In real-time distillation processes, the volumetric liquid holdups (or heights) in the reflux drum and column base are held almost constant by implementing conventional level controllers (proportional) to the manipulation of distillate and bottom product flow rates, respectively. But this is not the case for the internal trays. Distefano (1968) has suggested to use Equation (14.22) for all trays of a batch distillation column except the still-pot. Again Luyben (1990) preferred to simulate the total continuity equations for the calculation of liquid holdups on the internal trays of a multicomponent continuous distillation column. But he considered constant volumetric liquid holdups in the condenser–accumulator as well as in the reboiler–column base system.

In order to predict the holdup dynamics in the condenser–reflux drum and reboiler–column base systems, the molal holdups may be represented according to the approach explained above as:

For Condenser–Reflux Drum System

$$m_D = \frac{mv_D \rho_{LD}}{\mathrm{MW}_D} \qquad (14.23a)$$

For Reboiler–Column Base System

$$m_B = \frac{mv_B \rho_{LB}}{\mathrm{MW}_B} \qquad (14.23b)$$

where subscripts '*D*' and '*B*' refer, respectively, to the distillate and bottoms. For the debutanizer column, Equations (14.23a) and (14.23b) will be used for the computations of m_D and m_B respectively, and internal tray holdups will be calculated simulating the total continuity equations.

Calculation of volumetric liquid holdup

The volumetric liquid holdup can be calculated as:

$$mv = A_l h_l \qquad (14.24a)$$

Knowing the tray geometry, it is straightforward (Holland, 1981; Gomez et al., 2006) to determine the active area (A_l) of a tray. The height of liquid on the tray (h_l) is the sum of the weir height[1] (h_w) and the height of liquid over the weir (h_{ow}).

1 Weir height is less than 15% of the tray spacing.

$$h_l = h_w + h_{ow} \qquad (14.24b)$$

The height over the weir in millimetre is determined from a form of the Francis equation (McCabe et al., 1993) for a straight segmental weir as:

$$h_{ow} = 43.4 \left(\frac{L}{W_L} \right)^{2/3} \qquad (14.24c)$$

where L denotes the flow rate of liquid (m^3/min) and W_L the weir length[2] (m). Another form in units of inches and gal/min is as follows:

2 For segmental downcomers, the chord length (Sinnott, 2005) is normally between 0.6 and 0.85 of the column diameter.

$$h_{ow} = 0.48\left(\frac{L}{W_L}\right)^{2/3} \qquad (14.24d)$$

It should be noted that each downcomer generally occupies 10 to 15% of the column cross section, leaving 70 to 80% of the column area for bubbling or contacting. The relation between weir length and downcomer area is also presented graphically in a book by Sinnott (2005).

14.2.3 Predictions of Enthalpy and Equilibrium Coefficient

The multistage multicomponent separation processes are extensively used in chemical, petroleum and related industries. Simulation of these processes requires accurate and consistent thermodynamic properties such as enthalpies [H^L (for liquid) and H^V (for vapour) values] and equilibrium coefficients (k values) over a wide range of conditions. In general, enthalpies in a high-pressure operating system are calculated from an equation of state model. Equations of state are also used to predict adequately the vapour–liquid equilibrium properties of a highly nonideal system. Alternatively, the nonidealities in the liquid phase alone can be estimated using the activity coefficient models.

The Benedict–Webb–Rubin (BWR), Peng–Robinson (PR), Soave–Redlich–Kwong (SRK), Redlich–Kwong (RK) and universal quasi-chemical functional group activity coefficients (UNIFAC) methods are very effective and most useful in industrial practice to predict the thermodynamic properties. The performances of these thermodynamic methods on several complex processes have been compared by Angel, Marmur and Kehat (1986). They have suggested, based on their observations, that the activity coefficient-based UNIFAC method should not be used when the operating pressure is above the critical pressure of any of the light components. Additionally, except for low pressure, a fugacity correction for the vapour phase at the operating pressure is very much essential.

Since the sample debutanizer column will be operated at sufficiently high pressure, the equation of state model is the natural choice for use to predict accurate and consistent thermodynamic properties of pure components and their mixtures in liquid as well as in vapour phase. It is required now to select a state model for the prescribed multicomponent distillation process. It should be such that the selected equation of state model can provide satisfactory results in addition with simplicity in application.

Although the BWR equation of state has been used to predict satisfactorily the thermodynamic properties of hydrocarbons and their mixtures even at cryogenic conditions, this state model has eight adjustable constants. Evaluation of these constants requires extensive experimental pressure–volume–temperature (*P-V-T)* data, and several sets of constants may give equally good representation of the data. Hence extension of the BWR equation or any of the modifications of the BWR equation with a large number of constants and associated non-uniqueness of parameters to a complex mixture of unknown hydrocarbons becomes cumbersome. Therefore, two constant equations such as SRK and PR equations of state have been used to predict consistent thermodynamic properties for light hydrocarbons and their mixtures at cryogenic conditions as well as for heavy hydrocarbons and their mixtures at high temperatures. As these equations contain only two adjustable parameters, it is easy to extend them to complex mixtures of unknown hydrocarbons and apply them for calculations involved in the separation processes. Based on these well-known observations as described above, we have selected the SRK equation of state to employ for the predictions of enthalpies and VLE coefficients in the concerned multicomponent column.

SRK algorithm

Detailed representation of the SRK equation of state model is given in Chapter 13. In the present study,

the required computational steps are highlighted for the development of the debutanizer simulator. Note that the following steps (denoted by ☆) are actually involved in the SRK algorithm but these steps are not given here in the sequential order.

- Using the following correlations, determine the values of several parameters at specified temperature[3] (T) for all pure components:

[3] This bubble point temperature varies with time in each tray.

$$a_i = 0.42747 \frac{R^2 T_{ci}^2}{P_{ci}} \qquad \text{[from Equation (13.66)]}$$

$$b_i = 0.08664 \frac{RT_{ci}}{P_{ci}} \qquad \text{[from Equation (13.67)]}$$

$$A_i = \frac{a_i^{0.5} \alpha_i^{0.5}}{RT} \qquad \text{[from Equation (13.68)]}$$

$$B_i = \frac{b_i}{RT} \qquad \text{[from Equation (13.52)]}$$

$$\alpha_i^{0.5} = 1 + m_i(1 - T_{ri}^{0.5}) \qquad \text{[from Equation (13.69)]}$$

$$m_i = 0.480 + 1.574 w_i - 0.176 w_i^2 \qquad \text{[from Equation (13.70)]}$$

Values of critical temperature (T_{ci}), critical pressure (P_{ci}) and Pitzer acentric factor (w_i) are known (given in Table 13.4) for every pure component i. T_{ri} represents the reduced temperature ($=T/T_{ci}$) for component i and R is the universal gas constant.

- Determination of compressibility factor (Z) for liquid phase (Z_L) as well as for vapour phase (Z_V) based on the following cubic equation:

$$Z^3 - Z^2 + [A^2P - BP(1 + BP)]Z - A^2PBP = 0 \qquad \text{[from Equation (13.53)]}$$

For vapour phase

For vapour phase, the above equation becomes:

$$Z_v^3 - Z_v^2 + [A_v^2 P - B_v P(1 + B_v P)]Z_v - A_v^2 P B_v P = 0 \qquad (14.25)$$

where

$$A_v = \sum_{i=1}^{N_c} y_i A_i \qquad \text{[from Equation (13.43)]}$$

$$A_v^2 = \left(\sum_{i=1}^{N_c} y_i A_i \right)^2 = \sum_{i=1}^{N_c} \sum_{j=1}^{N_c} y_i y_j A_i A_j \qquad \text{[from Equation (13.60)]}$$

$$B_v = \sum_{i=1}^{N_c} y_i B_i \qquad \text{[from Equation (13.44)]}$$

The solution of Equation (14.25) yields three roots. The first root (Z_{v1}) is obtained by solving the cubic Equation (14.25) applying any numerical iterative technique. If the Newton–Raphson convergence method is used, then the iteration steps involved in the solution technique are as follows:

I. Guess Z_{v1} (say, at time step t)

II. Calculate F_{Zv} from the following form of equation:

$$F_{Zv} = Z_{v1}^3 - Z_{v1}^2 + [A_v^2 P - B_v P(1 + B_v P)]Z_{v1} - A_v^2 P B_v P \quad (14.26)$$

III. Calculate the derivative of F_{Zv} with respect to Z_{v1} based on the following equation:

$$F'_{Zv} = \frac{dF_{Zv}}{dZ_{v1}} = 3Z_{v1}^2 - 2Z_{v1} + A_v^2 P - B_v P(1 + B_v P) \qquad (14.27)$$

IV. Compute Z_{v1} at the next time step ($t + 1$) by using:

$$(Z_{v1})_{t+1} = (Z_{v1})_t - \frac{F_{Zv}}{F'_{Zv}} \qquad (14.28)$$

V. Check whether the absolute value of $(Z_{v1})_{t+1} - (Z_{v1})_t$ is less than the specified tolerance limit? If yes, note down the root as Z_{v1} and go to next step, otherwise go to Step (II) to continue the calculations for the next iteration.

VI. Stop.

So far, one real root (Z_{v1}) of Equation (14.25) is known. Then Equation (14.25) yields a quadratic equation. The roots of a quadratic equation (say Z_{v2} and Z_{v3}) are easily determined. For example, the following form of a quadratic equation,

$$AZ_v^2 + BZ_v + C = 0 \qquad (14.29)$$

has two roots as:

$$Z_{v2} = \frac{-B + \sqrt{B^2 - 4AC}}{2A} \qquad (14.30)$$

and

$$Z_{v3} = \frac{-B - \sqrt{B^2 - 4AC}}{2A} \qquad (14.31)$$

where A ($\neq 0$), B and C are the coefficients. Quadratic equations always have two roots, which can either be real or imaginary (conjugate). Now, among the three roots (Z_{v1}, Z_{v2} and Z_{v3}), the largest real root (when all the roots are real) is taken for the vapour phase as vapour root (Z_v). If a single real root and two conjugate imaginary roots are there, then follow the rules as explained in Chapter 13 (Subsection 13.5.1).

For example the debutanizer column, the Fortran (90) code is given in Program 14.1 to compute the

vapour root, which is needed at every time step and for all trays. Note that nomenclature of some terms in the program differs from that used in the text.

PROGRAM 14.1 *Computer Program* (*subroutine*) *for Vapour Root Calculations*

```
! Determination of first root (Z1) of the following equation (same with
! Equation (14.25))!
!——————————Z*Z*Z-Z*Z+(Ca-Cb-Cb*Cb)*Z-(Ca*Cb) = 0.0——————————!
!————————————here, Ca = Av*Av*P and Cb = Bv*P————————————!

! Inputs: TTR (degree R), P (Psi), Y (mole fraction)
! Outputs: Z1, Ca, Cb

! NC = Number of components
! P = Pressure in a tray
! Pc = Critical pressure in Psi
! R = Universal gas constant in Btu/(lbmol)(degree R)
! TcF = Critical temperature in degree F
! TcR = Critical temperature in degree R
! TTR = Temperature in a tray
! W = Acentric factor
! Y = Mole fraction in vapour-phase

SUBROUTINE First_Root_Z_Vap(TTR,P,Y,Z1,Ca,Cb)
IMPLICIT NONE
INTEGER::i,j,LOOP
INTEGER,PARAMETER::NC=8
REAL*8,INTENT(IN)::TTR,P
REAL*8,DIMENSION(NC),INTENT(IN)::Y
REAL*8,INTENT(OUT)::Z1,Ca,Cb
REAL*8::am(NC,0:NC),bm,fc,df
REAL*8,PARAMETER::R=1.987 D0, GA=0.42747 D0,GB=0.08664 D0
REAL*8::ZV,ZV1
REAL*8,DIMENSION(NC)::W,Ym,TR,TcF,TcR
REAL*8,DIMENSION(NC)::Pc,af,ac,bc,A,B

!——Initialization——!

W(1)=0.098 D0
W(2)=0.152 D0
W(3)=0.176 D0
W(4)=0.193 D0
W(5)=0.227 D0
W(6)=0.251 D0
W(7)=0.296 D0
W(8)=0.394 D0

TcF(1)=90.32 D0
TcF(2)=206.24 D0
TcF(3)=274.9 D0
TcF(4)=305.6 D0
TcF(5)=369.32 D0
TcF(6)=385.88 D0
TcF(7)=453.92 D0
TcF(8)=564.44 D0
DO i=1,NC
 TcR(i)=TcF(i)+460.0
END DO

Pc(1)=708.34 D0
Pc(2)=616.41 D0
Pc(3)=529.54 D0
```

```
Pc(4)=550.56 D0
Pc(5)=490.225 D0
Pc(6)=488.775 D0
Pc(7)=430.76 D0
Pc(8)=359.69 D0

DO i=1,NC
 Ym(i)=0.480+(1.574*W(i))-(0.176*W(i)*W(i))
 TR(i)=TTR/TcR(i)
 af(i)=1+(Ym(i)*(1-(TR(i)**0.5)))
 ac(i)=GA*R*R*TcR(i)*TcR(i)/Pc(i)
 bc(i)=GB*R*TcR(i)/Pc(i)
 A(i)=((ac(i)**0.5)*af(i))/(R*TTR)
 B(i)=bc(i)/(R*TTR)
END DO

DO i=1,NC
am(1:NC,0)=0.00 D0
 DO j=1,NC
 am(i,j)=am(i,j-1)+(Y(i)*Y(j)*A(i)*A(j))
 END DO
END DO
Ca=(am(1,NC)+am(2,NC)+am(3,NC)+am(4,NC)+
& am(5,NC)+am(6,NC)+am(7,NC)+am(8,NC))*P

bm=0.00 D0
DO i=1,NC
 bm=bm+(Y(i)*B(i))
END DO
Cb=bm*P

LOOP=0
ZV=0.01 D0 ! guess value
100 LOOP=LOOP+1
IF(LOOP .GT. 1000) GO TO 300 ! maximum number of iterations = 1000
fc=(ZV*ZV*ZV)-(ZV*ZV)+((Ca-Cb-Cb*Cb)*ZV)-(Ca*Cb)
df=(3.0*ZV*ZV)-(2.0*ZV)+(Ca-Cb-Cb*Cb)
ZV1=ZV-(fc/df)
Z1=ZV1
IF(ABS(ZV1-ZV) .LT. 0.00001)RETURN ! tolerance limit = 1.0E-5
ZV=ZV1
GO TO 100
300 STOP
END SUBROUTINE First_Root_Z_Vap

!————————————Determination of vapour root (Z_vap)————————————!
!———Knowing one root (Z1), one can calculate the other two roots (Z2
! and Z3) by———!
!————————————solving (Z-Z1)(A*Z*Z+B*Z+C) = 0.0————————————!
!————————————here, A = 1, B = C1 and C = C2————————————!

! Inputs: Z1, Ca, Cb
! Outputs: Z2, Z3, Z_vap

SUBROUTINE Optimum_Z_Vap(Z1,Ca,Cb,Z2,Z3,Z_vap)
IMPLICIT NONE
REAL*8,INTENT(IN)::Z1,Ca,Cb
REAL*8,INTENT(OUT)::Z2,Z3,Z_vap
REAL*8::Z,C1,C2,delta

C1=Z1-1.00
C2=(Ca*Cb)/Z1
delta=(C1*C1)-(4.0*C2)
```

```
IF(delta>=0.0)THEN
Z2=(-C1+(delta**0.5))/2.0
Z3=(-C1-(delta**0.5))/2.0
 IF(Z2>0.0)THEN
 IF(Z2<=Z1)THEN
 Z_vap=Z1
 ELSE
 Z_vap=Z2
 END IF
 ELSE
 Z_vap=Z1
 END IF
Z=Z_vap

 IF(Z3>0.0)THEN
 IF(Z3<=Z)THEN
 Z_vap=Z
 ELSE
 Z_vap=Z3
 END IF
 ELSE
 Z_vap=Z
 END IF

ELSE
Z_vap=Z1
END IF

END SUBROUTINE Optimum_Z_vap
```

For liquid phase

The calculation of compressibility factor for liquid phase is very similar to that for vapour phase. This involves the following equation:

$$Z_L^3 - Z_L^2 + [A_L^2 P - B_L P(1 + B_L P)]Z_L - A_L^2 P B_L P = 0 \qquad (14.32)$$

where

$$A_L = \sum_{i=1}^{N_c} x_i A_i \qquad \text{[from Equation (13.47)]}$$

$$A_L^2 = \left(\sum_{i=1}^{N_c} x_i A_i \right)^2 = \sum_{i=1}^{N_c} \sum_{j=1}^{N_c} x_i x_j A_i A_j \qquad \text{[from Equation (13.64)]}$$

$$B_L = \sum_{i=1}^{N_c} x_i B_i \qquad \text{[from Equation (13.48)]}$$

The smallest real root obtained by solving Equation (14.32) is considered as liquid root (Z_L). As stated, the solution technique is similar to the method that described for the computation of vapour root. Therefore, the computer program is not given for this case and a similar Program 14.1 is reported for the vapour root computations.

It is noteworthy to mention here that the vapour and liquid roots are required for enthalpy, equilibrium vapour composition and equilibrium feed flash (details in Chapter 12) calculations. In all the three

calculations, the compressibility factors are different, except the liquid roots used in enthalpy and equilibrium vapour composition (at final iteration step) calculations. This is because of the difference in either phase composition or temperature or pressure or any two/three of these; only these three variables play the role to determine the compressibility factors.

- Calculation of enthalpy departure function ( ): For the computation of enthalpy, the enthalpy departure function and ideal gas enthalpy are needed. The enthalpy departure functions for both vapour phase (v) and liquid phase (L) are calculated from the SRK equation of state model.

For vapour phase

$$\Omega_v = RT(Z_v - 1) + \frac{RTA_v^2}{B_v}\left[\frac{2T}{A_v^2}\sum_{i=1}^{N_c} y_i \bar{A}_{vi}^2 \left(\frac{1}{\alpha_i^{0.5}}\frac{d\alpha_i^{0.5}}{dT}\right) - 1\right]\ln\left(1 + \frac{B_v P}{Z_v}\right)$$

[from Equation (13.58)]

where

$$\bar{A}_{vi}^2 = A_i \sum_{j=1}^{N_c} y_j A_j \qquad \text{[from Equation (13.61)]}$$

For liquid phase

$$\Omega_L = RT(Z_L - 1) + \frac{RTA_L^2}{B_L}\left[\frac{2T}{A_L^2}\sum_{i=1}^{N_c} x_i \bar{A}_{Li}^2 \left(\frac{1}{\alpha_i^{0.5}}\frac{d\alpha_i^{0.5}}{dT}\right) - 1\right]\ln\left(1 + \frac{B_L P}{Z_L}\right)$$

[from Equation (13.62)]

where

$$\bar{A}_{Li}^2 = A_i \sum_{j=1}^{N_c} x_j A_j \qquad \text{[from Equation (13.65)]}$$

- Calculation of ideal gas enthalpy (H^0) using the following empirical correlation:

$$H^0 = A + BT + CT^2 + DT^3 + ET^4 + FT^5 \qquad \text{[from Equation (13.30)]}$$

where A, B, C, D, E and F are the coefficients. These coefficients are reported for several components in Table 13.2 when the enthalpy is in Btu/lb and the temperature in °R.

The vapour phase and liquid phase enthalpies can be computed by combining the respective enthalpy departure function with the ideal gas enthalpy as illustrated in Chapter 13. The Fortran (90) code is given in Program 14.2 for the computations of both the liquid and vapour enthalpies.

PROGRAM 14.2 *Computer Program* (*subroutine*) *for Enthalpy Calculations*

```
! Inputs: TF (degree F), P (Psi), X (mole fraction), Y (mole fraction)
! Outputs: HL (Btu/lbmol), HV (Btu/lbmol)
```

```
! Const1, Const2, Const3, Const4, Const5, Const6 = Coefficients of
! Equation (13.30)
! HL = Liquid-phase enthalpy
! HV = Vapour-phase enthalpy
! MW = Molecular weight
! NC = Number of components
! P = Pressure in a tray
! Pc = Critical pressure in Psi
! TcF = Critical temperature in degree F
! TcR = Critical temperature in degree R
! TF = Temperature in a tray
! TR = Reduced temperature
! TTR = Temperature in a tray in degree R
! W = Acentric factor
! X = Mole fraction in liquid phase
! Y = Mole fraction in vapour phase

SUBROUTINE ENTH(TF,P,X,Y,HL,HV)
IMPLICIT NONE
INTEGER::i,j
INTEGER,PARAMETER::NC=8
REAL*8,INTENT(IN)::TF,P
REAL*8,DIMENSION(NC),INTENT(IN)::X,Y
REAL*8,INTENT(OUT)::HL,HV
REAL*8::TTR,VAR,LAR,ZV1,CaV,CbV,AAv,Bv,ZV2,ZV3,Z_Vap
REAL*8,DIMENSION(NC)::Ym,W,TR,TcF,TcR,Pc,af,ac,bc,A,B
REAL*8,DIMENSION(NC)::AbarV,AbarL,dafdT
REAL*8::Sumation_V,VAR1,VAR2,VAR3,VAR4,dhV
REAL*8::I_Enthal_Liq,I_Enthal_Vap
REAL*8::Sumation_L,LAR1,LAR2,LAR3,LAR4
REAL*8,DIMENSION(NC)::h_ig,Const1,Const2,Const3,Const4,Const5
REAL*8,DIMENSION(NC)::Const6,MW
REAL*8::ZL1,ZL2,ZL3,Z_Liq,CaL,CbL,AAL,BL,dhL
REAL*8,PARAMETER::R=1.987 D0,GA=0.42747 D0,GB=0.08664 D0

!——Initialization——!

W(1)=0.098 D0
W(2)=0.152 D0
W(3)=0.176 D0
W(4)=0.193 D0
W(5)=0.227 D0
W(6)=0.251 D0
W(7)=0.296 D0
W(8)=0.394 D0

TcF(1)=90.32 D0
TcF(2)=206.24 D0
TcF(3)=274.9 D0
TcF(4)=305.6 D0
TcF(5)=369.32 D0
TcF(6)=385.88 D0
TcF(7)=453.92 D0
TcF(8)=564.44 D0
DO i=1,NC
 TcR(i)=TcF(i)+460.0
END DO

Pc(1)=708.34 D0
Pc(2)=616.41 D0
Pc(3)=529.54 D0
Pc(4)=550.56 D0
```

```
Pc(5)=490.225 D0
Pc(6)=488.775 D0
Pc(7)=430.76 D0
Pc(8)=359.69 D0

MW(1)=30.069 D0
MW(2)=44.096 D0
MW(3)=58.123 D0
MW(4)=58.123 D0
MW(5)=72.151 D0
MW(6)=72.151 D0
MW(7)=86.178 D0
MW(8)=114.232 D0

Const1(1)=-0.76005 D0
Const1(2)=-1.22301 D0
Const1(3)= 13.28660 D0
Const1(4)= 29.11502 D0
Const1(5)= 27.62342 D0
Const1(6)= 27.17183 D0
Const1(7)= 32.03560 D0
Const1(8)= 29.50114 D0

Const2(1)= 0.273088 D0
Const2(2)= 0.179733 D0
Const2(3)= 0.036637 D0
Const2(4)= 0.002040 D0
Const2(5)=-0.031504 D0
Const2(6)=-0.002795 D0
Const2(7)=-0.023096 D0
Const2(8)=-0.022402 D0
Const3(1)=-0.042956 D-3
Const3(2)= 0.066458 D-3
Const3(3)= 0.349631 D-3
Const3(4)= 0.434879 D-3
Const3(5)= 0.469884 D-3
Const3(6)= 0.440073 D-3
Const3(7)= 0.461333 D-3
Const3(8)= 0.459712 D-3
Const4(1)= 0.312815 D-6
Const4(2)= 0.250998 D-6
Const4(3)= 0.005361 D-6
Const4(4)=-0.081810 D-6
Const4(5)=-0.098283 D-6
Const4(6)=-0.086288 D-6
Const4(7)=-0.097402 D-6
Const4(8)=-0.098062 D-6

Const5(1)=-1.389890 D-10
Const5(2)=-1.247461 D-10
Const5(3)=-0.298111 D-10
Const5(4)= 0.072349 D-10
Const5(5)= 0.102985 D-10
Const5(6)= 0.081764 D-10
Const5(7)= 0.103368 D-10
Const5(8)= 0.104754 D-10

Const6(1)= 2.007023 D-14
Const6(2)= 1.893509 D-14
Const6(3)= 0.538662 D-14
Const6(4)=-0.014560 D-14
```

```
Const6(5)=-0.029485 D-14
Const6(6)=-0.019715 D-14
Const6(7)=-0.030643 D-14
Const6(8)=-0.031355 D-14

TTR=TF+460.0
DO i=1,NC
 Ym(i)=0.480+(1.574*W(i))-(0.176*W(i)*W(i))
 TR(i)=TTR/TcR(i)
 af(i)=1+(Ym(i)*(1-(TR(i)**0.5)))
 ac(i)=GA*R*R*TcR(i)*TcR(i)/Pc(i)
 bc(i)=GB*R*TcR(i)/Pc(i)
 A(i)=((ac(i)**0.5)*af(i))/(R*TTR)
 B(i)=bc(i)/(R*TTR)
END DO

!——For Vapour——!

VAR=0.0 D0

DO j=1,NC
 VAR=VAR+(Y(j)*A(j))
END DO

DO i=1,NC
 AbarV(i)=A(i)*VAR
END DO

!——For Liquid——!

LAR=0.0 D0

DO j=1,NC
 LAR=LAR+(X(j)*A(j))
END DO

DO i=1,NC
 AbarL(i)=A(i)*LAR
END DO

CALL First_Root_Z_Liq(TTR,P,X(1:NC),ZL1,CaL,CbL)
CALL Optimum_Z_liq(ZL1,CaL,CbL,ZL2,ZL3,Z_Liq)
CALL First_Root_Z_Vap(TTR,P,Y(1:NC),ZV1,CaV,CbV)
CALL Optimum_Z_Vap(ZV1,CaV,CbV,ZV2,ZV3,Z_vap)

AAL=CaL/P
AAV=CaV/P
BL=CbL/P
BV=CbV/P

!——Calculation of daf/dT——!

DO i=1,NC
 dafdT(i)=(-Ym(i))/(2*((TcR(i)*TTR)**0.5))
END DO

!——Calculation of enthalpy departure function (dhV) for vapour phase
! (Btu/lbmol)——!

Sumation_V=0.0 D0
DO i=1,NC
 Sumation_V=Sumation_V+(Y(i)*AbarV(i)*dafdT(i)/af(i))
END DO
VAR1=R*TTR*(Z_Vap-1)
VAR2=2*TTR/AAv
```

```
VAR3=DLOG(1+(Cbv/Z_vap))
VAR4=R*TTR*AAv/Bv
dhV=VAR1+(VAR4*((VAR2*Sumation_V)-1)*VAR3)

!——Calculation of enthalpy departure function (dhL) for liquid phase
! (Btu/lbmol)——!

Sumation_L=0.0 D0
DO i=1,NC
 Sumation_L=Sumation_L+(X(i)*AbarL(i)*dafdT(i)/af(i))
END DO
LAR1=R*TTR*(Z_Liq-1)
LAR2=2*TTR/AAL
LAR3=DLOG(1+(CbL/Z_Liq))
LAR4=R*TTR*AAL/BL
dhL=LAR1+(LAR4*((LAR2*Sumation_L)-1)*LAR3)

!——Calculation of ideal gas enthalpy (h_ig) (Btu/lbmol)——!

DO i=1,NC
h_ig(i)=(Const1(i)+(Const2(i)*TTR)+(Const3(i)*TTR*TTR)+
& (Const4(i)*(TTR**3))+(Const5(i)*(TTR**4))+
& (Const6(i)*(TTR**5)))*MW(i)
END DO

I_Enthal_Vap= (Y(1)*h_ig(1)) + (Y(2)*h_ig(2)) + (Y(3)*h_ig(3)) +
& (Y(4)*h_ig(4)) + (Y(5)*h_ig(5)) + (Y(6)*h_ig(6)) +
& (Y(7)*h_ig(7)) + (Y(8)*h_ig(8))

I_Enthal_Liq= (X(1)*h_ig(1)) + (X(2)*h_ig(2)) + (X(3)*h_ig(3)) +
& (X(4)*h_ig(4)) + (X(5)*h_ig(5)) + (X(6)*h_ig(6)) +
& (X(7)*h_ig(7)) + (X(8)*h_ig(8))

HV=dhV+I_Enthal_Vap
HL=dhL+I_Enthal_Liq

END SUBROUTINE ENTH
```

- For a mixture, the calculation of partial fugacity coefficients in vapour phase $(\hat{f}_i^V/Py_i)$ and in liquid phase $(\hat{f}_i^L/Px_i)$ is carried out based on the following equations, respectively:

$$\ln\frac{\hat{f}_i^V}{Py_i}=\frac{B_i}{B_v}(Z_v-1)-\frac{A_v^2}{B_v}\left(\frac{2\bar{A}_{vi}^2}{A_v^2}-\frac{B_i}{B_v}\right)\ln\left(1+\frac{B_vP}{Z_v}\right)-\ln(Z_v-B_vP)$$

[from Equation (13.59)]

$$\ln\frac{\hat{f}_i^L}{Px_i}=\frac{B_i}{B_L}(Z_L-1)-\frac{A_L^2}{B_L}\left(\frac{2\bar{A}_{Li}^2}{A_L^2}-\frac{B_i}{B_L}\right)\ln\left(1+\frac{B_LP}{Z_L}\right)-\ln(Z_L-B_LP)$$

[from Equation (13.63)]

Note that the values of Z_v, B_v, A_v^2 and $\bar{A}_{vi}^2$ used in the above Equation (13.59) are not same with the values of these terms used in the calculation of vapour-phase enthalpy. Here, these useful terms (Z_v, B_v, A_v^2 and $\bar{A}_{vi}^2$) are computed based on the equilibrium vapour-phase composition, whereas the same terms are required to calculate for vapour-phase enthalpy taking actual vapour-phase

composition. In case of liquid phase, no such dissimilarity exists for a particular tray. However, more understandable explanation is provided in Subsection 14.2.4.

- Computation of vapour–liquid equilibrium coefficient (k_i) according to the following correlation:

$$k_i = \frac{\hat{f}_i^L / Px_i}{\hat{f}_i^V / Py_i} \qquad \text{[from Equation (13.17)]}$$

14.2.4 Equilibrium Relationship

The equilibrium relation between a vapour-phase and a liquid-phase is represented by

$$y_{n,i}^* = k_{n,i} x_{n,i} \qquad (14.33)$$

The vapour–liquid equilibrium coefficient, $k_{n,i}$ is determined for nth plate from Equation (13.17). The equilibrium coefficient is usually a function of phase compositions (only liquid-phase composition when the liquid-phase nonideality is considered), temperature and pressure. The composition of each component in the liquid-phase is easily determined by simulating the component continuity equation. In addition, for the debutanizer column example, the pressure in each tray is specified. Now, the tray temperature (better to say, bubble-point temperature) and equilibrium vapour composition are required to be calculated. The temperature of nth tray is computed using any iterative convergence method such that

$$\sum_{i=1}^{N_c} y_{n,i}^* = 1.0 \qquad (14.34)$$

For a particular tray, the following problem deals with the calculation of equilibrium vapour-phase composition of every component and bubble-point temperature.

Problem statement:

Given: liquid-phase composition (x_i), pressure (p).

Unknowns: equilibrium vapour-phase composition (y_i^*), bubble-point temperature (T).

Solution technique: We wish to consider a mixture having nonidealities both in vapour phase and in liquid phase. The computational steps, which are involved in the solution algorithm, are described below.

Step 1: Guess the initial value for tray temperature T. We have assumed that the guessed value for T at present time step is equal to the value of T at previous time step.

Step 2: For each component i, calculate the vapour pressure (P_i^S) using Equations (13.115), (13.116) and (13.117) based on the guessed temperature, and known acentric factor (w_i), critical temperature (T_{ci}) and critical pressure (P_{ci}). Then compute the vapour–liquid equilibrium coefficient assuming ideal mixture from:

$$k_i = \frac{P_i^S}{P} \qquad (14.35)$$

Step 3: Calculate the equilibrium vapour-phase composition for each component (y_i^*) present in the ideal mixture from:

$$y_i^* = k_i x_i \qquad (14.36)$$

Now the assumed value for T (in Step 1) and calculated value for y_i^* (in Step 3) will be considered as guessed values for T and y_i^* respectively in the subsequent global iteration.

Global iteration (Step 4 to Step 8):

Step 4: Calculate the compressibility factors for both vapour and liquid phases according to the method described in Subsection 14.2.3.

Step 5: Now calculate k_i for the nonideal mixture according to Equation (13.17).

Step 6: Compute y_i^* from $y_i^* = k_i x_i$ [Equation (14.36)].

Step 7: Check whether the absolute value of $\left(\sum_{i=1}^{N_c} y_i^* - 1\right) \leq$ tolerance limit? If yes, note down the temperature and equilibrium vapour compositions, and go to Step 9, otherwise go to Step 8.

Step 8: Update T. The Muller convergence technique based on second-degree equation is used for the debutanizer column. Continue the global iteration until the necessary condition (as stated in Step 7) is satisfied.

Step 9: Stop.

The Fortran (90) code is given in Program 14.3 to carry out the bubble-point calculations for the example debutanizer distillation process.

PROGRAM 14.3 *Computer Program* (*subroutine*) *for Bubble-point Calculations*

```
! Inputs: Tguess (degree F), X (mole fraction), P (Psi)
! Outputs: T (degree F), Y (mole fraction)

! Kay = Vapour-liquid equilibrium coefficient
! NC = Number of components
! P = Pressure in a tray
! Pc = Critical pressure in Psi
! Pckp = Critical pressure in kPa
! Pvp = Vapour pressure in Psi
! R = Universal gas constant = 1.987 Btu/(lbmol)(degree R)
! TcF = Critical temperature in degree F
! TcK = Critical temperature in degree K
! TcR = Critical temperature in degree R
! T = Tray temperature
! Tguess = Guessed value for T
! TTR = Tray temperature in degree R
! W = Acentric factor
! X = Mole fraction in liquid-phase
! Y = Mole fraction in vapour-phase

SUBROUTINE BUBPT(T,Tguess,X,Y,P)
IMPLICIT NONE
INTEGER::i,j,K
INTEGER,PARAMETER::NC=8,iter=1000
REAL*8,DIMENSION(NC),INTENT(IN)::X
REAL*8,INTENT(IN)::P,Tguess
REAL*8,DIMENSION(NC),INTENT(OUT)::Y
REAL*8,INTENT(OUT)::T
REAL*8,DIMENSION(iter)::TTR,TF,func,deviation,Lemda,delta
REAL*8,DIMENSION(iter)::GO,CO,PAR,PAR1,PAR2
```

```
REAL*8::VAR,LAR,ZL1,CaL,CbL,ZL2,ZL3,Z_liq
REAL*8::ZV1,CaV,CbV,ZV2,ZV3,Z_vap
REAL*8,DIMENSION(NC)::Kay,Ym
REAL*8,DIMENSION(NC)::W,TR,TcF,TcR,af,ac,Pc,bc,A,B
REAL*8,DIMENSION(NC)::AbarV,AbarL
REAL*8,PARAMETER::GA=0.42747 D0,GB=0.08664 D0
REAL*8,PARAMETER::R=1.987 D0
REAL*8::AAL,AAV,BL,BV,SUMY
REAL*8,DIMENSION(NC)::VAR1,VAR2,VVAR
REAL*8::VAR3,LAR3,VAR4,LAR4
REAL*8,DIMENSION(NC)::LAR1,LAR2,LLAR
REAL*8::TK
REAL*8,DIMENSION(NC)::TcK,TRK
REAL*8,DIMENSION(NC)::Pi,Pvp,Pckp,Press1,Press2,Press3,Press4

!——Initialization——!

W(1)=0.098 D0
W(2)=0.152 D0
W(3)=0.176 D0
W(4)=0.193 D0
W(5)=0.227 D0
W(6)=0.251 D0
W(7)=0.296 D0
W(8)=0.394 D0

TcF(1)=90.32 D0
TcF(2)=206.24 D0
TcF(3)=274.9 D0
TcF(4)=305.6 D0
TcF(5)=369.32 D0
TcF(6)=385.88 D0
TcF(7)=453.92 D0
TcF(8)=564.44 D0
DO i=1,NC
 TcR(i)=TcF(i)+460.0
 TcK(i)=((5.0/9.0)*(TcF(i)-32.0))+273.0
END DO

Pc(1)=708.34 D0
Pc(2)=616.41 D0
Pc(3)=529.54 D0
Pc(4)=550.56 D0
Pc(5)=490.225 D0
Pc(6)=488.775 D0
Pc(7)=430.76 D0
Pc(8)=359.69 D0
DO i=1,NC
 Pckp(i)=Pc(i)*6.89479
END DO

TF(1)=Tguess-15.0
TF(2)=Tguess
TF(3)=Tguess+15.0
DO i=1,3
 TTR(i)=TF(i)+460.0
END DO

Tk=((5.0/9.0)*(TF(1)-32.0))+273.0
DO i=1,NC
 TRK(i)=TK/TcK(i)
 Press1(i)=5.92714-(6.09648/TRK(i))-(1.28862*DLOG(TRK(i)))+
```

```
 & (0.169347*(TRK(i)**6))
 Press2(i)=15.2518-(15.6875/TRK(i))-(13.4721*DLOG(TRK(i)))+
 & (0.43577*(TRK(i)**6))
 Press3(i)=Press1(i)+(W(i)*Press2(i))
 Press4(i)=Pckp(i)*EXP(Press3(i))
 Pvp(i)=0.145037*Press4(i)
 Kay(i)=Pvp(i)/P
 Y(i)=Kay(i)*X(i)
END DO

DO i=1,NC
 Ym(i)=0.480+(1.574*W(i))-(0.176*W(i)*W(i))
END DO

!————————Global Iteration——————————!
!————————————————————————————!

DO K=1,iter                        ! Starting of global iteration loop
IF(K .GT. 1000)GO TO 333

DO i=1,NC
 TR(i)=TTR(K)/TcR(i)
 af(i)=1+(Ym(i)*(1-(TR(i)**0.5)))
 ac(i)=GA*R*R*TcR(i)*TcR(i)/Pc(i)
 bc(i)=GB*R*TcR(i)/Pc(i)
 A(i)=((ac(i)**0.5)*af(i))/(R*TTR(K))
 B(i)=bc(i)/(R*TTR(K))
END DO

VAR=0.0 D0
DO j=1,NC
 VAR=VAR+(Y(j)*A(j))
END DO
DO i=1,NC
 AbarV(i)=A(i)*VAR
END DO

LAR=0.0 D0
DO j=1,NC
 LAR=LAR+(X(j)*A(j))
END DO
DO i=1,NC
 AbarL(i)=A(i)*LAR
END DO

CALL First_Root_Z_Liq(TTR(K),P,X(1:NC),ZL1,CaL,CbL)
CALL Optimum_Z_liq(ZL1,CaL,CbL,ZL2,ZL3,Z_Liq)
CALL First_Root_Z_Vap(TTR(K),P,Y(1:NC),ZV1,CaV,CbV)
CALL Optimum_Z_Vap(ZV1,CaV,CbV,ZV2,ZV3,Z_vap)

AAL=CaL/P
AAV=CaV/P
BL=CbL/P
BV=CbV/P

DO i=1,NC
 VAR1(i)=(B(i)/Bv)*(Z_vap-1)
 VAR2(i)=(AAv/Bv)*((2*Abarv(i)/AAv)-(B(i)/Bv))
 VAR3=DLOG(1+(Cbv/Z_vap))
 VAR4=DLOG(Z_Vap-Cbv)
 VVAR(i)=EXP(VAR1(i)-(VAR2(i)*VAR3)-VAR4)
END DO
```

```
DO i=1,NC
 LAR1(i)=(B(i)/BL)*(Z_liq-1)
 LAR2(i)=(AAL/BL)*((2*AbarL(i)/AAL)-(B(i)/BL))
 LAR3=DLOG(1+(CbL/Z_liq))
 LAR4=DLOG(Z_Liq-CbL)
 LLAR(i)=EXP(LAR1(i)-(LAR2(i)*LAR3)-LAR4)
END DO

!——Vapour-liquid equilibrium coefficient——!

DO i=1,NC
 Kay(i)=LLAR(i)/VVAR(i)
END DO
SUMY=0.00 D0
DO i=1,NC
 Y(i)=Kay(i)*X(i)
 SUMY=SUMY+Y(i)
END DO

func(K)=SUMY-1
IF(DABS(SUMY-1) .LT. 0.00001)RETURN
IF(K>=3)THEN
 deviation(k-1)=TTR(k-1)-TTR(k-2)
 deviation(k)=TTR(k)-TTR(k-1)
 Lemda(k)=deviation(k)/deviation(k-1)
 delta(k)=1+Lemda(k)
 GO(k)=((Lemda(k)**2)*func(k-2))-
 & ((delta(k)**2)*func(k-1))+
 & ((Lemda(k)+delta(k))*func(k))
 CO(k)=Lemda(k)*((Lemda(k)*func(k-2))-
 & (delta(k)*func(k-1))+func(k))
 PAR(K)=((GO(K)**2)-(4*delta(k)*func(k)*CO(k)))**0.5
 PAR1(k)=((-2)*delta(k)*func(k))/(GO(k)+PAR(k))
 PAR2(k)=((-2)*delta(k)*func(k))/(GO(k)-PAR(k))

 IF(DABS(PAR1(K)) > DABS(PAR2(K)))THEN
 Lemda(k+1)=PAR2(k)
 ELSE
 Lemda(k+1)=PAR1(k)
 END IF

 TTR(K+1)=TTR(K)+(Lemda(K+1)*(TTR(K)-TTR(K-1)))
 T=TTR(K+1)-460.0
END IF

END DO                                  ! End of global iteration loop

333 STOP
END SUBROUTINE BUBPT
```

14.3 MODEL VERIFICATION

The model of the representative column proposed above is verified using the plant data reported in literature (Shah and Bishnoi, 1978) for a debutanizer unit that was operated in a natural gas processing plant in the province of Alberta (Canada). Although a few specifications are different between the prescribed column and the real process, a comparison is made between the simulation results and the plant data in Table 14.3. In addition, the results of a debutanizer model developed by Shah and Bishnoi (1978) are also compared.

Table 14.3 Comparison of simulation results with plant data at steady state

Items	*Simulation results*		*Plant data* (Shah and Bishnoi, 1978)
	Proposed model	*Reported model* (Shah and Bishnoi, 1978)	
Number of stages	15 (theoretical)	31 (theoretical)	38 (actual)
Reflux ratio	1.588	1.7235	1.7235
Eighth component	Octane (nC_8)	Hyp-Comp[1]	Hyp-Comp
Temperature (°F)			
Top stage	140.496	138.740	129.920
Reflux	134.880	135.140	82.040[2]
Bottom point	257.654	270.320	251.960
Feed rate (lbmol/h)	880.56 (same in all three cases)		
Feed composition	Given in Table 14.2 (same in all three cases)		
Feed pressure (Psi)	110.01 (same in all three cases)		
Feed temperature (°F)	180	150.08	150.08
Distillate composition			
C_2	0.0022396	0.0021436	0.0021436
C_3	0.0125736	0.0120578	0.0120580
iC_4	0.4277434	0.4294212	0.4295284
nC_4	0.5143382	0.5554394	0.5562700
iC_5	0.0341264	0.0008842	—
nC_5	0.0089300	0.0000536	—
nC_6	0.0000507	—	—
Eighth component	0.000000082	—	—

[1]Hyp-Comp is treated as a hypothetical component with a normal boiling point temperature of 240.8°F (= 116°C).
[2]Reflux in the plant is suspected to be subcooled.

14.4 APPLICATION OF CONTROL ALGORITHM

In the debutanizer column, the control objective is to remove impurities (C_5^+ components) in the distillate and maintain minimum possible amount of butane in the bottom product to maximize the yield of butane. Accordingly, nC_5 composition in the distillate (x_{DnC_5}) and nC_4 composition in the bottom product (x_{BnC_4}) are considered as controlled variables, and reflux flow rate (R) and vapour boil-up rate (V_B) are the respective manipulated inputs. Liquid holdups in the column base (m_B) and reflux drum (m_D) are controlled by manipulating the flow rate of bottom (B) and overhead (D) products, respectively. The conventional proportional integral (PI) controller has been used in all four cases and they are given below.

14.4.1 Dual-loop PI Structure for Composition Control

Two single-loop PI controllers, which are employed around the multicomponent distillation process, are

as follows:

$$R = R_S + K_{C1}\left(e_1 + \frac{1}{\tau_1}\int e_1\,dt\right), \text{ where } e_1 = x_{DnC_5SP} - x_{DnC_5} \tag{14.37}$$

$$V_B = V_{BS} + K_{C2}\left(e_2 + \frac{1}{\tau_2}\int e_2\,dt\right), \text{ where } e_2 = x_{BnC_4SP} - x_{BnC_4} \tag{14.38}$$

Here, e denotes the error to the controller and it is calculated by subtracting controlled variable value from its desired set point value.

14.4.2 Dual-loop PI Structure for Holdup Control

Two conventional PI controllers are implemented to control the holdups in reflux drum and column base by manipulating the distillate and bottom product flow rates, respectively. The controller equations are as follows:

$$D = D_S + K_{CD}\left(e_D + \frac{1}{\tau_D}\int e_D\,dt\right), \text{ where } e_D = m_{DSP} - m_D \tag{14.39}$$

$$B = B_S + K_{CB}\left(e_B + \frac{1}{\tau_B}\int e_B\,dt\right), \text{ where } e_B = m_{BSP} - m_B \tag{14.40}$$

14.4.3 Control Performance

In order to investigate the control performance, the dual-loop composition and level controllers have been employed. The values of the tuning parameters used are given in Table 14.4. Steady state values, R_S, V_{BS}, D_S and B_S, are included in Table 14.1.

In the servo performance study, two consecutive set point step changes in x_{DnC_5} have been introduced and the results are presented in Figure 14.2. Along with the composition dynamics, the profiles of manipulated variables are also shown in the figure. It is evident from this simulation that although the step change is considered in the top composition loop, the bottom composition loop does not remain at its original state. The bottom loop is originally affected by the top loop and this fact reminds the interaction of two control loops we studied in process control course.

Table 14.4 Controller tuning parameter values

Controller	*Tunable parameter*
Composition controller Level controller	$K_{C1} = 90.2$, $\tau_1 = 3.0$; $K_{C2} = -98.28$, $\tau_2 = 2.91$ $K_{CD} = -250.0$, $\tau_D = 58.5$; $K_{CB} = -250.0$, $\tau_B = 60.0$ [Integral time constant (τ) is given in min]

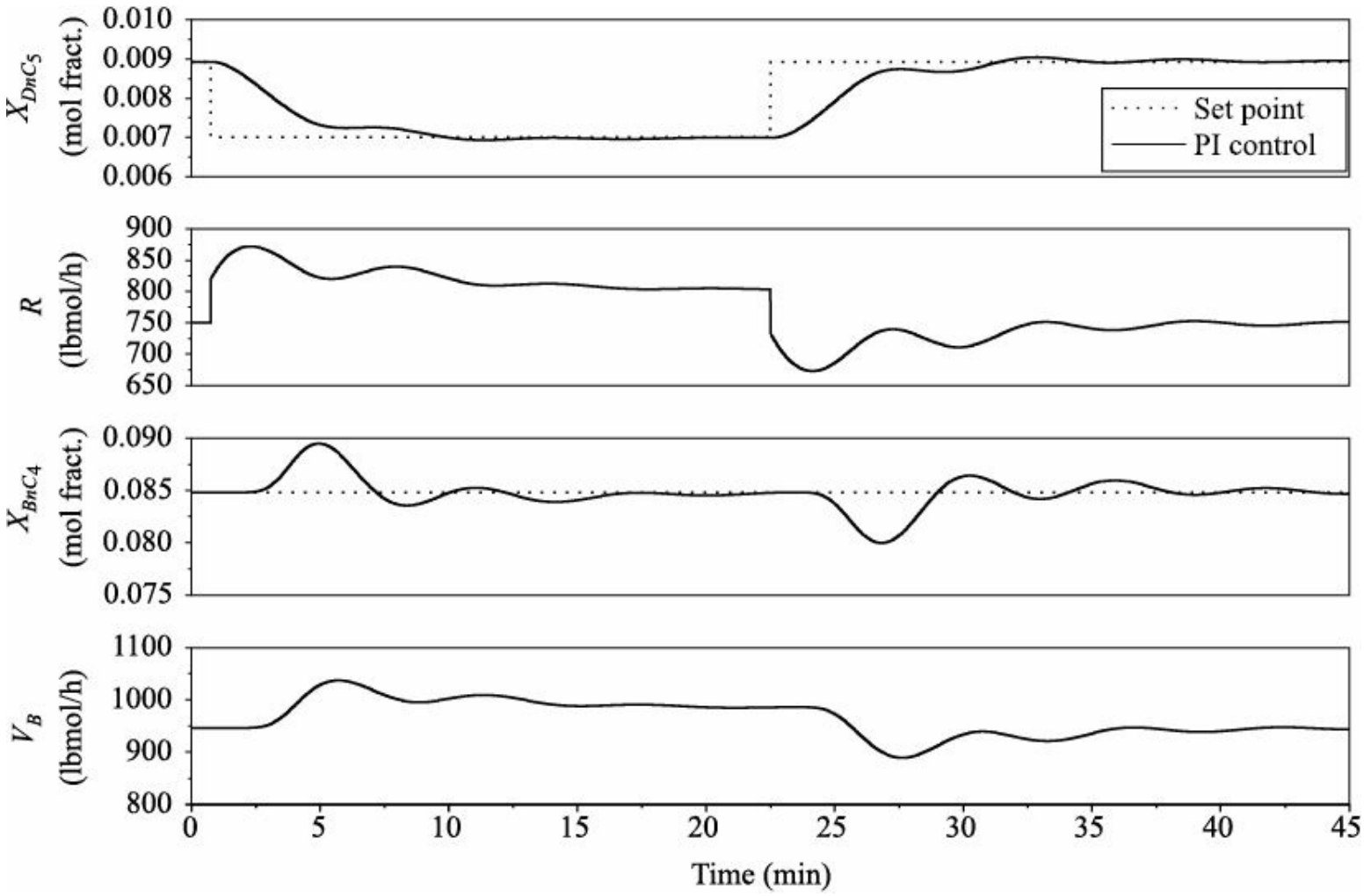

FIGURE 14.2 Servo performance with set point step changes in x_{DnC5} (changed from 0.00893 to 0.007 at time = 0.75 min and then from 0.007 to 0.00893 at time = 22.5 min).

Figure 14.3 depicts the regulatory performance of the control scheme against two subsequent step changes in feed flow rate. In this simulation experiment, the loop interaction is also prominent. To minimize the effect of loop interaction, the *decoupler* is recommended to include with the PI control law.

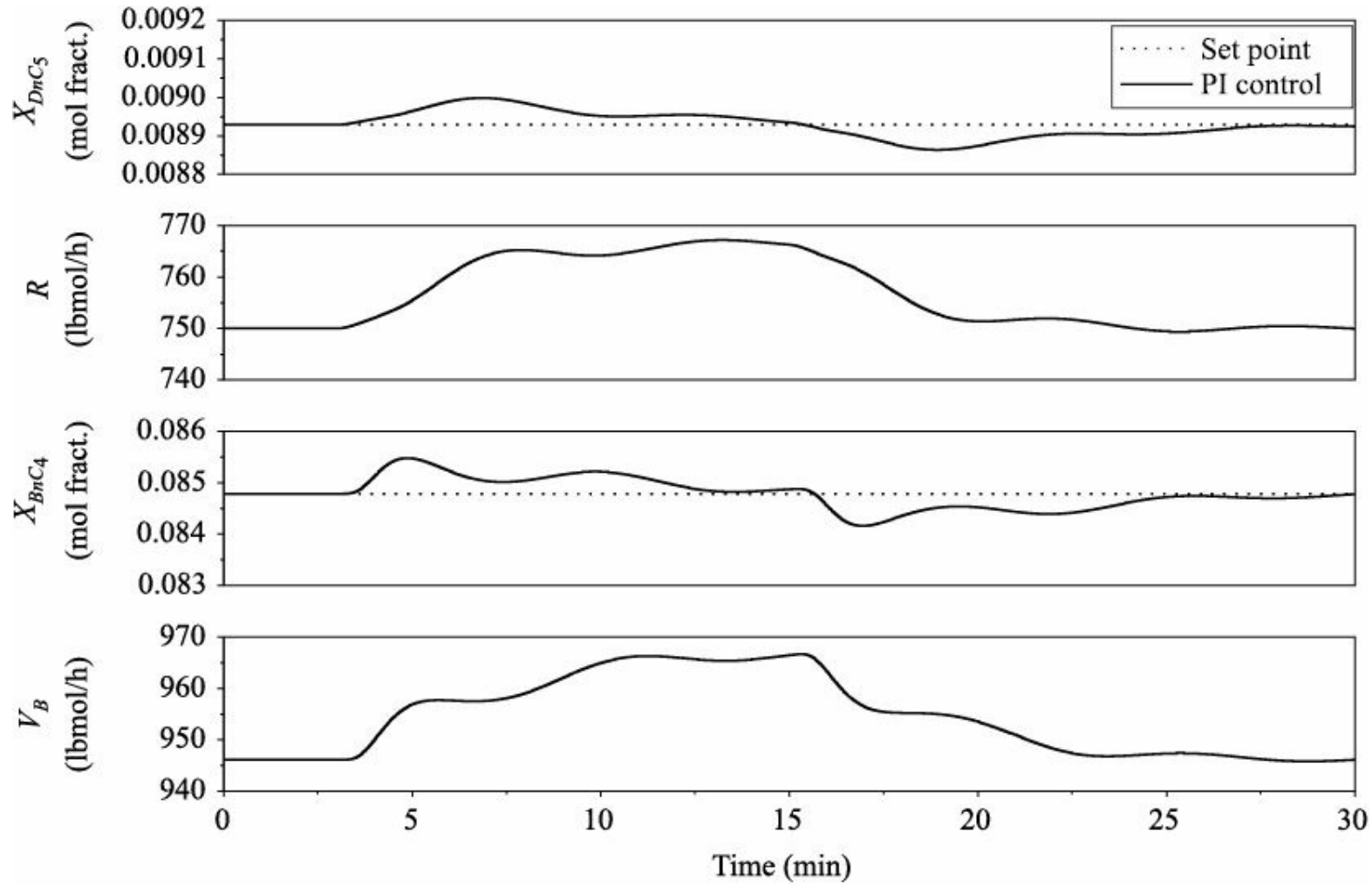

FIGURE 14.3 Regulatory performance with step changes in feed rate
(changed from 880.56 to 900 lbmol/h at time = 3 min and then
from 900 to 880.56 lbmol/h at time = 15 min).

14.4.4 A Few Practical Issues and Recommendations

From practical point of view, some modifications/additions to the control algorithm discussed above are suggested. The most important ones are as follows:

(i) The controlled variables m_D and m_B should be replaced by mv_D and mv_B (or respective liquid height), respectively.

(ii) It is appropriate to manipulate the reboiler duty (Q_R) instead of vapour boil-up rate (V_B). However, a simple steady state correlation can easily be developed between Q_R and V_B neglecting the thermal dynamics around the reboiler.

(iii) One fundamental concept in distillation column control is to prevent rapid changes in pressure. If the increase of pressure is too fast, vapour rates through the trays decrease, which can cause weeping and dumping. On the other hand, when the decrease of pressure is too rapid, vapour rates increase, which can cause flooding. Therefore,
fairly tight pressure control is necessary. Either vapour distillate flow rate or coolant flow rate in the overhead condenser is usually adjusted to control the column top pressure.

(iv) Sometimes, the need for temperature control becomes necessary since the composition analyzers require high investment and maintenance costs and deliver delayed responses.

14.5 SUMMARY AND CONCLUSIONS

Debutanizer column is widely used as a separation unit in petroleum refineries. The refinery industries are among the main contributors of pollution to the environment. Recently, ever-growing interest has been shown in production quality standards and pollution phenomena in industrial environments. Government laws enforce hard limits on pollutant and product specifications. Therefore, we need an adequate knowledge on process behaviours and the increasingly efficient control policies.

With these objectives in mind, in the present chapter, a rigorous model of a multi-component debutanizer column is developed and verified with real plant data. The study also includes the dynamic simulation of the complex column. The model defines a set of ODEs and of algebraic equations/correlations. The value of Murphree vapour-phase tray efficiency, as discussed in Chapter 9, is used to calculate the actual component composition in the vapour-phase since the vapour and liquid leaving a tray are not in phase equilibrium. The average molecular weight and density of the tray liquid in addition to the tray hydraulics can be computed within the process simulator as discussed in Chapter 11 for the multicomponent batch distillation. Detailed calculations of the equilibrium feed flash (isothermal) involved in the simulated debutanizer column are given in Chapter 12. Finally, a control algorithm is devised and applied on the sample process. The closed-loop control performance is investigated with conducting servo and regulatory tests.

It is not necessary to provide repeatedly the values of few common terms (e.g., acentric factor, critical temperature, critical pressure, etc.) in all subroutines (computer programs) as reported in this chapter. The values may be given once in the *main program* and utilized in all subroutines.

Finally it can be concluded that the work presented in this chapter can be easily implemented on a computer and constitutes an efficient tool for education, industrial or research purposes.

EXERCISES

14.1 Why is the multicomponent distillation column that is prescribed in this chapter called the debutanizer column?

14.2 Why is the sample column operated at high pressures?

14.3 Develop the computer programs (subroutines) for the sample debutanizer column to calculate:

(i) average molecular weight and density of the tray liquid
(ii) compressibility factor for liquid phase (liquid root)
(iii) internal liquid flow rates.

14.4 Mention the computational steps that are involved in the bubble-point calculations using the Secant method.

14.5 Develop the debutanizer simulator that is exampled in the present chapter predicting the liquid-phase and vapour-phase enthalpy, and vapour–liquid equilibrium coefficient by use of:

(i) the PR equation of state model
(ii) the BWR equation of state model.

14.6 Which one is the light key (LK) and which one is the heavy key (HK) among the constituent components of the hydrocarbon mixture that is fractionated in the prescribed debutanizer?

14.7 Why has the cubic Equation (13.53) either three real roots or one real root and two conjugate imaginary roots?

14.8 What is LPG? How does the petroleum gas remain at liquid state in the gas cylinder? What are the main constituent hydrocarbons of LPG?

14.9 What is unstabilized naphtha and why is it called so?

REFERENCES

Angel, S., Marmur, A., and Kehat, E. (1986). Comparison of methods of prediction of vapour–liquid equilibria and enthalpy in a distillation simulation program, *Comput. Chem. Eng.*, 10, 169–180.

Billingsley, D.S., and Boynton, G.W. (1971). Iterative methods for solving problems in multicomponent distillation at the steady state, *AIChE J.*, 17, 65–68.

Distefano, G.P. (1968). Mathematical modeling and numerical integration of multicomponent batch distillation equations, *AIChE J.*, 14, 190–199.

Friday, J.R., and Smith, B.D. (1964). An analysis of the equilibrium stage separation problem. Formulation and convergence, *AIChE J.*, 10, 698.

Gani, R., Ruiz, C.A., and Cameron, I.T. (1986). A generalized model for distillation columns-I; model description and applications, *Comput. Chem. Eng.*, 10, 181–198.

Goldstein, R.P., and Stanfield, R.B. (1970). Flexible method for the solution of distillation design problems using the Newton–Raphson technique, *Ind. Eng. Chem. Process Des. Dev.*, 9, 78–84.

Gomej, J.M., Reneaume, J.M., Roques, M., Meyer, M., and Meyer, X. (2006). A mixed integer nonlinear programming formulation for optimal design of a catalytic distillation column based on a generic nonequilibrium model, *Ind. Eng. Chem. Res.*, 45, 1373–1388.

Holland, C.D. (1981). *Fundamentals of Multicomponent Distillation*, 1st ed., McGraw-Hill, New York.

Ishii, Y., and Otto, F.D. (1973). A general algorithm for multistage multicomponent separation calculations, *Can. J. Chem. Eng.*, 51, 601–606.

Lewis, W.K., and Matheson, G.I. (1932). Studies in distillation design of rectifying columns for natural and refinery gasoline, *Ind. Eng. Chem.*, 24, 494–498.

Luyben, W.L. (1990). *Process Modeling, Simulation, and Control for Chemical Engineers*, 2nd ed., McGraw-Hill Book Company, Singapore.

McCabe, W.L., Smith, J.C., and Harriott, P. (1993). *Unit Operations of Chemical Engineering*, 5th ed., McGraw-Hill, New York.

Naphtali, L.M., and Sandholm, D.P. (1971). Multicomponent separation calculations by linearization, *AIChE J.*, 17, 148–153.

Shah, M.K., and Bishnoi, P.R. (1978). Multistage multicomponent separation calculations using thermodynamic properties evaluated by the SRK/PR equation of state, *Can. J. Chem. Eng.*, 56, 478–486.

Sinnott, R.K. (2005). *Chemical Engineering Design*, Coulson & Richardson's Chemical Engineering Series, Vol. 6, 4th ed., Elsevier, Oxford, UK.

Sujata, A.D. (1961). Absorber–stripper calculations: made easier, *Hydrocarbon Processing*, 40, 137–140.

Thiele, E.W., and Geddes, R.L. (1933). Computation of distillation apparatus for hydrocarbon mixtures, *Ind. Eng. Chem.*, 25, 289.

Tomich, J.F. (1970). A new simulation method for equilibrium stage processes, *AIChE J.*, 16, 229–232.

Wang, J.C. and Henke, G.E. (1966). Tridiagonal matrix for distillation, *Hydrocarbon Processing*, 45,

155–163.

15

Reactive Distillation Column

15.1 INTRODUCTION

What is reactive distillation?

Reactive distillation (RD) combines the principles of reaction engineering and separation technology in a single vessel. The combination of chemical reaction and distillation is called reactive distillation.

How does an RD column operate?

We have studied the operation of nonreactive distillation in several previous chapters of this book. Now, we wish to know about the operation of an RD. A portion of RD column may contain a catalyst for performing the desired reaction. The catalyst may be present as a solid-phase packing or may be in the same phase as the reacting species. RD is usually a single-feed or double-feed column and the feed(s) is introduced near to the catalyst section (above and/or below, depending on volatility). The reaction takes place, generally in the liquid phase, on the catalyst. The reaction products are withdrawn continuously and the reagents are kept in the column. A typical layout of an RD column is shown in Figure 15.1.

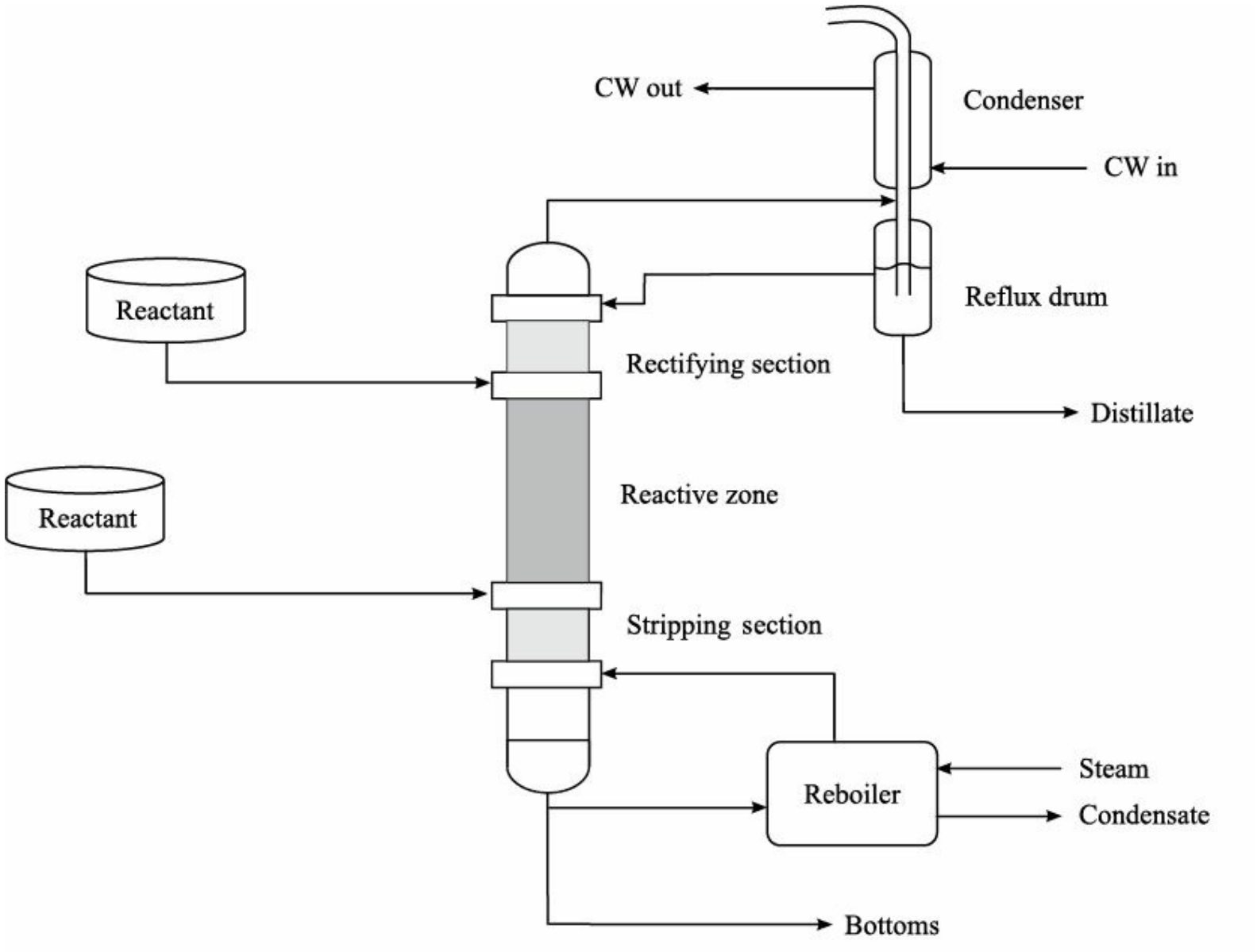

FIGURE 15.1 Schematic of an RD column.

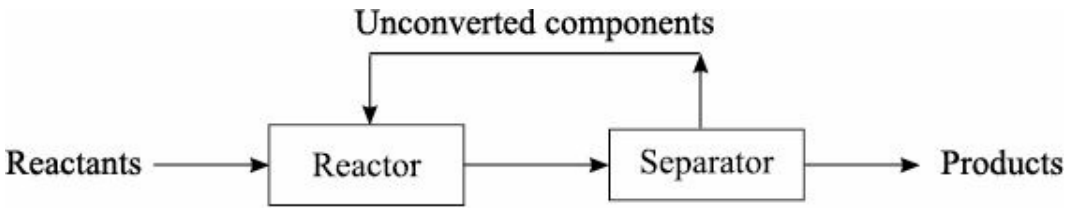

FIGURE 15.2 Schematic of a reactor-followed-by-separator process.

When is it called as catalytic distillation?

RD can be classified into homogeneous RD and heterogeneous RD. The former is either auto-catalyzed or homogeneously catalyzed. In the heterogeneous RD column, the reaction is catalyzed by a solid catalyst. The term *catalytic distillation* is used for such systems where a catalyst (homogeneous or heterogeneous) is employed for accelerating the reaction.

Why should we prefer RD?

In many chemical industries, reaction and separation take place separately in a reactor followed by a separator. In this type of process (Figure 15.2), the reactants are introduced to the reactor, where the reaction occurs and reaches equilibrium. Next, a distillation train is needed to separate the individual products and to separate them from the unconverted components that are recycled back to the reactor. Compared to the conventional reactor-followed-by-distillation scheme, an RD column offers several

potential advantages. The most important ones are summarized as follows:

1. By performing the reaction and distillation in a single unit, the capital investment can be reduced significantly. This integration leads to lower costs in pumps, piping and instrumentation.
2. By the continuous removal of products from the reactive zone, the reactant conversion can approach 100% by affecting the chemical equilibrium.
3. In a fixed-bed reactor followed by a separator system, the distillate or bottom of the reaction mixture is recycled to the reactor inlet. But in the RD scheme, the increase in conversion gives a benefit in reduced recycle costs.
4. If the reaction occurred in the RD column is exothermic, the reaction heat can be utilized for the evaporation of the liquid-phase component. By this way, the energy cost can be reduced by the reduction of reboiler duties.
5. The maximum temperature attained in the reactive section does not exceed the boiling point temperature of the reaction mixture. Therefore, the tendency of hot spot formation on the catalyst is reduced substantially.
6. The probability of side reactions can be lowered to improve the product selectivity (the ratio of the quantity of desired product formed to the quantity of undesired material formed) by the fast removal of products or reactants from the reactive
   zone.
7. In a conventional reactor-separator arrangement, when the reactor product is a mixture of species that can form several azeotropes with each other, the separation scheme would require multiple distillation units and use of entrainers to break the azeotropes. Careful choice of RD conditions can allow the azeotropes to be *reacted away* in a single piece of equipment.

Major constraints

Major constraints for the substitution of conventional processes by RD are given in the following:

1. The reagents and products must have suitable volatility such that high concentrations of reactants and low concentrations of products can be maintained in the reactive zone.
2. The necessary conditions (e.g., temperature) for the reaction must match those of distillation.
3. The reaction has to take place entirely in the liquid-phase because of the necessity of wet catalyst pellets.
4. If the residence time for the reaction is long, a large column size and large tray hold-ups are required. In such a situation, it may be more economic to use a reactor-separator scheme.

Note that the endothermic reactions are not suitable for the RD technology because of vapour condensation. Although the endothermic reactions require more reboiler duty and therefore exhibit no large energy savings, there are no restrictions to the application of RD operation (Tuchlenski et al., 2001).

It is now obvious that the RD is a very promising alternative to the conventional reaction-distillation flow scheme. However, the suitability of RD for a particular reaction is dependent on the various factors mentioned above. It clearly indicates that the use of RD column for each and every reaction may not be feasible.

Challenges

Due to the combination of reaction and separation, the RD exhibits complex behaviours (Khaledi and Young, 2005), such as steady-state multiplicity, process gain sign changes (bidirectionality) and strong interactions between process variables. These complexities lead to challenging problems in design, operation and control. Moreover, an RD column offers more limited flexibility than a traditional reactor-separator process because of the smaller number of manipulated variables available for adjustment.

15.2 MODELLING OF A REACTIVE TRAY: IN GENERAL

There are two modelling techniques in use for the RD processes. They are the equilibrium stage model and the nonequilibrium-based (or rate-based) model. The former model is relatively simple and easy to employ, whereas the latter one is rigorous and involves additional effects owing to mass and heat transfer. It should be noted that the modelling of a packed column can also be performed based on the equilibrium stage concept. For that, the reactive as well as the nonreactive zones of a packed distillation column can be modelled as a multi-stage column with finding the height equivalent to a theoretical plate (HETP)[1].

[1] The HETP is an experimentally determined quantity characteristic for individual packing. The HETP varies not only with the category and size of the packing material but also very strongly with flow rates of each fluid and for every system with concentration as well.

The mathematical modelling of a reactive tray is very similar to that of a nonreactive tray. The difference is only due to the reaction occurred in a reactive tray. The scheme of a typical nth reactive tray is shown in Figure 15.3. The tray is fed with a liquid feed mixture having flow rate F_n and composition $z_{n,i}$. Side streams are withdrawn in a state of both liquid (flow rate S_n^L and composition $x_{n,i}$) and vapour (flow rate S_n^V and composition $y_{n,i}$). The outgoing liquid and vapour streams from nth tray are L_n (composition $x_{n,i}$) and V_n (composition $y_{n,i}$), respectively. The incoming streams are obviously L_{n+1} and V_{n-1}. The model of the nth tray consisting of MESH (Material balance, vapour-liquid Equilibrium, mole fraction Summation and Heat balance) equations is presented below under some specific assumptions.

Total mole balance:

$$\dot{m}_n = L_{n+1} + V_{n-1} + F_n - (L_n + S_n^L) - (V_n + S_n^V) + R_f \sum_{j=1}^{N_r} \sum_{i=1}^{N_c} (\delta_{i,j} r_{j,n} \varepsilon_n) \qquad (15.1)$$

Component (i) *mole balance:*

$$\dot{m}_n \dot{x}_{n,i} = L_{n+1} x_{n+1,i} + V_{n-1} y_{n-1,i} + F_n z_{n,i} - (L_n + S_n^L) x_{n,i} - (V_n + S_n^V) y_{n,i} + R_f \sum_{j=1}^{N_r} (\delta_{i,j} r_{j,n} \varepsilon_n) \qquad (15.2)$$

Energy balance:

$$\dot{m}_n \dot{H}_n^L = L_{n+1} H_{n+1}^L + V_{n-1} H_{n-1}^V + F_n H_n^F - (L_n + S_n^L) H_n^L - (V_n + S_n^V) H_n^V + R_f \sum_{j=1}^{N_r} (r_{j,n} \varepsilon_n \Delta H_{rj,n}) - Q_n \qquad (15.3)$$

Equilibrium:

$$y_{n,i} = k_{n,i}\, x_{n,i} \qquad (15.4)$$

Summation:

$$\sum_{i=1}^{N_c} x_{n,i} = 1 \qquad (15.5a)$$

$$\sum_{i=1}^{N_c} y_{n,i} = 1 \qquad (15.5b)$$

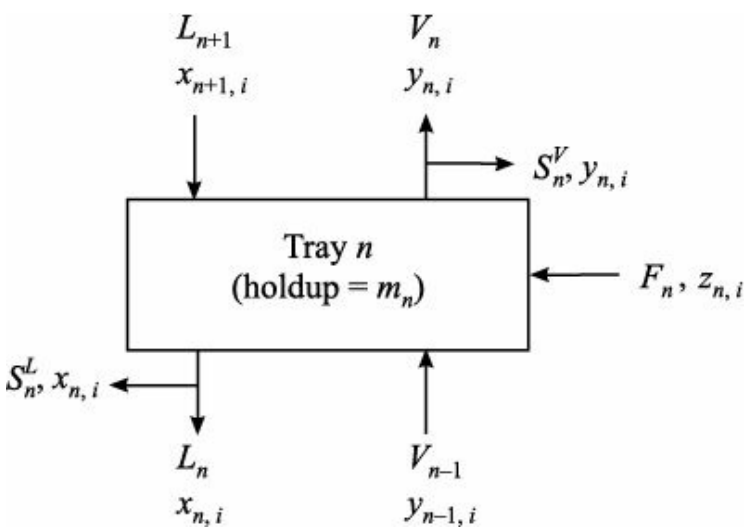

FIGURE 15.3 Quantities associated with a typical *n*th tray.

Here, N_c represents the total number of components, N_r the total number of reactions, H_n^L the enthalpy of a liquid stream leaving *n*th tray, H_n^V the enthalpy of a vapour stream leaving *n*th tray, $H_{rj,n}$ the heat of reaction for *j*th reaction and *n*th tray, $k_{n,i}$ the vapour-liquid equilibrium coefficient for *i*th component on *n*th tray, m_n the liquid holdup on *n*th tray, Q_n the heat loss from *n*th tray, $r_{j,n}$ the rate of *j*th reaction and *n*th tray, W_n the volume or weight of the catalyst for *n*th tray, $\nu_{i,j}$ the stoichiometric coefficient of *i*th component and *j*th reaction. R_f is a multiplication factor which takes values equal to zero for nonreactive and one for reactive tray. The dot symbol (.) is used to represent the time derivative.

In the simulation, algebraic form of equations is usually used to compute the vapour and liquid enthalpies. In many cases, no side streams $(S_n^L = S_n^V = 0)$ are involved. Negligible heat loss[2] from a stage to the surroundings ($Q_n = 0$) is also assumed for theoretical RD columns. It is worthy to mention that for a batch distillation, values of feed flow rate (F) and bottom product flow rate are taken as zero.

2 For practical column, a linear relationship between the temperature and the heat loss can be established based on experimental results. Usually, one relationship for each section and one for reboiler are derived.

Heat of reaction

Considering no phase change and no pressure effect, the specific enthalpy change from the reference state is given (Himmelblau, 1989) for a single component '1' as:

$$\Delta H_1 = \Delta H_{f1}^0 + \int_{T_{\text{ref}}}^{T} C_{p1}\, dT \quad \text{(per unit mole)} \qquad (15.6)$$

where ΔH_f^0 designates the heat of formation[3] at standard state [superscript '0' represents the standard state (298 K and 1 atm)] and C_p is the heat capacity. If standard heat of formation is not taken into account, then

[3] The heat of formation ($\equiv H_f$) is defined as the enthalpy change when one mole of a substance is formed from its constituent elements.

Similarly, the standard heat of formation ($\equiv H_f^0$) is defined as the enthalpy change when one mole of a substance is formed in its standard state from its constituent elements in their standard states.

$$\Delta H_1 = \int_{T_{\text{ref}}}^{T} C_{p1}\, dT \qquad (15.7)$$

For a stream consisting of say two components, namely 1 and 2, we write:

$$\Delta H_{\text{stream}} = \sum_{i=1}^{N_c=2} n_i \Delta H_{fi}^0 + \sum_{i=1}^{N_c=2} \int_{T_{\text{ref}}}^{T} n_i C_{pi}\, dT$$

$$= \underbrace{[n_1 \Delta H_{f1}^0 + n_2 \Delta H_{f2}^0]}_{\text{Heat of formation}} + \underbrace{[\int_{T_{\text{ref}}}^{T} (n_1 C_{p1} + n_2 C_{p2})\, dT]}_{\text{Sensible heat}} \qquad (15.8)$$

Here, n_i denotes the number of moles of component i. Now, we can easily develop the similar expression of $\equiv H_{\text{stream}}$ for any number of components.

The heat of reaction at constant pressure ($\equiv H_r$) is defined as the enthalpy change of the process and obviously it is the difference between the enthalpies of products and reactants:

$$\equiv H_r = (\equiv H_{\text{stream}})_{\text{products}} - (\equiv H_{\text{stream}})_{\text{reactants}} \qquad (15.9)$$

Let components 1 and 2 enter the system, then react and produce components 3 and 4 that finally leave the system. Using Equations (15.8) and (15.9), we have

$$\Delta H_r = (\Delta H_{\text{stream}})_{\text{products}} - (\Delta H_{\text{stream}})_{\text{reactants}} = [(n_3 \Delta H_{f3}^0 + n_4 \Delta H_{f4}^0) - (n_1 \Delta H_{f1}^0 + n_2 \Delta H_{f2}^0)]$$

$$+ \left[\int_{T_{\text{ref}}}^{T_{\text{out}}} (n_3 C_{p3} + n_4 C_{p4})\, dT - \int_{T_{\text{ref}}}^{T_{\text{in}}} (n_1 C_{p1} + n_2 C_{p2})\, dT \right]$$

$$= \left[\sum_{\text{products}} n_i \Delta H_{fi}^0 - \sum_{\text{reactants}} n_i \Delta H_{fi}^0 \right] + \left[\int_{T_{\text{ref}}}^{T_{\text{out}}} (n_3 C_{p3} + n_4 C_{p4})\, dT - \int_{T_{\text{ref}}}^{T_{\text{in}}} (n_1 C_{p1} + n_2 C_{p2})\, dT \right]$$

(15.10a)

It is interesting to note that if there is no reaction (i.e., no generation of components 3 and 4) involved, Equation (15.10a) becomes:

$$\Delta H_r = (\Delta H_{\text{stream}})_{\text{out}} - (\Delta H_{\text{stream}})_{\text{in}}$$

$$= \left[\int_{T_{\text{ref}}}^{T_{\text{out}}} (n_1 C_{p1} + n_2 C_{p2})\, dT - \int_{T_{\text{ref}}}^{T_{\text{in}}} (n_1 C_{p1} + n_2 C_{p2})\, dT \right] \qquad (15.10b)$$

The heat of reaction at standard state (ΔH_r^0) implies $T_{\text{in}} = T_{\text{out}} = T_{\text{ref}} = 298$ K. Accordingly, Equation (15.10a) yields:

$$\Delta H_r^0 = \left[\sum_{\text{products}} n_i \Delta H_{fi}^0 - \sum_{\text{reactants}} n_i \Delta H_{fi}^0 \right] \qquad (15.11)$$

Therefore, Equation (15.10a) becomes:

$$\Delta H_r = \Delta H_r^0 + \left[\int_{T_{\text{ref}}}^{T_{\text{out}}} (n_3 C_{p3} + n_4 C_{p4})\, dT - \int_{T_{\text{ref}}}^{T_{\text{in}}} (n_1 C_{p1} + n_2 C_{p2})\, dT \right] \qquad (15.12)$$

The heat of reaction at any temperature $T(\equiv H_rT)$ with respect to an arbitrary reference temperature T_0 gets the following form:

$$\Delta H_{rT} = \Delta H_{rT_0} + \left[\int_{T_0}^{T} (n_3 C_{p3} + n_4 C_{p4})\, dT - \int_{T_0}^{T} (n_1 C_{p1} + n_2 C_{p2})\, dT \right] \qquad (15.13)$$

Equation (15.13) is obtained when we put $T_{\text{in}} = T_{\text{out}} = T$ and replace T_{ref} by T_0 in Equation (15.12).

If *phase change* is involved, Equation (15.6) can be modified to represent the specific enthalpy change for a single component 1 as:

$$\Delta H_1 = \Delta H_{f1}^0 + \int_{T_{\text{ref}}}^{T_{BP}} C_{pL1}\, dT + \lambda_{T_{BP}1} + \int_{T_{BP}}^{T} C_{pV1}\, dT \text{ (per unit mole)} \qquad (15.14)$$

Here, suffix BP denotes the boiling point, L the liquid and V the vapour. Alternatively, the phase difference can be included in ΔH_f^0. Say, for example, water vapour is the product. So, use ΔH_f^0 for water vapour, not for liquid water. Then automatically the phase change from liquid water at 298 K to water vapour at 298 K is taken into account.

Usually, the heat of reaction depends not only on the reaction stoichiometry but also on the number of moles that react, the reaction temperature, the phases of the reactants and products, and the pressure. The *effect of pressure* upon heats of reaction is relatively negligible under most conditions. However, if exceedingly high pressures are encountered, we need to consider the necessary corrections as explained in any standard text on thermochemistry.

15.3 SIMULATION ALGORITHM: IN GENERAL

The simulation steps given here in sequence for the model described earlier are similar to those described in Chapter 10 of this book.

Step 1: Input data on the column size (number of total trays and column diameter), weir dimensions (weir height and weir length), feed (components, flow rate, composition and temperature), feed tray location, pressure profile, tray efficiency, reaction information, vapour pressure data, etc.

Step 2: Input data for variables at time $t = 0$. The variables include the liquid-phase compo-sitions (x_i) and liquid holdups (m) for all trays.

Step 3: Either input the values of reflux rate, distillate rate, bottoms rate and reboiler duty (or vapour boil-up rate) or manipulate these variables employing the suitable controllers. Recall that in batch operation, the start-up phase runs under total reflux condition and at production phase, the manipulated inputs are adjusted using the controllers.

Step 4: Compute the equilibrium vapour-phase composition and temperature (T) for each tray based on bubble point algorithm. The Newton–Raphson convergence method can be used in the bubble point calculations. Subsequently, calculate the actual vapour-phase composition (y_i) employing Murphree relationship [Equation (9.19)].

Step 5: Calculate the liquid- and vapour-phase enthalpies for each tray using the algebraic form of equations.

Step 6: Compute the reaction rate.

Step 7: Calculate the internal liquid flow rates using the Francis weir formula [Equation (9.18)] and the vapour flow rates solving the energy balance equations. Note that the three different approaches for calculating the vapour flow rate are discussed later. In the open-loop simulation, we use the steady state values of reflux rate and reboiler duty, and we calculate the distillate rate and bottoms rate assuming constant holdups in reflux drum and column base, respectively.

Step 8: Calculate the liquid holdup on each tray for the future time step ($t + \Delta t$) by solving the total mole balance equation.

Step 9: Compute the liquid-phase compositions on all trays for the future time step ($t + \Delta t$) by solving the component mole balance equations.

Step 10: To continue the process simulation for the next time step, go back to Step 3.

Algorithm for calculating the vapour flow rate

In the distillation model, the energy balance has the following form:

$$d(mH)/dt = f(\text{variables}) \qquad (15.15)$$

In general, the left term $d(mH)/dt$ has three kinds of forms for simulation. They are:

(a) $d(mH)/dt = 0$: the enthalpy change of the stage [$= d(mH)$] is negligible.
(b) $d(mH)/dt = H\, dm/dt$: dH/dt is assumed negligible.
(c) $d(mH)/dt = H\, dm/dt + m\, dH/dt$: the rigorous energy balance is assumed.

Unlike option (a) or (b), (c) has the dH/dt term, and the computation of dH/dt needs to estimate variables at future time step ($t + \Delta t$). It implies that the computation involving option (c) requires a yet more complicated algorithm than that involving (a) or (b). It can be said that the simulation assuming (c) can describe the actual phenomena more accurately but at the expense of much longer computation time.

Calculation of vapour flow rate using option (c)

Like internal liquid flow rate, vapour rate is also used in the simulation of each stage. In the following,

the vapour flow rate (V_n) calculation steps for a particular tray n are shown.

(i) Guess V_n at time $t = 0$.

(ii) Compute $x_{n,\,i}$ at next time step ($t + \Delta t$) solving component mole balance equation.

(iii) Calculate bubble point temperature at time step $t + \Delta t$.

(iv) Calculate $dH_n^L/dt\ \{\approx [H_n^L(t + \Delta t) - H_n^L(t)]/\Delta t\}$ using algebraic enthalpy equations.

(v) Set $V_t = V_n$, where V_t is a temporary variable for calculation.

(vi) Compute V_n from the following equation [derived from Equations (15.1) and (15.3)]:

$$V_n = \frac{1}{H_n^L - H_n^V}\left\{H_n^L\left[L_{n+1} + V_{n-1} + F_n - S_n^V + R_f\sum_{j=1}^{N_r}\sum_{i=1}^{N_c}(\delta_{i,j}r_{j,\,n}\varepsilon_n)\right] - L_{n+1}H_{n+1}^L - V_{n-1}H_{n-1}^V - F_nH_n^F + S_n^VH_n^V - R_f\sum_{j=1}^{N_r}(r_{j,n}\varepsilon_n\Delta H_{rj,n}) + Q_n + m_n\frac{dH_n^L}{dt}\right\} \tag{15.16}$$

(vii) If $|(V_n - V_t)/V_t| < 10^{-4}$ or so (tolerance limit), stop here; otherwise, go back to Step (ii).

Option (a) has been considered in several chapters, including the RD column exampled in the next section, of this book. Option (b) is also relatively simple and not discussed further. Interested readers may find the application of option (c) in literature papers [e.g., Jhon and Lee (2003); Kathel and Jana (2010)].

15.4 BATCH REACTIVE DISTILLATION: AN EXAMPLE

Now, we will consider an example of a batch reactive rectifier. The modelling, simulation and control are the three issues to be discussed here. It is well known that the batch reactors and batch distillations are very common in the chemical and petroleum industries. Their combination in RD is a process alternative that allows to combine the benefits of RD and batch processes, providing a significant reduction of capital investment and additional flexibility.

The sample batch RD column is shown in Figure 15.4. The representative process has total 8 trays, excluding the reboiler and total condenser. The trays are counted from bottom to top; bottom tray is the 1st tray and top tray is the 8th tray. Subindex *D* and *B* have been used throughout this chapter for distillate and bottom, respectively.

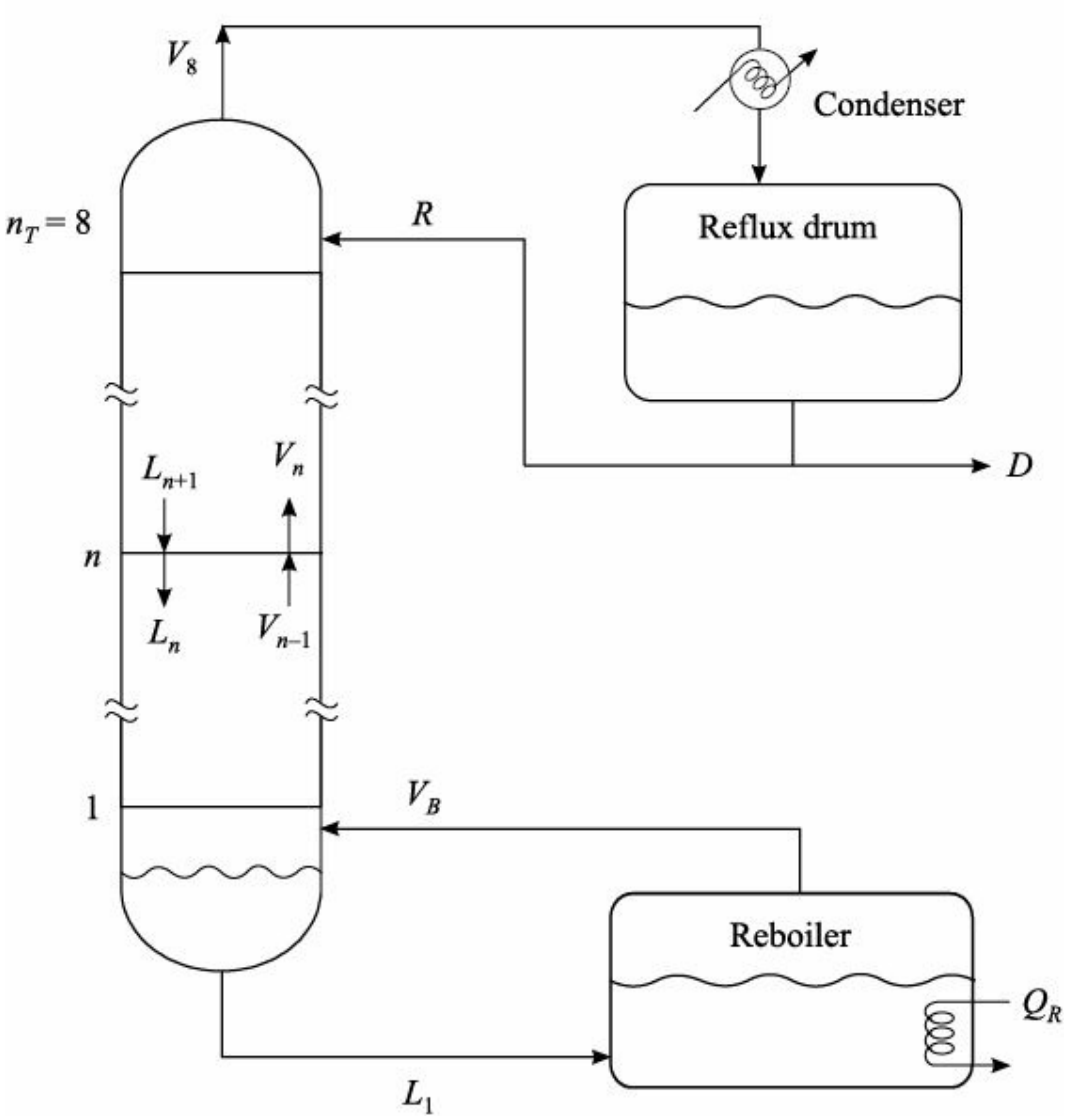

FIGURE 15.4 Schematic representation of the batch reactive rectifier.

The concerned process produces ethyl acetate and water by the esterification of ethanol with acetic acid. The reaction scheme and the boiling temperatures are mentioned in the following:

acetic acid + ethanol ⇌ ethyl acetate + water

(1) (2) (3) (4)

Boiling point (K) ⟶ 391.1 351.5 350.3 373.2

The reversible reaction takes place in the liquid phase. For the ethanol esterification reaction, the kinetic data taken from Bogacki et al. (1989) are listed in Table 15.1.

Table 15.1 Column specifications and reaction kinetic data

Column specifications	
System	acetic acid/ethanol/ethyl acetate/water
Total feed charge, kmol	30.0
Feed composition (start-up), mol fraction	0.45/0.45/0.0/0.1
Tray holdup (start-up), kmol	0.075
Reflux drum holdup, kmol	0.6
Heat input to the still pot, kJ/min	3200
Distillate flow rate (production phase), kmol/min	0.06
Distillate composition (steady state), mol fraction	0.9344
Column diameter, inch	18
Integration time interval = 0.005 min	
Kinetic data	
Rate of reaction [gmol/(l min)]: $r = k_1 C_1 C_2 - k_2 C_3 C_4$	

Rate constants: $k_1 = 4.76 \times 10^{-4}$; $k_2 = 1.63 \times 10^{-4}$
where C_i = concentration (gmol/l) for the ith component

The main product, ethyl acetate, is the lightest component in the mixture. The continuous withdrawal of ethyl acetate as distillate shifts the chemical equilibrium further to the right
and consequently, the reactant conversion is improved. This will also proportionately increase the yield.

The model structure of the example of batch reactive rectifier has been developed based on the following assumptions:

- Negligible tray vapour holdups
- Variable liquid holdup in each tray
- Perfect mixing and equilibrium on all trays
- No chemical reactions in the vapour phase
- Reactions occurred on the trays, and in the condenser and reboiler
- Fast energy dynamics [i.e., $d(mH)/dt = 0$]
- Constant operating pressure (atmospheric) and tray efficiencies (Murphree vapour-phase efficiency = 75%)
- Total condensation with no subcooling
- Raoult's law and Dalton's law for describing the liquid and vapour phase, respectively [Equation (9.24)]
- No heat loss to the surroundings
- No azeotropes formation
- Nonlinear Francis weir formula [Equation (9.18)] for liquid hydraulics calculations
- Constant liquid holdup in the reflux drum [perfectly controlled by a conventional proportional (P-only) controller with a proportional gain of – 0.01 and D_S (bias signal) of 0.06 kmol/min]

15.4.1 Modelling Equations

The representative batch reactive rectifier is modelled using a detailed tray-to-tray model. The modelling equations for nth tray are summarized as follows:

nth Tray

Total mole balance:

$$\dot{m}_n = L_{n+1} + V_{n-1} - L_n - V_n + \sum_{i=1}^{N_c} \delta_i r_n \varepsilon_n \tag{15.17}$$

Component mole balance:

$$\dot{m}_n \dot{x}_{n,i} = L_{n+1} x_{n+1,i} + V_{n-1} y_{n-1,i} - L_n x_{n,i} - V_n y_{n,i} + \delta_i r_n \varepsilon_n \tag{15.18}$$

Energy balance:

$$\dot{m}_n \dot{H}_n^L = L_{n+1} H_{n+1}^L + V_{n-1} H_{n-1}^V - L_n H_n^L - V_n H_n^V + r_n \varepsilon_n \Delta H_{r,n} \tag{15.19}$$

Equilibrium:

$$y_{n,i} = k_{n,i} x_{n,i} = \frac{P^S_{n,i}}{P_t} x_{n,i} \qquad (15.20)$$

Summation:

$$\sum_{i=1}^{N_c} x_{n,i} = 1 \qquad \text{[from Equation (15.5a)]}$$

$$\sum_{i=1}^{N_c} y_{n,i} = 1 \qquad \text{[from Equation (15.5b)]}$$

Here, $_{\text{en}}n$ stands for the volume of the tray liquid (L), P_t the total pressure (mm Hg) and P_i^S the vapour pressure of component i (mm Hg). All flow rates are in kmol/min, enthalpies in kJ/kmol, heat of reaction in kJ/kmol and liquid holdups in kmol. The unit of rate of reaction used in the above model equations must be kmol/(l.min).

15.4.2 Computer Simulation

In the simulation, algebraic form of equations (Yaws, 1996) has been used to compute the vapour and liquid enthalpies. The heat of reaction in all energy balance equations is omitted, because heat of formation at the standard conditions is used as a base for enthalpy calculations. Values of Antoine constants given in Chapter 9 have been used in determining the vapour pressure of any component i(P_i^S) in mm Hg. Accordingly, the total pressure (P_t) must be in mm Hg in Equation (15.20).

The model and system characteristics are reported in Table 15.1. As mentioned in the earlier discussion on batch distillation, at the beginning of batch operation, the reboiler, all the trays, and the reflux drum are filled with the liquid feed that ensure consistent initialization of the DAE (differential and algebraic equation) system used here. The 4% of the total feed
charge is used as the total column holdup. Half of this holdup is taken as reflux accumulator holdup and the rest is equally divided for the tray holdups. Note that the computer code developed for simulating the modelling equations of the example column is not provided. This is left for you.

15.4.3 Open-loop Process Dynamics

Now we will discuss the simulation results of the reactive batch rectifier operated in an open-loop fashion. In a standard reactive column, both the reaction and separation take place simultaneously. Among the reactants and product components of the representative system, ethyl acetate has the lowest boiling temperature. Naturally, the ethyl acetate enriched mixture comes out as the distillate product.

Although we have simulated the batch distillation processes in Chapters 9 and 11, at this moment it is good to revisit shortly the following points: In a typical batch distillation operation, first the column may be brought to the steady state by following the total reflux start-up procedure. Then the production phase is begun with switching on the controller aiming to maintain the specified product purity. In some cases, however, the product is withdrawn as soon as the overhead composition reaches its desired value, without waiting for the steady state to be attained. It is noteworthy that immediately after the production phase is started, the controller responses may be aggressive enough. It happens because of the following two reasons:
(i) immediate withdrawal of the distillate product, and (ii) the change of distillate composition (controlled variable) from the process value to the set point value. This results in severe spiking of the

reflux rate (manipulated variable). To avoid this occurrence, the reflux flow rate may be passed through a rate-of-change filter (Seborg et al., 1989). Alternatively, one could consider filtering the set point, as described in Henson and Seborg (1991). Next, we will discuss the results by creating various situations in the simulator.

Start-up profile with no reaction

At the very beginning of the start-up mode of batch operation, the sample column operates under total reflux condition without having esterification reaction. In such a situation, the batch distillation process, originally a nonreactive ternary (acetic acid/ethanol/water) batch process, reaches at steady state within about 11 min. This observation is depicted in Figure 15.5 showing the profile of component compositions in the top and bottom.

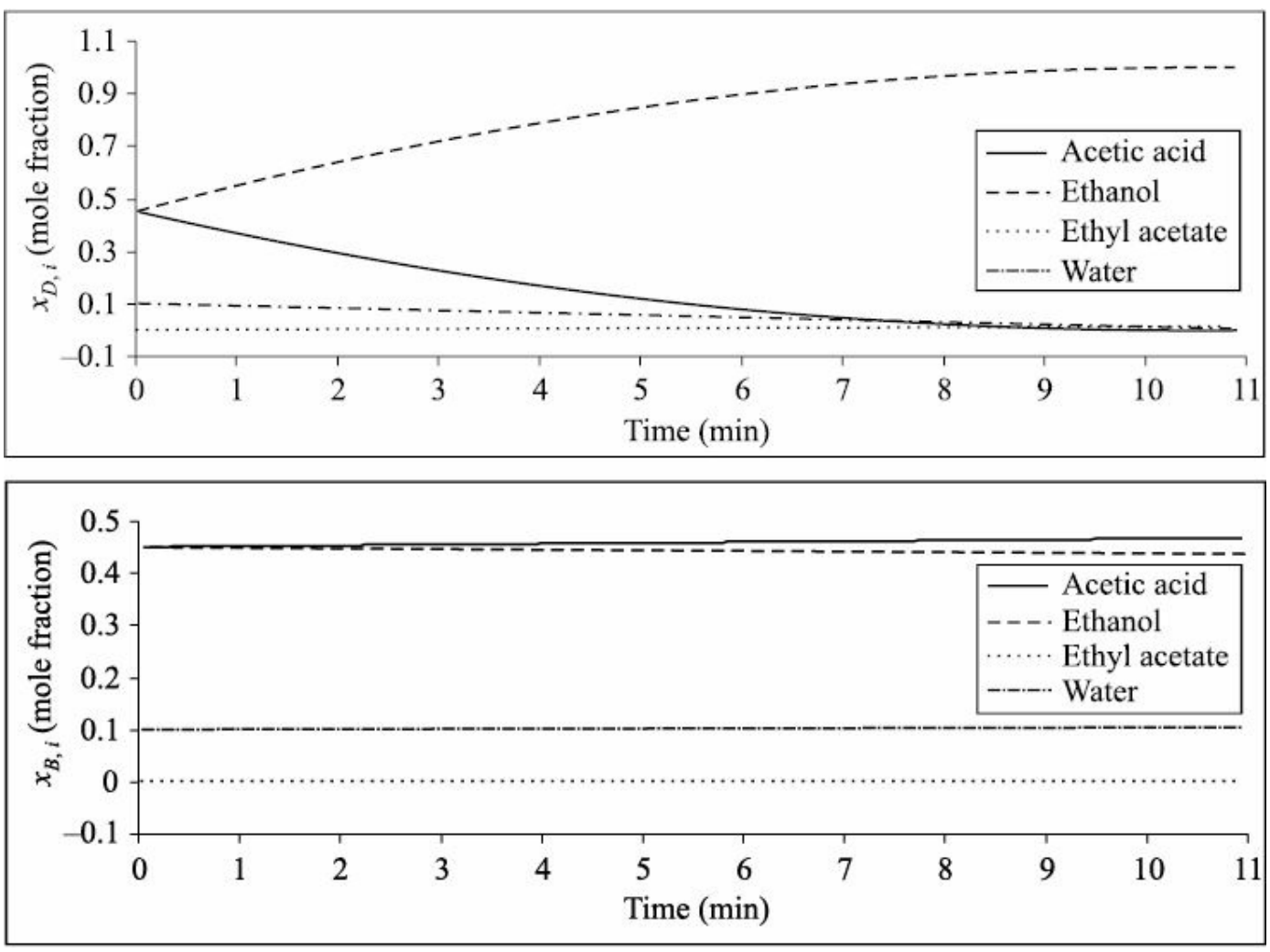

FIGURE 15.5 Open-loop process dynamics at the start-up phase under complete reflux condition without having reaction.

Complete start-up profile

In the above, the start-up profile of the nonreactive batch column is demonstrated. The next part of the start-up phase runs under complete reflux condition but with having esterification reaction. At the end of the start-up period, the reactive batch column attains another steady state with the ethyl acetate composition of 0.9344. This composition data imposes an upper limit in the achievable product purity under batch operation. Figure 15.6 presents the dynamics in
terms of uncontrolled compositions of the sample batch reactive rectifier throughout the entire start-up phase.

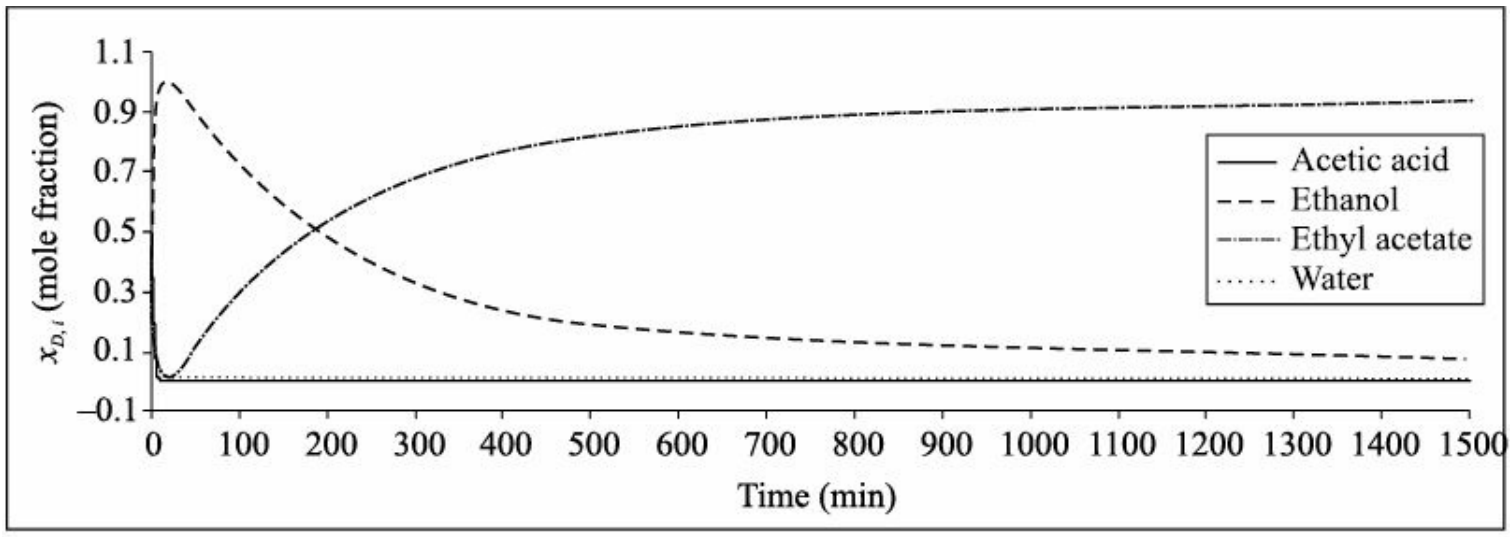

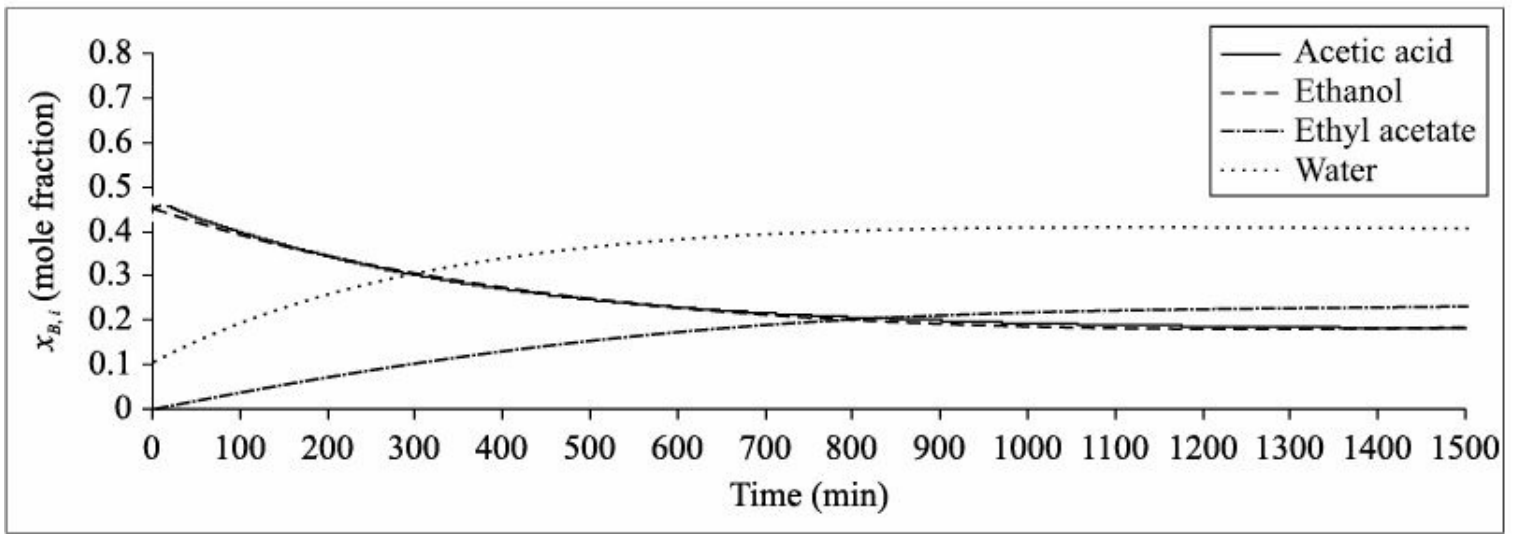

FIGURE 15.6 Open-loop process dynamics at the entire start-up phase under total reflux condition with having reaction (no reaction only in the first 11 min).

15.4.4 Closed-loop Process Dynamics

Why is controller required for the example batch process?

Before going to study the process dynamics under a control scheme, we are curious to know about the need of a controller for the example batch reactive rectifier. For this purpose,
Figure 15.7 is produced to display the uncontrolled process dynamics at the production phase in terms of ethyl acetate composition in the distillate stream ($x_{D,3}$). In this simulation experiment, a reflux ratio ($RR = R/V_8$) of 0.875 is considered throughout the production period. It is evident from the figure that as time progresses, the product purity decreases. From this fact we realize, therefore, that the batch distillation will necessitate a controller mainly for maintaining the product purity at a specified value under different conditions.

Application of control algorithm

The control objective is to produce the overhead product with a specified purity of ethyl acetate. The manipulated input is the reflux flow rate[4]. As mentioned, the reflux drum holdup is remained almost unchanged by the employment of a traditional P-only controller. For the concerned column, a gain-scheduled proportional integral (GSPI) control system is chosen to be used for regulating the ethyl acetate composition at the top.

[4] Reflux ratio (internal/external) can also be considered as the manipulated input.

Why GSPI controller?

The batch rectifier is truly an integrating system. The depletion of light components with the progress of batch operation (see Figure 15.7) takes a role somewhat like a ramp load and produces a control problem (Finefrock et al., 1994). The column experiences a great deal of changes from a low-plant-gain composition space (i.e., the steady-state space) to a high-plant-gain composition space. This indicates that the control gain must be increased appropriately during the batch operation. It is, therefore, suggested that to obtain tight control of the distillate composition, the controller having variable gain (e.g., GSPI and adaptive controller) must be preferred.

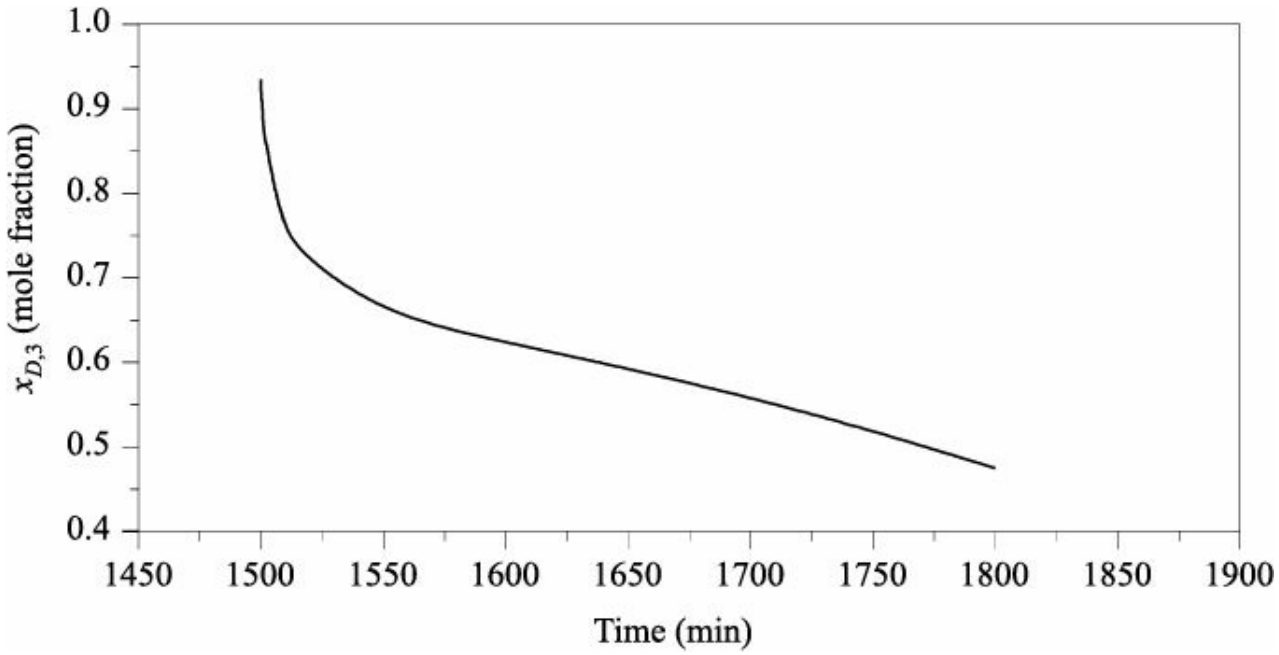

FIGURE 15.7 Open-loop process dynamics at the production phase in terms of ethyl acetate composition in the distillate ($x_{D,3}$).

GSPI control algorithm

For the representative process, the GSPI structure (Bequette, 2003) can be described with the following form:

$$R = R_s + K_c(x_{D,i})\left(e + \frac{1}{\tau_i}\int e\ dt\right) \qquad (15.21)$$

Here, R_S denotes the bias signal for the reflux rate (R) and $x_{D,\,i}$, distillate composition of any component i, is the scheduling variable. The controller gain, K_c, is varied aiming to keep K_cK_p constant, which then keeps the stability margin constant. When the process gain (K_p) is characterized as a function of the scheduling variable, $K_p(x_{D,\,i})$, then the controller gain can be scheduled as:

$$K_c(x_{D,i}) = \frac{K_c(x_{D0,i})\,K_p(x_{D0,i})}{K_p(x_{D,i})} \qquad (15.22)$$

where $x_{D0,\,i}$ is the nominal operating value of $x_{D,\,i}$ ($= x_{DSP,\,i}$). The gain of the GSPI control scheme used has the following forms:

Case 1: When $x_{D,\,i} > x_{D0,\,i}$,

$$K_c(x_{D,i}) = K_{c0}\frac{1 - x_{D0,i}}{1 - x_{D,i}} \qquad (15.23)$$

where $K_p(x_{D,i}) = 1 - x_{D,i}$ and $K_c(x_{D0,i}) = K_{c0}$.

Case 2: When $x_{D,i} < x_{D0,i}$

$$K_c(x_{D,i}) = K_{c0} \qquad (15.24)$$

It is worthy to mention that this is a *one-way* approach. Since the process gain increases with lower purity, maintaining a constant controller gain speeds up the response when the distillate is less pure. Values of controller tuning parameters used are as follows: $K_{c0} = 1.16$ and $\tau_i = 0.15$ min.

GSPI control performance

Constant composition control

Figure 15.8 illustrates the closed-loop performance of the GSPI scheme for maintaining the top product composition of the concerned batch reactive rectifier at the value of 0.9344 (reference/steady state composition). The figure also includes the manipulated input profile. The controller takes about 30 min to return the process near to its reference state. It is clear that just after the starting of product withdrawal, the control action is aggressive for the reason(s) described earlier.

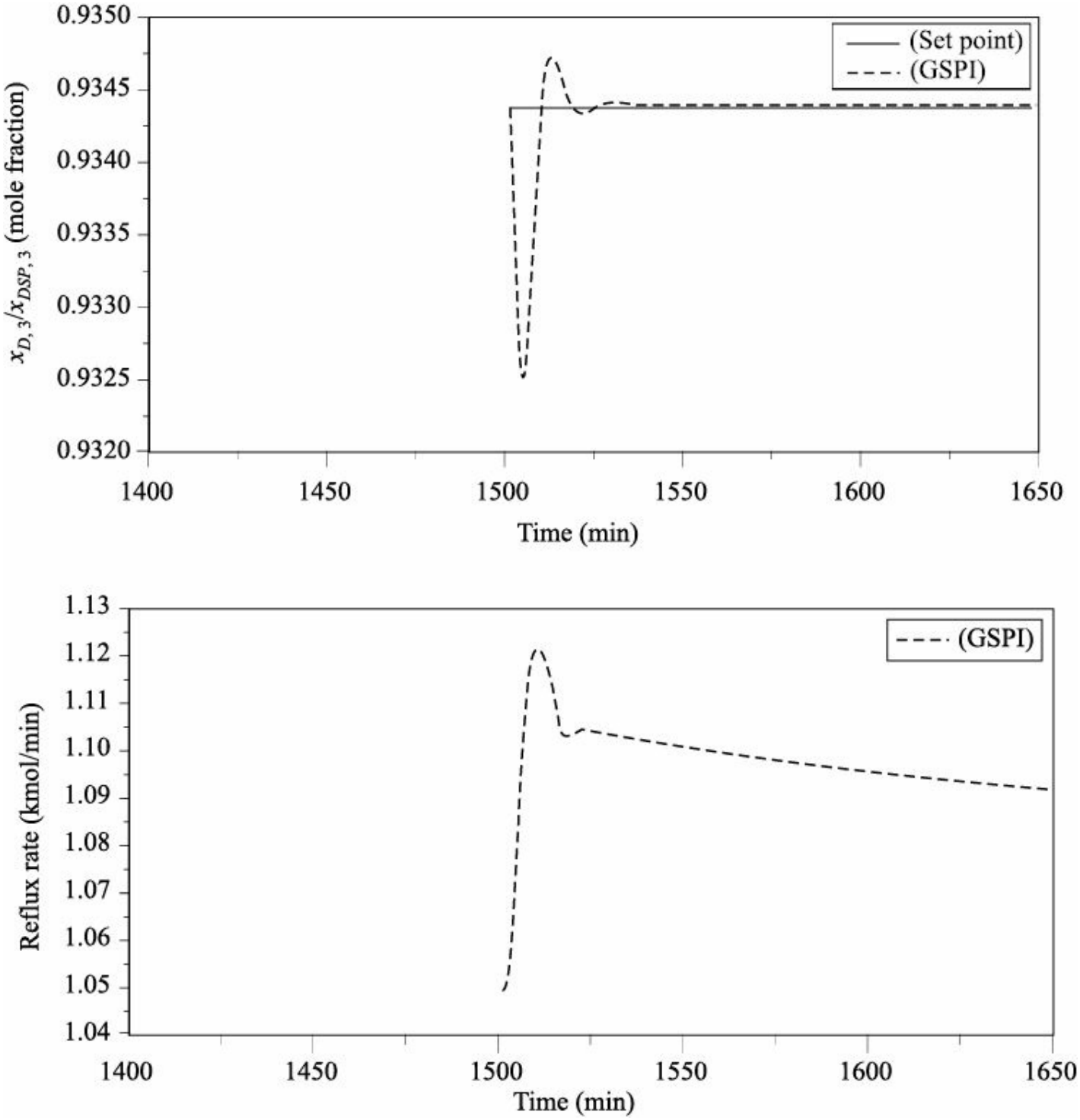

FIGURE 15.8 Performance of the gain-scheduled PI controller for constant composition control ($x_{DSP,3}$ = 0.9344) (suffix 3 indicates the 3rd component that is ethyl acetate).

15.5 SUMMARY AND CONCLUSIONS

This chapter introduces the concept of RD. Several potential merits and demerits of RD column have been discussed. After detailing the theory involved in modelling an RD process, a batch RD column is exampled for the production of ethyl acetate. The model structure is developed for equilibrium stages. Computer coding part is left for the students. This chapter presents the open-loop process dynamics for both reactive and nonreactive cases. Finally, the GSPI control law has been devised for the example column and the closed-loop control performance has been investigated.

EXERCISES

15.1 In what sense is an RD column comparable with a reactor-followed-by-distillation scheme?

15.2 Select the correct and incorrect statements from the followings:

Benefits offered by the RD technology include:

(i) increased yield, because of overcoming chemical and thermodynamic equilibrium limitations

(ii) increased selectivity via suppression of undesired side reactions

(iii) reduced energy consumption via direct heat integration, in the case of exothermic reactions

(iv) avoidance of hot spots by simultaneous liquid evaporation

(v) ability to separate wide boiling components

15.3 A continuous-flow reactive distillation process produces methyl acetate and water by the esterification of methanol with acetic acid. The reversible liquid-phase reaction is given as:

$$\text{methanol} + \text{acetic acid} \rightleftarrows \text{methyl acetate} + \text{water}$$

	(MeOH)	(HOAc)	(MeOAc)	(H_2O)
Boiling point (°C)	64.7	118.1	56.9	100

The example process operates at a pressure of 1 atm. Though the esterification reaction is self-catalyzed, consider ion-exchange resin (e.g., Amberlyst-15) as an external catalyst to enhance the reaction rate. The rate of reaction described in the following is developed (Song et al., 1998) by utilizing the Langmuir–Hinshelwood–Hougen–Watson (LHHW) isotherm.

$$R_{\mathrm{MeOAc}} = \frac{M_{\mathrm{cat}} k_1 \left(a_{\mathrm{HOAc}}\, a_{\mathrm{MeOH}} - \dfrac{a_{\mathrm{MeOAc}}\, a_{\mathrm{H_2O}}}{K_{\mathrm{eq}}} \right)}{\left(1 + K_{\mathrm{HOAc}}\, a_{\mathrm{HOAc}} + K_{\mathrm{MeOH}}\, a_{\mathrm{MeOH}} + K_{\mathrm{MeOAc}}\, a_{\mathrm{MeOAc}} + K_{\mathrm{H_2O}} a_{\mathrm{H_2O}}\right)^2} \tag{15.25}$$

$$k_1 = 6.942 \times 10^9 \exp\left(\frac{-6287.7}{T}\right) \tag{15.26}$$

$$K_{\mathrm{eq}} = 2.32 \exp\left(\frac{782.98}{T}\right) \tag{15.27}$$

$$a_i = \text{▭}_i x_i \tag{15.28}$$

With $K_{\mathrm{HOAc}} = 3.18$, $K_{\mathrm{MeOH}} = 4.95$, $K_{\mathrm{MeOAc}} = 0.82$ and $K_{\mathrm{H2O}} = 10.5$. Here, a_i is the activity, ▭_i the liquid activity coefficient, x_i the liquid mole fraction, k_1 the reaction rate constant [mol/(g cat h)], M_{cat} the mass of the catalyst per stage (g) and T the temperature (K). The catalyst holdup on each tray is 2 kg. The UNIQUAC thermodynamic model can be adopted with parameters given by Tang et al. (2005).

Making necessary assumptions, derive the modelling equations of the methyl acetate RD column and investigate the process dynamics using the data given in Table 15.2.

Table 15.2 Operating conditions of the methyl acetate RD column

Number of stages	20
[excluding total condenser (Tray 1) and reboiler (last tray)]	
Stripping stages	4
Rectifying stages	5

Feed 1 (pure acetic acid) stage	6
Feed 1 flow rate (mol/s)	1
Feed 2 (pure methanol) stage	16
Feed 2 flow rate (mol/s)	1
Feed temperature (K)	325
Distillate composition (methyl acetate)	0.9972
Bottoms composition (water)	0.99
Reboiler duty (J/s)	22,000
Column pressure (atm)	1
Murphree tray efficiency	75%

15.4 A continuous RD column (Singh et al., 2005) shown in Figure 15.9 is employed for the production of methyl *tert*-butyl ether (MTBE) according to the following reaction:

$$\textit{iso}\text{-butene} + \text{methanol} \rightleftarrows \text{MTBE}$$

The etherification of *iso*-butene (IB) with methanol (MeOH) forms MTBE in the presence of a strong acid catalyst. The base case operating conditions and design parameters are mentioned in the figure. Assume ideal vapour phase and use the Wilson activity coefficient model for liquid phase. The Wilson parameters are reported in Table 15.3. An activity-based rate expression used to model the reaction kinetics is given as:

$$r = k_r \left(\frac{a_{\text{IB}}}{a_{\text{MeOH}}} - \frac{a_{\text{MTBE}}}{K_a a_{\text{MeOH}}^2} \right) \tag{15.29}$$

The reaction rate constant and equilibrium constant are modelled as:

$k_r = 1.8 \times 10^{13} \exp(-11110/T)$ mol/(s.kg catalyst)

$K_a = \exp(-16.33 + 6820/T)$ and $a_i = \gamma_i x_i$

Develop the model structure for the MTBE RD column operated at 11 atm and simulate the model for dynamics study.

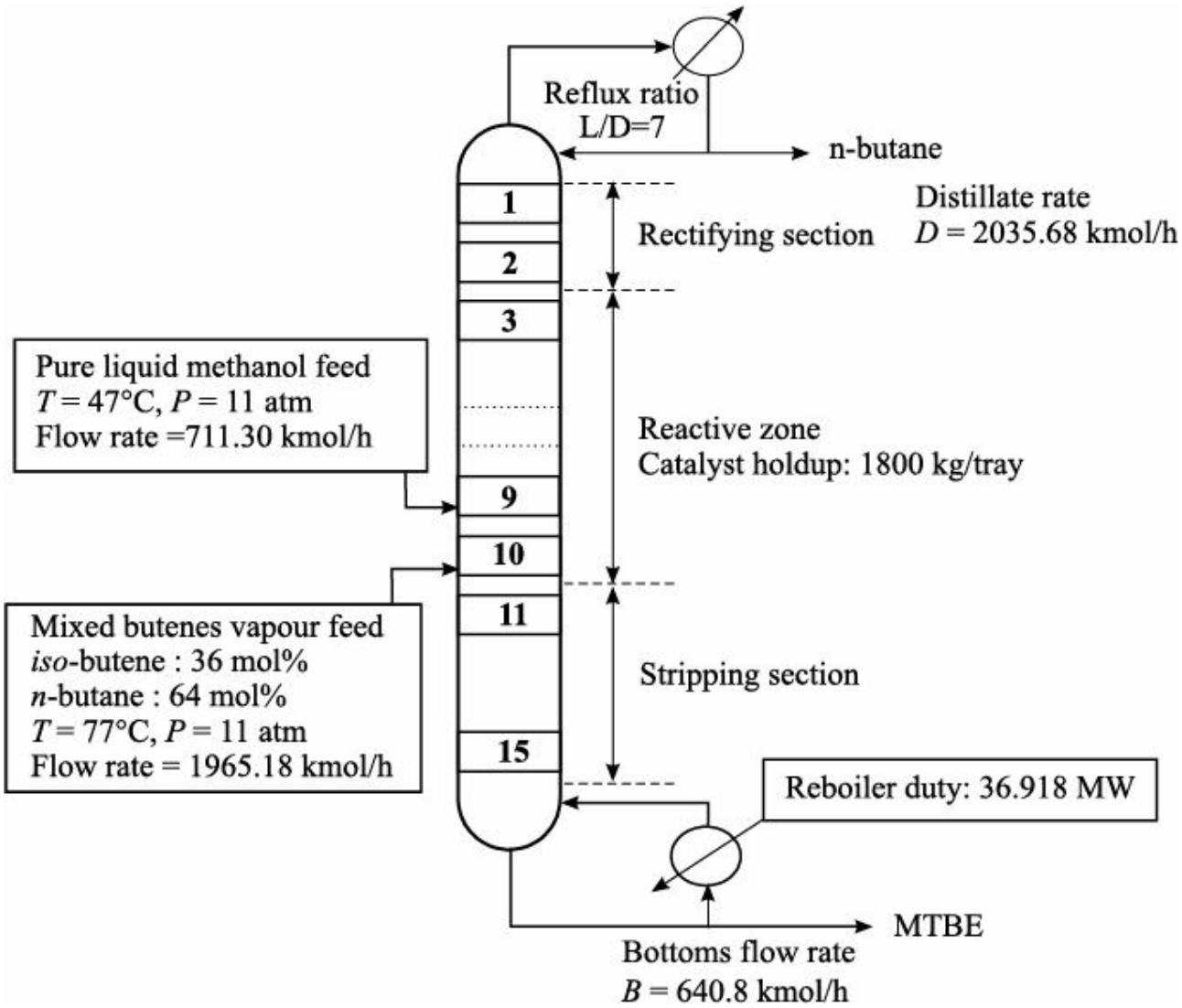

FIGURE 15.9 An MTBE RD column.

Table 15.3 Wilson binary interaction parameters

	iso-butene	*Methanol*	MTBE	*n-butane*
iso-butene	0	2576.853	271.567	0
Methanol	169.995	0	– 406.390	382.343
MTBE	– 60.108	1483.248	0	0
n-butane	0	2283.873	0	0

15.5 Consider a total reflux reactive distillation column (Ciric and Miao, 1994) shown in Figure 15.10 for the production of ethylene glycol (EG) from ethylene oxide (EO) and water (W). The representative process has total 10 stages (excluding the bottom reboiler and total condenser). The trays are counted from bottom up; bottom tray is the 1st stage and top one is the 10th stage. The example column has two sections, namely the reactive section (5th to 10th stage) and the nonreactive section (1st to 4th stage). Of course, the separation occurs in both sections. In the top six stages, the following exothermic liquid-phase reaction takes place:

$$\underset{C_2H_4O}{\text{ethylene oxide}} + \underset{H_2O}{\text{water}} \rightarrow \underset{C_2H_6O_2}{\text{ethylene glycol}}$$

	C_2H_4O	H_2O	$C_2H_6O_2$
Boiling point (K)	283.5	373.2	470.4

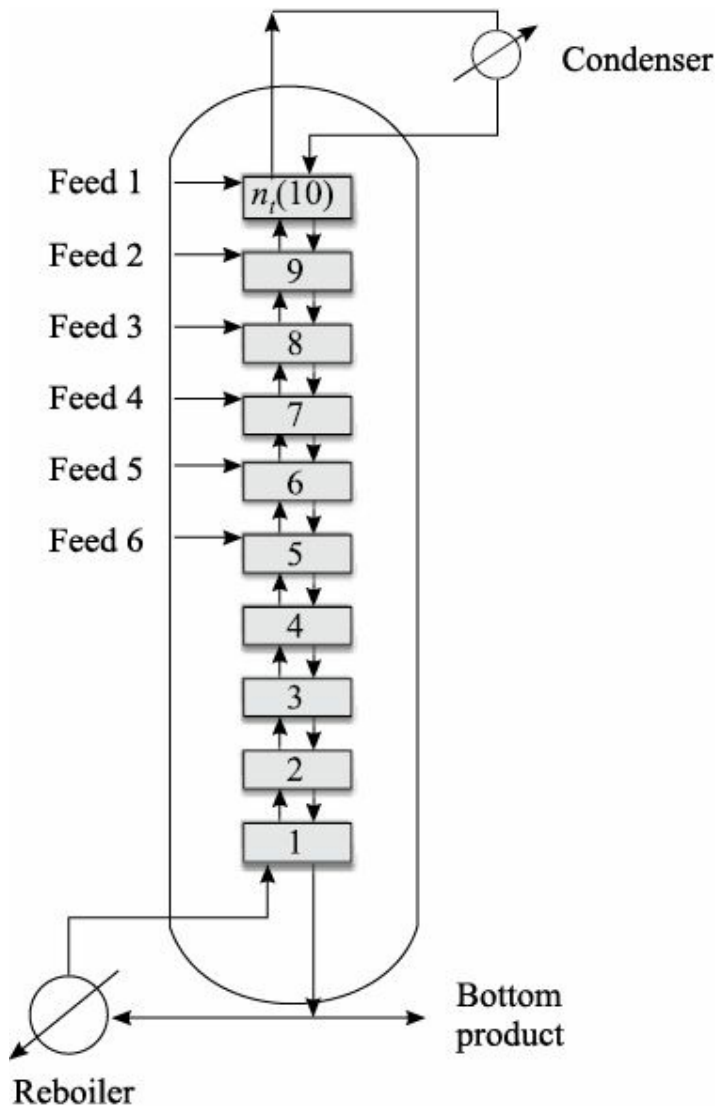

FIGURE 15.10 The ethylene glycol RD column.

The mathematical model of the multiple-feed RD column is asked to derive under the following assumptions: negligible tray vapour holdup compared to liquid holdup, variable tray liquid holdup, perfect mixing and equilibrium on all trays, fast energy dynamics, top stage pressure of 1 atm (= 101.33 kPa) with a stage pressure drop of 0.3 kPa, constant tray efficiency (Murphree vapour-phase efficiency = 70%), no side reaction, and Wilson model to predict the vapour–liquid equilibrium.

Column and system specifications are reported in Table 15.4. Table 15.5 includes the property data. Reaction volumes are distributed unevenly between stages 5 and 10. Pure water with a flow rate of 26.3 kmol/h is introduced onto the top stage and a total feed of 27.56 kmol/h of pure EO is distributed among stages 5 and 10. Among the three species, EO is the lightest, water is the intermediate and EG is the heaviest one. Accordingly, the product EG is taken out from the bottom. The overhead vapour, a highly pure EO (99.7 mol%) stream, is totally converted to liquid state in a condenser. The only product that is withdrawn at the bottom contains 94 mol% EG.

Table 15.4 Column and system specifications

Pure EO feed rates (kmol/h) [from stages 5 to 10]	4.89/4.76/4.69/4.97/0.2/8.05
Pure water feed rates (kmol/h) [from stages 5 to 10]	0.0/0.0/0.0/0.0/0.0/26.3
Reaction volume (m^3)	0.551/0.481/0.447/0.371/1.447/0.011

[from stages 5 to 10]	
Bottoms composition (EO/W/EG)	0.053/0.007/0.94
Bottoms rate (kmol/h) (EO/W/EG)	1.4604/0.2011/26.099
Column diameter (m)	1.3

Reaction kinetics (Ciric and Miao, 1994)

Reaction rate (kmol/m^3.h): $r = \exp\left(37.0 - \frac{9547.7}{T}\right) x_{EO} x_W$, where temperature ($T$) is in K

Heat of reaction = – 80 kJ/mol
Heat of vaporization = 40 kJ/mol

Table 15.5 Property data

Antoine equation and coefficients (Ciric and Miao, 1994):

$$P_i^S = A_{1i} \exp\left(A_{2i} \frac{T - A_{3i}}{T - A_{4i}}\right)$$ (where P_i^S is in atm and T is in K)

Component	A_{1i}	A_{2i}	A_{3i}	A_{4i}
Ethylene oxide	71.9	5.72	469	35.9
Water	221.2	6.31	647	52.9
Ethylene glycol	77	9.94	645	71.4

Wilson binary interaction parameters (Chen et al., 2000):

	Ethylene oxide	*Water*	*Ethylene glycol*
Ethylene oxide	0.0	1905.77	635.82
Water	124.96	0.0	–1265.74
Ethylene glycol	–79.47	1266.01	0.0

Derive the modelling equations for the ethylene glycol RD column and simulate the model structure to inspect the dynamic process behaviour.

REFERENCES

Bequette, B.W. (2003). *Process Control: Modeling, Design, and Simulation*, 1st ed., Prentice-Hall of India, New Delhi.

Bogacki, M.B., Alejski, K., and Szymanowski, J. (1989). The fast method of the solution of a reacting distillation problem, *Comput. Chem. Eng.*, 13, 1081–1085.

Chen, F., Huss, R.S., Malone, M.F., and Doherty, M.F. (2000). Simulation of kinetic effects in reactive distillation, *Comput. Chem. Eng.*, 24, 2457–2472.

Ciric, A.R., and Miao, P. (1994). Steady state multiplicities in an ethylene glycol reactive distillation column, *Ind. Eng. Chem. Res.*, 33, 2738–2748.

Finefrock, Q.B., Bosley, J.R., and Edgar, T.F. (1994). Gain scheduled PID control of batch distillation to overcome changing system dynamics, *AIChE Annual Meeting*, San Francisco, CA.

Henson, M.A., and Seborg, D.E. (1991). An internal model control strategy for nonlinear systems, *AIChE J.*, 37, 1065.

Himmelblau, D.M. (1989). *Basic Principles and Calculations in Chemical Engineering*, 5th ed., Prentice-Hall of India, New Delhi.

Jhon, Y.H., and Lee, T.H. (2003). Dynamic simulation for reactive distillation with ETBE synthesis, *Sep. Purif. Technol.*, 31, 301–317.

Kathel, P., and Jana, A.K. (2010). Dynamic simulation and nonlinear control of a rigorous batch reactive

distillation, *ISA Trans.*, 49, 130–137.

Khaledi, R., and Young, B.R. (2005). Modeling and model predictive control of composition and conversion in an ETBE reactive distillation column, *Ind. Eng. Chem. Res.*, 44, 3134–3145.

Seborg, D.E., Edgar, T.F., and Mellichamp, D.A. (1989). *Process Dynamics and Control,* 1st ed., John Wiley & Sons, New York.

Singh, B.P., Singh, R., Kumar, M.V.P., and Kaistha, N. (2005). Steady-state analyses for reactive distillation control: An MTBE case study, *J. Loss Prevention in the Process Industries*, 18, 283–292.

Song, W., Venimadhavan, C., Manning, J., Malone, M., and Doherty, M. (1998). Measurement of residue curve maps and heterogeneous kinetics in methyl acetate synthesis, *Ind. Eng. Chem. Res.*, 37, 1917–1928.

Tang, Y.T., Chen, Y.W., Hung, S.B., Huang, H.P., Lee, M.J., and Yu, C.C. (2005). Design of reactive distillations for acetic acid esterification, *AIChE J.*, 51, 1683–1699.

Tuchlenski, A., Beckmann, A., Reusch, D., Dussel, R., Weidlich, U., and Janowsky, R. (2001). Reactive distillation–industrial applications, process design & scale-up, *Chem. Eng. Sci.*, 56, 387–394.

Yaws, C.L. (1996). *The Yaws Handbook of Thermodynamic Properties for Hydrocarbons and Chemicals,* Vol. 1, 1st ed., Gulf Publishing Company, Texas.

Part IV

Vaporizing Processes

There are typically two principal types of vaporizing processes (Kern, 1997) used in industrial practice: boilers and vaporizing exchangers. *Boilers* are directly fired equipments that primarily convert fuel energy into latent heat of vaporization. On the other hand, *vaporizing exchangers* are unfired and they convert the sensible or latent heat of one fluid into the latent heat of vaporization of another. The three common types of vaporizing exchangers are: evaporator[1], reboiler[2] and vaporizer[3].

1 used to evaporate water or an aqueous solution

2 used to supply heat at the bottom of a distilling column

3 other than evaporator and reboiler

16

Vaporizing Exchangers

16.1 INTRODUCTION

As stated, the three common types of vaporizing exchangers are: reboiler, vaporizer and evaporator. The distillation reboiler has been discussed in several chapters of this book (e.g., Chapter 10). This chapter is devoted for detailing a vaporizer followed by an evaporation system. In the present study, the vaporizer model will also be used to represent a boiler for steam production.

16.2 VAPORIZER

A typical layout of a vaporizer is shown in Figure 16.1. It is a jacketed vessel, in which a liquid (feed) enters at the bottom with a volumetric flow rate F_i and temperature T_i, and the produced vapour is taken out from the top. Steam is supplied from the external source as a heating medium. Due to the continuous input of heat (Q) to the vaporizer, the liquid temperature gradually rises and finally reaches the boiling point. The boiling of a liquid starts at some temperature (and composition if more than one component is present) when the vapour pressure of the liquid (P) tends to exceed the pressure in the vapour phase above it (P_V). An infinitesimal difference between these two pressures is sufficient to provide the vapour flow. At this point it is worthy to mention that the vapour boil-up rate ($\dot{m}_B$) is proportional to the driving force $P–P_V$, i.e., $\dot{m}_B = k(P - P_V)$. At equilibrium, $P = P_V$, which indicates very large gain (mass transfer coefficient), k. Recall the well-known fact that the system temperature does not rise beyond the boiling point when there is no resistance to the departure of the produced vapour.

16.2.1 Model Development

The model for a vaporizer is constructed based on the following assumptions:

- The liquid is pure, incompressible and perfectly mixed in the vessel.
- The heat losses are assumed negligible.
- The density (ρ) and heat capacity (C_p) remain constant.
- The liquid and vapour phases are in equilibrium. It implies that
  (a) the temperatures of liquid and vapour are identical (i.e., $T_L = T_V = T$) and no energy balance is required for the vapour phase.
  (b) the vapour pressure of liquid (pure) and the pressure in the vapour phase are identical (i.e., $P = P_V$).
- The temperature is the same (T_S) everywhere in the jacket.
- The perfect gas law is used.

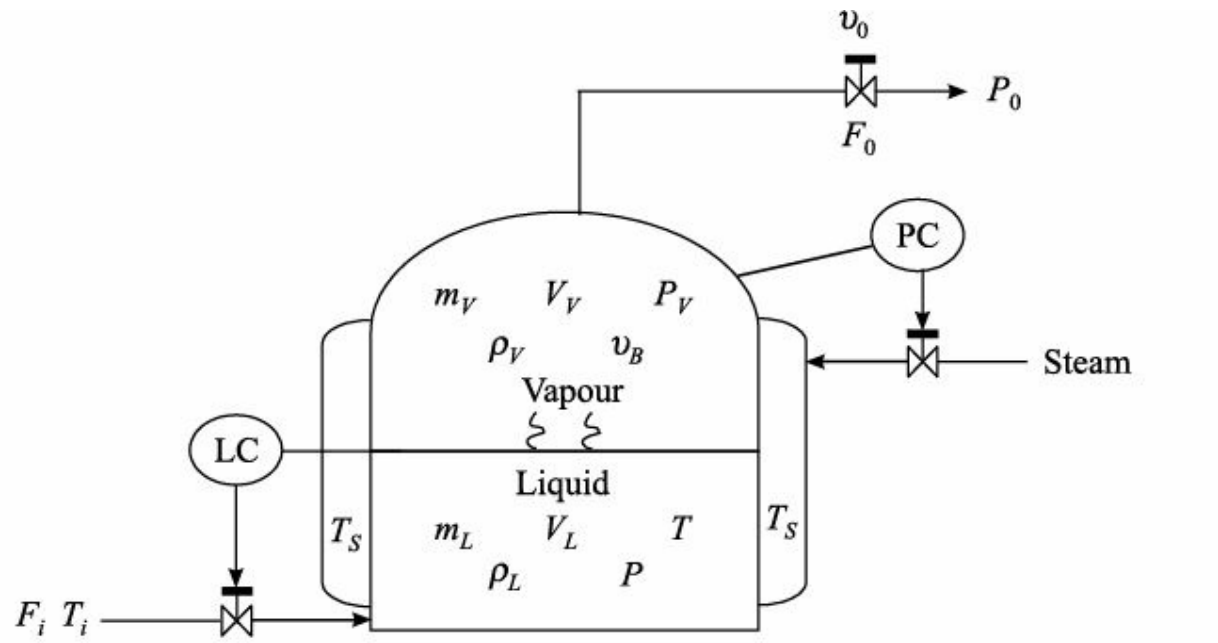

FIGURE 16.1 Schematic representation of a vaporizer.

The balance equations for the representative system are presented in the following:

Mass balance (*liquid phase*)

$$\frac{dm_L}{dt} = \frac{d(\rho_L V_L)}{dt} = F_i \rho_L - \upsilon_B \qquad (16.1)$$

Mass balance (*vapour phase*)

$$\frac{dm_V}{dt} = \frac{d(\rho_V V_V)}{dt} = \upsilon_B - F_0 \rho_V \qquad (16.2)$$

where V_L denotes the volume of liquid, V_V the volume of vapour, F_0 the volumetric vapour outflow through exit valve, m_L the mass in liquid phase and m_V the mass in vapour phase.

Energy balance (*liquid phase*)

$$\frac{d(\rho_L V_L C_p T)}{dt} = F_i \rho_L C_p T_i - \upsilon_B(\lambda + C_p T) + Q \qquad (16.3)$$

with

$$Q = UA(T_S - T) \qquad (16.4)$$

Obviously, the reference temperature (T_{ref}) is considered here zero. In the above equations, ¬ is the latent heat of vaporization at the system temperature, U the overall heat transfer coefficient, A the heat transfer area and Q the heat supplied by the steam. Using the following equation, the steam temperature (T_S) in degree Celsius can be determined knowing the pressure (P_{steam}) in bara:

$$P_{\text{steam}} = \exp\left(11.6859 - \frac{3822.3186}{227.47 + T_S}\right) \qquad \text{[from Equation (2.83)]}$$

Energy balance (*vapour phase*)

$$T_L = T_V = T \qquad (16.5)$$

Equation of state (*vapour phase*)

$$P_V V_V = \frac{m_V RT}{MW} \qquad (16.6)$$

with

$$V_V = V - V_L \qquad (16.7)$$

Here, V represents the total volume of the system and MW the molecular weight.

Valve equation (*gas flow*)

Considering $\tilde{\nu}_0 = \hat{\nu}_V F_0$,

$$\upsilon_0 = K_V \sqrt{P_V (P_V - P_0)} \qquad (16.8)$$

where K_V is the valve constant and P_0 the exit pressure.

Vapour pressure (*boiling relation*)

$$\ln P = A - \frac{B}{T + C} \qquad \text{[Antoine equation, i.e., Equation (9.28)]}$$

Note that it is straightforward to calculate the boiling point temperature, T and pressure, P ($= P_V$) by solving simultaneously Equation (16.6) and the Antoine equation. As shown in Figure 16.1, two controllers can be employed for the example system. One is for maintaining the liquid level in the vessel by the manipulation of feed inflow rate and the other one can control the pressure by adjusting the steam flow rate.

16.2.2 Simulation Algorithm with a Boiler Example

So far, we have discussed a process model that can be used for a boiler. Now, consider a boiler that aims to produce steam by receiving heat (Q) from external firing. In order to simulate the boiler model, required data are documented in Table 16.1. In this problem, neglect the left-hand side of Equation (16.3) because this differential term is negligible with respect to Q. The simulation algorithm in step-wise fashion is given in the following. The development of computer code and the dynamics study are left for the students. Investigate the closed-loop performance as well implementing the P-only controller for maintaining both the level and pressure.

Table 16.1 Given data for a boiler

$Q = 5000$ kcal/h
$\bar{\lambda} = 475$ cal/g
$C_p = 1$ cal/g.°C
$T_{ref} = 0$°C
$T_i = 20$°C
$F_i = 1000$ l/h
$\hat{\rho}_L = 1$ g/cc
$V = 5500$ l
V_L (at $t = 0$) $= 2800$ l
m_V (at $t = 0$) $= 9$ kg
$K_V = 40$ kg/h.bara
$P_0 = 10$ bara
$MW = 18$
$R = 1.987$ cal/gmol.K

Simulation steps

Step 1: Compute V_V from Equation (16.7) knowing V and V_L (at $t = 0$).

Step 2: Knowing m_V (at $t = 0$), R, MW and V_V, calculate T and P by simultaneously solving the boiling relation (Antoine) and Equation (16.6).

Step 3: Solve Equation (16.3) with left-hand side equals zero for finding $\dot{m}_B$ based on the known information of F_i, x_L, C_p, T_i, T, T and Q.

Step 4: Compute $\dot{m}_0$ from Equation (16.8) at given K_V and P_0. P is available.

Step 5: Update m_V (at $t + 1$) using Equation (16.2). $\dot{m}_B$ and $\dot{m}_0$ ($= x_V F_0$) are obtained previously.

Step 6: Update V_L (at $t + 1$) using Equation (16.1).

Step 7: Go to Step 1 until the steady state has reached.

16.3 COMMERCIAL DOUBLE-EFFECT EVAPORATOR: TOMATO JUICE

16.3.1 Introduction

Evaporation technique is used for removing the solvent as vapour from a solution or slurry. For most of the evaporation systems, the solvent is water. The purpose of an evaporation process is to produce a concentrated solution (thick liquor or slurry) by vaporizing a portion of the solvent. In many situations, evaporators operate under a vacuum. For this, a vacuum pump or jet ejector vacuum system is needed on the last effect. Evaporators are widely used in food, paper and pulp, and chemical industries.

In evaporation, no attempt is made to separate components of the vapour and this distinguises evaporation from distillation method. Evaporation differs from drying in that the residue is always a liquid, which may be highly viscous or a slurry. Again it is distinguised from crystalization in that evaporation technique is employed for concentrating a solution rather than producing or building crystals.

Evaporator may have a single unit, called single-effect, or multiple units, called multiple-effect. Most important advantage of multiple-effect over the single-effect evaporator is the *economy*[1]. Multiple-effect scheme evaporates more water per kilogram of steam fed to the unit by reusing the vapour from one effect as the heating medium for the next. Note that the multiple-effect scheme provides lower *capacity*[2] than the single-effect evaporator. To know more about evaporators, the reader can consult any standard textbook on heat transfer
(e.g., McCabe et al., 1993).

1 Economy is the number of kilograms vaporized per kilogram of steam fed to the evaporator.

2 Capacity is the number of kilograms of water vaporized per hour.

In this chapter, a systematic simulation study is conducted on a commercial double-effect tomato paste evaporator. The dynamic process model, consisting of mass balance, energy balance and empirical correlations, is derived in the form of differential-algebraic equations. The validation of this model is reported in literature (Runyon et al., 1991). The simulation of the model structure is performed here for open-loop process dynamics. For closed-loop dynamics, the three single-loop proportional integral (PI) control strategies along with two level controllers (P-only) have been employed around the interactive evaporation system.

16.3.2 The Process

The example process shown in Figure 16.2 is a double-effect evaporator with backward feeding arrangement used for tomato concentrate. The two effects are numbered[3] from left to right as Tank1 and

Tank2, respectively. The raw juice (feed) having flow rate F, composition X_f and temperature T_f enters Tank2, and the steam with flow rate S and temperature T_S enters Tank1. The mass holdups in the two tanks are defined as M_1 and M_2. V_1 and V_2 are the vapour flow rates from the overhead of two tanks with temperature T_1 and T_2, respectively. P_1 and P_2 are the product flow rates from the two effects with composition X_p and X_2, and temperature T_1 and T_2, respectively. The steady state and parameter values are listed in Table 16.2.

3 Effects are always numbered according to decreasing pressure (steam flow), irrespective of the feeding pattern.

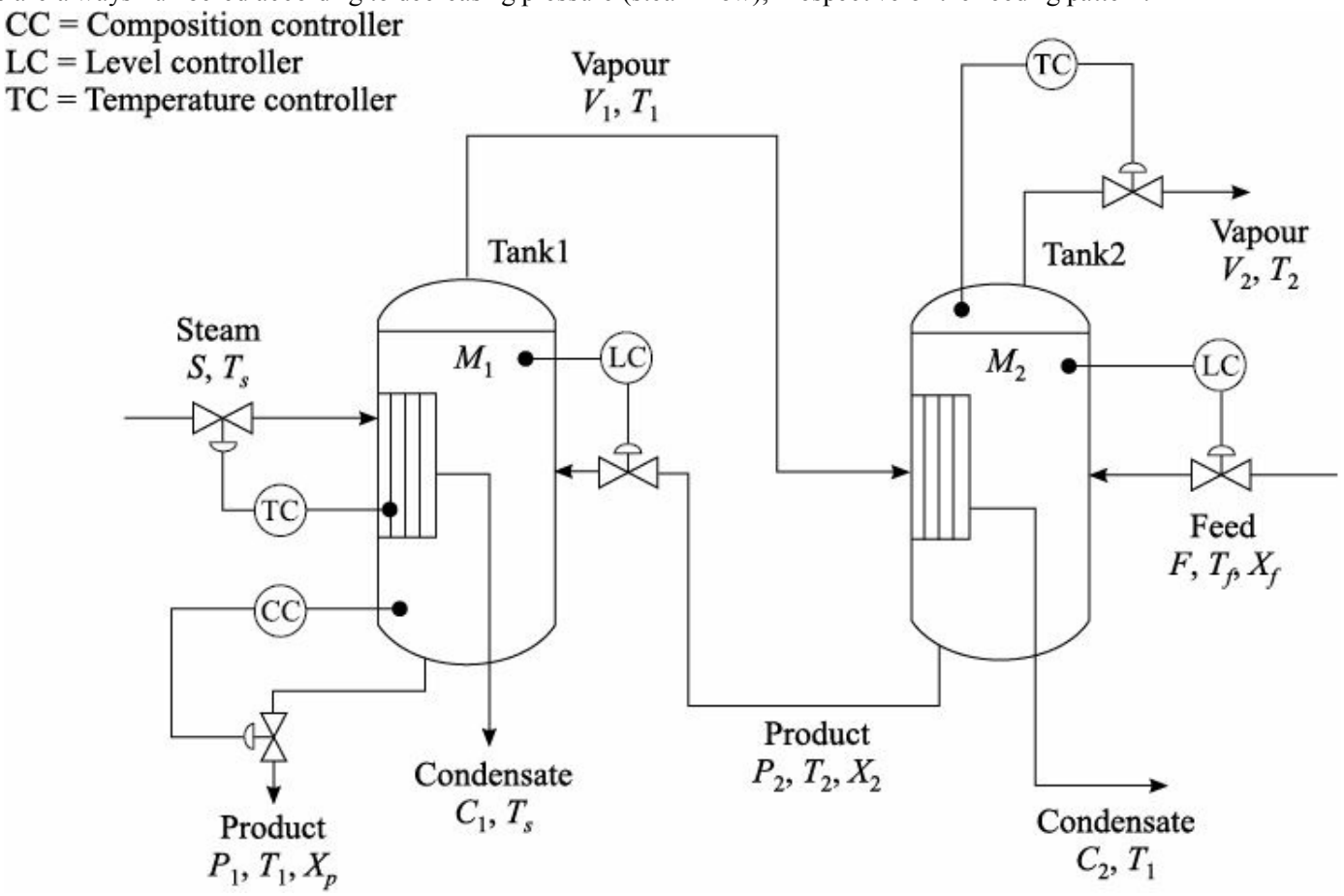

FIGURE 16.2 Schematic representation of a double-effect evaporator.

Table 16.2 Steady state* and parameter values

Term	*Abbreviation (unit)*	*Value*
Tank1 mass holdup	M_{10} (kg)	2268
Tank2 mass holdup	M_{20} (kg)	2268
Input feed flow rate	F_0 (kg/h)	26,103
Input steam flow rate	S_0 (kg/h)	11,023
Tank1 liquid product flow rate	P_{10} (kg/h)	5006
Tank2 liquid product flow rate	P_{20} (kg/h)	14,887
Vapour flow rate from Tank1	V_{10} (kg/h)	9932
Vapour flow rate from Tank2	V_{20} (kg/h)	11,165
Feed composition	X_{f0} (kg/kg)	0.05
Tank1 composition	X_{p0} (kg/kg)	0.2607
Tank2 composition	X_{20} (kg/kg)	0.0874
Steam temperature	T_{S0} (°C)	115.7
Feed temperature	T_{f0} (°C)	85.0
Temperature in Tank1	T_{10} (°C)	74.7
Temperature in Tank2	T_{20} (°C)	52.0
Heat transfer area in Tank1	A_1 (m^2)	102
Heat transfer area in Tank2		412

Overall heat transfer coefficient for Tank1	A_2 (m^2)	5826
Overall heat transfer coefficient for Tank2		2453
	U_1 (kJ/h.m^2.°C)	
	U_2 (kJ/h.m^2.°C)	

*suffix 0.

Model development

An evaporation process involves mass and heat transfer. The tomato juice is considered as a binary solution of water and soluble solids (Miranda and Simpson, 2005), both considered inert in a chemical sense. The macroscopical evaporator model has been constructed based on conservative laws and empirical relationships. It should be noted that only the juice phase is considered for modelling. The assumptions involved in the formulation of the mathematical model are listed below. A separate 'Notation' section is given at the end of the discussion to define the terms used.

- Negligible heat losses to the surroundings
- Homogeneous composition and temperature inside each effect
- Variable liquid holdup and negligible vapour holdup
- Overhead vapours considered as pure steam
- Latent heat of vaporization varied with temperature

Total mass balance

$$\text{First effect: } \frac{dM_1}{dt} = P_2 - P_1 - V_1 \qquad (16.9)$$

$$\text{Second effect: } \frac{dM_2}{dt} = F - P_2 - V_2 \qquad (16.10)$$

Component (*solids*) *mass balance*

$$\text{First effect: } \frac{d(M_1 X_p)}{dt} = P_2 X_2 - P_1 X_p \qquad (16.11)$$

$$= \qquad M_1 \frac{dX_p}{dt} + X_p \frac{dM_1}{dt} = P_2 X_2 - P_1 X_p \qquad (16.12)$$

$$= \qquad M_1 \frac{dX_p}{dt} = P_2 X_2 - P_1 X_p - X_p \frac{dM_1}{dt} \qquad (16.13)$$

Substituting Equation (16.9), we obtain

$$M_1 \frac{dX_p}{dt} = P_2 X_2 - P_1 X_p - X_p (P_2 - P_1 - V_1) \qquad (16.14)$$

$$= \qquad M_1 \frac{dX_p}{dt} = P_2 X_2 - P_1 X_p - X_p P_2 + X_p P_1 + X_p V_1 \qquad (16.15)$$

$$= \quad \frac{dX_p}{dt} = \frac{P_2(X_2 - X_p) + X_p V_1}{M_1} \tag{16.16}$$

Second effect: $\frac{d(M_2 X_2)}{dt} = FX_f - P_2 X_2$ (16.17)

Simplifying and rearranging, finally we get

$$\frac{dX_2}{dt} = \frac{F(X_f - X_2) + X_2 V_2}{M_2} \tag{16.18}$$

Energy balance

The steam flow rate to the first effect is obtained through the energy balance on the first effect heat exchanger as:

$$S\lambda(T_S) = U_1 A_1 (T_S - T_1) \tag{16.19}$$

That means,

$$S = \frac{U_1 A_1 (T_S - T_1)}{\lambda(T_S)} \tag{16.20}$$

Similarly, the vapour flow rate to the second effect is derived from the energy balance on the second effect heat exchanger as:

$$V_1\lambda(T_1) = U_2 A_2 (T_1 - T_2) \tag{16.21}$$

$$= \quad V_1 = \frac{U_2 A_2 (T_1 - T_2)}{\lambda(T_1)} \tag{16.22}$$

In the following, the energy balance equations are derived.

First effect: $\frac{d[M_1 h(T_1, X_p)]}{dt} = P_2 h(T_2, X_2) + S\lambda(T_S) - P_1 h(T_1, X_p) - V_1 H(T_1)$

(16.23)

$$= M_1 \frac{dh(T_1, X_p)}{dt} + h(T_1, X_P) \frac{dM_1}{dt} = P_2 h(T_2, X_2) + S\lambda(T_S) - P_1 h(T_1, X_p) - V_1 H(T_1)$$

(16.24)

$$= M_1 \frac{dh(T_1, X_p)}{dt} = P_2 h(T_2, X_2) + S\lambda(T_S) - P_1 h(T_1, X_p) - V_1 H(T_1) - h(T_1, X_p) \frac{dM_1}{dt}$$

(16.25)

Substituting Equation (16.9), we obtain

$$M_1 \frac{dh(T_1, X_p)}{dt} = P_2 [h(T_2, X_2) - h(T_1, X_p)] + S\lambda(T_S) - V_1 [H(T_1) - h(T_1, X_p)]$$

(16.26)

Using Equation (16.19), we obtain

$$M_1 \frac{dh(T_1, X_p)}{dt} = P_2[h(T_2, X_2) - h(T_1, X_p)] + U_1A_1(T_S - T_1) - V_1[H(T_1) - h(T_1, X_p)]$$

(16.27)

$$= \frac{dh(T_1, X_p)}{dt} = \frac{P_2[h(T_2, X_2) - h(T_1, X_p)] + U_1A_1(T_S - T_1) - V_1[H(T_1) - h(T_1, X_p)]}{M_1}$$

(16.28)

Second effect: $\frac{d[M_2h(T_2, X_2)]}{dt} = Fh(T_f, X_f) + V_1\lambda(T_1) - P_2h(T_2, X_2) - V_2H(T_2)$

(16.29)

Simplifying and rearranging, finally we have

$$\frac{dh(T_2, X_2)}{dt} = \frac{F[h(T_f, X_f) - h(T_2, X_2)] + U_2A_2(T_1 - T_2) - V_2[H(T_2) - h(T_2, X_2)]}{M_2}$$

(16.30)

Empirical correlations

The enthalpy of the product (tomato juice) is represented as (Heldman and Singh, 1981):

$$h(T, X) = (4.177 - 2.506X)T \qquad (16.31)$$

The pure solvent vapour (steam) enthalpy is computed using a polynomial regression equation of values from the steam tables as:

$$H(T) = 2495.0 + 1.958T - 0.002128T^2 \qquad (16.32)$$

For the condensate streams, the pure solvent liquid enthalpy is also obtained from the steam tables as:

$$h(T) = 4.177T \qquad (16.33)$$

So, the latent heat of vaporization has the following form:

$$\neg(T) = H(T) - h(T) = 2495.0 - 2.219T - 0.002128T^2 \qquad (16.34)$$

Using the above correlations, the energy balance equations [Equations (16.28) and (16.30)] have the following final forms:

$$\frac{dT_1}{dt} = \frac{P_2(4.177 - 2.506X_2)(T_2 - T_1) - U_2A_2(T_1 - T_2) + U_1A_1(T_S - T_1)}{M_1(4.177 - 2.506X_p)}$$

(16.35)

$$\frac{dT_2}{dt} = \frac{F(4.177 - 2.506\,X_f)\,(T_f - T_2) + U_2A_2(T_1 - T_2) + V_2[4.177\,T_2 - H(T_2)]}{M_2(4.177 - 2.506X_2)}$$

(16.36)

In the following, the open-loop as well as the closed-loop dynamics are discussed.

16.3.3 Application of Control Algorithm

Control objectives

The control objectives for an evaporation system are selected taking into account the product specifications, operational constraints and cost considerations. For the concerned process, the primary objective is to maintain the product solids concentration (or product viscosity) at its desired value. In addition to the product specifications, the following aspects need to be taken care of:

- To prevent the overflow or drying out of evaporator tubes, liquid mass holdup is required to control.
- To avoid the product degradation or damage, temperature is required to maintain at the desired value.
- Steam economy should be maximized.

Degrees of freedom analysis

The evaporator model presented earlier includes 15 independent variables (V) [F, P_1, P_2, M_1, M_2, T_f, T_S, T_1, T_2, S, V_1, V_2, X_f, X_p and X_2] and eight independent equations (E) [(16.9), (16.10), (16.16), (16.18), (16.20), (16.22), (16.35) and (16.36)]. We know that the number of degrees of freedom (f) is given as

$$f = V - E \tag{16.37}$$

The process is said to be:

Case A: exactly specified when $f = 0$
Case B: underspecified when $f > 0$
Case C: overspecified when $f < 0$.

It should be noted that for an underspecified system having f degrees of freedom, we require f number of additional equations to make the system completely specified. On the other hand, f number of equations has to be removed for the overspecified case.

Underspecified systems are quite common. To make them exactly specified, there are, however, two possibilities:

(i) Specify the values of disturbance variables mostly through direct measurements.

(ii) Include control equations selecting best possible control pairs[4].

4 A control pair is a pair between a controlled variable and a manipulated input.

At this point, it is important to mention that the implementation of the above two strategies must be done judiciously and care must be taken to avoid the overspecification of the system.

For the representative evaporation system, the number of degrees of freedom is seven (= 15 – 8), i.e., $f > 0$ (underspecified). In order to have a completely determined process, as stated, the number of its degrees of freedom should be zero. For this purpose and to meet the control objectives, five control pairs have been selected and two input variables, namely X_f and T_f, are to be treated as known disturbances.

Selection of control pairs

A control pair is selected taking into consideration the following:

(i) The manipulation has a direct and rapid effect on the controlled variable.
(ii) The dead-time is as small as possible between the manipulated input and controlled variable.
(iii) For multi-input/multi-output system, the loop interaction is minimal.

The detailed analysis with the consideration of above issues in selecting the control loops is beyond the scope of this course. For the example of tomato paste evaporator, the following are chosen as controlled variables: (i) the final product composition (X_p), (ii) the temperature of the inlet steam (T_S), (iii) the temperature of the second effect (T_2), (iv) the liquid mass holdup in the first effect (M_1), and (v) the liquid mass holdup in the second effect (M_2). The corresponding manipulated inputs are chosen based on experience as: (i) the product flow rate from the first effect (P_1), (ii) the steam flow rate (S), (iii) the vapour flow rate from the second effect (V_2), (iv) the product flow rate from the second effect (P_2), and (v) the feed flow rate (F). Figure 16.2 and Table 16.3 define all these control pairings.

Table 16.3 Control pairings and corresponding controllers used

Controlled variable	*Manipulated variable*	*Controller type*
X_p	P_1	PI
T_S	S	PI
T_2	V_2	PI
M_1	P_2	P-only
M_2	F	P-only

Control laws

As shown in Table 16.3, the three single-loop classical PI controllers and two P-only controllers have been employed on the interactive evaporator system. The general form of a classical PI control law is given in Chapter 3. It is well known that for a P-only controller, there is no integral part. The controller tuning parameter values used are reported in Table 16.4.

Table 16.4 Tuning parameter values

Tuning parameter	*Value*
K_{p1}	30,000 kg/h
K_s	15 kg/h.°C
K_{v2}	1250 kg/h.°C
K_{p2}	800 h^{-1}
K_f	1000 h^{-1}
τ_{p1}	0.05 h
τ_s	0.35 h
τ_{v2}	0.03 h

16.3.4 Simulation Results

Computer codes have been developed (not reported here, left for your homework) to produce simulation results. The fourth-order Runge–Kutta method (see Chapter 2) is used to solve the differential equations contained in the model. In the subsequent discussion, the open-loop followed by the closed-loop evaporator performance is covered.

Open-loop performance

Figure 16.3 illustrates the effect of Tank2 product flow rate on the main product composition. The two consecutive step changes have been introduced in the product flow rate (step increase: 14,887 $\rightarrow$ 15,200

kg/h at time = 5 h; step decrease: 15,200 ⟶ 14,887 kg/h at time = 10 h).
As a consequence, the final product purity gets disturbed and the process attains a new steady state against each step change. This result confirms that the sample evaporator is open-loop stable.

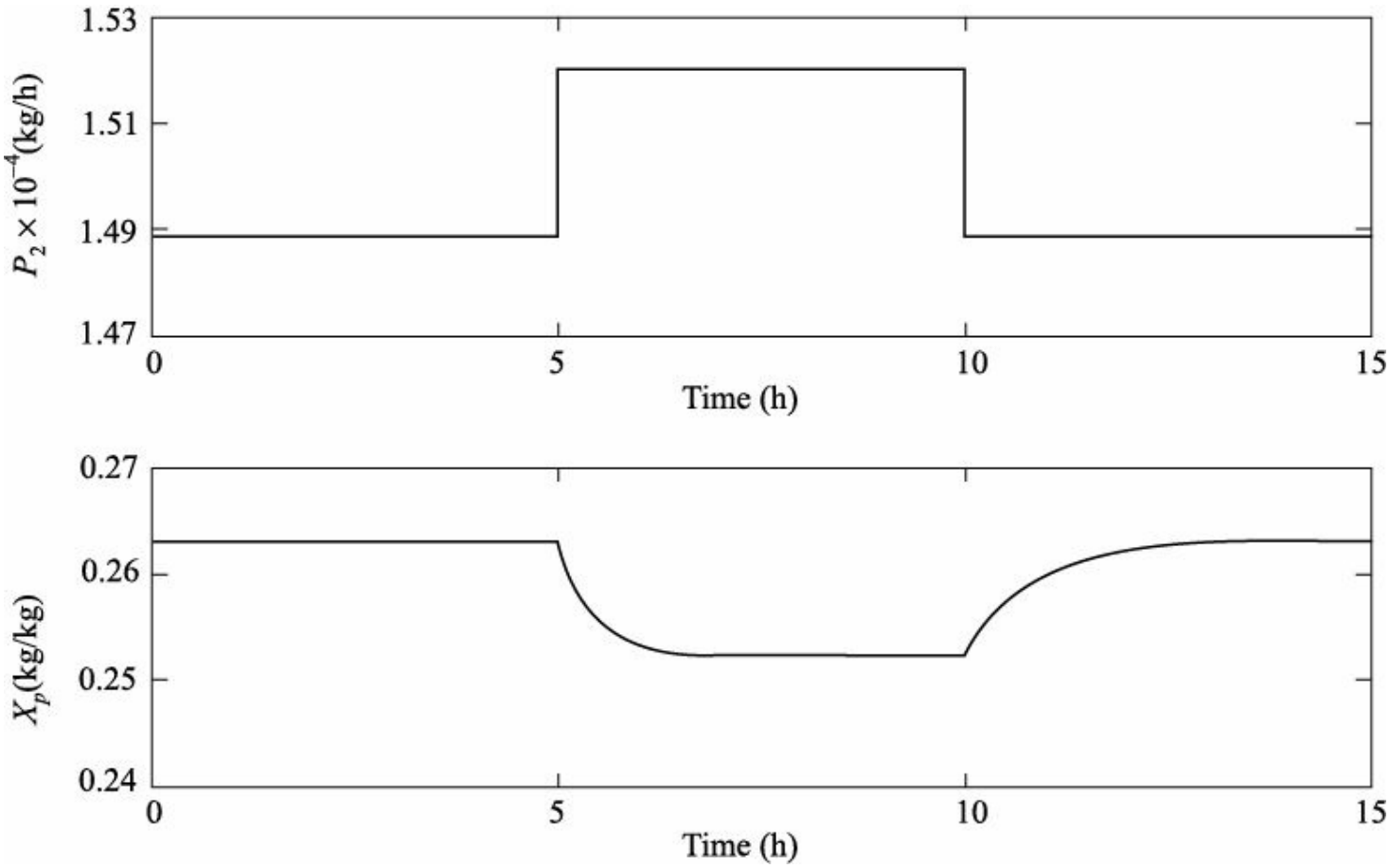

FIGURE 16.3 Effect of a pulse input change in Tank2 product flow rate (changed from 14,887 to 15,200 kg/h at time = 5 h and then from 15,200 to 14,887 kg/h at time = 10 h).

Closed-loop performance

Regulatory performance

The regulatory performance is depicted in Figure 16.4 introducing a pulse input change in feed composition (step increase: 0.05 ⟶ 0.0525 kg/kg at time = 5 h; step decrease: 0.0525 ⟶ 0.05 kg/kg at time = 15 h). The figure does not show the results of all five control loops; the control performance in terms of final product composition and liquid mass holdup in Tank1 is demonstrated. It is obvious from the simulation results that both the composition and level controllers take action for reducing the effect of disturbance.

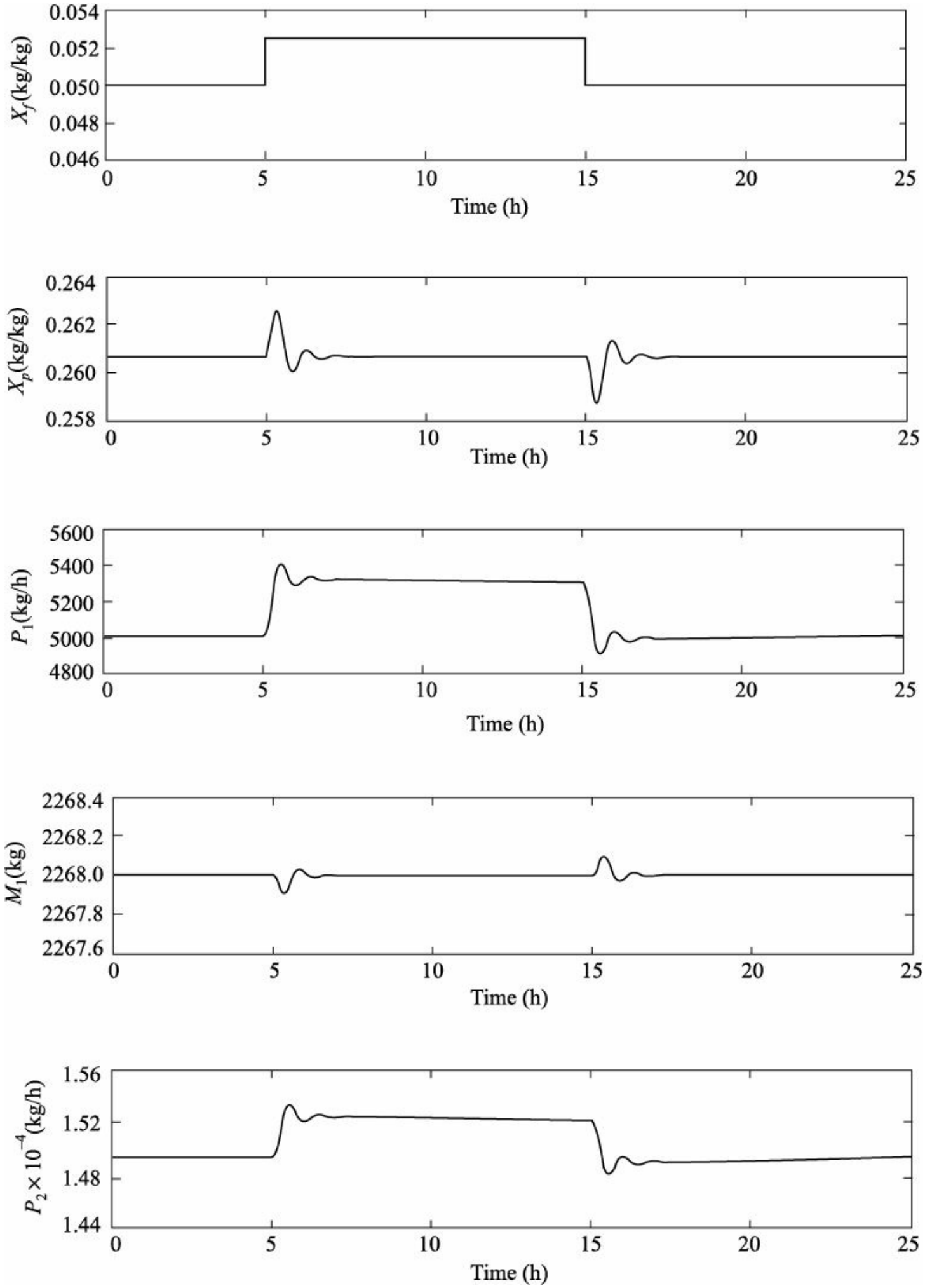

FIGURE 16.4 Effect of a pulse input change in feed composition (changed from 0.05 to

0.0525 kg/kg at time = 5 h and then from 0.0525 to 0.05 kg/kg at time = 15 h).

Servo performance

Figure 16.5 displays the servo performance against a pulse change in set point value of the final product composition (step increase: 0.2607 ₀ 0.27 kg/kg at time = 5 h; step decrease: 0.27 ₀ 0.2607 kg/kg at time = 15 h). In the figure, the controller outputs are also recorded. In this simulation experiment, the interaction between the control loops is also prominent.

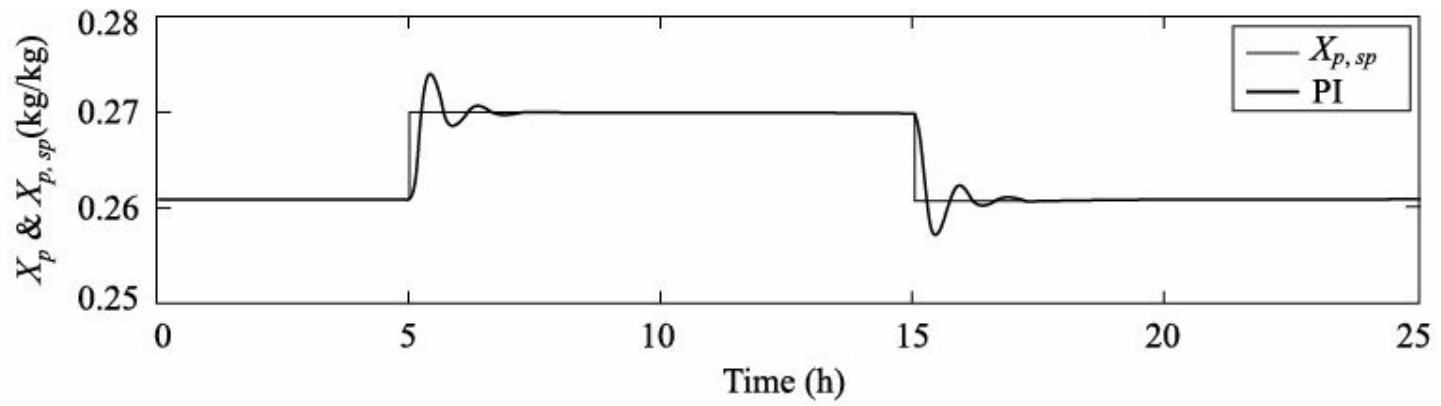

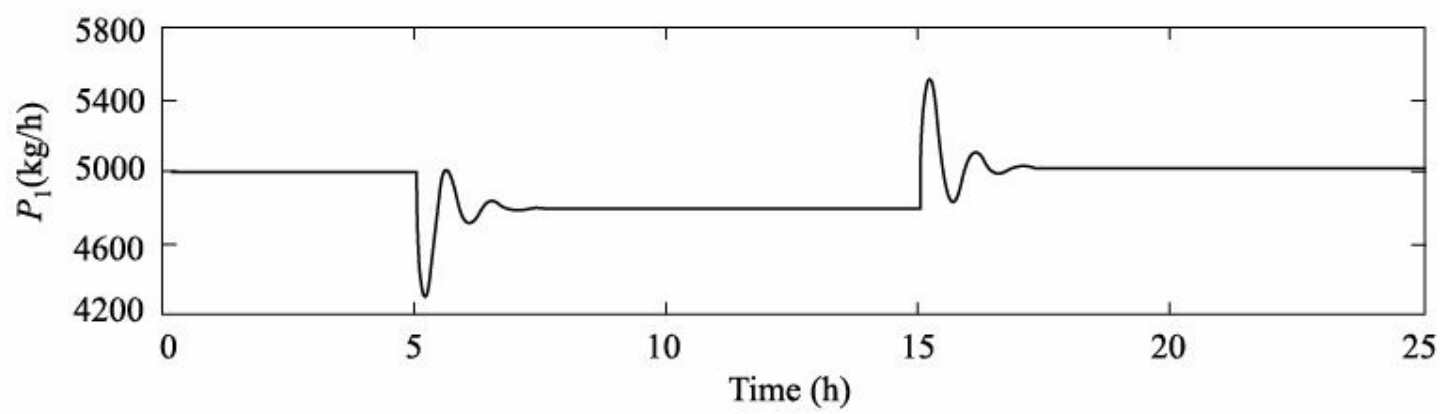

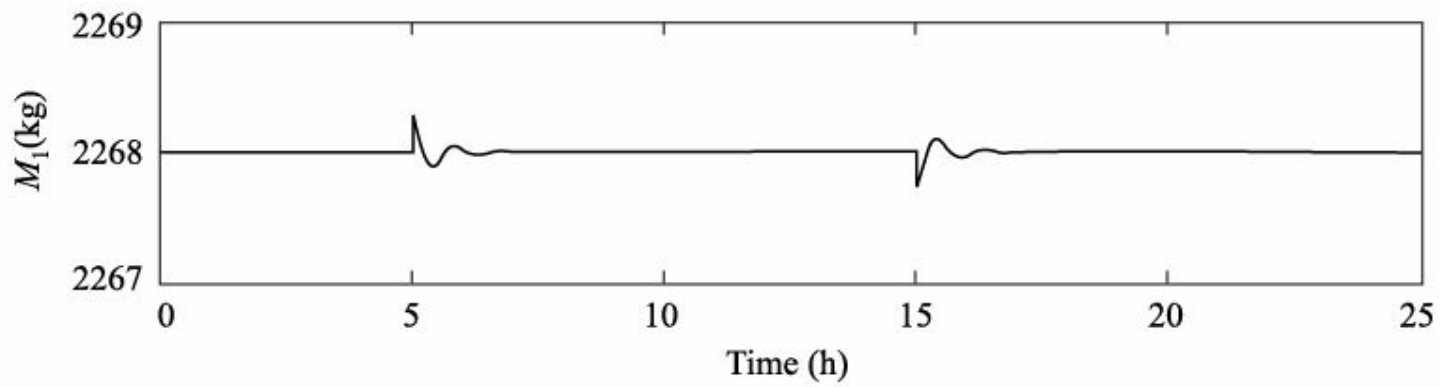

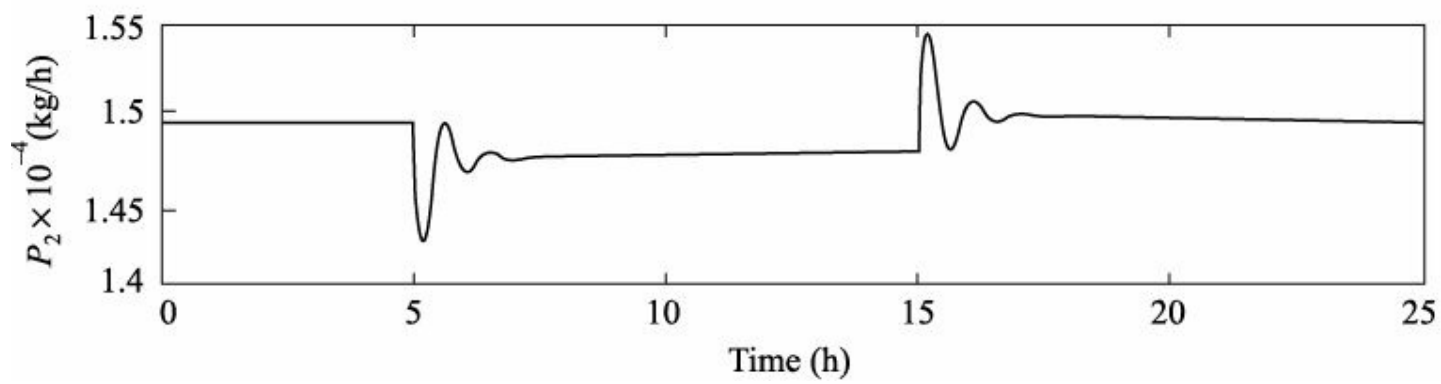

FIGURE 16.5 Effect of a pulse set point change in final product composition (changed from 0.2607 to 0.27 kg/kg at time = 5 h and then from 0.27 to 0.2607 kg/kg at time = 15 h).

16.4 SUMMARY AND CONCLUSIONS

This chapter discusses two vaporizing exchangers, namely vaporizer and evaporator. A vaporizer model is developed first and then the simulation steps are explained. It is suggested to use the two control loops for maintaining the liquid level and vaporizer pressure. The next part of the chapter includes the open-loop as well as the closed-loop operation of a commercial double-effect tomato paste evaporation system. The model structure is developed based on backward feeding approach. Open-loop simulation shows that the sample evaporator is a stable process. The three conventional PI controllers along with two level (P-only) controllers have been simulated to investigate the closed-loop performance. The control performance has been tested based on servo and regulatory response.

Notations for the Evaporator

$h(T)$	Enthalpy of pure liquid solvent (condensate) at temperature T (kJ/kg)
$h(T, X)$	Enthalpy of liquid product (tomato juice) at temperature T and composition X (kJ/kg)
$H(T)$	Enthalpy of pure vapour solvent (saturated steam) at temperature T (kJ/kg)
K	Proportional gain
t	Time (h)
$\varkappa$	Integral time constant (h)
Subscripts	
f	Feed
p	Final product
p_1	Product stream from the first effect in control study
p_2	Product stream from the second effect in control study
s	Steam
v_2	Vapour stream from the second effect in control study
sp	Set point
0	Steady state
1	Tank1/first effect
2	Tank2/second effect

EXERCISES

16.1 What are the different types of vaporizing exchangers?

16.2 Can we call a shell-and-tube heat exchanger as a vaporizing exchanger?

16.3 What are the merits and demerits of a multi-effect evaporator with respect to its single-effect counterpart?

16.4 What do you mean by evaporator capacity and economy?

16.5 Define the individual heat transfer resistances between the steam and the boiling liquid.

16.6 Give an example of a multicomponent vaporizing exchanger.

16.7 Develop the model structure for a double-effect evaporator based on the forward feeding approach. Simulate the model for dynamics study using the data given in this chapter. Discuss the possible control pairings.

REFERENCES

Heldman, D.R., and Singh, R.P. (1981). *Food Process Engineering*, 2nd ed., AVI Publishing Company, Westport, Connecticut.

Kern, D.Q. (1997). *Process Heat Transfer*, 2nd reprint, Tata McGraw-Hill, New Delhi.

McCabe, W.L., Smith, J.C., and Harriott, P. (1993). *Unit Operations of Chemical Engineering*, 5th ed., McGraw-Hill, Singapore.

Miranda, V., and Simpson, R. (2005). Modeling and simulation of an industrial multiple effect evaporator: tomato concentrate, *Journal of Food Engineering*, 66, 203–210.

Runyon, C.H., Rumsey, T.R., and McCarthy, K.L. (1991). Dynamic simulation of a nonlinear model of a double effect evaporator, *Journal of Food Engineering*, 14, 185–201.

Appendix

Thermodynamic Processes

Thermodynamic Process	*Meaning*
Adiabatic	no heat added to or removed from system
Isothermal	constant temperature
Isobaric	constant pressure
Isochoric	constant volume
Isenthalpic	constant enthalpy
Isentropic	constant entropy

Universal Gas Constants (R)

1.987 kcal/(kmol)(K)
1.987 cal/(gmol)(K)
1.987 Btu/(lbmol)(°R)

8.314 (kPa)(m^3)/(kmol)(K)
8.314 J/(gmol)(K)

82.06 (cm^3)(atm)/(gmol)(K)
0.08206 (l)(atm)/(gmol)(K)

10.73 (psia)(ft^3)/(lbmol)(°R)

21.9 (in Hg)(ft^3)/(lbmol)(°R)

0.7302 (ft^3)(atm)/(lbmol)(°R)

Index

Second Edition

Chemical Process Modelling and Computer Simulation

AMIYA K. JANA

This comprehensive and thoroughly revised text, now in its *second edition*, continues to present the fundamental concepts of how mathematical models of chemical processes are constructed and demonstrate their applications to the simulation of two of the very important chemical engineering systems: the **chemical reactors** and **distillation systems**.

The book provides an integrated treatment of process description, mathematical modelling and dynamic simulation of realistic problems, using the robust process model approach and its simulation with efficient numerical techniques. Theoretical background materials on activity coefficient models, equation of state models, reaction kinetics, and numerical solution techniques—needed for the development of mathematical models—are also addressed in the book.

The topics of discussion related to tanks, heat exchangers, chemical reactors (both continuous and batch), biochemical reactors (continuous and fed-batch), distillation columns (continuous and batch), equilibrium flash vaporizer, and refinery debutanizer column contain several worked-out examples and case studies to teach students how chemical processes can be measured and monitored using computer programming.

The new edition includes two more chapters—**Reactive Distillation Column** and **Vaporizing Exchangers**—which will further strengthen the text.

This book is designed for senior level undergraduate and first-year postgraduate level courses in "Chemical Process Modelling and Simulation". The book will also be useful for students of petrochemical engineering, biotechnology, and biochemical engineering. It can serve as a guide for research scientists and practising engineers as well.

THE AUTHOR

AMIYA K. JANA (PhD) is Assistant Professor at IIT Kharagpur. He received his BE degree in chemical engineering in 1998 from Jadavpur University, M.Tech. in chemical engineering (specialization: Petroleum Refining Engineering and Petrochemicals) in 2000 from IIT Kharagpur, and PhD in chemical engineering (specialization: Control Systems) in 2004 from IIT Kharagpur.

Professor Jana has also authored another book *Process Simulation and Control Using ASPEN™* , published by the same publisher. His areas of research include nonlinear control, modelling and simulation, and energy engineering.

ISBN:978-81-203-4477-8

9 788120 344778

₹ 325.00

www.phindia.com